SEISMIC ASSESSMENT AND RETROFIT OF PRE-1970S REINFORCED CONCRETE FRAME STRUCTURES

A Thesis
Submitted in Partial Fulfilment
of
the Requirements for the Degree
of Doctor of Philosophy in Civil Engineering
at the
University of Canterbury
Christchurch
New Zealand

by
Aizhen Liu

2001

ABSTRACT

The seismic assessment of an existing reinforced concrete building designed to pre-1970s codes during a major earthquake focuses on investigating the global post-elastic responses of the building. The global post-elastic response of a reinforced concrete building can be studied based on the local post-elastic behaviour of the individual structural components.

In this study, simulated seismic loading tests were conducted on as-built reinforced concrete beam-column joint subassemblages in order to obtain the information on the post-elastic behaviour of as-built reinforced concrete components. Simulated seismic loading tests included two as-built full-scale interior beam-column joint units, four as-built full-scale exterior beam - column joint units and one retrofitted as-built exterior beam-column joint unit. The as-built test units contained the plain round longitudinal reinforcement and had the reinforcing details typical of an existing reinforced concrete structure constructed in the late 1950s in New Zealand.

The two as-built interior beam-column joint units, Unit 1 and Unit 2, were identical. Unit 1 was tested with zero column axial load and Unit 2 was tested with a compressive column axial load of $0.12A_g f_c'$. According to the current codes, the two as-built interior beam-column joint units would develop premature shear failure in the joints, beams and columns. Both units when tested showed that, unlike the conclusion reached by the theoretical assessment using the current code method, the premature shear failure was precluded in the joint and members of the test units. For both units, the post-elastic behaviour of the reinforced concrete components was limited to the fixed-ends at the beam-column interfaces of the members, and it was in the form of a major flexural crack at the beam-column interfaces. Due to the plain round longitudinal reinforcement used, severe bond slip along the plain round longitudinal reinforcement occurred within and adjacent to the joint, resulting in significantly degrading flexural behaviour at the beam-column interfaces of the members. For both units tested, the available structural stiffness and strength were low, especially the stiffness, and the degradation of the stiffness and strength was significant. Column bar buckling was also apparent, especially when the compressive axial load was present in the column.

The four as-built exterior beam-column joint units, Units EJ1 to EJ4, were identical except for the beam bar hook details in the exterior columns. Identical units EJ1 and EJ3 had the beam bar hooks bent away from the joint cores. Identical units EJ2 and EJ4 had the beam

bar hooks bent away from the joint cores. Units EJ1 and EJ2 were tested with zero column axial load but Units EJ3 and EJ4 were tested with a compressive column axial load of about $0.25A_gf_c'$ present. The retrofitted unit was the original as-built unit EJ1 with the beam bar hooks bent away from the joint core, and the retrofit was achieved by wrapping the column areas immediately above and below the joint core using fibre-glass after tested to test an alternative force path across the joint core. According to the current code method, the premature shear failure would occur in the joint of Unit EJ1 and in the beams of all the four as-built exterior beam-column joint units. Examination of the member force transfer across the joint showed that effective column transverse confinement within the beam bar hook range was critical in restraining the opening of the beam bar hooks and actuating the force transfer across the joint core, and an alternative force path across the joint core, in the case of the beam bar hooks bent away from the joint core in the exterior columns, could be actuated if sufficient column confinement above and below the joint core was available.

The as-built units when tested with zero axial column load demonstrated very poor force strength and stiffness behaviour. The final failures were dominated by the concrete tension cracking along the outer layer of column main bars adjacent to the joint core, which was initiated by the interaction between the opening of the beam bar hooks and the column bar buckling, irrespective of the beam bar hook details. The configuration of the beam bar hooks bent into the joint core was found to result in better seismic performance compared to that with the beam bar hooks bent away from the joint core in the case of zero axial column load and small amount of column transverse reinforcement provided. The as-built units when tested with constant compressive axial column load of about $0.25A_g f_c'$ present demonstrated that the presence of compressive axial column load totally prevented the concrete tension cracking along the beam bar hooks, and the post-elastic behaviour of the test units was limited to the fixed-ends of the beams, in the form of a big beam fixed-end rotation. Generally, the compressive column axial load greatly improved the overall stiffness and force strength of the units. In this case the effects of different beam bar hook details on the seismic performance of the as-built exterior beam-column joint units became very insignificant. The test on the retrofitted as-built unit showed that fibre-glass jacketing in the column areas adjacent to the joint core restrained the opening of the beam bar hook and actuated the postulated alternative the force transfer path across the joint

when the axial column load was low, leading to much improved stiffness and force strength performance.

Overall, for the as-built reinforced concrete members reinforced by plain round longitudinal reinforcement, the post-elastic seismic behaviour was governed by the degrading flexural behaviour at the member fixed-end at the beam-column interfaces, in the form of big fixed-end rotations. A rotational ductility factor at the fixed-end, rather than a curvature ductility factor associated with a plastic hinge length, became a more useful index to the member post-elastic flexural deformation. Member flexural strength and stiffness were lower than the theoretical estimations, and they were significantly influenced by the force transfer mechanism across the joint core. Typically, the compressive column axial load at the same joint resulted in much improved flexural behaviour at the beam fixed-end. Based on the test evidence, a method was tentatively proposed for allowing for the beneficial effect on the member flexural behaviour at the fixed-end of the compressive axial load on the transverse members at the same joint.

After obtaining the information on the post-elastic behaviour of as-built structural components, non-linear static and dynamic analyses were conducted for the subject building represented by the as-built test units. The non-linear static analysis showed that the earthquake-resisting capacity of similar structures do not satisfy the current design code requirements, a failure mechanism was very unlikely to form and the local member deformation capacity limited the structural performance during a major earthquake. No structural ductility can be relied on and the structural assessment has to be based on elastic response. Allowance for the masonry infills meant that the structural earthquake-resistant capacity was more inadequate. In this case, a soft storey failure mechanism could form, no ductility can be relied on. The non-linear dynamic analysis conducted for the subject building showed that similar existing reinforced concrete structures would survive during an earthquake with similar characteristics and magnitudes to the 1940 El Centro NS record.

ACKNOWLEDGEMENTS

The research work reported in this thesis was carried out in the Department of Civil Engineering at the University of Canterbury, New Zealand.

I wish to express my deepest gratitude to Dr. Carr and Prof. Park, supervisors of this project, for their invaluable advice and patience.

Thanks are also extended to the technical staff, Mr. G.E. Hill and Mr. N.J. Hickey, of the Department of Civil Engineering for their assistance with the construction and testing in the experimental programme.

The research funding provided by the Earthquake Commission of New Zealand for this project and the Doctoral Scholarship provided by the University of Canterbury are gratefully acknowledged. The financial support provided by Shanxi Province, P.R. China is also acknowledged. In addition, the contribution of the fibre-glass jacketing by Mr. Rob Irwin of Construction Technique Ltd, Auckland, is also gratefully acknowledged.

Finally, I wish to thank my family for their understanding and encouragement during the past years.

CONTENTS

NOTATION

f_c' = concrete compressive cylinder strength (MPa)

f_y = yield strength of longitudinal reinforcement (MPa)

f_{yt} = yield strength of transverse reinforcement (MPa)

N^* = compressive axial column load (N)

A_g = gross area of column section (mm^2)

b = width of beam (mm)

d = distance from extreme compression fiber of beam to centroid of beam tension reinforcement (mm)

p = ratio of area of the top beam longitudinal bars to bd of beam

p' = ratio of area of the bottom beam longitudinal bars to bd of beam

p_t = ratio of area of the total column longitudinal bars to column gross area

ε_y = steel yield strain

d_b = diameter of longitudinal steel (mm)

s = spacing of transverse reinforcement

ϕ = the strength reduction factor, being unity here

h_b = beam depth (mm)

h_c = column depth (mm)

ϕ_u = ultimate curvature (mm^{-1})

ϕ_y = yield curvature (mm^{-1})

v_{jh} = the nominal horizontal joint shear stress (MPa)

V_{jh} = the imposed horizontal joint shear force (N)

A_j = effective joint area (mm^2)

δ_{cr} = the rigid horizontal movement due to the deformation within the test rig (mm)

V_c = the equivalent storey shear (N)

P_r = the vertical shear applied to the right beam end (N)

P_l = the vertical shear applied to the left beam end (N)

l_1 = the loading span of the left beam of 1755 mm

l_2 = the loading span of the right beam of 1755 mm

γ_j = the joint shear distortion

l_j = the initial length of the diagonal in the joint core (mm)

δ_j = the change in the length of one diagonal in the joint core (mm)

$\delta_{j'}$ = the change in the length of the other diagonal in the joint core (mm)

α_j = the angle of the diagonal to the horizontal axis

K_e = the measured initial stiffness (N/mm)

$\Delta_{y,\,test}$ = the measured first yield displacement (mm)

μ_Δ = the imposed displacement ductility factor, defined as the imposed displacement

divided by the first yield displacement

Δ_{co} = the equivalent storey deflection (mm)

Δ_{bl} = the imposed vertical displacement at the left beam end (mm)

Δ_{br} = the imposed vertical displacement at the right beam end (mm)

l_c = storey height of 3200 mm

l_b = beam span of 3810 mm

V_i = theoretical strength of the unit in terms of storey shear, based on the flexural strength of the members

V_b = theoretical strength of beam in terms of beam shear, based on the flexural strength of the beam

Δ_c = estimated storey displacement (mm)

$\Delta_{c,b}$ = contribution of beam deformation to the storey displacement (mm), referred as Beam Displacement Component (mm)

$\Delta_{c,c}$ = contribution of column deformation to the storey displacement, referred as Column Displacement Component (mm)

$\Delta_{c,j}$ = contribution of joint deformation to the storey displacement, referred as Joint Displacement Component (mm)

$\theta_{b,i}$ = rotation angle over the beam region S_i

$\theta_{c,j}$ = rotation angle over the column region R_j

${}_t\delta_i$ = measurement of the top beam curvature potentiometer over the region S_i

${}_b\delta_i$ = measurement of the bottom beam curvature potentiometer over the region S_i

${}_r\delta_j$ = measurement of the right column curvature potentiometer over the region R_j

${}_l\delta_j$ = measurement of the left column curvature potentiometer over the region R_j

${}_t\delta_1$ = the top displacement measured by beam curvature linear potentiometer at the fixed-end interface

${}_b\delta_1$ = the bottom displacement measured by beam curvature linear potentiometer at the fixed-end interface

${}_R\delta_1$ = measurement of the right column curvature linear potentiometer at the fixed-end interface

${}_L\delta_1$ = measurement of the left column curvature linear potentiometer at the fixed-end interface

${}_E\delta_{bf}$ = the flexural deformation of east beam

${}_W\delta_{bf}$ = the flexural deformation of west beam

${}_U\delta_{cf}$ = the flexural deformation of upper column

${}_B\delta_{cf}$ = the flexural deformation of bottom column

${}_b\delta_{fe}$ = the deformation due to beam fixed-end rotation

${}_c\delta_{fe}$ = the deformation due to column fixed-end rotation

$\phi_{b,i}$ = measured average curvature over the region S_i

$\phi_{c,j}$ = the measured average curvature over the region R_j

h_i = vertical distance between the top and bottom beam curvature linear potentiometers over the region S_i

s_i = longitudinal length of the region S_i

r_j = longitudinal length of the column region R_j

d_j = the horizontal distance between the right and the left column curvature potentiometers over the region R_j

l_1 = the distance from column face to the centre of west beam end pin (==1755 mm)

l_2 = the distance from column face to the centre of east beam end pin (==1755 mm)

$l_b' = l_1 = l_2 =$ the distance from the column face to the centre of the beam end pin.

l' = the distance from the beam face to the pin center of the upper column

$l_c' = l'$ = the distance from the beam face to the column end pin center

x_i = the distance from column face to the centre of the region i

y_j = the distance from the beam face to the center of the region j

γ_j = the joint shear distortion

h_b = the beam depth

h_c = the column depth

$\theta_{b,fe}$ = the beam fixed-end rotation

$\theta_{c,fe}$ = the column fixed-end rotation

h_1 = the vertical distance between the two fixed-end beam curvature linear potentiometers

$\Delta_{b,fe}$ = the equivalent storey displacement due to fixed-end rotation of the beam

$\Delta_{c,fe}$ = the component of storey displacement due to column fixed-end rotations

d_1 = the horizontal distance between the two linear potentiometers over the column fixed-end zones

μ = a coefficient of friction used in estimating the shear strength of the masonry panels

h_m = the height of the masonry panel

L_m = the length of the masonry panels

A_m = the area of the masonry panels in the horizontal plane

τ_O = bond shear strength of masonry panels

CHAPTER 1

INTRODUCTION

1.1 THE NEED FOR SEISMIC ASSESSMENT AND RETROFIT OF EXISTING REINFORCED CONCRETE STRUCTURES

Seismic design procedures for concrete structures have advanced significantly since about the 1970s around the world, such as in New Zealand and the United States, and the main advances have been in the understanding of the factors influencing the post-elastic dynamic behaviour of structures, the introduction of capacity design philosophy and the methods for detailing reinforcement in reinforced concrete structures to achieve the structural ductile behaviour necessary to survive severe earthquakes [P1, P2, N1]. These developments have brought the realisation that many reinforced concrete structures constructed before 1970s may be deficient according to the seismic requirements of current codes.

The need for the seismic assessment of existing reinforced concrete building structures designed to outdated seismic codes, and to retrofit if necessary, has been further emphasised by the damage observed as a result of major earthquakes. Several recent earthquakes, such as the 1985 Mexico Earthquake [J2, N2] and 1989 Loma Prieta Earthquake in California, USA [B2], caused severe collapse and/or damage to existing reinforced concrete structures designed to outdated codes. The 1985 Mexico earthquake with unique ground motions resulted in huge damage to about 2300 buildings, among which about 210 existing reinforced concrete structures collapsed, and left thousands dead [N2]. Once again, the damage caused by the 1995 Hyogo-ken Nanbu Earthquake in Kobe provided renewed impetus for seismic assessment and retrofit of existing reinforced concrete building structures. In the 1995 Hyogo-ken Nanbu Earthquake, the earthquake damage to reinforced concrete buildings was much more severe for buildings built before 1981 when the most recent Japanese seismic code came into effect. Most reinforced concrete buildings built after 1981 suffered only minor damage in the 1995 Hyogo-ken Nanbu Earthquake [P7].

As a result, there have been increased activities in many countries in the seismic assessment of existing reinforced concrete buildings and retrofit where necessary to improve their seismic performance. Several seismic assessment procedures have been

developed in many countries in recent years, and they are established on the basis of different principles. Most of the current seismic assessment procedures only check the dimensions and reinforcing details of each individual member, and they do not consider the post-elastic response of the whole structure, which is the fundamental revolution in the understanding of structural seismic performance during a major earthquake. Basically, the principles on which theses procedures are developed is still the working stress design concept. There are more advanced seismic assessment procedures, which incorporate the capacity design philosophy and consider the global structural behaviour in post-elastic range. Also a number of experimental researches into the possible seismic behaviour of pre-1970s reinforced concrete structures have been carried out and the majority of the experimental work is to study the cyclic loading behaviour of reinforced concrete components designed to now out-dated code. The information on cyclic loading behaviour of individual members is needed for investigating the post-elastic seismic behaviour of the whole structure.

1.2 BACKGROUND OF THIS RESEARCH PROJECT

A research program on Seismic Assessment and Retrofit of Existing Reinforced Concrete Structures has been under way at the University of Canterbury for several years sponsored by the Earthquake Commission of New Zealand. An existing reinforced concrete frame building constructed in 1950s in New Zealand has been thoroughly investigated. Following this investigation, a number of cyclic loading tests on as-built reinforced concrete columns and beam-column joint subassemblages with reinforcing details typical of the 1950s construction in New Zealand have been conducted [R2, H1, W1]. Although the tests on the columns used plain round bars for longitudinal reinforcement [R1], the previous tests on beam-column joints used deformed bars for longitudinal reinforcement [H1, W1]. Actually, plain round bar reinforcement was used in New Zealand until about the mid 1960s when deformed bar reinforcement became widely available. The bond strength of plain bar reinforcement is low, compared with deformed bar reinforcement, particularly during cyclic loading. Bond strength between the longitudinal reinforcement and the surrounding concrete plays a vital role in the performance of reinforced concrete members. Conventional theory for flexure and shear was established on the basis of the assumption of perfect bond between the longitudinal reinforcement and the surrounding concrete. Hence, plain round reinforcing bars when used for longitudinal reinforcement

may lead to very different seismic performance from the theoretical prediction, and the information obtained from the tests with deformed longitudinal reinforcement when used for assessing the seismic performance of reinforced concrete members with plain round longitudinal reinforcement may give misleading results.

In addition, these previous beam-column joint tests were conducted with zero axial column load, and this was considered to be the most unfavourable condition for the joint core. It is necessary to investigate the influence of axial column load on the seismic performance of beam-column joint regions, especially on the bond performance of the beam bars passing through the joint core and the joint shear capacity. This is of particular importance when plain round bars are used for longitudinal reinforcing bars. The presence of the compressive axial column load can enhance the force transmission by bond within the joint core, introducing larger forces into the joint core and hence accelerating the joint shear failure.

1.3 OBJECTIVES OF THIS RESEARCH PROJECT

The objectives of this research project are:

(1). To obtain, by tests, the information on the cyclic behaviour of as-built reinforced concrete components with plain round longitudinal reinforcement, which is needed for the seismic assessment of pre-1970s reinforced concrete frame structures. Emphasis is placed on identifying the weakest failure mode and its associated cyclic behaviour of the as-built reinforced concrete components reinforced by plain round bars. This is to be achieved by conducting simulated seismic loading tests on beam-column joint assemblies, which are reinforced by plain round longitudinal bars and have reinforcing details typical of the pre-1970s construction in New Zealand.

(2). To testify an effective method for strengthening and repair of existing reinforced concrete building frames for earthquake loading.

(3). To develop a proper structural analytical method for assessing the seismic performance of existing reinforced concrete moment - resisting frame structures (pre-1970s constructions) with plain round longitudinal bars. After employing the information obtained from the tests conducted in this project, a proper member modelling method,

which is capable of capturing the on-linear behaviour of as-built reinforced concrete components with plain round longitudinal reinforcement, is to be proposed.

1.4 ORGANIZATION OF THE THESIS

This thesis, which consists of 11 chapters, is classified into 6 parts.

Part 1, which includes chapters 2 and 3, reviews the available seismic assessment procedures and the previous research projects relevant to this project conducted at the University of Canterbury. Review of the available seismic assessment procedures is to clarify the needed information on local behaviour of reinforced concrete components for conducting the seismic assessment of existing reinforced concrete structures, and the review of the previous researches at the University of Canterbury relevant to this project is to identify what has been done in this research program and what needs to be done in this project.

In Part 2, which includes chapters 4 to 5, the test scheme proposed in this project is described first. A detailed seismic assessment of the as-built test units is then conducted according to the current New Zealand design standard NZS3101: 1995 [N1] and the capacity design based seismic assessment procedure, leading to the identification of critical design deficiencies. The predicted design deficiencies in this way will be compared with the test observations later on in order to identify the effectiveness of the current code method and the current seismic assessment method in assessing the seismic performance of existing reinforced concrete structures reinforced by plain round longitudinal reinforcement. Following that, the influence of the beam bar hook details on the shear mechanism of exterior beam-column joints is examined, and the possible retrofit methods in existing exterior beam-column joint regions are proposed.

In part 3, which includes chapters 6 and 7, test results are presented. Chapter 6 introduces the results from the tests on two as-built interior beam-column joint units and chapter 7 introduces the results from four as-built exterior beam-column joint units and one retrofitted existing exterior beam-column joint unit. Emphasis is placed on studying the effects of plain round bars used and axial column load on the seismic behaviour of existing reinforced concrete structures. In addition, the effectiveness of fibre-glass

jacketing technique as a retrofit technique in improving the structural strength and stiffness properties of existing exterior beam-column joint components is investigated.

Part 4, which is chapter 8, outlines the characteristics of the observed local post-elastic behaviour of the as-built members with plain round longitudinal reinforcement in order to generalise the information on modelling the post-elastic behaviour of the as-built members. A method was proposed for determining the flexural capacity at the fixed-end of an as-built member, which is the dominant factor of the member post-elastic behaviour. The information on the post-elastic behaviour of the as-built members is the fundamental element in the seismic assessment of an existing reinforced concrete structure.

In Part 5, which includes chapters 9 and 10, the seismic performance of the subject structure is assessed by conducting global non-linear analyses. Chapter 9 does not consider the influence of masonry infills so the subject structure is considered to be a bare frame. The proposed analytical models are developed based on the observed test evidence. Non-linear static and dynamic analysis is carried out for the structure to assess the possible seismic performance of the structure in a major earthquake. Chapter 10 allows for the effect of masonry infills. The masonry infills are considered to be non-integral infills as common for New Zealand construction. Non-linear static analysis is conducted for the subject structure. Then the possible effects of masonry infills on the seismic performance of existing reinforced concrete frame structures are identified.

Part 6, which has only chapter 11, summarises the conclusions reached in this project and then gives the suggestions for future research.

CHAPTER 2

REVIEW OF PAST RESEARCH INTO SEISMIC ASSESSMENT AND RETROFIT OF PRE-1970S REINFORCED CONCRETE STRUCTURES

2.1 INTRODUCTION

As stated in section 1.1 "THE NEED FOR SEISMIC ASSESSMENT AND RETROFIT OF EXISTING REINFORCED CONCRETE STRUCTURES", the significant developments of design procedures for concrete structures since about 1970s brought about the realisation that existing reinforced concrete structures designed to pre-1970s codes may be deficient according to the seismic requirements of current codes. Consequently, several seismic assessment procedures have been developed, and extensive laboratory studies, which were aimed at obtaining the information on member strength and deformation/ductility capacities of pre-1970s reinforced concrete structures, as required by the seismic assessment procedures, have been carried out.

This chapter aims at reviewing the available seismic assessment procedures, the current methods for determining the member local behaviour and the possible retrofit methods. To achieve these aims, the typical design deficiencies present in pre-1970s reinforced concrete structures and the critical concerns in assessing the seismic performance of pre-1970s reinforced concrete structures are identified first following the review of code developments. Based on this, the reliabilities of different seismic assessment procedures are clarified. Subsequently, the current methods for determining the member capacity are outlined and the possible retrofit methods are briefly reviewed.

2.2 TYPICAL DESIGN DEFICIENCIES IN PRE-1970S REIFNORCED CONCRETE STRUCTURES

Code required proportions and details for reinforced concrete frame structures changed dramatically in the early 1970s. Hence many design deficiencies are present in pre-1970s reinforced concrete structures. To facilitate the identification of the possible inadequate aspects of existing reinforced concrete building structures constructed before 1970s when

responding to a major earthquake, a brief review of design code development is given below.

2.2.1 Development of Seismic Codes

In New Zealand, the first code NZSS 95 to require all buildings to be subject to seismic design requirements was published in 1935 after the 1931 Hawkes Bay earthquake. Although the concept of ductility was introduced into New Zealand codes in the 1960s, no specifications were given for detailing reinforced concrete structures to achieve the ductile behaviour. The year 1976 was the milestone date when the current generation of codes for the seismic design of building structures commenced to be introduced, starting with the code for general structural design and design loadings for buildings 4203:1976. This code was followed in 1982 by NZS 3101:1982 which gave specific design provisions for concrete structures. NZS 4203 was amended and reissued in 1984 and 1992. NZS3101 was amended and reissued in 1995. These current seismic codes, which were developed based on the capacity design philosophy, took into account the seismic performance of structures during cycles of lateral loading in the post-elastic range imposed by a severe earthquake. They focused on aspects of proportioning and detailing to achieve system overall strength and ductility by means of appropriate mechanisms of post-elastic behaviour, in order to survive severe earthquakes.

Other countries, such as the United States and Japan [A2], have undergone similar evolution but a difference exists with regard to the degree of capacity design used and ductility expected from structures.

The requirements of outdated and current codes are outlined below, in order to lead to the identification of general possible problem areas in existing reinforced concrete structures constructed before 1970s:

(1). For each individual structural element, the capacity design philosophy underlying the current codes has requirements for the relative strengths of different possible failure modes of the member. Current codes not only require that the element have adequate strength (as did NZSS 95), but also that the relative strengths of its different failure modes so as to preclude the occurrence of undesirable modes of inelastic deformation, such as may result from shear or anchorage failures. This can be achieved by ensuring that the strengths of these undesirable failure modes of the element exceed the actions associated

with its flexural capacity at overstrength. This latter feature, which is intended to achieve the required post-elastic mechanism and member local ductile behaviour, was not required by pre-1970s codes.

(2). For a whole reinforced concrete building frame, the capacity design philosophy underlying the current codes requires that the plastic hinge regions be well defined in order to lead to a preferred strong column-weak beam post-elastic failure mechanism where soft storey failures are precluded and regions of the structures other than plastic hinge regions remain essentially in the elastic range. For the potential plastic hinge regions, a generous supply of member transverse reinforcement is needed to ensure the expected ductile behaviour. This feature is intended to achieve the required global behaviour of the whole structure; namely, adequate overall load strength, deformation and ductility capacity of the post-elastic critical deformation mechanism of the whole structure. The now outdated codes, which were based on working stress design principles, had no requirements associated with the achievement of a satisfactory global structural behaviour.

Therefore it is apparent that the possible deficiencies in the seismic performance of existing (old) reinforced concrete structures designed to pre-1970s seismic codes have two major categories. One category includes the deficiencies resulting from lack of the design specifications associated with member local ductility capacity, and the other category includes the deficiencies associated with the structural global behaviour during the inelastic loading cycles. In a word, the post-elastic behaviour of existing reinforced concrete frame structures during a major earthquake is the greatest uncertainty in assessing the seismic performance of pre-1970s reinforced concrete frame structures.

2.2.2 Typical Problem Areas of Pre-1970s Existing Reinforced Concrete Structures

2.2.2.1 Beams

In existing, pre-1970s reinforced concrete frame structures, the beams often had the longitudinal bars with lap splices in the potential plastic hinge regions (see Figure 2.1). This means that yielding may concentrate over small lengths of bars outside the lap and/or slip of bars may occur at the lap, resulting in the inadequate member local ductility capacity.

Also the beams of pre-1970s reinforced concrete frame structures often had relatively sparse and inadequately-configured transverse reinforcement. This was because the design of beam transverse reinforcement according to pre-1970s codes was to resist the shear corresponding to code-specified lateral forces rather than the shear corresponding to the development of beam flexural plastic hinges, and the concrete was assumed to contribute to shear strength in plastic hinge regions. Current understanding is that transverse reinforcement in members is required not only for providing the shear force resistance but also for providing the lateral restraint against longitudinal bar buckling and the confinement of the compressed concrete. Hence the beams in pre-1970s reinforced concrete frame structures may end up with the occurrence of undesirable inelastic failure mode(s), resulting in a much reduced member local ductility capacity.

2.2.2.2 Columns

In existing, pre-1970s reinforced concrete frame structures, the quantity of column longitudinal reinforcement bars commonly was based on the bending moments obtained from code-specified lateral forces rather than the input moment strengths from the beams, as specified by current codes. The resulting columns may be weaker than the beams, possibly leading to undesirable column side sway mechanism, rather than the preferred beam sway mechanism. Consideration of the contribution of slab reinforcement to beam flexural strength in ways not originally envisioned further highlights the concern of the expected failure mechanism.

Again it is common to find column longitudinal reinforcement spliced just above the joint where the maximum moments develop, as shown in Fig.2.2. Splice lengths and transverse reinforcement along the splice were often determined assuming the splice acted only in compression, the resulting splice tensile strength and ductility are commonly inadequate for expected cyclic loadings. In this case, the column local ductility behaviour could be very inadequate.

Similar to the beams, column transverse reinforcement was spaced too widely and may be inadequately configured to restrain longitudinal bar buckling and confine the compressed concrete in the potential plastic hinge regions. As a result, the columns in pre-1970s reinforced concrete frame structures may perform in a very brittle manner.

2.2.2.3 Beam-Column Joints

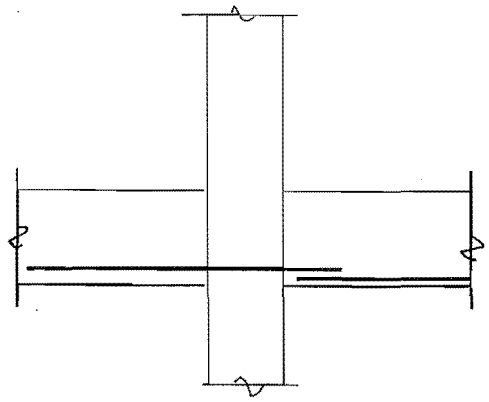

Fig.2.1 Lap splice of beam longitudinal bars in plastic hinge regions

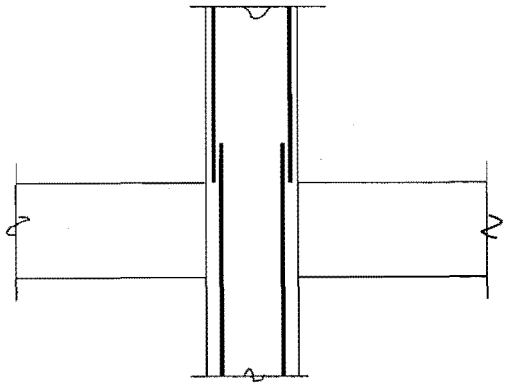

Fig.2.2 Lap splice of column longitudinal bars above joint

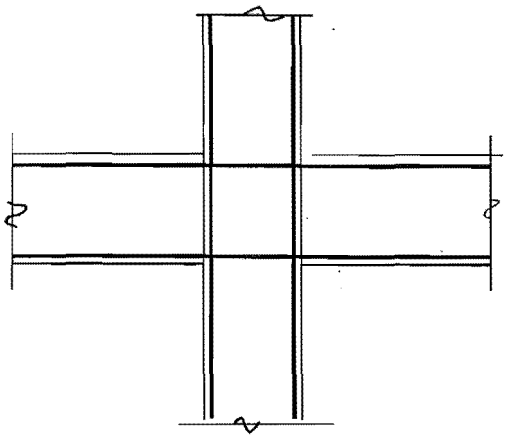

Fig.2.3 No horizontal shear reinforcement in joint

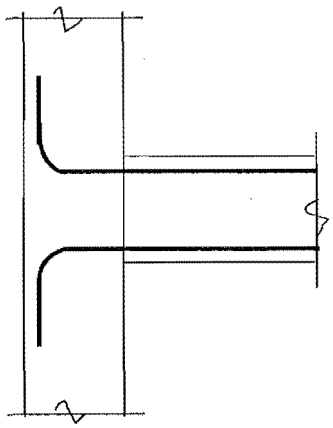

Fig.2.4 Beam bars bent away from joint in exterior columns

The greatest uncertainty when assessing the seismic performance of pre-1970s reinforced concrete frame structures is the likely behaviour of beam-column joints. Most frame structures designed before about 1970 did not have any shear reinforcement in the joint cores [P3, H1], as shown in Fig.2.3. Lack of joint transverse reinforcement may lead to reduced load strength and reduced ductility of the beam-column joint or the adjacent framing members.

It is also common to find the longitudinal beam bars of larger diameter passing through relatively small interior columns in pre-1970s reinforced concrete frame structures, resulting in high bond stresses and bar slip. This occurs as a result of seismic loading which causes the beam bar to be in compression on one side of the column and in tension on the other side, which in the limit may require twice the yield force of the bar to be transferred to the joint core by bond. This situation would be more critical should the existing reinforced concrete frames be reinforced by plain round bars. However, current concrete design codes do not allow for the bond performance when calculating the joint shear capacity. Qualitatively, if slippage does occur, the beam bars will be in tension through the joint core and the "compression" reinforcement in the beam on one side of the column may actually be in tension. In this case, the "compression" reinforcement will not act as compression reinforcement, with a resulting loss in the available beam ductility [P1] and a possible reduction in the attained flexural strength [H5, S8]. Bond failure in interior beam - column joints will reduce the stiffness of the building but it may improve the shear strength of the joint core, since the beam compressive forces will be introduced into the joint by concrete compression rather than by bond along compression reinforcement. Hence the shear carried by the diagonal compression strut will be increased, and the diagonal tension stress introduced into the joint core by bond forces will diminish, resulting in an increase in the shear strength of the joint core due to relatively sound joint core integrity. Thus some slip of beam bars through the joint, although resulting in less ductile behaviour of the beam, will actually increase the shear strength of the joint core.

In exterior beam-column joints of pre-1970s reinforced concrete frame structures, it is not uncommon for the beam longitudinal bars to be bent away from the joint cores in the exterior columns, as shown in Fig.2.4. Such an arrangement of the beam longitudinal reinforcement in the exterior columns does not provide the best configuration to enable the tensile steel force at the bend in the bar to be transferred into the diagonal compression strut which crosses the joint core. Current design codes require the hooks to be bent into the joint core so that the bearing stresses at the inside of the bend are at the end of the diagonal compression strut.

In addition, it is also not uncommon to find that the beam bottom longitudinal reinforcement terminated a short distance into the joint, creating the possibility of bar slip (or pullout) under moment reversals and thus leading to brittle structural performance.

In many cases the presence of lap splices of beam and column longitudinal reinforcement adjacent to but outside of the joint cores in adjacent framing members will limit the input actions from those members so that joint shear failure before failure of the adjoining members will be unlikely. However, if the lap splices or inadequate anchorage in adjacent members are strengthened as part of a seismic upgrade scheme, the joint actions may be increased to a point where the joint will require strengthening as well. This means that the investigation of structural global behaviour is necessary to preclude the occurrence of such problem shifting, instead of problem solving when the structure is to be retrofitted.

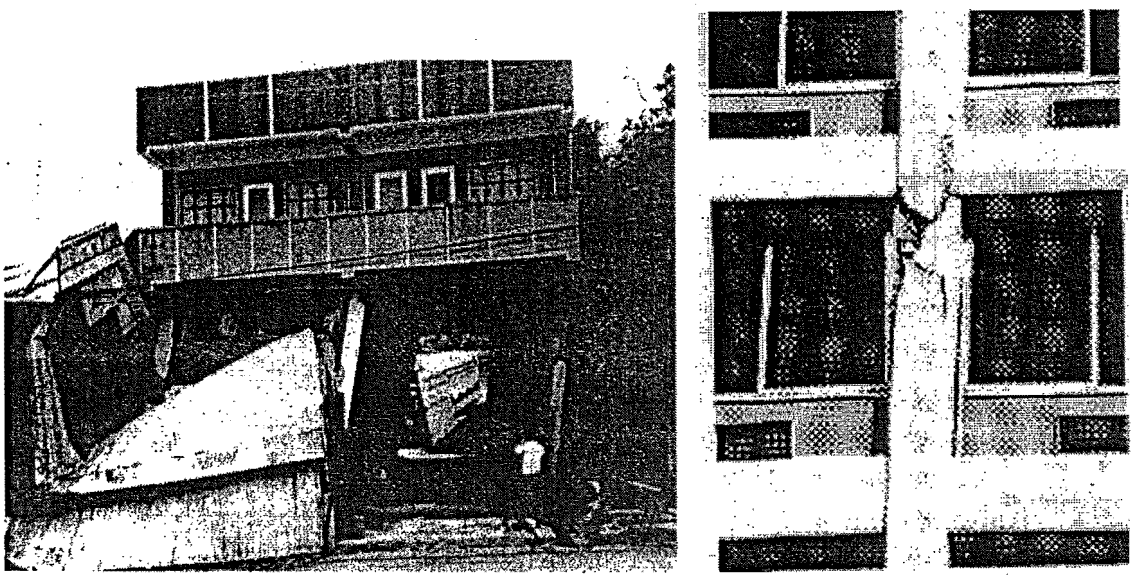

Fig. 2.5 Observed Column Failure

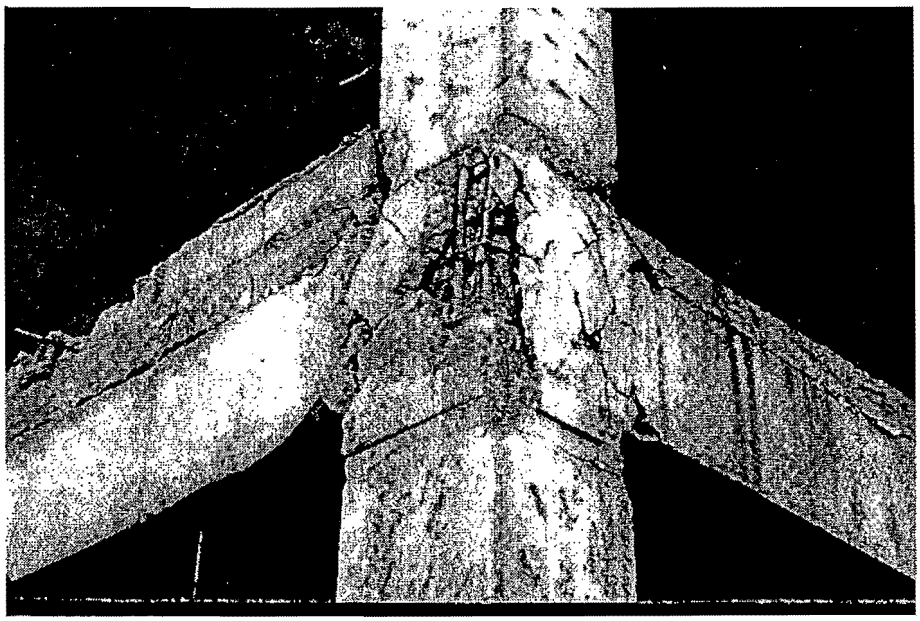

Fig. 2.6 Observed Joint Distress

2.3 OBSERVED EARTHQUAKE DAMAGE [M5, P11]

The most significant failings of existing reinforced concrete frames in past earthquakes have been attributed to failure of the columns, including column shear distress, spalling of column end regions, buckling of column longitudinal reinforcement, and formation of soft stories (Fig.2.5). Several collapses of one or more stories of buildings have been attributed to column failures.

Distress in beam-column connections has been observed following several earthquakes. In several cases, joint failure has contributed to building collapse. Fig. 2.6 shows a common example of joint distress.

Cases of observed distress in beams have been relatively few, in comparison with failures in columns and joints. Most cases have involved splice failure, shear failure, or flexural/shear failure where beam longitudinal reinforcement was curtailed prematurely.

Reinforced concrete building frames often are characterised by their relatively low lateral stiffness. One result among many is that lateral response of the frame can be influenced strongly by the interaction with the nonstructural elements. A common interaction is between the frame and the infill elements. Several building failures in past earthquakes have been attributed to overstressing of columns that were partially restrained by nonstructural infills. Presence of the partial infill increases the column stiffness and increases the column shear-moment ratio. Interaction may occur between the frames and other nonstructural elements such as stairways. Low lateral load stiffness and the resulting lateral displacements may also lead to excessive nonstructural damage, pounding between adjacent structures, and collapse.

Apparently, the observed earthquake damage to reinforced concrete frames in past earthquakes coincides with the possible problem areas covered in Section 2.2.2.

2.4 REVIEW OF SEISMIC ASSESSMENT PROCEDURES

The seismic assessment of an existing reinforced concrete frame structure can be carried out under the circumstance of the known reinforcing details, the known material strengths and the known cyclic loading properties of individual members and their connections.

In recent years, several seismic assessment procedures have been developed in many countries, such as in New Zealand, the United States of American and Japan, and they can

be classified into two categories, namely check-list type of procedures and capacity design based procedures.

2.4.1 Seismic Assessment of Existing Reinforced Concrete Buildings in Japan[A1, S5]

The first complete document in Japan for the evaluation of the seismic performance of existing reinforced concrete buildings was developed in 1977 as a result of the earthquake damage observed to low rise engineered reinforced concrete buildings in the 1968 Tokachioki earthquake, and it was named as "Standard for Seismic Capacity Evaluation of Existing Reinforced Concrete Buildings". This document was revised in 1990 [A1, S5, O5].

2.4.1.1 Basic Principles

The basic principle underlying this "Standard" was that the extent of the seismic forces resisted by shear walls was the most important factor in structural responses to a major earthquake, and supply of sufficient shear capacity for structural vertical elements was the most effective way of meeting the requirements.

The basic principle was based mainly on the observed earthquake damage as a result of the 1968 Tokachioki earthquake in Japan. The observed damage to the reinforced concrete frame structures in the 1968 Tokachioki earthquake was mainly the shear failure of columns and the earthquake damage statistics after the earthquake showed a close correlation between the load resisted by shear walls and the degree of damage.

2.4.1.2 Proposed Procedures

This Japanese procedure recommended three level screening procedures. The lower level procedure is simpler, and the result is believed to be more conservative for Japanese construction. The higher level procedure results in a less conservative conclusion, but involves more complicated analysis. The first level procedure is used to screen safe buildings while the second and third level procedures are used subsequently only for those buildings, which are found not to be satisfactory by the first level procedure. In general, the second and the third level procedures are of a similar complexity of analysis.

For all three level procedures, the safety level of the existing buildings is assessed by comparing the 'Seismic Index' I_s with the 'Seismic Protection Index' I_{so}. The 'Seismic

Index' I_s is the total earthquake resisting capacity of a storey, and it includes information on the basic strength and deformation/or ductility capacity of a certain storey, the stiffness distributions in the plan and/or vertical extents of the buildings, the strength and stiffness deterioration with time and geological conditions. The 'Seismic Protection Index' I_{so} is a direct indicator of the degree of earthquake damage, and it is determined totally based on the earthquake damage observed in past earthquakes in Japan.

The main difference in determining the 'Seismic Index' I_s for different levels of screening is in the determination of basic strength and deformation/or ductility capacity of a certain storey. The first and second level procedures assess the strength of a storey by only considering the vertical lateral-resisting elements, but they have different complexities of estimation of the strength capacity of the vertical elements. The third level procedure not only considers the vertical lateral-resisting elements but also allows for the effect of the beams in determining the total strength of a certain storey. The highlight of the importance of the vertical lateral-resisting elements in determining I_s is mainly because the observation of earthquake damage proves a good correlation between the earthquake damage and the amount of walls relative to total floor area during the past earthquakes in Japan. However it needs to be noted that all three level procedures assume completely rigid beam-column joint cores because of the lack of evidence of earthquake damage due to the insufficient strength of beam-column joints in Japan. This observation is most likely due to the large member sizes used in Japan.

2.4.1.3. Discussion

Evidently, the Japanese Standard above reviewed has two characteristics as follows:
Firstly, it is clear that the Standard was developed in such a way as to specifically apply to Japanese low rise reinforced concrete buildings because both the basic principles, on which the Standard was developed, and the determination of the 'Seismic Index' and the 'Seismic Protection Index' were based on the earthquake damage to the reinforced concrete buildings of Japanese construction, observed in previous earthquakes experienced in Japan. Direct application to buildings of other countries certainly may not give satisfactory prediction.

Secondly, this Standard ignores the evaluation of beam-column joints and ignores the influence of the horizontal elements on structural deformation and/or ductility capacity.

Especially it has no investigation into the post-elastic critical mechanism as well as the two-level limit states, resulting in failure to identify critical areas. Basically this approach is still based on the working stress concept, and is not in accordance with the capacity design philosophy. Once the specified earthquake intensity is exceeded, how much reserve structural capacity remains is still unknown.

In addition, the damage indices were developed by relating damage levels of specific classes of structures to seismic intensity based on experience in past earthquakes, and it is inappropriate to use such damage indices in determining seismic risk of individual buildings. Also the application of a mean value from a data set with extremely wide scatter will provide little insight beyond indicating that there is a need for more detailed structural calculations.

Hence this approach could only be applied in Earthquake Disaster Preparation Projects which only require a check as to whether the investigated structure is sufficient in a given earthquake, rather than determining the available capacity of the structure. Evidently this approach could not be used in retrofit type of projects because, for retrofit projects, it is important that the retrofit schemes do not shift the problem areas to somewhere else. Hence the investigation of the post-elastic critical mechanism of the structure after retrofitting would be necessary.

2.4.2 Seismic Assessment of Existing Reinforced Concrete Buildings in the USA

In the United States of America, the most comprehensive assessment methodology is based on documents prepared by the Applied Technology Corporation ATC22[A3]. ATC 22 is an ultimate limit state assessment procedure, and it provides a screening process to decide if further investigation is required. Priestley and Calvi have reviewed it in detail [P4].

2.4.2.1 Basic Principles

The basic principles on which the ATC22 method was developed are as follows:

(1). Concern is related only to life-safety: consequently, only an ultimate limit state is considered.

(2). An ultimate strength of 67% of that required by the NEHRP design recommendation is accepted.

(3). A calculation of seismic demand and seismic capacity is performed, together with checks to ensure that excess shear strength is provided, and that specially vulnerable elements are protected.

2.4.2.2 Proposed Procedures

The basic assessment procedure of the ATC22 method is to check if a series of statements is true or false. Any "false" result identifies an issue requiring further investigation. "Further investigation" means essentially applying normal design procedures for a new building with the base shear scaled to 67% of NEHRP requirements. Also, quick check relationships are suggested for the evaluation of story shear and story drift.

2.4.2.3 Discussion

Priestley [P4] pointed out a few aspects which deserve comment as follows:

(1). The use of a 67% NEHRP "new building" coefficient, which is based on historical precedent, is hard to justify on a rational basis. It is particularly inappropriate where the probability of occurrence of a major earthquake on a given fault (e.g., the Hayward fault, San Francisco) is assessed to be high.

(2). The discussion of some behaviour issues, such as the presence or absence of a strong column / weak-beam design should not be considered independent of reinforcement details.

(3). The assessment of unsatisfactory detailing is handled in a simplistic fashion, as is the issue of the significance of masonry infills.

(4). The assessment is directed towards delineation between " satisfactory " and "unsatisfactory". Although this is of prime importance to a regulatory authority, it is less complete information than may be required by a building owner.

2.4.3 Seismic Assessment of Existing Reinforced Concrete Buildings in New Zealand [N3, N4]

In New Zealand, a document "Guidelines for the Seismic Assessment of pre-1975 Reinforced Concrete Structures and Structural Steel Buildings" [N3] was prepared for the Building Industry Authority by a study group of the New Zealand National Society for Earthquake Engineering in 1994, and this document, after being refined, became "The Assessment and Improvement of the Structural Performance of Earthquake Risk

Buildings, Draft for General Release" in 1996 [N4], which is referred to as "Draft" in the following.

2.4.3.1 Basic Principles

The basic principles on which the "Draft" was developed are as follows:

(1). The "Draft" concentrates on matters relating to life safety, that is to say, performance at the ultimate limit state;

(2). The "Draft" accepts a higher level of risk for pre-1975 reinforced concrete buildings, compared with those constructed to modern seismic design codes. Typically for Category IV pre-1975 reinforced concrete buildings, the risk factor is two-thirds of the corresponding risk factor for the new reinforced concrete buildings. This indicates an increase in risk for an existing reinforced concrete building of between two and three times over that of an equivalent new building for the same design life. The structural performance factor in assessing pre-1975 reinforced concrete buildings is 0.85, rather than 0.67 as given in NZS4203: 1992 for structural design. Typically for Category IV pre-1975 reinforced concrete structures, the combination of the modified risk factor and structural performance factor indicates that the numerical requirement for the assessment of a non-ductile existing reinforced concrete structure is 85% of that for designing a new structure, noting that there are offsetting factors on the resistance or strength side of the equation such as the use of probable strengths.

2.4.3.2 Proposed Procedures

The "Draft" recommends a two-stage seismic assessment procedure; that is, the rapid evaluation and the detailed assessment.

The rapid evaluation is established on the recognition and ranking of various building structure characteristics that are known to affect earthquake vulnerability, and is based on the observed damage characteristics of buildings in earthquakes. The rapid evaluation largely follows the process of ATC-21 [A4], but allowing for the features of New Zealand construction. When an existing reinforced concrete structure is assessed using the rapid evaluation method, the structural score needs to be obtained. The structural score is the sum of the indicatives of a number of potential damage parameters. The final assessment is expressed as a plot of the structural score and building area, and the decision whether or not the detailed assessment is needed is made based on such a plot. For a given structure

score, a detailed assessment is recommended if a building has an area larger than that shown in the plot.

For the detailed assessment of an existing reinforced concrete structure, the "Draft" recommends two general procedures, force-based and displacement-based procedures. Both the force-based and the displacement-based procedures are based on the capacity design philosophy, and the major difference between these two procedures is the end product. Whereas the force-based procedure suggests comparing the structural demand and structural capacity in terms of forces, the displacement-based procedure suggests comparing the structural demand and structural capacity in terms of displacement. The detailed review of the two capacity design based assessment procedures will be conducted in section 2.4.4.

2.4.3.3 Discussion

Basically, the rapid evaluation procedure recommended in the "Draft" has similar characteristics to ATC procedure and the detailed assessment procedures recommended in the "Draft" are the capacity-design based seismic assessment procedures, including the force-based and the displacement-based seismic assessment procedures, which were developed and discussed by Priestley et al [P5] and Park [P6].

2.4.4 Capacity Design Based Seismic Assessment Procedures

The seismic assessment procedure based on the capacity design philosophy, which has been developed in recent years, emphasises the overall (global) post-elastic performance of the structure, rather than the member local behaviour only.

The capacity design based seismic assessment procedure was initially suggested by Priestley and Calvi in 1991[P4]. The procedure, when originally proposed in 1991, suggested comparing the structural demand and capacity in terms of forces, referred to as the forced-based seismic assessment procedure. This is the same concept as adopted by current codes. In 1995, Priestley [P5] introduced into the original force-based procedure a new idea, which was to compare the structural demand and capacity in terms of displacements, referred to as the displacement-based seismic assessment procedure. In 1997, the displacement-based seismic assessment approach [P5] was further discussed by Priestley and Calvi [P21], and by Priestley [P22].

The displacement-based approach has apparent advantages over the force-based approach.

Although many designers prefers to assess earthquake-induced structural actions in terms of static equivalent loads or forces, it must be appreciated that actual seismic response is dynamic and is related primarily to imposed deformation rather than forces. Priestley et al pointed out that failure of a ductile system occurs not when the strength is reached but when the ductility capacity (i.e., the ultimate displacement) is reached and the developed strain, therefore the attained displacement, is clearly a better indicator of the structural damage level. The displacement-based approach is hence more rational than the force-based approach, especially for the seismic assessment of reinforced concrete structures. The weaknesses of the force-based approach, outlined by Priestley et al in references P5 and P21, include: (1). the improper assumption of the relationships between ductile response and elastic response of the system, namely, the use of the force reduction factor as in current forced-based seismic design codes; (2). the lack of consideration of hysteretic energy dissipation characteristics, namely, the use of the initial elastic stiffness. The use of initial elastic stiffness and the force reduction factors in the force-based approach could lead to, in terms of seismic risk, a change in probability of damage of as much as an order of magnitude, under a given event [P21]. The key element of the displacement-based assessment procedure is that a substitute structure, as suggested by Shibata and Sozen [S7] is constructed and the stiffness and damping of the substitute structure are characterized by the secant properties at the maximum response, rather than initial elastic properties as for force-based procedure, leading to the elimination of the problems associated with the use of initial elastic stiffness and the use of force reduction factor. Meanwhile, in 1997, Park [P6] further discussed the force-based seismic assessment procedure, and outlined, in detail, the static procedure for assessing the likely seismic performance of existing reinforced concrete moment-resisting frame structures. Park [P6] agreed that the displacement-based seismic assessment procedure has apparent advantages over the force-based approach, but pointed out [Park 1997] that since the current New Zealand design standard recommends seismic design in terms of design seismic forces and the associated ductility demand, and most engineers at present will prefer to use a force-based approach for seismic assessment of pre-1975 existing reinforced concrete structures until the New Zealand standard adopts the displacement based design.

2.4.4.1 Basic Principles

The basic principles underlying the capacity design based seismic assessment procedure are as follows:

(1). Two limit states, namely serviceability limit state and ultimate limit state, are considered.

The force-based seismic assessment procedure defines the two limit states in exactly the same way as in current seismic design codes. The serviceability limit state is defined to be the state corresponding to the yield displacement (or yield curvature), -- i.e., a displacement ductility of μ_s =1. A serviceability limit corresponding to μ_s =1, while generally conservative, provides a very uneven protection against damage [P17]. The ultimate limit state is defined to correspond to the formation of the critical post-elastic failure mechanism of the structure.

The displacement-based seismic assessment procedure defines the two limit states based on strain criteria. The serviceability limit state corresponds to the concrete cracking and acceptable large residual crack widths, as is suggested by Priestley and Calvi [P21] to be a maximum concrete strain of ε_c=0.004 and a maximum reinforcement tensile strain of ε_s=0.015, whichever is reached first. Hence, unlike the force-based approach, the displacement-based approach enables a consistent level of assessment to be achieved. The ultimate limit state also is defined to correspond to the formation of the post-elastic failure mechanism of the structure.

(2). The probability of exceedance for each limit state is determined by comparison with reference spectra representing code-specified seismicity, or a site-specific design spectrum.

2.4.4.2 Proposed Procedures

The seismic assessment procedures are summarised in Fig.2.7 and Fig. 2.8, for the force-based procedure and the displacement-based procedure, respectively, and they have been respectively described in detail by Park [P6] and Priestley [P21].

1. Seismic Assessment at the Serviceability Limit State

The structural response at the serviceability limit state is expected to be essentially elastic, hence elastic methods, such as modal analysis, are used to analyse the overall structural response at this state.

Once the best estimation of elastic flexural and shear strengths of beams and columns as well as the best estimation of elastic shear strengths in the beam-column joints are

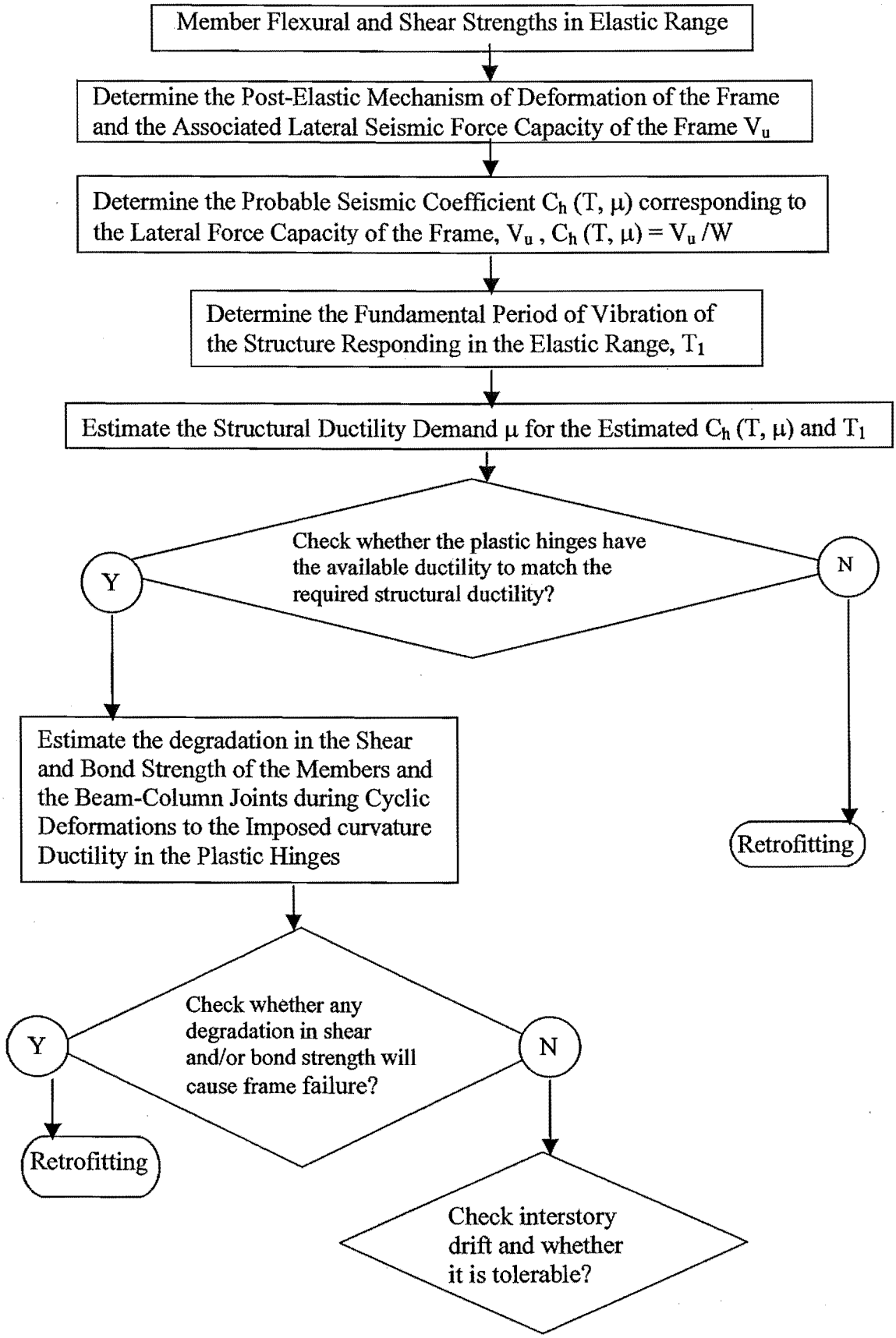

Fig. 2.7 Procedures of Force-Based Seismic Assessment Approach

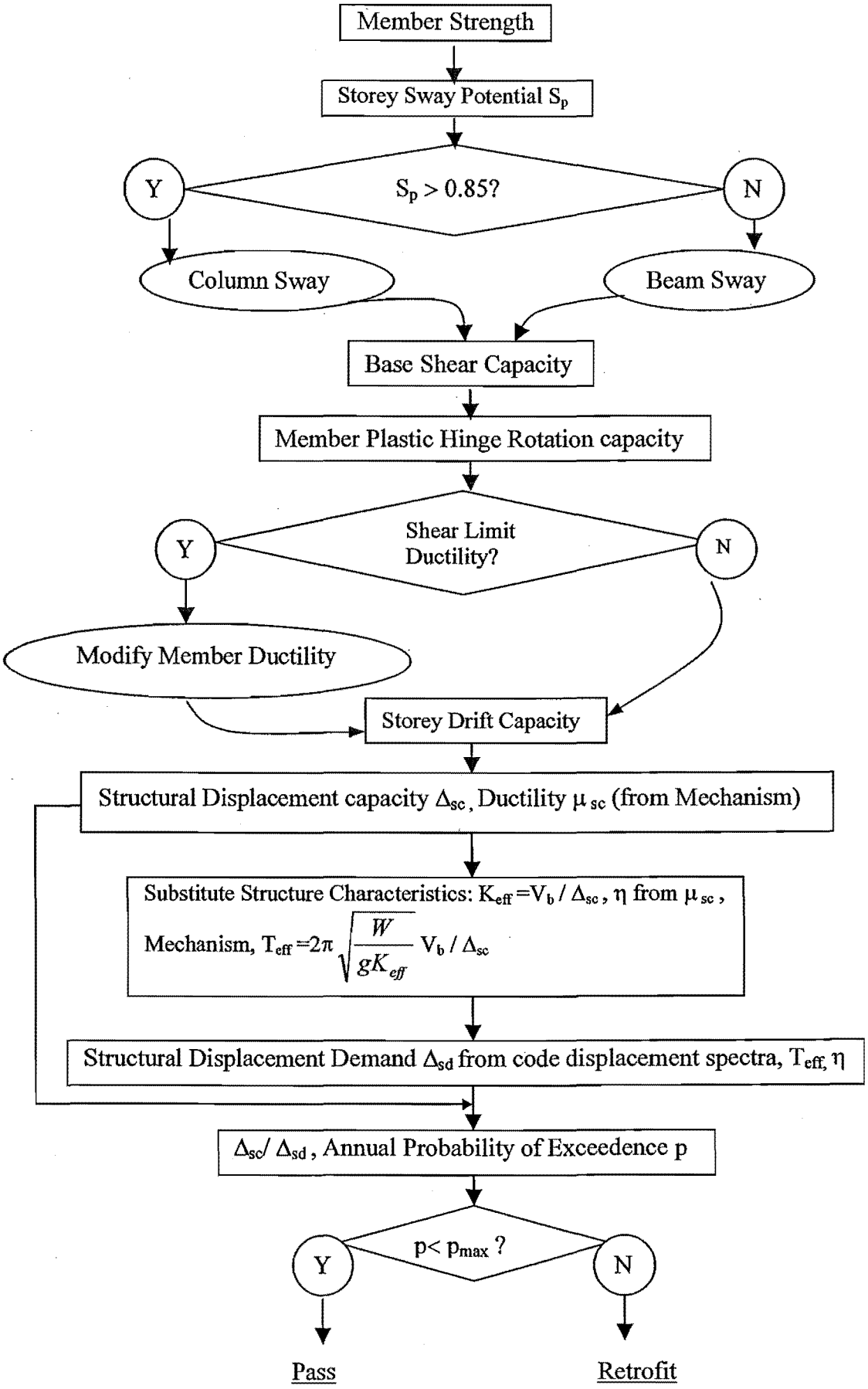

Fig.2.8 Procedures of Displacement-Based Seismic Assessment Approach

available, the serviceability limit state assessment can be carried out realistically. Here the elastic strengths are the strengths without considering strength degradation.

The quality of the seismic assessment results depends on the quality of the estimation of member strengths. Apart from the utilisation of realistic material strengths, proper methods to estimate member strengths should be used, and provisions in current design codes should not always be used for the purpose of seismic assessment because these provisions are only applicable to the design of new buildings and usually very conservative. A brief review of the determination of material strength can be seen in section 2.5.

2. Seismic Assessment at the Ultimate Limit State

As seen in Figs. 2.7, for the force-based assessment procedure, the system lateral load strength and the overall structural deformation capacity of the post-elastic collapse mechanism need to be found, and the combination of the system lateral load strength and the overall structural ductility capacity of the post-elastic collapse mechanism gives an equivalent elastic response force level, which, by comparison with the design elastic response spectrum, could be used to determine annual probability of exceedence corresponding to development of structural capacity.

Similar to the force-based assessment procedure, for the displacement-based assessment procedure, the system lateral load strength and the overall structural ductility capacity of the post-elastic collapse mechanism are also needed in order to construct the substitute structure, as seen in Fig. 2.8.

In major earthquakes, a structure is expected to develop large non-linear deformations, and hence the fundamental aspect in the seismic assessment of an existing reinforced concrete structure using capacity design based assessment procedures is the determination of the post-elastic collapse mechanism of the system and the estimation of its associated lateral load strength and the structural ductility capacity (or displacement capacity).

2.4.4.3 Determination of the Critical Post-Elastic Collapse Mechanism

According to capacity design philosophy, the ductile behaviour of the critical post-elastic failure mechanism at the ultimate limit state is achieved by inelastic flexural deformations in well defined plastic hinge regions (mainly in the beams), and the relative strengths of

undesirable failure modes should be high enough to preclude the occurrence of undesirable failure modes of inelastic deformation. A series of provisions regarding structural proportioning and reinforcing details are specified in current codes to achieve the desired structural ductile behaviour. However, for the existing reinforced concrete structures, the ductile structural response of the critical post-elastic collapse mechanism may be hampered by the occurrence of undesirable failure modes, as a result of lack of capacity design philosophy in now outdated seismic codes.

The capacity design based seismic assessment procedure suggests that the determination of the critical post-elastic collapse mechanism be determined by using a modified form of capacity design principle which allows some local element failure provided that the overall structural integrity is not jeopardised. This will involve the identification of the critical collapse mechanism, the determination of the available lateral load strength and the overall structural ductility capacity of the post-elastic collapse mechanism and the check to see whether the occurrence of the undesirable failure modes of the element is possible [P5, P6].

Park outlined in detail the methods for determining the post-elastic collapse mechanism of the system [P6 by Park in 1997], and it is reviewed below.

1. Identification of the Critical Post-Elastic Collapse Mechanism

Many older reinforced concrete frame buildings can be expected to have a mixed post-elastic mechanism, instead of simply a beam sidesway mechanism or a column sidesway mechanism (see Figure 2.9). The consequences of particular failures need to be assessed relative to each other. For example, column shear failure is very serious, since it is associated with the loss of gravity load capacity and could result in total collapse of the structure. Joint shear failure is less likely to result in catastrophic collapse. It must also be recognised that the shear strength of beams and columns in plastic hinge regions is dependent on the level of flexural ductility imposed. Hence a mechanism which initiates with flexural plastic hinges may degenerate into plastic hinges with shear failure as the ductility demand increases.

To investigate whether the plastic hinges form in the beams or columns at a particular joint, the sum of the probable flexural strengths of the beams and the columns at the joint centroid can be compared, (see Fig. 2.10). The flexural strength ratio at the joint may be defined as:

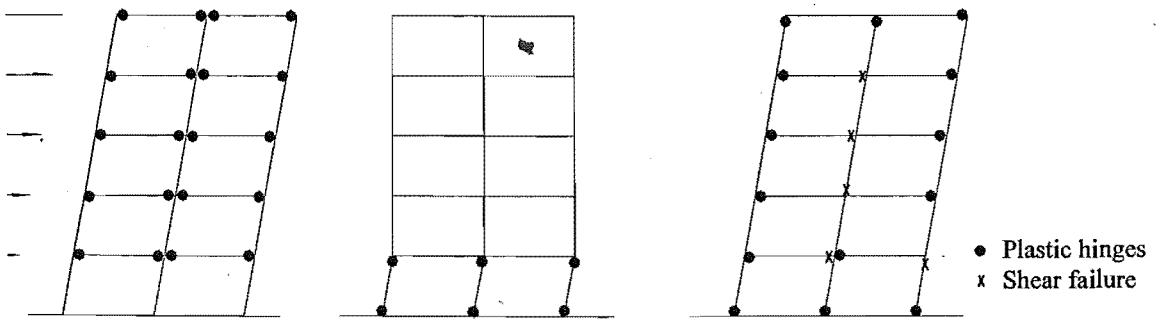

(a) Beam sidesway mechanism

(b) Column sidesway mechanism

(c) Mixed sideway mechanism with plastic hinges and shear failure

Fig. 2.9 Mechanisms of Post-Elastic Deformation of Seismically Loaded Moment Resisting Frames

$$S_r = \frac{M_{bl} + M_{br}}{M_{ca} + M_{cb}}$$

where M_{bl} and M_{br} = beam flexural strengths at the left and the right of the joint, respectively, at the joint centroid, and M_{ca} and M_{cb} =column flexural strengths above and below the joint, respectively, at the joint centroid.

When $S_r > 1$ plastic hinges in the columns can be expected.

To investigate whether a column sway mechanism (soft story) can be expected, a sway potential index S_i can be defined as the sum of all the S_r values for the beam-column joints at a floor level. Thus at a floor level,

$$S_i = \sum S_r$$

If the value of the flexural strength ratio S_r for the beam-column joints at the floors above and below a storey are all greater than 1.0, a column sidesway mechanism can be assumed to occur in that storey since plastic hinges can form at the top and bottom of all columns in that storey.

If the sway potential index S_i for the beam-column joints of the floors above and below a storey are both greater than 1.0, it is possible that a column sidesway mechanism will occur. However, the presence of some joints with a flexural strength ratio S_r<1.0 will prevent a column sidesway mechanism even if S_i>1.0.

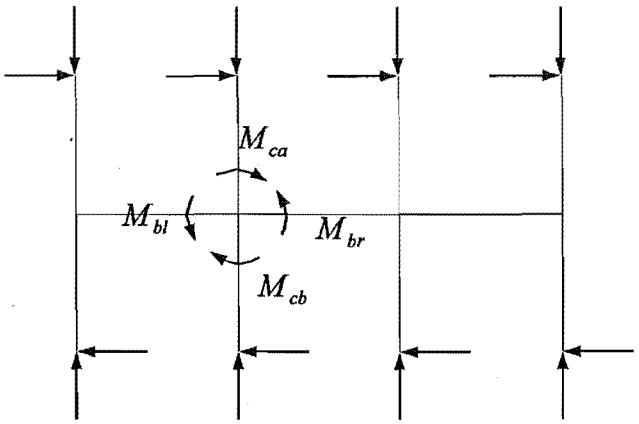

Fig.2.10 Bending Moments Acting at a Beam-Column Joint at a Floor Level

Due to the possible increase in column moments due to higher mode effects, it is suggested that column plastic hinges can be assumed to form if S_r>0.8.

The probable lateral seismic load capacity of the critical post-elastic collapse mechanism of the frame in the general case can be found by assuming that the structural performance is dominated by flexure only. Whether the undesirable failure modes hamper the maintenance of the flexural strengths with the development of displacement will be checked later on.

Park suggested three possible methods for determining the lateral load strength of the corresponding mechanism, when the probable lateral seismic load capacity of the frame is only dependent on the flexural strengths of members.

- Method 1

Linear elastic structural analysis is used to determine the lateral seismic force corresponding to the development of the first plastic hinge. For this method, the equivalent static earthquake forces are increased from zero until the first plastic hinge forms. The

lateral seismic force corresponding to the development of the first plastic hinge gives a lower bound to the probable lateral force capacity of the critical collapse mechanism, and this will be equal to or less than the actual lateral force capacity. In reality, moment redistribution in the post-elastic range will permit higher lateral seismic forces to be resisted while further plastic hinges form until a mechanism develops.

- Method 2

If the mechanism of post-elastic deformation is obvious from the onset, the lateral seismic force capacity corresponding to the critical collapse mechanism can be calculated directly. This estimate gives an upper bound to the probable lateral force capacity of the frame and will be always equal to or greater than the actual lateral force capacity. The danger of calculating the lateral force capacity by the upper bound approach is that the lateral force capacity may be overestimated as a result. The mechanism giving the least lateral force capacity is the correct one and must be sought.

- Method 3

The most complete approach is to use nonlinear push-over structural analysis. That is, the lateral seismic forces acting on the frame are gradually increased until the mechanism forms. The behaviour of the frame is in the elastic range until the first plastic hinge forms and then the post-elastic deformations at the plastic hinges need to be taken into account. The number of plastic hinges forming increases with the increase in the lateral force until a mechanism develops, giving the actual probable lateral force capacity.

2. Determination of the Ductility Capacity of the Critical Post-Elastic Collapse Mechanism

The available structural ductility can be estimated by taking into account the plastic hinge rotation capacity and /or section ductility according to the level of detailing.

Park suggested three methods for determining the available structural ductility [P6].

- Method 1:

A simplistic approach is to compare the detailing of the structure with that recommended by current codes for ductile structures and to assess the available ductility on that basis.

Typically for a structure where a beam sidesway mechanism is expected, when the transverse reinforcement detailing in the potential beam plastic hinge regions meets the

current code requirement, an available displacement ductility factor of $\mu = 6$ may be assumed for the frame, but when the transverse reinforcement detailing in the potential beam plastic hinge regions are very sparse and poorly anchored, an available displacement ductility factor of $\mu = 2$ may be assumed for the frame. For the intermediate situation, interpolation method is used for determining the available displacement ductility factor.

For potential plastic hinge regions at the base of columns where a beam sidesway mechanism is shown to be likely, or for frames of one or two storeys in height, where a column sidesway mechanism is likely, if the transverse reinforcement detailing is satisfactory according to current design code, an available structural ductility factor of μ =6 may be assumed; and if the transverse reinforcement is not well anchored and has a big spacing, typically greater than 16 times the bar diameter, an available structural ductility of 2 may be estimated. For the frame structures of more than two storeys in height where the column sidesway mechanism is likely, an available μ of 1.5 can be assumed if the transverse reinforcing details are poor.

- Method 2

A more accurate method would be to first determine the available curvature ductility factors at the plastic hinge regions taking into account the amount of transverse reinforcement present. The available structural ductility may then be found from the mechanism by pushing the mechanism laterally until the critical available curvature ductility is reached.

This is an approximate approach since not all the plastic hinges in the mechanism form simultaneously because for one reason, the vertical profile of horizontal displacement of the frame will not be linear, for example, as a result of the effect of the higher modes of vibration. That is, the drift (lateral displacement of a storey divided by the storey hight) will not be the same for each storey.

- Method 3

The most complete approach for determining the available displacement ductility μ is to use a nonlinear structural push-over analysis in which lateral seismic forces on the frame are gradually increased until the available ultimate curvature is reached first at the critical plastic hinge.

This method is believed to be essential for frames in which mixed sidesway mechanisms form as shown in Fig.2.9 (c), since such frames can not be easily analysed by the simpler methods.

3. Check the Possibility of Occurrence of Undesirable Member Failure Modes

It needs to be realised that the determination of the lateral seismic load strength and the overall ductility capacity of the critical post-elastic collapse mechanism, described above, is based on the assumption that the flexural strengths of members dominated the seismic performance of the frame structures at the ultimate state. Whether or not the other non-ductile failure modes possibly dominate the post-elastic performance of the system needs to be identified. Cyclic loading tests frequently demonstrate that the final failures of existing reinforced concrete members reinforced by deformed bars are likely to be dominated by shear failure due to the observed degradation in shear strength at plastic hinges and beam-column joints with the increase in the imposed ductility level. A mechanism which initiates with flexural plastic hinges may degenerate into plastic hinges with shear failure as the ductility demand increases. Hence the strength degradation associated with other failure modes (such as, shear failure and bond/anchorage failure) with increase in the imposed ductility levels needs to be checked to make sure that the degradation of the non-desirable failure modes (for example, shear strength and bond strength) in the plastic hinges does not hamper the maintenance of the flexural strength.

2.4.4.4 Discussion

As revealed by outlining the development of seismic design codes in section 2.2.1, the structural design without incorporation of capacity design philosophy, as was the case before mid 1970s around the world, contributes greatly to the uncertainty of the structural post-elastic behaviour. Therefore, the key point in assessing the seismic performance of an existing reinforced concrete structure is to investigate the global structural behaviour, that is, the structural lateral load capacity and structural ductility of the critical post-elastic mechanism of the structure, rather than only local behaviour. This is especially true for an existing reinforced concrete building frame where the post-elastic critical mechanism is a mixed sidesway mechanism with the development of the beam hinges, columns and shear failures likely at different locations within the frames. In this case, a simple check-list assessment procedure, which compares the local member details of the as-built reinforced concrete structures with the requirements of current seismic codes, will rarely be

successful. Furthermore, the evidence of tests and analysis as well as observed earthquake damage demonstrate that not all structures designed to now outdated codes will response poorly to severe earthquakes, even when according to current standards the detailing of reinforcement in some regions is substandard [P3].

Apparently, capacity design based seismic assessment procedures are more realistic and more adequate, compared to check list procedures. Especially, if the decision to retrofit the structure has been made after structural assessment using a check list type of procedure, the prevention of problem shifting rather than problem solving resulting from one potential retrofit technique only can be fulfilled by using capacity design based seismic assessment procedures. This is apparently a prominent advantage of capacity design based seismic assessment procedures over the check-list type of procedures.

To investigate the global structural behaviour in the post-elastic range, the required information on local behaviour of individual members includes the members' strength and deformation capacity. On important aspect in the consideration of member local behaviour is to investigate the strength degradation of undesirable failure modes. For reinforced concrete members containing deformed bars, the major concern is the shear strength degradation of members and beam-column joints.

Obviously, the quality of the seismic assessment of existing reinforced concrete structures greatly depends on how realistic are the estimation of the probable member strength and deformation capacity and the estimation of the strength degradation of undesirable failure modes. Hence the assessment of member strength and deformation capacity by test and analysis becomes fundamental in achieving the best seismic assessment of structures.

2.4.5 Summary

Check list assessment procedures, such as, "Standard" in Japan, ATC method in USA and the rapid evaluation method in New Zealand, assess the seismic performance of existing reinforced concrete structures by referring to the earthquake damage of structures of similar structural type observed in past earthquakes. Core element of check-list procedures is the statistical relationship between potential earthquake vulnerable factors and the earthquake damage in the past earthquakes. Check list procedures only take into account the local behaviour of the individual concrete elements, and inadequately represent the interactions between the actions of different members, which is the key advance of current

design codes compared to the old design codes. Hence, the check-list seismic assessment procedures are basically based on working stress philosophy. However, the check-list seismic assessment procedures are easy to follow, and so can be used for City Earthquake Disaster Prevention and Preparation Programs.

In contrast, capacity design based assessment procedures, force-based and displacement-based procedures, aim at investigating the available strength and deformation capacity of the post-elastic failure mechanism of the system, and hence realistically assess the structural post-elastic response. The information needed for conducting seismic assessment using capacity design based seismic assessment procedures includes the initial strength of individual existing reinforced concrete members and the strength degradation with the increase in the imposed displacement level. Typically, premature shear failure in members (beams and columns) and beam-column joints could occur when deformed bars are used for longitudinal reinforcement, hence shear strength degradation with the increase in the imposed displacement level should be investigated in this case.

Current design code equations are considered not to be suitable for determining the shear strengths of existing reinforced concrete members, and the information on probable strength and strength degradation of existing reinforced concrete components should be obtained from cyclic tests on as-built reinforced concrete components.

2.5 METHODS FOR DETERMINING MEMBER STRENGTH AND DEFORMATION CAPACITY

The determination of the post-elastic collapse mechanism is based on a knowledge of member's post-elastic behaviour in terms of member strength and deformation capacity, as seen from Figs. 2.7 and 2.8. The basis of a realistic assessment should be to obtain a "best estimate" of member strength and deformation properties. Hence, apart from using realistic values of material strengths, proper methods rather than code design equations need to be used for determining member strength and deformation capacity.

For the design of each individual concrete member, capacity design philosophy requires that its relative strengths of the different failure modes preclude the occurrence of undesirable modes of inelastic deformation, such as may result from shear or anchorage failures. Hence, for existing reinforced concrete members, the study on member strength and deformation performance should identify the dominant failure mode, determine the probable flexural strengths of members and investigate whether the strength

corresponding to the most critical non-ductile failure mode could hamper the development of the post-elastic deformation due to the possible strength degradation with the progress of post-elastic cyclic deformations.

When the deformed longitudinal reinforcement is used, the shear performance of the as-built concrete members and beam-column joints was often observed to dominate the final failure [H1]. This occurred due to the shear strength degradation with the increase in the imposed displacement level in the post-elastic range. In this case, the degradation of shear strength with the increase in the imposed displacement level apparently needs to be investigated in order to find whether the degradation in shear strength can hamper the development of post-elastic deformation. Some laboratory testing has been carried out to study the shear strength degradation of as-built concrete components and beam-column joints reinforced by deformed bars in the post-elastic range. As a result, the methods for estimating the available shear strength and the shear strength degradation of as-built concrete members and beam-column joints have been tentatively developed.

Representatives of the current methods, for determining the probable flexural strength and the shear strength degradation of as-built concrete members and beam-column joints when using deformed longitudinal bars, are the methods proposed respectively by Priestley et al [P5] and by Park [P6].

2.5.1 Material Strengths

To achieve the best estimate of member strength and performance properties, it is inappropriate to use nominal or specified material strengths and strength reduction factors. This has been addressed by many researchers [C6, P5, P6].

2.5.1.1 Reinforcement

Site sampling and testing in pre-1970s reinforced concrete structures frequently showed that the reinforcement used is likely to possess a characteristic yield strength, which is significantly greater than the specified value. For instance, Chapman [C6] reported that the reinforcement in New Zealand construction built during the 1930 to 1970 period is likely to possess a characteristic yield strength, which is 15 to 20% greater than the nominal value, which was 250 to 275 MPa at that time. Whenever possible, samples of steel from the structure should be tested to obtain a better estimation of the probable yield

strength of the reinforcement. Otherwise, a value of $1.1 f_y$ should be adopted as the probable reinforcement yield strength, where f_y is the nominal yield strength [P22].

A further consideration is whether the longitudinal reinforcement is from deformed or plain round bars. For instance, plain round bars were commonly used before the mid-1960s in New Zealand. The use of plain round longitudinal reinforcement would result in very different structural performance, when compared with the case with deformed longitudinal reinforcement. This can be seen later from the test results of this research project.

2.5.1.2 Concrete

The actual concrete compressive strength of old reinforced concrete buildings is likely to considerably exceed the nominal value as a result of conservative mix design, age and the less finely ground cement particles. Results on the concrete of 30 year old bridges in California consistently showed compressive strengths approximately 1.5 times to twice the nominal strength [P22]. Concrete from the columns of the Thorndon overbridge in Wellington has a measured compressive strength about 30 years after construction of about 2.3 times the specified value of 27.5MPa [P6].

The increase in concrete strengths usually has not a significant influence on a member's flexural and shear capacity. For instance, an increase of 50% in concrete compressive strength could only result in about 5 to 10% increase in flexural and shear capacities of beams and columns. Therefore the utilisation of 1.5fc' for probable concrete strength is accurate enough in seismic assessment of existing reinforced concrete structures when there is a lack of information on the actual concrete compressive strength.

In addition, the quality of the concrete should be inspected since if compaction was poor a lower concrete compressive strength may need to be assumed.

2.5.2 Flexural Strengths of Beams and Columns

The probable flexural strengths of beams and columns were suggested by Priestley [P5] and Park [P6] to be calculated using the probable material strengths, standard theory for flexural strengths, and assuming a strength reduction factor of unity.

2.5.3 Shear Strength of Reinforced Concrete Columns

Priestley, based on extensive laboratory testing, proposed a method for estimating the probable shear strength of columns. Priestley recommended using a shear strength reduction factor of 0.75 and he suggested that the probable shear strength of columns is the sum of components due to concrete contribution (V_c), transverse reinforcement (V_s) and axial load (V_n). Thus,

$$V_p = V_c + V_s + V_n \quad (1)$$

In which,

$$V_c = v_c \ 0.8 \ A_g = k\sqrt{f_c'} \ 0.8 \ A_g \quad (2)$$

$$V_s = \frac{A_v f_{yt} d''}{s}(\cot 30°) \text{ for rectangular sections} \quad (3a)$$

$$V_s = \frac{\pi}{2} \frac{A_{sp} f_{yt} d''}{s}(\cot 30°) \text{ for circular sections} \quad (3b)$$

and

$$V_n = N^* \tan \alpha \quad (4)$$

where:

k = 0.29 prior to shear strength degradation

v_c = nominal shear stress carried by the concrete mechanisms,

A_g = gross area of the column,

f_c' = probable concrete compressive cylinder strength,

A_v = total area of hoops and cross ties in the direction of the shear force at spacing s

A_{sp} = area of spiral or circular hoop bar,

f_{yt} = probable yield strength of the shear reinforcement,

d'' = depth of the concrete core measured in the direction of the shear force for rectangular hoops and the diameter of the concrete core for spiral or circular hoops.

N^* = the axial load acting on the column

α = for a cantilever beam, the angle between the longitudinal axis of the column and the straight line between the centroid of the column section at the top and the centroid of the concrete compressive force of the column section at the base, and for a column in double curvature α is the angle between the longitudinal axis of the column and the straight line between the centroids of the concrete compressive forces of the column section at the top and bottom of the column.

Evidently, Priestley assumed that the critical diagonal tension crack is inclined at 30° to the longitudinal axis of the column in calculating the shear resisted by transverse reinforcement, see Equations 3a and 3b.

The degradation of shear strength of concrete members is due to the decrease in the contribution of the concrete mechanism with the increase in the imposed flexural displacement level. The degradation of shear strength of columns proposed by Priestley [P5] is depicted in Fig. 2.11, in terms of the degradation of k.

Park [P6] suggested using a shear strength reduction factor of 0.85, rather than 0.75 of Priestley. The general expression proposed by Park for estimating the probable shear strength of columns is exactly the same as equation (1) by Priestley. The determination of V_c and V_n are also by equations 2 and 4 respectively. However, Park suggested that V_s be given as follows:

$$V_s = \frac{A_v f_{yt}(d'' - c)}{s}(\cot 30°) \text{ for rectangular sections} \qquad (3a')$$

$$V_s = \frac{\pi}{2}\frac{A_{sp} f_{yt}(d'' - c)}{s}(\cot 30°) \text{ for circular sections} \qquad (3b')$$

where:

c = distance from neutral axis to the extreme compression fibre of the section

A_v, A_{sp}, f_{yt}, and d'' have the same meanings as for Equations 3a and 3b.

It is seen that the method proposed by Priestley and the method proposed by Park for estimating the probable shear strength of columns are basically the same, and the only difference is that Park uses d'' - c, rather than d'' as for the method proposed by Priestley [P5], in calculating the shear resisted by the shear reinforcement. Park[P6] points out that

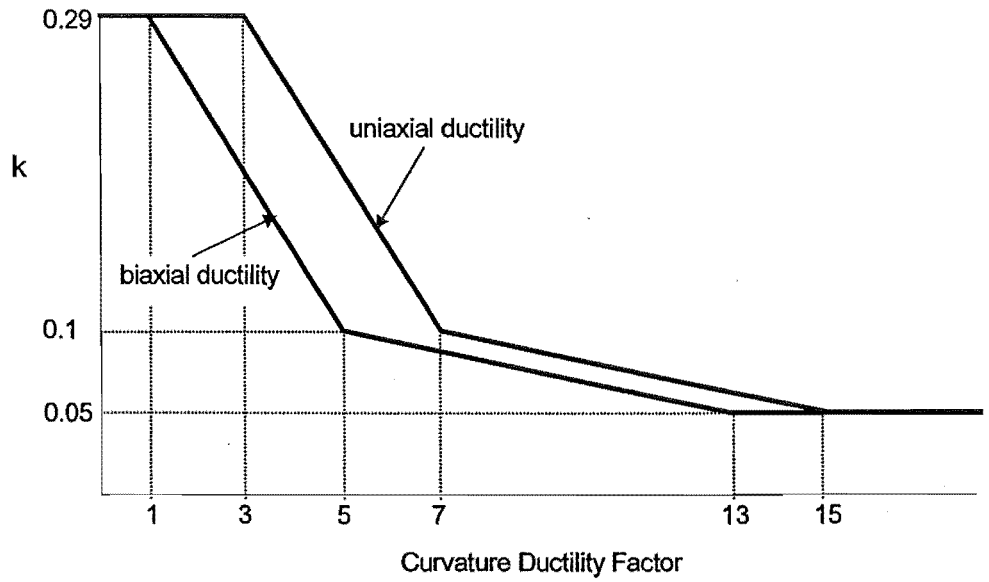

Fig.2.11 Degradation of Concrete Shear Strength with Ductility for Columns [P22]

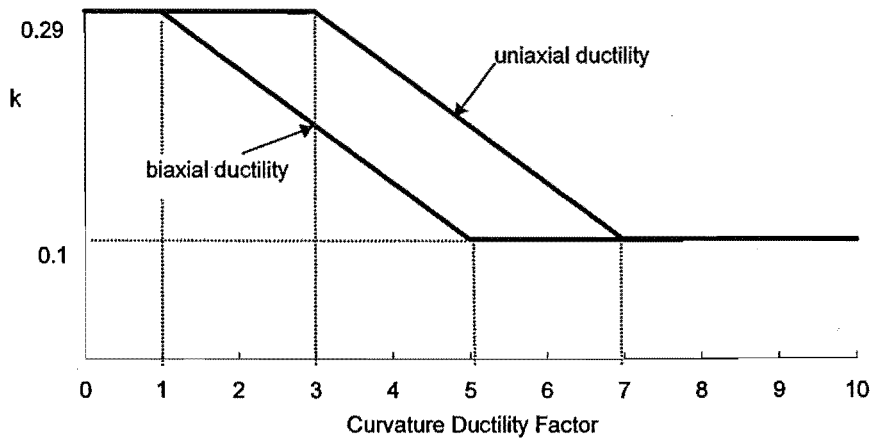

Fig.2.12 Degradation of Concrete Shear Strength with Ductility for Columns [P6]

such a modification is based on the suggestion made by Kowalsky, which indicates only the portion of the transverse reinforcement on the tensile side of the neutral axis crossing the potential shear failure plane.

Proposed degradation of concrete shear strength with ductility for reinforced concrete columns by Park [P6] is depicted in Fig. 2.12.

In a word, Priestley and Park proposed basically the same method for estimating the shear strength of columns, except that they recommended using different shear strength reduction factors in estimating the column shear strength.

2.5.4 Shear Strength of Reinforced Concrete Beams

Priestley directly extended his model for estimating the shear strength of reinforced concrete columns to reinforced concrete beams [P22]. Priestley recommended that the probable shear strength of reinforced concrete beams with rectangular stirrups or hoops be given by:

$$V_p = \mathrm{k}\sqrt{f_c'}\ 0.8\ A_g + \frac{A_v f_{yt}(d-d')}{s}(\cot 30°) \qquad (5)$$

where:

f_c' = probable concrete compressive cylinder strength,

A_g = gross sectional area of beams,

A_v = area of transverse shear reinforcement at spacings,

f_{yt} = probable yield strength of the shear reinforcement,

d = effective depth of beam,

d' = thickness of the concrete cover,

The degradation of beam shear strength suggested by Priestley, expressed in terms of coefficient k, is described in Fig.2.13, and it is based on Hakuto's tests with deformed longitudinal bars.

Park [P6] used an approach similar to the New Zealand code equation [NZS3101:1995] for estimating beam shear strength. Park recommended that the probable shear strength of beams with rectangular stirrups or hoops be given by:

$$V_p = \mathrm{k}\sqrt{f_c'}\ b_w \mathrm{d} + \frac{A_v f_{yt} d}{s} \qquad (5')$$

where b_w is the width of beam, and the other parameters have the same meanings as in Eq.(5).

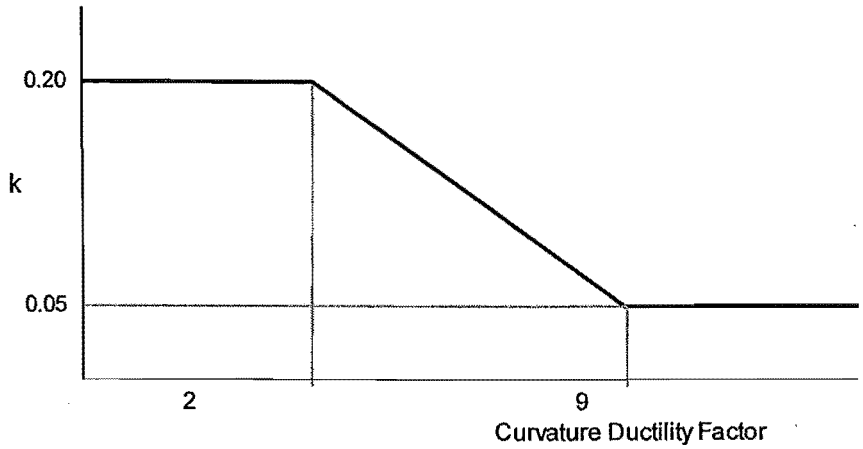

Fig.2.13 Degradation of Concrete Shear Strength with Ductility for Beams

The suggested degradation model for beam concrete shear resisting mechanism by Park [P6] is the same as depicted in Fig.2.13 by Priestley.

Comparison of equations (5) and (5') shows that a major difference between the method proposed by Priestley and the method proposed by Park is the assumed inclination angles of the critical diagonal tension cracks. Priestley [P5] believes that there should not be much conceptual difference in the shear resisting mechanisms between a beam and a column with zero axial load, and that the critical diagonal tension cracks are inclined at 30° to the longitudinal axis of the beam, similar to that for the columns. However, Park [P6] assumes that the critical diagonal tension cracks are inclined at 45° to the longitudinal axis of the beam, as is in NZS3101: 1995.

As for columns, Priestley and Park suggested different shear strength reduction factors. The shear strength reduction factors were 0.75 and 0.85 respectively for the methods proposed by Priestley and Park.

2.5.5 Shear Capacity of Reinforced Concrete Beam-Column Joints

It is very common that there is no, or insignificant, transverse reinforcement in the beam-column joint cores in pre-1970s reinforced concrete frame structures. In this case, NZS3101: 1995 implies that the shear strength of the joint core is negligible. However, Hakuto et al[Hakuto 1995] and Priestley [P22] pointed out that the beam-column joints without any, or insignificant, transverse reinforcement in the joint cores, do have some

shear strength, particularly if the joint core is uncracked or if plastic hinges undergoing cyclic deformations in the post-elastic range do not occur adjacent to the joint core.

Conceptually, the shear resisting mechanisms between interior and exterior beam-column joints are different. Hence the probable shear strength of the interior beam-column joints is expected to be different from that of the exterior beam-column joints.

2.5.5.1 Interior Beam-Column Joints

Having reviewed the vast body of test data, useful in this regard, assembled by Japanese, New Zealand and USA researchers, Priestley proposed tentative recommendations to estimate the shear strength of interior beam-column joints.

Priestley [P5] outlined that the joint shear failure is due to either the principal tension stress or the principal compression stress in the joint concrete.

When the beam longitudinal reinforcement is light or high column axial forces exist, the critical parameter is the principal tension stress in the joint, rather than the shear stress level. In this case, Priestley recommended using the model as shown in Fig.2.14, which was developed by Hakuto, Park and Tanaka, based on tests on as-built beam-column joints with deformed longitudinal reinforcement. The degradation of joint shear strength is expressed in terms of k in Fig.2.14. Hakuto et al [H1] suggested that for beam-column joints without shear reinforcement the maximum probable horizontal joint shear force that can be resisted is:

$$V_{jh} = v_{ch}\, b_j \mathrm{h} = \mathrm{k}\sqrt{f_c'}\,\sqrt{1+\frac{N^*}{A_g k\sqrt{f_c'}}}\, b_j \mathrm{h} \qquad (6)$$

where v_{ch}=nominal horizontal joint shear stress carried by a diagonal compressive strut crossing the joint, b_j=effective width of the joint, h = depth of column, N^* is the axial load on columns, and other parameters have the same meanings as before.

When the shear stress level is high in the joint, interior beam-column joints tend to fail in shear, regardless of the amount of joint shear reinforcement. In this case, the failure is as a result of the principal compression stress. The model proposed by Priestley for estimating the joint shear strength in this case is the principal compression model. The postulated principal compression model is shown in Fig.2.15, which was deduced by setting the

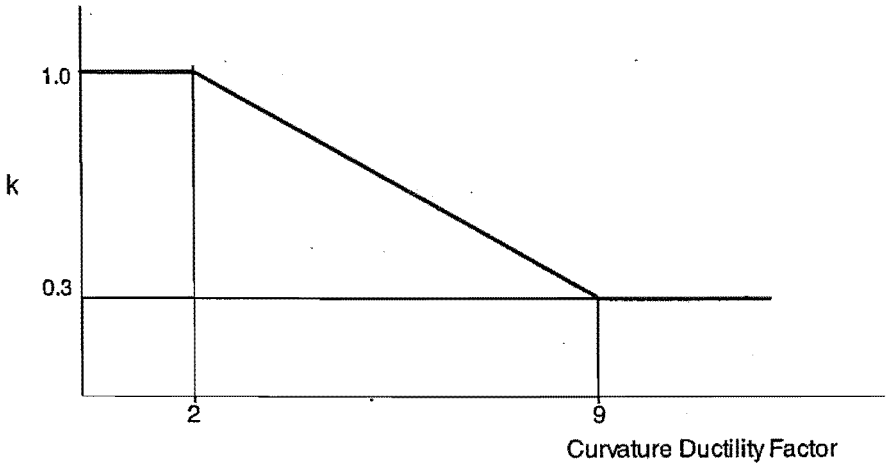

Fig.2.14 Principal Tension Model of Degradation of Concrete Shear Resisting Mechanism of Interior Beam-Column Joints [Hakuto et al 1995]

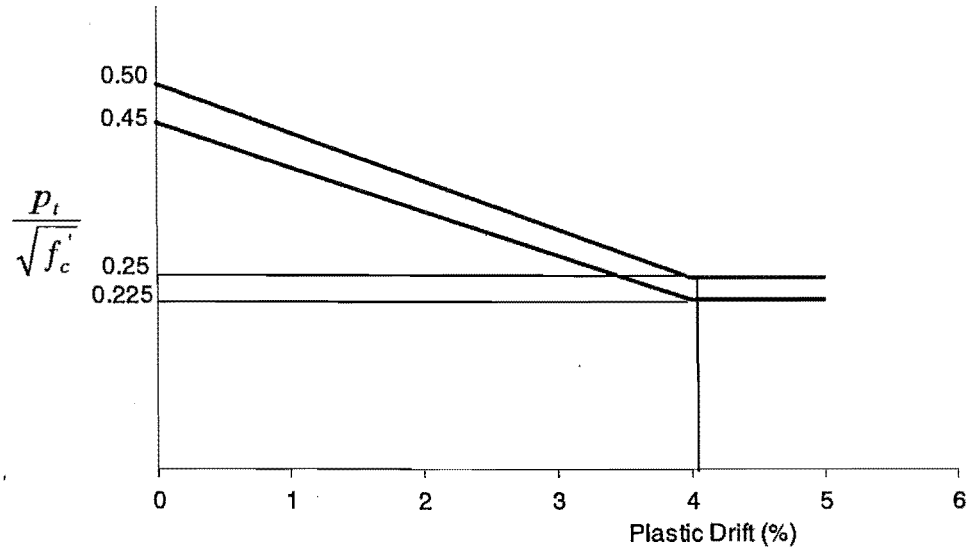

Fig.2.15 Principal Compression Model of Degradation of Concrete Shear Resisting Mechanism of Interior Beam-Column Joints [P22]

upper limit in association with the principal compression stress not greater than 0.5 concrete compression strength.

However, Priestley did not give clear definition for principal tension failure and principal compression failure.

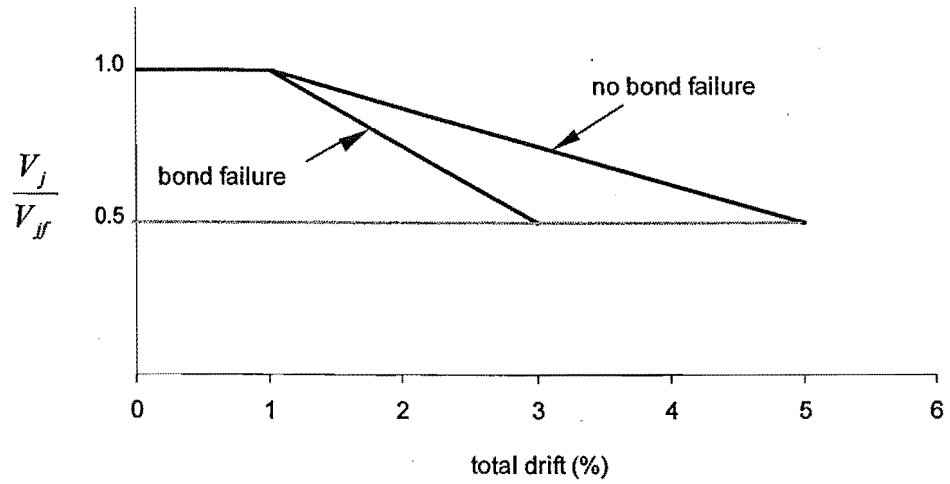

Fig.2.16 Possible Shear Strength Model of Interior Beam-Column Joints [P22]

In addition, Priestley also postulated a simpler model as shown in Fig.2.16 in order to allow for the influence of bond performance on the joint shear strength degradation. The degradation is assumed to start at 1% drift, regardless of poor bond or adequate bond and regardless of the actual shear stress or principal stress level. However, this model has no support from test results.

Park also recommended using the model developed by Hakuto et al as shown in Fig. 2.14 for degradation of shear strength resisted by the concrete mechanism of interior beam-column joints without joint horizontal shear reinforcement, but without clarifying the failure type of the joints. This model is clearly the principal tension model Priestley used.

Apparently, more testing needs to be conducted to identify different failure modes of the joints and develop reliable models for estimating the degradation of joint shear strength correspondingly.

2.5.5.2 Exterior Beam-Column Joints

Similar to interior beam-column joints, the maximum probable horizontal joint shear force that can be resisted by exterior beam-column joints without shear reinforcement is suggested to be calculated by equation 6.

The degradation of the horizontal joint shear strength, when expressed in terms of k, is proposed to be represented by Fig. 2.17 by Priestley, and it was based on the tests of unreinforced exterior and corner joints. The degradation of the horizontal joint shear force,

when expressed in terms of k, is proposed by Park to be represented by Fig.2.18, and it was based mainly on test results of Hakuto et al.

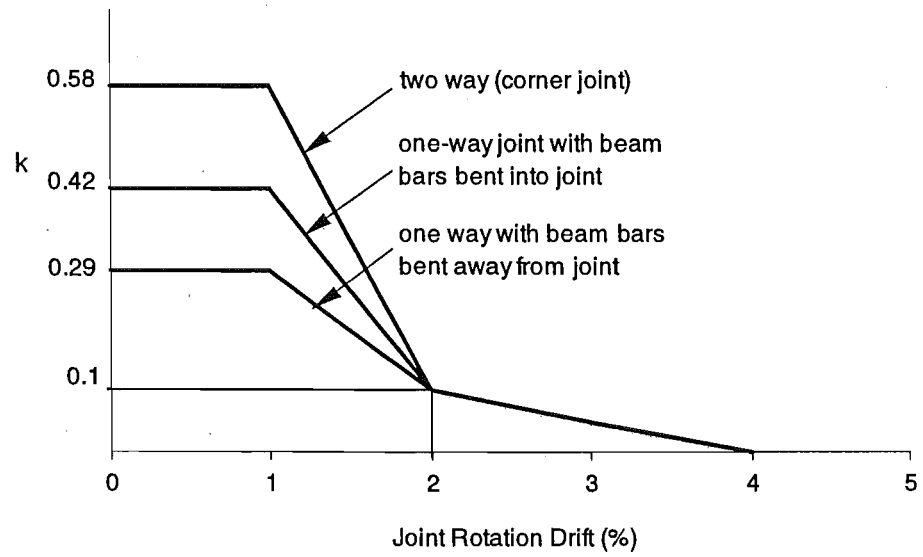

Fig. 2.17 Degradation of Joint Shear Force Resisted by Concrete Mechanism for Exterior Beam-Column Joints [Prietley P22]

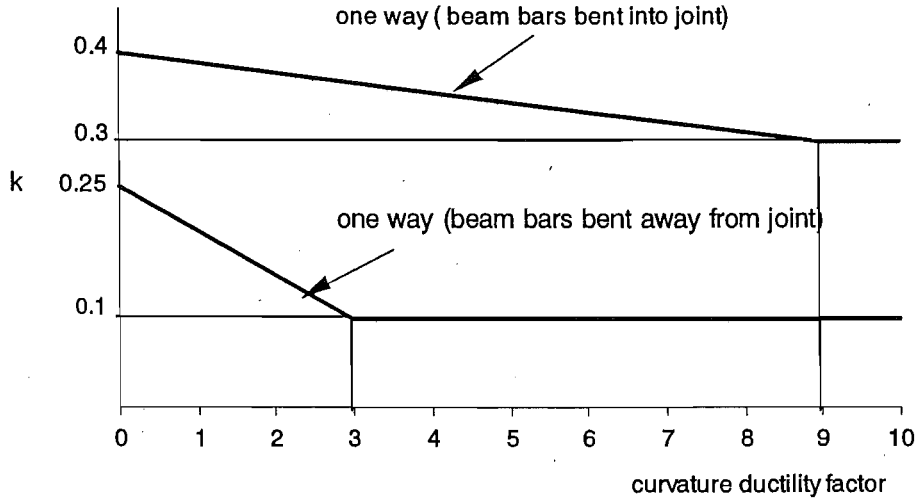

Fig. 2.18 Degradation of Joint Shear Force Resisted by Concrete Mechanism for Exterior Beam-Column Joints [Park, P6]

Both the model proposed by Priestley and the model proposed by Park assumed that the joint shear failure in exterior beam-column joints is as a result of large principal tension stress. A significant difference of the model proposed by Priestley, from the model proposed by Park is that Priestley prefers to use drift as an index of the post-elastic deformation.

It is noted that the models proposed by Priestley and Park are based on very limited test results. Evidently, more tests on as-built beam-column joints are needed in order to refine the models.

2.5.6 Flexural Deformation Capacity in Plastic Hinges

Assessment of the displacement ductility capacity of the structures needs to define the plastic rotation capacity of beams and columns. Rotational capacity of plastic hinges is given by

$$\theta_p = (\phi_u - \phi_y) l_p \qquad (7)$$

where:

ϕ_u and ϕ_y are respectively the ultimate and yield curvatures of the members, and l_p is the equivalent plastic hinge length.

Priestley [P22] and Park [P6] proposed exactly the same methods for determining l_p, ϕ_u and ϕ_y.

l_p is calculated by:

$$l_p = 0.08L + 0.022\ f_y\ d_b \qquad (8)$$

where:

f_y is the yield strength of the longitudinal reinforcement,

d_b is the diameter of the longitudinal reinforcement

and L is the distance from the critical section to the point of contraflexure.

In calculating the ultimate curvatures of beams and columns, the ultimate concrete strain ε_{cu} for unconfined concrete is suggested to be 0.005, and that for confined concrete is given by:

$$\varepsilon_{cu} = 0.004 + 1.4\ \rho_s f_{yh} \varepsilon_{su} / f'_{cc} \qquad (9)$$

$$\rho_s = 1.5\ \frac{A_v}{b_c s} \qquad (10)$$

where:

A_v =total area of transverse reinforcement in a layer at spacing s

b_c = width of member core measured from centre to centre of the peripheral transverse reinforcement in the web

f_{yh} = the yield strength of transverse reinforcement

ε_{cu} = the strain of the transverse reinforcement at maximum stress

and $f_{cc}^{'}$ = the compression strength of the confined concrete

2.5.7 Summary

To realistically estimate member strength and deformation capacity, probable material strength rather than nominal material strength should be used. In the case of the lack of information on the actual material strength, 1.1 times the nominal steel yield strength and 1.5 times the nominal concrete compression strength should be used.

Unlike modern reinforced concrete structures designed to current codes, premature shear failure of members (beams and columns) and joints of existing reinforced concrete structures, when reinforced by deformed longitudinal reinforcement, is observed to degrade with the increase in the imposed flexural deformation. As a result, a mechanism which initiates with flexural plastic hinges may degenerate into plastic hinges with shear failure as the ductility demand increases. Consideration of degradation of shear strength is very critical in this case. Design code equations are considered to be not suitable in estimating the member strength and deformation capacity.

The current method for estimating member flexural strength is basically the same as code equation, except that probable material strength and a strength reduction factor of unity are used.

The current method for estimating the initial column shear strength and its degradation with the increase in the imposed flexural deformation is based on extensive test results, and one major difference from design code equation is that the influence of column axial load on the enhancement of column shear strength is taken as the horizontal component of the column compressive strut.

Meanwhile, the current method for estimating the initial beam shear strength and its degradation has not been adequately testified. There is no agreement for the assumed angles of the critical diagonal tension cracks to the longitudinal axis of the beam.

Estimation of shear strength of beam-column joints is still the most difficult task. Current models for predicting joint shear strength and deformation capacity propose to use different models for different failure modes, but only the principal tension models, which assume that the joint shear failure is due to large principal tension stress generated in the joint concrete, were established based on very limited test data. Apparently, the failure mechanism of beam-column joints is still unclear.

A major concern is that the current methods are based on the tests with deformed longitudinal reinforcement. When plain round longitudinal bars are used, reinforced concrete components may have different critical failure modes. The strength and deformation capacity of correspondent critical failure modes in this case needs to be investigated.

2.6 Retrofit of Existing Reinforced Concrete Structures

2.6.1 General

In most cases retrofit methods are associated with an increase in the strength and stiffness of regions of the structure. Possible retrofit measures need to be carefully assessed to ensure that the seismic characteristics of the structure will be improved. Seismic assessment procedures based on capacity design can be used in this regard provided the information on the strength and deformation capacity of retrofitted members is available.

Retrofit methods typically involve adding new structural components to the existing structure, such as movement restrainers, walls, steel bracing, and jacketing [A7, H1, P23, P24, P25, R1, R2, S9].

2.6.2 RETROFITTING OF COLUMNS

Columns are particularly vulnerable elements in buildings. Several methods for increasing the strength and/or ductility of existing columns have been developed, tested and used in the United States and New Zealand. These methods include jackets of new concrete containing longitudinal and transverse reinforcing [R2, S9], grouted site welded circular thin jackets [P23], site welded elliptical thin steel jackets filled with concrete, grouted stiffened or built-up rectangular steel jackets, grouted composite fiberglass/epoxy jackets [P25], or prestressing steel wrapped under tension[P23]. Methods for calculating the required size of jackets are given elsewhere, for example reference P23.

The column retrofit can be designed so as not to increase the flexural strength, but to provide only additional transverse reinforcement for concrete confinement, restraint against buckling of existing longitudinal bars, shear resistance and restraint against bond failure of lap splices of longitudinal reinforcement. In such case the strengthening is not continued beyond the ends of the column, so that the flexural strength of the column ends is not increased. Alternatively, the strengthening can be continued beyond the ends of the column so that the flexural strength of the column ends is increased. This requires passing longitudinal reinforcement through the floors in the case of a building.

The most successful technique for providing additional transverse reinforcement, without additional longitudinal reinforcement, has been the use of thin steel jackets[P23]. For circular columns the thin jacket is constructed slightly oversize in two semi circular halves which are welded up vertical seams in situ. The jacket is terminated about 25 mm from the face of the beams or footing at the column ends. The gap between the steel jacket and the column is subsequently pressure filled with a cement-based grout which contains a small quantity of water reducing expansive additive. For rectangular columns an elliptical thin steel jacket is used to provide continuous confinement, with concrete placed between the jacket and the column. A rectangular thin steel jacket would not be so effective for confinement, due to the sides bowing out when dilation of the concrete occurs during a major earthquake, resulting in confinement applied mainly in the column corners.

The use of fiberglass/epoxy jackets for columns of buildings and bridges is becoming common in New Zealand. Typically the fiberglass sheets with epoxy are wrapped around the columns and are not grouted.

2.6.3 RETROFITTING OF BEAM-COLUMN JOINTS

Beam-column joint regions can be retrofitted by jacketing, using either external steel jacketing[A7] or jacketing with new reinforced concrete [P23]. This can be a very labour intensive and costly procedure, due to the drilling of holes through the existing joint to pass new reinforcement through. One solution, which has been proposed as a result of tests on full scale beam-column joint assemblies is to enlarge the existing beam-column joints without placing new hoops [A7]. It has been found that no new hoops are required in the added jacket if the resulting nominal horizontal shear stress in the enlarged joint core is reduced to less than $0.3\sqrt{f_c'}$ MPa [A7,H1].

Another solution, which has been adopted for beam-column joints, has been to remove the existing concrete joints and to replace the whole joint region with new reinforced concrete.

2.7 Conclusions

The possible design deficiencies in existing reinforced concrete structures designed to pre-1970s seismic design codes are as a result of two major failings in outdated seismic design codes. One is that the now outdated seismic codes did not have the design specifications associated with the member local ductility behaviour, the other is that the now outdated seismic codes did not have the design specifications associated with the global structural behaviour during the post-elastic loading cycles. As a consequence, the greatest uncertainty of the seismic performance of existing reinforced concrete structures is the post-elastic behaviour in a major earthquake.

There are currently two types of assessment procedures, the check list type and the capacity design type procedures. Check list seismic assessment procedures emphasise the statistical study of the observed earthquake damage in past earthquakes and emphasise member local behaviour, but do not identify the critical post-elastic failure mechanism, failing in adequately assessing the global structural post-elastic seismic performance, which is the core element needed to be investigated. Hence, check list assessment procedures could give irrational results. However, check list procedures are easy to follow, are suitable for statistical study of earthquake damage because of the procedures' nature. Therefore they can be used for City Earthquake Disaster Prevention and Preparation Programs.

Capacity design based seismic assessment procedures aim at investigating the post-elastic response of existing reinforced concrete structures, and thus can realistically assess the seismic performance of the structures.

When capacity design based seismic assessment procedures are used for the seismic assessment of an existing reinforced concrete structure, the required information is member strength and deformation capacity in post-elastic range, namely, member local behaviour. The fundamental aspects here are to determine the most critical failure mode of the member and to determine the strength degradation of identified critical failure mode with the increase in the imposed flexural deformation.

When deformed bars are used for longitudinal reinforcement, shear failure in members (beams and columns) and beam-column joints is observed to be very critical. In this case, the determination of degradation in shear strength of members and joints is of particular importance. Several models for determining the post-elastic shear strength degradation of members and beam-column joints are developed, but they are based on very limited test results. This is especially true for the models for reinforced concrete beams and beam-column joints designed to now outdated seismic codes. More testing is urgently needed to refine the current models.

Variety of seismic retrofit techniques have been developed, some retrofit techniques aim at improving the member strength and/or ductility capacity, and the others aim at improve the structural global behaviour during the post-elastic loading cycles. One needs to investigate the post-elastic performance of the upgraded structure during a major earthquake to make sure that the used retrofit technique did not shift the problem.

Steel type (deformed bars or plain round bars) can make a big difference in the critical failure mode of the members and the associated strength and deformation performance in the post-elastic range. Therefore, the critical concern of the post-elastic response of existing reinforced concrete members reinforced by plain round longitudinal bars needs to be identified based on laboratory testing and proper models for estimating the corresponding strength and deformation capacity need to be studied.

CHAPTER 3

REVIEW OF PREVIOUS RESEARCH PROJECTS RELEVANT TO THIS PROJECT AT UNIVERSITY OF CANTERBURY

The research program "Seismic Assessment and Retrofit of Existing Reinforced Concrete Structures" started in 1989 at the University of Canterbury sponsored by the Earthquake Commission of New Zealand. Four research projects have been conducted since then and the proposed project here is a continuation of the previous four research projects.

3.1 THE INVESTIGATED STRUCTURE

The subject structure of the previous four research projects was a seven-storey reinforced concrete frame structure constructed in Christchurch, New Zealand, in the 1950s, and it has been thoroughly investigated. The typical deficiencies identified of this reinforced concrete frame building are as follows [H1]:

(1). Columns with inadequate longitudinal reinforcement to ensure strong column-weak beam behaviour.

(2). Columns and beams with inadequate transverse reinforcement for concrete confinement and prevention of premature buckling of longitudinal compression bars, and/or inadequate transverse reinforcement for shear resistance.

(3). Small quantities of joint shear reinforcement or no joint shear reinforcement at all.

(4). Greater diameter of the beam longitudinal reinforcement passing through the joints than that required by NZS3101: 1995 [N1], hence significant loss of anchorage of reinforcement would occur in that region if ductile structural behaviour is required.

(5). Poor anchorage details of longitudinal beam bars in exterior columns.

(6). Longitudinal beam and column bars with lap splices in potential plastic hinge regions near beam-column joints.

3.2 ANALYSIS OF THE AS-BUILT STRUCTURE

Hakuto, Park, and Tanaka [H1] carried out a static analysis of the whole as-built building using the current code approach to estimate the lateral load capacity of the structure, and the shear and ductility demands of the members and beam-column joints; in addition they also conducted a non-linear dynamic analysis using the two-dimensional time-history non-linear frame analysis program "RUAUMOKO" of the whole building to investigate the drift demand of the structure, and the shear and ductility demands of the members and joints under the El Centro and the Bucharest earthquake records. The analysis of this reinforced concrete frame building indicated that the available lateral load strength of the complete structure approached the design seismic force, assuming an elastic response, required by the current New Zealand standards. The inelastic failure mechanism of the frame was identified to be a mixture of flexural and shear failures in the beams and columns.

A critical aspect with respect to shear was found to be the behaviour of the beam-column joints with little or no shear reinforcement, as a result of the relatively large joint shear forces. The estimated maximum nominal joint shear stresses in the lower storey by the static analysis, calculated from the beam face moments and column shear forces acting on the joints, ranged from $1.2\sqrt{f_c'}$ MPa to $1.5\sqrt{f_c'}$ MPa for the interior beam-column joints, and ranged from $0.6\sqrt{f_c'}$ MPa to $1.0\sqrt{f_c'}$ MPa for exterior beam-column joints. These, by far, exceeded the joint shear stress level associated with the estimated joint shear strength reached at the stage of initial diagonal tension cracking of the joint core. Typically the maximum exterior joint shear capacity is $0.25\sqrt{f_c'}$ MPa for the case with the beam longitudinal reinforcing bars bent away from the joint core if estimated using the proposed procedures by Park [P6]. Hence, the seismic performance of the early reinforced concrete frames was likely to be governed by joint shear failure.

The estimated maximum axial column load level obtained by the static analysis was 0.24 for the interior column and 0.3 for the exterior column, in the first storey respectively, when the roof horizontal displacement was 1% of the total height. The estimated maximum axial column load level from the dynamic analysis was 0.26 and 0.31 for the interior column and exterior column in the first storey respectively. The axial column load

level was expressed as $N^* / A_g f_c^{'}$. Evidently, axial column load was very significant in some cases, and neglecting its influence on the seismic behaviour of the beam-column joint units could give misleading results.

The maximum inter-storey drift angle found by the static analysis using the code approach was approximately 1.20%, and the maximum interstorey drift angle found by the dynamic analysis was 0.7% under the El Centro record and 2.9% under the Bucharest record.

3.3 THE FIRST STAGE OF THE RESEARCH SERIES - COLUMNS

The first stage of the experimental research series involved the simulated seismic loading tests on four near full-scale column replicas of the first storey of the subject building at the University of Canterbury [R1, R2]. The aim of this project was to investigate the seismic performance of as-built columns and the increase of strength, stiffness, and ductility which can be achieved by jacketing existing damaged or undamaged reinforced concrete columns with new reinforced concrete. The as-built columns, which were 350 mm square, were reinforced by plain round reinforcement and contained low quantities of transverse reinforcement. The column units represented the column region between the mid-heights of successive stories. Two columns units were tested as-built to study the seismic behaviour and damage during major earthquakes, and then repaired and strengthened by reinforced concrete jacketing and retested. The other two column units were strengthened by reinforced concrete jacketing before being damaged and then tested. The new longitudinal reinforcement in concrete jacket was placed through the floor slab. Two arrangements of transverse reinforcement in the jacket were devised to properly tie the longitudinal reinforcement. The as-built columns displayed low available ductility and significant degradation of strength during testing due to inadequate column transverse reinforcement and severe bar slip owing to the utilisation of plain round longitudinal bars. The jacketed columns behaved in a ductile manner with higher strength and much reduced strength degradation during testing. The retrofit of columns using reinforced concrete jackets was found to be successful but labour intensive.

3.4 THE SECOND STAGE OF THE RESEARCH SERIES –INTERIOR BEAM-COLUMN JOINT ASSEMBLIES

The second stage of this experimental research series involved the simulated seismic loading tests on three full-scale replicas of the interior beam-column joint region of the perimeter frame of the subject building in order to investigate the seismic performance of existing reinforced concrete structures and the effectiveness of reinforced concrete jacketing as a repair and strengthening measure [H1, H2].

The test units were identical to that part of the frame between the mid-span of the beams and the mid-height of the interior columns of the as-built reinforced concrete frame structure as described previously [H1]. The reinforcing details in the members and joints were as in the as-built structure, and hence did not meet the requirements of the current New Zealand concrete design code NZS 3101:1995. Deformed reinforcement was used for longitudinal reinforcement.

One of the interior beam-column joint replicas was tested as-built subjected to simulated seismic loading. The test confirmed that the performance of the as-built beam-column joint region would be poor in a major earthquake, mainly due to the lack of joint shear reinforcement and poor anchorage of longitudinal beam bars in the beam-column joint region. The damaged (tested) beam-column joint unit and the other two undamaged (not tested) beam-column joint units were then retrofitted by jacketing with new reinforced concrete to increase the strength and ductility of the existing frame. All retrofitted interior beam-column joint units were then tested subjected to simulated seismic loading and performed in a very satisfactory manner. It was found that the concrete jacketing technique could be used for extending the life of existing reinforced concrete structures and for the repair of damage arising from major earthquakes.

3.5 THE THIRD STAGE OF THE RESEARCH SERIES - INTERIOR AND EXTERIOR BEAM-COLUMN JOINT UNITS

The third stage of the research series involved the seismic load testing and analysis of four full-scale replicas of other beam-column joint regions of the 1950s building frame [H1, H3]. Deformed longitudinal reinforcing bars were used for longitudinal reinforcement again. Two of the subassemblies were further interior beam-column joint subassemblies which lacked joint shear reinforcement. These two specimens had different column depth

to beam bar diameter ratios and were tested mainly to investigate the effect of the bond conditions along the beam bars passing through the joint on the seismic behaviour of beam-column joints without joint shear reinforcement. Changing the beam bar diameter to column depth ratio from 1/25 to 1/18.75 was found not to have a significant effect on the seismic performance of joints without joint transverse reinforcement. The other two specimens were exterior beam-column joints with limited shear reinforcement and with different arrangements of beam bar hooks in the joint core. One exterior beam-column joint specimen had the beam bar hooks bent away from the joint core, as was common in many early frames; and the other exterior beam-column joint specimen had the beam bar hooks bent into the joint core, as is the current practice. Tests demonstrated that the seismic performance of the exterior beam-column joints with little shear reinforcement was significantly influenced by the directions in which the tails of the beam bars in the joint core were bent. It was found that the exterior beam-column joint subassemblies of early frames in which the tails of the beam bars were bent out of the joint core would behave unsatisfactorily during a major earthquake.

3.6 THE FOURTH STAGE OF THE RESEARCH SERIES - INTERIOR BEAM-COLUMN JOINT UNITS

Two additional full-scale replicas of interior beam-column joints in which the longitudinal beam bars were lap spliced in the plastic hinge regions of the beams were also tested by Wallace 1996 [W1]. One specimen contained plain round longitudinal bars and the other contained deformed longitudinal bars. Tests illustrated very limited ductility available from this poor detail during seismic loading, especially when plain round bars were used.

3.7 SUMMARY

Evidently, the research work in this research program conducted so far has been focused on the study of the possible seismic performance and retrofit methods of as-built reinforced concrete frame structures, with the emphasis on the use of deformed bar reinforcement. Actually, plain round bar reinforcement was used in New Zealand until about the mid 1960s when deformed bar reinforcement became widely available. The reliability of using the obtained information in the past research stages for the existing reinforced concrete structures reinforced by plain round bars apparently needs to be re-

examined. The observed evidence of severe bond slip for the tests on as-built columns conducted in the first stage already suggested the need for the investigation of the seismic performance of existing reinforced concrete structures with plain round longitudinal bars.

In addition, these previous beam-column joint tests were conducted with zero axial column load. The estimated maximum column axial load level by Hakuto et al was as high as 0.31, the influence of so high axial column load on the seismic behaviour of the actual structural performance is apparently significant, and needs to be allowed for.

CHAPTER 4

TEST UNITS AND THEORETICAL CONSIDERATIONS

4.1 INTRODUCTION

Review of the researches at the University of Canterbury into the seismic assessment and retrofit of pre-1970s reinforced concrete frame structures, conducted in Chapter 3, indicates that the as-built beam-column joint subassemblies tested in the previous research projects used deformed longitudinal reinforcement and the resulting information on the member local behaviour is only applicable to the situations where deformed bars are used for longitudinal reinforcement. There is an urgent need for obtaining the information on the local behaviour of beam-column joint subassemblies, which are reinforced by plain round bars and designed to now outdated seismic design codes.

The experimental work conducted in this current research project studied the seismic behaviour of as-built beam-column joint subassemblies with plain round longitudinal bars, including the weakest failure mechanism, the attainment and maintenance of the strength and stiffness with the increase in the imposed post-elastic deformations. The effective retrofit methods of as-built beam-column joint subassemblies reinforced by plain round bars are also tested where necessary. Emphasis is placed on the effect of the plain round longitudinal bars, when compared to the cases with deformed longitudinal reinforcement.

This chapter introduces the units tested in this current research project.

4.2 DETAILS OF TEST UNITS

4.2.1 General

The as-built beam-column joint subassemblies, reinforced by deformed bar reinforcement and representing the subject frame building constructed in 1950s in New Zealand, have been tested under simulated seismic loading by Hakuto et al at University of Canterbury [H1]. The beam-column joint test units in the current research project were designed to be identical to the test units conducted by Hakuto et al [H1], except that the plain round bars were used for the longitudinal reinforcement. Such a test unit design aimed at identifying the effect of the use of plain round longitudinal reinforcement by comparing the observed test evidence in this project with the test evidence observed by Hakuto [H1].

The current project involved six as-built full-scale beam-column joint test units and one retrofitted exterior beam-column joint unit. The six as-built test units include two interior beam-column joint units and four exterior beam-column joint units.

4.2.2 Details of the Interior Beam-Column Joint Units

Two identical one-way interior beam-column joint units were constructed, each full-scale in size, containing plain round longitudinal reinforcement and with reinforcement details typical of the 1950s construction in New Zealand. These two units were identical to Hakuto's Unit O1 except that Hakuto used deformed longitudinal bars, and were referred to as Unit 1 and Unit 2. The overall dimensions and reinforcing details of the two identical as-built interior beam-column joint units are shown in Fig. 4.1.

The beams were 500 mm in depth and 300 mm in width, and the columns were 300 mm in depth and 460 mm in width. The test units were identical to that part between the mid-span of the beams and the mid-height of the columns of a seven-storey existing reinforced concrete frame structure constructed in the 1950s in New Zealand, which has been described previously [H1].

The beams were unsymmetrically reinforced, contained four 24 mm diameter Grade 300 plain round bars in the top (p =0.013) and two 24 mm diameter Grade 300 plain round bars in the bottom (p'=0.0068). The beam transverse reinforcement was from 6 mm diameter Grade 300 plain round bars placed at 380mm centres, and the first stirrup was 300 mm from the column face. The columns were symmetrically reinforced, and contained three 24 mm diameter Grade 300 plain round bars on both sides (p_t = 0.02). The column transverse reinforcement was from 6 mm diameter Grade 300 plain round bars placed at 230 mm centres, and the first tie was 100 mm from the beam face. The beam-column joint cores contained no transverse reinforcement or intermediate column bars (at the mid-depth of the columns).

The concrete for Units 1 and 2 was normal weight. The units were cast in one stage in the horizontal plane. Table 4.1 lists details of concrete compressive cylinder strengths of Units 1 and 2 at the time of testing the units and the axial load ratios applied to the columns during testing. For both units, all R24 plain round longitudinal reinforcing bars were taken from the same steel batch. Similarly, all R6 transverse reinforcement was taken from the same steel batch. Table 4.2 lists details of the reinforcement for Units 1 and 2.

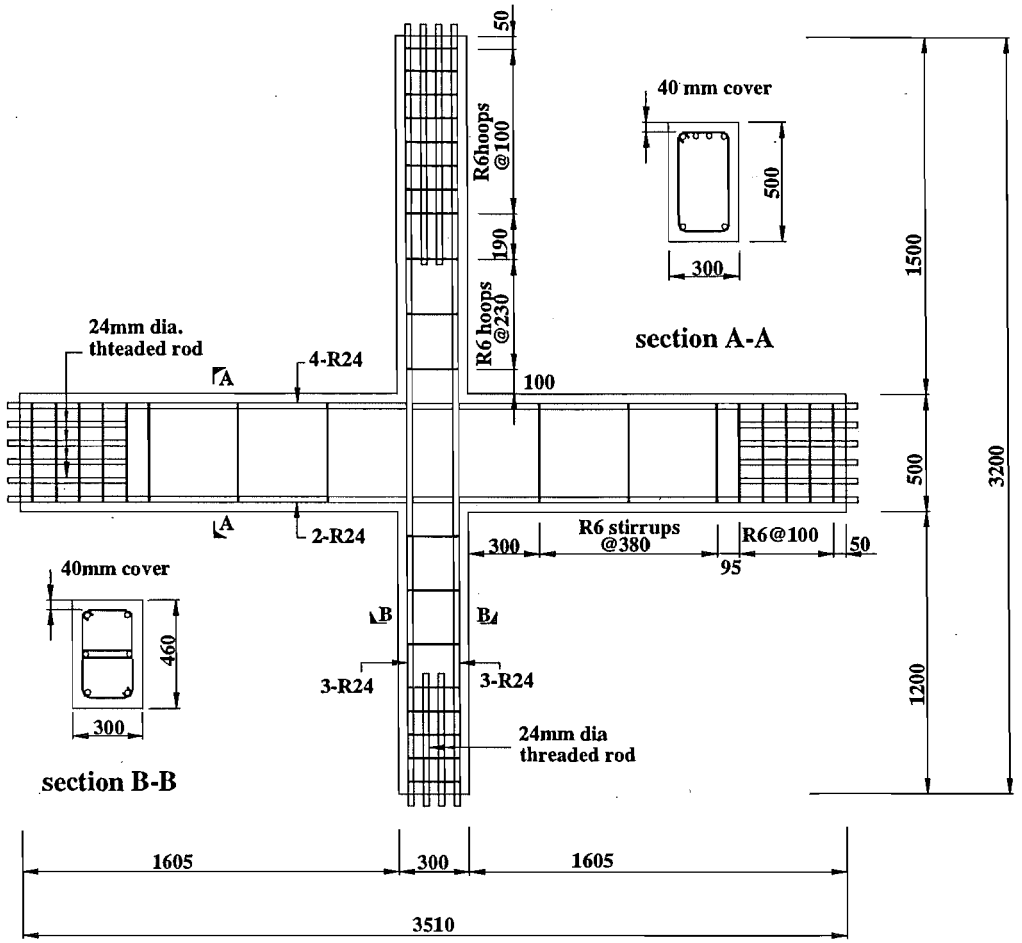

Fig.4.1 Reinforcement Details of the Two Interior Beam-Column Joint Specimens

Table 4.1 Compressive strengths of concrete at the time of testing the Units

Unit	f_c'(MPa)	$N^*/A_g f_c'$
Unit 1	44	0
Unit 2	49	0.12

Table 4.2 Details of Reinforcement in the Units

Part of Unit	Longitudinal Reinforcement						Transverse Reinforcement		
	d_b (mm)	f_y MPa	ε_y $x10^{-6}$	p %	p' %	p_t %	d_b (mm)	f_{yt} (MPa)	s (mm)
Beam	24	321	1560	1.36	0.68		6	318	380
Column	24	321	1560			1.97	6	318	230

4.2.3 Details of the Exterior Beam-Column Joint Units

Four one-way exterior beam-column joint units, which were identical to each other except for the anchorage of the beam longitudinal bars in the exterior columns, were constructed. Each unit contained plain round longitudinal reinforcement and had other reinforcement details typical of the 1950s construction in New Zealand.

The first two exterior beam-column joint units were identical to each other, and had beam bar hooks bent away from the joint core in exterior columns. The straight extension of the beam bars beyond the bends was four times the bar diameter, as was typical of pre-1970s construction in New Zealand. These two units are referred to as Units EJ1 and EJ3. Unit EJ1 and Unit EJ3 were identical to Hakuto's Unit O7 except that Hakuto used deformed longitudinal reinforcement. The overall dimensions and reinforcing details of the as-built test units EJ1 and EJ3 are shown in Fig.4.2 (a). The other two exterior beam-column joint units were also identical to each other, and had the beam bar hooks bent into the joint core in the exterior columns. The straight extension of the beam bars beyond the bends was twelve times the bar diameter, as is the current practice [N1]. These two units are referred to as Units EJ2 and EJ4. Unit EJ2 and Unit EJ4 were identical to Hakuto's Unit O6 except that Hakuto used deformed longitudinal reinforcement. The overall dimensions and reinforcing details of the as-built test units EJ2 and EJ4 are shown in Fig. 4.2 (b).

The beams of each exterior beam-column joint unit were 500 mm in depth and 300 mm in width and the columns were 460 mm square. The size of these units are identical to those of the perimeter planar frame of a seven-storey existing reinforced concrete frame structure constructed in the 1950s in New Zealand, which has been described previously [H1].

The beam was unsymmetrically reinforced, contained three 24 mm diameter Grade 300 plain round bars in the top ($p = 0.01$) and two 24 mm diameter Grade 300 plain round bars in the bottom ($p' = 0.0066$). The beam transverse reinforcement was from 6 mm diameter Grade 300 plain round bars placed at 380 mm centres. The columns were symmetrically reinforced, contained two 24 mm diameter Grade 300 plain round bars on both sides ($p_t = 0.0085$). The column transverse reinforcement was from 6 mm diameter Grade 300 plain round bars placed at 305 mm centres outside the joint region and at 250 mm centres within the joint region. The first column tie was 305 mm from the beam face.

The concrete was normal weight for all exterior beam-column joint units. The four units were cast in one stage in the horizontal plane. The R24 plain round longitudinal reinforcing bars of the four units were taken from the same steel batch. Similarly, all R6 transverse reinforcement of the four units was taken from the same steel batch. Table 4.3 lists details of concrete compressive cylinder strengths of Units EJ1, EJ2, EJ3 and EJ4 at the time of testing and the axial load ratios applied to the columns during testing. Table 4.4 lists details of the reinforcement for Units EJ1, EJ2, EJ3 and EJ4.

Table 4.3 Compressive strengths of concrete at the time of testing the Units

Unit	f_c' (MPa)	$N^* / A_g f_c'$
Unit EJ1	33.7	0
Unit EJ2	29.2	0
Unit EJ3	34	0.25
Unit EJ4	36.5	0.23

Table 4.4 Details of Reinforcement in the Units of EJ1, EJ2, EJ3 and EJ4

Part of Unit	Longitudinal Reinforcement						Transverse Reinforcement		
	d_b (mm)	f_y MPa	ε_y $x10^{-6}$	p %	p' %	p_t %	d_b (mm)	f_{yt} (MPa)	s (mm)
Beam	24	321	1605	1.0	0.66		6	318	380
Column	24	321	1605			0.85	6	318	305

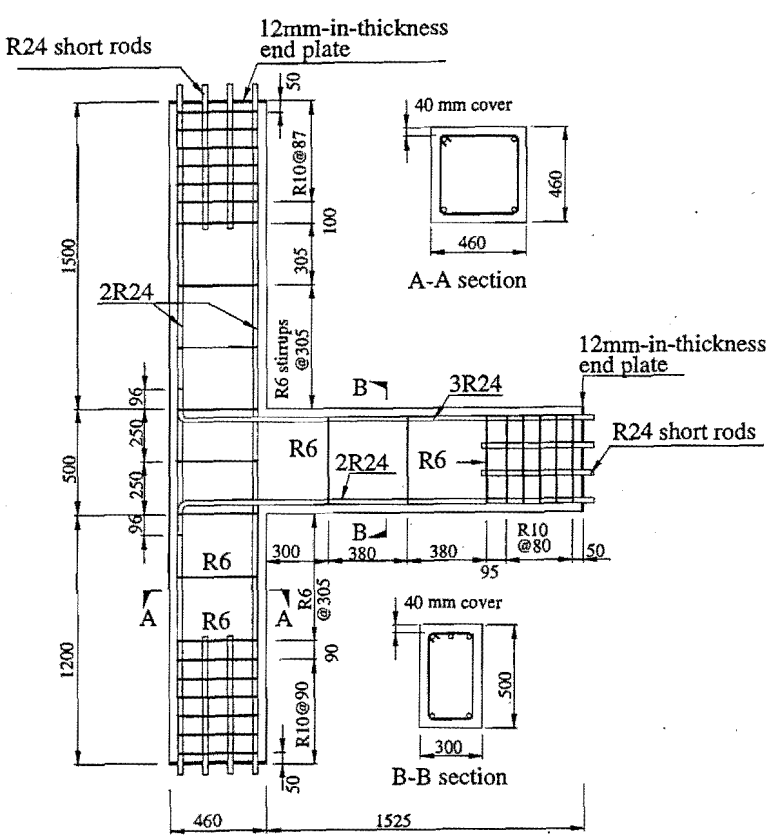

(a) Units EJ1 and EJ3 with Beam Bar Hooks Bent Away from Joint

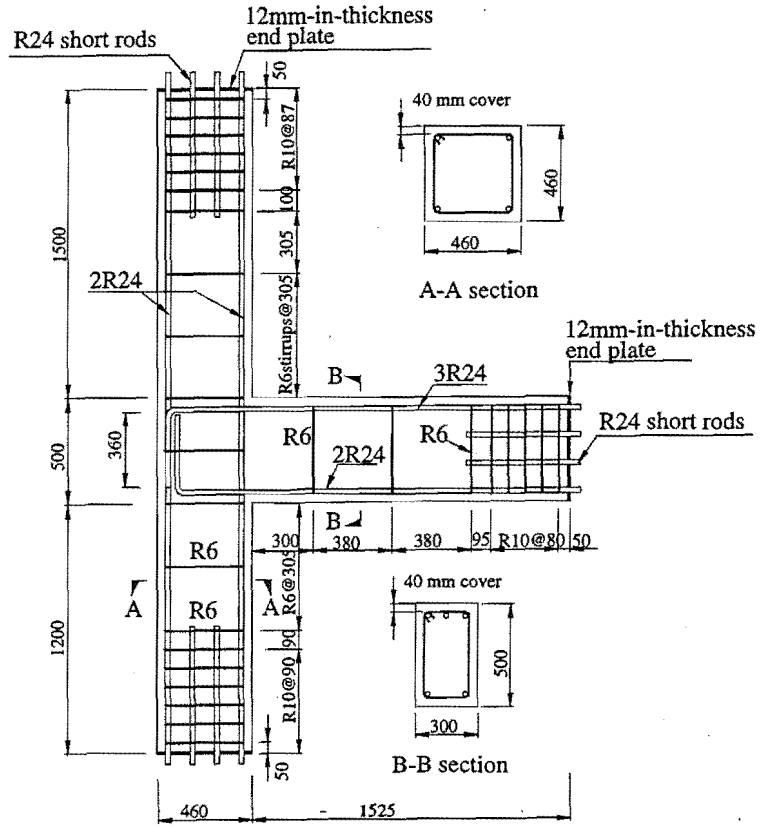

(b) Units EJ2 and EJ4 with Beam Bar Hooks Bent into Joint

Fig. 4.2 Overall Dimensions and Reinforcing Details of Exterior Beam-Column Joint Units

4.3 SEISMIC ASSESSMENT OF AS-BUILT TEST UNITS

The probable seismic performance of the as-built test units were assessed theoretically. This assessment includes the identification of the critical failure mechanism, the calculation of the theoretical flexural strengths and the curvature ductility capacity of the members, the estimation of the probable shear strength capacity of beams, columns and beam-column joints. It also included the investigation of the anchorage details of longitudinal reinforcement especially within the beam-column joints. The details of the theoretical assessment of the as-built interior and exterior beam-column joint units can be seen in Appendix A.

4.3.1 Interior Beam-Column Joint Test Units

4.3.1.1 Theoretical Flexural Strengths

Table 4.5 Theoretical Flexural Strengths and Curvature Properties of Members

		Flexural strengths (kN-m)	Yield curvature ϕ_y (mm^{-1}) ($\times 10^{-6}$) +	Ultimate curvature ϕ_u (mm^{-1}) ($\times 10^{-5}$) +	Curvature ductility factor ϕ_u / ϕ_y +	$\frac{\sum M_{column}}{\sum M_{beam}}$
Unit 1	Beam negative	250	5.0	8.3	16	0.63
	Beam positive	129	4.4	10.3	23	
	Column *	108	8.6	10.6	12	
Unit 2	Beam negative	251	5.0	8.0	16	1.16
	Beam positive	129	4.4	10.8	25	
	Column **	198	10.7	6.4	6.0	

+ Calculated assuming no bond slip of longitudinal bars

* with zero axial column load present ** with axial column load present of $0.12 A_g f_c'$ (=800kN)

The flexural strengths of the beams and columns were calculated for the two interior beam-column joint units using the measured material strengths, assuming an extreme fibre concrete compressive strain of 0.003 and a rectangular compressive stress block as recommended by NZS3101: 1995 [N1] and a strength reduction factor ϕ of unity. The calculation was made on the basis of the assumption of perfect bond between steel and concrete. The curvatures at first yield and at ultimate for the beams and the columns were also calculated for both units assuming no bond slip of longitudinal bars using standard

theory [P1]. The ultimate curvature was calculated assuming that the ultimate compressive strain of the concrete was 0.004, which is a lower limit for the strain just before crushing and spalling of the compressed concrete. The theoretical flexural strengths, yield curvatures, ultimate curvatures and curvature ductility factors of the members are summarised in Table 4.5. From Table 4.5, it is evident that Unit 1 would develop plastic hinges in the columns and Unit 2 would develop plastic hinges in the beams during simulated seismic loading test. The storey shear at the theoretical flexural strengths of the critical members of the units was 80 kN for Unit 1 and 128 kN for Unit 2.

4.3.1.2 Investigation of Amount of Transverse Reinforcement

The investigation of the amount of transverse reinforcement in the members and the joints of existing reinforced concrete structures is of particular interest because out-dated seismic codes did not specify capacity design philosophy. The amount of transverse reinforcement according to NZS 3101: 1995 [N1] not only has to meet the requirement associated with the shear strength, but also has to meet the requirement associated with the confinement of the compressed concrete and prevention of the longitudinal bars from buckling.

In order to investigate the amount of transverse reinforcement associated with the shear strength, the imposed shear forces on the members and the joints during testing, which are associated with the above calculated theoretical flexural strengths of the units, are compared with the available shear strengths of the members and the joints in Table 4.6. The available shear strength of the plastic hinge regions were calculated using the methods of NZS3101: 1995 [N1] for structures designed for ductility, using the measured material strengths and assuming a strength reduction factor ϕ of unity. The shear strengths of the other regions were calculated using the non-seismic provisions of NZS3101: 1995. It is to be noted that NZS3101 does not give a method for calculating the shear strength of existing beam-column joints. The amount of transverse reinforcement needed to restrain the longitudinal bars against premature buckling in plastic hinge regions according to NZS 3101:1995 for structures designed for ductility are also compared with the actual quantities in Table 4.6. For the units, the column axial load ratios were low. Hence, the transverse reinforcement required to confine the compressed concrete of the columns was not as critical as that required for preventing the longitudinal bar buckling.

Table 4.6 Shear Forces Imposed and Shear Capacities of Beams, Columns, and Joints and Lateral Restraints of Longitudinal Bars

Parts of Units	Shear Requirement				Transverse Reinforcement for Lateral Restraint of Longitudinal Bars in Plastic Hinge Zones			
	Max. Imposed Shear Force (kN)		Shear Force Capacity (kN)		Required amount		Actual amount	
	Unit 1	Unit 2	Unit 1	Unit 2	Spacing (mm)	Area per set (mm^2)	Spacing (mm)	Area per set (mm^2)
beam	67	143	146 (204)	22 (70)	115	91	380	57
column	80	128	41 (134)	250 (358)	75	60	230	113
joint (H)	483	744	(268)	(550)	200	79	∞	0

Note: 1. (H) = horizontal direction

2. Maximum imposed shear forces and shear force capacities are calculated assuming that the plastic hinges formed in the columns of Unit 1 and in the beams of Unit 2; and the maximum imposed shear forces are calculated assuming that the Units reached their flexural strengths at the plastic hinges.
3. Shear force capacities shown without brackets are those calculated using the methods of NZS3101:1995 [N1] for ductile frames at the plastic hinges and for elastic behaviour elsewhere.
4. Shear force capacities shown with brackets are those calculated using the methods of Reference P6 assuming curvature ductility factor greater than 10 at the plastic hinges and elastic behaviour elsewhere. That is, the values of k used were:

   Unit 1 : For beams k = 0.2, columns k = 0.1 and joint k = 0.3
   Unit 2 : For beams k = 0.05, columns k = 0.29 and joint k = 0.3

5. The nominal shear stresses at the theoretical flexural strength of the columns of Unit 1 was $0.10\sqrt{f_c'}$ in the columns and $0.073\sqrt{f_c'}$ MPa in the beams;

   The nominal shear stresses at the theoretical flexural strength of the beams of Unit 2 was $0.15\sqrt{f_c'}$ in the columns and $0.15\sqrt{f_c'}$ MPa in the beams.

6. The nominal horizontal joint shear stresses at the theoretical flexural strength of the columns of Unit 1 was $0.5\sqrt{f_c'}$ MPa, and that at the theoretical flexural strength of the beams of Unit 2 was $0.8\sqrt{f_c'}$ MPa.

From Table 4.6, it is apparent that, for both units, both the spacing and the diameter of the beam and column transverse reinforcement in the plastic hinge regions met neither the requirement of NZS3101: 1995 [N1] for shear strength nor the requirements for the prevention of longitudinal bar buckling for structures designed for ductility.

Also shown in brackets are the shear force capacities of the beams, columns and beam-column joints calculated using the method recommended by Park [P6]. It is evident that the shear force capacities calculated using the methods proposed by Park are greater than those calculated using the methods of NZS3101: 1995 [N1]. For the two interior beam-column joint units, the shear force capacities calculated using the method recommended by Park [P6] were adequate except for the beams of Unit 2 and the beam-column joints of the units.

4.3.1.3 Anchorage Development of the Longitudinal Reinforcement

The development length of longitudinal reinforcing bars within the joint region is of concern, especially when plain round longitudinal reinforcement is used. The ratio of column depth to beam bar diameter, for both beam-interior column joint units, was $\frac{h_c}{d_b}$=12.5. According to NZS3101: 1995 [N1], the ratio of column depth to beam bar diameter when deformed longitudinal bars are used should not be less than 14.7 for Unit 1 assuming that plastic hinges form in the columns and 17.4 for Unit 2 assuming that plastic hinges form in the beams. The use of plain round longitudinal bars would require at least twice this needed development length, and on this approximate basis the ratio of column depth to beam bar diameter should not have been less than at least 30 for Unit 1 and 35 for Unit 2. Therefore, the available development length of the plain round beam bars was quite inadequate.

NZS3101: 1995 also has a requirement for the development length of column longitudinal reinforcing bars within the joint region. The ratio of the beam depth to the column bar diameter for both interior beam-column joint units was 20.8. According to NZS3101: 1995, for ductile frames, the ratio of beam depth to column bar diameter, when deformed longitudinal bars are used, should not be less than 15.1 for Unit 1 assuming that plastic hinges form in the columns and 11.5 for Unit 2 assuming that plastic hinges form in the beams. As before, the use of plain round longitudinal bars would require at least twice this needed development length, and this means that the ratio of beam depth to column bar

diameter should not have been less than at least 30 for Unit 1 and 23 for Unit 2. Again, the available development length of the plain round column bars was inadequate.

Hence significant bond degradation, resulting in slip along the longitudinal bars, would be expected within the beam-column joint region of both units. Bond deterioration along the longitudinal reinforcement within the joint region may reduce the flexural strength and stiffness of the linear members and reduce ductility capacity of the whole building, but it may improve the shear strength of the joint core due to easier actuation of the joint concrete strut mechanism. The investigation into the joint performance is of particular importance because the beam-column joint cores of the as-built reinforced concrete structure were identified to be very critical in shear by the analysis of the whole structure.

4.3.1.4 Discussion of the Seismic Assessment

The seismic assessment of the two as-built interior beam-column joint units identified three design deficiencies for Units 1 and 2.

(1). The amount of transverse reinforcement in the plastic hinge regions was not adequate for the prevention of the longitudinal bar buckling, according to current seismic code NZS3101: 1995.

(2). The shear force resisting capacities in the beam-column joint cores of both units and in the beams of Unit 2 were inadequate.

(3). Significant bar slip within the beam-column joint regions along the longitudinal reinforcement would be expected. This was due to the combined effects of relatively small anchorage development lengths of the longitudinal reinforcement and the use of the plain round longitudinal bars.

However, it is to be noted that both the current seismic code NZS 3101: 1995 and the seismic assessment procedure proposed by Park [P6] are only applicable to the situations where the deformed longitudinal reinforcement was used, especially the procedure proposed by Park [P6], which was derived from limited experimental evidence obtained from beam-column joint assemblies reinforced by deformed longitudinal reinforcement. The predicted significant bar slip along the longitudinal reinforcement within the beam-column joint regions may improve the shear behaviour of the beam-column joint cores. This occurs due to the enhanced joint shear capacity resulting from the easier concrete

crack closing in the flexural compression side of the framing members. Also when plain round longitudinal reinforcement is used, the main shear resisting mechanism in linear reinforced concrete members becomes the robust concrete thrust, which is very different from the ones with deformed longitudinal bars, so the beams of Unit 2 may be not critical in shear.

As a result, the most critical design aspects of the units became large fixed-end rotations, due to severe bond degradation and slip along the longitudinal reinforcement within the joint core and/or inadequate transverse reinforcement required for preventing the longitudinal bar buckling and confining the compressed concrete, especially for preventing the longitudinal bar buckling in this case with relatively low level of column axial load.

4.3.2 Exterior Beam-Column Joint Test Units

4.3.2.1 Theoretical Flexural Strengths

As for the case of the interior beam-column joint units, the flexural strengths curvatures at first yield and at ultimate of the beams and columns of the four exterior beam-column joint units were calculated assuming no bond degradation and using the measured material strengths, a rectangular compressive stress block as recommended by NZS3101: 1995 [N1] and a strength reduction factor ϕ of unity. Again the ultimate compression strain of the concrete was assumed to be 0.004 in calculating the ultimate curvature and 0.003 in calculating the flexural strengths of the members. The detailed investigation of the amount of transverse reinforcement in the members can be found in Appendix A. The theoretical flexural strengths, yield curvatures, ultimate curvatures and curvature ductility factors of the members are summarised in Table 4.7 for the four units. From Table 4.7, it is evident that all the four units would develop plastic hinges in the beams during simulated seismic load testing. The strengths of the test units in terms of storey shears at the theoretical flexural strength of the critical member, the beam, of Units EJ1, EJ2, EJ3 and EJ4 were about the same, being about 67 kN when governed by the beam negative flexural strength, and 45 kN when governed by the beam positive flexural strength. This was because the variation of concrete compressive strength has only a small effect on the flexural strengths of members, as described by Brunsdon and Priestley in 1975 [B1], and the yield strength of the longitudinal reinforcement dominates the flexural strength of the members. The

longitudinal reinforcement steel used in Units EJ1, EJ2, EJ3 and EJ4 was from the same steel batch and was of the same steel property.

Table 4.7 Theoretical flexural strengths and curvature properties of members for exterior beam-Column Joints EJ1, EJ2, EJ3 and EJ4

Unit	Component of the Unit	Flexural strength of members (kN-m)	ϕ_y (mm^{-1}) $(\times 10^{-6})$	ϕ_u (mm^{-1}) $(\times 10^{-5})$	μ_ϕ $(=\frac{\phi_u}{\phi_y})$	$\frac{\sum M_{column}}{M_{beam}}$
EJ1	beam	129 (+) 190 (-)	4.5 (+) 4.9 (-)	9.9 (+) 8.6 (-)	22 (+) 18 (-)	2.07 (+)
	Column*	120	4.8	11.3	24	1.40 (-)
EJ2	beam	128 (+) 189 (-)	4.6 (+) 5.0 (-)	9.8 (+) 8.2 (-)	21 (+) 16 (-)	2.07 (+)
	column*	119	4.9	10.9	22	1.40 (-)
EJ3	beam	129 (+) 190 (-)	4.5 (+) 4.9 (-)	10 (+) 8.7 (-)	22 (+) 18 (-)	6.76 (+)
	column**	392	7.9	2.4	3	4.59 (-)
EJ4	Beam	129 (+) 190 (-)	4.5 (+) 4.9 (-)	10 (+) 8.7 (-)	22 (+) 18 (-)	6.90 (+)
	column***	400	7.7	2.5	3	4.68 (-)

\+ beam positive bending direction
\- beam negative bending direction
* with zero axial column load present
** with axial column load present of 0.25 $f_c' A_g$
*** with axial column load present of 0.23 $f_c' A_g$

4.3.2.2 Investigation of Amount of Transverse Reinforcement

Similar to the case for the interior beam-column joint units, the amount of transverse reinforcement in the members and the joints is also investigated for the four exterior beam-column joint units, and details can be seen in Appendix A.

The imposed shear forces on the members, which are associated with the above-calculated theoretical flexural strengths of the units, are compared with the available shear strengths of the members in Table 4.8. The available shear strengths of the members are calculated using the measured material strengths and assuming a strength reduction factor ϕ of unity.

Table 4.8 Shear, concrete confinement and anti-buckling

	Part of Units	Maximum Imposed Shear (kN)				Shear Force Capacity (kN)			
		EJ1	EJ2	EJ3	EJ4	EJ1	EJ2	EJ3	EJ4
Shear strength requirement	beams	113	113	113	113	22 (62)	22 (59)	22 (62)	22 (63)
	columns	67.5	67.2	67.5	67.5	156 (325)	147 (304)	255 (512)	257 (528)
	joint (H)	368	368	368	368	(141)	(361)	(505)	(933)

Concrete confinement and anti-buckling	Part of Units	Required Amount		Actual Amount	
		Spacing (mm)	Area (mm^2)	Spacing (mm)	Area (mm^2)
	beam	115	68	380	56.6
	columns	153	43	305	56.6
	joint (H)	200	79	250	56.6

1. H means horizontal joint shear.
2. The imposed horizontal shear force on the joint at the attainment of the theoretical strength of the units would result in a nominal horizontal joint shear stress $v_{jh} = V_{jh} / A_j$ of $0.05 f_c'$ MPa, $0.06 f_c'$ MPa, $0.05 f_c'$ MPa and $0.05 f_c'$ MPa, for Units EJ1, EJ2, EJ3 and EJ4, respectively. These v_{jh} values are also equivalent to $0.3\sqrt{f_c'}$ MPa, $0.3\sqrt{f_c'}$ MPa, $0.3\sqrt{f_c'}$ MPa and $0.3\sqrt{f_c'}$ MPa, for Units EJ1, EJ2, EJ3 and EJ4, respectively.
3. The maximum nominal shear stresses in the beams of all the Units at the negative flexural strengths of the beams were 0.82MPa, being $0.14\sqrt{f_c'}$ MPa for EJ1, $0.15\sqrt{f_c'}$ MPa for EJ2, $0.14\sqrt{f_c'}$ MPa for EJ3 and $0.14\sqrt{f_c'}$ MPa for EJ4.
4. The maximum nominal shear stresses in the columns were 0.35MPa, being $0.06\sqrt{f_c'}$ MPa for Units EJ1, EJ2, EJ3 and EJ4.
6. The values with brackets are the estimated shear force capacities using the seismic assessment proposed in Reference P6, and the values without brackets are the estimated shear force capacities using current code method of NZS3101: 1995.

The available shear force strengths of the beams were calculated using the method of NZS3101: 1995 for structures designed for ductility because the beams of all the four tests were expected to form plastic hinges, and the available shear force strengths of the

columns were calculated using the non-seismic provisions of NZS3101: 1995, since they were not expected to develop plastic hinges. In addition, the available shear strengths of the members were also calculated using the seismic assessment procedures suggested by Park [P6], and the values are shown in brackets in Table 4.8. Table 4.8 shows that the shear force capacities of the members estimated using the method of current code NZS3101: 1995 are very conservative, compared to those estimated using the seismic assessment procedures proposed by Park [P6]. It is apparent from Table 4.8 that, for all the four exterior beam-column joint units, the available beam shear force strengths were quite inadequate according to both the NZS3101 method and the seismic assessment procedure proposed by Park [P6]. The beam shear performance was hence expected to be very critical for all the four exterior beam-column joint tests.

The imposed shear forces on the joints during testing are calculated at the theoretical strengths of the units and are compared with the available joint shear strengths in Table 4.8 as well. The available shear strengths of the beam-column joints are estimated for the four exterior beam-column joint units only using the procedure proposed by Park [P6] because current code NZS3101 does not give a method for calculating the available shear force capacities of existing beam-column joints. Evidently, the available joint shear strengths estimated using the method proposed by Park [P6] are adequate except the joint shear capacity of Unit EJ1, which was tested with zero axial column load and had the beam longitudinal reinforcement bent away from the joint core.

Finally, the amount of transverse reinforcement needed for the confinement of the compressed concrete and for the prevention of the longitudinal bars from buckling by NZS3101: 1995 [N1] was also calculated and compared with the actual quantities in Table 4.8. The seismic assessment procedure proposed by Park [P6] gives no method for assessing the required amount of transverse reinforcement for preventing the longitudinal bar buckling and confining the compressed concrete. Table 4.8 illustrates that neither the spacing nor the cross sectional area of the beam and column transverse reinforcement met the requirement of NZS3101: 1995 for confinement of the compressed concrete and for the prevention of longitudinal bar buckling. In this case, significant bar buckling might take place, especially when high axial column load is present. For the tests, the axial column load was low, the column transverse reinforcement is more needed for anti-buckling than for confining the compressed concrete.

Another issue of concern could be the distance between the first set of ties in the column and that within the joint core for column bars not restrained against buckling by beam. NZS3101: 1995 requires this distance not to be greater than 6 times the diameter of the column bar, namely, 124 mm. The actual distance was 305 mm, and this again indicates possible bar buckling of the outer column bars in the vicinity of the joint core.

4.3.2.3 Anchorage of Beam Longitudinal Reinforcement in Exterior Columns

The anchorage detail of the beam longitudinal bars in exterior column plays an important role in the transfer of the member forces across the joint core for exterior beam-column joint assemblies. NZS3101: 1995 requires the deformed beam longitudinal reinforcement to be bent into the joint core in exterior columns in order to engage the diagonal compression strut and hence to achieve the best force transmission path across the joint core, that is, corner to corner joint diagonal concrete compression strut. Apparently, the bending configuration of the beam longitudinal reinforcement in the exterior columns of Units EJ2 and EJ4 satisfied the current code requirement, but the used steel type did not satisfy the current code requirement. For Units EJ1 and EJ3, neither the used steel type of the longitudinal reinforcing bars nor the bending configuration of the beam longitudinal reinforcing bars in exterior columns met the requirements of the current seismic code NZS3101: 1995. As a result, two questions arise: one is how the member forces can be transferred across the joint cores of Units EJ1 and EJ3, and the other is how the use of the plain round bars affects the postulated joint shear force path for Unit EJ2 and Unit EJ4.

4.3.2.4 Discussion of the Seismic Assessment

In summary, the conducted seismic assessment of units EJ1, EJ2, EJ3 and EJ4 identified three critical issues.

(1). The beam transverse reinforcement was not adequate according to the requirement for shear resistance.

(2). The amount of transverse reinforcement in the beams and columns was inadequate for the prevention of buckling of the longitudinal reinforcement.

(3). The beam bar hook details of Unit EJ1 and Unit EJ3 did not provide the best force transfer across the joint cores and this is further aggravated by the use of the plain round longitudinal bars.

As stated in Section 4.3.1.4, severe bond degradation along the longitudinal reinforcement due to the use of plain bar reinforcement could cause the shear resisting mechanism in linear reinforced concrete members and the joint cores to be very different from the postulated ones with the deformed bar reinforcement. The current seismic design and assessment procedures were established on the basis of the experimental data with deformed bars. Hence, the shear performance of the beam-column joint core of Unit EJ1 and the shear performance of the beam of the units may be not critical.

Regarding the effects of the beam bar hook details in the exterior columns and the use of the plain round longitudinal bars, the joint shear resisting mechanisms of the exterior beam-column joints are examined in detail in Section 4.4 in order to facilitate the understanding of the possibility of actuating an alternative joint force path when the beam bar hooks were bent away from the joint cores and also to facilitate the understanding of the effect of the use of plain round longitudinal bars.

4.4 SHEAR RESISTING MECHANISMS OF THE EXTERIOR BEAM-COLUMN JOINTS

4.4.1 Joint Shear Mechanisms of Exterior Beam-Column Joints EJ2 and EJ4

In designing exterior beam-column joints according to NZS3101: 1995[N1], the deformed beam longitudinal bars are required to be bent into the joint cores in exterior columns and adequate joint shear reinforcement needs to be provided. The postulated joint shear resisting mechanisms in this case by NZS3101: 1995 are a corner to corner joint concrete strut mechanism and one joint truss mechanism as shown in Fig. 4.3 (a) and 4.3(b).

As shown in Fig. 4.3, the resistance to the postulated joint concrete strut D induces lateral concrete tensile stresses around the beam bar hooks. This tendency is further exacerbated by the forces transmitted by the beam bar hooks to the outer layer of column longitudinal reinforcement, resulting in possible premature concrete failure due to tension cracking induced by the beam bar hooks. If this does occur, the beam bar hooks will open, similar to that of 90° stirrups after concrete cover spalling occurs, as suggested by the dotted line in Fig. 4.3 (c).

For well-designed exterior beam-column joint assemblies, deformed beam bar hooks are bent into the joint core and adequate joint horizontal hoop reinforcement is provided in the region of the beam bar hooks. Part of the beam tension force is transmitted to the joint

core concrete by bond and resisted by the postulated joint truss mechanism shown in Fig. 4.3(b). Even if concrete tension cracking occurs along the beam bar hooks, adequate *joint horizontal shear reinforcement* can well restrain the opening action of the beam bar hooks, and an effective concrete strut mechanism can be activated within the joint core.

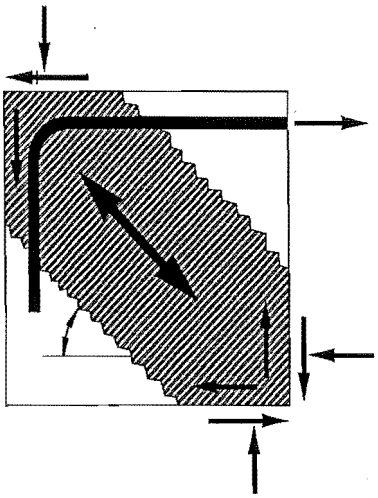

(a) Concrete Strut Mechanism

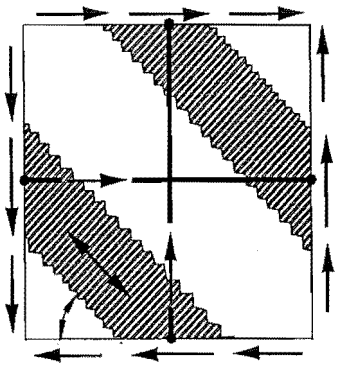

(b) Truss Mechanism

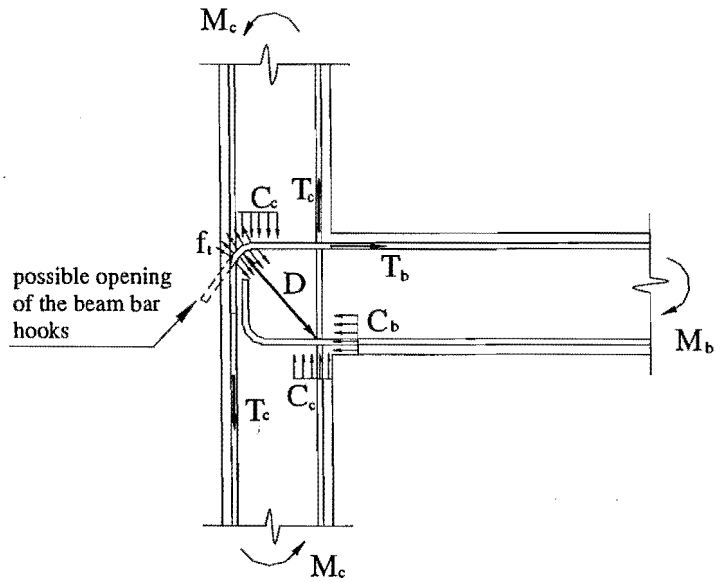

(c) Potential Straightening Action of the Beam Bar Hook

Fig.4.3 Shear Resisting Mechanism in Exterior Beam-Column Joints with the Beam Bar Hooks Bent into the Joint Core

The postulated joint concrete strut mechanism in Fig. 4.3(a) of exterior beam-column joint assemblies can only be actuated if the premature failure associated with the opening action of the beam bar hooks can be prevented.

For Units EJ2 or EJ4, typical design deficiencies were the use of plain bar reinforcement and very limited joint horizontal shear reinforcement present. Regarding the use of plain bar reinforcement, the resulting severe bond degradation and slip from the use of plain round bar reinforcement along the beam longitudinal bars within the joint core could increase the demand for transmitting the beam steel tension force at the bends of the beam longitudinal bars by the joint diagonal concrete strut, enhancing the possible premature concrete tension cracking failure initiated by the beam bar hooks and leading to increased demand for the joint horizontal shear reinforcement to prevent such a failure, compared to the case with deformed reinforcing bars. However the joint core of Units EJ2 or EJ4 contained only limited joint shear reinforcement and therefore premature failure associated with the opening action of the beam bar hooks could control the seismic performance of the system. As a consequence, the effectiveness of the joint concrete strut mechanism could diminish.

Evidently, the exterior beam-column joint assemblies reinforced by plain round longitudinal reinforcement and with the beam bar hooks bent into the joint cores, as was the case for Unit EJ2 or Unit EJ4, emphasise the need for joint horizontal shear reinforcement within the beam bar hooks.

4.4.2 An Alternative Joint Model for the Exterior Beam-Column Joints EJ1 and EJ3

As stated in section 4.3.2.2, for Units EJ1 or EJ3, neither the arrangement of the beam bar hooks in exterior column nor the plain round bars used satisfied the requirements of NZS3101: 1995. Apart from this, the amount of column transverse reinforcement was very inadequate according to NZS3101: 1995 requirements for anti-buckling, especially above and below the joint core.

When the beam longitudinal bars are bent out of the joint cores in exterior columns as for Units EJ1 or EJ3, the beam steel tensile force transfer within the bend has to be as illustrated in Fig. 4.4 (a). The resistance within the bend to the beam steel tension force could potentially cause the concrete tension cracking in the columns initiated by the beam bar hooks, and such concrete tension cracking could be further enhanced by column bar buckling above and below the joint core. If this does occur, the beam bar hooks will open

up as suggested in Fig. 4.4 (a). To restrain the opening of the beam bar hooks of Units EJ1 or EJ3 and to develop the concrete compressive struts, extensive *column transverse reinforcement immediately above and below the joint core* is required in the region of the beam bar hooks.

Due to the use of plain bar reinforcement for Units EJ1 and EJ3, severe bond degradation and bar slip would be expected along the longitudinal reinforcement. As a result, column bar buckling adjacent to the joint core along the outer layer of longitudinal column bars which are not restrained by the lateral beam would be enhanced. Also the beam steel tension forces at the column inner face would be mainly transmitted within the bend of the beam bars. Hence the possibility of the above described premature failure associated with the interaction of column bar buckling and the opening action of the beam bar hooks would increase, and the need for column transverse reinforcement above and below the joint core would further increase as well. However, the seismic performance of the whole system would be *independent of the amount of joint core shear reinforcement* in this case, contrary to Units EJ2 or EJ4.

For the exterior beam-column joint Units EJ1 or EJ3, column transverse reinforcement was sparse and the first set of column transverse reinforcement was far away from the beam faces. Column bar buckling, especially along the outer layer of the column longitudinal bars, above and below the joint core, would be unavoided. As a result, concrete cover spalling could take place in this region, enhancing the opening of the beam bar hooks and leading to the premature concrete cracking failure associated with the interaction of column bar buckling and the opening of the beam bar hooks.

However, an alternative force path with the beam bar hooks bent out of the joint cores in exterior columns could be developed should sufficient column transverse confinement be provided adjacent to but outside of the joint core [P9], as illustrated in Fig.4.4(b). Extensive column transverse confinement within the region of the beam bar hooks can not only control the above described premature concrete tension cracking failure, but also generate at the outer column face clamping forces which are necessary for the formation of the inclined concrete compression strut actions of D across the joint core and D_1 in the columns. It should be appreciated that sufficient column compressive area beyond the beam bar hooks would make the actuation of the alternative joint force path more comfortable, as shown in Fig.4.4(c). In this case, the effective force path for transmitting the member forces across the joint core is a steeper concrete strut D running

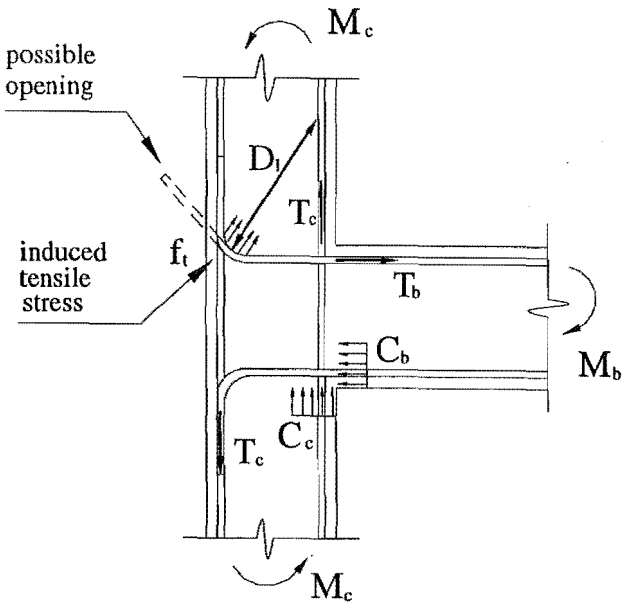

(a). Potential Straightening Action of the Beam Bar Hooks

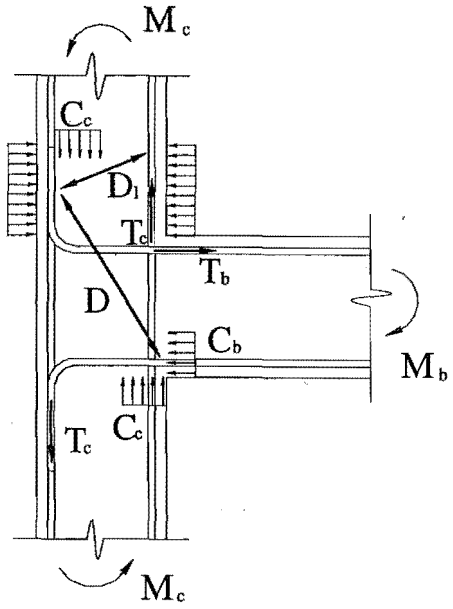

(b). An Alternative Force Path across the Joint Core

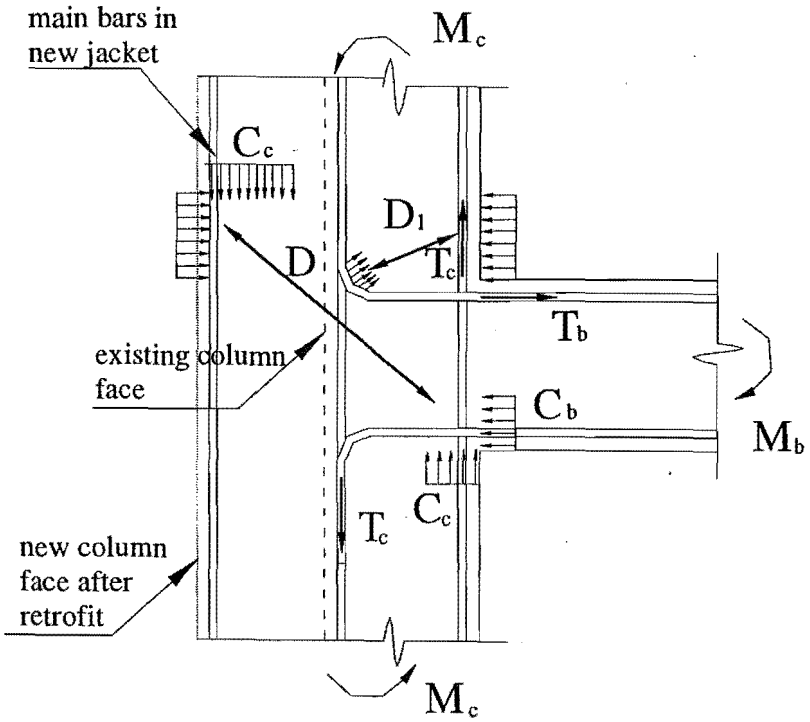

(c). the Alternative Joint Force Path after Increasing Column Depth

Fig.4.4 An Alternative Force Path across the Joint Cores of Units EJ1 and EJ3

from one joint corner to the midway of the confined column zone, rather than corner to corner joint diagonal strut. This is illustrated in Fig. 4.4 (b) and Fig.4.4(c). Actuation of the strut action, D_1, would lead to reduced column flexural strength, but the provided transverse confinement would significantly enhance the bond strength along the plain round column longitudinal bars, leading to the increase in the available column flexural strength.

4.5 RETROFIT SCHEME USED FOR UNIT REJ1

As explained in section 4.4.2, the fundamental element of retrofitting the exterior beam-column joint assemblies with the beam bar hooks bent away from the joint core is to provide extensive column transverse confinement above and below the joint core. The increase of the column depth would facilitate the actuation of the suggested alternative joint force path in Fig.4.4. Many retrofit methods can achieve this effect, for instance, external ordinary or prestressed reinforced concrete jacketing of the exterior columns, fibre-glass jacketing et al. Prestress reinforced concrete jacketing would give a much better effect of the retrofit.

In this research project, the postulation for achieving the alternative joint force path shown in Fig.4.4 was testified by conducting simulated seismic loading test on the retrofitted Unit REJ1, which was the damaged Unit EJ1 and retrofitted by external fibre-glass jacketing.

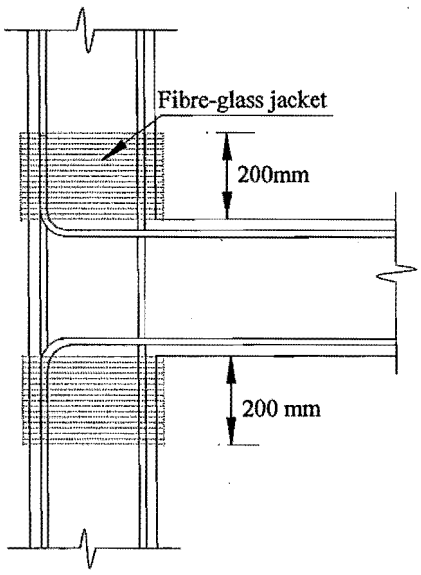

Fig.4.5 Retrofit Scheme Using Fibre-Glass Jacketing

Table 4.9 Properties of fibre-glass

Ultimate tensile strength	400 MPa
Design tensile strength	100 MPa
Elastic Modulus	20000 MPa
Cross sectional area per wrap	508 mm^2

A fibre-glass jacket of eight layers, which gave a cross sectional area per wrap of 508 mm^2, was used to wrap the column areas of 200 mm immediately above and below the joint core of the damaged Unit EJ1 (see Fig.4.5). The Unit then became Unit REJ1. The material properties of fibre-glass are shown in Table 4.9. Resin injection was used before the fibre-glass jacketing in order to enhance the damaged bond strength and to repair the cracked regions.

4.6 EFFECT OF AXIAL COLUMN LOAD

Should compressive axial load be present in the column, as for the tests on Units EJ3 and EJ4, the depths of column flexural compression zones will increase, leading to enhanced concrete strut capacity and also leading to enhanced force transmission of the beam steel tensile forces to the concrete by bond within the joint core. Due to enhanced force transmission from the beam tension steel to the concrete by bond, the portion of the beam steel tensile forces to be transmitted at the bend in the form of the resistance to D_1 reduces and the possibility of the premature failure caused by interaction of column bar buckling and the opening action of the beam bar hooks diminishes as well. At some stage when the axial column load is large enough, the concrete cracking initiated by the beam bar hooks may be totally avoided. In this case, retrofit using external passive confinement method in the column areas above and below the joint core will not make any difference in the seismic behaviour, compared with the seismic behaviour of the as-built units. However, the beneficial effect of column compressive axial load is not limitless. When the column axial load is large, the compressive strength of joint concrete compressive strut will govern the performance of the system.

4.7 CONCLUSIONS

In this chapter, the overall dimensions and the reinforcing details of all the test units involved in this study were described. Possible seismic performance of the as-built beam-column joint test units was assessed according to the code method and the capacity design based seismic assessment approach. In addition, the force transfer path across the joint core in as-built exterior beam-column joint subassemblages was examined and the alternative force path to transfer the steel force across the joint core of the exterior beam-column joint unit with the beam bar hooks bent away from the joint core was postulated.

Based on that, the retrofit method for the as-built exterior beam-column joint with the beam bar hooks bent away from the joint core was proposed.

The current project involved two as-built full-scale interior beam-column joint units, four as-built exterior beam-column joint units and one retrofitted as-built exterior beam-column joint unit. As-built beam-column joint units contained plain round longitudinal reinforcement and represented an existing reinforced concrete frame structure constructed in the later 1950s in New Zealand. Two as-built interior beam-column joint units were identical but tested under simulated seismic loading with different column axial load. The four as-built exterior beam-column joint units were identical except the beam bar hook details in the exterior columns and the four units were tested under simulated seismic loading with different column axial load.

1. Seismic assessment conducted for the as-built interior beam-column joint units led to the following conclusions:

(a). According to the New Zealand code NZS3101: 1995, the available shear force capacity in the columns was 51% of the shear demands at developing the theoretical strength of the unit, when the unit was tested with zero column axial load, and the available shear force strength of the beams was only 15% of the shear demands at developing the theoretical strength of the unit, when the unit was tested with the column compressive axial load of $0.12A_gf_c'$ present.

(b). The shear force capacities in the joint according to the seismic assessment method proposed by Park was respectively 55% and 74% of the shear demands for the case with zero column axial load and for the case with the column compressive axial load of $0.12A_gf_c'$ present.

(c). The diameters of the plain round longitudinal bars passing through the joint core were larger than the code permitted value, and severe bond degradation would be expected within the joint region.

(d). The transverse reinforcement in the beams and columns were very inadequate, according to the code requirements for anti-buckling and concrete confinement.

2. Seismic assessment conducted for the as-built exterior beam-column joint units led to the following conclusions:

(a). The beam and column transverse reinforcement was inadequate for all the as-built exterior beam-column joint units, according to the requirement for preventing the longitudinal reinforcement from buckling and confining the compressed concrete, and/or the requirement for providing the shear force strengths. For all the as-built exterior beam-column joint units, the available beam shear force capacity was only 20% of the shear demand at developing the theoretical force strength of the unit, according to NZS3101: 1995.

(b). The shear force capacities of the as-built exterior beam-column joint cores were adequate except for the unit, which had the beam bar hooks bent away from the joint core and was tested with zero axial column load.

(c). The first set of column stirrups was not close enough to the beam face, according to NZS3101: 1995. As a result, column bar buckling would be expected adjacent to the joint core.

3. Examination of the force transfer across the exterior beam-column joint core led to the following conclusions:

(a). Due to the use of plain round longitudinal reinforcement and only small amount of column transverse reinforcement within the beam bar hook range, premature concrete tension cracking failure along the beam bar hooks could occur.

(b). Different beam bar hook details were expected to actuate different joint force transfer paths and therefore would emphasise the need for column transverse reinforcement at different locations. When the beam bar hooks are bent away from the joint core in the exterior columns, an alternative joint force path would be possible should sufficient column transverse confinement be available just above and below the joint core. Increase in the column depth, for instance, by external reinforced concrete jacketing of the exterior columns, would facilitate the actuation of the postulated alternative joint forced path.

CHAPTER 5

TESTS ON THE INTERIOR AND EXTERIOR BEAM-COLUMN JOINT UNITS

5.1 LOAD APPLICATION AND REACTION

Testing was carried out on the Structural Laboratory's Reinforced Concrete Strong Floor at the University of Canterbury. Each hold down point of the strong floor has a tensile capacity of 10 tonnes.

For the two identical interior beam-column joint units, Unit 1 was tested under simulated seismic loading with zero axial column load and Unit 2 was tested under simulated seismic loading with a constant axial column load of 800 kN, producing a column axial load ratio of 0.12 for Unit 2. The column axial load ratio is calculated by $N^*/f_c^{'}A_g$, where N^* is the axial column compressive load; $f_c^{'}$ is the measured concrete compressive cylinder strength; and A_g is the column gross cross-sectional area.

For the exterior beam-column joint units, as-built Units EJ1 and EJ3 as well as the retrofitted Unit REJ1 were tested under simulated seismic loading with zero axial column load, and as-built Units EJ2 and EJ4 were tested under simulated seismic loading with a constant compressive axial column load N^* of 1800kN, which produced a column axial load ratio of 0.25 and 0.23 respectively for Unit EJ3 and Unit EJ4, based on the measured concrete compressive cylinder strengths

Independent loading rigs were designed to accommodate the simulated seismic loading and the constant compressive axial load on the top of the columns, respectively.

Seismic loading was simulated by applying vertical forces at the beam ends while the column ends were prevented from displacing horizontally by holding the columns in position using a horizontal strut to connect the top of column with the steel reaction frame (see Fig.5.1) in order to induce the desired moment reversed across the joint as sketched in Fig. 5.2. The ends of the beams and columns were free to rotate, and the ends of the beams were also free to move axially. For the tests on interior beam- column joint units, two independent hydraulic jacks were used to apply vertical forces at two beam-ends.

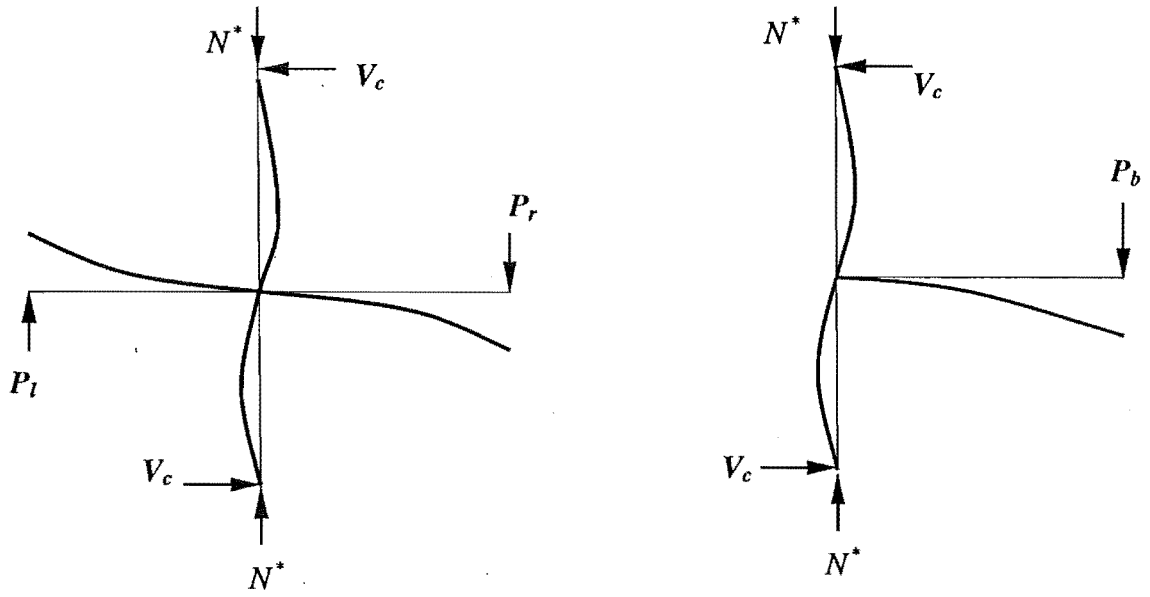

Fig. 5.1 Method of Loading Exterior Beam-Column Joints

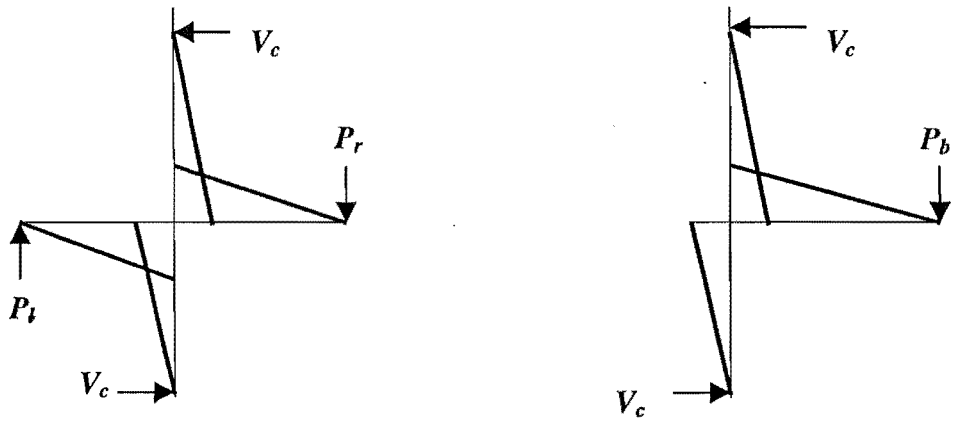

(a). Interior Beam-Column Joints (b) Exterior Beam-Column Joints

Fig. 5.2 Moment Reversed across the Joint Core during Earthquakes

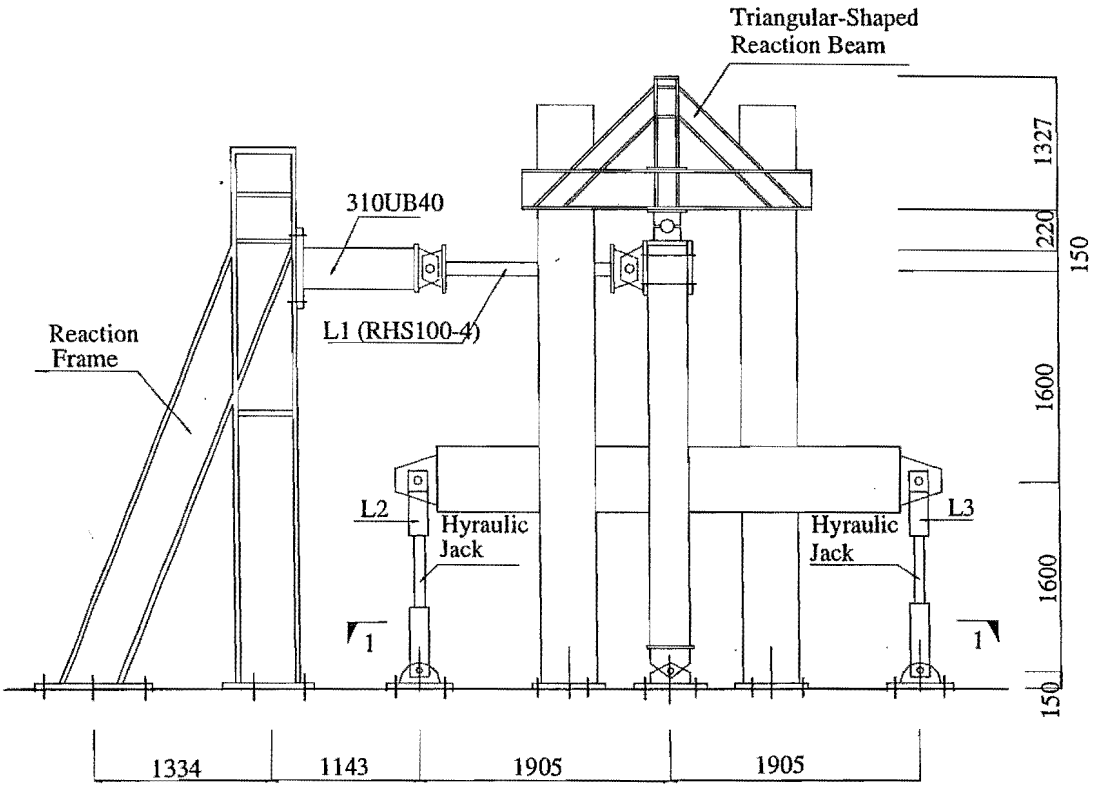

(a) Elevation

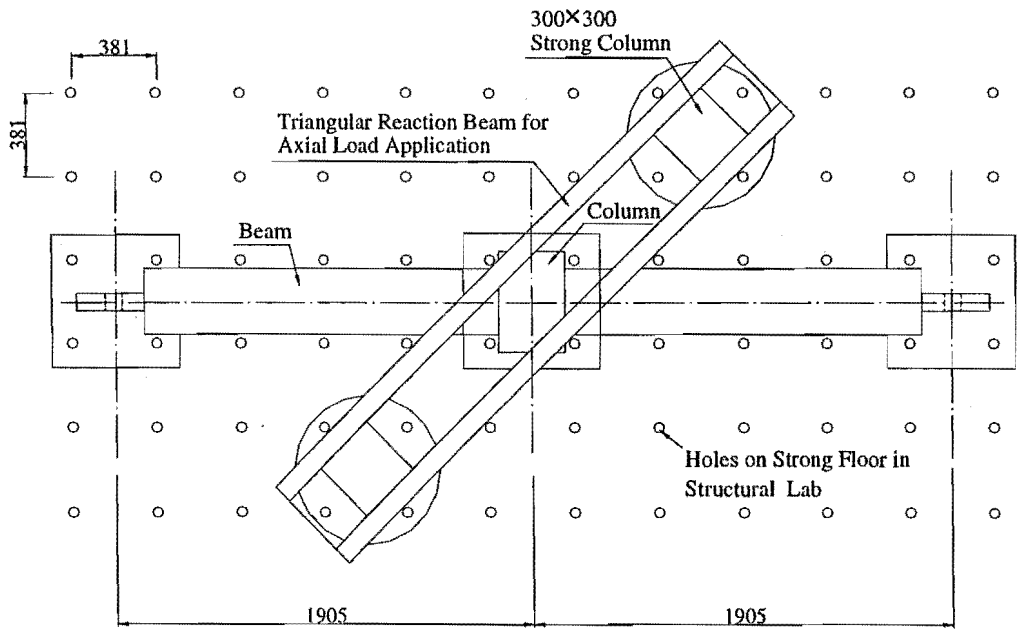

(b). Section 1-1 (Layout Plan)

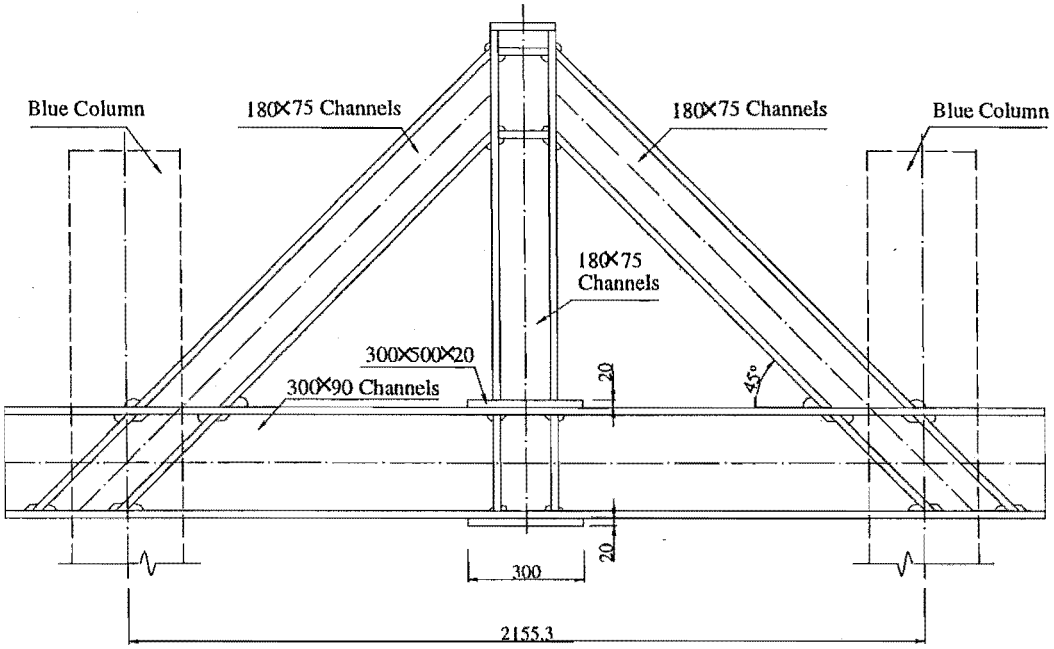

(c) Triangular-Shaped Reaction Beam

Fig.5.3 Overall Configuration of Loading Rigs for Testing Interior Beam-Column Joint Units

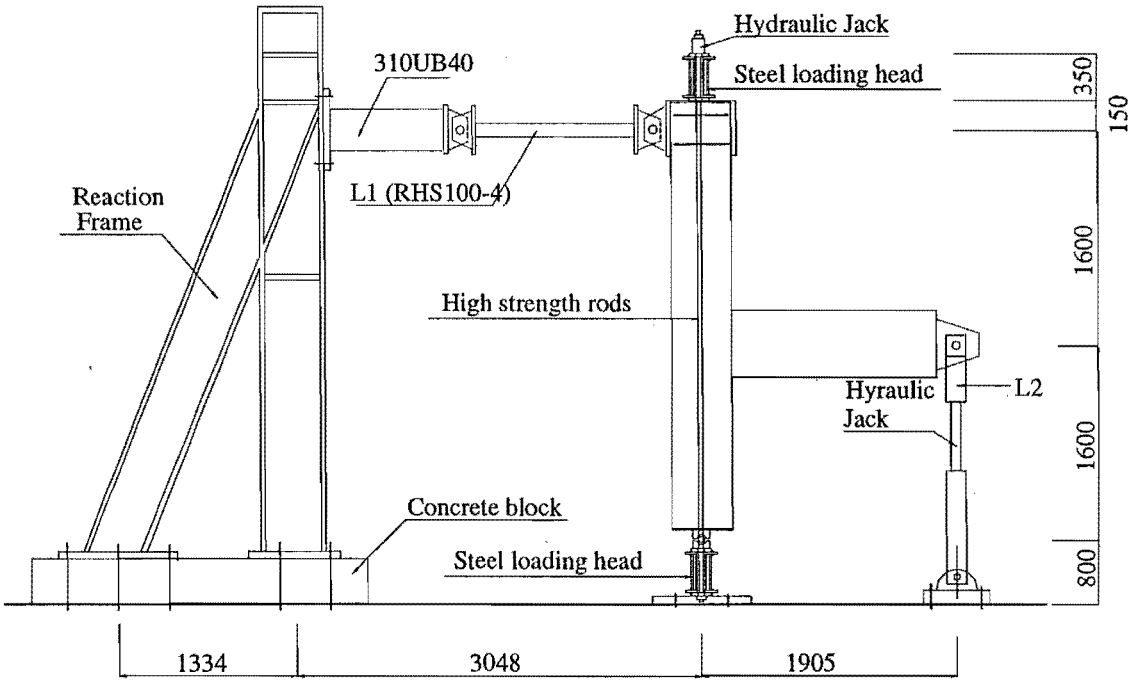

(a) Elevation

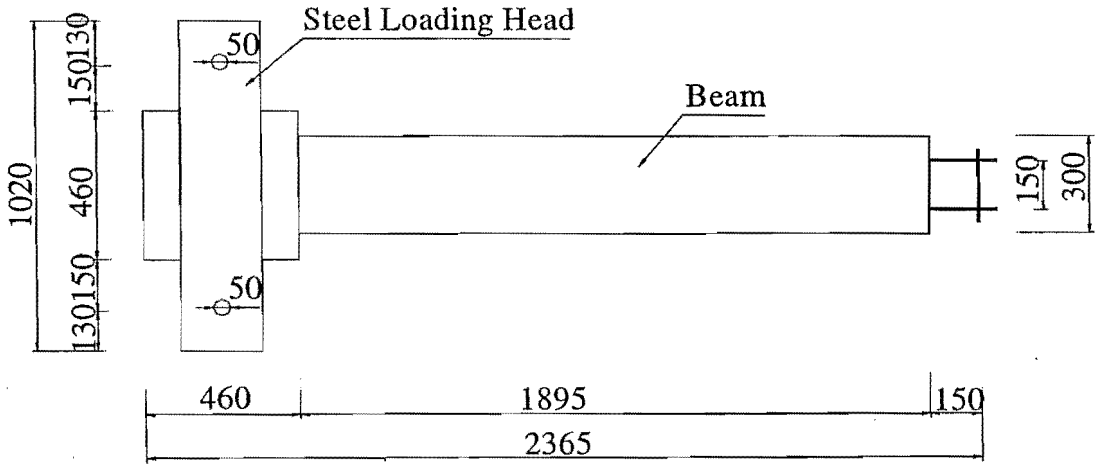

(b) Layout Plan

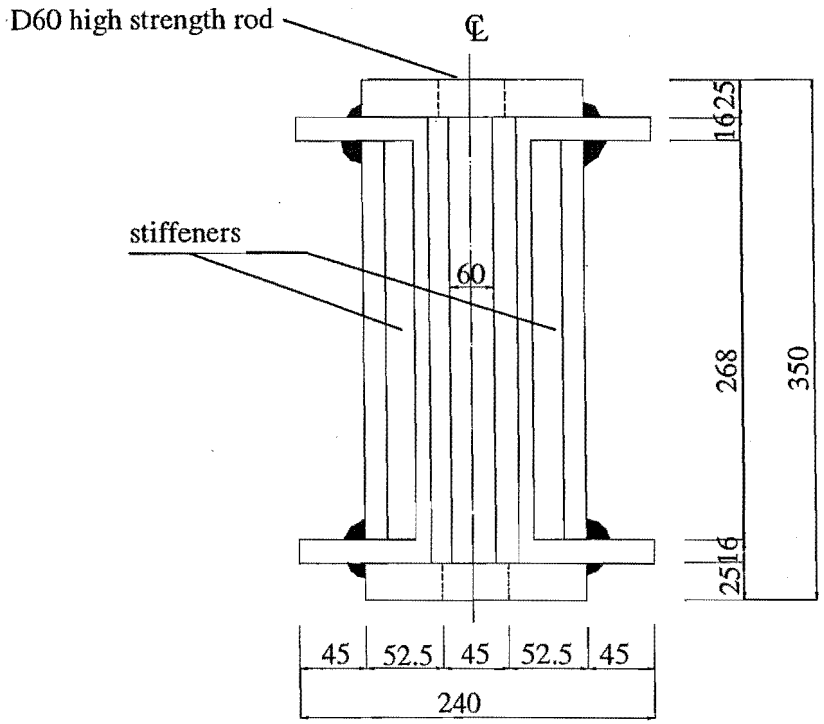

(c) Details of Steel Loading Heads (Steel Reaction Beams)

Fig. 5.4 Overall Configuration of Loading Rigs for Testing Exterior Beam-Column Joint Units EJ2, EJ2, EJ3 and EJ4

Vertical displacement of each beam end was maintained equal but opposite during displacement-controlled loading stages. For the tests on the exterior beam-column joint units, one hydraulic jack was used to apply a vertical force at the beam-end.

Apart from simulated seismic loading, a constant compressive axial load of 800 kN was applied to the column of Unit 2 by the axial loading rig which ran 45° to the lateral loading plane across the specimen and comprised of a triangular-shaped steel reaction beam and two strong steel reaction columns. Each of the two strong steel reaction columns in the axial loading rig was connected with the reinforced concrete strong floor by four high strength bolts to transmit the induced reaction forces to the strong floor. Maximum tensile capacity of each bolt in the strong floor is 10 tonnes, and it meant that the maximum tensile axial load capacity of each steel reaction column was 400 kN and hence that the maximum possible compressive axial load applied to the columns of Unit 2 was 800 kN. The specified concrete compressive cylinder strength was 30 MPa for Unit 2, and this meant a column axial load ratio of 0.2 for test of Unit 2. However, the measured concrete compressive cylinder strength at the time of testing Unit 2 was 48.9 MPa, and it was 60% higher than the specified concrete compressive strength. Hence the axial column load of 800 kN gave only an column axial load ratio of 0.12 for Unit 2. The overall configuration of the loading rigs for testing interior beam-column joint units is shown in Fig. 5.3, where both the simulated seismic loading rig and the axial loading rig were employed. When Unit 1 was tested, the axial loading rig was removed.

Similarly, a constant compressive axial load of 1800 kN was applied to the columns of Unit EJ3 and Unit EJ4 by a self-contained steel loading rig, which consisted of the top and bottom steel loading heads (reaction beams), hydraulic rams as well as two high strength tension rods. The measured concrete compressive cylinder strength at the time of testing was 34 MPa for Unit EJ3, and 36.5 MPa for Unit EJ4. Hence, the constant compressive axial column load of 1800 kN produced a column axial load ratio of 0.25 for test of Unit EJ3 and 0.23 for test of EJ4. The overall configuration of the loading rigs for testing exterior beam-column joint units is shown in Fig. 5.4, where both the simulated seismic loading rig and the axial loading rig were employed. When Units EJ1 and EJ2 and REJ1 were tested, axial loading rig was removed.

To accommodate the column end rotations and maintain a vertical axial column load during testing, a rock seat was used for test of Unit 2 between the top of the column and the bottom surface of the triangular reaction beam. Similarly, a rock seat was used for tests of EJ3 and EJ4 between the bottom of the column and the top surface of the bottom steel reaction beam of the axial loading rig.

5.2 INSTRUMENTATION

5.2.1 Measurement to Determine the Hysteresis Loops

A property that needs to be appreciated in the evaluation of structural seismic performance is the force-displacement hysteretic response. The force-displacement hysteretic response indicates the energy dissipation capacity of the structure by considering the area encompassed by the hysteresis loops. In this study, the beam end loads (beam shears) and the correspondent beam end displacements were measured. The storey shear and the storey displacement could be found by considering the equilibrium criteria and the geometry of the unit on the basis of the measured beam end forces and displacements as described in the following. Hence the measurements of the beam end load(s) and the corresponding beam end displacement(s) enables the acquisition of the hysteretic responses of both the individual beam and the whole test units. For the purpose of a check, the storey (column) shear force was also directly measured during testing for both the interior and the exterior beam-column joint tests.

5.2.1.1 Force Measurement

For each interior beam-column joint unit, three load cells were used to measure loads. Load cell L1 was used to measure storey (column) shear force, and Load cells L2 and L3 were used to measure beam end loads, as shown in Fig.5.3 (a).

For each exterior beam-column joint unit, two load cells were used to measure loads. Load cell L1 was used to measure storey (column) shear force, and load cell L2 was used to measure the beam end load, as shown in Fig.5.4 (a).

Load cell L1, which was used to measure the storey shear force, was made in this laboratory by placing 8 strain gauges on the horizontal strut in such a way that a full bridge

circuit was developed and the effects of flexure could be eliminated [H4]. Load cell L1 was calibrated in an Avery Universal Testing Machine.

The beam end load cells, L2 and L3, have built-in electrical circuits, giving a total resistance of 700 ohms. Each beam end load cell was connected in series with a hydraulic jack and had two outputs. One output of each beam end load cell was read directly using a strain indicator against which the load cell had been calibrated in an Avery Universal Testing Machine. Therefore it was possible to apply load during load-controlled stages by directly reading the load from the strain indicator. The other output of the beam end load cell was used to drive the Y-axis of the X-Y plotter. The X-axis of the X-Y plotter was driven by the signal from a linear potentiometer that measured the correspondent beam vertical displacement, see Section 5.2.1.2 below. Hence it was possible to obtain an instantaneous plot of beam end vertical force versus beam end lateral displacement for each beam.

5.2.1.2 Displacement Measurement

The displacement instrumentation for the interior and exterior beam-column joint tests is shown in Fig.5.5 and Fig.5.6 respectively. For all the tests on both interior and exterior beam-column joint units, two linear potentiometers of 300 mm travel were used to measure the vertical displacements at each beam end, and the linear potentiometer closer to the beam pin end was connected with the correspondent X-Y plotter to drive its X-axis. It was therefore possible for the X-Y plotter to give instantaneous plots of the beam-end lateral load versus beam-end displacement correspondingly. Meanwhile each linear potentiometer to drive the X-axis of X-Y plotter was also connected in parallel with a Digital Voltage Meter (DVM). Readings from the DVM manually gave immediately the value of the gross beam deflection, which was used to monitor the imposed beam end displacement in the displacement-controlled loading stages.

However, the recorded beam end load versus beam end displacement curves given by each of the X-Y plotters only served as a reference for monitoring the overall progress of the test unit, for the following reasons:

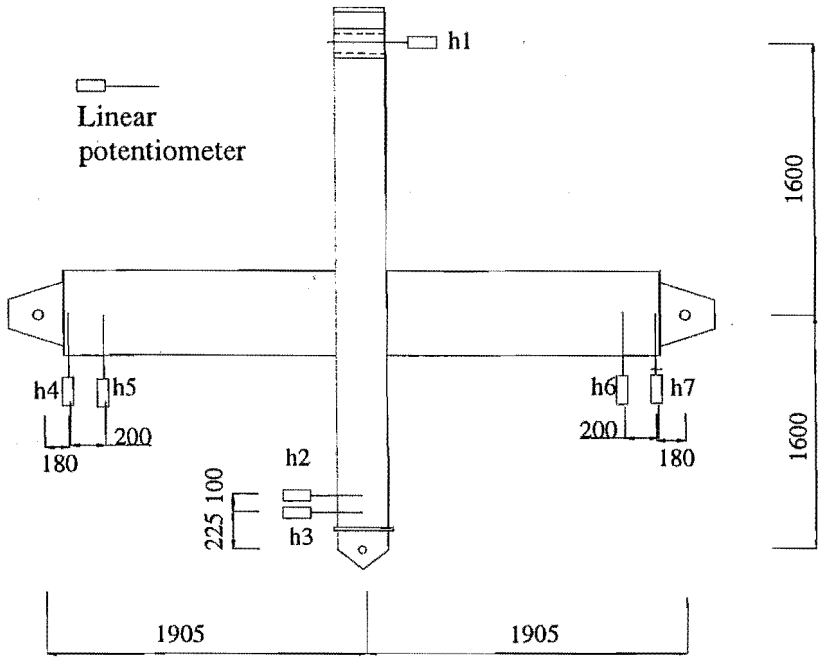

Fig.5.5 Displacement Measurement Method Using Linear Potentiometers for Interior Beam-Column Joint Unit 1 and Unit 2

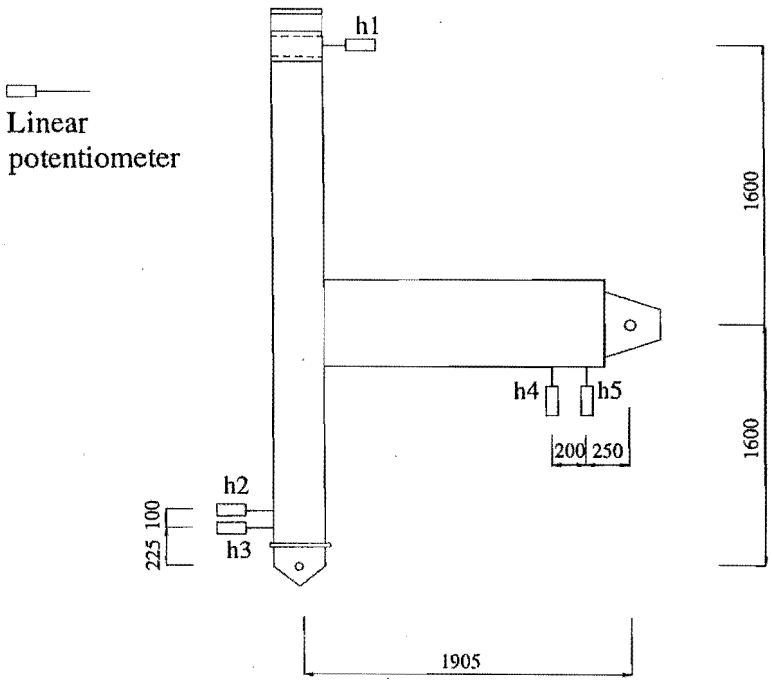

Fig.5.5 Displacement Measurement Method Using Linear Potentiometers for Exterior Beam-Column Joint Unit 1 and Unit 2

At first, the target positions for beam end displacement measurements are some distance away inward from the beam end pin positions, hence the measurements must be converted into beam end displacements at end pin positions by extrapolating. Also, the measured beam deflections included the components due to the sidesway of the seismic loading rig. The real displacement should be relative to the line joining the two column end-pins.

The horizontal movements of the beam-column joint assemblies referred as to be the sidesway of the seismic loading rig were detected by the linear potentiometers, h_1, h_2 and h_3 as shown in Fig.5.5 and Fig.5.6. The horizontal movement at the column top pin position was measured directly by potentiometer h_1, but the horizontal movement at the column bottom pin position was found by extrapolating the measurements of potentiometers h_2 and h_3. With the horizontal movements at the column top and bottom pin positions known, the movement of the centre of column top pin position relative to the centre of column bottom pin position, δ_{cr}, could be reasonably estimated by:

$$\delta_{cr} = (h_1 + h_3) + (h_3 - h_2) \times 225/100 \qquad (5.1)$$

The equivalent storey drift, Δ_{co}, and the equivalent storey shear force, V_c, can be found by considering the geometrical and equilibrium relationships of the frame, as shown in Fig. 5.7. According to the imposed vertical displacements and lateral forces at the beam ends, the equivalent storey displacements and storey (column) shear force can be found as follows:

The equivalent storey displacement is as follows:

$$\Delta_{co} = \left[\frac{\Delta_{bl} - \Delta_{br}}{l_b} \right] l_c \qquad \text{for interior beam-column joint tests} \quad (5.2)$$

$$\Delta_{co} = \frac{\Delta_b}{l_b} l_c \qquad \text{for exterior beam-column joint tests} \quad (5.2)'$$

The equivalent storey (column) shear force is

$$V_c = \frac{P_l l_1 - P_r l_2}{l_c} \qquad \text{for interior beam-column joint tests} \quad (5.3)$$

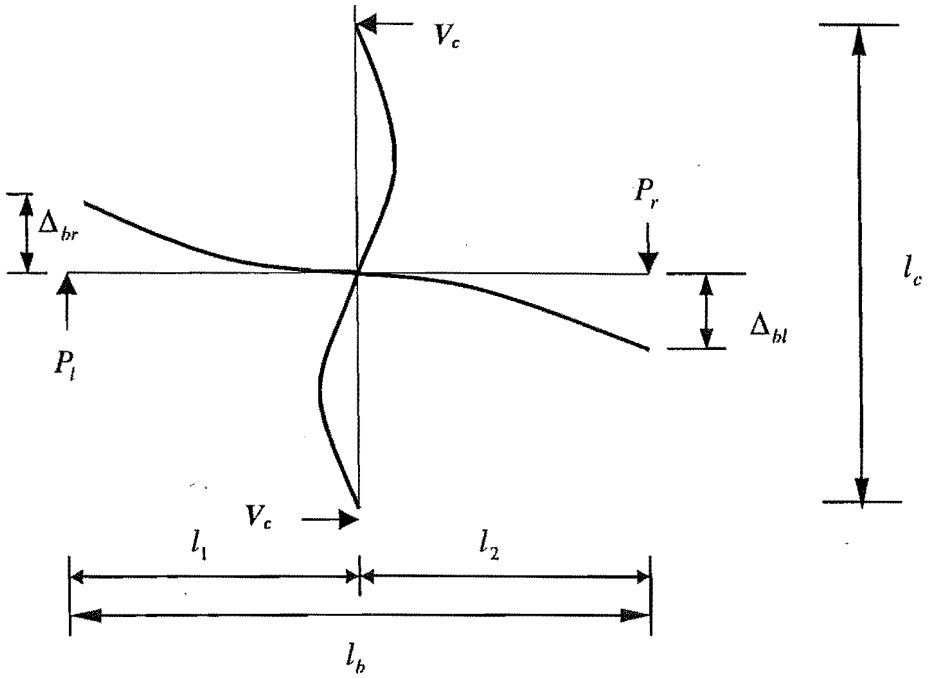

(a). Interior Beam-Column Joint Units

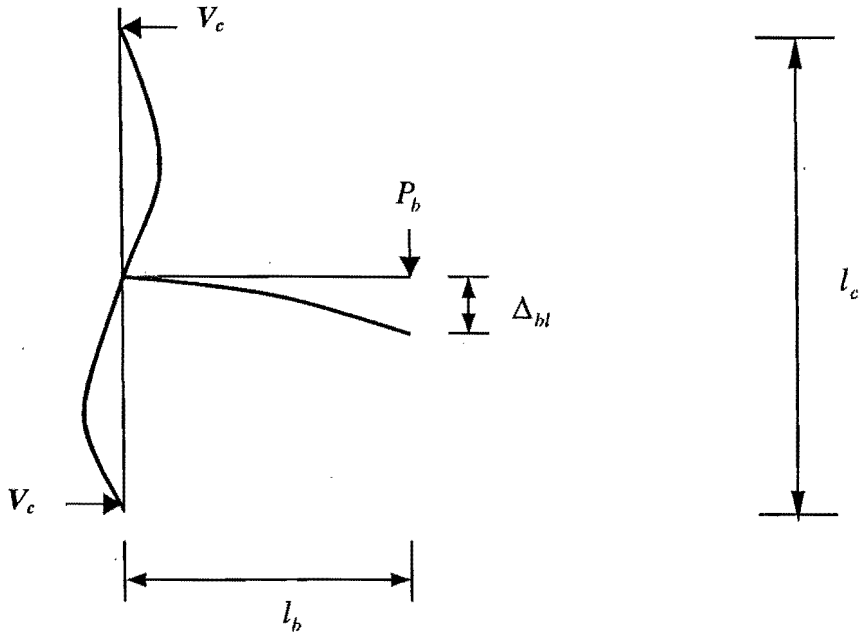

(b) Exterior Beam-Column Joint Units

Fig. 5.7 Determination of Equivalent Storey Shear and Storey Displacement

$$V_c = \frac{P_b l_b}{l_c}$$ for exterior beam-column joint tests (5.3)'

where :

l_c = the storey height, which is 3200 mm for all test units

l_b = the beam span, being 3810 mm for the interior beam-column joint unit and 1905 mm for the exterior beam-column joint unit

Δ_{bl} and Δ_{br} = the imposed vertical displacements at the pin ends of the left beam and the right beam, respectively (negative downwards) for the interior beam-column joint units

Δ_b = the imposed vertical displacements at the beam pin end for the exterior beam-column joint units.

l_1 and l_2 = the loading spans of the left beam and the right beam, respectively, being 1905 mm for both interior beam-column joint units.

P_r and P_l = the lateral shears applied to the right beam and left beam, respectively (negative downwards), for interior beam-column joint units.

P_b = the lateral load applied to the beam end for exterior beam-column joint units.

Δ_{co} = the equivalent storey drift

V_c = the equivalent storey shear force

Upward acting forces and displacements, as shown in Fig.5.7, which is causing the hogging beam moments, are taken positive, while downward loads and displacements, which is causing sagging beam moments, are taken negative.

The equivalent storey drift % is then given by Δ_{co} /32 for both interior beam-column joint tests and exterior beam-column joint tests.

The real storey displacements should be obtained by deducting the components due to the deformations within the loading rig, δ_{cr}. This was necessary for plotting storey shear versus storey drift curves because considerable horizontal movement of the test unit was caused by the sidesway of the steel reaction frame.

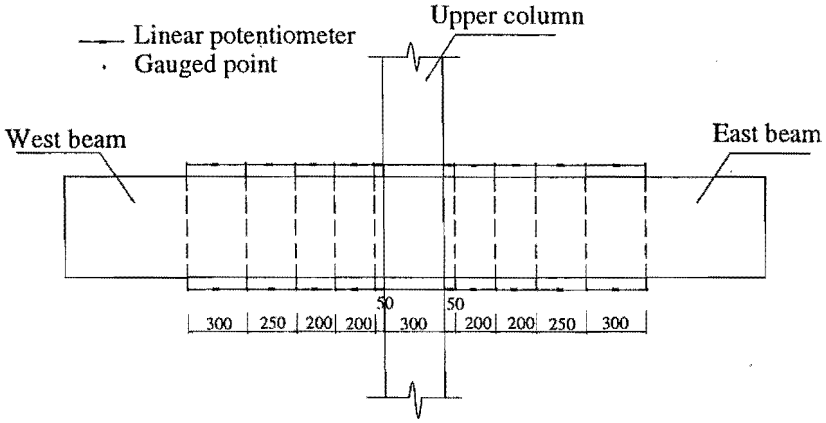

(a) Arrangement of Linear Potentiometers to Measure Beam Curvatures for Unit 1 & 2

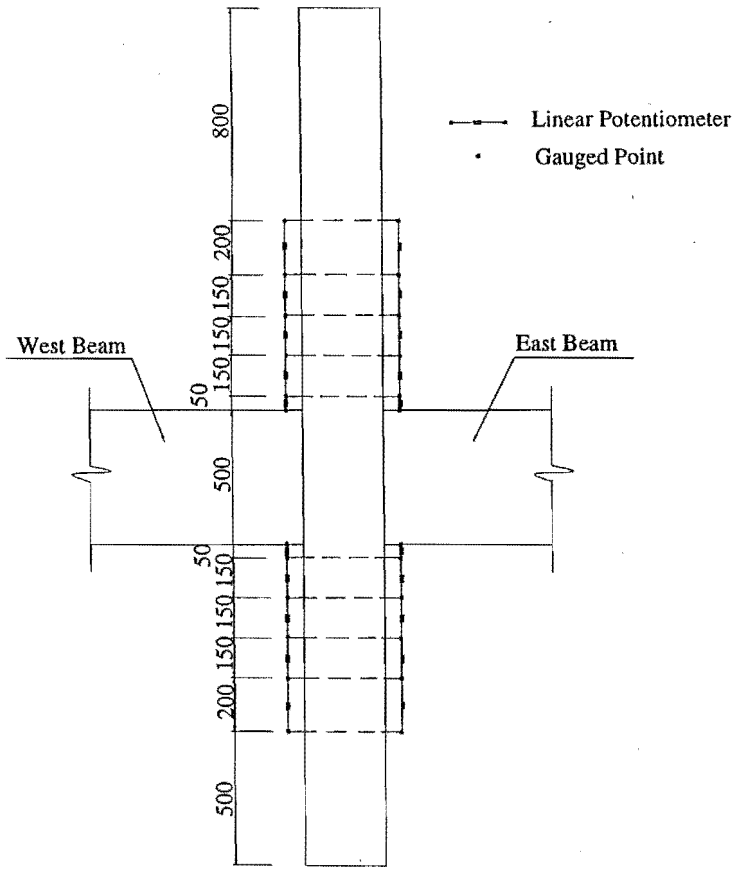

(b) Arrangement of Linear Potentiometers to Measure Column Curvatures for Units 1 and 2

Fig.5.8 Member Curvature Measurements for Interior Beam-Column Joint Units

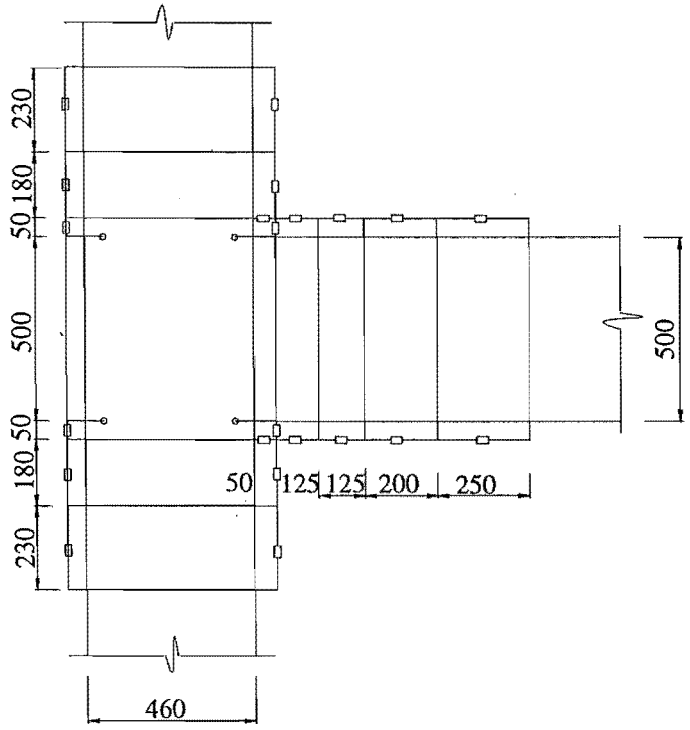

(a). for Test of EJ1

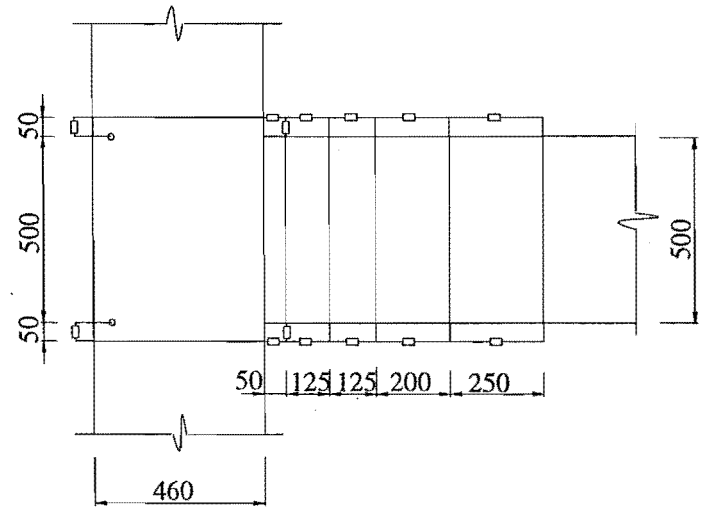

(b) for Tests of Unit EJ2, EJ3 and EJ4

Fig.5.9 Member Curvature Measurements for Exterior Beam-Column Joint Units

5.2.2 Force Measurement to Determine the Axial Load on Column

For the interior beam-column joint Unit 2, a compressive axial load of $0.12 A_g f_c'$ (= 800 kN) was applied to the column using a 100-tonne hydraulic jack and maintained constant during simulated seismic loading of that unit.

For the exterior beam-column joint Units EJ3 and EJ4, a compressive axial load of 1800 kN was applied to the column using two 100-tonne hydraulic jacks and maintained constant during simulated seismic loading of the units.

The maintenance of the constant column compressive axial load was monitored by a pressure gauge calibrated against a Universal Avery Testing Machine.

5.2.3 Measurement of Average Curvatures

A number of linear potentiometers of 30 mm or 50 mm travel were used to monitor member curvatures.

Each beam and each column employed several pairs of linear potentiometers in measuring the member curvatures within the gauged regions, and each pair of linear potentiometers were attached to the two ends of a steel rod embedded in the concrete. Fig. 5.8 (a) and Fig. 5.8(b) illustrate the arrangement of the curvature linear potentiometers for the beams and columns of the interior beam-column joint units, respectively. Fig.5.9 (a) and Fig.5.9 (b) illustrate the arrangement of the curvature linear potentiometers for test of Unit EJ1 and the other three exterior beam-column joint units, respectively. All steel rods were fixed into the mould using external steel brackets to hold them firm during concreting.

5.2.4 Measurement of Joint Shear Distortion and Joint Expansion

The average joint shear distortions and expansions were monitored by two diagonally placed linear potentiometers on the joint core as shown in Fig. 5.10.

The average joint shear distortion γ_j can be found by

$$\gamma_j = \gamma_1 + \gamma_2 = \frac{\delta_j - \delta_{j'}}{2l_j}(\tan\alpha_j + \frac{1}{\tan\alpha_j}) \qquad (5.4)$$

where δ_j and $\delta_{j'}$ are the changes in the lengths of the diagonals AB' and A'B respectively, l_j is the initial length of the diagonal in the joint core and α_j is the angle of the diagonal to the horizontal axis.

The joint core expansion index is defined as the average value of the length changes of the two diagonals, that is, $(\delta_j + \delta_{j'})/2$, because the joint expansion index so obtained is proportional to the increase in the volume of the joint core concrete. Evidently, the joint expansion index so obtained also can be used as an indicator of the joint core concrete failure.

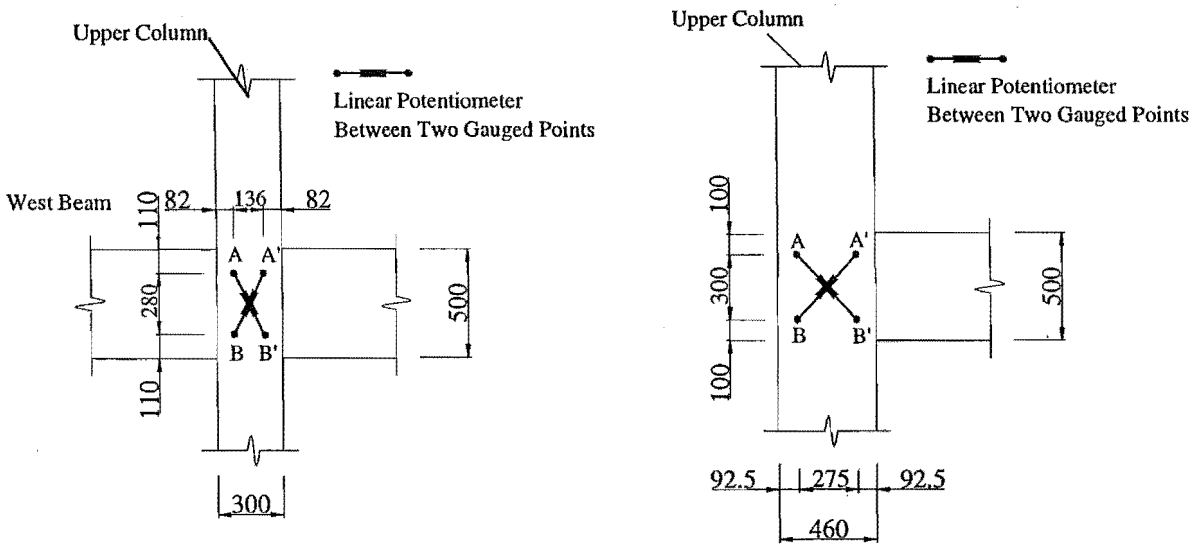

(a) Interior Beam-Column Joints (b) Exterior Beam-Column Joints

Fig.5.10 Estimation of Joint Shear Distortion

5.2.5 Measurement of Reinforcement Strains

Both electrical resistance strain gauges and linear potentiometers were used to measure reinforcement strains.

5.2.5.1 Measurements by Electrical Resistance Strain Gauges

The arrangement of electrical resistance strain gauges was exactly the same for the two interior beam-column joint units, and it is shown in Fig. 5.11. Eighty - six Showa 120-ohm electrical resistance strain gauges (Type N11 – FA – 120-11) were used to

monitor steel strain variations along the longitudinal and transverse reinforcement in the beams, columns and the joints of each unit.

The arrangement of electrical resistance strain gauges was also the same for the four exterior beam-column joint units, and it is shown in Fig.5.12. Fifty-three Showa 120-ohm electrical resistance strain gauges (Type N11-FA-120-11) were used for each Unit to monitor steel strain variation along the longitudinal and transverse reinforcement in the beams, columns and the joint.

The electrical resistance strain gauges were put on two opposite faces at the same location within the joint region because the steel strains in the joint core were to be carefully investigated, and the average values were taken as the real steel strains. Elsewhere only one gauge was placed at each location.

The distributions of electrical resistance strain gauges are summarised in Table 5.1 for the test units.

Table 5.1 Distribution of Electrical Resistance Strain Gauges for Unit 1 and Unit 2

Test Units	Components	No. of Strain gauges
Interior Beam-Column Joint Units 1 and 2	Beam longitudinal bars (R-24)	42
	Column longitudinal bars (R-24)	28
	Beam transverse steel (R-6)	4
	Column transverse steel (R-6)	12
	Total	86
Exterior Beam-Column Joint Units EJ1, EJ2 EJ3 and EJ4	Beam longitudinal bars (R-24)	22
	Column longitudinal bars (R-24)	24
	Beam transverse steel (R-6)	2
	Column transverse steel (R-6)	5
	Total	53

5.2.5.2 Linear Potentiometer Arrangement

One objective of using linear potentiometers to measure steel strains was to obtain the information on bar slip along the reinforcing bars within the joint core.

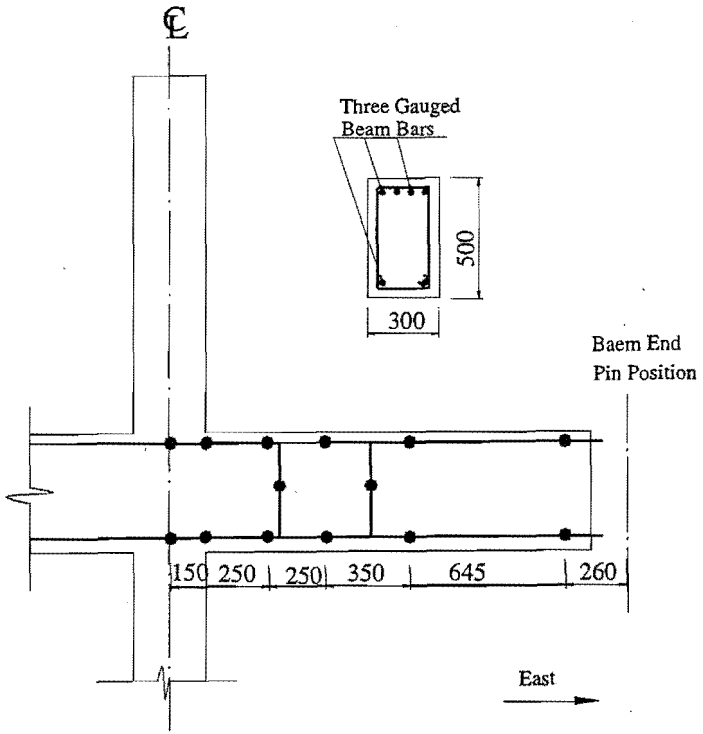

(a) Beam longitudinal and transverse reinforcement

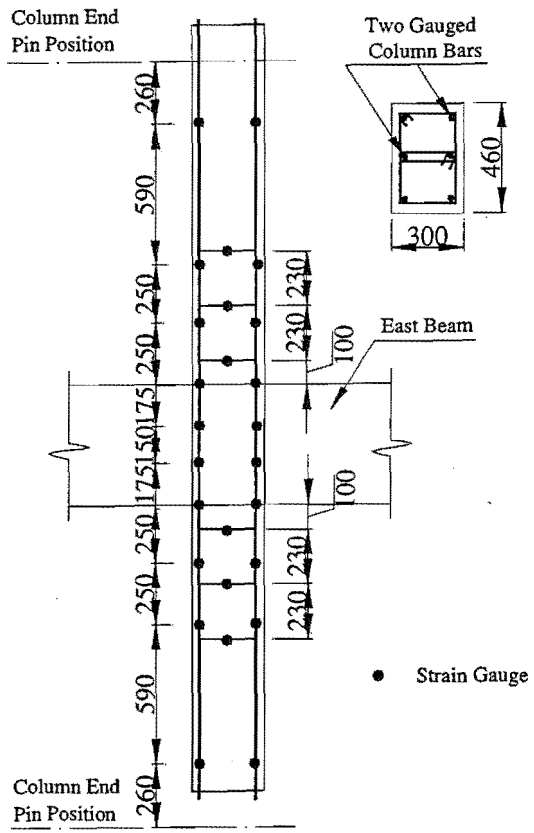

(b) Column longitudinal and transverse reinforcement

Fig.5.11 Arrangement of Electrical Strain Gauges for Interior Beam-Column Joint Units

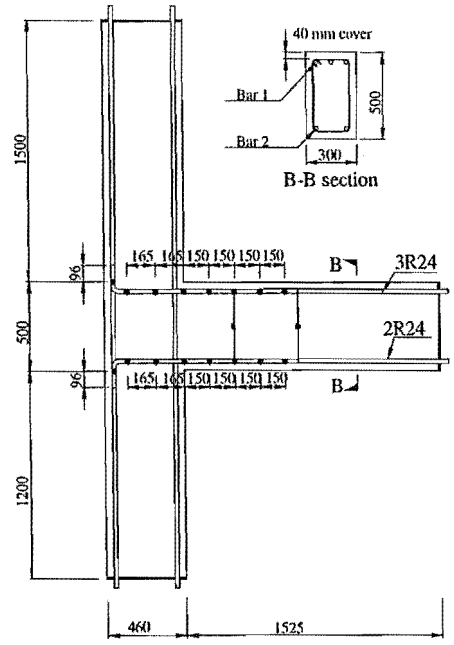

(a) Beam longitudinal and transverse (Units EJ1 and EJ3)

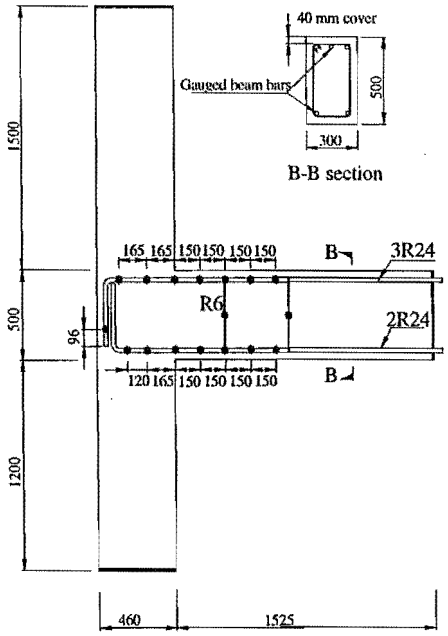

(b) Beam longitudinal and transverse reinforcement reinforcement (Units EJ2 and EJ4)

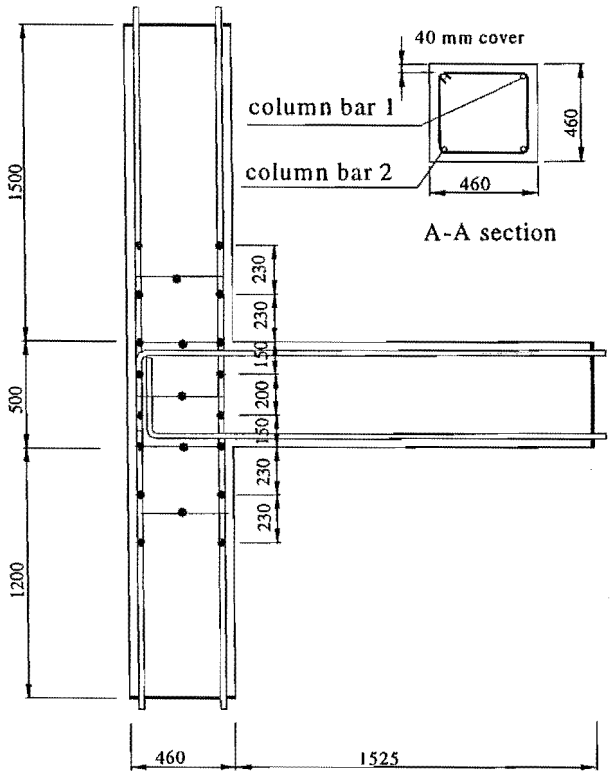

(d) Column longitudinal and transverse reinforcement

Fig.5.12 Arrangement of Electrical Resistance Strain Gauges for Exterior Beam-Column Joints with Beam Bar Hooks Bent into Joint

Each interior beam-column joint unit used thirty-six linear potentiometers to measure steel strain variations and bar slips within the joint core along the beam and column longitudinal reinforcing bars. Each exterior beam-column joint unit used fifteen linear potentiometers to measure steel strain variations and bar slips within the joint core along the beam and column longitudinal reinforcing bars.

The linear potentiometers for measuring steel strains were mounted to 10 mm steel rods welded to the beam and column main reinforcing bars. Therefore the measurements of the linear potentiometers represents the elongation of the reinforcing bars between the two gauged points. This method enabled the strain distribution in the reinforcing steel to be detected. With two static targets embedded in the joint core concrete, the bar slips within the joint region can be also detected. Fig.5.13 and Fig.5.14 show the positions of steel rods for mounting the linear potentiometers for the interior beam-column joint units and the exterior beam-column joint units, respectively.

5.2.6 Data Acquisition

Each of the two interior beam-column joints Unit 1 and Unit 2 required 173 channels, for 3 load cells, 84 linear potentiometers and 86 electrical resistance strain gauges. Two data loggers, CEDACS of 64 channels and Metrabyte data logger of 128 channels, were therefore employed for each test.

For the exterior beam-column joint Units EJ1, EJ2, EJ3 and EJ4, the required channel numbers for each test was less than 128 channels, and only Metrabyte of 128 channels was employed for each exterior beam-column joint test.

Because each bank of the data logger is of the same amplification factor, each bank of the data logger contained either electrical resistance strain gauges of the same gain or linear potentiometers.

Two different gains of 200 and 1000 (which are in fact the amplification factors) were set up for the electrical resistance strain gauges at critical locations and the electrical resistance strain gauges at the non-critical locations respectively, since very different steel strains were expected at the critical and non-critical locations. In other words, the gain for the electrical resistance strain gauges within the expected plastic hinge

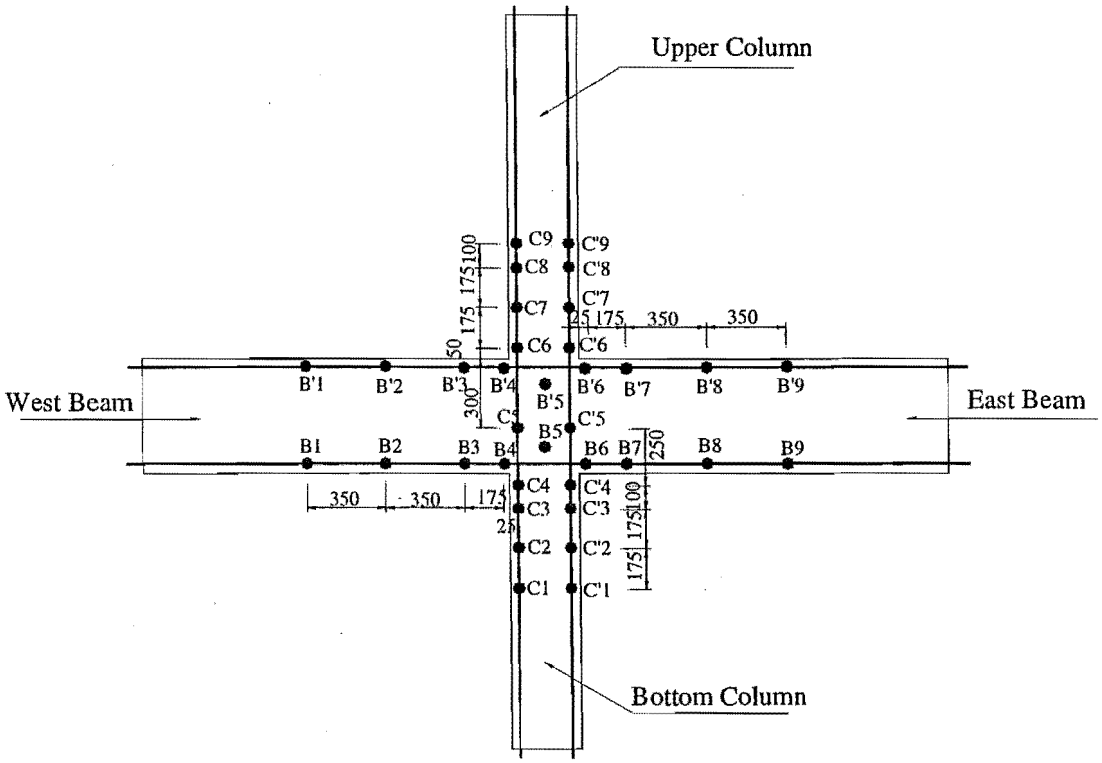

Fig.5.13 Positions of Steel Studs Welded on the Steel to Mount the Linear Potentiometers for Interior Beam-Column Joint Units

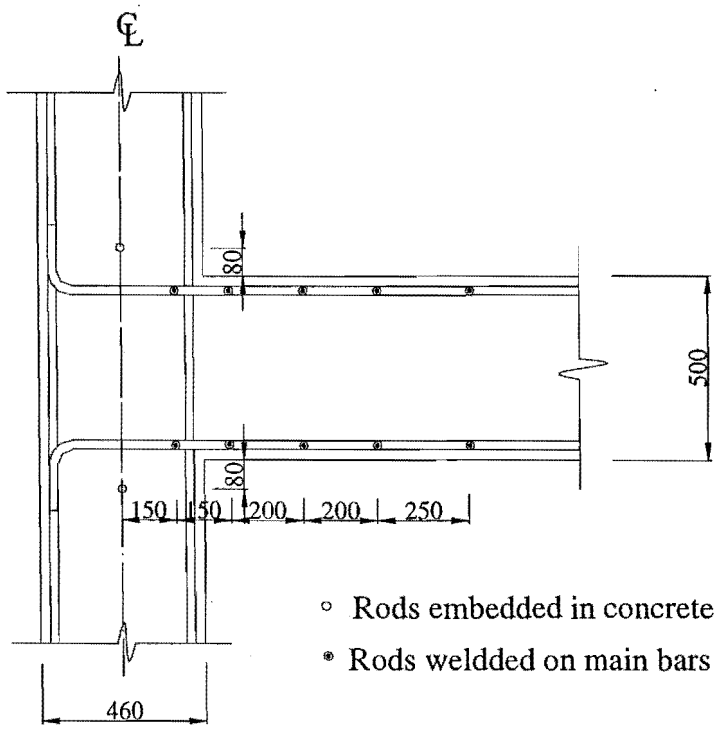

(a) Beam longitudinal reinforcement for Units EJ1 and EJ3

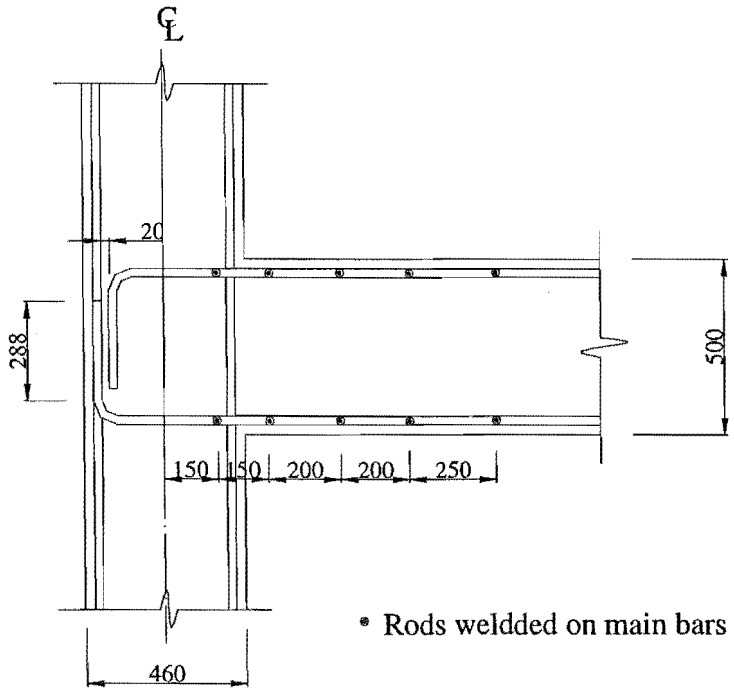

(a)

(b) Beam longitudinal reinforcement for Units EJ2 and EJ4

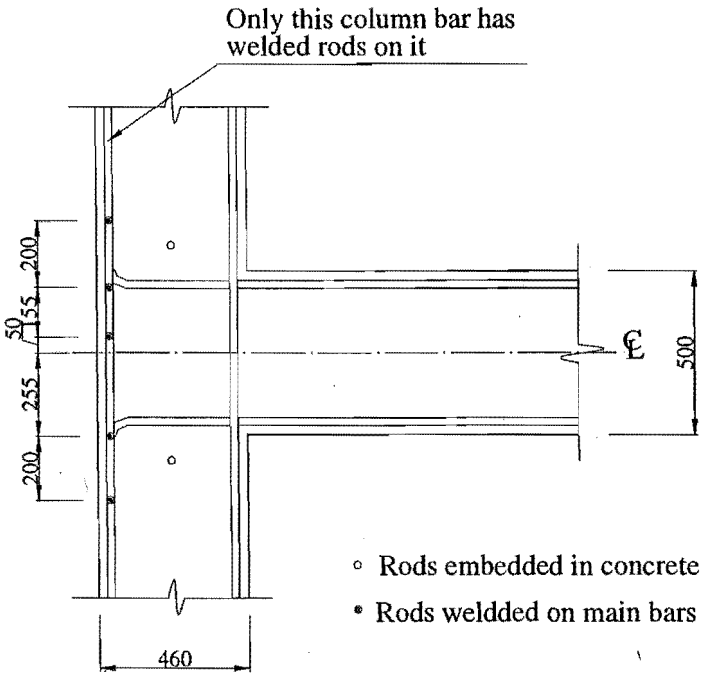

(c) Column longitudinal reinforcement of Units EJ1, EJ2, EJ3 and EJ4

Fig.5.14 Positions of Steel Studs Welded on the Steel to Mount the Linear Potentiometers for Exterior Beam-Column Joint Units

regions was set to be 200 since these gauges were expected to record large strains. In comparison, the gain for the electrical resistance strain gauges outside the expected plastic hinge regions was set to be 1000 because they were expected to record relatively low strains.

The linearity and repeatability of all linear potentiometers were checked after they were connected to the data loggers to make sure they would work properly during testing.

5.3 LOADING SEQUENCE

5.3.1 Cyclic Loading History

All the tests on the interior and exterior beam-column joint units followed the same quasi-static cyclic loading histories on the beam ends as depicted in Fig. 5.15 except that the compressive axial load of 800 kN was applied to the column for test on Unit 2 and the compressive axial load of 1800 kN was applied to the column for tests on Unit EJ3 and EJ4 in advance prior to cyclic loading. The first two loading cycles at the beam ends were load-controlled, including one cycle to 50% of the theoretical strength of the unit and one cycle to 75% of the theoretical strength of the unit. These two cycles in the elastic range were followed by a series of deflection-controlled inelastic cycles comprising two full cycles at displacement ductility factors of 1, 2 and 3. Each loading cycle included one half cycle clockwise loading and the other half anti-clockwise loading cycle. Clockwise loading for the interior beam-column joints meant downward loading at east (right) beam and upward loading at west (left) beam while clockwise loading for the exterior beam-column joints meant downward loading at the beam end.

5.3.2 Determination of Yield Displacement and Initial Stiffness

It is widely accepted in New Zealand that the "first yield" displacement, $\Delta y,test$, is found experimentally by extrapolating the measured stiffness at 75% of the theoretical strength linearly up to the theoretical strength of the unit. This method is graphically explained in Fig. 5.16, where Vi is the theoretical strength in terms of storey shear of

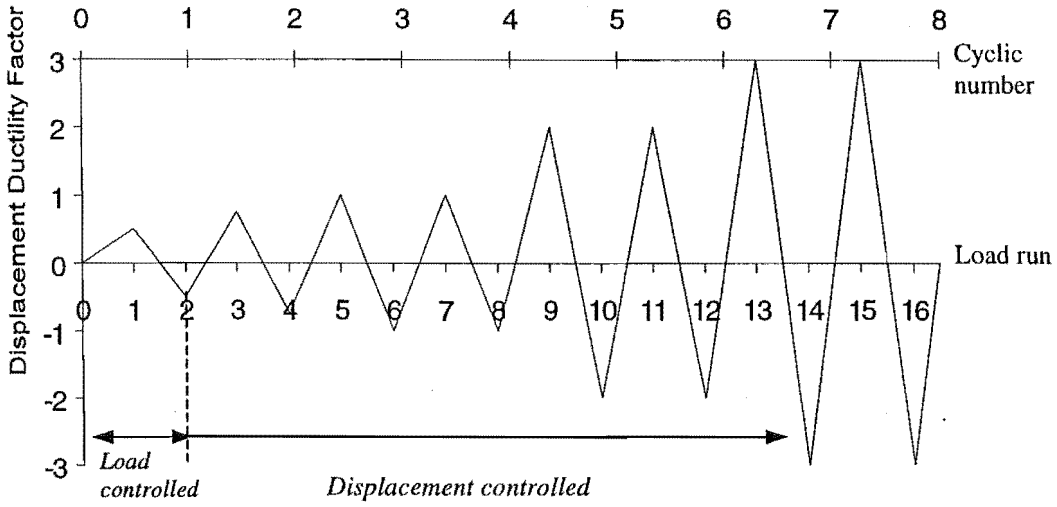

Fig. 5.15 Simulated Seismic Loading History

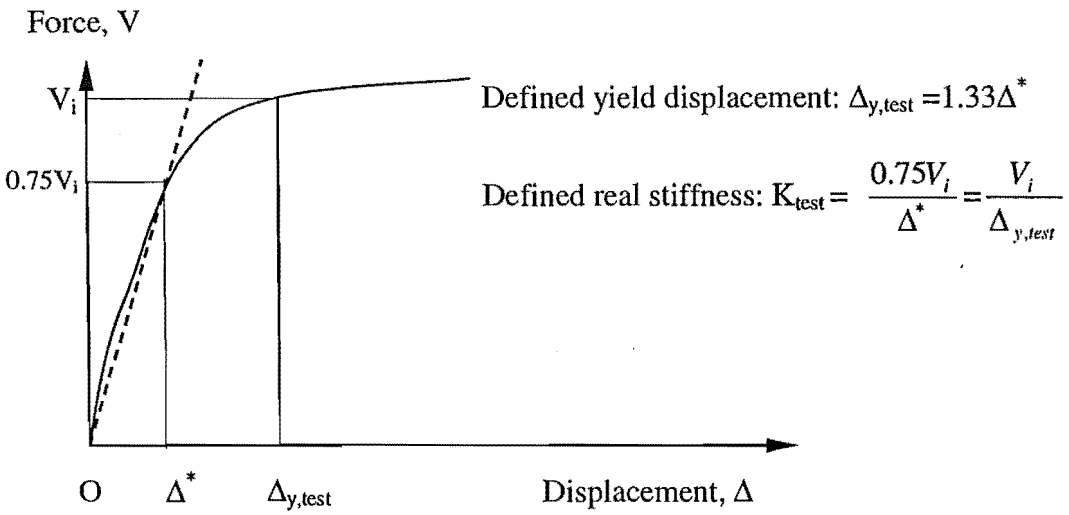

Fig.5.16 Experimental Determination of Displacement at First Yield

the unit. The imposed displacement ductility factor μ_Δ, which was to be used in displacement-controlled loading stages, was then defined to be the imposed displacement divided by the measured yield displacement $\Delta_{y,test}$. The measured initial stiffness of the unit, K_e, was then found to be:

$$K_e = V_i / \Delta_{y,test} \quad (5.5)$$

It is clear that, in situations when the measured displacement at first yield as defined above is much larger than the theoretically predicted first yield displacement, the attained storey drift is a more useful measure of deformation capacity of the subassemblage than the displacement ductility factor, since in that case high displacement ductility factors are associated with unrealistically high drifts. Alternatively, the imposed displacement ductility factor μ_Δ, which was to be used in displacement-controlled loading stages, should be defined to be the imposed displacement divided by the theoretical yield displacement $\Delta_{y,\,theoretical}$ in this case.

5.4 TEST PROCEDURE

Before any forces were applied to the test units, two complete sets of readings from all transducers were taken over 16 hours to check the stability of their readings.

After the specified compressive column axial load was applied to the test unit in advance, the cyclic vertical forces were applied to the beam-ends using hydraulic jacks. For the tests on interior beam-column joint units, the force application at the beam ends was coordinated manually to give equal rotations of the beams. The loading spans of the two beams were equal for the two interior beam-column joint units, hence equal beam rotations required equal amount of displacements applied at each beam end. In each load run, several force increments were taken before the target load or displacement was achieved so as to provide data for plotting continuous force-displacement curves.

After the maximum force or ductility level had been attained in each load run, unloading of the beams was carried out by two-step load control by removing 50% of the maximum force for that load run for the relevant beam.

At the peak of each load run, cracks on the front and the back faces were checked and the cracks on the front face were marked with felt-tip pens on the white painted surface. Photographs were taken usually at the peak of each load run, but also at other stages when it was felt necessary.

5.5 DISPLACEMENT COMPONENTS

5.5.1 General

As described in Section 5.1, seismic actions were simulated by applying vertical forces at the beam-end(s) of the test units while the equivalent storey (column) displacements and storey shears were calculated according to Eqs. 5.2 and 5.3. The storey (column) displacements were a combination of the elastic and inelastic deformations of the beams, the columns and the joint core. Namely,

$$\Delta_c = \Delta_{c,b} + \Delta_{c,c} + \Delta_{c,j} \qquad (5.6)$$

Where: Δ_c = the total storey displacement,

$\Delta_{c,b}$ = beam displacement component;

$\Delta_{c,c}$ = column displacement component;

$\Delta_{c,j}$ = joint displacement component.

Different displacement components can be estimated according to the measured member curvatures and the joint shear distortion, as stated in the following sections.

5.5.2 Deformations of the Beams

For the sake of the illustration of beam displacement estimation, the east beam in Fig. 5.8(a) is reproduced in Fig. 5.17.

The sign convention is defined as follows:

Beam positive curvatures and positive rotation angles were induced by beam positive bending moment, that is, beam positive curvatures and positive rotation angles corresponded to the bottom fibre in tension and the top fibre in compression. Similarly beam negative curvatures and rotation angles were induced by beam negative bending moment and corresponded to the top fibre in tension and the bottom fibre in compression.

The rotation over the region s_i is:

$$\theta_{b,i} = (_t\delta_i - _b\delta_i) / h_i \qquad (5.7)$$

The average curvature over the region s_i is

$$\phi_{b,i} = \theta_{b,i} / s_i \qquad (5.8)$$

where: h_i and s_i are shown in Fig. 5.17, ${}_t\delta_i$ and ${}_b\delta_i$ are the measurements of the top and bottom curvature linear potentiometers over the region i, and the measured compressive displacements by curvature linear potentiometers were taken as positive.

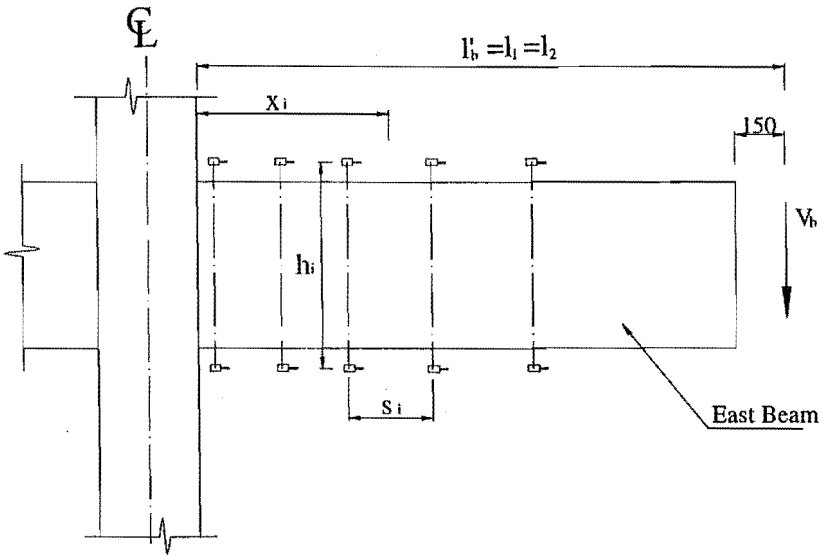

Fig.5.17 Estimation of Beam Deformation

The east beam end displacement ${}_E\delta_{bf}$ due to its flexural deformation only then can be found as follows:

$$ {}_E\delta_{bf} = \sum_i \theta_{b,i} (l_2 - x_i) \qquad (5.9) $$

where: l_2 is the distance from column face to the centre of the beam end pin (=1755mm), and x_i is the distance from column face to the centre of the region i.

The west beam end displacement ${}_W\delta_{bf}$ due to its flexural deformation only could be obtained in the same way, namely,

$$ {}_W\delta_{bf} = \sum_i \theta_{b,i} (l_1 - x_i) \qquad (5.9') $$

No instrumentation had been set up to measure the beam shear deformations because the beams were not expected to fail in shear owing to the use of plain round bars. This was later on verified by the test observations. Therefore, it was reasonable to neglect the shear deformations in beams.

The equivalent storey displacement (column displacement), $\Delta_{c,b}$, resulting from beam deformations, ${}_E\delta_{bf}$ and ${}_W\delta_{bf}$, is calculated as follows:

$\Delta_{c,b} = l_c / l_b \ ({}_W\delta_{bf} - {}_E\delta_{bf})$ for interior beam-column joint units (5.10)

$\Delta_{c,b} = - \delta_{bf} \ l_c / l_b$ for exterior beam-column joint units (5-10)'

where: l_c is the storey height, namely, vertical distance between the column end pins (3200mm) and l_b is the beam span or horizontal distance between the beam end pins (=3810mm for interior beam-column joint units, and = 1905 mm for exterior beam-column joint units).

In reality, the consequence of large beam deformations will complicate the structural force transfer path. Typically the increase in beam lengths will result in expansion of bay lengths of the frame structures, actuating the restraints against the beam deformations from columns. As a result, compressive axial beam load develops, then the beam flexural capacities are enhanced. This finally causes an adverse effect on the desired ratio of column moment capacities to beam moment capacities at the same joint.

5.5.3 Deformations of the Columns

The upper column of Fig. 5.8 (b) was reproduced in Fig.5.18.

Similar to the definition for the beams, it was defined that positive column curvatures and positive column rotations were associated with the column left fibre in tension and the column right fibre in compression, and the measured compressive displacements by linear curvature potentiometers were taken as positive.

Therefore, the average rotation over the column region R_j could be as follows:

$$\theta_{c,j} = ({}_r\delta_j - {}_l\delta_j) / d_j \qquad (4.11)$$

and the average curvature over this region R_j is

$$\phi_{c,j} = \theta_{c,j} / r_j \qquad (4.12)$$

where: ${}_l\delta_j$ and ${}_r\delta_j$ are the measurements of the left and right column curvature linear potentiometers over the region j, and d_j and r_j are as seen in Fig. 5.18.

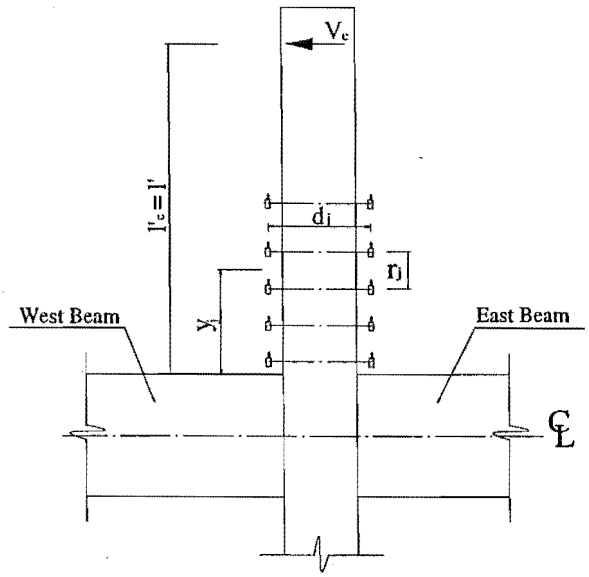

Fig.5.18 Estimation of Column Deformation

The flexural deformation of the upper column, ${}_U\delta_{cf}$, then can be derived as follows:

$${}_U\delta_{cf} = \sum_j \theta_{c,j}(l' - y_j) \qquad (5.13)$$

where: d_j, r_j, y_j and l' are shown in Fig. 5.18.

Like beams, column shear deformations were thought to be insignificant and were hence neglected. The observed test evidence during the testing also supported this assumption.

Similar schedules were used to find the deformations of the bottom column, ${}_B\delta_{cf}$.

The equivalent storey displacement, $\Delta_{c,c}$, resulting from the column deformations, ${}_U\delta_{cf}$ and ${}_B\delta_{cf}$, is calculated as follows:

$$\Delta_{c,c} = ({}_U\delta_{cf} - {}_B\delta_{cf})(l_c'/l_c) \qquad (5.14)$$

where: l_c' =1350mm, and l_c =3200mm

5.5.4 Deformations Due to Joint Shear Distortion

The equivalent storey displacement due to joint shear distortion, $\Delta_{c,j}$, can be obtained in the following way:

$$\Delta_{c,j} = \gamma_j \ (l_c - h_b - l_c \times h_c / l_b) \qquad (5.15)$$

where: γ_j is the joint shear distortion defined in Section 5.2.4, l_c is the storey height (=3200mm), l_b is the beam span (=3810mm), h_b is the depth of beam and h_c is the overall depth of the column.

5.5.5 Beam Fixed-End Rotation

The fixed-end rotation of the members adjacent to the joint is caused by the tensile strain or slip of the longitudinal bars anchored in the joint core. For these beam-column joint test units, significant bar slip would be anticipated due to the use of the plain round bars for longitudinal reinforcement and/or insufficient anchorage lengths within the joint core. Hence beam fixed-end rotations could be quite large.

In this test series, the fixed-end rotations of the beams were estimated by a pair of linear potentiometers located next to the column faces. From Fig. 5.17, the beam fixed-end rotation $\theta_{b,fe}$ can be derived by:

$$\theta_{b,fe} = ({}_t\delta_1 - {}_b\delta_1) / h_1 \qquad (5.16)$$

where: ${}_b\delta_1$ and ${}_t\delta_1$ are the bottom and the top displacement measured at the fixed-end interfaces and h_1 is the vertical distance between the linear potentiometers at the fixed-end interface.

The deformation due to beam fixed-end rotation, ${}_b\delta_{fe}$, can be obtained as:

$${}_b\delta_{fe} = \theta_{b,fe} \, l_b' \qquad (5.17)$$

where: $\theta_{b,fe}$ is the beam fixed-end rotation defined above and l_b' is the distance from the column face to the centre of the beam end pin.

The equivalent storey displacement due to fixed-end rotation of the beam, $\Delta_{b,fe}$, can be obtained as:

$$\Delta_{b,fe} = \text{-}_b\delta_{fe}\ l_c / l_b \qquad (5.18)$$

where: $\Delta_{b,fe}$ is the equivalent horizontal storey displacement due to beam fixed-end rotation, l_c is the storey height (=3200mm), and l_b is the beam span (=3810mm for interior beam-column joint units, and =1905 mm for the exterior beam-column joint units).

Although the linear potentiometers were placed as close as possible to the column faces, the fixed-end rotation so obtained includes some rotation due to elongation of the longitudinal bars over that region.

5.5.6 Column Fixed-End Rotation

Similar to beam fixed-end rotations, column fixed-end rotations were also monitored during testing because big column fixed-end rotations were anticipated.

In this test series, the component of equivalent storey displacement due to column fixed-end rotations were monitored by a pair of linear potentiometers located next to the beam faces, see Fig.5.18, the fixed-end rotation $\theta_{c,fe}$ can be derived by:

$$\theta_{c,fe} = ({}_r\delta_1 - {}_l\delta_1) / d_1 \qquad (5.19)$$

where: ${}_l\delta_1$ and ${}_r\delta_1$ are the measurements of the left and right column curvature linear potentiometers at the fixed-end interfaces;

d_1 is the distance between the two linear potentiometers.

The component of storey displacement due to column fixed-end rotations, $\Delta_{c,fe}$, is

$$\Delta_{c,fe} = \theta_{c,fe}\ l_c' \qquad (5.20)$$

where: l_c' is the distance from the beam face to the centre of the column end pin;

and $\Delta_{c,fe}$ is the storey displacement due to column fixed-end rotation.

CHAPTER 6

TEST RESULTS OF INTERIOR BEAM-COLUMN JOINTS

6.1 TEST OF UNIT 1

6.1.1 Introduction

This test program involved two as-built full-scale interior beam-column joint units, Unit 1 and Unit 2. Unit 1, which was tested under simulated seismic loading with zero axial column load, was characterised by an expected weak column-strong beam mechanism, the use of plain round longitudinal and transverse reinforcement, low quantities of transverse reinforcement in the beams and the columns, no shear reinforcement in the joint core at all, and large diameter longitudinal bars passing through the joint core, as was typical of 1950s construction in New Zealand. Test on Unit 1 was identical to Hakuto's test on Unit O1 except the use of plain round reinforcing bars. Such a test design aimed at investigating the seismic performance of existing reinforced concrete moment resisting frame structures and the possible effect of steel type used on the seismic performance of existing reinforced concrete moment resisting frame structures.

According to the theoretical considerations conducted in Chapter 4, the emphasis is placed on the investigations into the effects of bond degradation and bar slip along the longitudinal bars and column bar buckling, and into the shear performance of the beams, columns and the joint core when plain round longitudinal bars are used.

6.1.2 Cracking and Damage

Fig. 6.1 shows the final appearance of Unit 1 at the end of testing. As illustrated by photograph in Fig. 6.1, the two columns of Unit 1 had major cracking at the final stage and the damage to Unit 1 was mainly limited to the columns. Evidently, a weak column - strong beam failure mechanism formed during testing as predicted theoretically in Table 4.5.

The damage to the columns tended to mainly concentrate in column horizontal flexural cracks above and below the joint panel although some damage was also observed in the form of vertical cracks running along both layers of the column longitudinal bars across the joint core. The damage concentration in two major column horizontal cracks above and

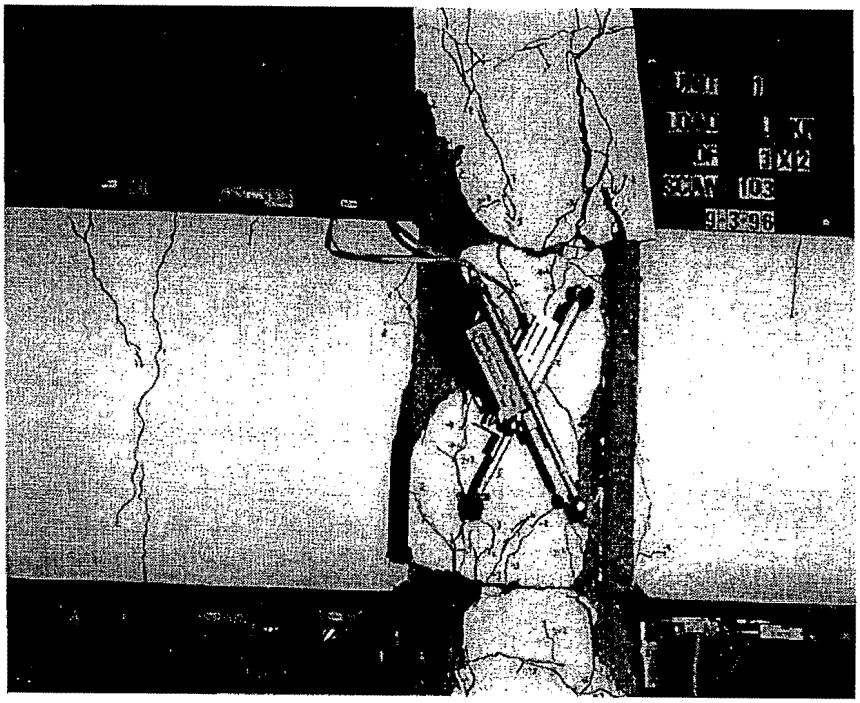

Fig. 6.1 Final Appearance of As-Built Interior Beam-Column Joint Unit 1

below the joint core for Unit 1 occurred as a result of rapidly increased column fixed-end rotations, which were associated with significant bond degradation and slip of the column longitudinal bars within the joint core. The damage in the form of column vertical cracks along the column longitudinal bars across the joint core occurred as a consequence of column bar buckling resulting from bar slip and inadequate lateral restraint against column bar buckling.

The damage observed to the beams was by way of beam vertical flexural cracks adjacent to the joint panel, but it was not so pronounced as that for the columns, indicating that bond degradation and slip along the beam main bars within the joint core were not so critical as for the columns for this weak column-strong beam system.

The joint panel performed satisfactorily during testing although the theoretical consideration showed that the joint shear performance would be very critical due to lack of joint horizontal shear reinforcement. Joint diagonal tension cracks did not develop with the increase in the imposed displacement level during testing, and the condition of the joint panel remained excellent till the completion of the testing, demonstrating that the joint shear failure did not govern the final failure.

No beam and column shear cracks were observed throughout the whole test history although the theoretical analysis showed insufficient column shear capacity, indicating that the use of plain round bars as was the case for Unit 1 led to a reduced demand for member transverse reinforcement in resisting shear. This is because bond degradation resulting from the use of plain round reinforcing bars changed the shear resisting mechanism in linear members into a thrust mechanism rather than a truss mechanism as was the case with deformed bars. The actuation of a thrust mechanism, unlike a truss mechanism, does not need the participation of transverse reinforcement in resisting shear. This was also reported by Maffei, J. 1997 [M1, M2].

In a word, the bond degradation and bar buckling of the plain round longitudinal bars, especially in the columns, were believed to initiate the final failure of Unit 1. The member transverse reinforcement was more needed for preventing longitudinal bar buckling than for providing shear capacity when plain round bars are used for longitudinal reinforcement.

Whereas in the case of Hakuto's test of Unit O1 the final failure was due to the joint shear failure and severe bond degradation along the column and beam longitudinal bars within the joint core, the final failure of Unit 1 was attributed to more severe bond degradation along the column longitudinal reinforcement within the joint region and column bar buckling. The appearance of the joint of Unit 1 at the final stage was of much better integrity than Hakuto's Unit O1. Hakuto's Unit O1 was identical to Unit 1 except that Hakuto's Unit O1 used deformed reinforcing bars. Evidently, the use of plain round reinforcing bars as was the case of Unit 1 increased the need of column transverse reinforcement for anti-buckling but led to greatly improved shear performance in the members and the beam-column joint.

6.1.3 Hysteretic Response

Fig.6.2 shows the storey (horizontal) shear force versus storey (horizontal) displacement hysteretic response measured for Unit 1. Also shown is the ideal theoretical storey shear strength of the unit, V_i, which was governed by the theoretical column flexural strengths calculated using the New Zealand code approach [N1] but using the measured material strengths and assuming a strength reduction factor of unity as previously described. Figs. 6.3 and 6.4 show the vertical deflections at the beam-ends plotted against the

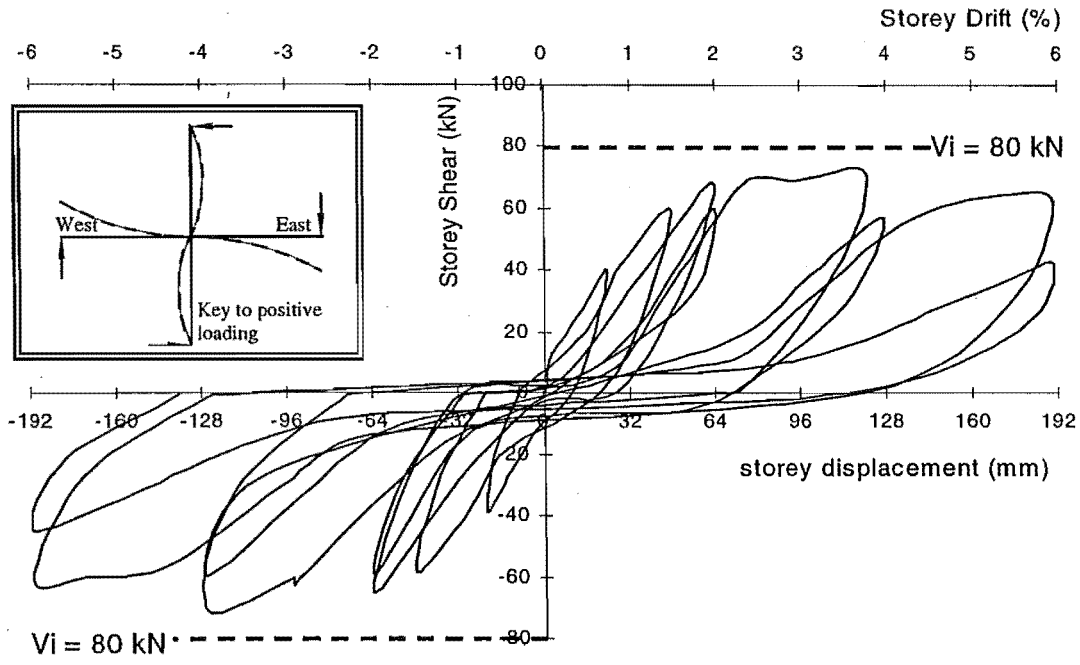

Fig.6.2 Storey Shear versus Storey Displacement Hysteresis Loops of Unit 1

corresponding beam shears for Unit 1. These plots confirm the poor seismic behaviour of the unit as a whole.

The first yield displacement measured for the test of Unit 1 using the method described in section 5.3.2 was 57 mm. This was equivalent to a storey drift of 1.8% and 2.7 times the predicted first yield displacement of 21 mm. The predicted first yield displacement was based on member curvature distribution and assuming that the columns just reached yield but the beams were still in the elastic range. Also of interest is that the first yield displacement measured for the test of Unit 1 was 1.5 times the value obtained in a previous test on an otherwise identical beam-column joint assembly but reinforced by deformed bars in which the storey drift was 1.2% at the measured first yield displacement [H1]. Hence, when existing reinforced concrete structures use plain round bars for longitudinal reinforcement, the available stiffness of the structures would be much smaller than the predicted value due to severe bond degradation along the longitudinal bars within and adjacent to the joint cores. As a result, the type of structure tested would become extremely flexible. On this basis the displacement ductility factor calculated using the measured first yield displacement becomes meaningless. In this case, the displacement ductility should be calculated using the theoretically predicted first yield

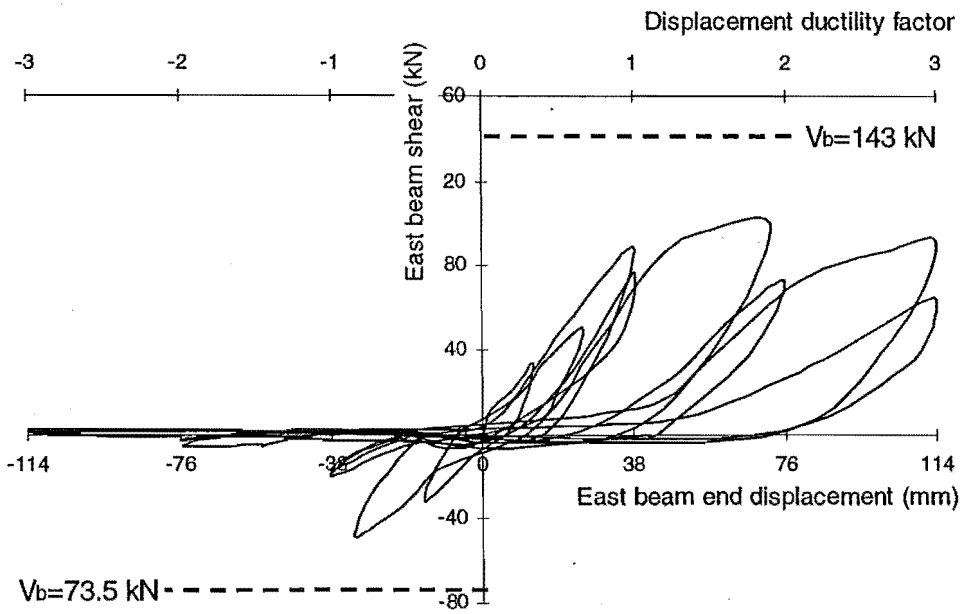

Fig.6.3 Hysteresis Loops of East Beam of Unit 1

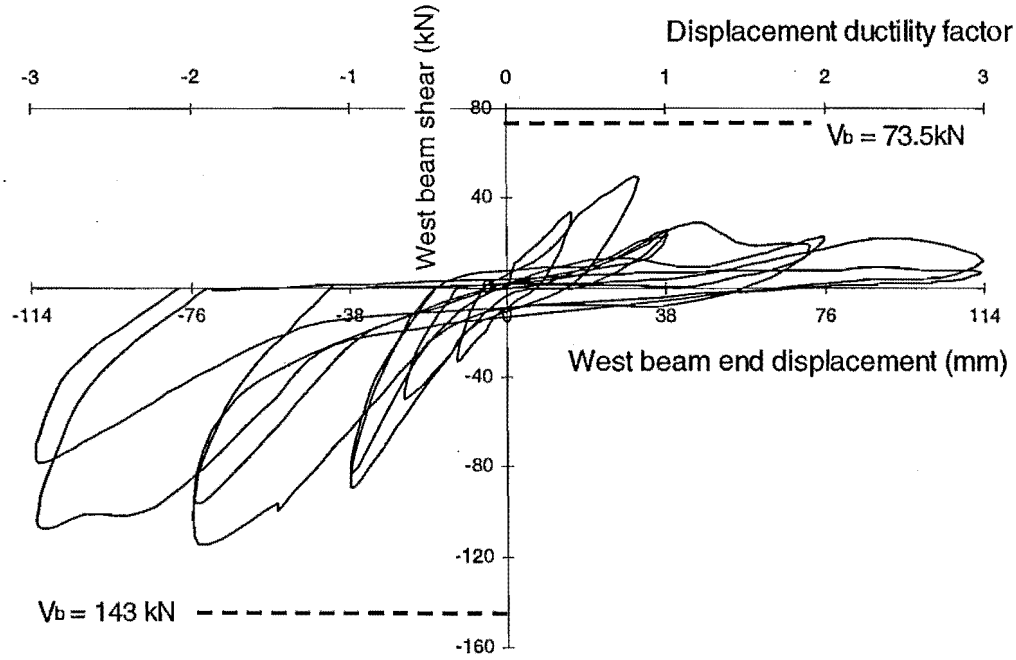

Fig.6.4 Hysteresis Loops of West Beam of Unit 1

displacement. Alternatively, a storey drift can be a much better index of the displacement of existing beam-column joint subassemblages. The use of the storey drift index for the imposed displacement level is also supported by the evidence that different beam-column joint test units achieved their maximum strengths at a similar drift level of 2% [A6, B3].

Significant pinching of the loops is evident in Figs. 6.2, 6.3 and 6.4, indicating very poor energy dissipating capacity of Unit 1. The pinching started at the early loading stages and became more and more pronounced with the imposed displacement levels. The softness of the test unit at the beginning of each loading run occurred at the stage before the commencement of the concrete contribution to the flexural compression. The softness was due to the major open flexural cracks adjacent to the joint core in the compression zones of the columns and beams caused by tension in the previous loading run. These wide flexural cracks adjacent to the joint core occurred due to the significant bond degradation and bar slip of the longitudinal reinforcement within the joint region and at the adjacent ends of the members. After the two faces of the major cracks closed together, shear and compression could be transferred along and across these cracks and the stiffness increased rapidly again.

Fig. 6.2 shows that, unlike well-designed beam-column joint units where the theoretical strength or even the overstrength can be attained, the maximum storey shear strength measured for Unit 1, which was attained in the first loading run at a storey drift of almost 4%, was about 10% less than the theoretical storey shear strength of Unit 1 of 80 kN. In comparison, the theoretical storey shear strength of Hakuto's Unit O1 was reached during testing. The low attainment of the storey shear strength for Unit 1 was due to severe bond degradation and slip of the longitudinal reinforcing bars, especially in the columns, which caused the plane section theory to overestimate the actual flexural strengths of the members at the plastic hinges, similar to the findings reported by Lees and Burgoyne [L2] and by Hakuto, Park and Tanaka [H5].

Figure 6.2 also shows that Unit 1 demonstrated a significant reduction in strength with increase in the imposed displacements after the maximum strength was attained. Apart from this, the second loading cycle had very significant strength degradation compared with the first cycle at the same displacement level, due to progressive bond slip and buckling of the longitudinal column bars under cyclic loading. Hence cyclic loading effect

on the strength degradation is of concern when the members contain plain round reinforcement.

It was also noticed from the hysteresis loops of each individual beam measured for Unit 1 in Figs. 6.3 and 6.4 that the attained strength of each beam at a certain displacement level for two loading directions was not proportional to their theoretical flexural strengths. Typically, for Unit 1, the beam which was experiencing downward displacement balanced a higher percentage of the column bending moments imposed on the same joint while the beam which was experiencing upward displacement balanced a lower percentage of the imposed column bending moments. This occurred due to much more severe bond degradation along the bottom beam bars than that along the top beam bars resulting from the initial higher bond stresses in the bottom beam bars during load-controlled elastic loading stages. Hence it is concluded that the more severe the bond degradation along the longitudinal bars, the less the attained strength in terms of the percentage of the corresponding theoretical flexural strength.

In summary, Unit 1 reached storey shears that were approximately 15% and 10% less than the theoretical storey shear strengths at storey drifts of approximately 2% and 4%, respectively, accompanied by a great deal of softening with cyclic loading and pinching of the hysteresis loops. Bond degradation and bar slip along the longitudinal bars played the major rule in the attainment of the member flexural stiffness and strength.

6.1.4 Column Behaviour

6.1.4.1 Column Deformation Characteristics

Fig.6.5 illustrates the measured average column curvature profiles by linear potentiometers for Unit 1. In Fig.6.5, the average column curvatures are calculated using the method described in Section 5.5.3, the positive column curvatures mean the column left side in tension and the column right side in compression, and the negative column curvatures mean the column left side in compression and the column right side in tension as defined in Section 5.5.3. In the legend of Fig.6.5, + and - represent positive and negative loading respectively, 0.5, 0.75, 1 and so on represent the loading cycle of 0.5 V_i, 0.75V_i and ductility 1 so on. The theoretical column curvatures at first yield are the same for both loading directions and they are 8.6E-06. Columns of Unit 1 were expected to develop plastic hinges.

Measured column curvature profile shown in Fig.6.5 is characterised by the following:

1. Heavy concentration of column deformation in the column fixed-ends

For a well-designed reinforced concrete member, the progress of the member post-elastic deformation is due to the steel yielding penetration within the member over a region called as "plastic hinge region", which has a length of about 50% to 100% member depth. At the ultimate stage, the generated curvature over the plastic hinge region is many times larger than the yield curvature and spreads over the whole plastic hinge region. In this case, the available curvature ductility over "plastic hinge region" in association with a certain plastic hinge length is an important index to the member non-linear deformation capacity.

Fig.6.5 shows that the column post-elastic deformation distribution for Unit 1 was different from that described above. In Fig.6.5, the column post-elastic deformation heavily concentrated on the fixed-ends. This becomes more evident in Fig.6.6, which shows the measured column deformation components attributed to the fixed-ends and the other regions, referred as to be "elastic portion" here. Deformation component of column fixed-ends increased as the loading progress, suggesting that column fixed-ends were the major source of column non-linear deformation and the deformation over the "elastic portion" can be neglected. Column fixed-end regions were very small and actually the observed column deformation occurred mainly in the major flexural cracking at beam-column interfaces (see Fig.6.1), which had a length much smaller than ordinary plastic hinge length. In this case, a better index to member non-linear deformation capacity is the rotational ductility in the fixed-ends, rather than its curvature ductility associated with a certain plastic hinge length.

It needs to be highlighted that member non-linear flexural deformation in the form of lumped fixed-end rotation as observed for Unit 1 is different in nature from that in the form of spreading over well-defined plastic hinge regions as for well-designed members. The non-linear deformation within the well-designed plastic hinge region is due to the yield penetration within the member and it is independent on the cross sectional details and actions of the other members framing into the same joint. However, the deformation in the fixed-ends occurs mainly due to severe bond degradation along the plain round longitudinal bars within the joint region, namely outside the member, and it is closely related to the force transfer mechanism from the member longitudinal reinforcement

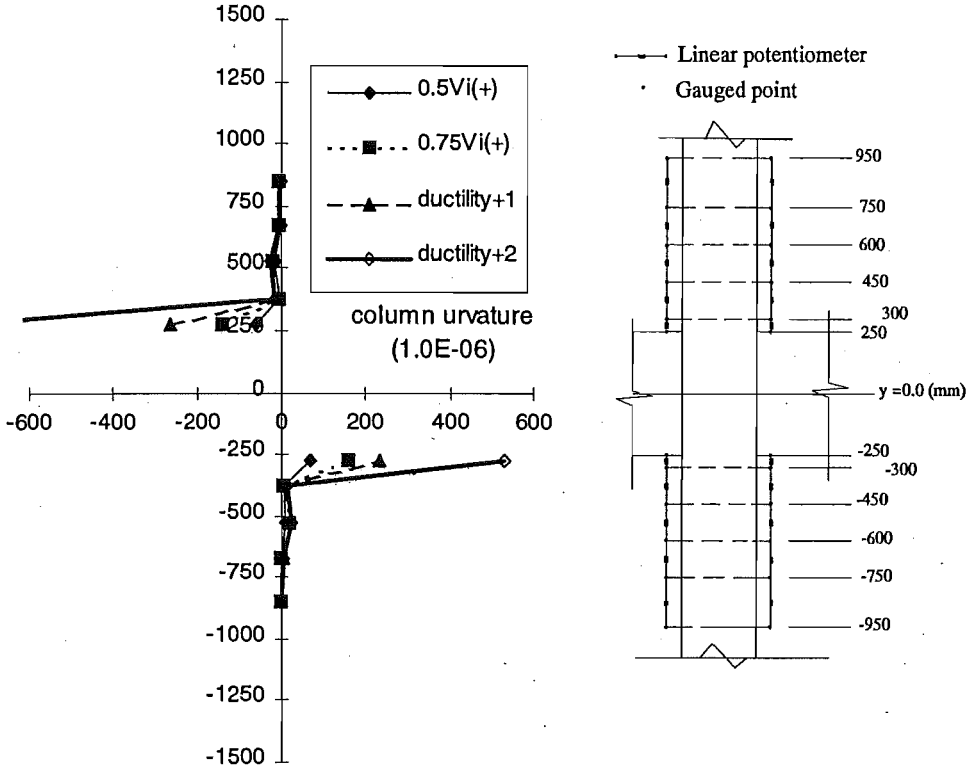

Fig. 6.5 Column Curvature Profile Measured at Clockwise Loading Peaks for Unit 1

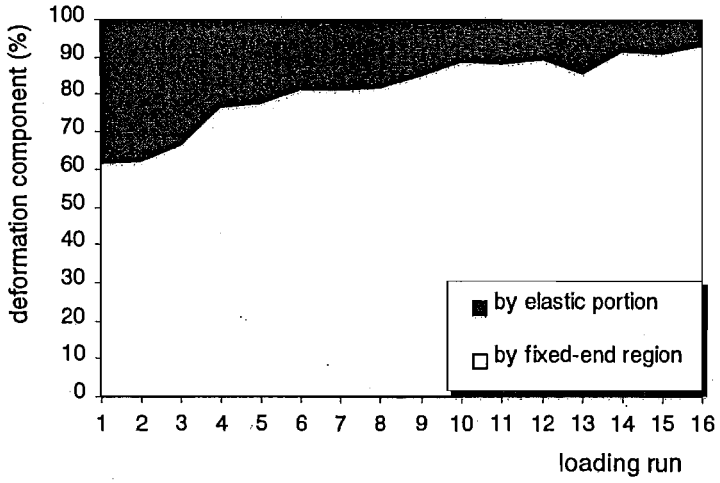

Fig. 6.6 Measured column deformation components

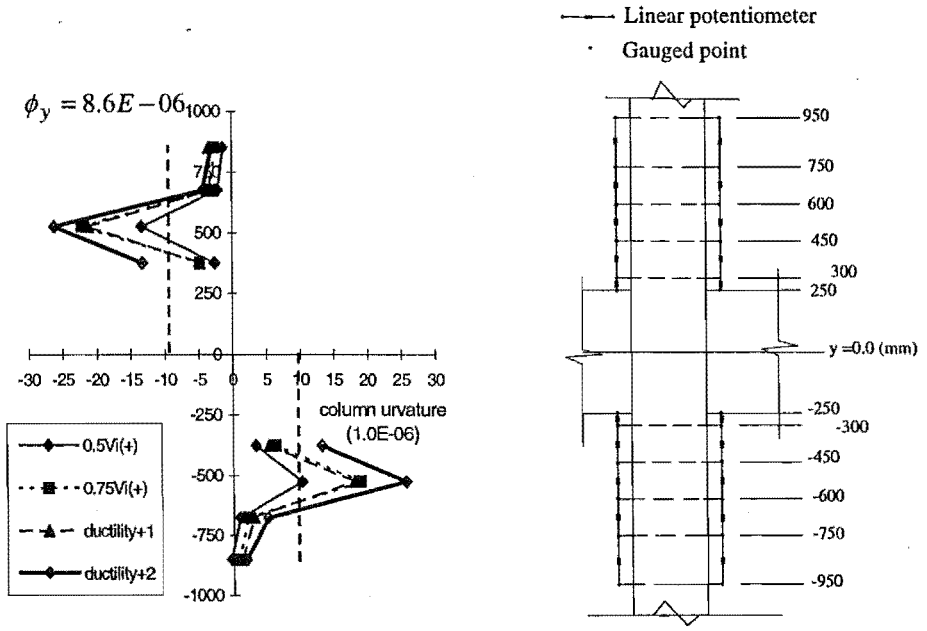

(a) Column curvature at clockwise loading peaks

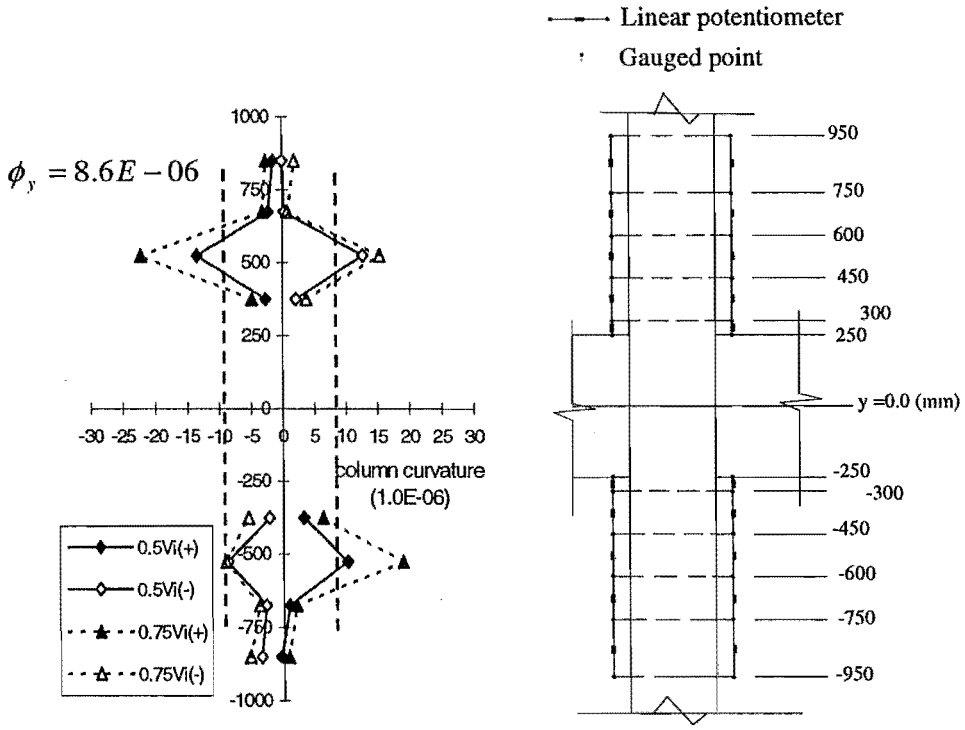

(b) Column curvature for the first two loading cycles

Fig.6.7 Column Curvature Profile of Unit 1 without Fixed-End Regions Included

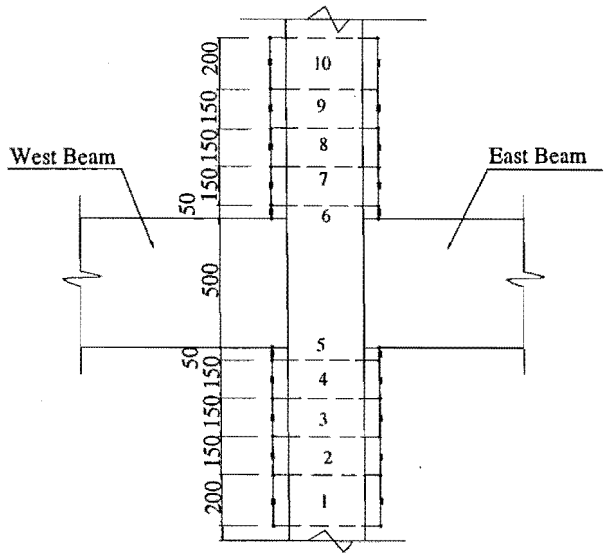

Fig.6.8 Numbering of Gauged Regions to Measure Column Curvature

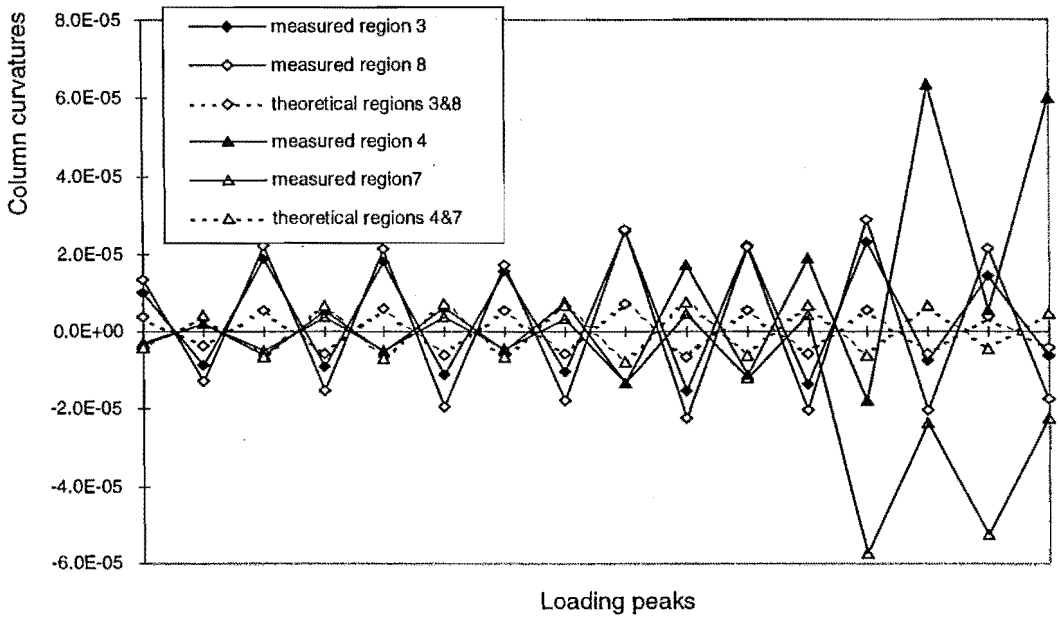

Fig. 6.9 Discrepancies between Measured Column Curvatures and Theoretical Ones

across the joint core. Hence, the deformation in the fixed-ends is dependent on the cross sectional details and the actions of the discussed member itself and the members framing into the same joint. Current computer programs cannot cope with such interaction between the beams and columns at the same joint. Therefore, there is a need for developing a new member model, which is capable of interrelating the member's fixed-end rotation with the

sectional details and actions on the other members framing into the same joints. This will be further discussed in chapter 8.

2. Violation of Plane Section Assumption

Although the column deformation was observed to be mainly in its fixed-ends, the column deformation over the rest regions is still studied here in detail to facilitate the understanding of the effect of severe bond degradation along the member longitudinal reinforcement on its curvature properties.

Fig. 6.7 shows the measured column curvature profiles without the inclusion of the fixed-end regions for the sake of explicit illustration. Form Figs.6.5 and 6.7, it is seen that big discrepancies existed in the magnitudes of the measured column curvatures and the theoretical predictions. The theoretical curvatures are based on plane section assumption and the measured member shear force. For instance, the measured column curvatures over fixed-end regions as well as some other regions in the loading to clockwise $0.5V_i$ were much larger than the theoretical column curvatures at first yield of 8.6E-06. The imposed bending moments over those regions at this stage were much smaller than the theoretical column moment capacity at first yield.

Fig. 6.9 shows the discrepancies at the specified loading stages for regions 3, 4, 7 and 8, using the region definition in Fig.6.8. From Fig.6.9, it is seen that the measured column curvatures were generally larger than the theoretical predictions, and the discrepancies increased as the loading progressed. In comparison, the discrepancy was especially pronounced over the column fixed-end regions. The measured column curvature over the fixed-end regions in Fig.6.5 reached up to about 150 times the theoretical prediction obtained using conventional flexural theory and plane section assumption.

The cause of the above-described discrepancies could be well explained by looking at the curvature measurement method used as described in Section 5.2.3. It is to be realised that the measurements of the linear potentiometers in measuring the column curvatures include the concrete deformations and the widths of cracks within the gauged regions. Severe bond degradation violated plane section assumption and led to wider concrete cracks as a result of the sustained large steel strain; hence the induced column curvatures would be generally larger than the theoretical predictions. Bond degradation along the column longitudinal bars was much more significant within the fixed-end regions, so the discrepancies between

the measured column curvature and the theoretical prediction were much larger over the fixed-end regions.

3. Summary

Flexural deformation of existing concrete members reinforced by plain round reinforcement was mainly limited to the fixed-ends and this was due to severe bond degradation along the member longitudinal reinforcement within and adjacent to the joint core. In this case, a suitable index to member post-elastic deformation behaviour is the rotational ductility in the fixed-ends, rather than the curvature ductility associated with a certain plastic hinge length. The characteristic of such a flexural deformation is that is depends on not only the member itself but also the other members framing into the same joint. Hence it is different in nature from that for a well-designed member. In addition, severe bond degradation along the member longitudinal reinforcement caused violation of ordinary plane section assumption, leading to generally larger member curvatures than the theoretical predictions.

6.1.4.2 Column Non-linear Behaviour

For well-design concrete members, the non-linear deformation spreads over a plastic hinge region and the force strengths of other non-ductile failure modes in plastic hinge regions do not degrade significantly with the progress of imposed non-linear deformation. Consequently, the force strength can be well maintained as the imposed non-linear deformation increases, leading to ductile member behaviour. Member deformation capacity in this case is evaluated by means of the available curvature ductility.

However, as described above, the observed evidence of column deformation behaviour for Unit 1 suggests that a better index to member non-linear deformation capacity be the rotational ductility in terms of its fixed-end rotation, rather than its curvature ductility associated with a certain plastic hinge length. So the maintenance of column force strength with the progress of non-linear deformation in the fixed-ends becomes a major concern.

The method for determining the rotational ductility in the fixed-ends is described as follows:

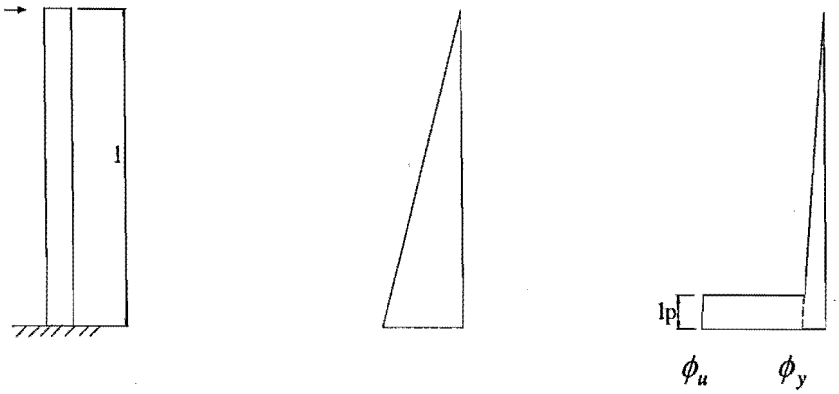

Cantilever Moment diagram Curvature distribution

(a) For a well-designed reinforced concrete cantilever column

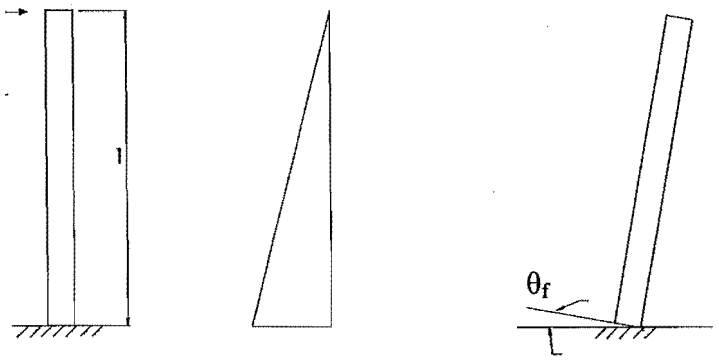

Cantilever Moment diagram Fixed-end rotation

(b) For an existing reinforced concrete cantilever column

Fig.6.10 Non-linear Deformation Characteristics of A Cantilever Column

Fig.6.10 illustrates the difference in the non-linear deformation characteristics for well-designed concrete members and existing concrete members, with reference to the cantilever column with a lateral load at the end.

For well-design reinforced concrete column, the lateral deflections at the top at the first yield and at the ultimate moment are respectively

$$\Delta_y = \frac{\phi_y l}{2}\frac{2l}{3} \qquad (6\text{-}1)$$

$$\Delta_u = (\frac{\phi_y l}{2}\frac{2l}{3}) + (\phi_u - \phi_y) l_p (l - l_p/2) \qquad (6\text{-}2)$$

where l = length of column and l_p = equivalent length of the plastic hinge.

The curvature ductility is

$$\mu_\phi = \frac{\phi_u}{\phi_y} \qquad (6\text{-}5)$$

The displacement ductility is

$$\mu_\Delta = \frac{\Delta_u}{\Delta_y} = 1 + (\frac{\phi_u - \phi_y}{\phi_y})\frac{l_p(l - l_p/2)}{l^2/3} \qquad (6\text{-}6)$$

For an existing reinforced concrete cantilever column, the lateral deflections at the top at the first yield is still estimated using equation 6-1, that is,

$$\Delta_y = \frac{\phi_y l}{2}\frac{2l}{3} \qquad (6\text{-}1)'$$

Theoretically, the total rotation over the full length of the column is

$$\theta_{y,theoretical} = \frac{\phi_y l}{2} \qquad (6\text{-}7)$$

However, the observed evidence is that the member flexural deformation prior to first yield is also lumped in the fixed-ends. Assuming that the total deformation is due to the rotation in the fixed-end at first yield, the rotation in the fixed end at first yield is

$$\theta_y = \Delta_y / l = \frac{\phi_y l}{3} \qquad (6\text{-}8)$$

The lateral deflection at the top at the ultimate state is calculated by allowing for the rotation in the fixed-end only, as observed from the tests, namely,

$$\Delta_u = \theta_f \, l \qquad (6\text{-}9)$$

Using the yield rotation given by Eq.6-8, the displacement ductility in this case is equal to the displacement ductility, that is,

$$\mu_\Delta = \frac{\Delta_u}{\Delta_y} = \frac{\theta_f l}{\theta_y l} = \mu_\theta \qquad (6\text{-}10)$$

Should the yield rotation be given by Eq.6-7, the resulting rotational ductility would be two-thirds the rotational ductility given by Eq.6-7. In this study, the yield rotation is calculated using Eq.6-8.

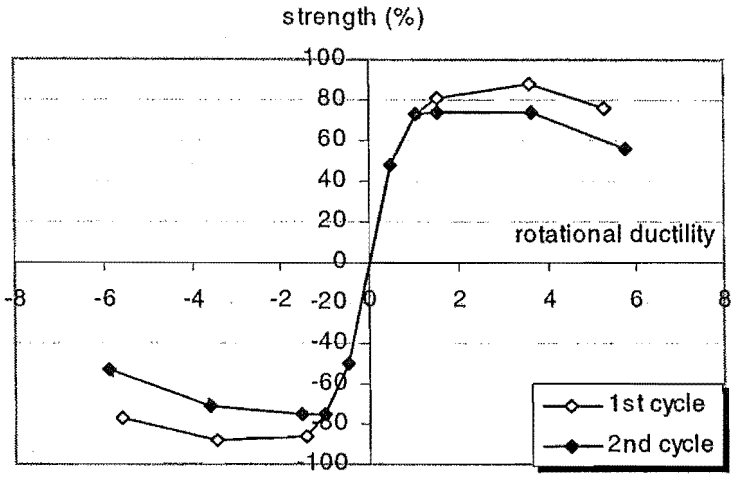

Fig.6.11 Measured column force strength versus the rotational ductility

Fig.6.11 shows the measured rotational ductility in column fixed-ends versus the measured column force strength for Unit 1. The attained column strength degraded at later stages as the deformation within column fixed-end regions increased. However a rotational ductility of 4 to 6 still can be achieved, although the columns were expected to behave in a brittle way.

6.1.4.3 Column Longitudinal Reinforcement Strains

As stated in Chapter 5, the column longitudinal reinforcement strains were monitored by both the electrical resistance strain gauges and the linear potentiometers.

1. Measurements by Electrical Resistance Strain Gauges:

The electrical resistance strain gauges behaved abnormally after the completion of displacement ductility factor of 1, so only the readings before the displacement ductility of 1 were studied here. It has to be pointed out that the electrical resistance strain gauge readings should be carefully explained in the case of severe bond degradation between the longitudinal steel and the concrete. Figs. 6.12 and 6.13 show the measured strains along the column longitudinal reinforcement by electrical resistance strain gauges for column bars 1 and 2 of Unit 1.

Figs. 6.12 and 6.13 show that the measured column reinforcing steel strains outside the joint region increased gradually as the test progressed due to the corresponding increase in

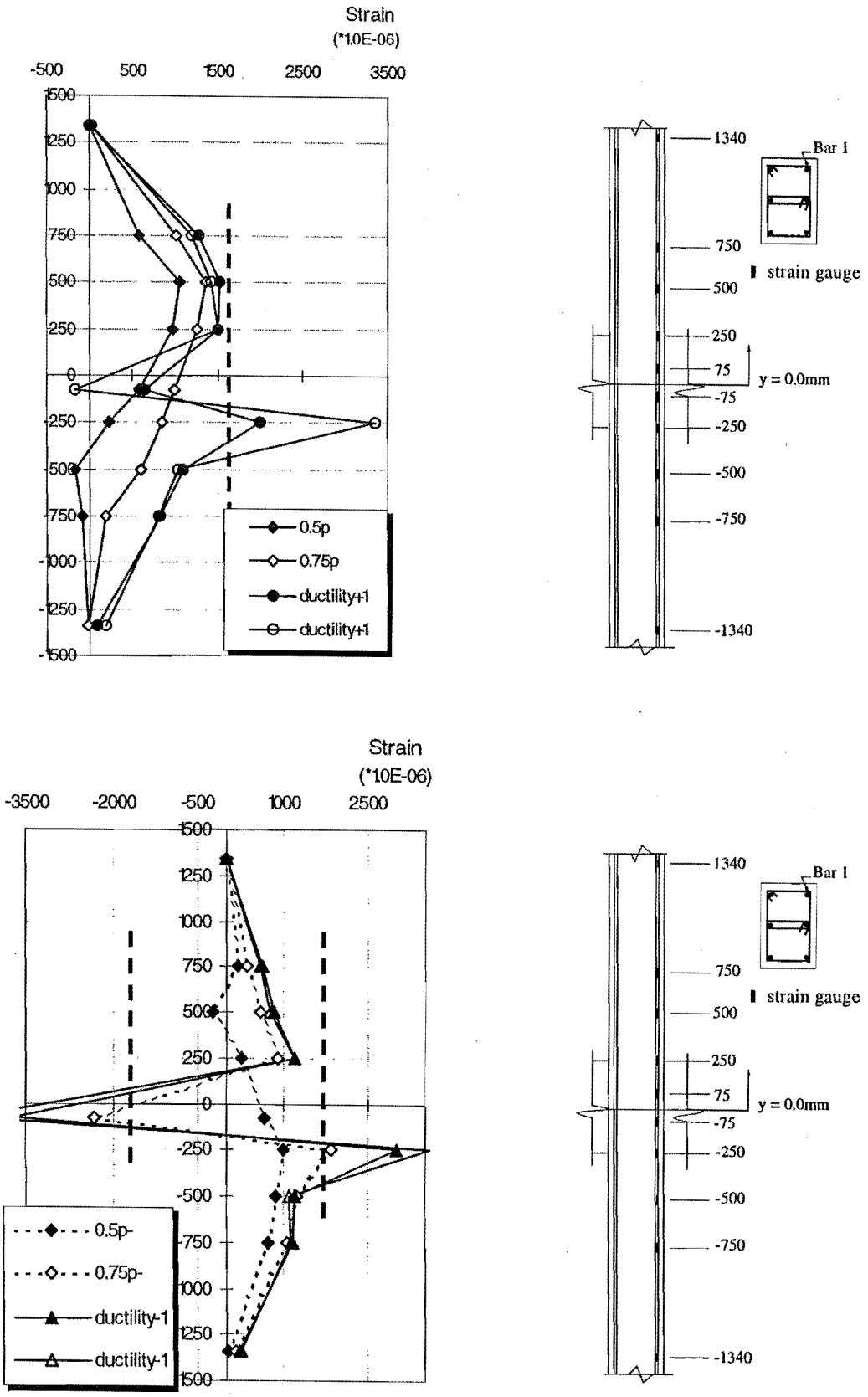

Fig.6.12 Measured Strain Profile for Column Bar 1 of Unit 1

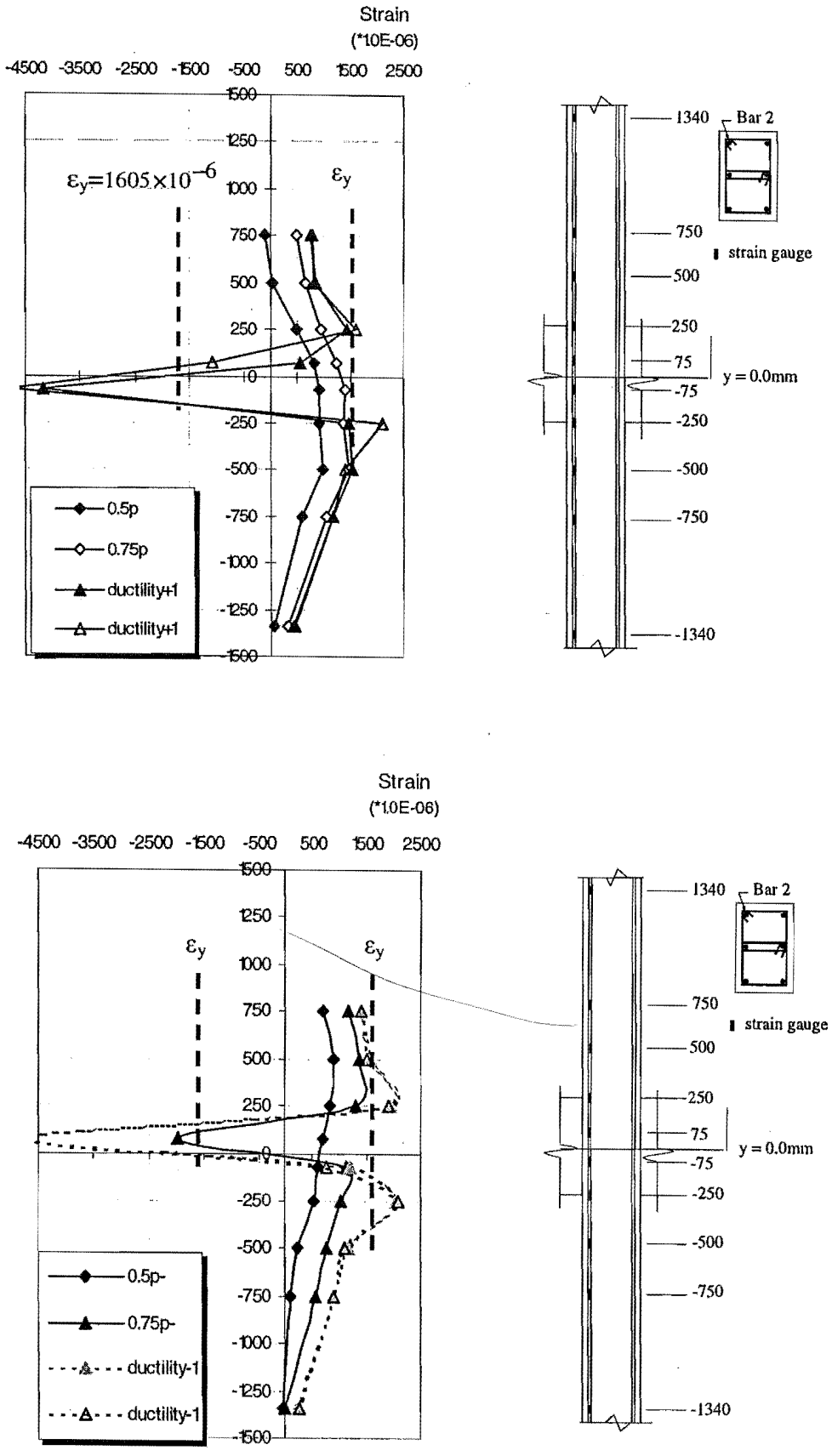

Fig.6.13 Measured Strain Profiles of Column Bar 2 of Unit 1

the imposed bending moment, and the column longitudinal steel strain distribution along the column longitudinal axis agreed with the imposed bending moment distribution. However the column longitudinal reinforcing steel strain profiles within the joint region displayed abnormal behaviour as the test progressed, and were characterised by the following features within the joint region:

- Severe bond degradation along column longitudinal reinforcing bars within the joint.

Figs. 6.12 and 6.13 demonstrate that severe bond degradation took place along the column longitudinal reinforcing bars within the joint region even at very early loading stages. As early as the loading stage of $0.5V_i$, the column longitudinal reinforcement had been in tension throughout the whole joint region due to inadequate bond strength within the joint region.

Compared to the test on an identical interior beam-column joint unit which used deformed bars [H1] where the column bars of the test unit were anchored at the opposite beam face (equal to 500 mm) at the loading stage of $0.5V_i$, the column bars of Unit 1 were observed to be anchored in the opposite column at a distance of about 1100mm from the considered beam face at the loading stage of $0.5V_i$, indicating that plain round bars require much longer anchorage length than that associated with the deformed bars. Severe bond degradation along the plain round longitudinal bars within the joint core caused very large column fixed-end rotations, greatly contributing to the enlarged first yield displacement.

- Discrepancies between the measured steel strains and the predicted steel strains

Figs 6.12 and 6.13 show that big discrepancies exist between the measured steel strains and the predicted steel strains along both flexural tensile bars and flexural compressive bars. The discrepancies for the flexural compression bars were obvious, and the column main bars on the flexural compression side were actually in tension at the beam face as a result of severe bond degradation and bar slip along the reinforcing bars within the joint core. The measured column flexural tension steel strains were generally larger than the theoretical ones. For example, the measured column flexural tension steel strains at beam faces reached yield at the displacement ductility of 1 while the imposed bending moment on this section was only about 80% of column theoretical yield strength. This once again illustrates that plane section assumption made in conventional flexural theory was violated due to severe bond degradation along the longitudinal reinforcement. However, when

compared with the measured curvature properties, the discrepancies for the measured steel stresses were much smaller.

However, it is to be realised that the maximum steel stress could not exceed steel yield strength, therefore the above evidence means that severe bond degradation due to the use of plain round reinforcing bars would cause the available strengths to be lower than the theoretical flexural strengths as was seen in the test of Unit 1. This is very important in assessing the available strength of existing reinforced concrete structures.

The above-described discrepancies will affect the estimation of the joint shear inputs because the joint vertical shear force input is estimated using plane section assumption on the basis of the column shear force and the estimated column flexural steel tension forces at beam faces. Bond degradation along the reinforcing bars within the joint core would cause the flexural compression steel force to be in tension, greatly reducing the joint shear input, but the larger measured steel strains caused by bond degradation would cause the joint shear input to increase. Evidently, the estimation of the actual joint shear inputs should take these two factors into account.

- Occurrence of column bar buckling

Figs. 6.12 and 6.13 also show the evidence of column bar buckling within the joint region after the loading cycle to $0.75V_i$. It was observed that the column reinforcing bars 1 and 2 were in tension throughout the whole joint region up to the loading to $0.75V_i$, but turned to be in significant compression in the lower part of the joint region after the completion of the loading to 0.75 V_i irrespective of the loading directions. Apparently, the remaining bond strength within the joint region after the loading to 0.75 V_i was not high enough to convert the column steel tension forces at beam face into such large compression forces, and it was local column bar buckling that caused the column bars to be in significant compression on the face with the gauges.

Hence it is concluded that, although the test of Unit 1 was conducted with zero axial column load, column bar buckling did occur at the later loading stages of the test due to inadequate amount of column transverse reinforcement, as predicted in Chapter 4 "Theoretical Consideration".

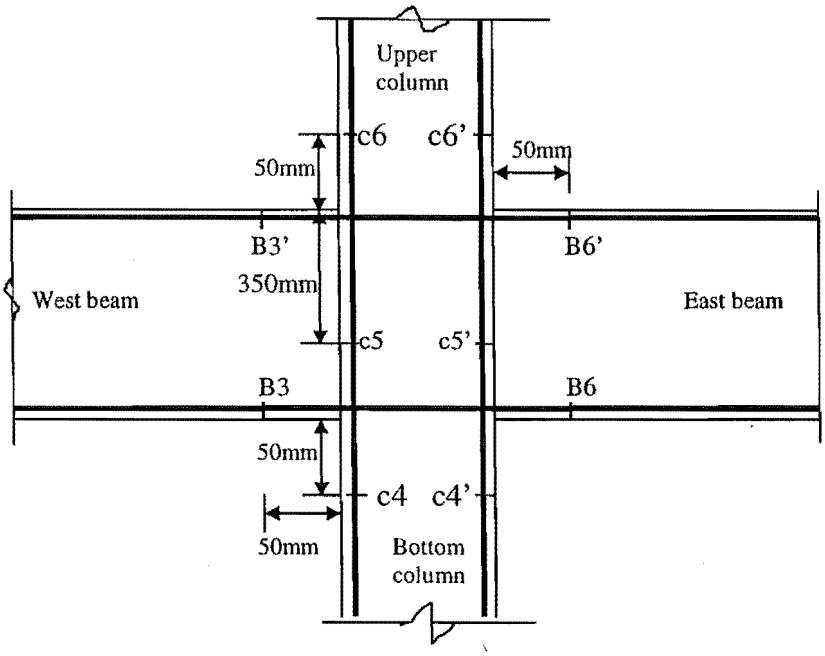

Fig. 6.14 Linear Potentiometers to Measure Column and Beam Bar Slip for Unit 1

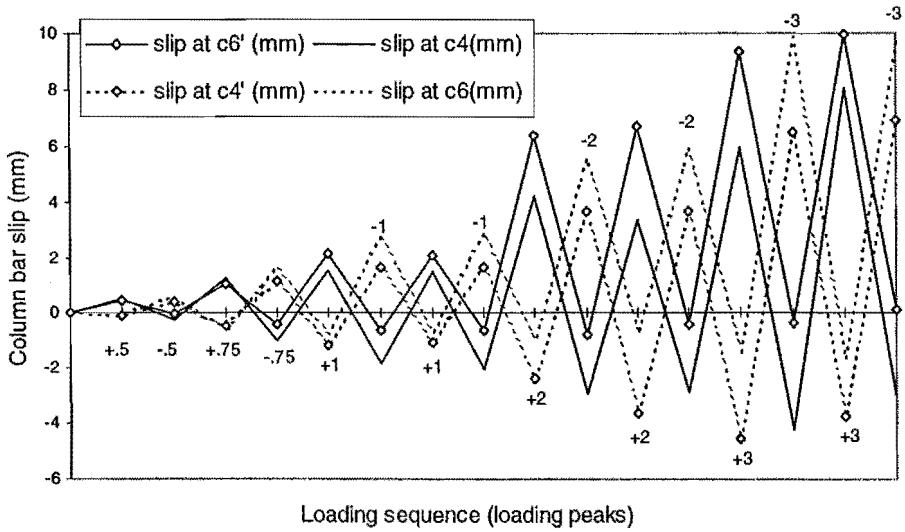

Fig. 6.15. Column Bar Slip Measured by Linear Potentiometers (mm)

2. Column Bar Slip Measured by Linear Potentiometers

Column bar slip within the joint core was found according to the measurements of linear potentiometers mounted on the steel rods welded on the column main bars, and this estimation is valid only if the joint core concrete deformation is negligible. The

instrumentation for estimating column bar slips is shown in Fig.5.13. The slips of the column bars at points c5 and c5' relative to the static point embedded in the concrete were estimated at first, the slips at points c6, c4, c6' and c4' can be found by adding the measured deformations at these points relative to the points c5 or c5' then. This is graphically demonstrated in Fig. 6.14.

Fig. 6.15 shows the column bar slips within the joint region estimated for Unit 1. The maximum slips measured for column bars within the joint core for Unit 1 were as much as 10 mm. This means that the use of plain round reinforcing bars led to very significant column bar slips within the joint core, then very large member fixed-end rotations.
Evidently a proper method for calculating the first yield displacement should take into account the estimation of fixed-end rotations.

6.1.4.4 Column Transverse Reinforcement Strains

The measured column transverse reinforcement strains were all well below the steel yield strain. This was because the use of plain round reinforcing bars actuated mainly arch action in resisting shear as described previously, and the transverse reinforcement does not engage in resisting shear in this case. Therefore the members reinforced by plain round bars are not shear critical and this is different from the case with deformed bars.

6.1.5 Beam Behaviour

6.1.5.1 Beam Curvature Distribution

Figs.6.16 shows the measured beam curvature profiles monitored using the methods described in Section 5.5.2. The positive and negative beam curvatures were defined to be induced by positive and negative beam bending moments, respectively, and the theoretical negative and positive beam curvatures at first yield are also shown. During testing, the beams of Unit 1 were theoretically expected to be in the elastic range.

The measured beam curvature behaviour generally has similar characteristics to the columns.

As shown in Fig.6.16, beam deformation was observed to be mainly in their fixed-end regions and the beam curvature over the fixed-end regions was very large, although the

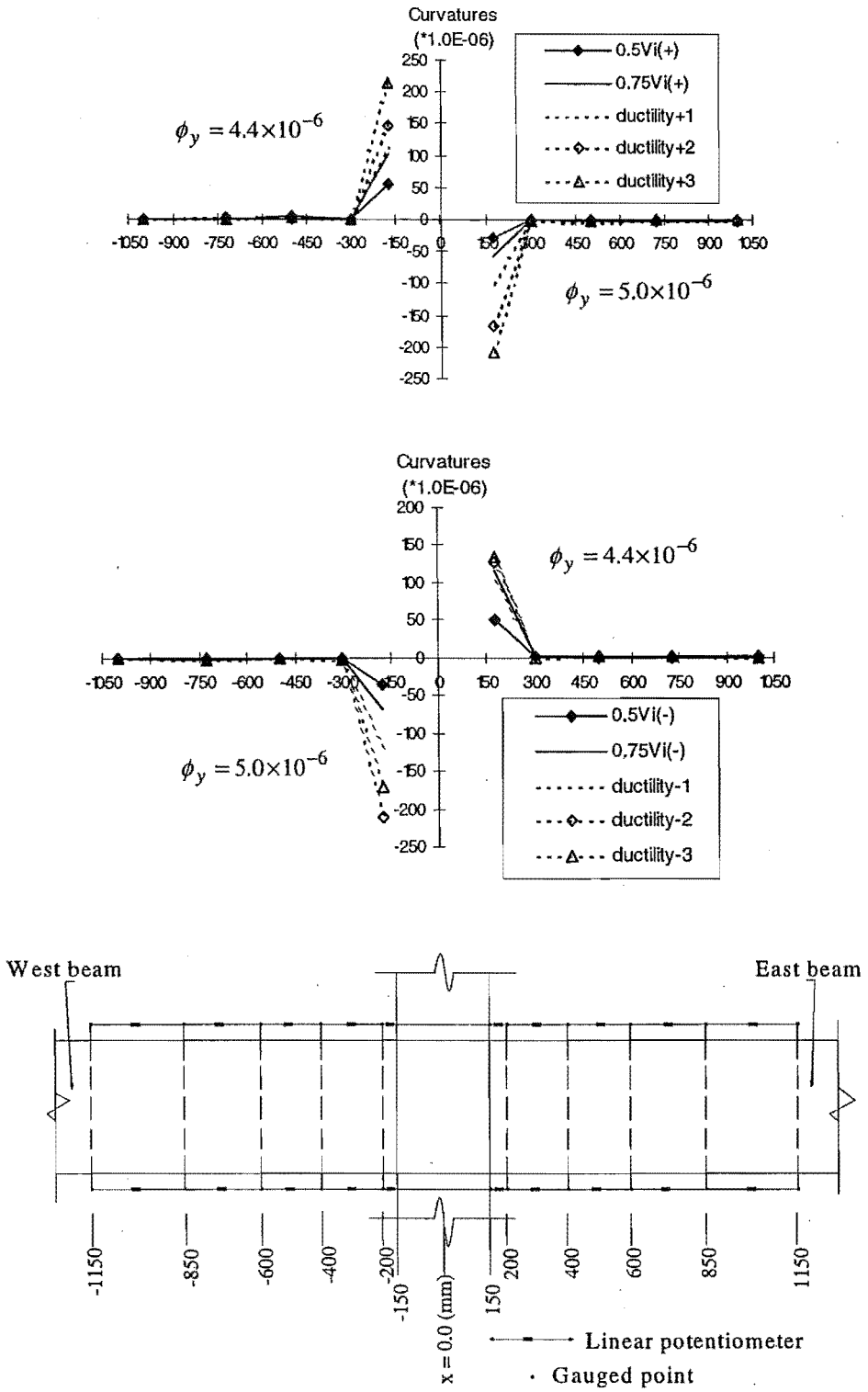

Fig.6.16 Beam Curvature Profile of Unit 1

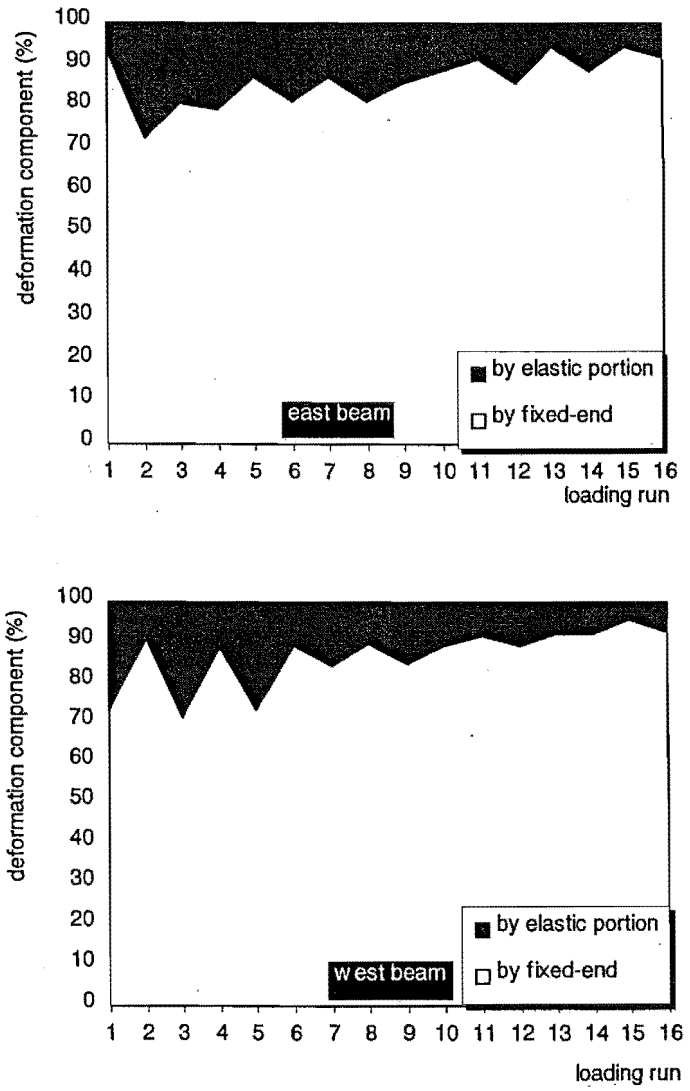

Fig.6.17 Beam deformation components measured for Unit 1

beams were expected to be in elastic range. This occurred due to significant bond deterioration of the beam bars within the joint region. Fig.6.17 shows the decomposition of measured beam deformation. Apparently, the deformation over the beam fixed-end regions can be adequately approximated to be the total beam deformation, even when the beams were supposed to be in elastic range.

Significant discrepancies exist between the measured beam curvatures and the theoretical predictions as revealed by the measured column curvature distributions for this test and the discrepancies were especially significant within beam fixed-end regions. The measured

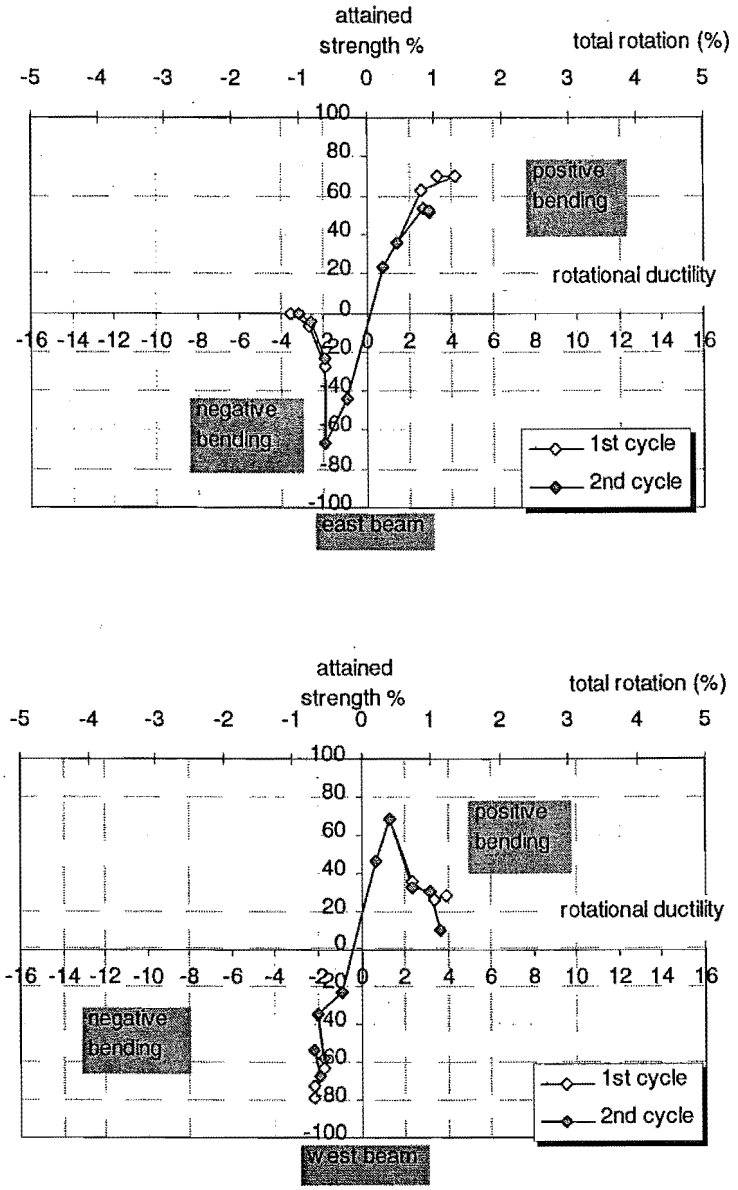

Fig.6.18 Beam rotational ductility versus attained force strength

beam curvatures over beam fixed-end regions in the first elastic loading cycle reached more than 20 times higher than the theoretical predictions, see Fig.6.16.

In addition, Fig. 6.17 shows the gradual decrease in the measured beam curvatures for Unit 1 with the loading progress, indicating that the beam failure did not initiate the final failure of the unit, as anticipated.

Fig.6.18 shows the measured rotational ductility in beam fixed-ends versus the beam force strength expressed as the percentages of the theoretical beam force strength at the

development of theoretical beam flexural strength. The beam deformation was by far beyond their theoretical yield deformation and the rotational ductility reached as high as 4, although the beams were expected to be in elastic range.

6.1.5.2 Beam Longitudinal Reinforcement Strains

The beam longitudinal reinforcement strains were monitored for Unit 1 by electrical resistance strain gauges as described in Section 5.2.5.1.

Figs. 6.19, 6.20 and 6.21 show the beam longitudinal steel strain profiles measured by electrical resistance strain gauges. Generally the recorded steel strains along the beam longitudinal bars had the similar features to the column longitudinal bars.

1. Better agreement between the measured beam steel strains and the imposed bending moments was seen, compared to the beam curvature properties. The measured beam flexural steel strains, although generally larger than the theoretical values predicted assuming plane section theory as was the case for the column bars, varied linearly from the column face toward the beam pin end as was the case for the imposed beam bending moment. For instance, the measured beam flexural tension steel strain at the column face was 0.00145 at the peak of the first clockwise displacement ductility 1 and this was 1.4 times the theoretical strain which was predicted using plane section theory and the measured west beam lateral load at this specific stage. However the measured curvature in beam fixed-ends reached up to 20 times the theoretical predictions. The amplification of the measured beam flexural steel strains was not caused by tension shift because of no observed diagonal tension cracks in the beams and columns, and it was due to the violation of plane section assumption by severe bond degradation along the flexural reinforcing bars. Severe bond degradation along the flexural reinforcing bars caused the longitudinal bars in the flexural compressive side not to be so effective in resisting compression as predicted, leading to larger demand on the concrete compressive force. As a result, the concrete compressive depth increases and the lever arm becomes smaller, leading to lower flexural strengths, when compared to the theoretical values.

2. Even at very early loading stage of $0.5V_i$, the beam flexural compression bars were actually in tension in the region adjacent to and within the joint region due to severe bond degradation along the beam longitudinal bars within the joint region. This is seen from Fig. 6.19 to Fig.6.21.

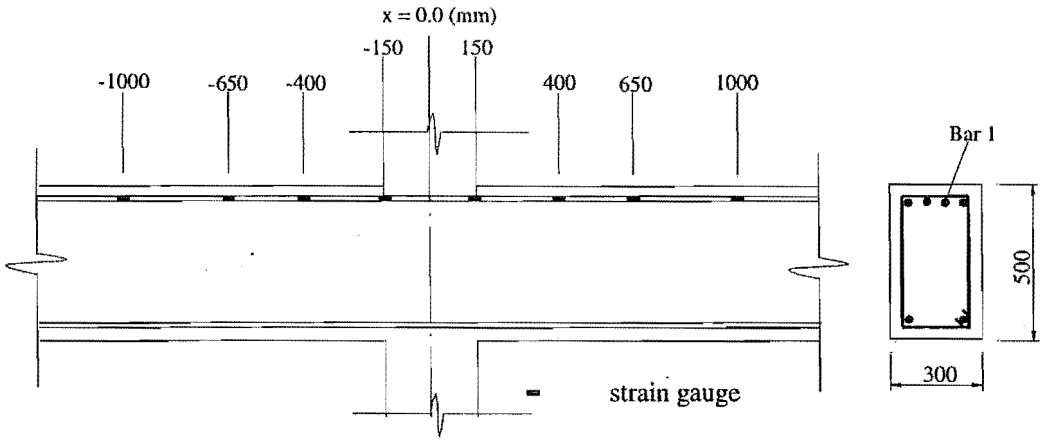

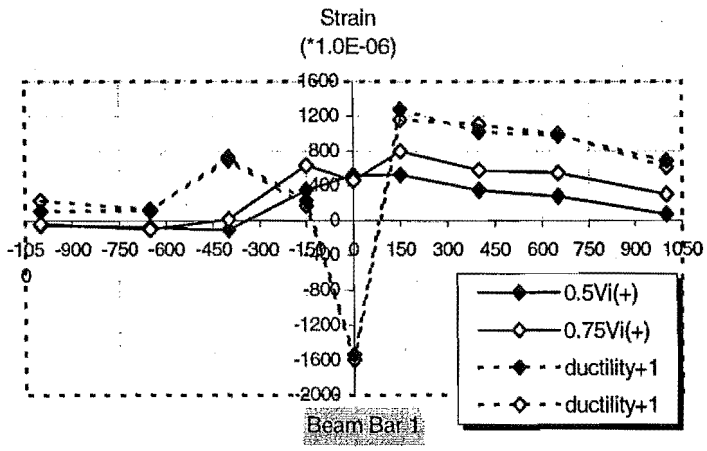

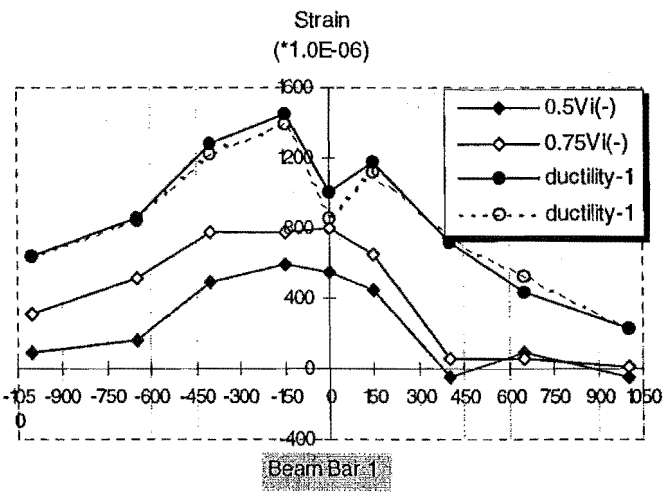

Fig. 6.19 Strain Profile of Beam Bar 1 by Electrical Resistance Strain Gauges

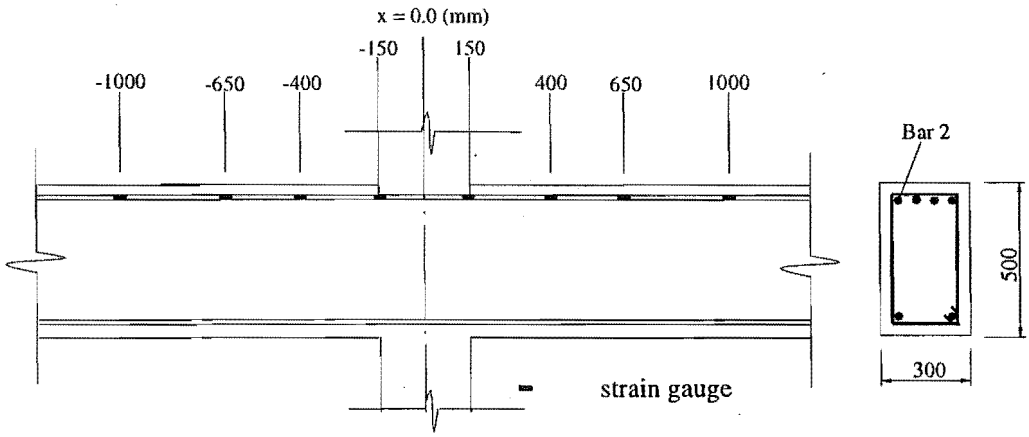

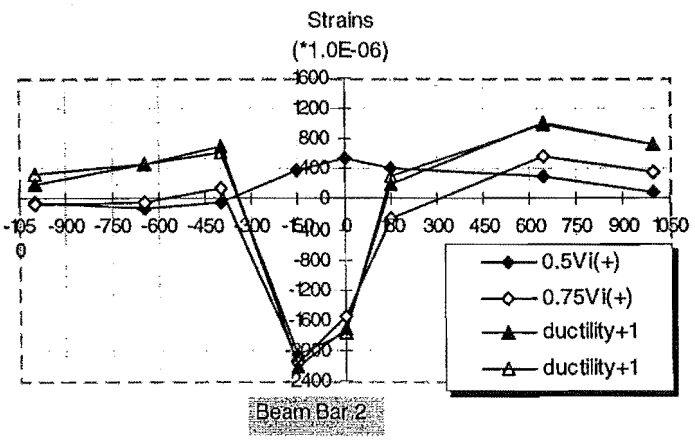

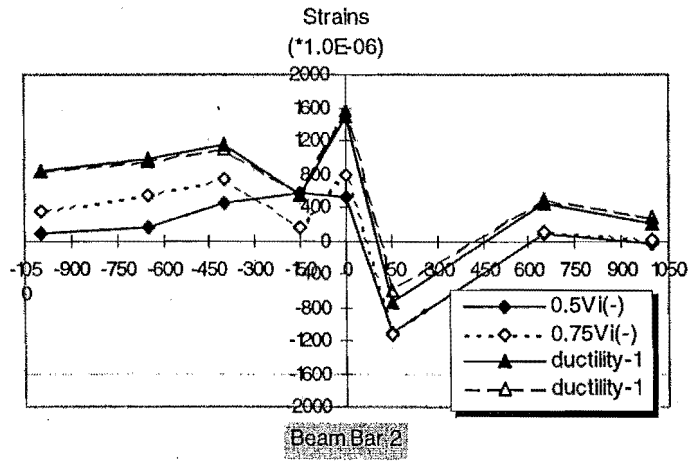

Fig.6.20 Strain profile of Beam Bar 2 by Electrical Resistance Strain Gauges

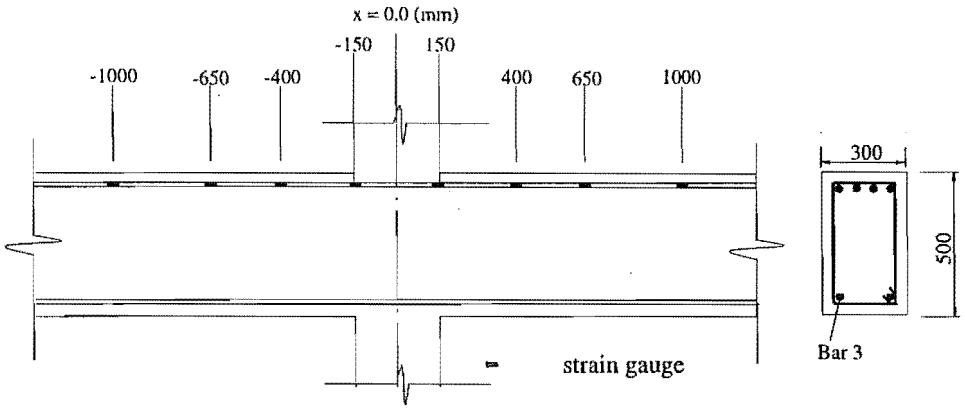

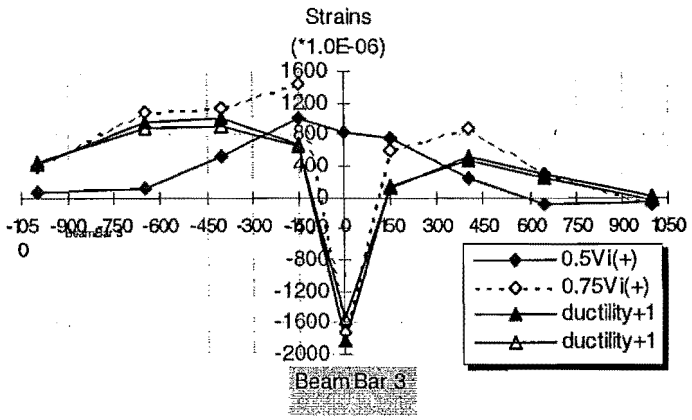

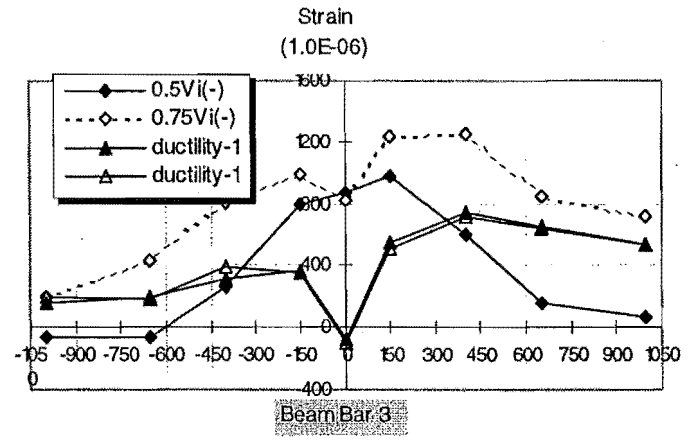

Fig.6.21 Strain Profiles of Beam Bar 3 by Electrical Resistance Strain Gauges

3. The measured beam steel strains were generally not larger within the joint core than those at the column faces, indicating that the beam flexural steel did not engage in the joint shear resisting mechanism. This evidence is different from the test observation of Hakuto's Unit O1, hence the joint shear mechanism associated with plain round bars was different from that associated with deformed bars.

6.1.6 Joint Behaviour

Fig. 6.22 illustrates the joint shear distortion γ_j and expansion $\frac{1}{2}(\delta_j + \delta_{j'})$ estimated using the method as described in Section 5.2.4. Theoretical considerations shows that the joint shear capacity was only 55% the maximum shear demand at developing the theoretical strength of the system.

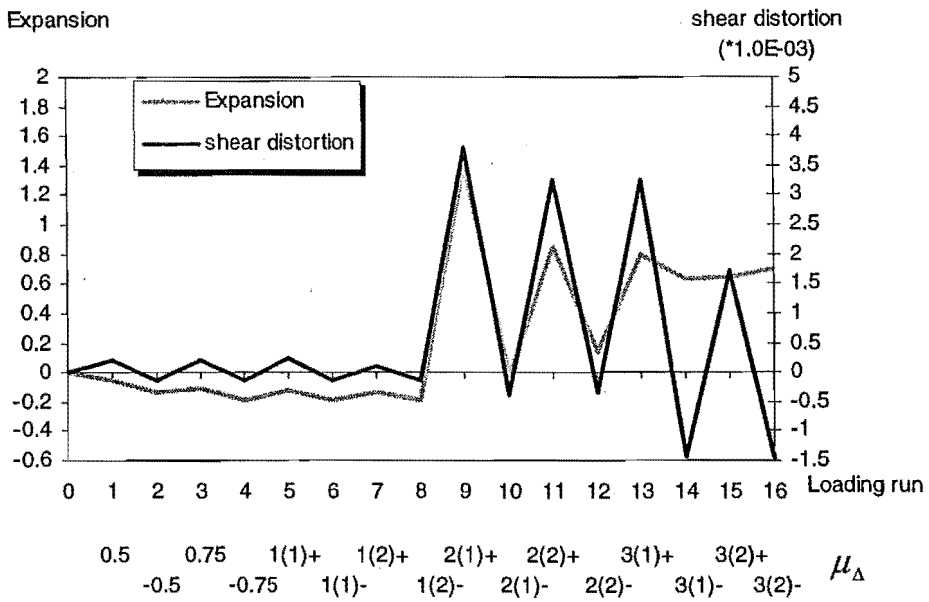

Fig. 6.22 Joint Shear Distortion and Expansion of Unit 1

The joint diagonal tension cracks initiated at the first clockwise ductility of 2, and this was also the stage of the attainment of the maximum force strength of Unit 1. The estimated nominal horizontal joint shear stress based on plane section theory at this stage was 3.2MPa, or $0.5\sqrt{f_c'}$ MPa for Unit 1. A common approach to assess the shear capacities of

beam-column joints without shear reinforcement at the stage of diagonal tension cracking of the joint cores is to use Mohr's circle for stress, and assume perfect bond and the diagonal tension strength of concrete of $0.3\sqrt{f_c'}$ MPa. This gives that the joint shear strength at developing the joint diagonal tension cracking, in terms of the nominal horizontal joint shear stress, is $0.3\sqrt{f_c'}$ MPa in the case without axial column load. Hence, the joint shear capacity measured for Unit 1 at diagonal tension cracking of the joint core was 1.7 times the theoretical prediction, indicating that the use of the above method derived from the cases with deformed longitudinal reinforcement would significantly underestimate the joint shear strength of existing reinforced concrete structures reinforced by plain round longitudinal bars.

Although rapid increases in the joint shear distortion and expansion was observed after the development of joint diagonal tension cracks, subsequent loading cycles caused gradual decreases in the measured joint shear distortion and expansion as seen in Fig. 6.22. Hence the joint shear performance did not govern the seismic performance of the test unit, although the theoretical assessment in Chapter 4 predicted very inadequate joint shear capacity, indicating that the current method for assessing the joint shear capacity cannot be used for existing beam-column joint with plain round longitudinal bars. Rapid increases in the joint shear distortion and expansion after the development of joint diagonal tension cracks were because joint diagonal elongation and expansion are mainly controlled by the joint shear reinforcement after joint tension cracking but the joint core of Unit 1 had no shear reinforcement.

The observed joint behaviour of Unit 1 is compared with that for Hakuto's Unit O1, which was identical to Unit 1 except the use of deformed reinforcing bars. Whereas in the case of Hakuto's Unit O1, the final failure was attributed to the joint shear failure, the observed joint performance for Unit 1 was excellent until the test completion. The attained maximum nominal horizontal joint shear stresses were $0.5\sqrt{f_c'}$ MPa or $0.075 f_c'$ MPa, for Unit 1, and $0.61\sqrt{f_c'}$ MPa or $0.095 f_c'$ MPa for Unit O1, and the induced maximum joint shear distortions were 0.37% for Unit 1 and 0.77% for Unit O1. Much improved joint shear performance of Unit 1 compared to Hakuto's Unit O1 was due to a much enhanced

joint concrete strut for Unit 1 resulting from severe bond degradation along the main beam bars.

Bearing in mind that bond degradation caused the actual steel stresses to be larger than the theoretical predictions, it could be concluded that the actual joint shear input may be larger than the theoretical predictions employed in the estimation of the nominal horizontal joint shear stress for Unit 1. Hence the attained maximum nominal horizontal joint shear stress or the attained nominal horizontal joint shear stress at developing joint diagonal tension cracking of Unit 1 may be actually larger than $0.5\sqrt{f_c'}$ MPa or $0.075\,f_c'$ MPa.

In a word, the use of plain round longitudinal reinforcement actually enhanced the joint concrete strut mechanism, leading to much improved joint shear performance. The current method, which was derived from limited tests with deformed longitudinal bars, would not give adequate prediction when used for assessing the joint shear capacity of existing reinforced concrete beam –column joints with plain round longitudinal bars.

6.1.7 Displacement Components

Fig. 6.23 illustrates the measured displacement components for the test of Unit 1 at the peaks of the loading cycles, in terms of percentages of the measured storey displacement. The methods for the estimations of displacement components were described in Section 5.5.

Figure 6.23 shows that the system deformation was mainly from the column fixed-end rotation. The contribution of the column fixed-end rotation to storey drift increased as the loading progressed, and reached up to about 81% of the storey drift at the final loading stages. In comparison, contributions of column flexural deformations outside the column fixed-end regions to storey drift were very small, only about 8% of the total storey drift at the final loading stages. In comparison, the contributions of the column fixed-end rotations and column flexure to the total storey displacement measured for Hakuto's Unit O1 were about 25% and 30% respectively. Evidently, the use of plain round longitudinal reinforcement resulted in significant concentration of member flexural deformation on the member fixed-ends, especially in the fixed-ends of weaker members.

The contribution of the beam deformation to the storey drift was small and fairly constant, and was about 10% throughout the whole loading history. In contrast, the beam displacement contribution measured for Hakuto's Unit O1 was about 22%, and it was also fairly constant.

The contribution of the joint deformation to the total storey drift reached its maximum value of about 7% of the total storey displacement at the stage of displacement ductility of 2 where the maximum storey force strength of the test unit was achieved, and it decreased at the later loading stages, indicating that the joint condition did not deteriorate as the loading progressed. In comparison, the displacement component of joint deformation measured for Hakuto's Unit O1 kept increasing as the loading progressed, and the maximum contribution of the joint deformation accounted for 31% of the total storey drift. This illustrated that bond deterioration along the longitudinal bars within and adjacent to the joint core of Unit 1 greatly enhanced the joint shear behaviour.

This meant that, when plain round reinforcement is used, the shear performance in the joint and the members is greatly enhanced and the current methods would significantly underestimate the shear capacity of the members and the joint. In this case, the deformation of the system is significantly concentrated in the fixed-ends of the weaker linear members.

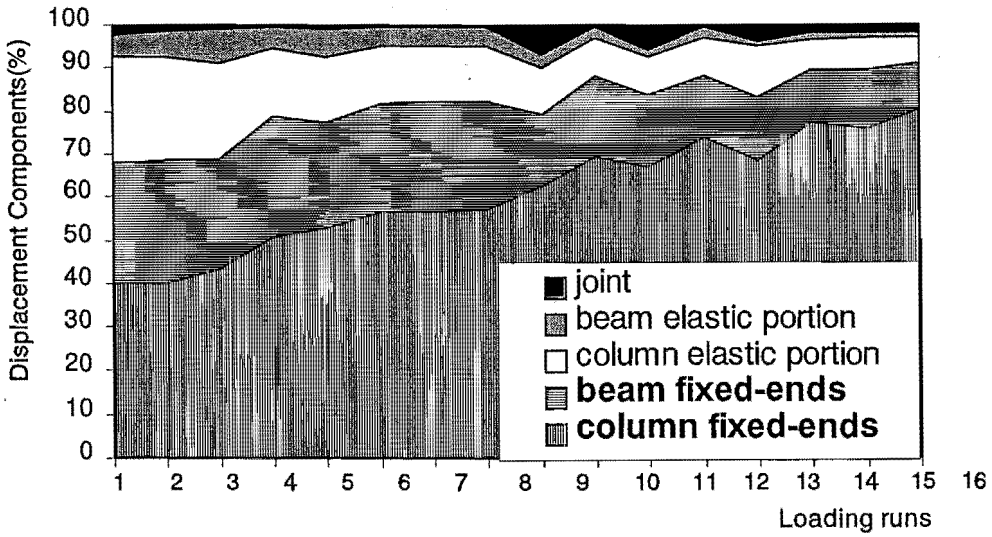

Fig. 6.23 Displacement Components of Unit 1

6.2 TEST OF UNIT 2

6.2.1 Introduction

As-built full-scale interior beam-column joint Unit 2 was identical to Unit 1 and it was tested under simulated seismic loading with the existence of a compressive axial column load of $0.12 A_g f_c^{'}$ in order to investigate the influence of the compressive axial load.

According to the theoretical considerations conducted in Chapter 4, Unit 2 was an expected marginal weak beam-strong column mechanism (the beam and column flexural strengths were almost identical, see Table 4.5). Theoretically, the quantities of transverse reinforcement in the beams and the columns were very inadequate for preventing bar buckling and resisting shear and the joint shear force capacity was also very inadequate. In addition, bond degradation along the longitudinal bars would be expected within the joint region due to larger diameter of the longitudinal reinforcement passing through the joint. Column bar buckling was anticipated to be more significant for Unit 2 than that for Unit 1.

6.2.2 Cracking and Damage

The appearance of Unit 2 at the end of testing is shown in Fig. 6.24.

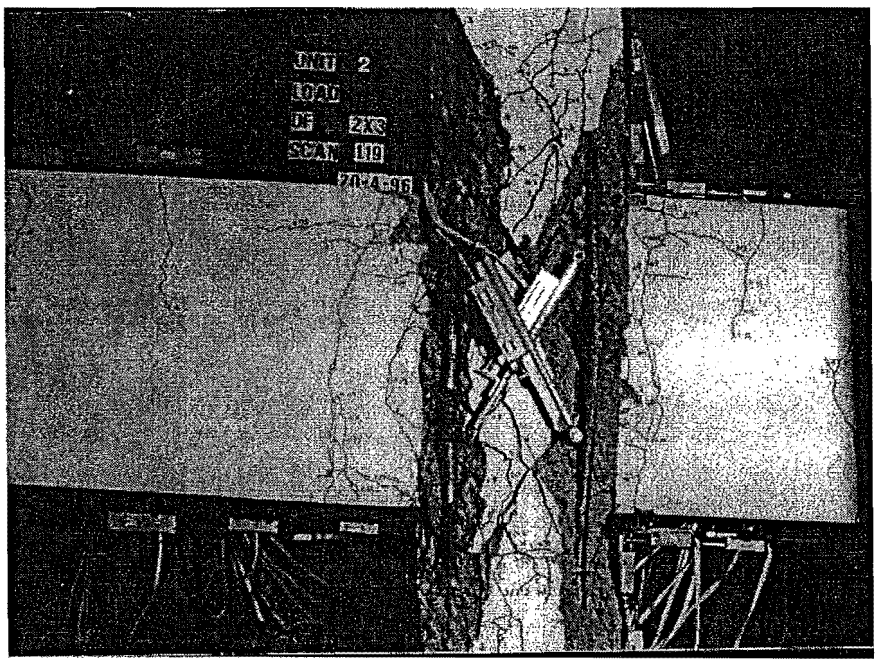

Fig.6.24 Final Appearance of Unit 2

Whereas in the case of Unit 1 the damage concentrated mainly in the columns and the column displacement component contributed as much as 90% of the total storey deflection at the final loading stage, the damage caused to Unit 2 spread throughout the whole test unit in the vicinity of the joint core. The measured column displacement component was 57% of the total storey deflection while the joint and beam displacement components contributed about equally to the rest of the total storey deflection at the final testing stage of Unit 2.

The damage to the columns of Unit 2 concentrated in the areas adjacent to the joint core as a result of concrete spalling caused by severe buckling of the column longitudinal bars which was associated with significant bar slip and the existence of the compressive axial column load. The damage to the columns progressed with the loading progress, indicating that the column failure triggered the final failure of the unit. The damage to the beams concentrated in the wide beam flexural cracks adjacent to the joint core, and it did not progress during later loading stages, indicating that beam failure did not trigger the final failure of this theoretically marginal weak beam-strong column system. The damage in the joint core was by way of extensive diagonal tension cracks. The compressive axial load on the columns enhanced the transmission of longitudinal beam bar forces to the joint region through bond. Bond force induced shear flow type of forces, leading to more concrete diagonal cracks in the joint core. In addition, the enhanced column bar buckling adjacent to the joint core due to the compressive axial load on the columns led to extensive concrete spalling adjacent to and within the joint core, weakening the joint force strength and increasing the joint deformation. As a consequence, the contribution of the joint core deformation to the total storey drift was much bigger, compared with the test of Unit 1. The damage to the joint core of Unit 2 progressed as the test progressed and the joint shear failure also attributed the final failure of the unit. Evidently, the observed joint shear behaviour is different from that where deformed longitudinal reinforcement is used. For instance, NZS3101: 1995 recognises the beneficial effect of the compressive column axial load on the joint shear strength. According to NZS3101: 1995, the joint performance of Unit 2 would be better than that of Unit 1.

As was the case in the test of Unit 1, no diagonal tension cracks were observed in the beams and columns of Unit 2 throughout the test, indicating that transverse reinforcement

in the members reinforced by plain round bars was more needed for preventing bar buckling than for providing shear strength.

In a word, column bar buckling, which was more significant for Unit 2 than for Unit 1 due to the compressive column axial load for Unit 2, initiated the final failure of Unit 2. Column bar buckling enhanced the failure of the columns and enhanced the damage to the joint core, facilitating the premature failure in the vicinity of the joint core of Unit 2.

6.2.3 Hysteretic Response

Fig. 6.25 shows the storey (horizontal) shear force versus storey (horizontal) displacement hysteresis loops for Unit 2. The measured hysteresis loops for each individual beam, in terms of beam shear and vertical displacement at beam end, are shown in Figs. 6.26 and 6.27 respectively. The measured hysteresis loops for Unit 2 in Figs. 6.25 to 6.27 confirm that the existence of the compressive axial column load could not improve the general performance of the test unit.

The measured first yield displacement for Unit 2 was equivalent to a storey drift of 2%, and this was about 2.6 times the theoretically predicted first yield displacement. The theoretical first yield displacement was predicted based on sectional moment- curvature analysis and assuming that the columns were in the elastic range and the beams just reached the first yield. The measured first yield displacement for Unit 2 was comparable with that for Unit 1. Hence, the existence of the compressive axial column load in Unit 2 did not improve the structural stiffness behaviour even for this initial weak column-strong beam unit and this disagreed with the observations made with deformed bars by Beres, White and Gergely in 1992 [B3, B4]. The compressive axial column load for Unit 2 did improve severe slip of longitudinal beam and column bars through the joint, reducing the contributions of beam and column deformations to the total storey deflection. At the same time, the compressive axial column load enhanced the column bar buckling in the vicinity of the joint panel and enhanced the beam steel force transfer by bond within the joint region, resulting in more joint diagonal tension cracks and thus a greater contribution of joint deformation to the total storey drift.

Significant pinching is observed in Figs.6.25 to 6.27. This occurred due to bar slip along the longitudinal reinforcement, premature column bar buckling and extensive joint diagonal tension cracking.

As shown in Figure 6.25, the maximum strength reached by Unit 2, which occurred in the first loading cycle at a storey drift of 2%, was 23% less than the theoretical strength of 128 kN for the unit. This can be compared with the test of Unit 1 where the achieved maximum strength at a storey drift of 2% was 15% less than the theoretical prediction. The lower percentage of the available force strength reached by Unit 2 was because the failure trigger, column bar buckling, was more severe for Unit 2 due to the presence of compressive axial column load and to the small amount of column transverse reinforcement.

The strength degradation after the maximum strength was attained, demonstrated by test of Unit 2 in Fig.6.25, was more significant, compared with that of Unit 1 in Fig. 6.2. This was again because the column bar buckling was accelerated by the existence of the compressive axial column load.

Compared with the test of Unit 1, pinching observed for test of Unit 2 in Figures 6.25 to 6.27 was more significant, the presence of the compressive column axial load caused earlier attainment of the maximum force strength of the unit, but more rapid strength degradation as reported in 1992 by Beres, White and Gergely [20, 21].

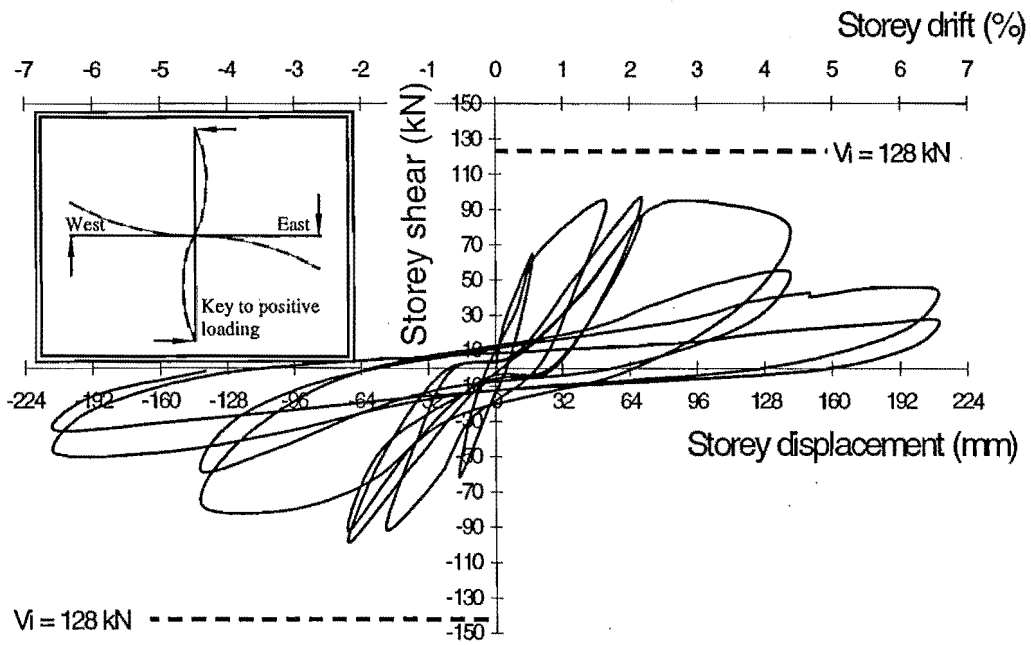

Fig. 6.25 Storey Shear versus Storey Displacement Hysteresis Loops of Unit 2

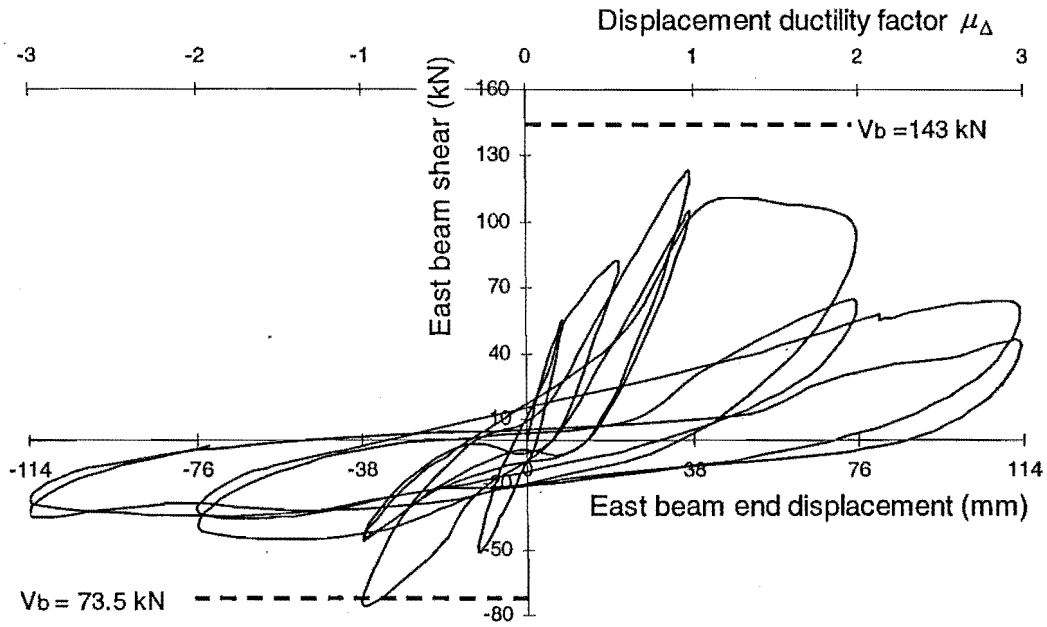

Fig.6.26 Hysteresis Loops of East Beam of Unit 2

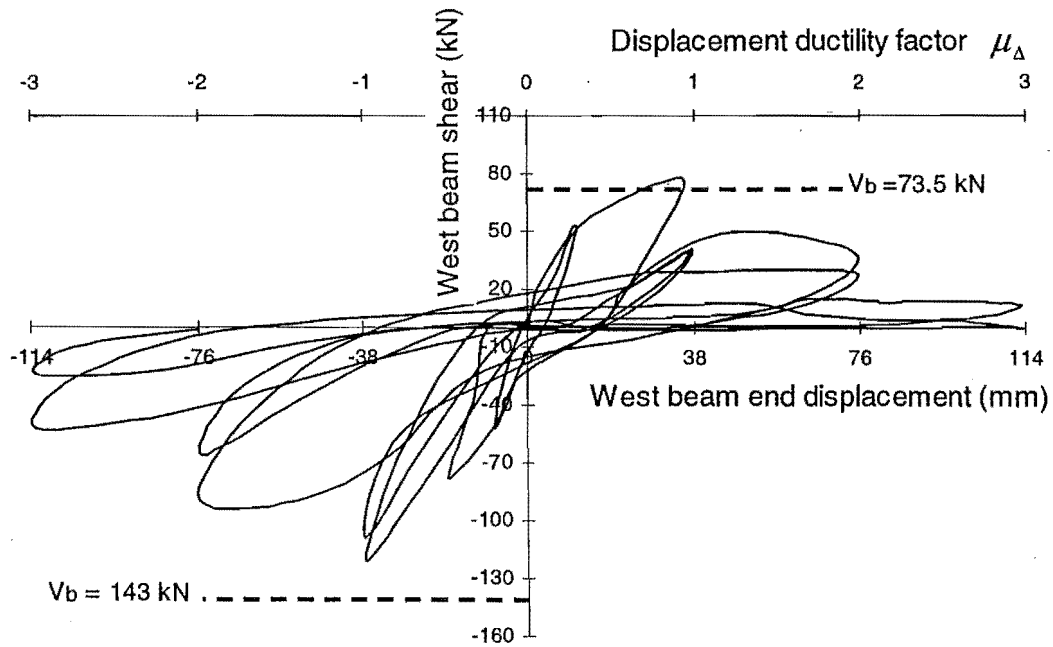

Fig. 6.27 Hysteresis Loops of West Beam of Unit 2

6.2.4 Column Behaviour

6.2.4.1 Column Curvature Distribution

Fig.6.28 illustrate the measured column curvature distributions using linear potentiometers for Unit 2, where the sign conventions were the same as for Unit 1. The theoretical column curvatures at first yield after taking the effect of axial column load into account are $10.7\times10^{-6}(mm^{-1})$ for either loading direction. Columns of Unit 2 were expected to be in elastic range.

The observed column curvature profiles for Unit 2 as illustrated in Fig.6.28 shows similar characteristics to Unit 1. Column deformation was mainly limited to the fixed-end regions.

The discrepancies also existed between the measured column curvatures and the theoretical column curvatures calculated based on plane section theory. The measured column curvatures in the column fixed-end regions at the loading peak to $75\%V_i$ were more than 7 times the theoretical prediction based on plane section assumption, demonstrating significant violation of plane section assumption. Hence, even for the members, which theoretically should respond in the elastic range, the member curvature properties would deviate significantly from the theoretical predictions when severe bond degradation occurred.

6.2.4.2 Column Longitudinal Reinforcement Strains

Figs.6.29 and 6.30 show the column longitudinal reinforcement strains monitored by the electrical resistance strain gauges for Unit 2.

The column longitudinal reinforcement strain profiles measured for Unit 2 show very severe bar buckling along the column flexural tension bars of Unit 2 as described in Section 6.2.2 "cracking and damage". Column bar buckling occurred in Unit 2 caused the measured steel strains along the column flexural "tension" steel to be well beyond steel yield strain in compression in Figures 6.29 and 6.30. Significant bond degradation under tension action caused the column bars to be less confined laterally at the side of the joint core subjected to column flexural tension action, and the flexural compression steel forces applied to these bars at the other side of the joint core forced these bar to buckle.

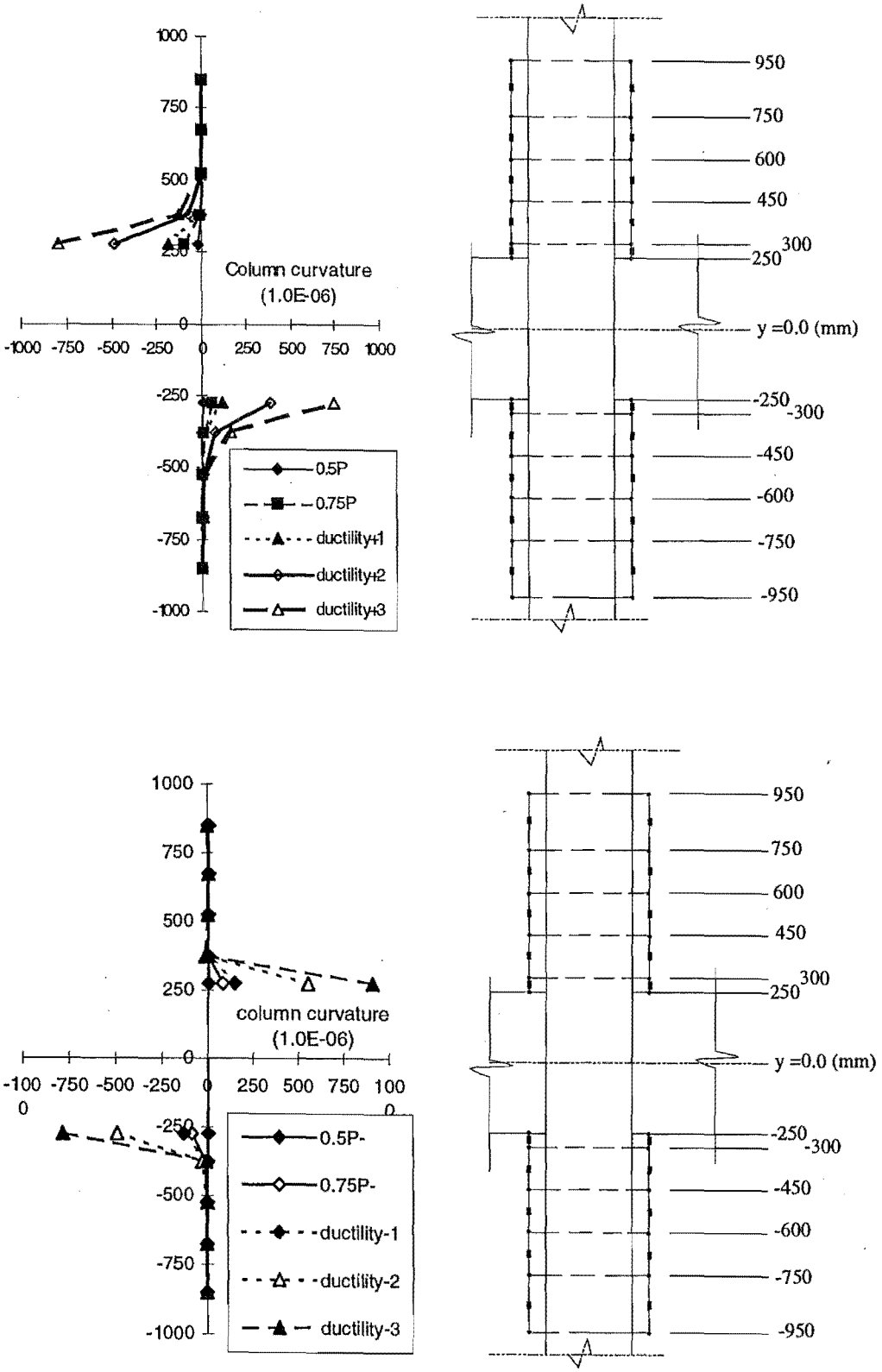

Fig. 6.28 Column Curvatures Measured of Unit 2

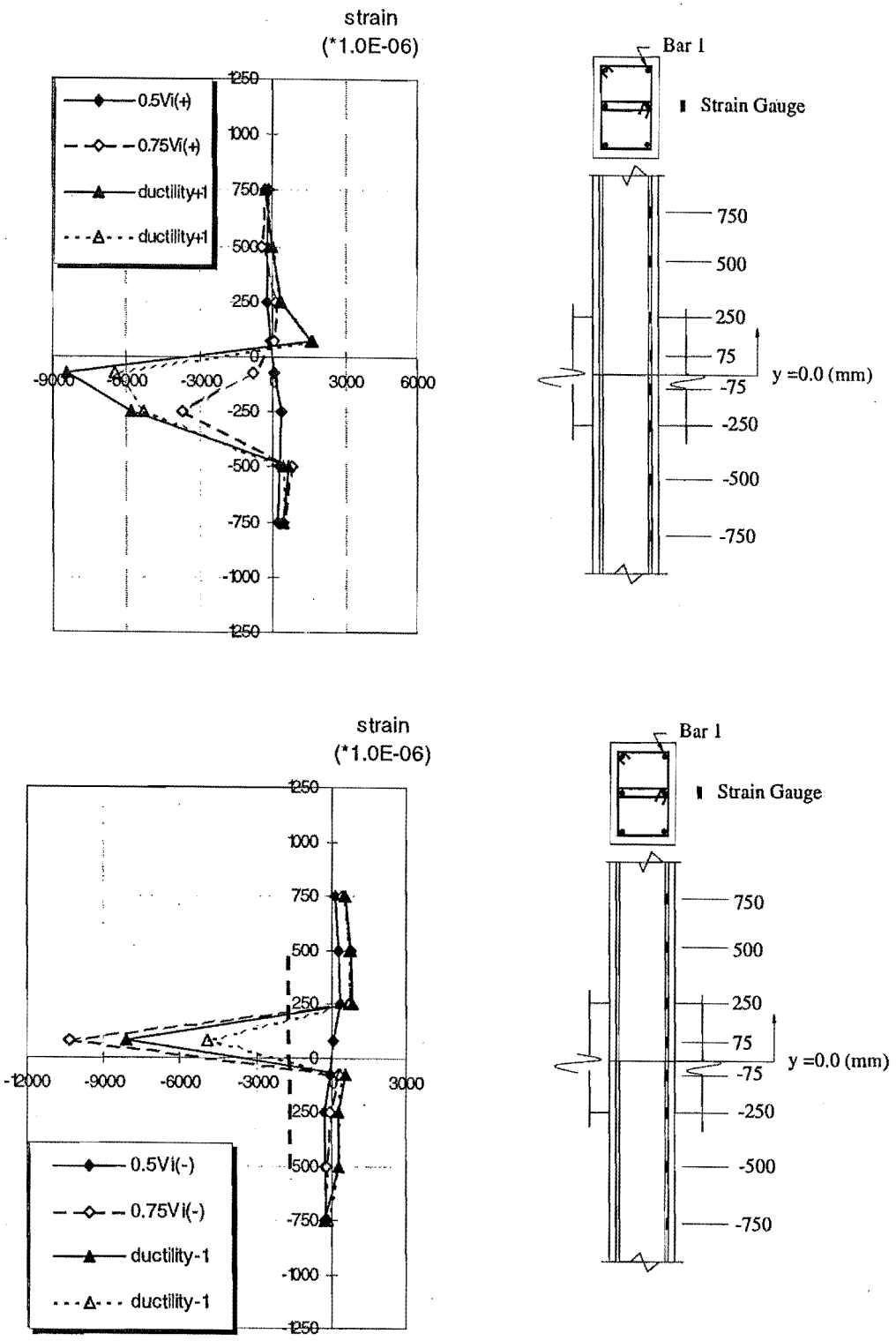

Fig.6.29 Strain Profile of Column Bar 1 of Unit 2

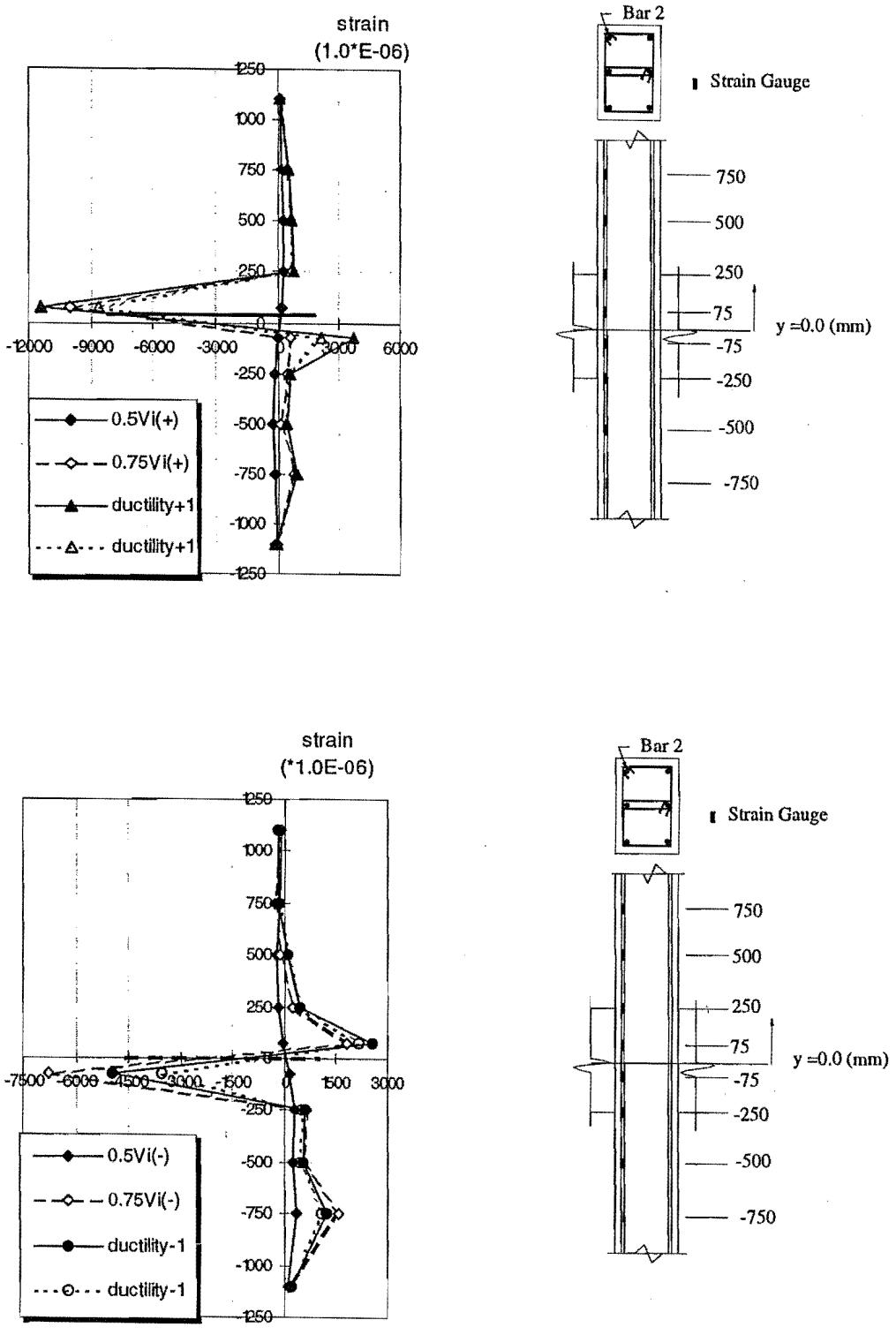

Fig.6.30 Strain Profile of Column Bar 2 of Unit 2

When compared with the test of Unit 1, the influence of column bar buckling on the column bar strains occurred earlier and spread to a bigger area due to the enhancement of column bar buckling by the column compressive axial load. Typically, the changes of column steel strains from tension to compression at the flexural tension side due to bar buckling for test of Unit 2 occurred after the completion of loading cycle of $0.5V_i$ instead of being after the completion of loading cycle of $0.75V_i$ as for Unit 1, indicating that more severe column bar buckling occurred for Unit 2. Regarding the column bar strains, the areas influenced by column bar buckling for Unit 2 spread to the joint region and the column areas adjacent to the joint core, see Fig. 6.30.

6.2.5 Beam Behaviour

6.2.5.1 Beam Deformation Characteristics

Unit 2 was a weak beam-strong column system and the beams were expected to develop plastic hinges. Fig.6.31 shows the measured beam curvature distributions for Unit 2. The theoretical beam curvatures at first yield were $\phi_y = 4.4\times10^{-6}$ for positive bending and $\phi_y = 5\times10^{-6}$ for negative bending respectively. The sign definition in Fig.6.31 is the same as for the beams of Unit 1.

In general, the beam curvature profiles measured for Unit 2 had similar trends to that of Unit 1.

Pronounced discrepancies between the measured beam curvature and the theoretical prediction exist, especially in the beam fixed-ends. Measured curvature over beam fixed-end regions in the anti-clockwise loading to $0.75V_i$ was 234×10^{-6} and 323×10^{-6} for positive and negative bending directions respectively, and they were 54 and 65 times the theoretically estimated curvatures at first yield. The theoretical member curvature at first yield was estimated at the attainment of the yield strain by the flexural tensile reinforcement based on plane section assumption. Such significant discrepancy between the measured member curvatures and the estimated curvatures was due to severe bond degradation along the beam longitudinal reinforcement within and adjacent to the joint core. The discrepancies between the measured member curvatures and the estimated curvatures were much smaller over the elastic portion due to much less significant bond degradation in that region. Evidently severe bond degradation along the beam flexural

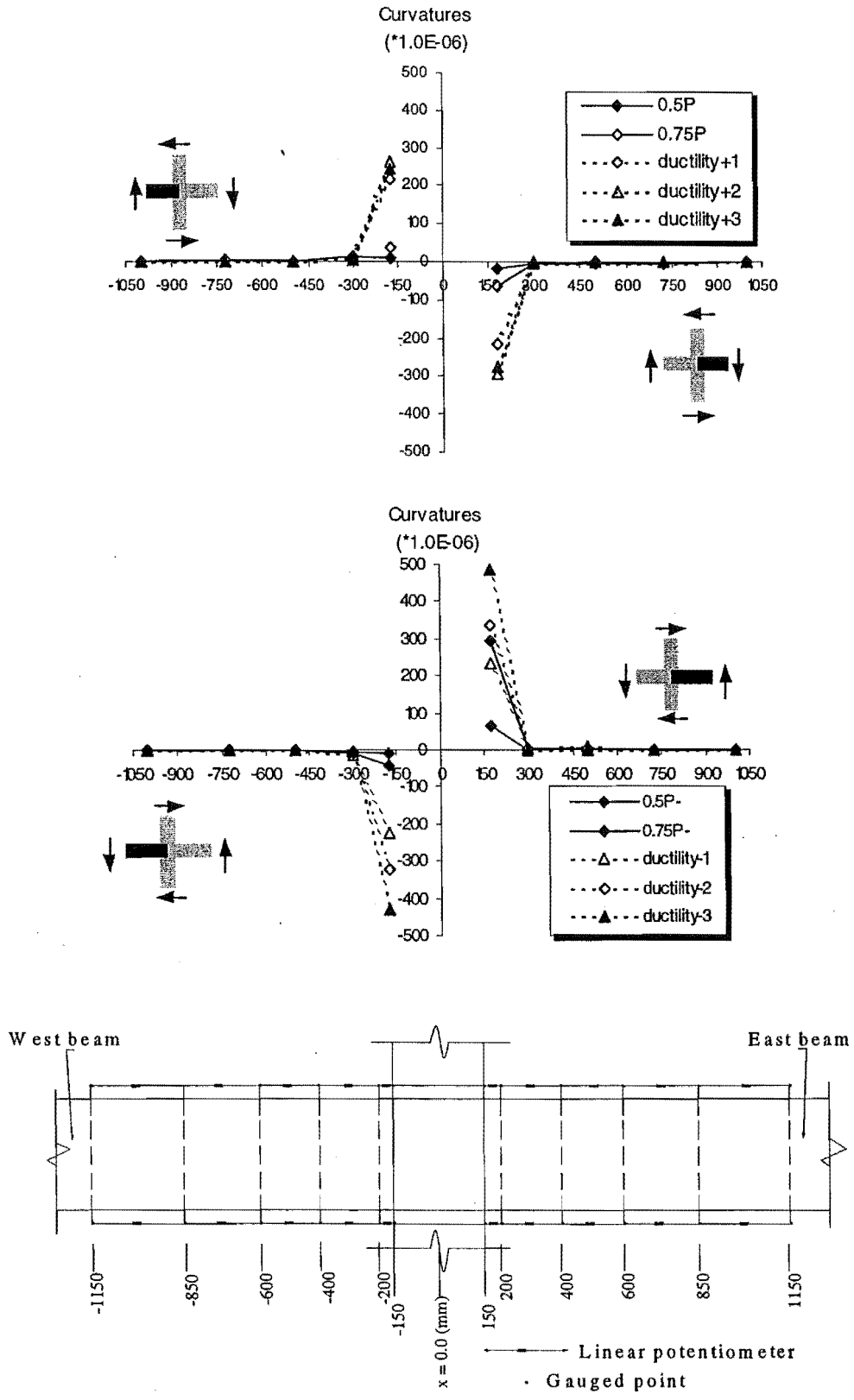

Fig.6.31 Measured Curvature Profile for Beams of Unit 2

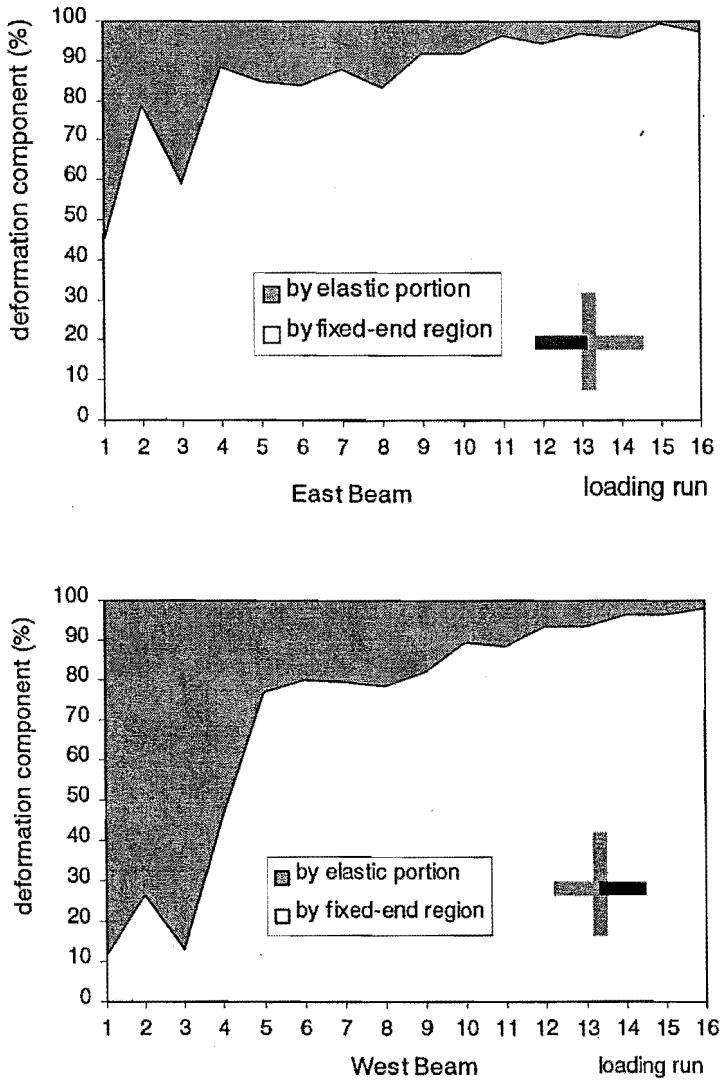

Fig.6.32 Measured beam deformation components

bars caused the plane section assumption to underestimate the member local curvatures, especially within the fixed-end significantly. Hence the detailed investigation on the local curvature ductility is not of much interest for this specific case.

Again, beam deformation was mainly limited to the fixed-ends, as seen in Fig.6.32, which shows the beam deformation components of fixed-ends and the other gauged regions, referred to as elastic portion. Hence, a rotational ductility, defined as the ratio of the rotation over the beam fixed-ends to the theoretical rotation over the whole beam at first yield as described before, is used here for the index to the member deformation.

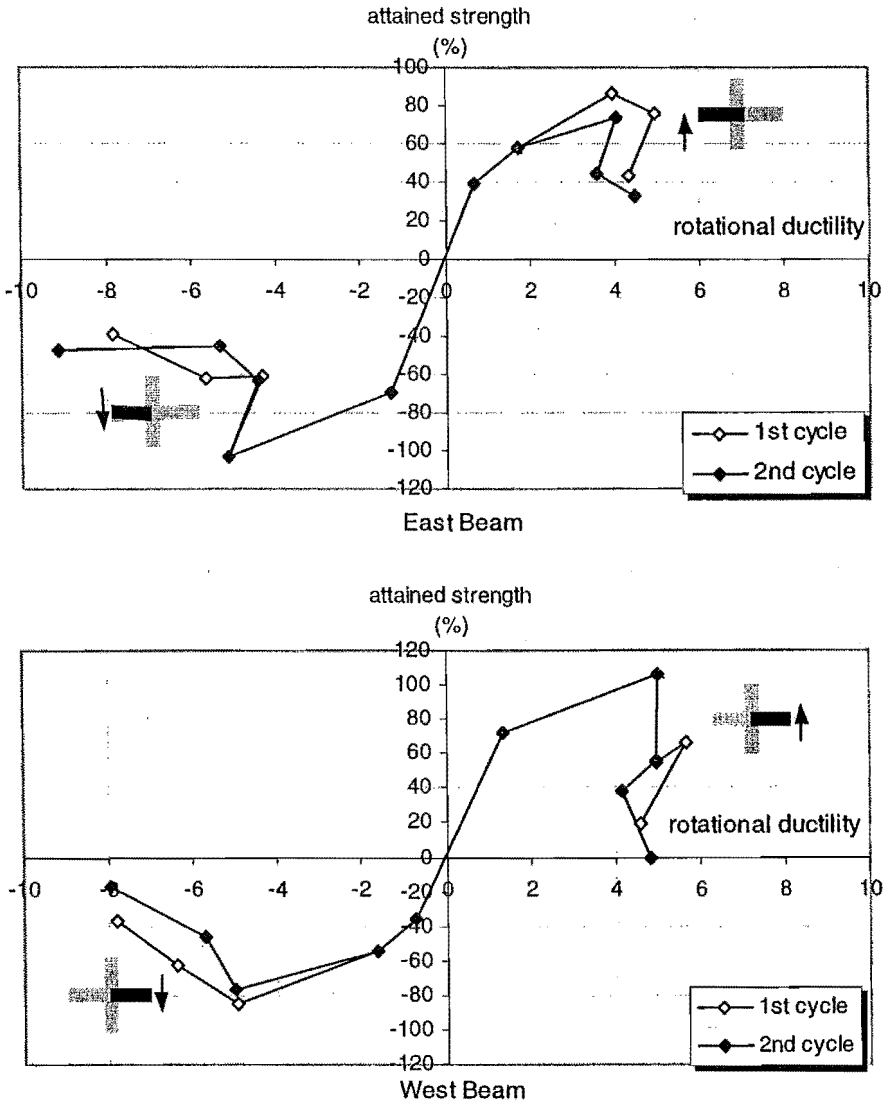

Fig.6.33 Measured beam force strength versus the rotational ductility for Unit 2

6.2.5.2 Beam Non-linear Behaviour

Theoretically, beams of Unit 2 were expected to develop plastic hinges. Rotational ductility index is used for the indicator of the beam non-linear deformation. Fig. 6.33 shows the observed beam non-linear behaviour. Fig.6.33 was plotted in terms of the measured beam rotational ductility and the attained beam force strength, expressed as the percentages of the measured beam force strength to the theoretical beam force strength at the development of the theoretical beam flexural strength.

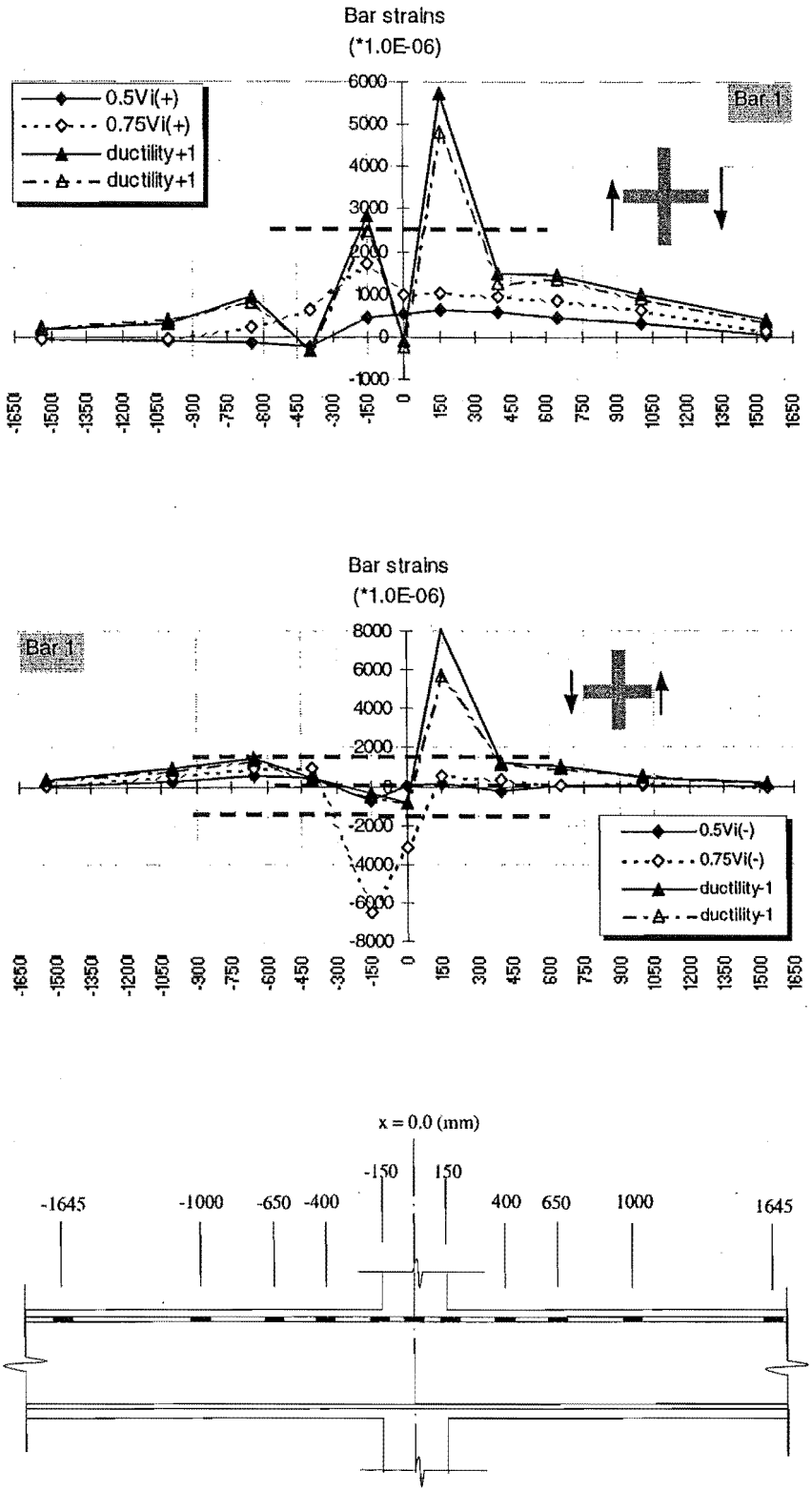

Fig.6.34 Strain Profile of Beam Bar 1 of Unit 2

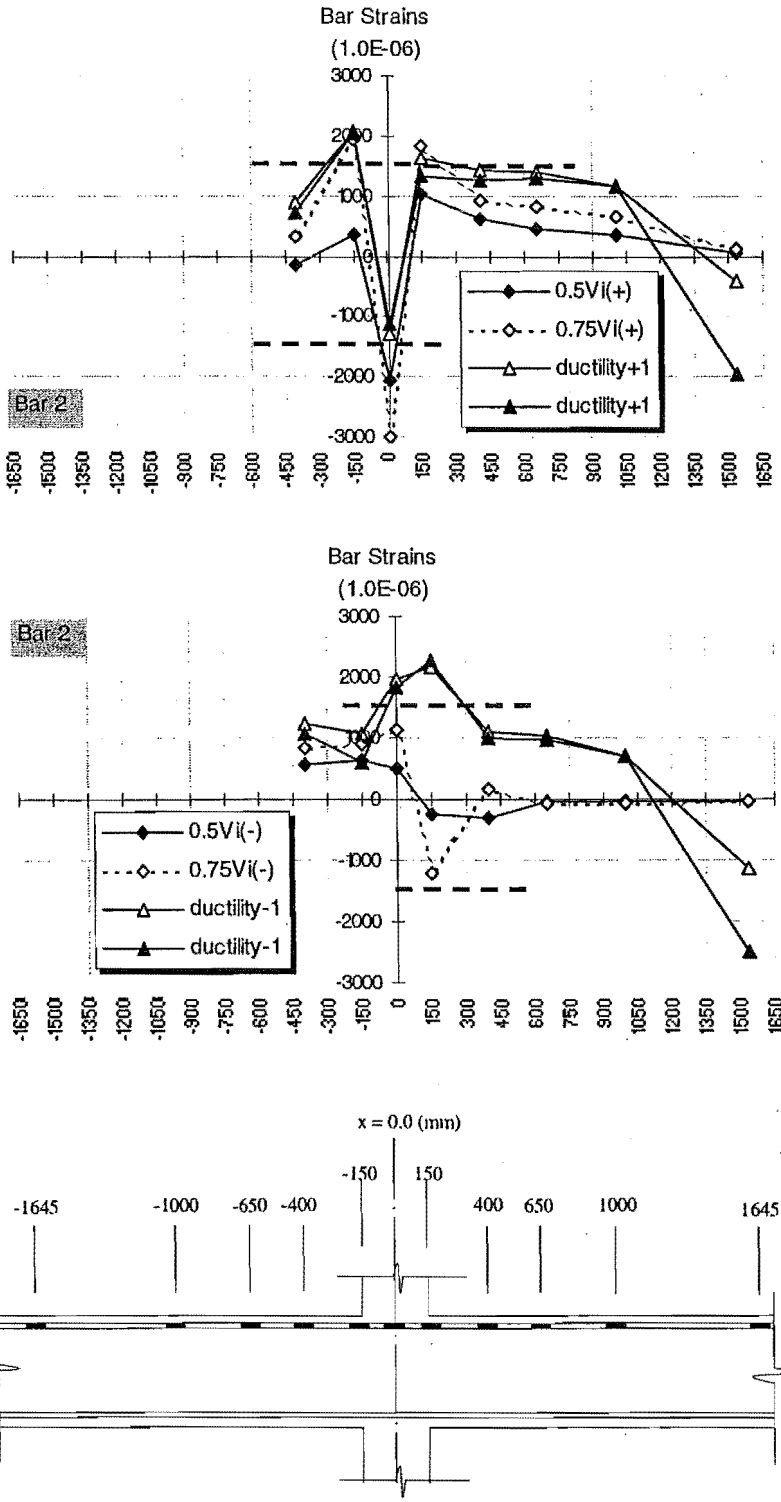

Fig.6.35 Strain Profile of Beam Bar 2 of Unit 2

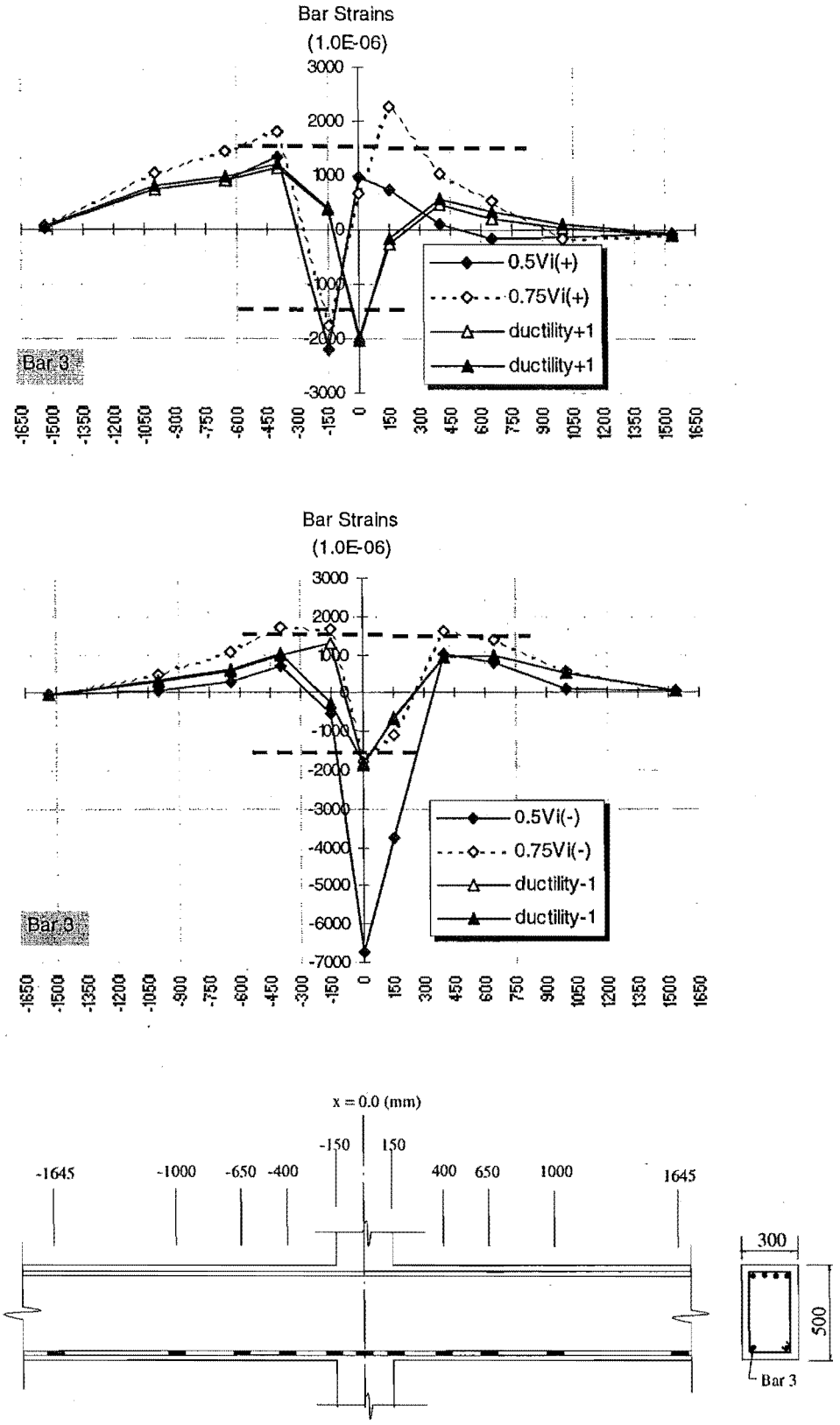

Fig.6.36 Strain Profile of Beam Bar 3 of Unit 2

6.2.5.3 Beam Longitudinal Reinforcement Strain

Figs 6.34 to 6.36 show the measured beam longitudinal steel strains along beam bars 1 2 and 3 of Unit 2 by electrical resistance strain gauges.

Similar to the test observations made for Unit 1, the measured beam longitudinal steel strains showed significant bond deterioration along the beam longitudinal reinforcement within and adjacent to the joint core. The measured strains along the beam reinforcement at the flexural compression side were in tension not only within the joint core but also adjacent to the joint core. This occurred as early as in the loading stage of $0.5V_i$ (Fig.6.34), at which the beams were supposed to behave in the elastic range. The measured beam longitudinal reinforcement strains at the centre-line of the joint core demonstrated a sudden change of the steel strain properties from tension to significant compression. This must have been attributed to local buckling. The limited bond strength could not have changed the large tensile strains into significant compression strains over such small region.

6.2.6 JOINT BEHAVIOUR

On the basis of plane section assumption and the measured beam lateral loads, the estimated nominal horizontal joint shear stress at joint diagonal tension cracking was $0.63\sqrt{f_c'}$ MPa or $0.09f_c'$ MPa. As described in section 6.1.6, the estimated joint shear strength at developing the joint diagonal tension cracking by assuming perfect bond and the diagonal tension strength of concrete of $0.3\sqrt{f_c'}$ MPa, in terms of the nominal horizontal joint shear stress, is $0.3\sqrt{f_c'}$ MPa in the case without axial column load. One approach to estimate the influence of compressive axial column load on the joint shear capacity is to use the equation $\sqrt{1+\frac{N^*}{0.3A_g\sqrt{f_c'}}}$, and this gave the joint shear capacity of $0.42\sqrt{f_c'}$ MPa for Unit 2, which was much smaller than the measured value of $0.63\sqrt{f_c'}$. Hence, when the applied compressive column axial load is lower than $0.12A_gf_c'$ as for Unit 2, the enhancement of the joint shear capacity associated with the concrete strut mechanism due to bond degradation along the longitudinal

reinforcement within the joint is still significant and the theoretical estimation based on current method would still significantly underestimate the joint shear strength of existing reinforced concrete structures reinforced by plain round longitudinal bars. However, the compressive column axial load of Unit 2 did enhance the bond mechanism along the longitudinal reinforcement within the joint and this resulted in more joint diagonal tension cracking. This can be seen below by comparing the observed joint shear deformation for Unit 2 with that for Unit 1.

Fig. 6.37 shows the measured joint shear distortion and the storey shear strength versus the joint displacement component hysteresis loops measured for Unit 2. Unlike the test evidence of Unit 1 where the joint diagonal tension cracks did not develop with the increase in the imposed displacement level, joint diagonal tension cracking, which initiated at the clockwise loading to $0.75V_i$, progressed with the loading for Unit 2, the joint shear distortion and the joint displacement component continued to increase after the maximum strength of the unit was reached at the displacement ductility of 1 as shown in Fig.6.37, indicating that joint shear failure did contribute to the final failure of Unit 2. Quantitatively, Fig. 6.38 compares the joint shear distortions measured for Unit 1 and Unit 2. The maximum joint shear distortion measured for Unit 2 was more than 10 times that measured for Unit 1. More severe joint shear failure of Unit 2 than that of Unit 1 was because the force transfer from the steel to the surrounding concrete within the joint region by bond was enhanced for Unit 2 by the compressive axial column load. Force transfer from the steel to the concrete by bond induced shear forces in the joint concrete. As a result, large diagonal principal tension stress was developed in the concrete, leading to extensive concrete diagonal tension cracking. In addition, more significant concrete spalling resulting from column bar buckling occurred in Unit 2 also contributed to the more severe joint shear failure of Unit 2.

The maximum joint displacement component was 7% of the total storey drift for Unit 1, but about 40 % of the total storey drift for Unit 2, illustrating much more severe joint shear failure for Unit 2 compared to Unit 1. The compressive column axial load for Unit 2 enhanced the force transmission from steel to the concrete by bond within the joint and enhanced column bar buckling within and adjacent to the joint core, leading to extensive concrete spalling. As a consequence, the compressive column

axial load for Unit 2 enhanced the joint shear cracking and resulted in large increase in the joint displacement component, compared to that of Unit 1.

The maximum nominal horizontal joint shear stress of Unit 2, which was reached at the first clockwise displacement ductility of 1, was $0.65\sqrt{f_c'}$ MPa or $0.09f_c'$ MPa.

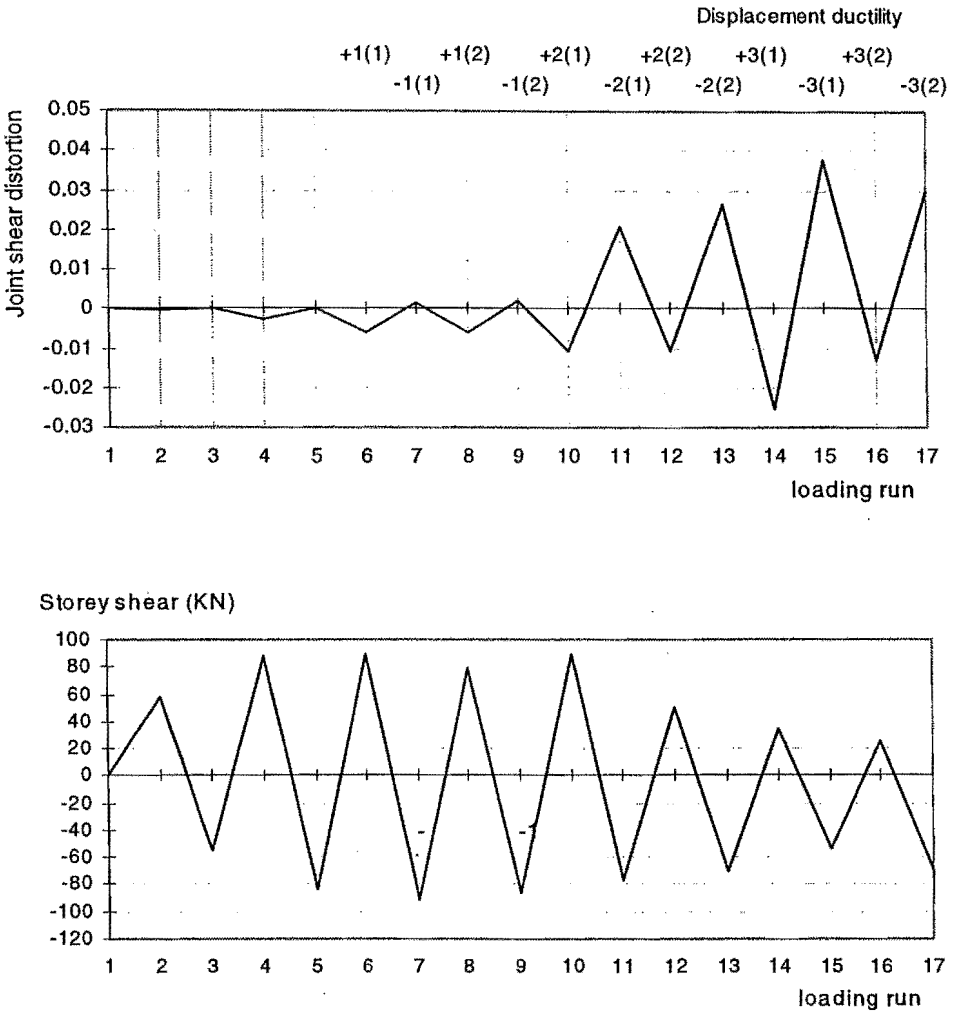

Note: In the above figures, + and – represent clockwise and anti-clockwise loading respectively, 1 and 2 in brackets represent the 1st and 2nd loading cycles at the same displacement level, 1, 2 and 3 outside brackets represent the displacement levels expressed as displacement ductility.

Fig. 6.37 Variation of measured joint shear distortion and storey shear strength for Unit 2

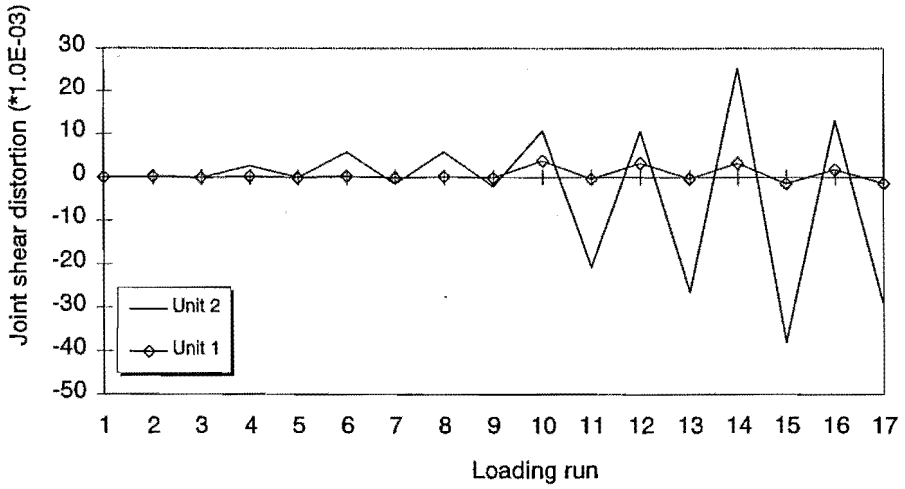

Figure 6.38 Comparison of Joint Shear Distortions of Unit 1 and Unit 2

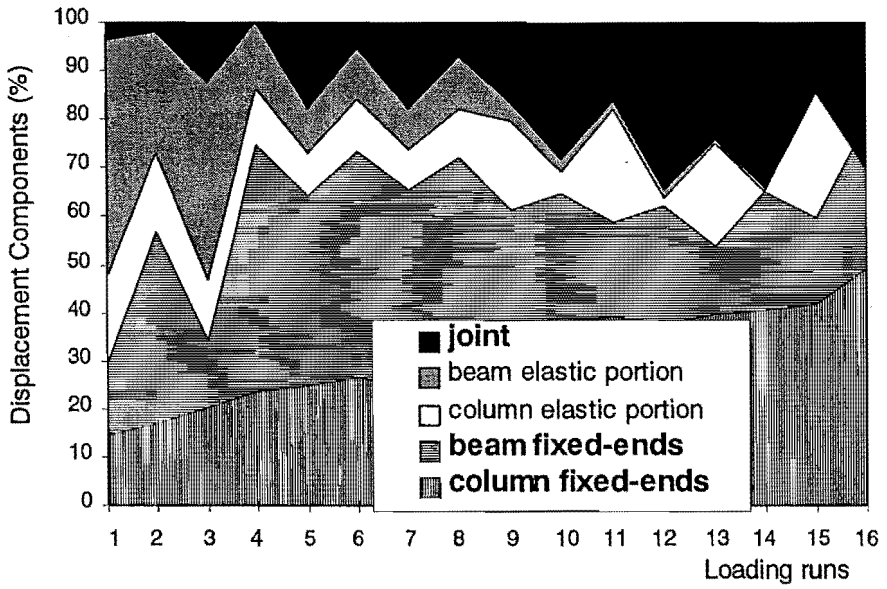

Fig. 6.39 Estimated displacement components for Unit 2

6.2.7 Displacement Components

Fig. 6.39 illustrates the measured displacement components for Unit 2 at the peaks of the loading cycles, expressed as percentages of the measured storey displacements. The displacement components were estimated as defined in Chapter 5.

Fig.6.39 shows that the column and joint displacement components, especially the component of column fixed-end rotation, progressed as the loading progressed. This indicates that the degrading column flexural behaviour in the fixed-end regions and the joint shear performance triggered the final failure of the unit.

For individual members, Fig.6.38 shows that the deformation components from member fixed-ends were much larger than that from their so-called elastic portions and such tendency of deformation lumping was more and more pronounced as the loading progressed, as revealed by the member deformation characteristics.

6.3 CONCLUSIONS FROM THE TESTS ON AS-BUILT INTERIOR BEAM-COLUMN JOINTS

Simulated seismic load tests were conducted on two identical as-built full-scale one-way interior beam-column joint units, Unit 1 and Unit 2. For the two units, the longitudinal and transverse reinforcement was from plain round bars, the beams and the columns had small amount of transverse reinforcement, the joint core had no shear reinforcement at all, and the diameter of the longitudinal bars passing through the joint core was larger than that permitted in NZS3101: 1995, as was typical of pre-1970s construction in New Zealand. Unit 1 was tested with compressive column axial load of zero but Unit 2 was tested with compressive column axial load of $0.12A_gf_c'$. For Unit 1, the beams were flexurally stronger than the columns. For Unit 2, the columns were marginally stronger than the beams due to the presence of compressive axial load. Theoretical consideration showed that the shear force capacity in the columns of Unit 1, the beams of Unit 2 and the joints of both units would be very inadequate. According to the New Zealand code NZS3101: 1995, the shear force capacities of the beams of Unit 2 and the columns of Unit 1 were only 15% and 51% of the shear demands at developing the theoretical strength of the units. The shear force capacities in the joint was 55% and 74% of the shear demands for Unit 1 and Unit 2 respectively, according to the method proposed by Park. The transverse reinforcement in the beams and columns were very inadequate, according to the code requirements for anti-buckling and concrete confinement.

Conclusions drawn from the two tests on as-built interior beam-column joint units are as follows:

1. The overall seismic performance of similar existing reinforced concrete structures designed to out-dated seismic codes would be very poor in terms of the attainment and maintenance of the stiffness and strength in a major earthquake. Severe

bond degradation, which occurred along the plain round longitudinal bars within and adjacent to the joint, and column bar buckling triggered the final failure of both tests.

The attained structural initial stiffness was about 40% of the theoretical predictions at first yield for both Unit 1 and Unit 2. The attained storey shear strength was about 10% and 23% less than the theoretical predictions for Unit 1 and Unit 2 respectively. The attainment of the force strength for Unit 1 and Unit 2 occurred at a storey drift of 4% and 2% respectively. Significant strength and stiffness degradation after the attainment of the maximum strength was observed.

2. Unlike the case with deformed longitudinal bars where compressive column axial load would enhance the system's overall performance and enhance the joint shear performance, the observed overall system performance for Unit 1 and Unit 2 showed totally different evidence. Compressive column axial load for Unit 2 did not improve the system's stiffness performance and led to more joint shear cracking. In addition, compressive column axial load for Unit 2 caused the attained system strength to be reduced if expressed as the percentage of the theoretical prediction, when compared to that for Unit 1.

For both tests, severe bond degradation occurred along the plain round longitudinal reinforcement within and adjacent to the joint core. The compressive column axial load for Unit 2, when combined with severe bond degradation, enhanced the premature column bar buckling within and adjacent to the joint core due to very small amount of column transverse reinforcement present, resulting in extensive concrete spalling adjacent to the joint core and larger damage areas adjacent to the joint core. As a result, the compressive column axial load for Unit 2 could not have improved the system's overall performance. Regarding the joint shear performance, the compressive column axial load for Unit 2 enhanced the force transfer from the longitudinal reinforcement to the surrounding concrete within the joint, resulting in more joint shear cracking, when compared with that for Unit 1.

3. For the as-built reinforced concrete members and beam-column joints, compared to the case with deformed longitudinal reinforcement, the use of plain round longitudinal bars resulted in severe bond degradation along the longitudinal reinforcement. As a result, the shear strength associated with the concrete compressive

strut mechanism was enhanced for both reinforced concrete members and the beam-column joints. Hence, the seismic performance of the system was much less shear critical, compared with the case with deformed longitudinal reinforcement. For the beams of Unit 2, their performance was observed to be totally dominated by flexure, although the theoretical prediction by New Zealand code NZS3101:1995 concluded that the shear force capacities were only 15% of the shear demands at developing the theoretical strength of the units. Evidently, the current code methods and other seismic assessment methods derived from the tests with deformed longitudinal reinforcement would significantly underestimate the shear force capacity in existing reinforced concrete members and joints, when the structures contain plain round longitudinal reinforcement.

However, the use of plain round longitudinal bars significantly facilitated the column bar buckling. The transverse reinforcement requirements for preventing the longitudinal bars from buckling and for confining the compressed concrete became much more critical than that for resisting shear.

Another consequence of severe bond degradation along the longitudinal reinforcement was that the member flexural behaviour was much less satisfactory and much less predictable, when compared to the cases with deformed longitudinal bars. Due to severe bond degradation along the longitudinal reinforcement, the plane section assumption was violated. Compared with the theoretical predictions based on the plane section assumption, member longitudinal reinforcement strains were higher and member flexural curvature deformations were larger. The discrepancies for the steel strains were smaller than for the deformation properties and this was compatible with the observation for the test units that the strength was slightly lower than the theoretical prediction but the stiffness was significantly lower than the theoretical prediction.

Of particular interest is that member post-elastic flexural deformation was limited to its fixed-ends at beam-column interfaces due to severe bond degradation within and adjacent to the joint core and a rotational ductility, rather than the curvature ductility associated with a certain plastic hinge length, became a proper index to member non-linear deformation. In this case, the force transfer of the member longitudinal

reinforcement within the joint, namely the joint force transfer mechanism, determined the flexural behaviour of the member. The determination of a member's flexural performance in this case could be strongly affected by the compressive axial actions and the cross sectional dimensions of transverse members framing into the same joint. This disagrees with the current understanding that the flexural performance of a reinforced concrete member is completely determined by the member itself.

CHAPTER 7

TEST RESULTS OF EXTERIOR BEAM-COLUMN JOINTS

7.1 GENERAL

Four full-scale one-way exterior beam-column joint units, named as EJ1, EJ2, EJ3 and EJ4, were constructed into two groups of two units each. The four units had identical overall dimensions and reinforcing details except the different arrangements of the beam bar hooks in the joint core. The longitudinal and transverse reinforcement was from Grade 300 plain round steel, the joint cores contained very limited shear reinforcement, and the columns and the beams contained small amount of transverse reinforcement, as was the case for pre-1970s construction in New Zealand.

For each two identical test units of each group, one unit was tested under simulated seismic loading with zero axial column load, and the other unit was tested under simulated seismic loading with the existence of a constant compressive axial column load of 1800 kN. The as-built exterior beam-column joint Unit EJ1 with the beam bar hooks bent away from the joint core was retrofitted by wrapping the column parts above and below the joint core using fibre-glass jacket after testing as-built with zero axial column load, in order to testify the alternative force path as described in Chapter 4. The retrofitted unit, named as REJ1, was tested again under simulated seismic loading with zero axial column load.

Seismic assessment of the test units conducted in Chapter 4 using New Zealand Code approach and the seismic assessment procedure proposed by Park shows that beam and column transverse reinforcement was inadequate for all the tests, according to the requirements for preventing the longitudinal reinforcement from buckling and confining the compressed concrete, and/or the requirement for providing shear force strength. Due to only small amount of column transverse reinforcement present above and below the joint core, the use of plain round longitudinal reinforcement and the inadequate anchorage configuration, which had the beam bar hooks bent away from the joint cores, meant that it was very critical to transfer the member forces across the joint core. Examination of exterior beam-column joint shear mechanisms conducted in Chapter 4 identified that different beam bar hook details could actuate different joint force transfer paths and therefore emphasise the need for column transverse reinforcement at different locations. Concrete tension cracking failure initiated by the opening of the beam bar hooks could

occur prior to the actuation of postulated joint force paths due to insufficient column transverse reinforcement within the beam bar hook ranges and the utilisation of plain round longitudinal reinforcement. Seismic assessment based on the method proposed by Park also showed that the shear force capacities of the beam-column joint cores were adequate except for the test of EJ1, which had the beam bar hooks bent away from the joint core and was tested with zero axial column load.

It is noted that the New Zealand code approach and the method proposed by Park are established on the basis of experimental results with deformed longitudinal reinforcement. Experimental evidence observed for the two as-built interior beam-column joint units reinforced by plain round longitudinal reinforcement conducted in this project revealed that reinforced concrete linear members (beams and columns) with small amount of transverse reinforcement are not shear critical if plain round longitudinal reinforcement is used. Reinforced concrete linear members designed according to a similar design philosophy, that is, to similar codes, must be of similar behaviour, irrespective of whether they are part of interior or exterior beam-column joint assemblies. Therefore for the exterior beam-column joint test units, beam and column behaviour would be more likely to be dominated by flexure, rather than by shear, but the member flexural behaviour would degrade significantly due to expected severe bond degradation along the longitudinal reinforcement. Hence, the member behaviour is studied with emphases on the member's degrading flexural behaviour. For the joints, the investigation emphasises the member force transfer across the joint core, the column transverse reinforcement strains at different locations, and the potential concrete tension cracking failure along the beam bar hooks. Of course the effects of different beam bar hook details and compressive axial column load are also investigated in a comparative way.

Similar to the tests on the two as-built interior beam-column joint tests conducted in this project, where big discrepancies between the measured member curvatures and the theoretical values were observed due to the violation of the plane section assumption and the flexural deformation of such linear members tended to concentrate on the fixed-end regions, the rotational deformation in the fixed-end of an existing reinforced concrete member, rather than the detailed member curvature properties along the member, becomes a proper index to the member's post-elastic flexural behaviour.

7.2 TEST OF UNIT EJ1

7.2.1 Introduction

As-built full-scale exterior beam-column joint unit EJ1 had the beam bar hooks bent away from the joint core and it was tested under simulated seismic loading with zero axial column load. Test on Unit EJ1 was identical to Hakuto's test on Unit O7 except that Hakuto used deformed longitudinal reinforcement. This test aimed at investigating the seismic performance of exterior beam-column joint components when reinforced by plain round longitudinal bars and containing reinforcing details typical of pre-1970 existing reinforced concrete moment resisting frame structures in New Zealand. Theoretically, test on Unit EJ1 would achieve a weak beam-strong column mechanism. The ratio of the column moment capacity to the beam moment capacity relative to the joint centre-line was 2.1 and 1.4 respectively when determined by the beam negative moment capacity and positive moment capacity. The theoretical storey shear strength of Unit EJ1 for clockwise loading, which was determined by the beam negative bending moment capacity was 67 kN, and the theoretical storey shear strength of the unit for anti-clockwise loading, which was determined by the beam positive moment capacity, was 45 kN.

7.2.2 Crack Development and Damage

The crack development and the final appearance of Unit EJ1 are illustrated in Fig. 7.1.

Concrete tension cracking, orientated by the anchorage configuration of the top beam bars, initiated above the joint core in the upper column as early as at the peak load attainment of clockwise $0.5V_i$ (loading run 1). This occurred due to the interaction of the column bar buckling and the opening action of the beam bar hooks in tension as described in Fig 4.4(a). The development of flexural cracks in the beam and columns at this specific stage was also observed and the beam and columns were still in the elastic range. In loading run 3, which attempted to achieve clockwise $0.75\ V_i$, the existing crack directed by the anchorage configuration of the top beam bars rapidly extended into the upper column as well as into the joint core although the storey shear strength remained nearly unchanged after it reached only $0.55V_i$. This was due to the failure in actuating the alternative joint shear model as a consequence of insufficient column transverse reinforcement adjacent to the joint core. In comparison, the observed development of the existing flexural

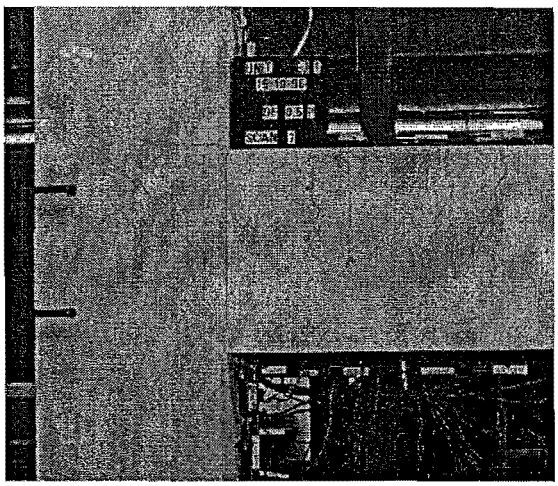

(a). Loading at Clockwise $0.5V_i$

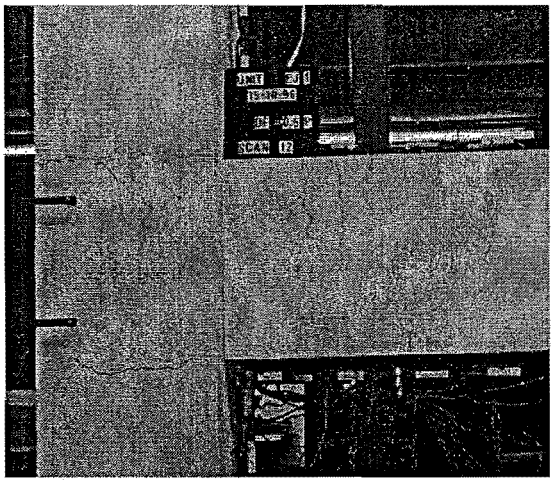

(b). Loading at Anti-Clockwise $0.5V_i$

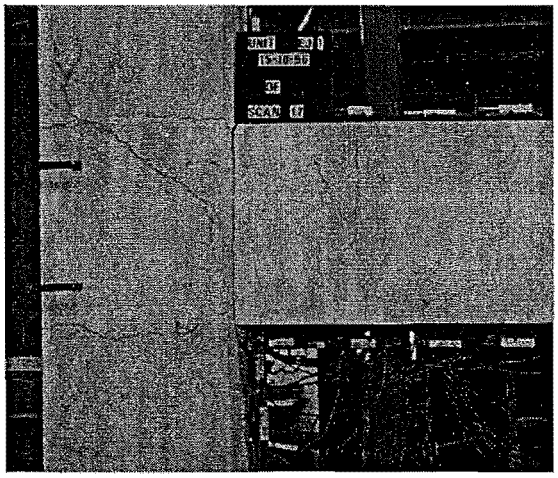

(c). Loading to Attain Clockwise $0.75V_i$

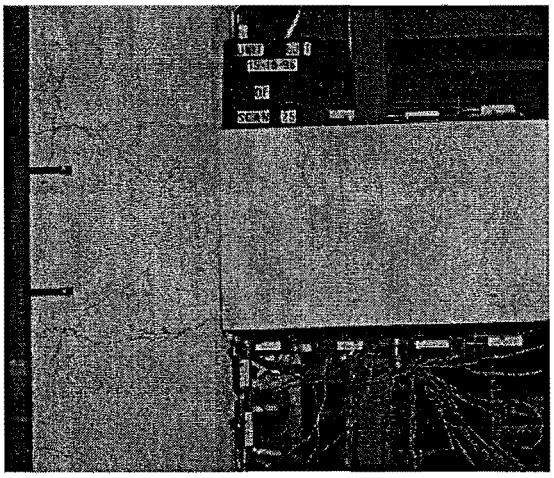

(d). Final Appearance

Fig.7.1 Crack Development and Final Appearance of EJ1 with Failure Initiated by Concrete Tension Cracking Orientated by Beam Bar Hooks

cracks was less apparent in loading run 3. Reversed anti-clockwise loading led to crack development similar to that with clockwise loading. In loading run 4 which attempted to achieve anti-clockwise $0.75V_i$, concrete tension cracking orientated by the bending configuration of the bottom beam bars initiated below the joint core in the column at the drift angle of 1% (see Fig.7.1(d)) and it rapidly developed into the bottom column in the vertical direction and into the joint core in the diagonal direction, although the observed increase in the storey shear strength was not significant after 60% of the theoretical storey shear strength in the anti-clockwise loading direction.

The testing of as-built Unit EJ1 was terminated after the completion of two loading cycles, and the peak loading of $0.75V_i$ was not attained in either directions. It was believed that subsequent loading could only cause further development of the cracks orientated by the anchorage configuration of the beam bar hooks without achieving any higher strength.

In general, the observed flexural cracks in the columns were much less pronounced than those in the beam, indicating the formation of a weak beam-strong column failure mechanism as theoretically predicted. The flexural cracks in the beam were sparsely spaced with one major flexural crack adjacent to the joint core as a result of severe bond degradation and slip along the beam longitudinal reinforcing bars within and adjacent to the joint core. No beam and column shear cracks were observed for Unit EJ1, similar to that observed for linear members of Units 1 and 2. The joint core of Unit EJ1 was observed to be of good integrity throughout the whole test, although the theoretical seismic assessment identified that the shear capacity of beam-column joint core of Unit EJ1 was only 38% the required strength at developing the theoretical strength of the unit (see *Table 4.8*). The seismic performance of individual members was therefore dominated by flexural failure, instead of shear failure. This demonstrated that both the current code method and the current seismic assessment procedure of Reference P6 could not give good prediction of the available shear strength for as-built linear members and as-built exterior beam-column joints should plain round longitudinal reinforcing bars be used, as revealed by other tests on concrete components reinforced by plain round bars [L1, M1, M2].

The influence of the steel type used on the overall seismic performance of exterior beam-column joint components is identified by comparing the observed test evidence of Unit EJ1 and Hakuto's Unit O7. Hakuto's Unit O7 was identical to Unit EJ1 except that Hakuto's Unit O7 used deformed longitudinal reinforcing bars, and both Unit EJ1 and Unit O7 were tested under simulated seismic loading with zero axial column load. For Hakuto's test on Unit O7, the final failure was due to the joint shear failure and the development of the joint diagonal tension cracks occurred earlier than the development of the crack orientated by the beam bar hook in the column. In comparison, the joint core of the as-built Unit EJ1 was of good integrity at the final stage, the development of joint diagonal tension cracks for Unit EJ1 occurred after the development of the crack

orientated by the beam bar hook in the column. The final failure of Unit EJ1 was attributed to concrete tension cracking failure along the beam bar hooks in tension, which was due to the interaction between the column bar buckling and the opening action of the tensile beam bar hooks.

This means that the use of plain round reinforcing bars enhanced the shear force capacities of the beam and beam-column joint, and this shear performance enhancement of the beam and beam-column joint reached a point where their seismic performance is governed by flexure, rather than by shear. However, the use of plain round reinforcing bars enhanced column bar buckling, facilitating concrete tension cracking failure associated with the opening action of the beam bar hooks and leading to an increased need for column transverse reinforcement within the beam bar hook range, compared to the case with deformed bars. Evidently, the member force transfer across the joint core is of more concern if plain round bars are used for longitudinal reinforcement.

7.2.3 Load-versus-Displacement Response Measured for Unit EJ1

Fig.7.2 shows the storey (horizontal) shear force versus storey (horizontal) displacement and storey drift hysteresis loops for the as-built unit EJ1. Also shown in Fig. 7.2 is the theoretical storey shear strength V_i of the unit at the attainment of the theoretical flexural strength of the unit, calculated using the New Zealand code approach but using the measured material strengths and assuming a strength reduction factor of unity as previously described. The plots in Fig. 7.2 confirm very poor general seismic behaviour of the as-built exterior beam-column joint unit EJ1.

The first yield displacement could not be obtained using the adopted method specified in Section 5.3.2 due to failure to attain the peak of $0.75V_i$. The stiffness measured at the loading cycle of $0.5V_i$ was 1.7 kN/mm, and this was only 42% of the theoretically predicted initial stiffness of 4.0 kN/mm. Significant stiffness degradation observed in the loading cycle of $0.75V_i$ indicated that the measured initial stiffness would be lower than 1.7 kN/mm should the loading peak of $0.75V_i$ be attained. Significant disparity between the measured stiffness and the theoretically predicted stiffness was partially because the theoretical prediction of the initial structural stiffness did not take the effect of member fixed-end rotations into account. The observed structural stiffness property of Unit EJ1

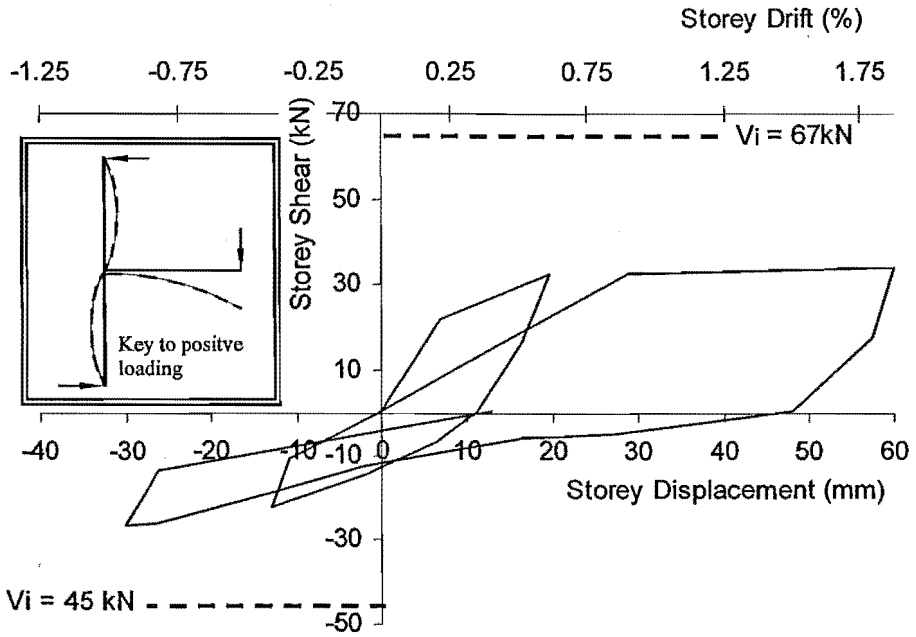

Fig.7.2 Storey Shear versus Storey Displacement Hysteretic Loops of Unit EJ1

also can be contrasted with the measured initial stiffness of Unit O7 tested by Hakuto et al [H1] which was otherwise identical but reinforced by deformed bars. The measured initial stiffness for Unit O7 at 75% of the theoretical storey horizontal load strength of the test unit was 3.4 kN/mm on average, being 2 times the measured stiffness for Unit EJ1 at $0.5V_i$. The use of plain round longitudinal reinforcement led to a more than 50% reduction in the initial stiffness, compared to the available stiffness with deformed longitudinal reinforcement. Compared to the test evidence of as-built interior beam-column joint Unit 1, where the initial stiffness observed was about 60% of that observed for an otherwise identical test but reinforced by deformed bars, the adverse effect resulting from the use of plain round longitudinal reinforcement on the structural stiffness property is more significant for as-built exterior beam-column joint subassemblages than for as-built interior beam-column joint subassemblages. This occurred because both the severe bond degradation along the beam longitudinal bars and the concrete tension cracking orientated by the beam bar hook configuration had contributed to large beam fixed-end rotation. This once again demonstrated that the type of structure tested would become very flexible when plain round bars are used for longitudinal reinforcement.

Fig. 7.2 shows that unlike well-designed exterior beam-column joint units where the theoretical strength or even the over-strength can be achieved [P13], the maximum storey

shear strengths measured for the as-built unit EJ1 in the clockwise loading direction and anticlockwise loading direction were respectively only 55% and 60% of the theoretical force strength of the unit, and they were attained at a storey drift of 2 % and 1% respectively. The low load capacity was attributed to failing to control the concrete tension cracking along the beam bar hook due to insufficient column transverse reinforcement above and below the joint core within the beam bar hook range. Comparison with the simulated seismic loading test on Hakuto's Unit O7 could lead to the identification of steel type with the seismic behaviour. The available strength of Unit EJ1 was only 70% of the available strength of Unit O7 after eliminating the influences of material strengths. The lower load capacity of Unit EJ1 compared to Hakuto's Unit O7 was due to severe bond degradation along the column and beam longitudinal bars of Unit EJ1. Severe bond degradation along the column longitudinal bars enhanced premature column bar buckling, and severe bond degradation along the beam longitudinal bars of Unit EJ1 increased the need for the joint concrete strut mechanism and increased the induced concrete lateral tensile stress around the beam bar bend. As a result, the capacity in association with premature concrete tension cracking orientated by the beam bar hooks was very low and it triggered the final failure of Unit EJ1.

Such low available load force strength and stiffness of the test unit EJ1 meant that investigation of other structural properties, such as, strength degradation and energy dissipating capacity, would be not meaningful.

7.2.4 Observed Steel Strains and Member Curvature Behaviour

The measured beam and column longitudinal reinforcement strains were below the steel yield values.

The beam of Unit EJ1 was expected to develop a plastic hinge and the columns of Unit EJ1 were expected to remain in the elastic range during testing. Fig.7.3 and Fig.7.4 show the measured curvature profiles for the beam and columns respectively.

In Figs.7.3 and 7.4, it is seen that the curvatures in the fixed-ends were much higher than the curvature over the elastic portion for the beam and columns although the beam and columns of the unit were expected to be still in the elastic range then, similar to the

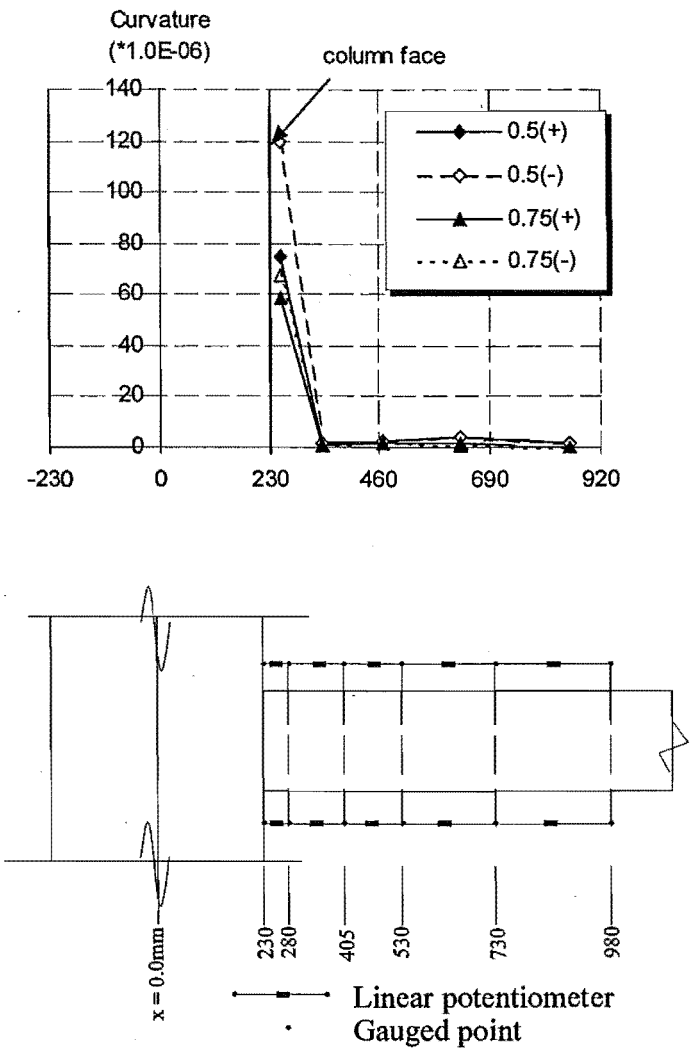

Fig.7.3 Beam curvature profile measured for Unit EJ1

member deformation characteristics observed for the as-built interior beam-column joint units. Fig.7.5 and Fig.7.6 show the deformation components measured for the beam and the columns, respectively. The measured beam fixed-end rotation contributed as high as 90% of the total beam flexural deformation and the column fixed-end rotation contributed about 98% of the measured total column deformation.

Apparently, for linear concrete members reinforced by plain round bars, the fixed-end rotation is the major source of the member deformation, irrespective of whether the member is in the elastic range or in the inelastic range.

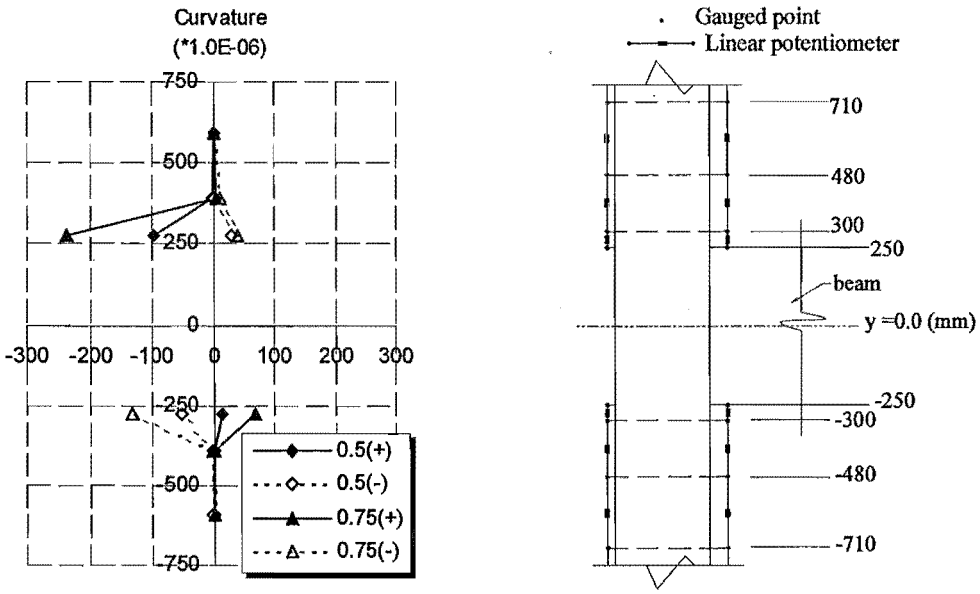

Fig.7.4 Measured column curvature profiles for Unit EJ1

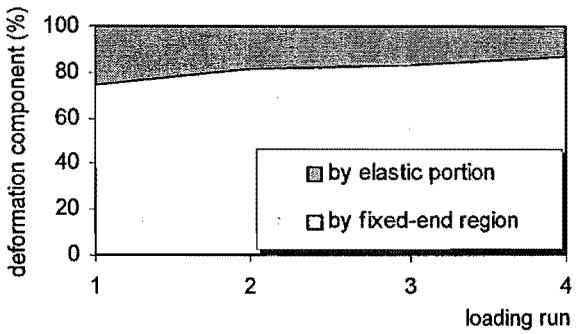

Fig.7.5 Deformation components measured for the beam of Unit EJ1

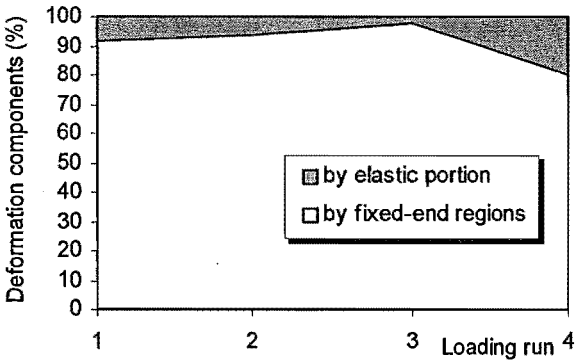

Fig.7.6 Deformation components measured for the columns of Unit EJ1

7.2.5 Joint Behaviour

7.2.5.1 Joint Shear Stress

The estimated maximum nominal horizontal joint shear stress for clockwise loading direction, based on the measured force strength and plane section theory, was 1.0 MPa, or $0.17\sqrt{f_c'}$ MPa. In comparison, the estimated maximum nominal horizontal joint shear stress for anti-clockwise loading direction was lower, being 0.72 MPa, or $0.12\sqrt{f_c'}$ MPa. For both clockwise and anti-clockwise loading directions, the attainment of the maximum nominal horizontal joint shear stresses coincided with the extension diagonally into the joint core of the cracks orientated by the hook configuration of the tensile beam bars in the columns.

If the shear force strengths of beam-column joints at the stage of diagonal tension cracking of the joint cores is assessed by using Mohr's circle for stress and the diagonal tension strength of concrete is assumed to be $0.3\sqrt{f_c'}$ MPa, the joint horizontal shear strength at the stage of joint diagonal tension cracking, in terms of the nominal horizontal joint shear stress, is $0.3\sqrt{f_c'}$ MPa when axial column load is zero as was for test on Unit EJ1. Evidently, the maximum joint shear input of $0.17\sqrt{f_c'}$ MPa in terms of the nominal horizontal joint shear stress would not have induced the concrete diagonal tension cracking in the joint core of Unit EJ1, should the unit contain the deformed longitudinal reinforcement. Due to severe bond degradation along the beam flexural tensile reinforcement resulting from the use of plain round longitudinal reinforcement, the beam steel tensile force was mainly transmitted into the concrete around the beam bar bend, resulting in high local concrete tensile action around the beam bar bend and subsequently inducing the concrete tension cracking, which initiated around the beam bar hook. In this case, the actual local concrete tensile stresses could be much higher than the estimated tensile action using the nominal horizontal joint shear stress. In addition, severe bond degradation along the beam flexural tensile reinforcement significantly violated the plane section assumption. As a result, the plane section theory would overestimate the

member flexural strength, namely, the actual tensile force along the beam flexural tensile reinforcement was larger than the theoretical value and the nominal horizontal joint shear stress calculated based on the plane section theory underestimated the shear input action in the joint. However, the latter cause was believed to be not so prominent as the former one.

Apparently, when plain round longitudinal reinforcement is used and the beam bar hooks are bent away from the joint core as for Unit EJ1, premature concrete tension cracking failure initiated at the beam bar bend due to the resistance to the beam steel tensile force, rather than the joint shear, is very critical.

Comparison of the joint behaviour of Unit EJ1 and Hakuto's Unit O7, which was identical to Unit EJ1 except the use of deformed reinforcing bars, could lead to the identification of the influence of steel type on the joint performance. The joint performance observed of Unit EJ1 was much better than that of Hakuto's O7 in terms of the final appearance, as seen in Fig.7.1. Whereas in the case of Unit O7 the nominal horizontal joint shear stress at which the crack running along the beam bar hooks initiated was about $0.23\sqrt{f_c'}$ MPa for the clockwise loading cycle and $0.21\sqrt{f_c'}$ MPa for the anti-clockwise loading cycle respectively, the estimated nominal horizontal joint shear stress at which the crack running along the beam bar hook initiated for Unit EJ1 was $0.17\sqrt{f_c'}$ MPa and $0.12\sqrt{f_c'}$ MPa for clockwise and anti-clockwise loading directions respectively, where f_c' is the measured concrete compressive strength. This illustrated that the use of plain round bars for longitudinal reinforcement enhanced the need to transmit the beam steel tension force at the bend, compared to the case with deformed bars. As a consequence, the failure associated with the concrete tension cracking orientated by beam bar hooks in tension was facilitated, which triggered the final failure of the test Unit EJ1.

7.2.5.2 Joint Shear Distortion

Fig. 7.7 illustrates the joint shear distortion and storey shear strength observed for Unit EJ1 using the method as described in Section 5.2.4.

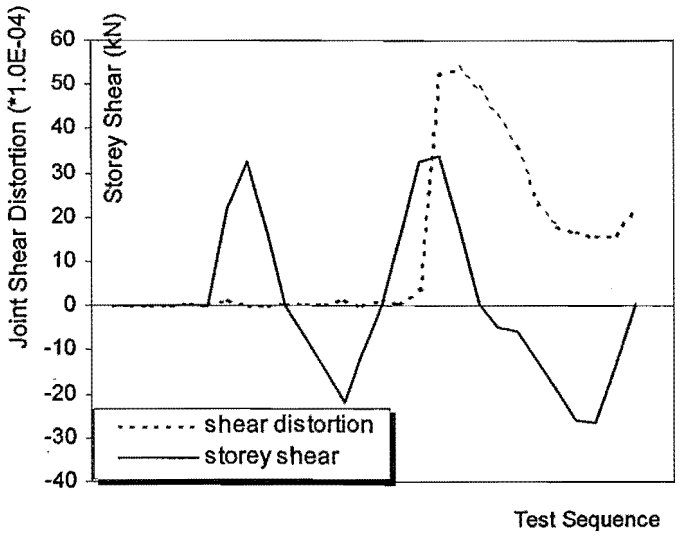

Fig.7.7 Joint shear distortion and storey shear strength measured for Unit EJ1

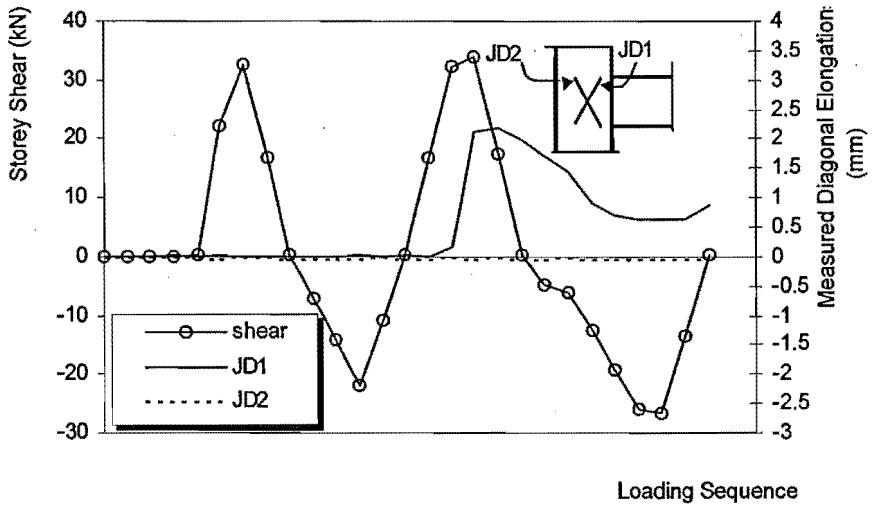

Fig.7.8 Storey Shear and Measured Elongation of Joint Diagonals for Unit EJ1

The induced maximum joint shear distortion was 0.52% for Unit EJ1 and it occurred at the achievement of the maximum storey shear strength when the existing crack was extending into the joint core. The maximum joint shear distortion measured for Unit EJ1 was only about 15% of the maximum joint shear distortion measured for Unit O7 by Hakuto et al, which was about 3.5% for both loading directions. Much better joint integrity observed for Unit EJ1 was attributed to less steel force transmitted into the concrete by bond within the joint core of Unit EJ1 due to more severe bond degradation and bar slip along the beam bars, compared to the test on Unit O7.

Fig.7.8 shows the storey shear force versus joint diagonal elongation measured for test on Unit EJ1. Evidently, the joint shear deformation was mainly a consequence of concrete tension cracking along the beam bar hooks and the concrete compressive strains along the supposed diagonal concrete strut was very small.

7.2.5.3 Joint Shear Reinforcement Strains

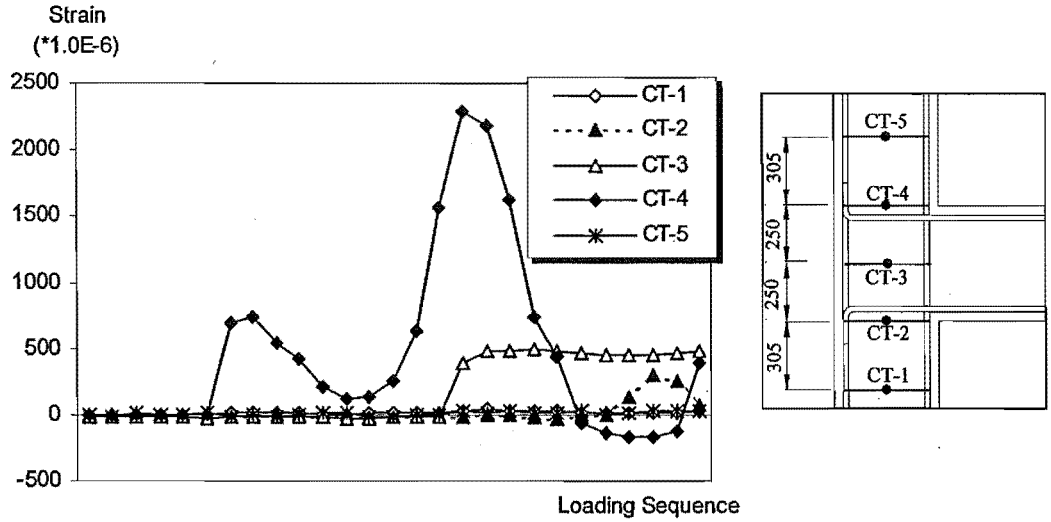

Fig.7.9 Measured Column Transverse Reinforcement Strains at Different Locations

The measured steel strains in the column transverse reinforcement during the test on Unit EJ1 by electrical resistance strain gauges were generally well below the steel yield strain. However, the measured strain of the column transverse reinforcement CT-4 at the top beam face was much larger than the steel yield strain of 1.59×10^{-6} , as shown in Fig.7.9. Due to the use of plain round longitudinal reinforcement for Unit EJ1, severe bond degradation along the beam longitudinal bars occurred and hence the beam tension steel force was mainly transferred within the bend. Due to the beam bar hooks bent away from the joint core, the member force transfer across the joint core for Unit EJ1 would follow the alternative force path as suggested by Fig. 4.4(b). The actuation of this alternative force path caused the column transverse reinforcement within the beam bar hook range to be significantly strained in tension. Because there was only one set of column stirrups within the beam bar hook range, the measured strain for CT-4 was very large.

7.2.6 Displacement Components

Fig. 7.10 shows the measured displacement components for Unit EJ1. The maximum beam and column displacement components accounted for about 70% and 40% respectively of the measured total storey displacement while the joint displacement component was less than 20%. It should be appreciated that concrete tension cracking orientated by the beam bar hook also contributed to the beam displacement component. Severe bond degradation and slip along the beam bars within the joint core not only enhanced the beam fixed-end rotations but also enhanced the concrete tension cracking orientated by the beam bar hook. Hence the utilisation of plain round reinforcing bars as was the case of Unit EJ1 enhances the beam displacement contribution significantly, but reduces greatly the joint displacement component.

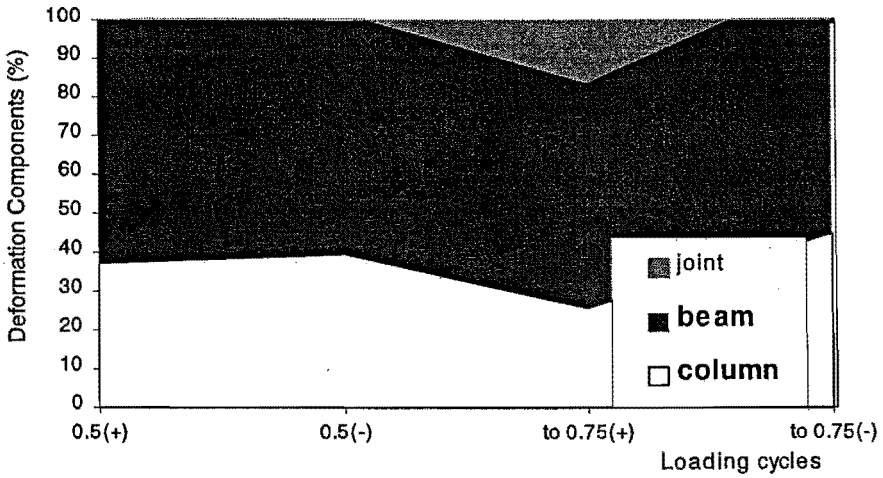

Fig. 7.10 Displacement components measured for Test of Unit EJ1

7.2.7 Summary

An as-built full-scale exterior beam-column joint unit EJ1 was tested under simulated seismic loading without axial column load. The design deficiencies of test unit EJ1 were (1). The beam longitudinal reinforcing bars were bent away from the joint core in the exterior column. As a result, the force transfer across the joint core was a critical concern. (2). The longitudinal reinforcement was from plain round bars. (3). The joint core contained very limited shear reinforcement and the estimated joint shear capacity was only 38% of the demand at developing the system's theoretical strength. (4). The transverse reinforcement in the beam and columns was very

inadequate according to the requirement for preventing the longitudinal reinforcement from buckling and/or for resisting shear. The tendency of the potential column bar buckling was further accelerated because the first set of transverse reinforcement was not close enough to the beam and column interface, according to current code requirement. The estimated beam shear strength was only 20% of the maximum shear demand.

Conclusions drawn from this test are as follows:

1. Very poor overall seismic performance

The overall performance of the unit was very poor. The experimental initial stiffness using the method described in section 5.3.2 could not be obtained due to being unable to attain 75% of the theoretical strength. The initial stiffness measured at the loading cycle of $0.5V_i$ was 1.7 kN/mm and this was only 42% of the theoretically predicted structural stiffness. The available strength of Unit EJ1 was also very low and it was only about 55% of the theoretical strength of the unit. The strength development of Unit EJ1 was governed by premature concrete tension cracking along the beam bar hooks, which occurred prior to the joint concrete diagonal tension cracking. Severe bond degradation between the longitudinal reinforcement and the surrounding concrete enhanced column bar buckling and enhanced the opening action of the beam bar hooks. Consequently, premature concrete tension cracking failure along the beam bar hooks, rather than the shear failure in the beam and/or the joint, triggered the final failure of the unit.

2. Enhanced need for hoop transverse reinforcement adjacent to the joint core

For the existing reinforced concrete exterior beam-column joint components with the beam bar hooks bent away from the joint core in the exterior columns, the column hoops adjacent to the joint core, rather than the ones in the centre of the joint, are highly stressed. This suggests that the column transverse reinforcement adjacent to the joint core is more needed than the joint hoops within the joint core. The plain round longitudinal reinforcement used facilitated the failure associated with the premature concrete tension cracking along the beam bar hooks, hence facilitating the need for the column transverse reinforcement adjacent to the joint core.

3. Significant concentration of member flexural deformation at the fixed-ends

The seismic performance of the beam and columns of Unit EJ1 was totally governed by flexure, rather than by shear. The flexural deformation of the beam and columns was significantly concentrated in the member fixed-ends even when the beam and columns were expected to remain in the elastic range. The contribution of the rotation in the fixed-end(s) was more than 90% of the total flexural deformation of the member. This indicates that allowance only for the member fixed-end rotation in estimating the member deformation is adequate.

4. More significant adverse effect due to the plain round longitudinal bars used

Comparison with an otherwise identical Unit O7 but reinforced by deformed bars showed that the use of plain round bars for the longitudinal reinforcement of as-built exterior beam-column joint assemblies not only caused the attained overall system strength to reduce by about 30% after eliminating the effect of material strengths, but also caused the attained stiffness of Unit EJ1 to reduce by more than 50%.

Compared with the test on as-built interior beam-column joint Unit 1, where the attained initial stiffness was about 60% of that observed for Hakuto's test of Unit O1 which was otherwise identical to Unit 1 but reinforced by deformed bars, the adverse effect of the utilisation of plain round longitudinal reinforcement on the structural stiffness property is more severe for as-built exterior beam-column joint assemblies. Hence the tested structure would be very flexible if plain round longitudinal reinforcement is used.

5. Enhanced shear performance of the members and the joint

Similar to the test evidence of the as-built interior beam-column joint units, the use of plain round longitudinal reinforcement for Unit EJ1 led to much improved joint shear performance due to severe bond degradation along the beam longitudinal reinforcement within the joint core. As a consequence, the problem area of as-built exterior beam-column joint unit was shifted from the joint shear failure for Unit O7 to concrete tension cracking orientated by the beam tensile steel hooks.

7.3 TEST OF RETROFITTED UNIT REJ1

7.3.1 Introduction

As-built Unit EJ1 was retrofitted by wrapping the column areas adjacent to the joint core using fibre-glass jacketing after tested as-built under simulated seismic loading with zero axial column load, and then became Unit REJ1. Unit REJ1 was tested under simulated seismic loading with zero axial column load in order to testify the actuation of the postulated alternative joint force transfer model in Section 4.4.2.

7.3.2 Crack Development and Damage

The crack development and the appearance of Unit REJ1 at the completion of testing are shown in Fig. 7.11.

The existing beam and column flexural cracks, which were repaired by injecting epoxy resin before jacketing the damaged as-built Unit EJ1 using fibre-glass, started to open again as early as in the loading cycle to $0.5V_i$, especially the beam flexural crack at the inner column face. Apart from this, a vertical crack along the outer layer of the column main bars was observed within the joint core in the later loading stages. This was associated with the reopening of the existing cracks orientated by the beam bar hook and the column bar buckling within the joint core. However, the development of this vertical crack within the joint core was not so pronounced as that of the major beam flexural crack at the column face.

Similar to the test observation for Unit EJ1, no concrete diagonal tension cracks were observed in the beam and columns of Unit REJ1. Hence the performance of individual linear members was dominated by flexural behaviour. There were no new joint diagonal tension cracks developed within the joint core of REJ1. It is noted that the theoretical seismic assessment conducted in section 4.3 "Seismic Assessment of As-built Test Units" showed that the provided horizontal joint shear force capacity was only 38 % of the imposed horizontal joint shear force at developing the beam negative theoretical flexural strength and the attained storey shear strength by test of REJ1 was 75% of the theoretical storey shear strength for both loading directions. Furthermore the theoretical seismic assessment conducted in Section 4.3 showed that the available shear force capacity of the beam of Unit EJ1 was only 20% and 55% of the imposed shear at developing the

theoretical strength of the unit by code approach and the approach suggested in reference P6 respectively. Hence both the current code method and the current seismic assessment method proposed in Reference P6 would underestimate the shear force capacity in linear concrete members and beam-column joints if plain round bars are used for longitudinal reinforcement.

Hence, the seismic performance of the test of REJ1 was totally governed by beam flexural behaviour. Beam flexural deformation concentrated in the major flexural crack at the column face due to severe bond degradation and slip along the beam main bars within and adjacent to the joint core of Unit REJ1 and beam fixed-end rotation became the major source of the beam flexural deformation.

Whereas in the case of the test on as-built unit EJ1 concrete tension cracking orientated by the beam bar hook configuration governed the strength attainment and triggered the final failure, test of Unit REJ1 evidently demonstrated that fibre-glass jacketing in the column areas adjacent to the joint core for Unit REJ1 controlled such premature concrete tension cracking and actuated the alternative force path postulated in Section 4.4.2. Consequently, the seismic performance of Unit REJ1 was governed by the flexural performance of the beam for this weak beam-strong column system.

7.3.3 Load-versus-Displacement Response Measured for Unit REJ1

Fig.7.12 shows the storey shear force versus storey displacement and storey drift hysteresis loops measured for the retrofitted as-built exterior beam-column joint unit REJ1. The theoretical storey shear strength of Unit REJ1, V_i, which was the same as that of the as-built unit EJ1, is also shown in Fig.7.12 for both loading directions. Compared to the hysteresis properties measured for Unit EJ1 in Fig.7.2, the hysteresis loops measured during the test of Unit REJ1 in Fig.7.12 demonstrated that wrapping the column parts above and below the joint core using fibre-glass greatly improved the seismic behaviour of as-built exterior beam-column joint assembly which had plain round beam longitudinal bar hooks bent away from the joint core in the exterior columns.

A large increase in the stiffness was observed for the test on Unit REJ1, when compared to the test on Unit EJ1. The stiffness measured at clockwise $0.5V_i$ for the test on Unit REJ1 was 4.26 kN/mm and it was 2.37 times the measured initial stiffness of 1.7 kN/mm

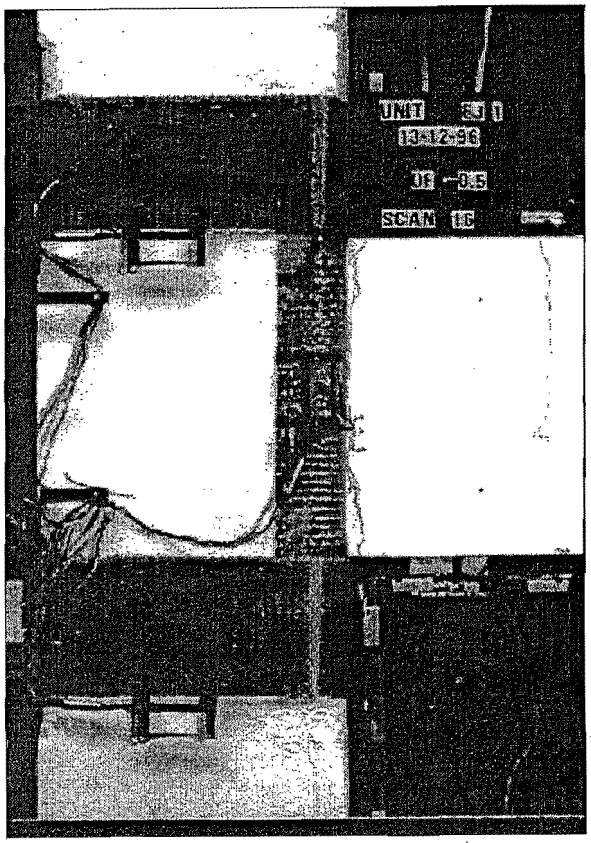

(a) Loading at 0.5Vi

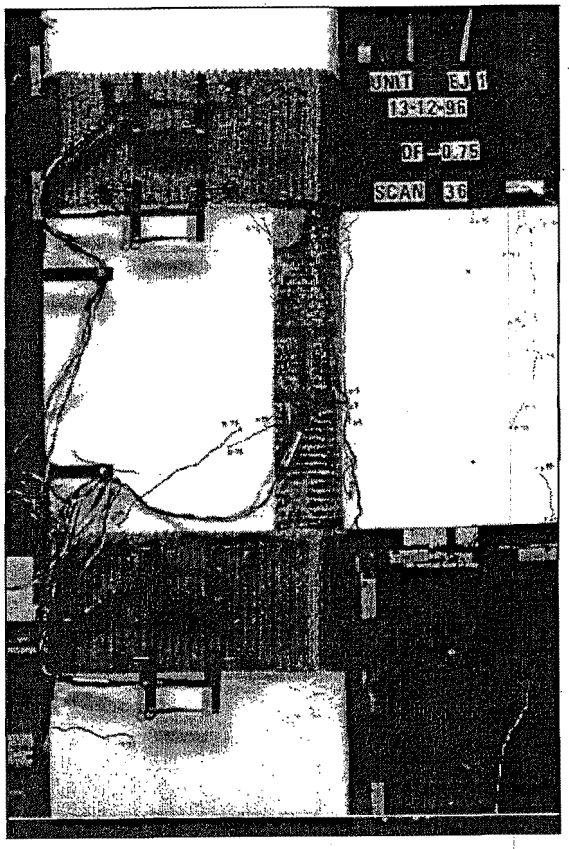

(b) Loading at 0.75Vi

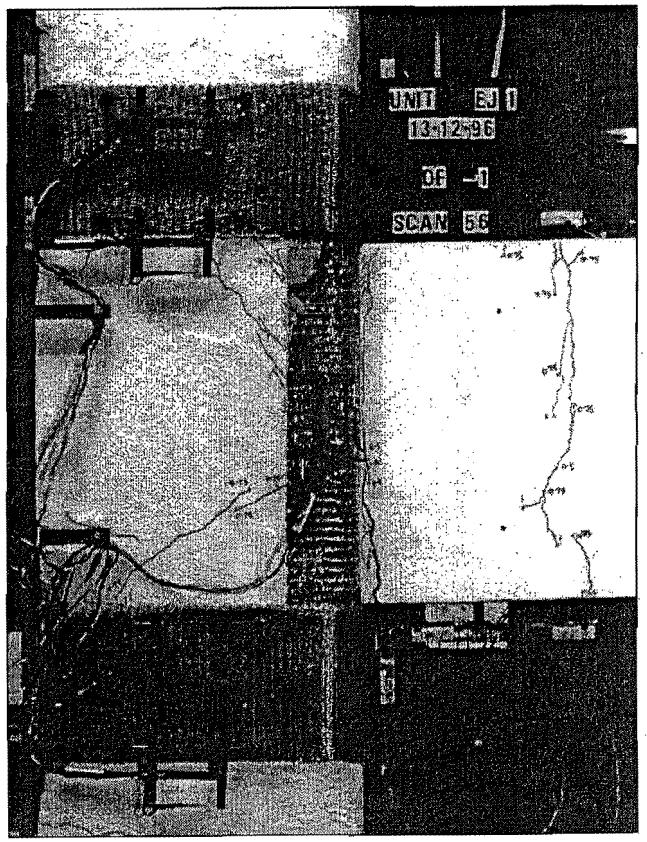

(c) End of Loading at Ductility 1

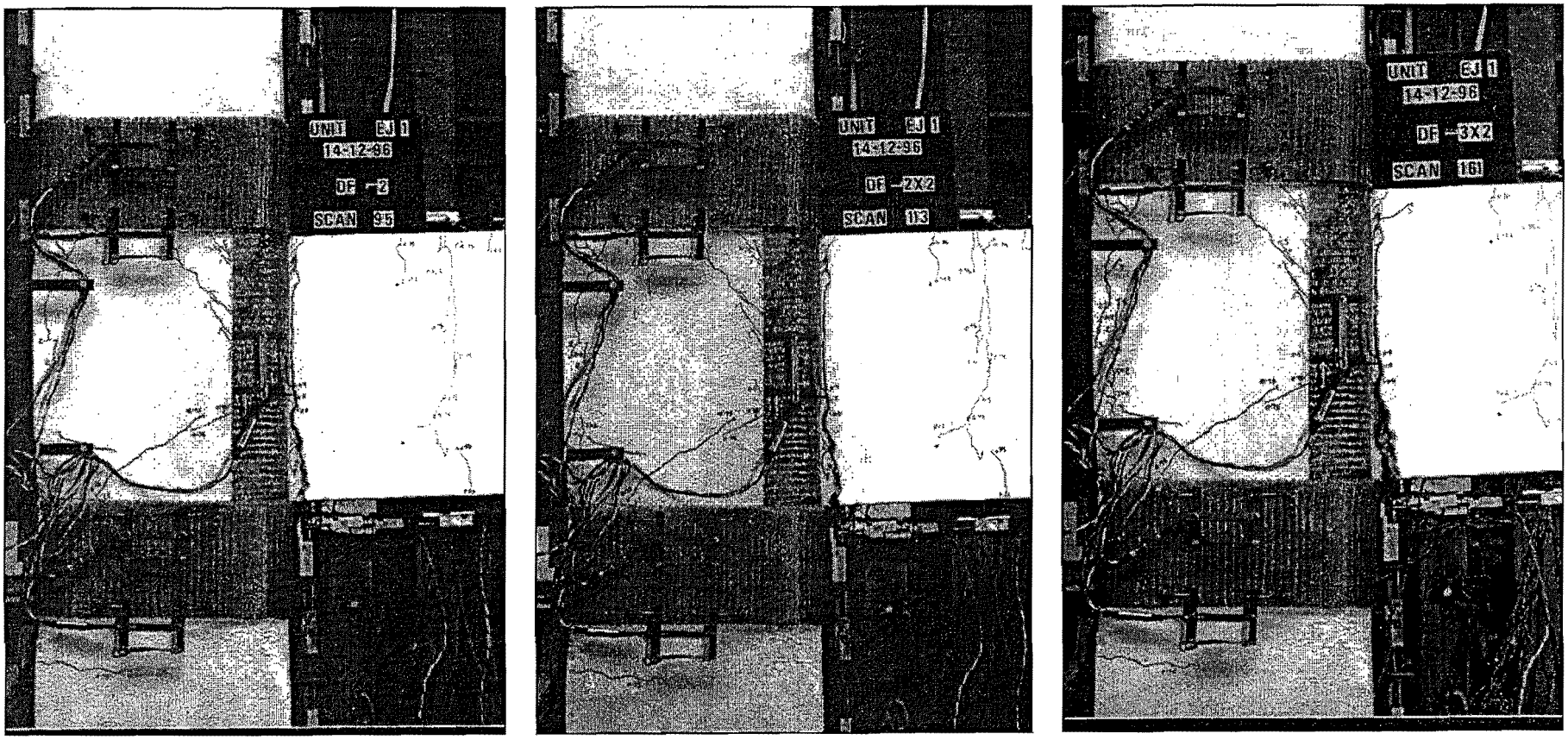

(d) End of Loading at Ductility 2 (e) End of Loading at Ductility 3 (f). Final Appearance

Fig.7.11 Crack Development and Final Appearance of Unit REJ1

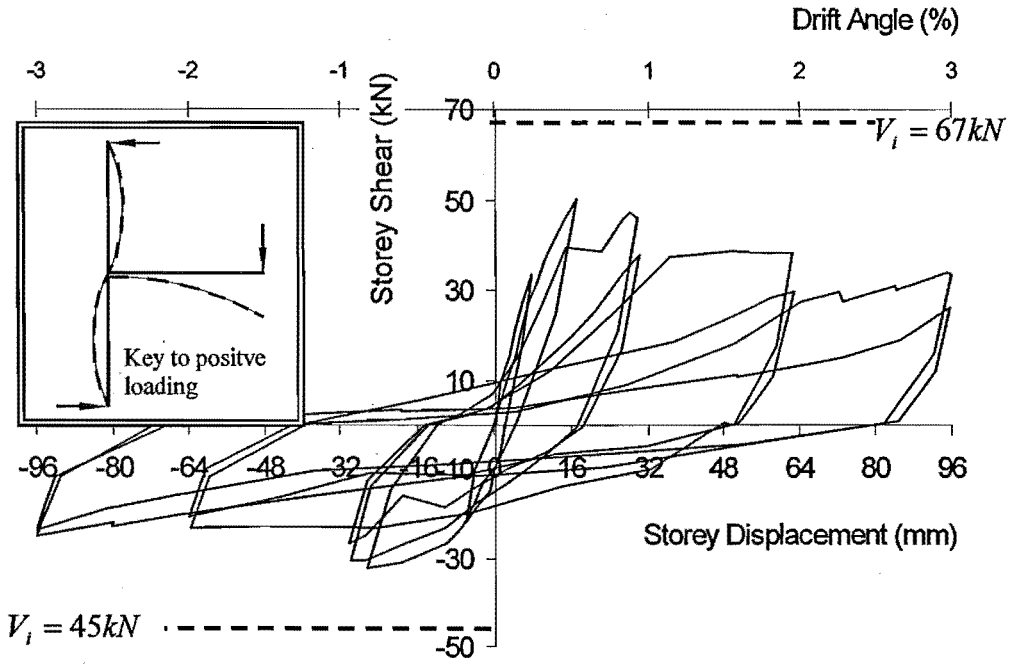

Fig.7.12 Storey Shear Versus Storey Displacement Hysteresis Responses of REJ1

for the as-built unit EJ1 at loading cycle of 0.5 V_i. This occurred because the development of concrete tension cracking orientated by the beam longitudinal bar hooks in exterior columns was controlled by the lateral confinement provided by fibre-glass jacketing. The average initial stiffness measured for Unit REJ1 at the loading cycle to 0.75 V_i was 2.1kN/mm, and this was about 50% of the theoretical prediction of the initial stiffness. Obviously the available stiffness of the retrofitted as-built exterior beam-column joint Unit REJ1 was still very low. The low stiffness was anticipated because of the following reasons: Firstly, the clamping actions in column areas adjacent to the joint core, which was necessary for actuating the alternative force path, was at the expense of large crack opening when passive jacketing, such as fibre-glass jacketing, is used as was the case as for REJ1. Secondly, severe bond deterioration along the beam longitudinal bars within and adjacent to the joint core must have led to a very low beam flexural stiffness.

Also observed was a large increase in the attained strength for Unit REJ1, in comparison with as-built Unit EJ1. The maximum storey shear strengths attained by Unit REJ1 for both clockwise and anti-clockwise loading directions, although still about 25% less than

the corresponding theoretical storey shear strengths of the unit, were more than 15% higher than the attained strengths by the as-built Unit EJ1. The lower strength of the unit was mainly due to severe bond degradation along the member longitudinal reinforcement. As revealed by the tests on Unit 1 and Unit 2, the plane section assumption could overestimate the available member flexural strength if severe bond degradation along the member longitudinal reinforcement occurs as was the case for Unit REJ1.

Significant pinching is also observed in the loops of Fig.7.12, and the pinching was observed to progress with the increasing level of the imposed displacement. The softness of the test unit at the beginning of each load run occurred due to the major beam flexural crack at the inner column face, which formed as a consequence of severe bond degradation and slip along the longitudinal beam reinforcement within and adjacent to the joint core.

In summary, the retrofitted Unit REJ1 demonstrated much better seismic performance. The attained initial stiffness, although only about 40% of the theoretical value based on the plane section assumption, was more than 2 times the measured initial stiffness for the as-built unit EJ1. The attained storey shear strengths occurred at storey drifts of approximately 0.86%, and although only about 75% of the theoretical storey shear strengths, were about 15% higher than that achieved by the as-built unit EJ1. However, the retrofitted unit still showed a great deal of strength and stiffness degradation.

7.3.4 Strains of Longitudinal Reinforcement Measured by Strain Gauges

The readings from electrical resistance strain gauges were checked first to verify their reliability. For a certain strain gauge, the variation of its readings was compared with the variation of the imposed member forces, as the testing progressed. If the strain gauge readings fluctuated in the same way as that of the imposed member forces, the strain gauge was thought to behave properly. Otherwise, the strain gauge readings were eliminated.

Fig.7.13 and Fig.7.14 show the measured strain profiles by electrical resistance strain gauges for beam bar 1 and beam bar 2, respectively. The beam bar strains were taken as the average values if two gauges were used at the same location. For beam bar 2, the

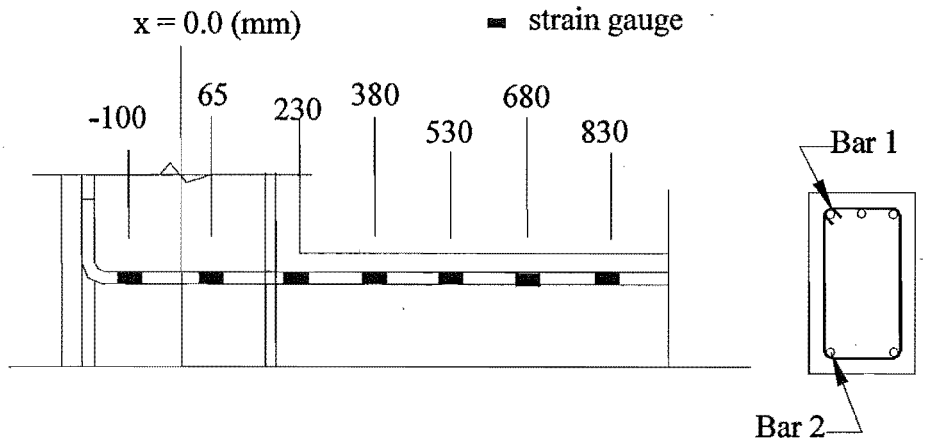

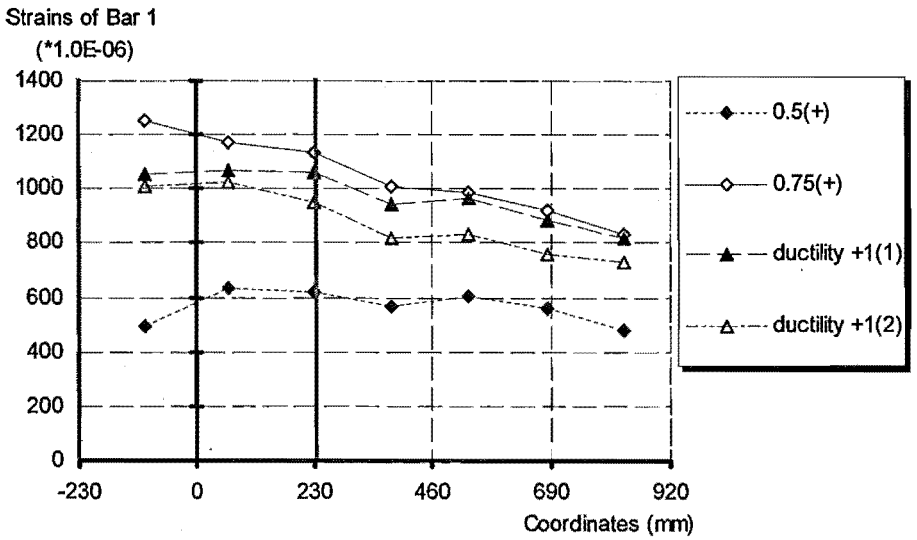

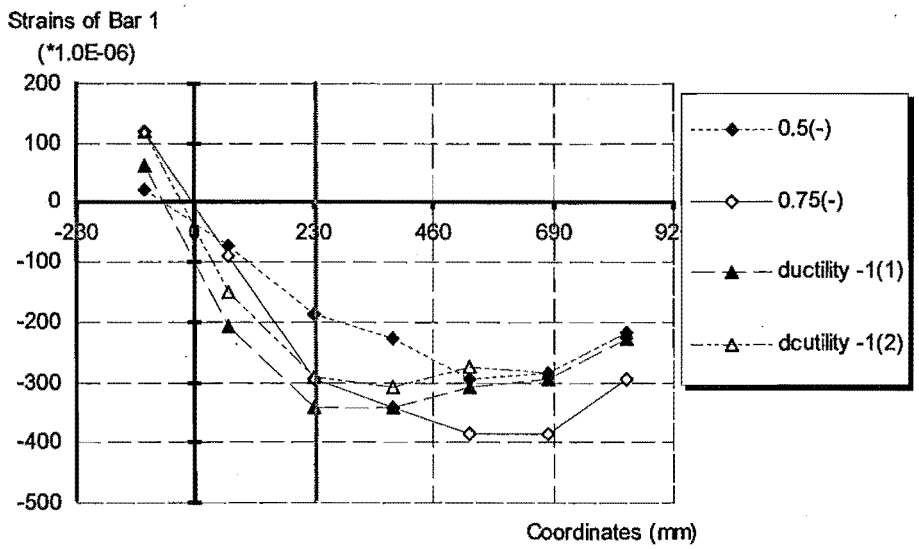

Fig.7.13 Strain Profile of Beam Bar 1 along Beam Axis

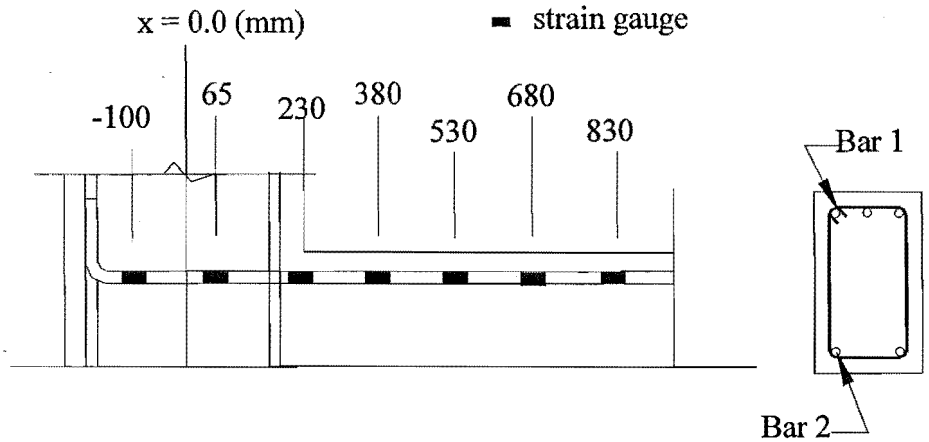

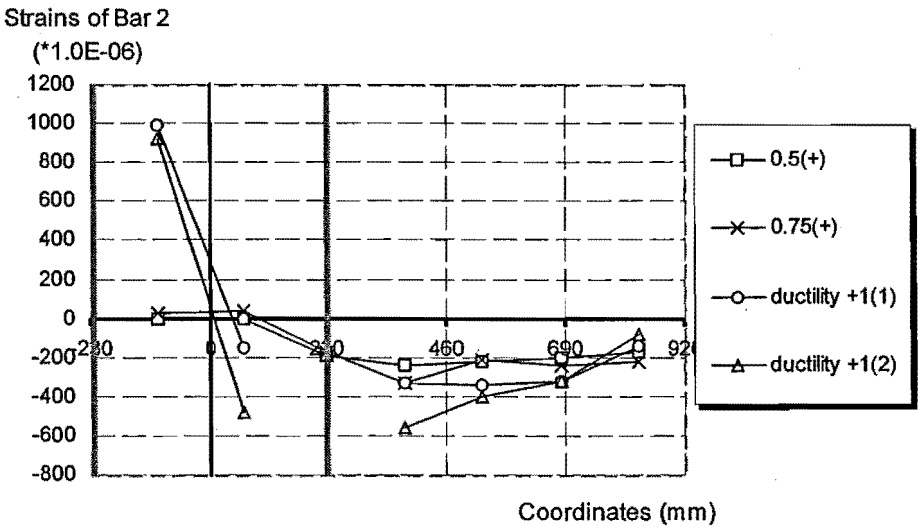

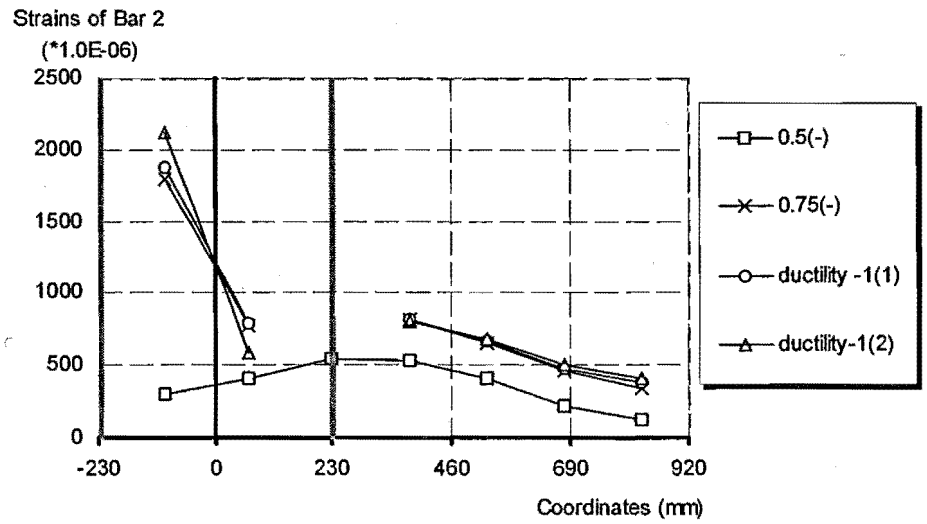

Fig.7.14 Measured Strain Profiles of Beam Bar 2

strain gauges glued at inner column face did not work properly, hence the strains of beam bar 2 at this location could not be obtained. It is seen from Fig.7.13 and Fig.7.14 that the measured tensile strains for beam bar 1 and beam bar 2 within the joint region did not apparently reduce, compared with the strains measured at inner column face throughout the testing history. Hence it could be said that very severe bond degradation must have taken place along the beam longitudinal bars 1 and 2 within the joint region.

Fig.7.15 compares the measured strains with the theoretical strains at the inner column face for beam bar 1 when beam bar 1 was in flexural tension in the early loading cycles until the completion of loading at ductility 1. After ductility 1, some strain gauges went out of order. Fig.7.15 shows that generally the measured beam steel strains matched reasonably well with the theoretical predictions at the inner column face. The measured steel strains were larger than the theoretical values at later stages. The theoretical values were predicted using the plane section assumption. Such a comparison could not be conducted for beam bar 2 because the readings from the strain gauges on beam bar 2 at inner column face did not make sense.

Measured strains along the column longitudinal bars were much smaller than the steel yield strain and theoretically the columns were expected to response in elastic range.

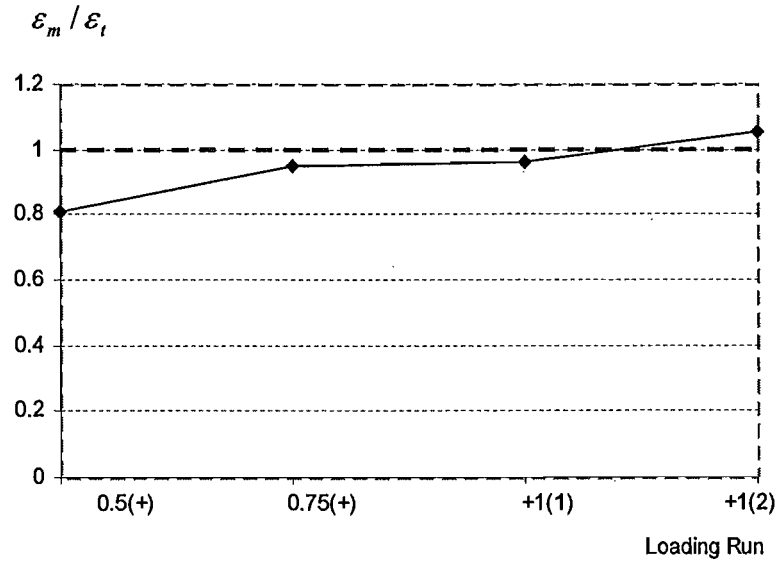

Fig.7.15 Comparison of measured strains with theoretical strains of beam bar 1 at inner column face

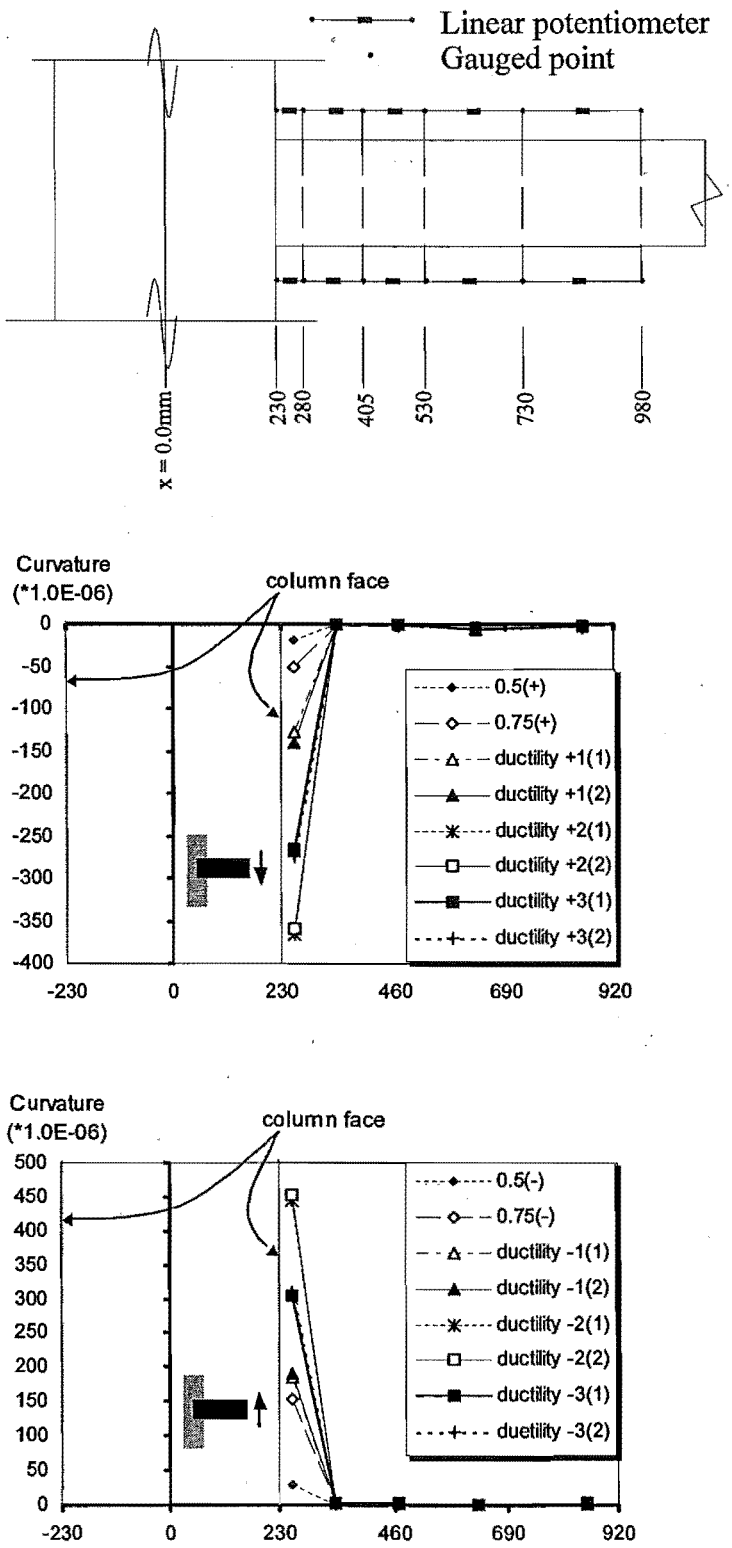

Fig.7.16 Measured Beam Curvature Profile for Unit REJ1

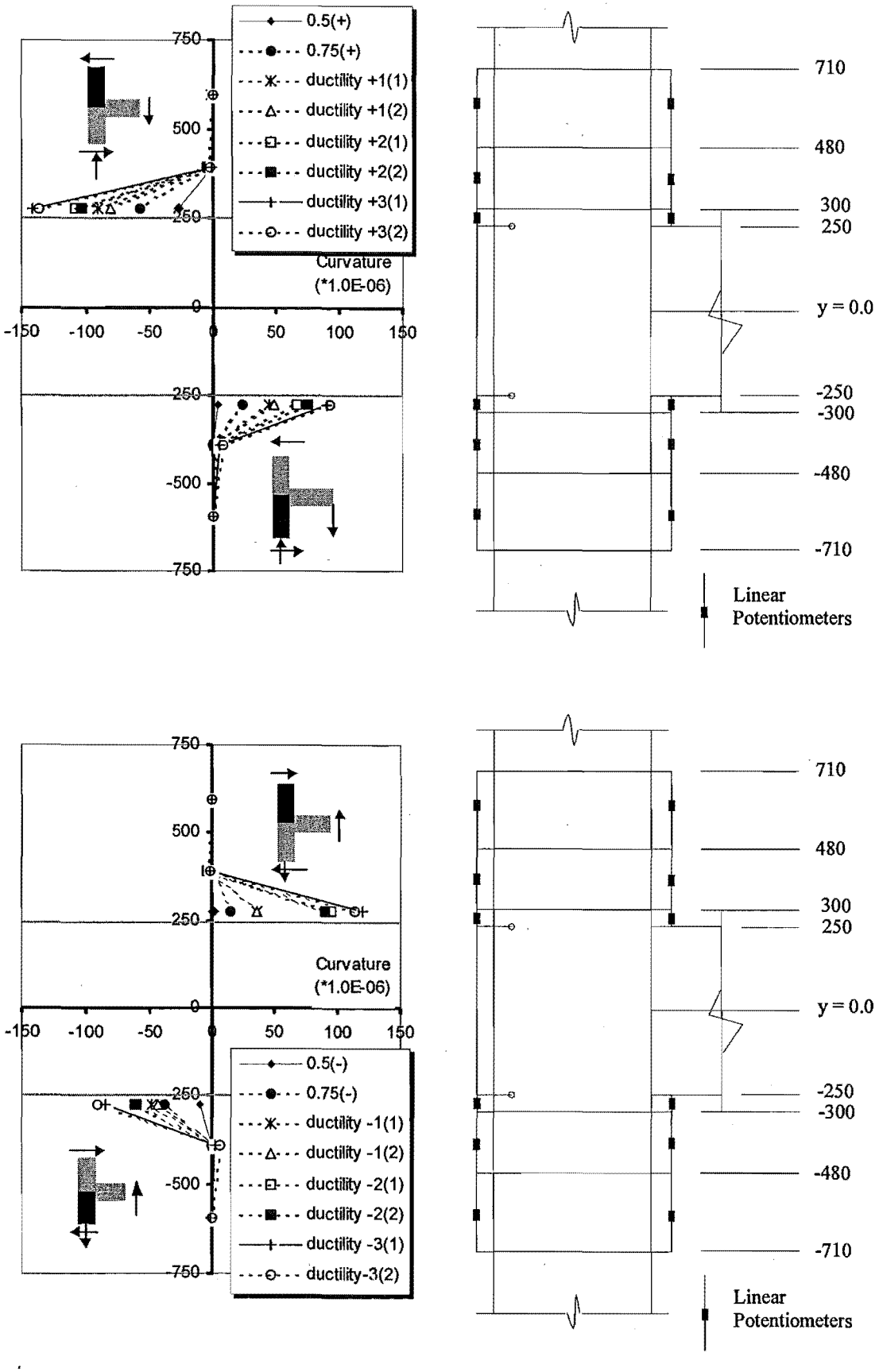

Fig.7.17 Measured Column Curvature Profile for Unit REJ1

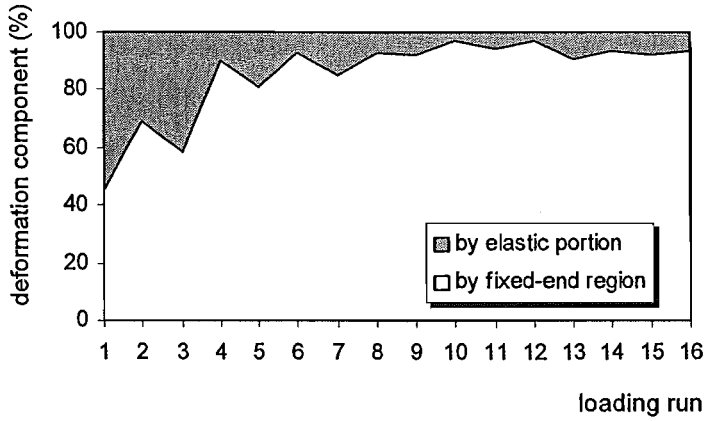

(a) Beam deformation components

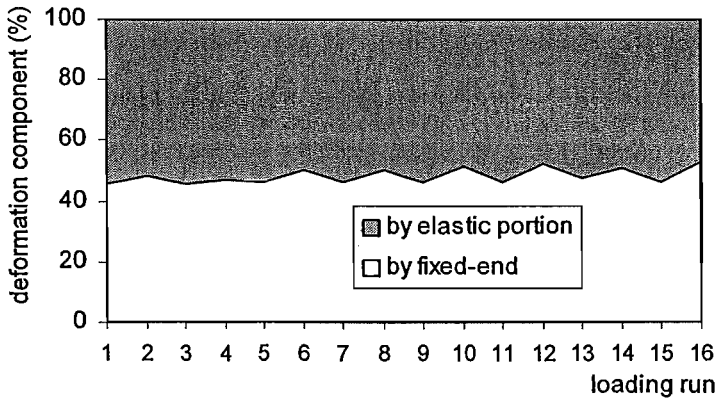

(b) Column deformation components

Fig.7.18 Deformation components measured for the beam of Unit REJ1

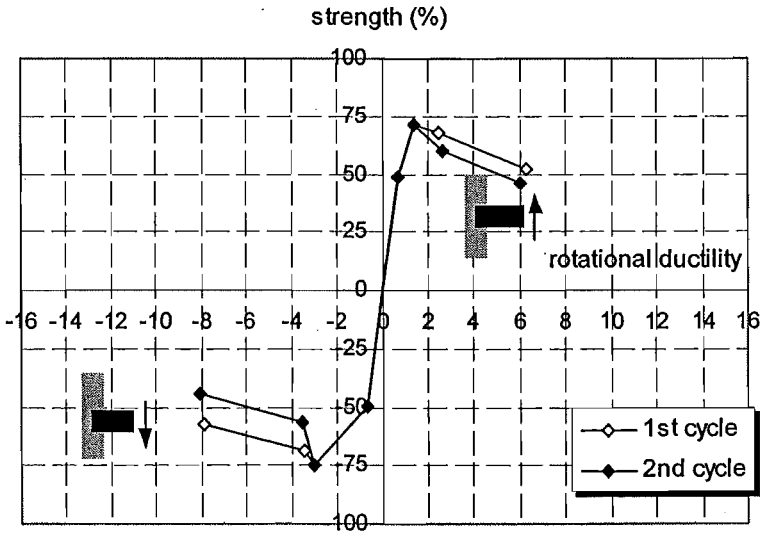

Fig.7.19 Rotational ductility in the beam fixed-end versus the beam force strength

7.3.5 Deformation Characteristics of Beam and Column Members

For the retrofitted as-built unit REJ1, the beam was expected to develop plastic hinges and the columns were expected to behave in the elastic range.

Fig.7.16 and Fig.7.17 show the measured curvature profiles for the beam and columns of Unit REJ1, respectively. It is evident that the measured curvatures over the fixed-end regions of the members were much larger than the curvatures measured elsewhere and the member flexural deformation was mainly limited to the fixed-end regions. For the columns, which were expected to behave in the elastic range, the measured curvatures over the fixed-ends reached up to 29 times the theoretically predicted yield curvature of 4.8E-06. The measured beam curvatures over the fixed-end regions reached up to nearly 100 times the theoretically predicted beam yield curvature although the attained beam flexural strength has never reached the theoretical strength. The theoretical beam yield curvature is 4.5E-06 for positive loading, and 4.9E-06 for negative loading.

Fig.7.18 shows the deformation components measured for the beam and columns of Unit REJ1. From Fig.7.18, it is evident that the tendency of the concentration of beam flexural deformation in the fixed-end became more significant, compared with the columns. The beam was weaker than the columns for Unit REJ1.

Fig.7.19 shows the beam rotational ductility in the fixed-end versus the beam strength of Unit REJ1 and the beam of Unit REJ1 was expected to develop plastic hinges. The strength degradation with the increase in the imposed displacement level is significant, but a rotational ductility of about 6 could still be achieved.

7.3.6 Joint Behaviour

7.3.6.1 Joint Shear Stress

The measured maximum nominal horizontal joint shear stress for Unit REJ1 was 1.37MPa or $0.23\sqrt{f_c'}$ MPa, based on the measured member forces and plane section theory. In comparison, the estimated maximum nominal horizontal joint shear stress for anti-clockwise loading direction was lower, being 0.9 MPa, or $0.15\sqrt{f_c'}$ MPa. Theoretically, the joint shear force at the development of the joint diagonal cracking was $0.3\sqrt{f_c'}$ MPa in the case of zero axial column load if expressed in terms of the nominal

horizontal joint shear stress. Evidently, the maximum nominal horizontal joint shear stress in Unit REJ1 was low enough to have no joint shear failure.

7.3.6.2 Measured Strains in Joint Shear Reinforcement and Fibre-Glass Jacketing

The strains in three joint hoops were measured by electrical resistance strain gauges, one set of the joint hoop was located at the centre of the joint core and the other two sets were located at the beam faces. The measured joint hoop strains were contrasted to the strains measured for column transverse reinforcement adjacent to the joint core in Fig.7.20, where the positions of the five sets of column transverse reinforcement were also illustrated in Fig.7.20.

For well-designed exterior beam-column joint subassemblages, the beam bar hooks are bent into the joint cores and the member forces will be transferred across the joint core by a concrete diagonal strut. Hence the joint horizontal hoops at the joint core centre will be subjected to higher tensile stresses due to Poisson's effect as for axially loaded columns in compression, compared to those close to beam faces [P13]. However, Fig.7.20 shows different behaviour, that is, the strain measured in the joint hoop CT-4 of Unit REJ1, which was located at the beam face, was much larger than the measured strains in CT-3, which was at the centre of the joint core. This was because the bending out configuration of the beam bars as was the case of Unit REJ1 required the actuation of an alternative force path as postulated in Chapter 4, and hence the joint hoops at the beam flexural tensile face were more stressed. Severe bond degradation in this case resulted in a greatly reduced joint shear force assigned to truss action. Hence the joint shear reinforcement provided at the centre of the joint core would make no difference to the shear performance of the as-built exterior beam-column joint components.

Fig.7.20 also shows clearly that CT-4 was subjected to a much higher tensile stress compared to column transverse reinforcement CT-1 and CT-5. Apparently the cause for the joint hoop at beam flexural tensile face to be highly stressed was not because of high column shear resistance demand, but was due to the requirement for control of concrete tensile cracking along the beam bar hook and the actuation of the alternative force path to transmit the member forces across the joint core.

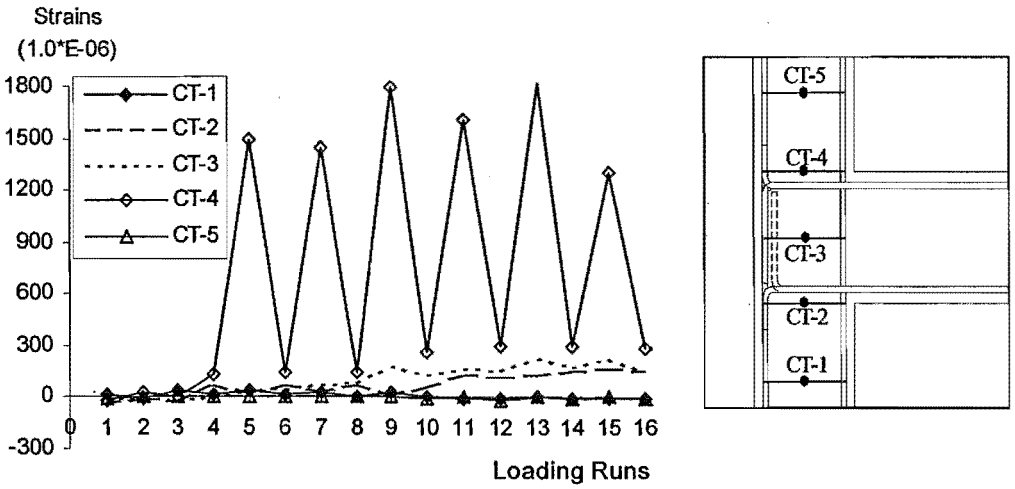

Fig.7.20 Joint Shear Reinforcement and Column Stirrup Strains of Unit REJ1

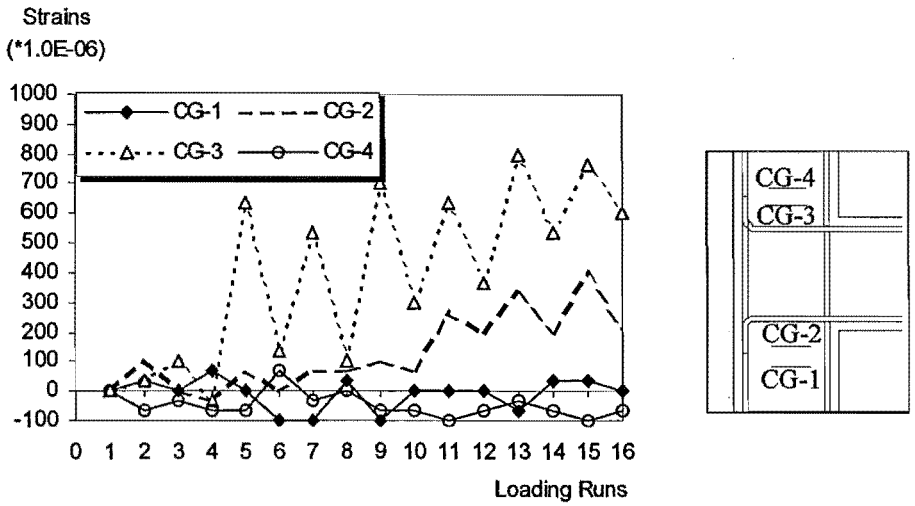

Fig.7.21 Measured Strains in Fibre-Glass Jacketing by Clip Gages for Unit REJ1

Fig.7.21 shows the measured strains in fibre-glass jacketing by clip gages, where positive strains represent tensile strains and negative strains represent compressive strains, similar to the definition of steel strains measured by electrical resistance strain gauges. Apparently, the fibre-glass jacketing was more stressed adjacent to the joint core as for CT-4, as seen from the measurement of clip gages 2 and 3, than that far away from the joint core as seen from the measurements of clip gauges 1 and 4. Severe

bond degradation caused the beam steel tension force to be mainly transmitted within the bend, hence the concrete tension cracking associated with the resistance to the beam steel tension force started from the beginning of the beam bar bend. The fibre-glass jacketing started to be stressed only after column concrete cracking within the confined column area. As a result, the fibre-glass jacket was more stressed in tension adjacent to the beam faces.

7.3.6.3 Joint Shear Distortion and Expansion

Whereas in the case of test on Unit EJ1 the measured maximum joint shear distortion was 5.38×10^{-3}, the measured maximum joint shear distortion for Unit REJ1 was 1.63×10^{-3}, which was much smaller, although the maximum horizontal nominal joint shear stress for Unit REJ1 was about 36% higher than that with Unit EJ1. Better joint shear performance of Unit REJ1 than that of Unit EJ1 occurred as a result of the actuation of a stiff concrete strut mechanism for Unit REJ1. Therefore in the case of the beam longitudinal bars being bent away from the joint core, the external jacketing in the column areas above and below the joint core can actuate an alternative concrete strut mechanism to transmit the member forces across the joint core as postulated in Section 4.4.2.

The influence of the used steel type on the joint shear behaviour also can be identified if the maximum joint shear distortion of Unit REJ1 was contrasted to that of Unit O7. The maximum joint shear distortion measured for Unit O7 was 35×10^{-3}, which was about 22 times the measured maximum joint shear distortion measured for Unit REJ1, although the two tests achieved similar storey shear strengths, being about 75% of the theoretical storey shear strengths. Severe bond degradation and slip along the beam longitudinal reinforcement within and adjacent to the joint core, although greatly increased the structural flexibility by causing a big beam fixed-end rotation, resulted in much improved joint integrity.

7.3.6.4 Discussion of Alternative Force Transfer across the Joint Core

As discussed above, the use of plain round longitudinal reinforcement enhances the concrete tension cracking failure along the beam bar hooks, resulting in an increased need for actuating the alternative force path when the beam longitudinal bar hooks are bent away from the joint core as for Unit EJ1. External fibre-glass jacketing for the columns above and below the joint core as used for Unit REJ1 is effective in improving the overall performance of as-built exterior beam-column joint components with the beam bar hooks bent away from the joint core and containing plain round longitudinal reinforcement.

However, the attainment of the strength and the stiffness of the retrofitted unit REJ1 was still low. It is believed that, should the external reinforced concrete column jacketing technique be used and the depth of the exterior columns be sufficiently enlarged, the improvement of the overall performance of the unit would have been more significant, compared to that of Unit REJ1. The generous increase in the column depth would resolve the complication incurred with the simultaneous formation of the strut D across the joint core and the strut D_1 (see Fig.4.4), and make the actuation of the alternative force transfer across the joint much easier.

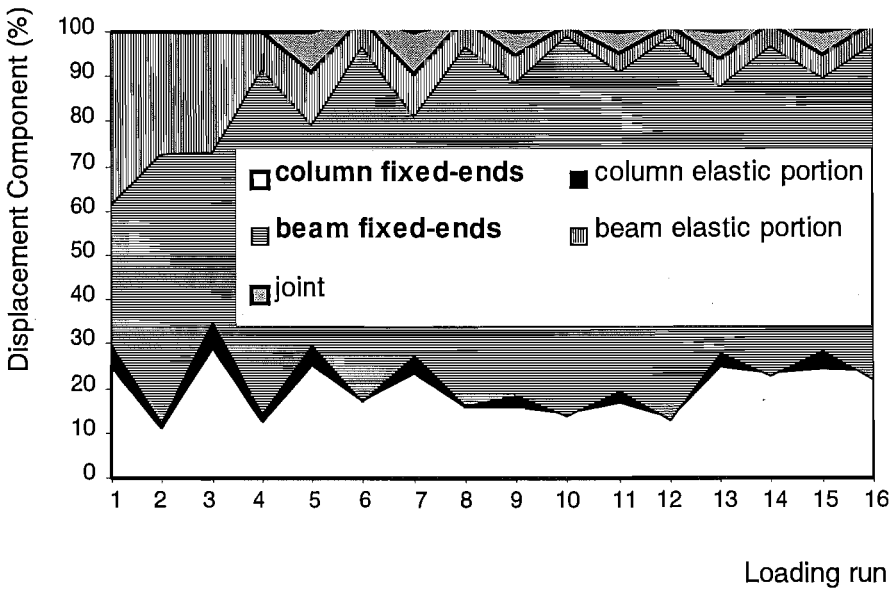

Fig.7.22 Displacement Components Measured for Unit REJ1

7.3.7 Displacement Components

Fig.7.22 shows the estimated storey horizontal displacement components, where the horizontal displacement components were expressed as percentages of the measured storey displacement at the peaks of the selected loading cycles. Fig.7.22 shows that, similar to the test of Unit EJ1, beam displacement component generally had been very large throughout the whole test, being about 85% of the storey displacement. As far as the beam deformation is concerned, the beam fixed-end rotation increased gradually with the loading while the beam curvature contribution decreased gradually. Evidently, the poor stiffness performance demonstrated by Unit REJ1 was mainly due to progress of the beam fixed-end rotation resulting from severe bond degradation along the beam bars within and adjacent to the joint core.

When compared with the test observation for Unit O7 where the contribution of joint shear distortion to the total storey displacements reached up to 66% for positive loading cycle and 68% for the negative loading cycle, the contribution of joint shear distortion estimated for Unit REJ1 was much smaller, being about 9.6% of the storey displacement although both tests achieved similar storey shear strength in terms of the percentages of the theoretical storey shear strength of the unit. Unit O7 was identical to Unit REJ1 except that Unit O7 was reinforced by deformed bars and Unit REJ1 was retrofitted by fibre-glass jacketing in the column areas above and below the joint core. The much smaller joint displacement component for Unit REJ1 was because of two reasons. One reason was that severe bond degradation along the beam main bars within the joint core of Unit REJ1 caused much less beam steel tension force transmitted into the joint core by bond, hence the joint shear deformation reduced significantly. The other reason was that wrapping the column areas adjacent to the joint core using fibre-glass jacketing actuated the postulated robust concrete strut mechanism, and concrete strut mechanism has much higher stiffness than truss mechanism with deformed bars. In this case, the critical part of the retrofitted exterior beam-column joint unit REJ1 was shifted to the beam fixed-end rotation.

7.3.8 Summary

The damaged as-built exterior beam-column joint unit was retrofitted by wrapping the column areas immediately above and below the joint core using fibre-glass jacketing, and it became Unit REJ1. Unit REJ1 was subjected to simulated seismic loading with zero axial column load, as for test on Unit EJ1. This test investigated the possibility of actuating the postulated alternative force path in Section 4.4.2 when the plain round beam longitudinal bars were bent away from the joint core in the exterior columns.

1. Test on Unit REJ1 demonstrated that fibre-glass jacketing in the column areas adjacent to the joint core significantly improved the general seismic performance of as-built exterior beam-column joint assemblies where the plain round beam longitudinal bars are bent away from the joint core. The fibre-glass jacketing in the column areas adjacent to the joint core controlled the concrete tension cracking along the beam bar hook, actuated the postulated concrete strut mechanism which could transmit the member forces across the joint core. As a result, the seismic performance of the test unit was governed by beam flexural behaviour, rather than by the premature concrete tension cracking along the beam bar hooks as for Unit EJ1.

2. The storey shear strength of the retrofitted unit REJ1 was 135% of the measured storey shear strength for as-built unit EJ1, but it was still 25% less than the theoretical storey shear strength of the unit, although the seismic performance of the unit was dominated by the beam flexure. Bond degradation along the beam longitudinal bars meant that the theoretical beam flexural strength estimated using ordinary flexure theory could not be attained.

3. The meausred initial structural stiffness for Unit REJ1 at loading of 75% of the theoretical storey shear strength of the unit was about 50% of the theoretical prediction, which was based on the sectional analysis and assuming that the beam was just yielding and the columns were still in elastic range. The stiffness measured at the loading of 50% of the theoretical storey shear strength was about 2.4 times that for as-built unit EJ1. Apparently, the enhancement for the stiffness achieved by wrapping the column areas adjacent to the joint core was more pronounced than that for the strength.

4. External column jacketing adjacent to the joint core activated the postulated joint shear force path, which was a robust concrete strut mechanism. Therefore, although the maximum joint horizontal shear input for Unit REJ1 was larger than that for as-built unit EJ1, due to the enhanced available storey shear strength, the joint shear performance was at least as good as that observed for Unit EJ1.

5. As far as the individual reinforced concrete beams and columns with plain round longitudinal reinforcement are concerned, the seismic performance is governed by flexure, rather than by shear. However, the theoretical flexural behaviour of the member was poor, especially the flexural stiffness.

6. Comparative study of the test results of Units EJ1, REJ1 and Unit O7 revealed the following findings:

(1). The most critical part of as-built exterior beam-column joint EJ1 with the plain round beam bar hooks bent out of the joint core was the failure associated with concrete tension cracking orientated by the beam bar hook if sufficient column transverse reinforcement is not available adjacent to the joint core. Under such circumstances, external column jacketing adjacent to the joint core as employed for test on Unit REJ1 could improve the overall seismic performance. Such a retrofit technique can control the concrete tension cracking orientated by the beam bar hook and mobilise the postulated concrete strut mechanism to transmit the member forces across the joint core. As a result, the overall performance of Unit REJ1 was no longer dominated by the concrete tension cracking in the column as was the case for test of EJ1, but it was dominated by the large beam fixed-end rotation.

It is believed that external column jacketing by using reinforced concrete jacketing technique would achieve better structural performance, in comparison with the external fibre-glass jacketing above and below the joint core as for Unit REJ1.

(2). The most critical part of as-built exterior beam-column joint deformation components with typical reinforcing details of pre-1970s construction became the joint shear failure in the case of using deformed bars for longitudinal reinforcing bars, as was the case of test of Hakuto's O7. However, the use of deformed reinforcement was not common at that time.

7.4 TEST OF UNIT EJ2

7.4.1 Introduction

As-built full-scale exterior beam-column joint unit EJ2 was otherwise identical to Unit EJ1 except that Unit EJ2 had the beam bar hooks bent into the joint core. As for Unit EJ1, Unit EJ2 was also tested under simulated seismic loading with zero axial column load. This test aimed at investigating the influence of the beam bar hook details in exterior column on the seismic performance of as-built reinforced concrete exterior beam-column joint components containing plain round longitudinal bars and other reinforcing details typical of pre-1970 existing reinforced concrete moment resisting frame structures in New Zealand. In addition, test on Unit EJ2 was identical to Hakuto's test on Unit O6 [H1] but Hakuto used deformed longitudinal reinforcement. Comparative study of test results of Units EJ2 and Hakuto's Unit O6 is conducted to identify the effect of the plain round bars used on the seismic performance of existing reinforced concrete frame structures.

7.4.2 Crack Development and Failure Mode

Fig. 7.23 shows the crack development and the final appearance observed for Unit EJ2.
In loading run 1, which was the peak of clockwise $0.5V_i$, flexural cracks initiated in the beam and columns as expected. Also observed in the loading run 1 was the development of the vertical crack running along the outer layer of the column longitudinal bars in the upper column adjacent to the joint core, and this occurred due to column bar buckling resulting from inadequate column transverse reinforcement adjacent to the joint core and bond degradation along the column longitudinal bars.

In the loading run 3 at the peak of clockwise $0.75V_i$ where the maximum storey shear strength was attained, the existing vertical crack extended vertically from the upper column into the joint core due to the progress of column bar buckling and the opening action of the beam bar hooks. The development of the existing vertical crack into joint diagonal tension cracks was also observed at this stage. The development of the beam and column flexural cracks was mainly limited to the beam and column interfaces due to severe bond degradation and slip along the longitudinal reinforcement within and adjacent to the joint core. The column flexural crack development was observed to be not so apparent as that for the beam, indicating that bond degradation was more severe along the

beam main bars than that along the column main bars as expected for a weak beam-strong column system.

Observed crack development during anti-clockwise loading was similar to that during clockwise loading, and the maximum storey shear strength of the unit was attained at anti-clockwise loading peak of $0.75V_i$.

During subsequent loading cycles after the loading cycle at $0.75V_i$, the attained storey shear strength degraded gradually, and the prominent crack development was in the major beam flexural crack at column face and in the damage resulting from interaction between the column bar buckling and the opening action of the beam bar hooks. Progressive bond degradation and slip along the beam bars within the joint core not only had caused the development of the major beam flexural crack at column face but also had caused the increase in the beam steel force needed to be transferred at the bend. Higher beam steel force required to be transmitted at the bend, together with outer joint concrete cover spalling resulting from progressive column bar buckling, enhanced the opening action of the beam bar hooks. Hence the degrading beam flexural performance and the damage caused by the column bar buckling and the opening action of the beam bar hooks governed the strength development of the unit and became the final failure triggers of Unit EJ2.

Throughout the whole test history of Unit EJ2, no diagonal concrete tension cracks were observed in the beam and columns, similar to the tests on Units EJ1 and REJ1. This indicates once again that the seismic performance of concrete members reinforced by plain round longitudinal bars is more likely to be dominated by flexure, rather than by shear.

The observed test evidence for Unit EJ2 was significantly different from that for Hakuto's Unit O6, which was identical to Unit EJ2 except that Hakuto's Unit O6 used deformed reinforcing bars. Whereas in the case of Hakuto's test on Unit O6 the final failure was due to the shear failure in the beam and in the joint, the joint core of Unit EJ2 only suffered minor concrete cracking, and the performance of its beam was totally governed by flexure.

Also, the observed joint crack orientation for Unit EJ2 was very different from that for retrofitted Unit REJ1. The observed joint shear cracks of Units EJ1 and REJ1 were about 45° to the horizontal axis and initiated from the midway of the beam bar hook, whereas the joint diagonal tension cracks observed of Unit EJ2 were approximately corner to corner

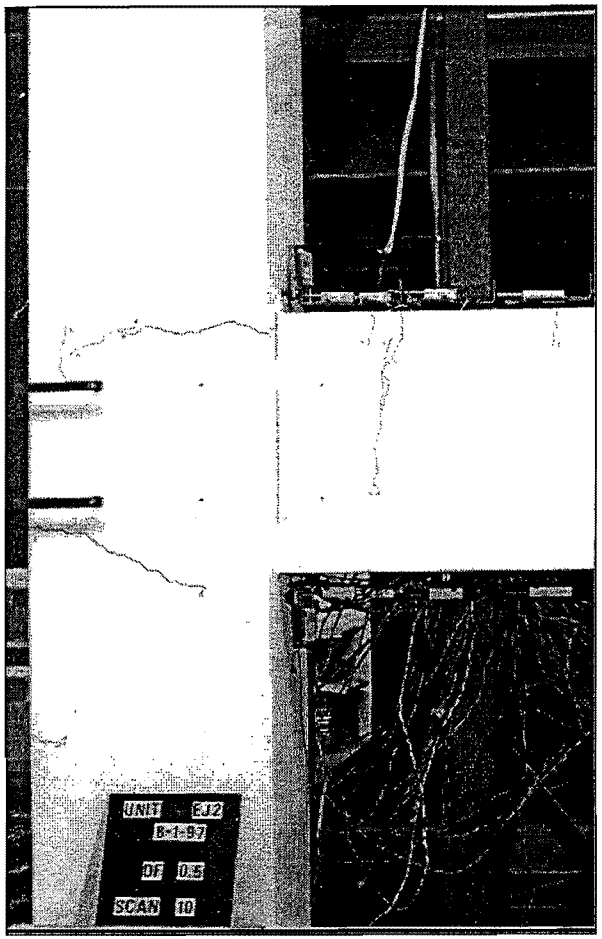

(a) Loading at 0.5Vi

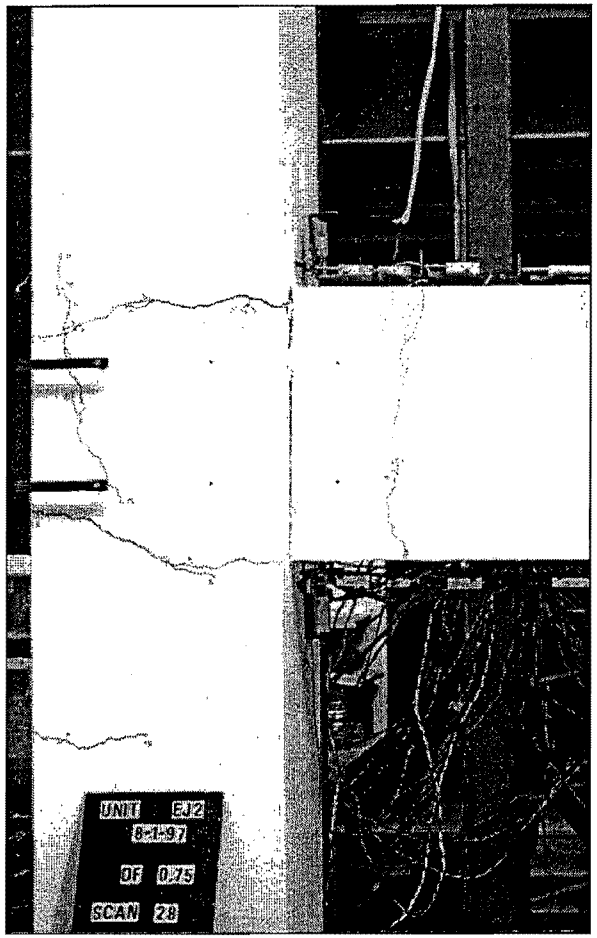

(b) Loading at 0.75Vi

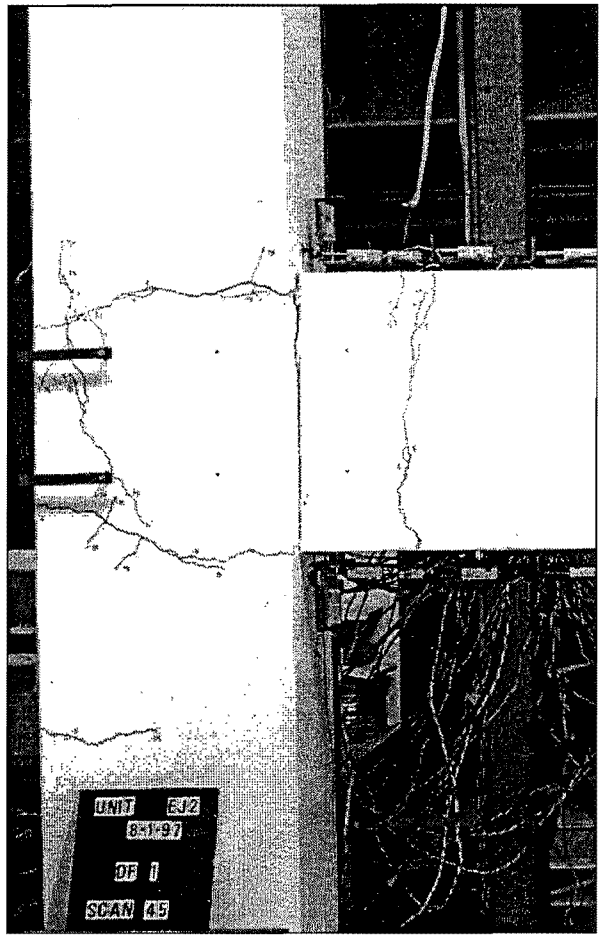

(c) End of Ductility 1

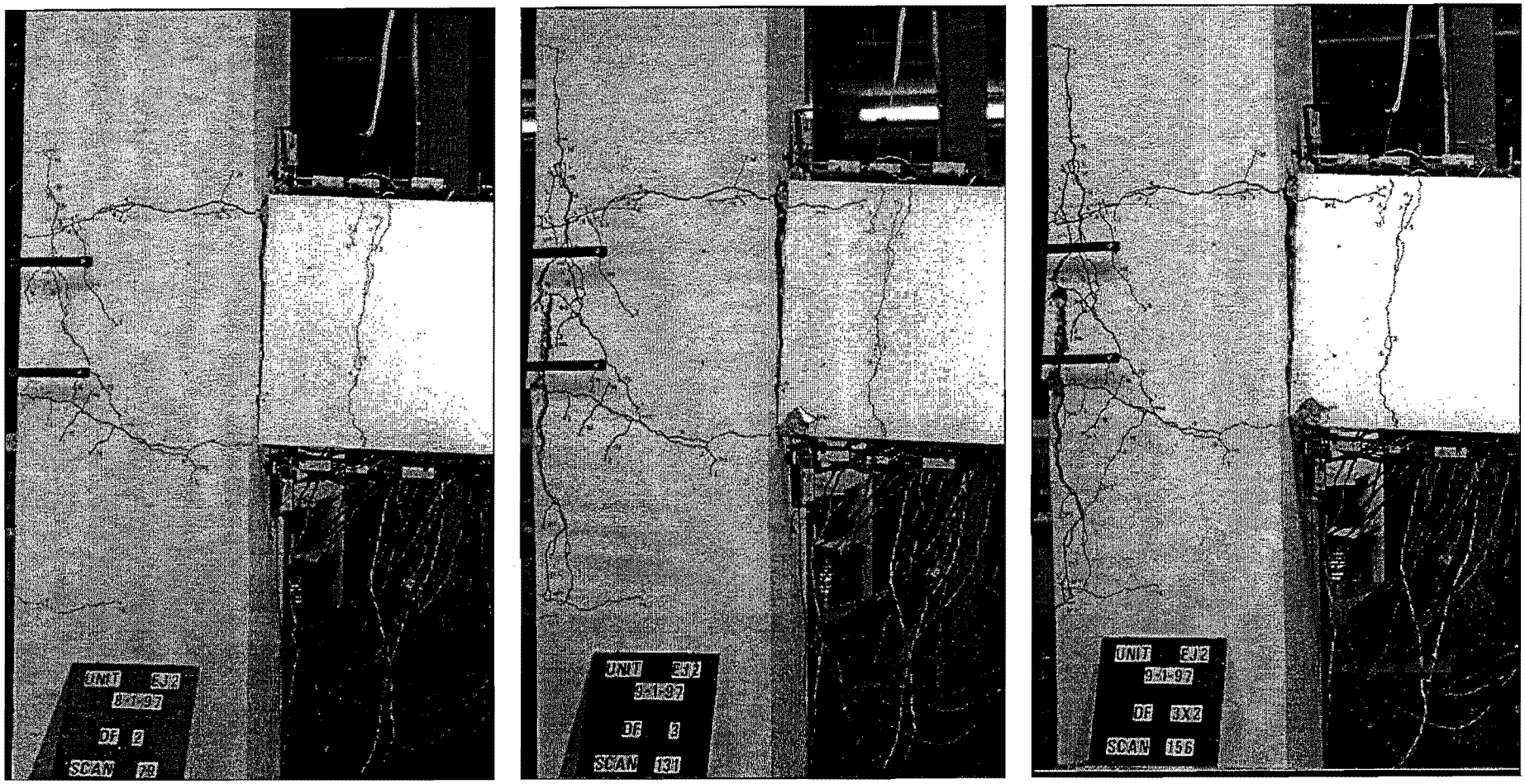

(d) End of Loading at Ductility of 2 (e) End of Loading at Ductility 3 (f) Final Appearance

Fig.7.23 Crack Development and Final Appearance of Unit EJ2

joint diagonal cracks. This led to the conclusion that the joint concrete strut mechanisms are of different orientations for different beam bar hook configurations in the exterior columns.

7.4.3 Load-versus-Displacement Response Measured for Unit EJ2

Fig.7.24 shows the measured storey shear versus storey displacement and drift hysteresis loops for Unit EJ2. Also shown in Fig.7.24 is the theoretical storey shear strength of the unit, V_i , at the attainment of the beam flexural strength for both clockwise and anti-clockwise loading directions. Fig. 7.24 demonstrates that the detail of the beam bar hooks bent into the joint core in the exterior columns greatly improved the seismic behaviour of exterior beam-column joint subassemblages, when compared with the similar test unit EJ1 with the beam bar hooks bent away from the joint core in the exterior columns.

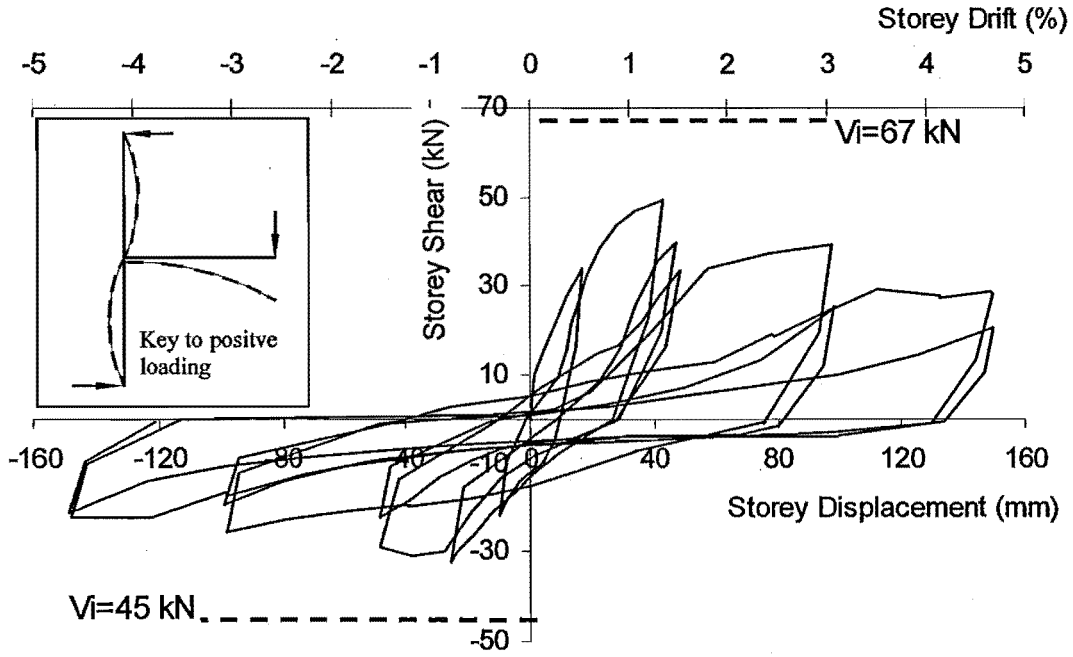

Fig. 7.24 Storey Shear versus Storey Displacement and Storey Drift Hysteresis Loops Measured of Unit EJ2

The maximum storey shear strength attained by Unit EJ2 was 75% of the theoretical storey shear strength for both loading directions and it occurred at a storey drift of approximately 1.3% in the loading cycle of $0.75V_i$. The storey shear strength achieved by Unit EJ2 was

higher than that by Unit EJ1, indicating that the bending configuration of the beam bars in the exterior columns will have significant effect on the available strength. The storey shear strength of Unit EJ2, if expressed as the percentages of the theoretical storey shear strength, was comparable to that of 75% for Unit REJ1, which was retrofitted by wrapping the column areas immediately adjacent to the joint core. Hence, for as-built exterior beam-column joint units, the inadequate anchorage configuration of the beam bar hooks bent away from the joint cores in the exterior columns will lead to a lower force strength if the column transverse reinforcement adjacent to the joint core is insufficient. But the inadequate anchorage configuration of the beam bar hooks when bent out of the joint cores in exterior column will not impair the available structural strength property of exterior beam-column joint components if sufficient column transverse reinforcement is available adjacent to the joint core. The strength behaviour observed for Unit EJ2 was also contrasted to that for Hakuto's Unit O6. Hakuto's Unit O6 attained the unit's theoretical storey shear strength. The lower load strength attainment of Unit EJ2 in comparison with Hakuto's Unit O6 was not only because of severe bond degradation along the beam longitudinal reinforcement but also because of premature concrete tension cracking along the beam bar hooks. Severe bond degradation along the beam longitudinal reinforcement resulting from the use of plain round longitudinal bars caused the available beam flexural strength to be lower than its theoretical prediction, as explained earlier. Premature concrete tension cracking along the beam bar hooks was associated with the interaction of the column bar buckling and the opening action of the beam bar hooks and it was facilitated by the use of plain round beam longitudinal bars. Consequently, the storey shear strength of Unit EJ2 was lower than that of Hakuto's Unit O6.

Measured first yield displacement was determined using the method described in Section 5.3.2 for the test of Unit EJ2, and it was equivalent to a storey drift of 1.5%. It is surprised to notice that the first yield displacement determined for Unit EJ2 was 3.6 times the displacement at first yield measured from Hakuto's test on Unit O6 [H1]. In Chapter 6, it was found that the use of the plain round longitudinal reinforcement caused an increase in the measured displacement at first yield by 50% for as-built interior beam-column joint units. Hence the adverse influence of the longitudinal steel type on the structural stiffness property is more significant for as-built exterior beam-column joint units, compared to as-built interior beam-column joint units. Also of interest is that the measured initial stiffness

for Unit EJ2 was 1.2kN/mm and it was only 57% of the average initial stiffness of 2.1 kN/mm measured for Unit REJ1 at loading cycle of 0.75 V_i. This demonstrated that, if the alternative force path across the joint core can be achieved, namely sufficient column transverse reinforcement is available adjacent to the joint core, the bending out configuration of the plain round beam bars in the exterior columns can result in similar strength and stiffness performance to that with the beam bar hooks bent into the joint core.

Significant pinching of the loops is evident in Fig. 7.24, similar to the test evidence of Unit EJ1, indicating very poor energy dissipating capacity of Unit EJ2. Pinching of the hysteresis loops is a typical feature of beam-column joint components reinforced by plain round longitudinal reinforcement because of the formation of a major beam flexural crack at the column face as a consequence of severe bond degradation along the plain round beam longitudinal reinforcement.

Fig. 7.24 also shows significant strength degradation after the maximum strength was attained for Unit EJ2. Strength degradation was also observed for the second loading cycle at the same deformation level, compared to the first loading cycle. This was mainly due to the progressive failure of the bond mechanism along the beam longitudinal bars within and adjacent to the joint core and the progressive failure associated with interaction of column bar buckling and the opening action of the beam bar hooks.

In summary, the test on Unit EJ2 attained a maximum storey shear that was approximately 25 % less than the theoretical storey shear strengths at a storey drift of approximately 1.3%. The measured hysteresis loops demonstrated significant pinching with cyclic loading. Configuration of the plain round beam bar hooks bent into the joint cores in exterior columns increased the available force strengths. The utilisation of plain round longitudinal reinforcement greatly improved joint shear performance, but caused the member flexural strengths and the structural stiffness to reduce a great deal, and the reduction in the available structural stiffness was especially significant, when compared to the available strength. However, the inadequate anchorage detail of the plain round beam bar hooks bent away from the joint cores will not impair the available strength and stiffness if sufficient column transverse reinforcement is provided adjacent to the joint core.

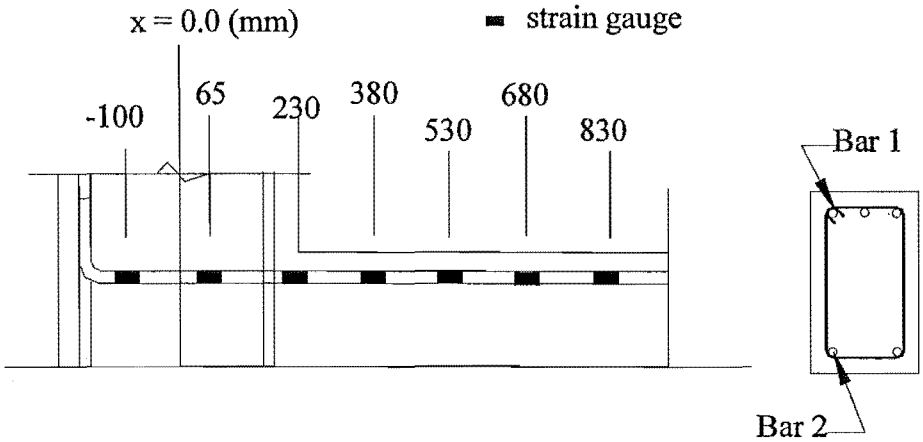

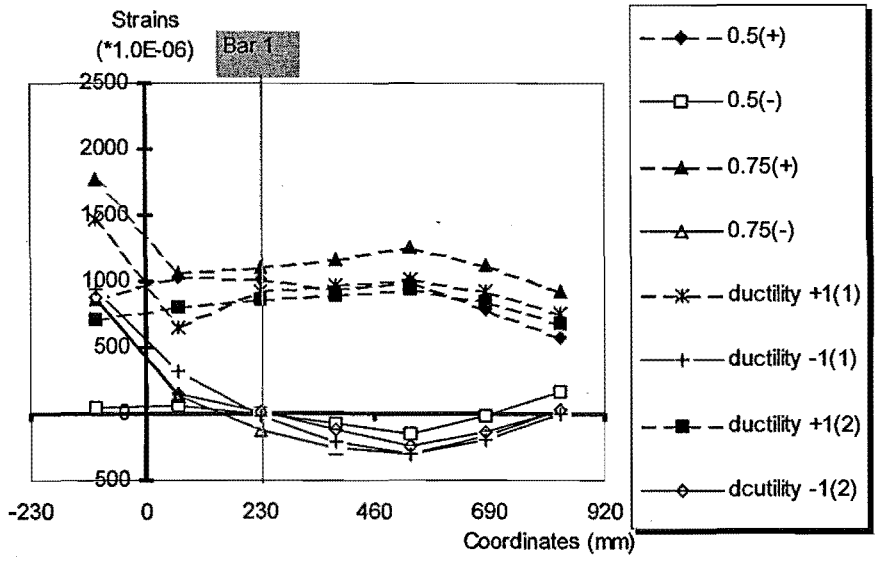

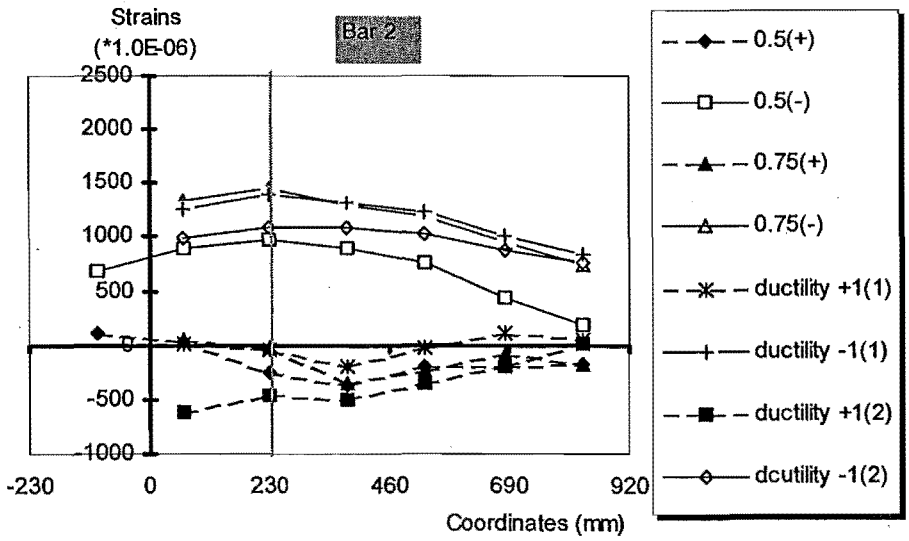

Fig.7.25 Strain Profiles of Beam Bars 1 and 2 Measured by Electrical Strain Gauges

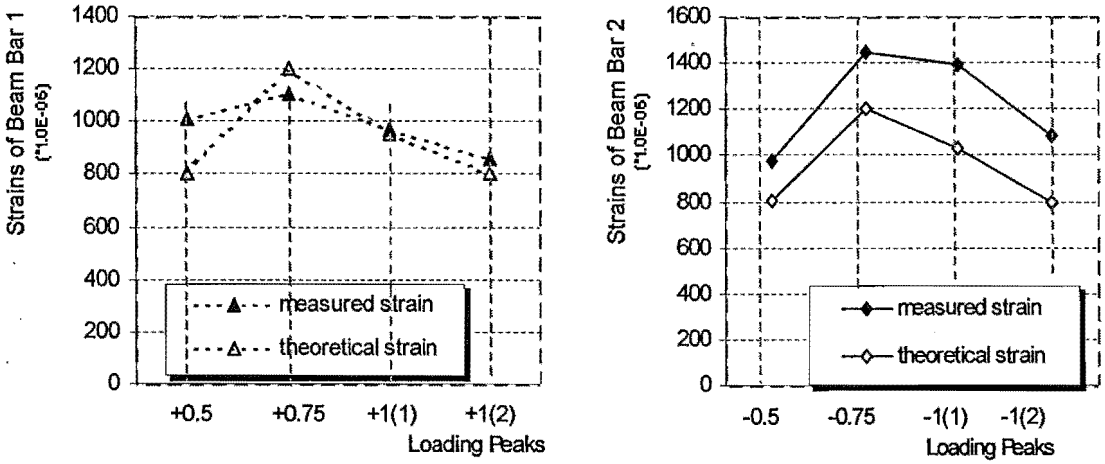

(a) Bar 1 (b) Bar 2

Fig.7.26 Comparison of measured and theoretical steel strains at column face

7.4.4 Measured Strains of the Longitudinal Reinforcement

Fig.7.25 shows the measured strain profiles by electrical resistance strain gauges for beam bar 1 and beam bar 2 respectively. Evidently, significant bond degradation and bar slip must have taken place within the joint core and adjacent to the joint core along the beam flexural tension bars. Measured steel stresses in the flexural beam tension bars were nearly the same from the point 65 mm away at the right from joint centre-line, to the point 100 mm at the left from joint centre-line in the beam. Fig.7.26 compares the measured steel strains with the theoretical strains for beam bars 1 and 2 at inner column face when the beam bars were in flexural tension in the early loading cycles until the completion of loading at ductility 1. For beam bar 1, the measured strains matched with the theoretical strain better than that for beam bar 2, and beam bar 2 tended to be more subjected to bond slip. However, the measured strains showed very big differences from the theoretical values, based on the plane section theory. The more severe the bond degradation along the member longitudinal bars is, the larger the measured steel tensile strains are, in comparison with the theoretical predictions.

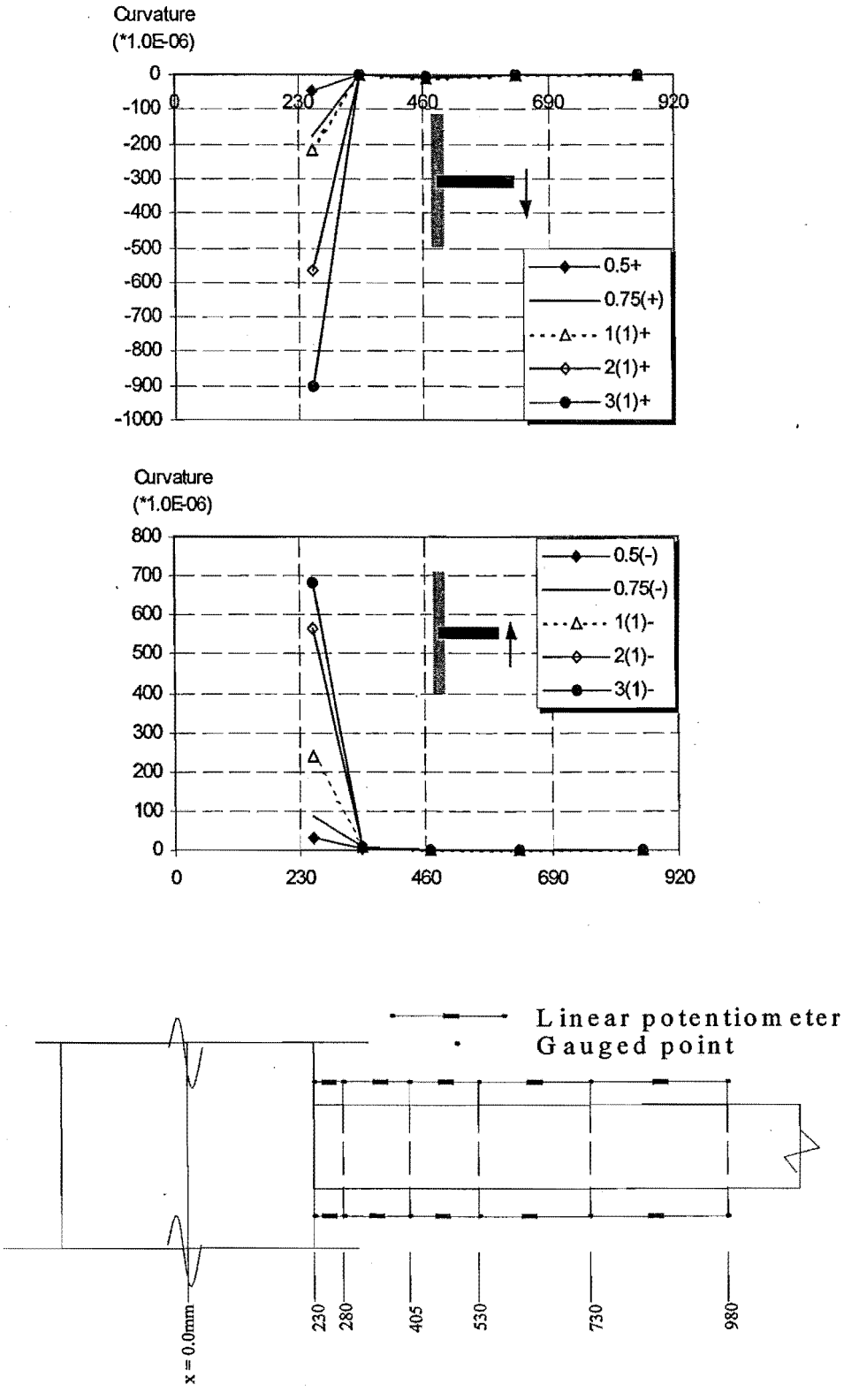

Fig.7.27 Measured beam curvature profiles for Unit EJ2

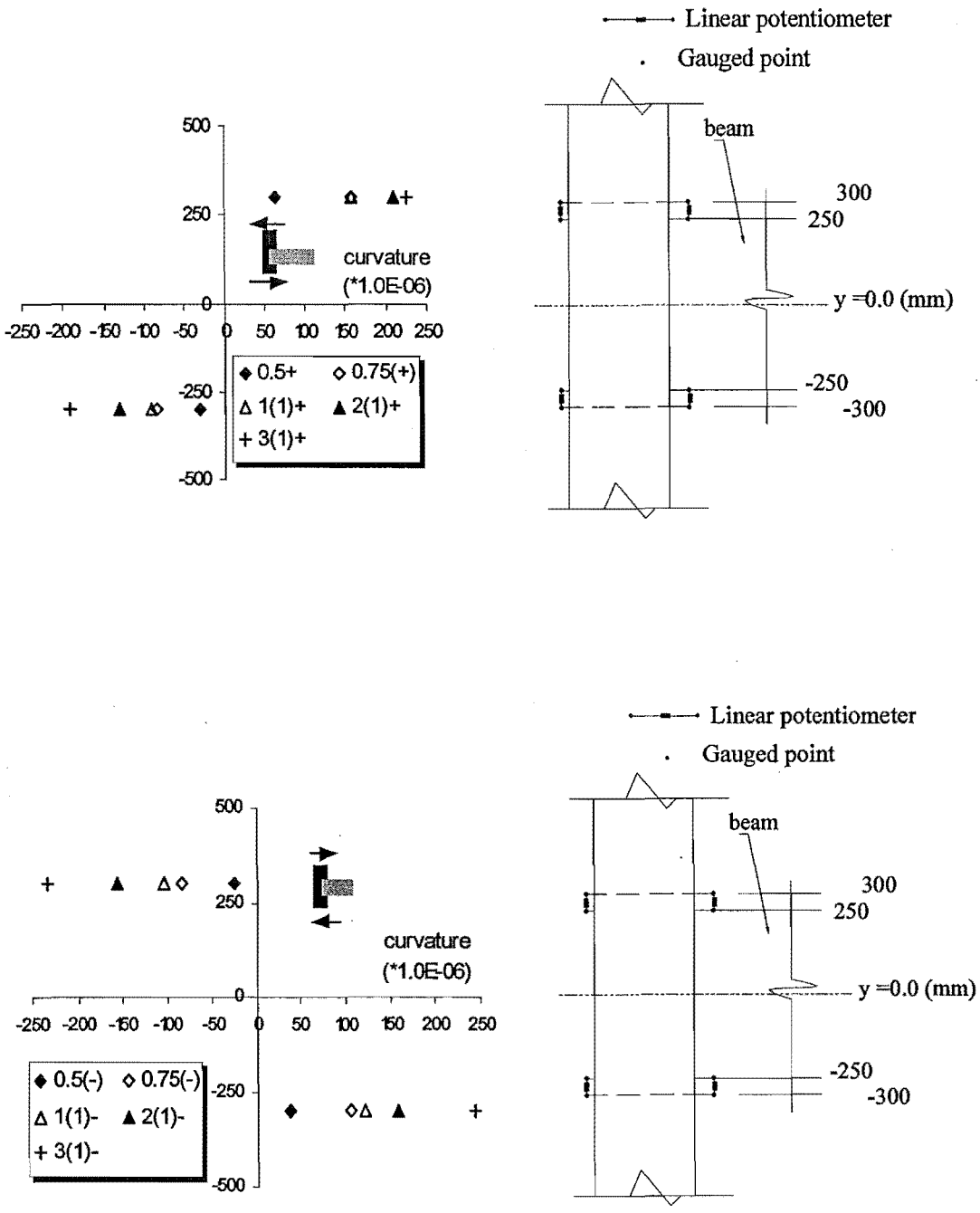

Fig.7.28 Measured curvature profiles in column fixed-ends for Unit EJ2

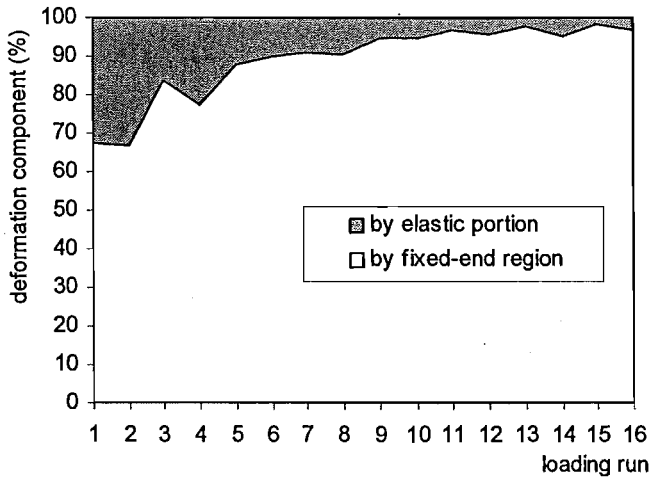

Fig.7.29 Beam deformation components

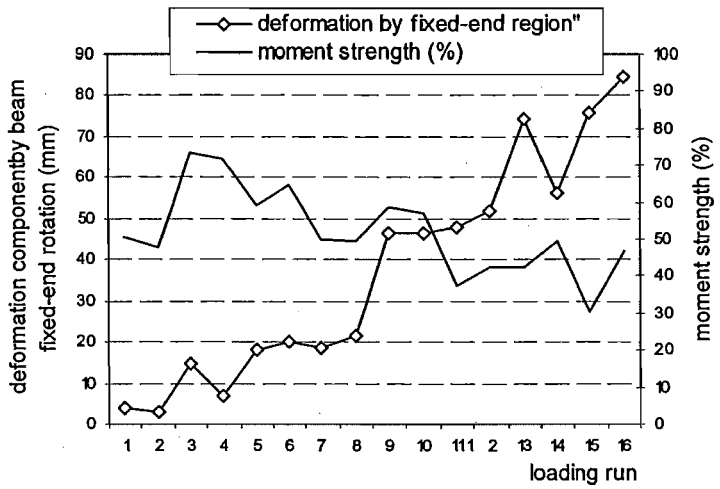

Fig.7.30 Measured beam fixed-end deformation versus beam force strength, expressed as the percentage of its theoretical strength

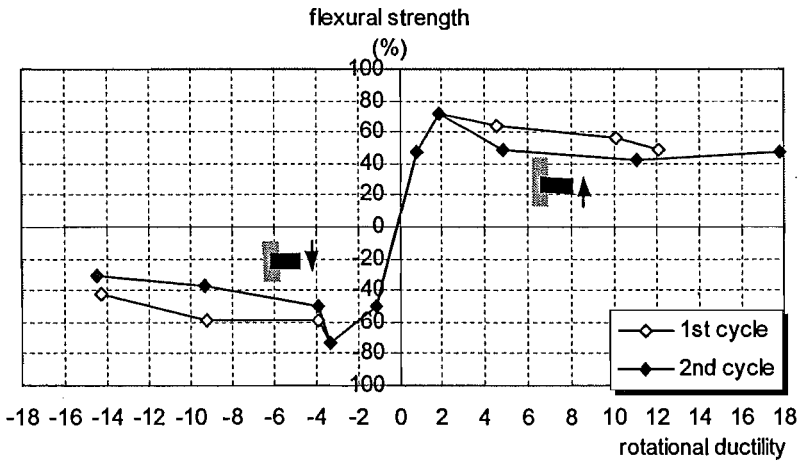

Fig.7.31 Measured beam rotational ductility versus beam force strength for Unit EJ2

Measured steel strains along the column longitudinal bars were small, and they disagreed with the theoretical prediction significantly, giving a signal that caution needs to be taken in using these measured steel strains. Slippage between the longitudinal reinforcement and the concrete could have damaged the strain gauges.

7.4.5 Member Deformation Characteristics

The beam of Unit EJ2 was expected to develop a plastic hinge and the columns were expected to remain elastic. Fig.7.27 and Fig.7.28 show the measured curvature profiles for the beam and columns respectively.

The beam flexural deformation was observed to be significant and again the beam deformation was mainly in the fixed-ends. The column deformation over the fixed-ends was much smaller than that of the beam. For the columns, only the curvatures over the fixed-ends were measured.

Fig.7.29 shows the measured beam deformation components and Fig.7.30 shows the beam fixed-end deformation versus the measured strength curves. In Fig.7.30, the deformation in the beam fixed-end increased even as the attained force strength decreased at later loading stages, indicating that the non-linear deformation occurred in the beam fixed-end and the non-linear performance of the system was governed by the non-linear behaviour in the beam fixed-end.

Fig.7.31 shows the measured beam rotational ductility in the fixed-end versus the measured beam force strength relationship for Unit EJ2. It is evident in Fig.7.31 that the beam flexural strength degraded with the cyclic loading progress more significantly when compared with the increase in the imposed displacement level. Available rotational ductility in the beam fixed-end was less than 4 after considering the adverse effect of the cyclic loading effect, should the force strength degradation be within 20%. Compared with the test evidence observed for the beam of the as-built interior beam-column joint unit, the available rotational ductility for the beam of the as-built exterior beam-column joint unit was smaller.

7.4.6 Joint Behaviour

7.4.6.1 Joint Shear Stress

The measured maximum nominal horizontal joint shear stress for Unit EJ2, based on the measured member forces and plane section theory, occurred when the joint core of Unit EJ2 developed diagonal tension cracking at the loading peaks of $0.75V_i$, and it was 1.37MPa or $0.23\sqrt{f_c'}$ MPa for the clockwise loading, and 0.9 MPa, or $0.15\sqrt{f_c'}$ MPa for anti-clockwise loading. Evidently, the attained maximum nominal horizontal joint shear stress was well below the theoretical joint shear capacity at diagonal tension cracking of $0.3\sqrt{f_c'}$ MPa in terms of nominal joint shear stress.

The development of the concrete diagonal tension cracks in the joint core of Unit EJ2 at such low shear input action was again due to the use of plain round longitudinal reinforcement, as described in section 7.2.5.1. The use of plain round bars for longitudinal reinforcement enhanced the local concrete tensile stress due to the concentration of steel force transfer to the beam bar bend, and increased the discrepancy between the actual local concrete tensile stresses and the estimated nominal horizontal joint shear stress, when compared to the case with deformed longitudinal bars. Hence, when plain round longitudinal reinforcement is used, concrete diagonal tension cracks develops when the estimated nominal horizontal joint shear stress is lower, compared with similar exterior beam-column joint unit with deformed longitudinal reinforcement.

7.4.6.2 Joint Shear Distortion

Fig. 7.32 illustrates the variations of the joint shear distortion, joint displacement component and storey shear with the loading estimated for Unit EJ2. The maximum joint shear distortion was only approximately 0.63 %. Gradual increases in the joint shear distortion and joint displacement components were observed as the loading progressed after the joint diagonal crack occurred at the loading of clockwise $0.75V_i$, but he joint shear distortion generally was very small.

The maximum joint shear distortion reached by test of Unit EJ2 was comparable to the maximum joint shear distortion of 0.52% measured for Unit EJ1. The joint cores of Units EJ2 and EJ1 were of sound integrity throughout the whole loading histories due to severe

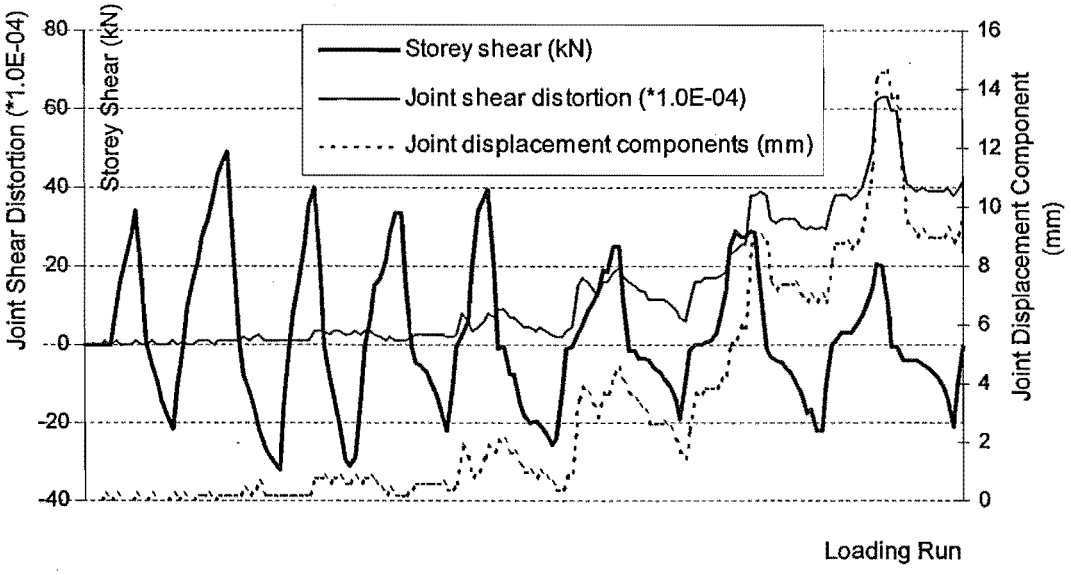

Fig.7.32 Joint shear distortion, joint displacement component and storey shear of Unit EJ2

bond degradation along the beam bars within the joint core resulting from the use of plain round longitudinal reinforcing bars. Whereas in the case of Hakuto's test on Unit O6 the maximum joint shear distortion was 1.5%, the maximum joint shear distortion observed for Unit EJ2 was only about 50% of that amount with Unit O6, indicating that the use of plain round longitudinal reinforcement led to much less cracked joint cores.

7.4.6.3 Joint Hoop Strains

The strains in three joint hoops, CT3, CT2 and CT-4, were measured by electrical strain gauges for Unit EJ2. CT-3 was located at the centre of the joint core and CT2 and CT4 were located at the beam faces. Two sets of column transverse reinforcement adjacent to the joint core of Unit EJ2 were also measured by electrical resistance strain gauges. Fig.7.33 shows the measured strains in joint hoops and two sets of column transverse reinforcement.

Evidently, the joint hoop at the centre of the joint core of CT-3 was subjected to higher tensile strain than the other joint hoops located close to the beam faces of CT-2 and CT-4. This evidence agrees with the evidence observed for exterior beam-column joint components with the beam bars bent into the joint core [P13, H1]. When the member forces are transferred across the joint core by the way of corner to corner joint diagonal

concrete strut, the diagonal strut behaves like a column, which is axially loaded in compression with loading heads at both ends. In this case, the lateral expansion of the column will reach the largest value at the mid-height of the column. However this evidence was different from the observed evidence for Unit EJ1 where the joint hoops at the beam faces were more stressed in tension compared to the joint hoop at the centre of the joint core. The difference between the test of Unit EJ1 and test of Unit EJ2 was the bending configuration of the beam bar hook.

Hence, when the beam bars of exterior beam-column joint components are not bent into the joint core, the joint hoops adjacent to the beam faces were more effective and the joint hoops within the joint core was not of much use for improving the force transfer across the joint core. However, when the beam bars of exterior beam-column joint components are bent into the joint core, the joint hoops at the centre of the joint core were very effective in providing the joint shear resistance, compared to the joint hoops located away from the joint core centre.

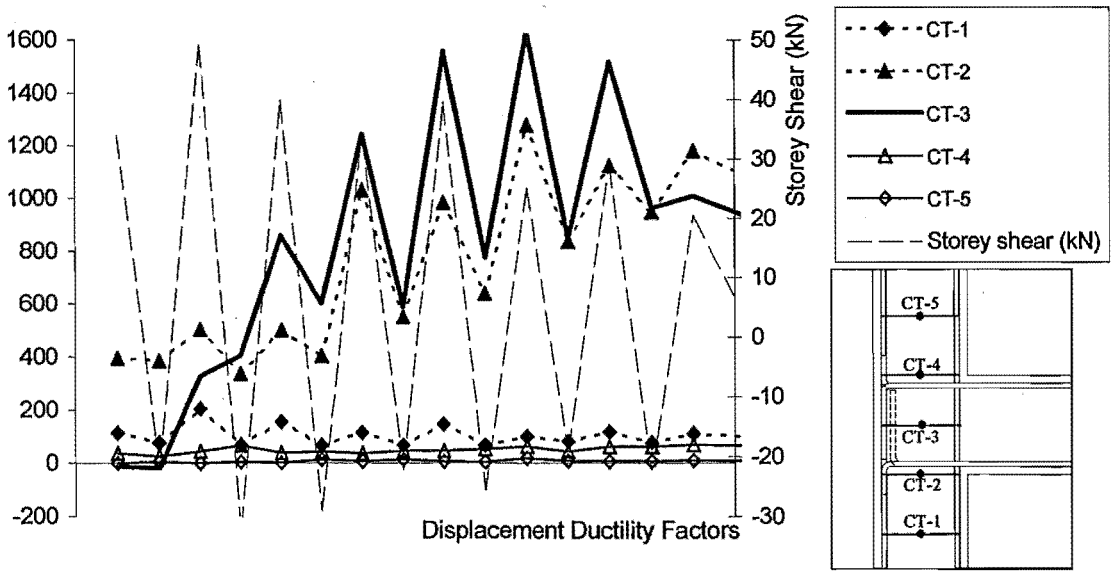

Fig.7.33 Joint Hoop Strains and Storey Shears Measured for Unit EJ2

7.4.7 Displacement Components

Fig.7.34 shows the displacement components estimated for Unit EJ2. Contribution to the total storey displacement by beam fixed-end rotation increased rapidly with the loading progress, and reached up to 80% of the total storey displacement. Contribution of the column fixed-end rotation to the total storey displacement, although was high at the beginning of the loading, decreased gradually with the loading progress, indicating the damage concentration in the beam due to the formation of a weak beam-strength column failure mechanism during the testing as predicted theoretically.

In general, the contributions of the beam curvatures and the joint shear distortions to the storey displacement were very small throughout the whole testing history.

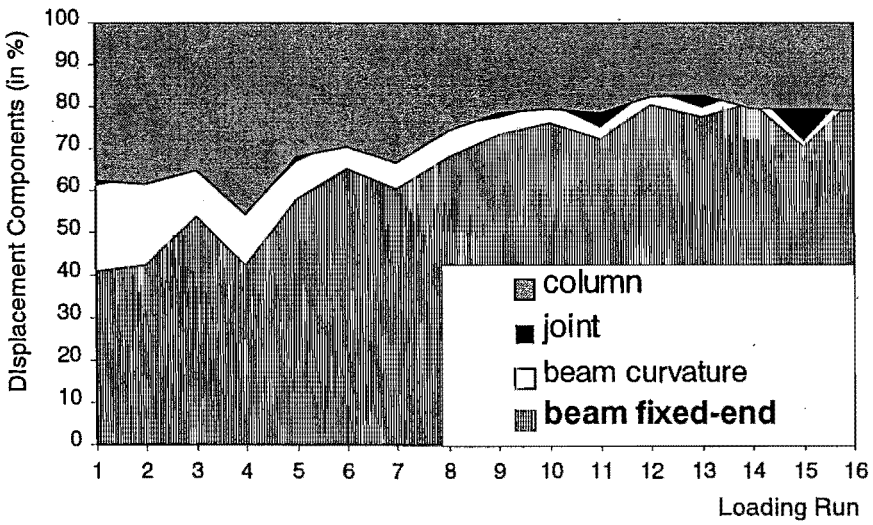

Fig. 7.34 Displacement Components Estimated for Unit EJ2

7.4.8 Summary

A full-scale one-way exterior beam-column joint unit EJ2, which was reinforced by plain round bars and had the beam bar hooks bent into the joint core, was tested under simulated seismic loading with zero axial column load in order to investigate the influence of the beam bar hook details on the overall performance of existing reinforced concrete frame structures. Unit EJ2 had small amount of transverse reinforcement in the beam and columns and contained only limited joint shear reinforcement. Unit EJ2 was identical to as-built exterior beam-column joint Unit EJ1 except the arrangement of the

beam bar hooks, and it was also identical to Hakuto's test Unit O6 except that Hakuto's Unit O6 used deformed longitudinal reinforcement.

Conclusions drawn from this test are as follows:

1. Poor overall seismic performance although the beam bars are bent into the joint

The overall performance of the test on Unit EJ2 was unsatisfactory in terms of the attainment and maintenance of the structural strength and stiffness properties. Seismic behaviour observed for Unit EJ2 was dominated by the beam flexural behaviour and the premature concrete tension cracking along the beam bar hooks. Premature concrete tension cracking along the beam bar hooks was associated with the interaction of column bar buckling adjacent to the joint core and the opening action of the beam bar hooks, due to inadequate joint horizontal shear reinforcement and severe bond degradation along the longitudinal reinforcement. Severe bond degradation along the longitudinal reinforcement not only caused the degrading beam flexural behaviour, but also facilitated column bar buckling and the opening action of the beam bar hooks, hence leading to the concrete tension cracking failure along the outer layer of the column bars adjacent to and within the joint core.

The storey shear strength was attained at storey drift of 1.5% by Unit EJ2, was about 25% less than the theoretical storey shear strength. Also observed was significant strength degradation for Unit EJ2 due to the development of bond degradation along the longitudinal beam bars as the loading progressed.

The initial stiffness attained of Unit EJ2 was 1.2 kN/mm. The initial stiffness measured for Unit EJ2 was only 30% of the theoretical prediction and it was equal to a storey drift of 1.5% at first yield. The adverse effect of the plain round longitudinal reinforcement on the structural stiffness is more significant for as-built exterior beam-column joint components than it was for interior beam-column joint components.

2. Violation of the plane section assumption in predicting the flexural behaviour

Observed individual beam and column behaviour was similar to that for interior beam-column joint units. The plane section assumption was violated and therefore it would overestimate the flexural strength and underestimate local curvature deformations.

Member deformation significantly concentrated in the fixed-ends. As a result, a rotational ductility in the member fixed-end is a better index to member deformation.

3. The test on Unit EJ2 demonstrated that the seismic performance of individual beam and columns was dominated by flexure only. The joint horizontal shear reinforcement is more needed for preventing the failure associated with the column bar buckling and the opening action of the beam bar hook than that for providing joint shear capacity.

4. Comparative study of the test results of Units EJ1 and EJ2 revealed the followings:

(1). The beam bar hook configuration in exterior column has an important influence on the available force strength property of exterior beam-column joint components when the columns contained small amount of transverse reinforcement adjacent to the joint core. The configuration of the beam bar hooks bent into the joint core as for Unit EJ2 led to about 25% increase in the available storey shear strength of the unit, when compared to that of Unit EJ1 which had the beam bar hooks bent away from the joint core.

(2). The overall seismic performance of existing exterior beam-column joint components is dependent on the amount of joint horizontal shear reinforcement at the centre of the joint core if the beam bar hooks are bent into the joint cores, but it is dependent on the column transverse reinforcement immediately above and below the joint cores if the beam bar hooks are NOT bent into the joint cores.

5. Comparative study of the test results of Unit EJ2 and Hakuto's Unit O6 identifies that the use of plain round longitudinal reinforcement for Unit EJ2, although leading to much better integrity of the joint core due to the occurrence of severe bond degradation along the beam longitudinal bars within the joint core for Unit EJ2, caused significant reduction in the available strength and stiffness of the unit, especially in the available stiffness. Compared with the case with deformed longitudinal reinforcement, exterior beam-column joints reinforced by plain round longitudinal reinforcement need more column transverse reinforcement adjacent to and within the joint core for preventing column bar buckling and controlling the opening action of the beam bars in tension.

7.5 TEST OF UNIT EJ3

7.5.1 General

As-built full-scale exterior beam-column joint unit EJ3 was identical to as-built exterior beam-column joint Unit EJ1, and it was tested under simulated seismic loading with the presence of a constant compressive axial column load of $0.25 A_g f_c^{'}$ in order to investigate the influence of compressive axial column load on the seismic performance of as-built exterior beam-column joint assemblies designed to out-dated seismic codes when the beam bar hooks are bent away from the joint core.

7.5.2 Crack Development and Damage

The crack development and the final appearance of Unit EJ3 are shown in Fig.7.35.

Throughout the whole testing histories, flexural cracks were only observed to develop in the beam, not in the columns, indicating the formation of the predicted weak beam-strong column failure mechanism. The beam flexural cracking was characterised by being sparsely spaced and having one major beam flexural crack adjacent to the joint core. This was due to severe bond degradation and bar slip along the beam longitudinal bars within and adjacent to the joint core. At the later stages of clockwise loading at displacement ductility of 2, a vertical crack along the outer layer of the column main bars was observed in the lower left corner of the joint core, but it was not so pronounced. The development of the vertical crack along the outer layer of the column bars occurred mainly due to column bar buckling. The final seismic performance of Unit EJ3 was controlled by the degrading beam flexural performance.

Evidently the test evidence of Unit EJ3 was very different from that of Unit EJ1. Test specimens EJ1 and EJ3 were identical, but one unit was tested with zero axial column load while the other unit was tested with the existence of constant column compressive axial load of $0.25 A_g f_c^{'}$. For test on Unit EJ1, the interaction of column bar buckling and the opening action of the beam bar hooks, which occurred due to inadequate column transverse reinforcement adjacent to the joint core and severe bond degradation along the longitudinal reinforcement, initiated the final failure of the unit.

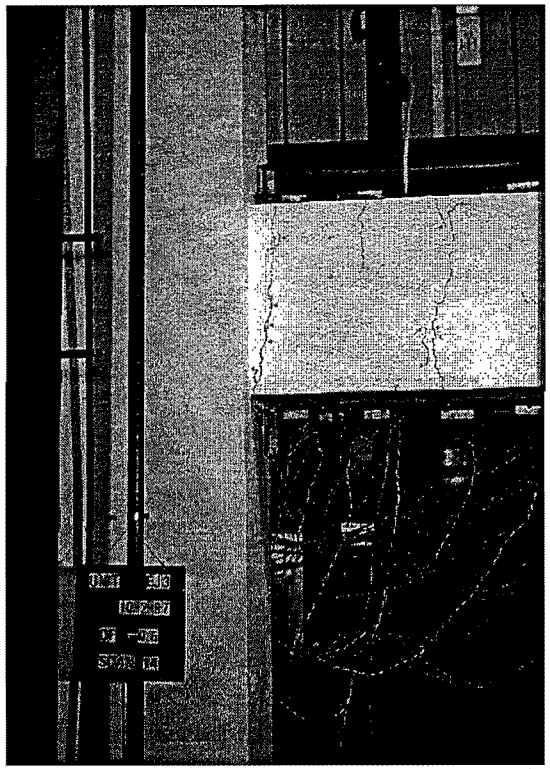

(a) Loading at 0.5Vi

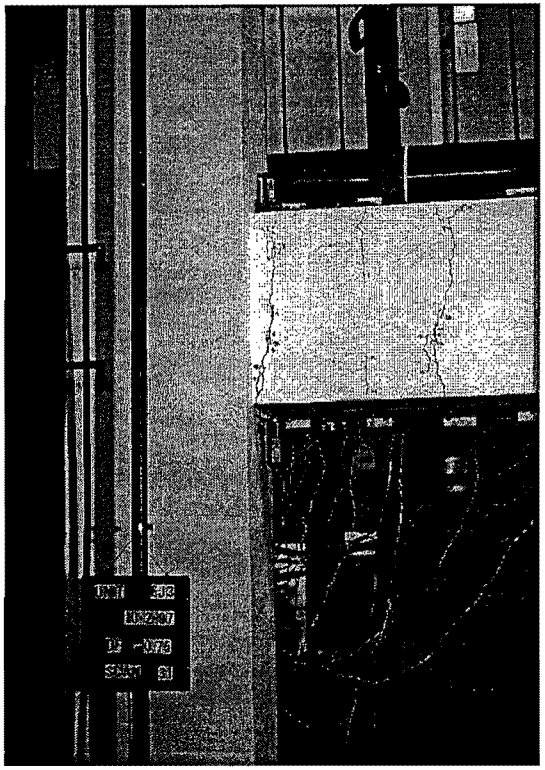

(b) Loading at 0.75Vi

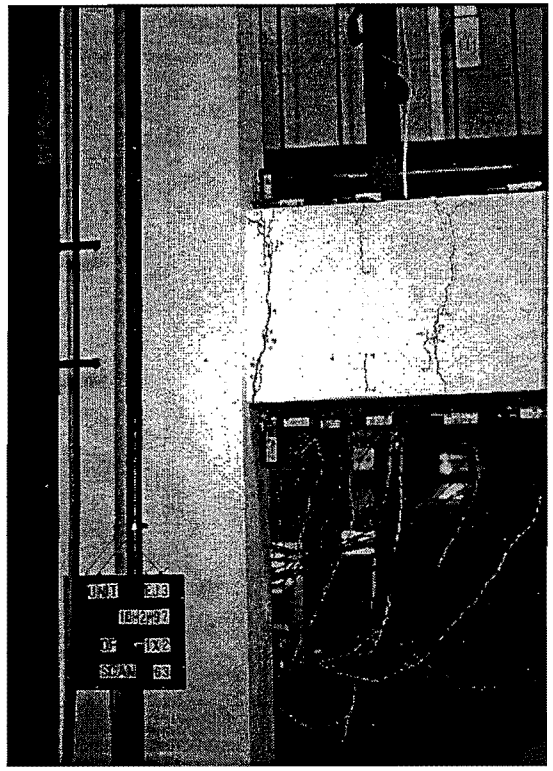

(c) End of Ductility 1

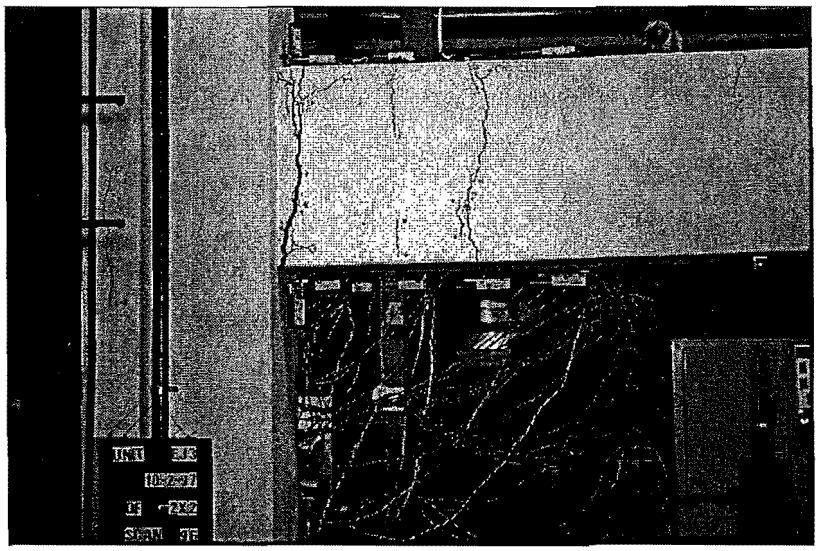

(d) End of Loading at ductility 2

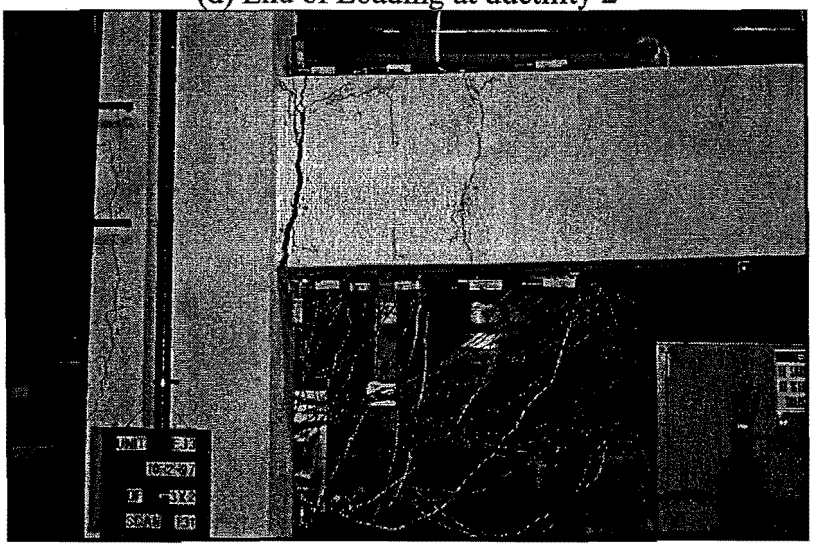

(e) End of loading at ductility 3

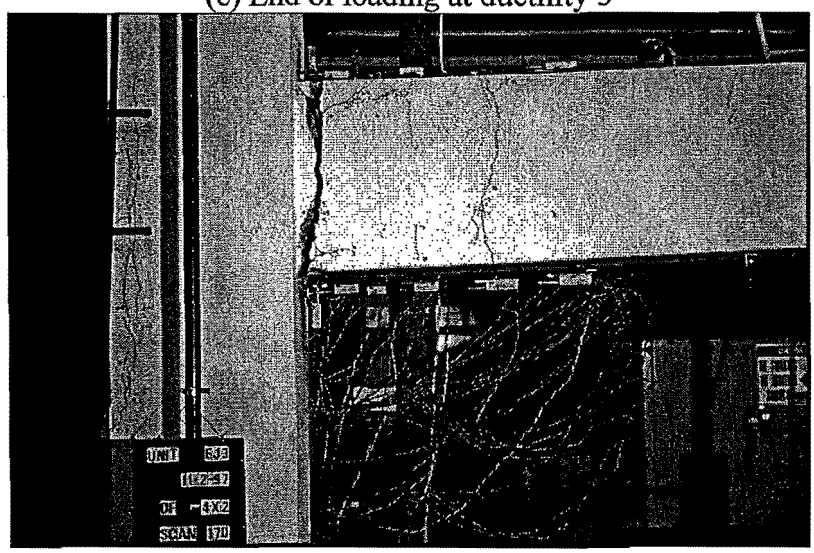

(f) Final appearance of Unit EJ3 with a major beam flexural crack at column face

Fig.7.35 Crack development and final appearance of Unit EJ3

Existence of constant compressive axial column load of $0.25 A_g f_c^{'}$ for test on Unit EJ3 enhanced the force transfer from the beam tension steel to the joint core concrete by bond within the joint region, resulted in a smaller proportion of the beam steel tension force to be transferred at the bend, consequently leading to much relieved opening action of the beam bar hooks. As a result, the development of concrete tension cracking orientated by the bending configuration of the beam longitudinal reinforcing bars in exterior columns was totally prevented for the test on Unit EJ3.

In addition, the compressive axial column load of $0.25 A_g f_c^{'}$ also prevented the development of the column flexural cracks for test of Unit EJ3, and greatly improved the stiffness performance of the columns.

Throughout the whole testing history of EJ3, no shear cracks were observed in members and the joint core although the theoretical considerations conducted in Chapter 4 indicated a possibility of very inadequate beam shear performance as seen in Table 4.8.

7.5.3 Observed Load versus Displacement Hysteresis Response

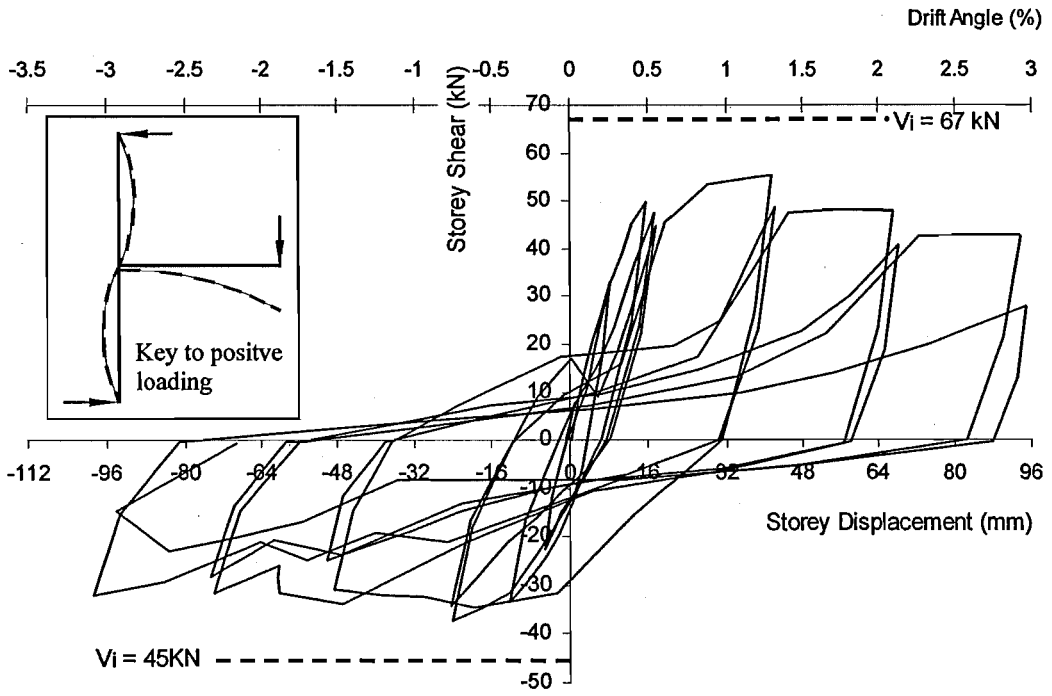

Fig. 7.36 Storey Shear versus Storey Displacement and Storey Drift Hysteresis Loops Measured for Unit EJ3

Fig.7.36 shows the storey (horizontal) shear versus storey (horizontal) displacement and storey drift hysteresis loops measured for Unit EJ3. Also shown in Fig.7.36 is the theoretical storey shear strengths of the unit, V_i, at the attainment of beam flexural strengths for both loading directions.

Fig.7.36 illustrates that the existence of constant compressive axial column load of $0.25 A_g f_c^{'}$ for test on Unit EJ3 resulted in much improved general seismic performance, compared to the test observations of Unit EJ1.

The displacement at first yield, which was measured using the method described previously, was equal to a storey drift of 0.66% and 0.51% respectively for clockwise loading and anti-clockwise loading. Alternatively, the measured initial stiffness was 3.19 kN/mm and 2.75 kN/mm for clockwise and anti-clockwise loading respectively. Compared to the measured initial stiffness of 1.7 kN/m for Unit EJ1 in the loading of clockwise loading at $0.5 V_i$, the measured initial stiffness for test on Unit EJ3 was about 1.88 times that observed for test on Unit EJ1. Significantly improved structural stiffness property observed for test of Unit EJ3 resulted from significant reduction in beam and column fixed-end rotations. Existence of constant compressive axial column load of $0.25 A_g f_c^{'}$ for test on Unit EJ3 greatly reduced the induced tensile strains in column longitudinal bars and enhanced the force transfer from the beam tension steel to the surrounding concrete by bond within the joint core. Compared to the test on Unit EJ2, which had the beam longitudinal bar hooks bent into the joint core, the measured maximum beam and column fixed-end rotations for Unit EJ3 were respectively only 70% and 40% of the measured values for Unit EJ2, although the attained force strength by Unit EJ2 was only about 88% of the attained strength by Unit EJ3.

During clockwise loading, the storey shear strength was attained by Unit EJ3 at a storey drift of 1.3% in the loading to displacement ductility of 2, and it was about 12% less than the corresponding theoretical storey shear strength of the unit at the attainment of the beam negative flexural strength. However, the storey shear strength of Unit EJ3 was about 1.6 times the storey shear force strength attained by Unit EJ1. During anti-clockwise loading, the storey shear force strength was attained by Unit EJ3 at a storey drift of 0.6% in the loading to displacement ductility of 1, and it was about 15 % less than the corresponding theoretical storey shear strength of the unit at the attainment of the

beam positive flexural strength. But this was about 1.5 times the storey shear force strength attained by Unit EJ1. Significant strength enhancement observed for EJ3 compared to test on Unit EJ1 was because the existence of constant compressive axial column load of $0.25 A_g f_c^{'}$ for test of Unit EJ3 suppressed the premature concrete tension cracking failure along the beam bar hooks.

Observed pinching of the hysteresis loops for the test on Unit EJ3 although still significant was much less pronounced when compared to that observed for similar exterior beam-column joint units but tested with zero axial column load, for example, Unit EJ2. Pinching of the hysteresis loops observed for test on Unit EJ2 occurred due to the major flexural cracks at beam and column interface. The existence of the compressive axial column load for test on Unit EJ3 resulted in a reduced beam fixed-end rotation and enhanced column stiffness performance, consequently leading to less pinched hysteresis loops for test of Unit EJ3.

In summary, the existence of compressive axial column load for the test on Unit EJ3 enhanced the available storey shear force strength and stiffness and improved the structural energy dissipating capacity. The test on Unit EJ3 reached the maximum storey shear that was approximately 15% less than the theoretical storey shear strengths at storey drift of approximately 1.3% for clockwise loading but at storey drift of 0.6% for anti-clockwise loading. Softening with cyclic loading and pinching of the hysteresis loops observed for test on Unit EJ3 were not so significant as that observed for similar tests but tested with zero axial column load. Existence of the compressive axial column load for the test on Unit EJ3 also enhanced the force capacity associated with the opening of the beam bar hooks in tension, shifting the weakest link of the unit to be the beam flexural behaviour.

7.5.4 Strains in Longitudinal Reinforcement of Beam and Columns

For Unit EJ3, the beam was expected to develop a plastic hinge. Fig.7.37 show the measured strain profiles by electrical resistance strain gauges along beam bar 1 and beam bar 2 respectively. Compared with the measured steel strain profile along the beam longitudinal bars of Unit EJ2, bond degradation and bar slip along the beam longitudinal bars of Unit EJ3 were improved within the joint region.

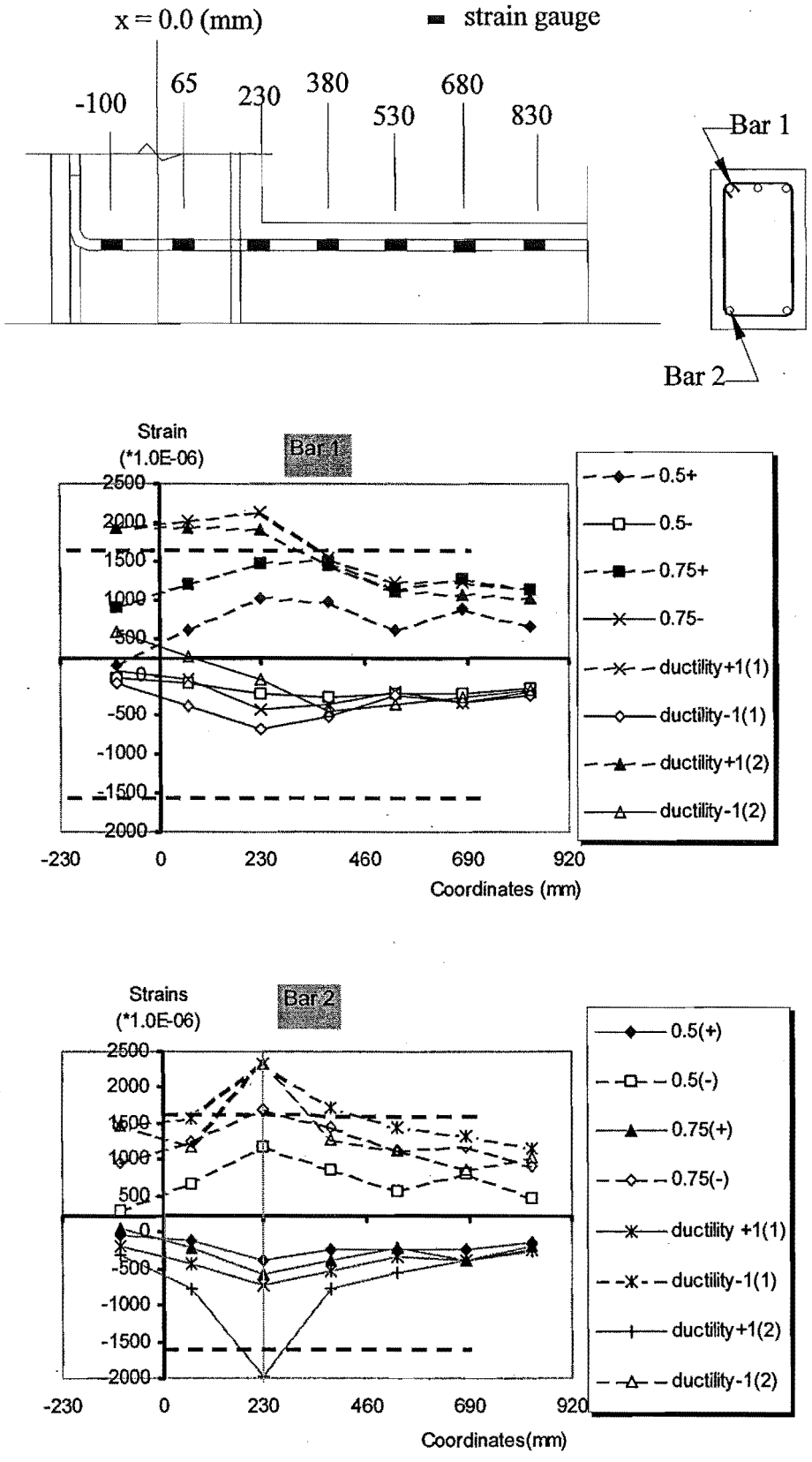

Fig.7.37 Strain Profiles of Beam Bars 1 and 2 Measured by Electrical Strain Gauges

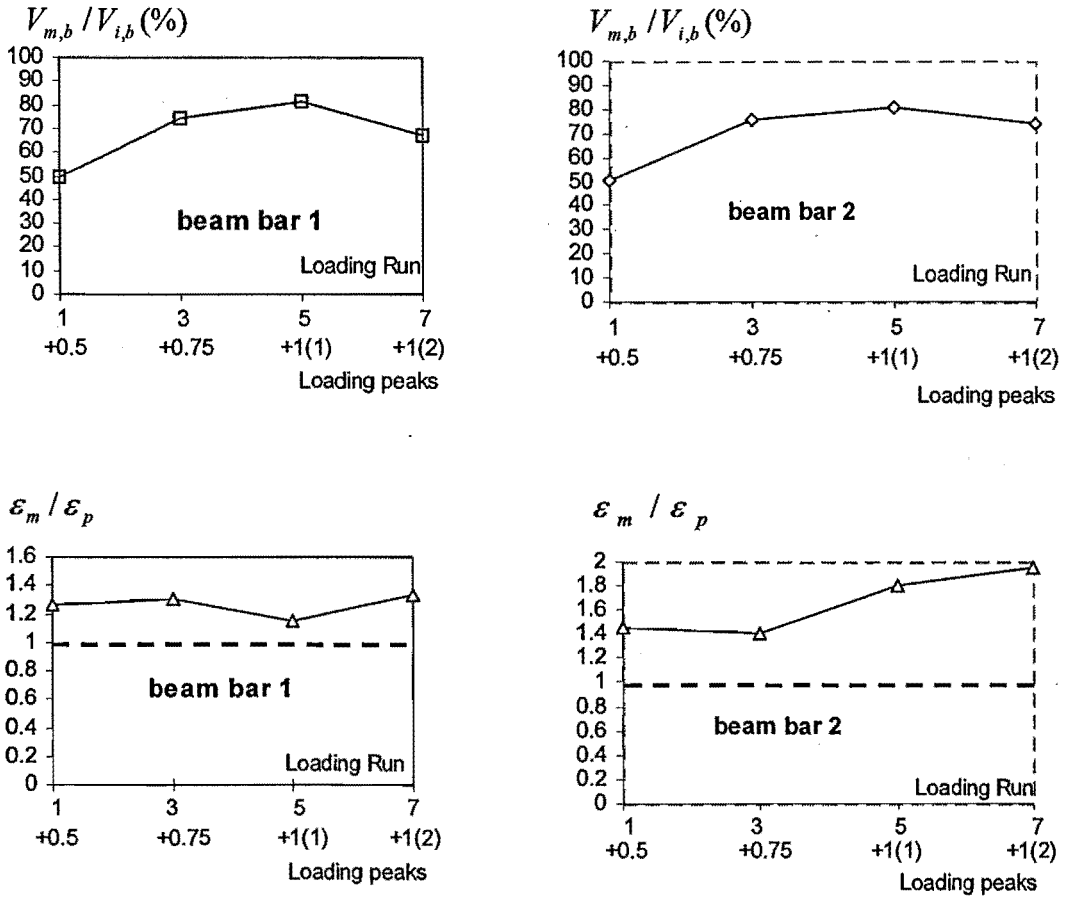

(a) Beam Bar 1 (b) Beam Bar 2

Fig.7.38 Comparison of measured and theoretical beam bar strains at column face

Fig.7.38 compares the steel strain discrepancies versus the imposed steel tensile stress level for beam bars 1 and 2 at inner column face when the beam bars were in flexural tension in the early loading cycles until the completion of loading at ductility 1. The steel strain discrepancies are expressed as the ratio of the measured steel strains, ε_m, to the theoretically predicted steel strains, ε_p. The imposed steel stress levels on the beam longitudinal bars were expressed as the ratios of the imposed beam shear to the theoretical beam shear strength, namely, $V_{m,b}/V_{i,b}$(%), where $V_{m,b}$ and $V_{i,b}$ are respectively the imposed shear on the beam and the theoretical beam shear strength calculated based on the beam flexural strength.

In Fig.7.38, it seems that the discrepancies between the measured steel strains with the theoretical strains for flexural tension bars at inner column face did not increase with the increase in the stress level of the beam longitudinal bars. Theoretically, the higher the reinforcement is stressed, the more severe the bond degradation along the reinforcement should be. This again meant that the readings from electrical resistance strain gauges could be wrong due to the slippage between the longitudinal reinforcement and the concrete.

7.5.5 Member Deformation Characteristics

Fig.7.39 shows the measured curvature profiles for the beam, which was expected to develop a plastic hinge. For the columns, only the curvatures over the fixed-ends were measured and the columns were expected to remain elastic.

Fig.7.39 shows that the beam deformation was mainly concentrated in the beam fixed-end and the tendency of the concentration of beam flexural deformation in the fixed-end became more and more evident as the loading progressed. The measured beam deformation components are shown in Fig.7.40. Hence the source of post-elastic beam deformation is in the fixed-end.

Fig.7.41 shows the measured beam rotational ductility in the fixed-end versus the measured beam force strength relationship for Unit EJ3. In Fig.7.41, the maximum beam force strength was attained, when the rotational ductility in the beam fixed-end was 3 and 4.8 for positive and negative beam bending respectively. More than 80% of the beam strength can be well maintained when the rotational ductility in the beam fixed-end was not larger than 6 in the first loading cycle, but the strength maintenance degraded significantly with the loading cycles. The rotational ductility in the beam fixed-end was similar to the beam displacement ductility defined to be the ratio of the imposed displacement to the theoretical yield displacement. Hence the strength maintenance and ductile behaviour of the beam was more affected by the cyclic effect of the loading than the increases in the imposed displacement levels, when the members contain plain round longitudinal reinforcement.

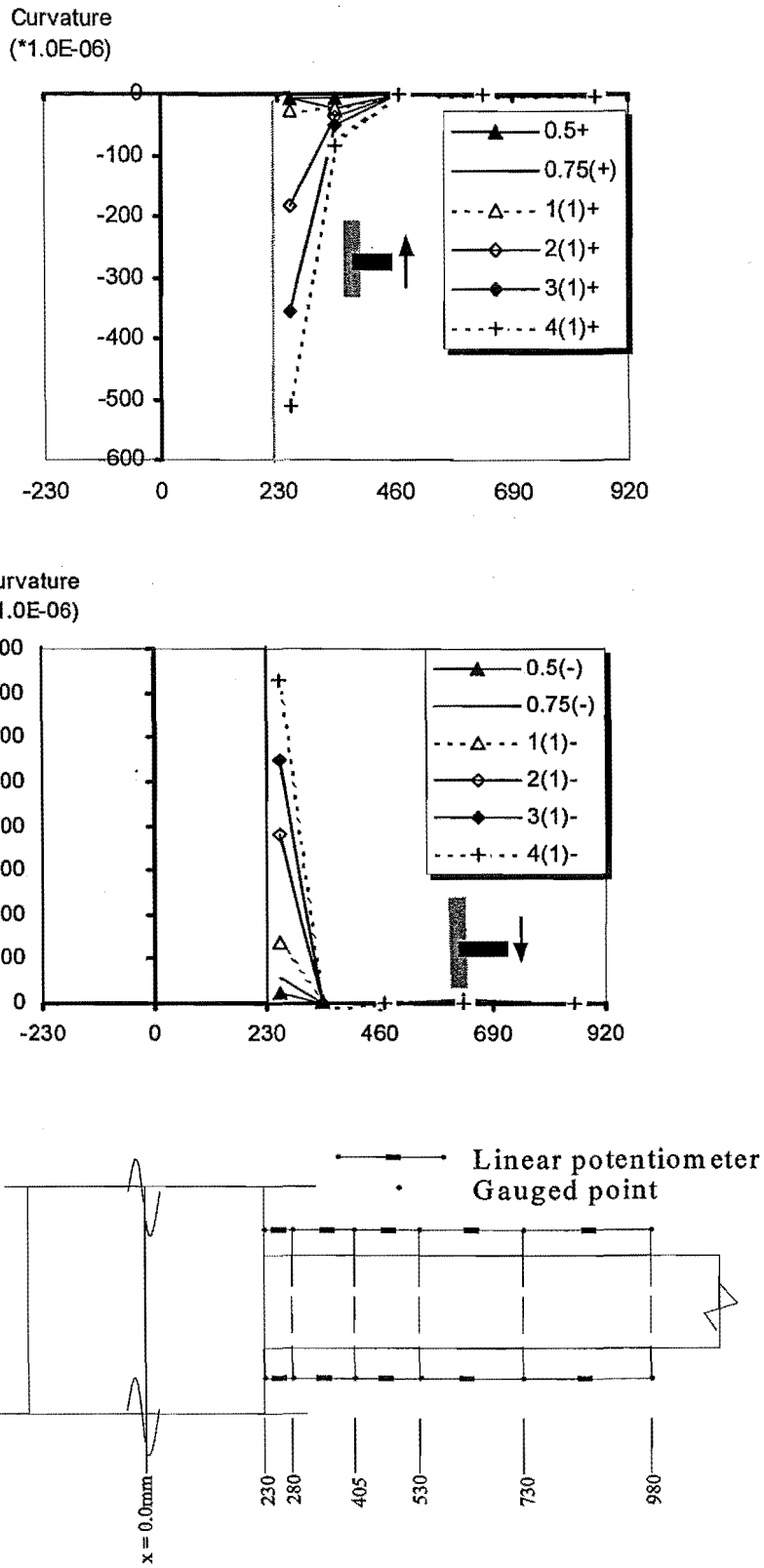

Fig.7.39 Measured beam curvature profiles for Unit EJ3

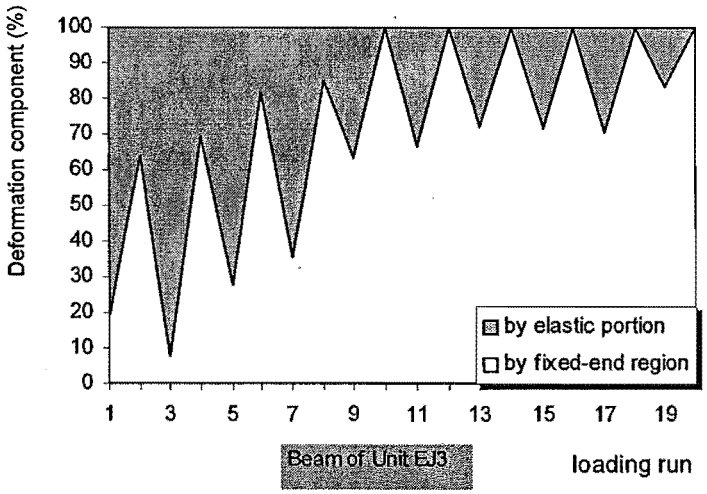

Fig.7.40 Beam deformation components measured for Unit EJ3

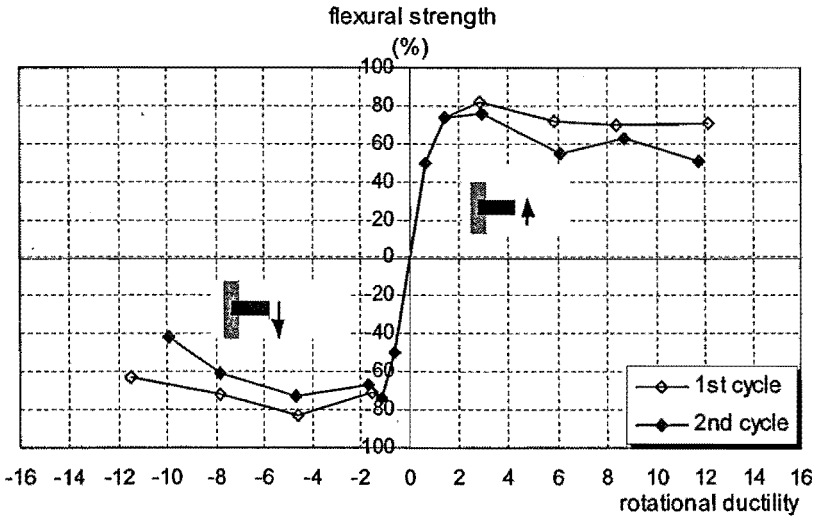

Fig.7.41 Rotational ductility versus beam force strength for Beam of Unit EJ3

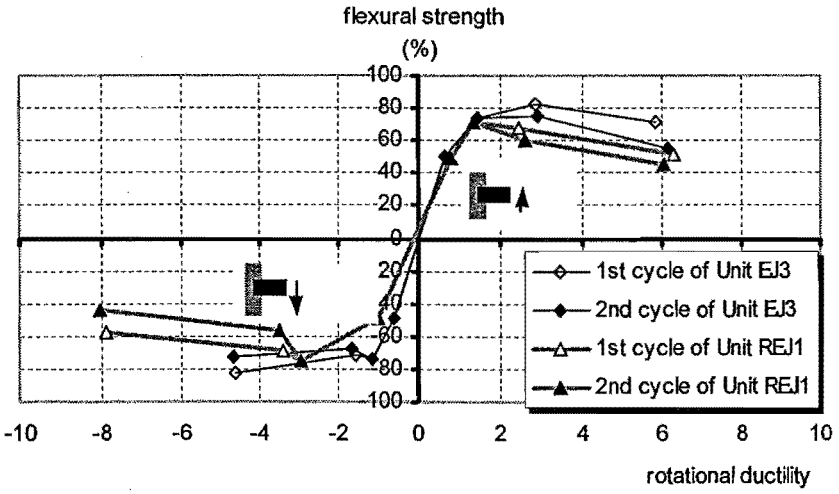

Fig.7.42 Comparison of strength and deformation relationships for the beams of Units EJ1 and EJ3

Fig.7.42 compares the observed beam behaviour for Units EJ1 and EJ3, in terms of rotational ductility in the fixed-end and the flexural force strength. The compressive axial column load of 0.23 $A_g f_c'$ for Unit EJ3 apparently enhanced the cyclic behaviour of the beam, when compared with the test evidence of Unit EJ1. In Fig.7.42, the initial stiffness observed for the beam of Unit EJ3, in terms of rotation in the fixed-end and the flexural force strength, was about 1.46 times that for Unit EJ1. The attained flexural strength for Unit EJ3 was 1.15 times that for Unit EJ1. Hence, due to the existence of the compressive axial column load for Unit EJ3, the beam post-elastic flexural behaviour in the fixed-end was significantly enhanced, especially the beam flexural stiffness behaviour. This disagrees with the current understanding that the beam flexural behaviour is completely determined by the overall dimensions and the reinforcing details of the discussed beam itself.

7.5.6 Joint Behaviour

7.5.6.1 Joint Shear Stress

The estimated maximum nominal horizontal joint shear stress for Unit EJ3 during clockwise loading occurred at a storey drift of 1.3% at displacement ductility of 2, and it was 1.6 MPa, or $0.27\sqrt{f_c'}$ MPa. In comparison, the estimated maximum nominal horizontal joint shear stress for anti-clockwise loading direction occurred at a storey drift of 0.6% at displacement ductility of 1, and it was 1.04 MPa, or $0.17\sqrt{f_c'}$ MPa. Evidently, the joint shear stress level of Unit EJ3 in both loading directions was well below the joint shear stress level of $0.78\sqrt{f_c'}$ MPa, which corresponds to the joint shear force strength at developing the diagonal tension cracking in the joint core concrete, estimated using Mohr's circle for stress and assuming the concrete diagonal tension strength of $0.3\sqrt{f_c'}$ MPa. This agrees with the observation that no joint diagonal tension cracks developed throughout the testing of Unit EJ3.

7.5.6.2 Joint Hoop Strains

Fig. 7.43 shows the joint hoop strains measured for Unit EJ3 using electrical resistance strain gauges.

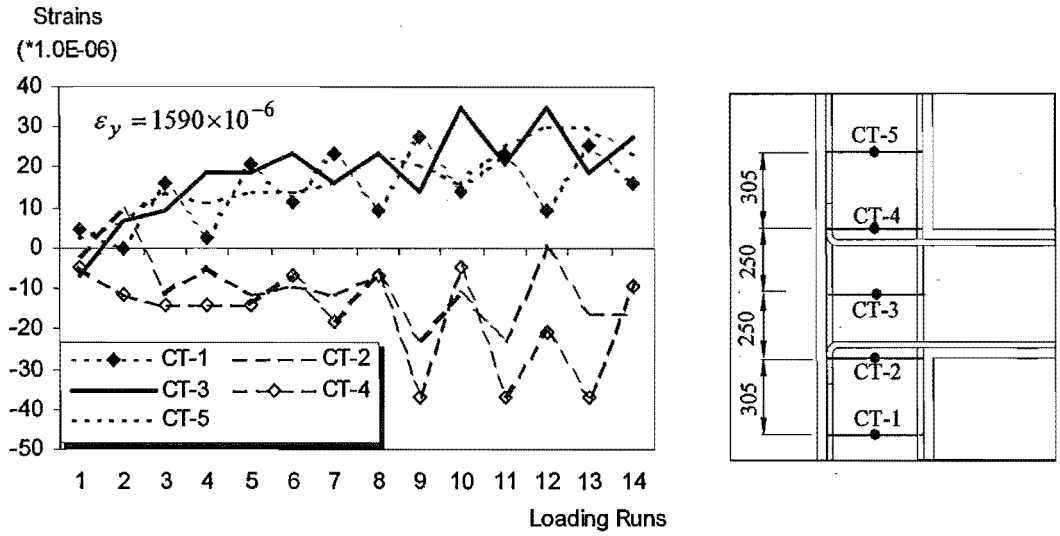

Fig. 7.43 Measured strains in joint hoops and column transverse reinforcement

Whereas in the case of test on Unit EJ1 the measured maximum strain in joint hoop CT-4 was well beyond the steel yield strain, the measured joint hoop strain in CT-4 for test of Unit EJ3 was very low, and it was less than 2.5% of the steel yield strain. Unit EJ1 and Unit EJ3 were identical but tested with different compressive axial column loads. Due to the existence of the constant compressive axial column load of $0.25A_gf_c'$ for test on Unit EJ3, the bond mechanism along the beam longitudinal bars was significantly enhanced, introducing the shear flow type of force input from the beam steel to the concrete. As a consequence, the transfer of the beam steel tensile force to the concrete was mainly in the form of shear flow to the joint core concrete, rather than in the form of the bearing around the bend within the column area. Prior to the concrete tension cracking as for Unit EJ3, the shear flow type of input can be resisted by a group of principal tension and compression stresses generated in the concrete and it is independent on the provided joint shear reinforcement [C1]. Apparently, there was no need for actuating the alternative joint shear mechanism as proposed in Chapter 4 to transfer the member forces across the joint core of Unit EJ3 and the joint shear reinforcement would not be highly stressed.

7.5.6.3 Joint Shear Distortion and Joint Expansion

For the test of EJ1, the induced maximum joint shear distortion was 0.52%. However, the maximum joint shear distortion measured for test of EJ3 was approximately zero (0.007%). For Unit EJ3, concrete diagonal tension cracking of the joint core was totally

prevented. In this case, the joint shear distortion was only attributed to the concrete deformation and it must be very small.

7.5.7 Displacement Components

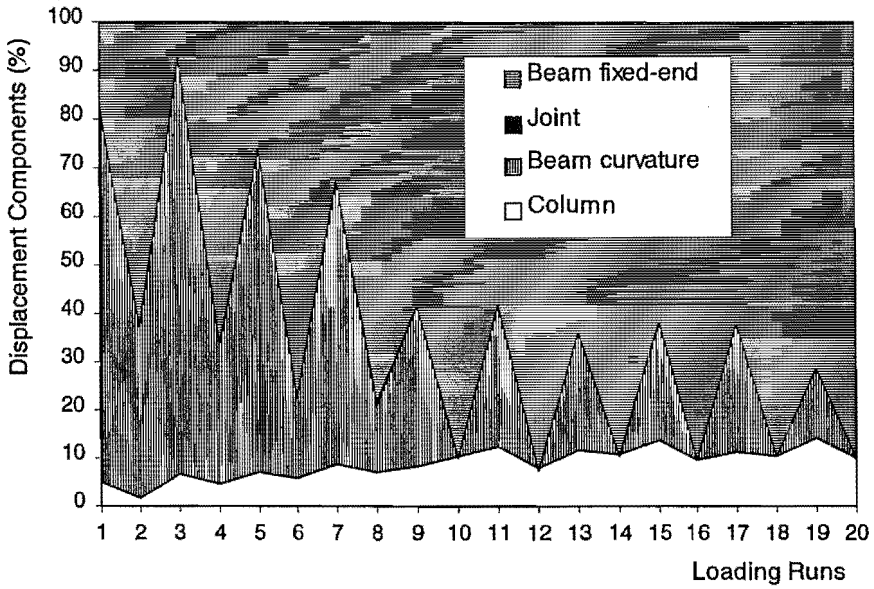

Fig. 7.44 Displacement Components Measured for Test of Unit EJ3

Fig. 7.44 shows the decomposition of different deformation components, expressed as percentages of the measured storey horizontal displacement.

Fig.7.44 shows that the beam fixed-end rotation was the major source of the structural deformation and it increased significantly as the loading progressed. The strength degradation behaviour in the post-elastic range of the unit was attributed to the degrading beam flexural behaviour in the fixed-end.

7.5.8 Summary

An as-built full-scale exterior beam-column joint unit EJ3 was constructed. Unit EJ3 was identical to as-built test Unit EJ1 but tested under simulated seismic loading with the presence of a constant compressive axial column load of $0.25 A_g f_c^{'}$. In addition, test on Unit EJ3 was identical to test on Unit EJ4 except that Unit EJ4 had the beam longitudinal bars bent into the joint core in the exterior column. The longitudinal and transverse reinforcement was from plain round bars. Theoretical considerations showed that transverse reinforcement in the members of Unit EJ3 was very inadequate, especially in

the beam, according to the requirement of shear force capacity and the requirement for preventing longitudinal bar buckling and confining the compressed concrete.

1. Simulated seismic loading test on Unit EJ3 showed that the overall seismic performance of Unit EJ3 was dominated by the beam flexural behaviour only, the degradation of the beam flexural performance with the loading was mainly limited in the major beam flexural crack at the column face. Compressive axial column load enhanced the force transfer by bond from the beam tension steel to the surrounding concrete ahead of the bend, and reduced the beam steel tension force transferred at the bend. In addition, the presence of compressive axial column load for test of EJ3 enhanced the joint shear capacity prior to the diagonal tension cracking, leading to perfect joint core integrity. As a result, premature concrete tension cracking resulting from the interaction between the column bar buckling and the opening action of the beam bar hooks as occurred for test on Unit EJ1 was entirely prevented for test on Unit EJ3, and the most critical area was shifted to the major beam flexural crack at the column face for Unit EJ3, which was associated with severe bond degradation along the beam longitudinal reinforcement adjacent to the joint core.

2. The presence of constant compressive axial column load of $0.25 A_g f_c^{'}$ greatly improved the strength and stiffness performance of the unit, especially the stiffness behaviour. The storey shear strength of Unit EJ3 was approximately 12% less than the theoretical storey shear strength for both clockwise and anti-clockwise loading. The storey shear strength of the unit was attained by unit EJ3 at storey drift of approximately 1.3% for clockwise loading but at storey drift of 0.6% for anti-clockwise loading. The attained displacement at first yield was equal to a storey drift of 0.66% and 0.51% respectively for clockwise loading and anti-clockwise loading.

Results of test on Unit EJ3 were compared with the results of test on Unit EJ1. Such a comparison revealed that the presence of compressive axial column load of $0.25 A_g f_c^{'}$ caused the initial stiffness to be about 1.8 times the measured initial stiffness for Unit EJ1 and the storey shear strength to increase by about 33% of the theoretical storey shear strength. In addition, the presence of compressive axial column load of $0.25 A_g f_c^{'}$ also greatly improved the energy dissipating capacity of the system.

3. A very interesting test observation for the test on Unit EJ3 was that the beam's post-elastic flexural behaviour was affected by the axial action imposed on the columns framing into the same joint. This disagrees with the current understanding that the member's flexural behaviour is completely determined by the overall dimensions and reinforcing details of the considered member itself and it is independent on the other members.

7.6 TEST OF UNIT EJ4

7.6.1 General

As-built full-scale exterior beam-column joint unit EJ4 had the beam bar hooks bent into the joint core and it was identical to the as-built full-scale exterior beam-column joint unit EJ2. Unit EJ4 was tested under simulated seismic loading with a constant compressive axial column load of $0.23 A_g f_c^{'}$ present in order to investigate the influence of compressive axial column load on the seismic performance of exterior beam-column joint components when the test units had the reinforcing details typical of pre-1970s reinforced concrete frame structures.

In addition, Unit EJ4 was identical to Unit EJ3 except the beam bar hook arrangement in the exterior columns and both Unit EJ4 and Unit EJ3 were tested under simulated seismic loading with a constant compressive axial column load of 1800 kN.

7.6.2 Crack Development and Damage

The crack development and the final appearance of Unit EJ4 at the end of testing are shown in Fig.7.45.

The observed damage throughout the whole testing for Unit EJ4 was mainly the flexural crack developed in the beam at the beam-column interface. A vertical crack also developed along the outer layer of column bars in the upper left corner of the joint core and it occurred in the loading at anticlockwise displacement ductility of 3. However, the development of this vertical crack was much less apparent compared to that of the major beam flexural crack at the column face. The beam flexural cracking at beam-column interface occurred due to the occurrence of severe bond degradation and bar slip along the beam longitudinal bars adjacent to and within the joint core. The development of the vertical crack along the outer layer of the column longitudinal reinforcement occurred

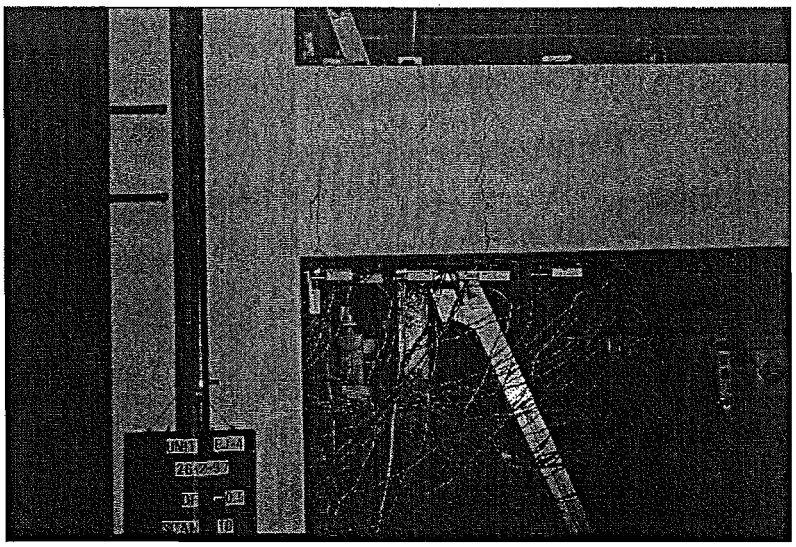

(a) Loading at 0.5Vi

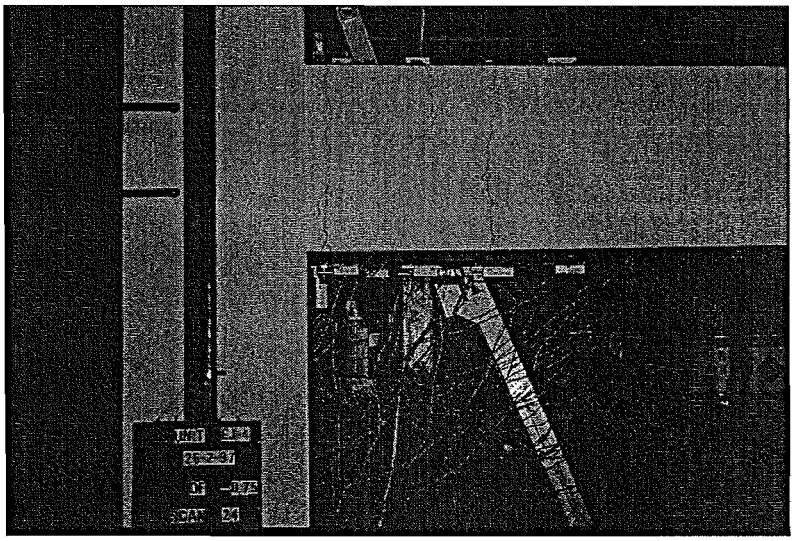

(b) Loading at 0.75Vi

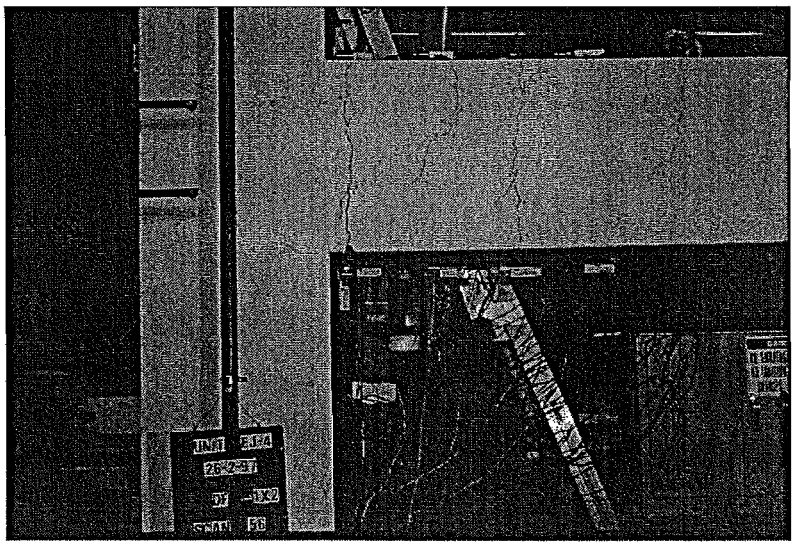

(c) End of loading at ductility 1

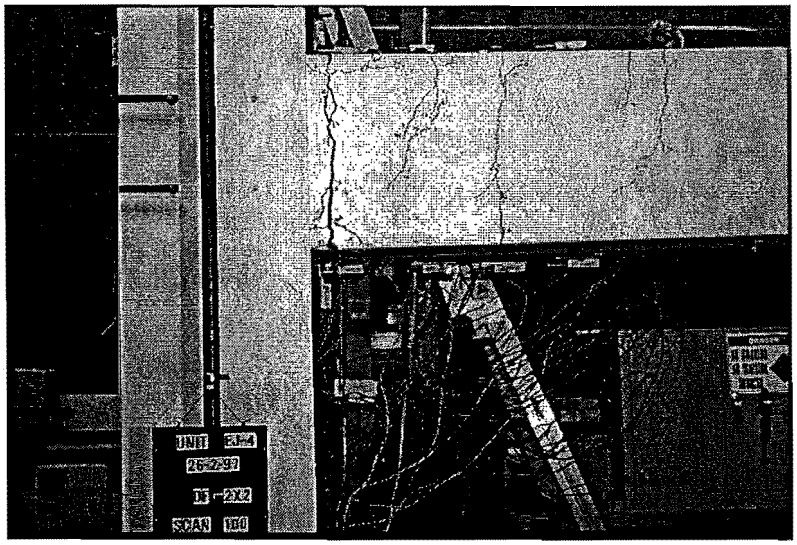

(d) End of loading at ductility 2

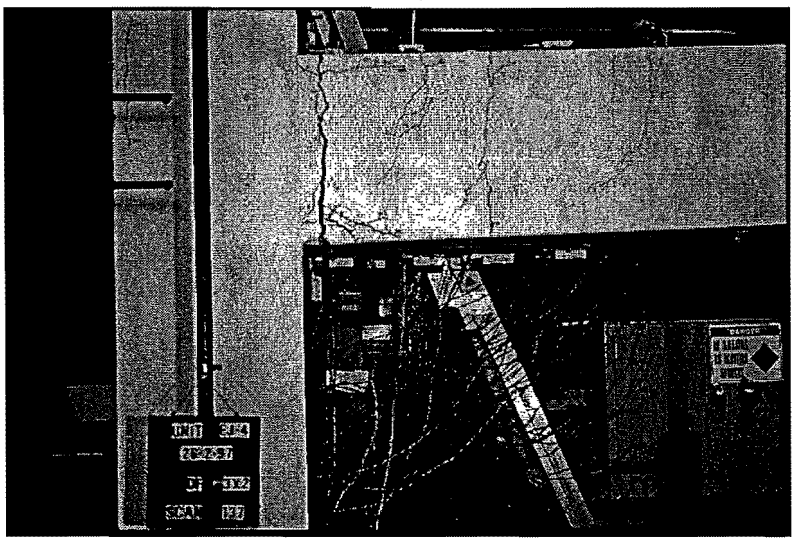

(e) End of loading at ductility 3

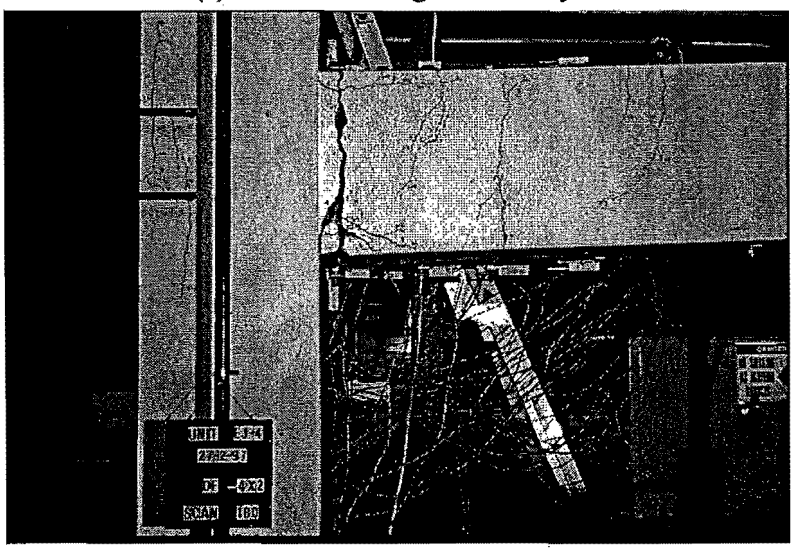

(f) Final appearance with damage mainly in the beam flexural crack at column face

Fig.7.45 Crack development and final appearance of Unit EJ4

because of column bar buckling, which was associated with severe bond degradation along the outer layer of the column bars. No damage was observed to the columns throughout the whole testing, and the final failure trigger for test on Unit EJ4 was due to the degraded beam flexural behaviour, which occurred due to the progressive bond degradation along the beam longitudinal bars adjacent to and within the joint core.

Throughout the whole testing of EJ4, no shear cracks developed in the members and the joint although theoretical consideration conducted in chapter 4 showed very inadequate beam shear performance (see Table 4.8). Hence the code method is too conservative when used for estimating the shear resisting capacity of reinforced concrete members containing plain round longitudinal bars.

The test evidence observed for test on Unit EJ4 was obviously very different from that for test on Unit EJ2. The prominent damage development observed for the test on Unit EJ2 was the damage resulting from the interaction between the column bar buckling and the opening action of the beam bar hooks due to inadequate column transverse reinforcement adjacent to and within the joint core. The difference in the observed evidence of tests of EJ2 and EJ4 was apparently attributed to the compressive axial column load. The existence of the constant compression axial column load for test of EJ4 enhanced the force transfer by bond within the joint region from the beam tension steel to the joint core concrete, hence greatly reduced the amount of the beam steel tension force needed to be transferred at the bend by bearing force, leading to much reduced possibility of the failure associated with the beam bar opening action.

7.6.3 Hysteretic Response of Test on Unit EJ4

Fig. 7.46 shows the measured storey shear versus storey displacement and drift hysteresis loops for Unit EJ4. Also shown in Fig. 7.46 is the theoretical strength of the unit in terms of the storey shear, V_i, at the attainment of beam flexural strength for both clockwise and anti-clockwise loading directions.

The general seismic performance of test on Unit EJ4 was greatly improved, compared with test on Unit EJ2. The evident improvement was mainly because the premature concrete tension cracking along the beam bar hooks in tension was entirely suppressed due to the compressive axial column load of $0.23 A_g f_c^{'}$. Also, the seismic performance demonstrated

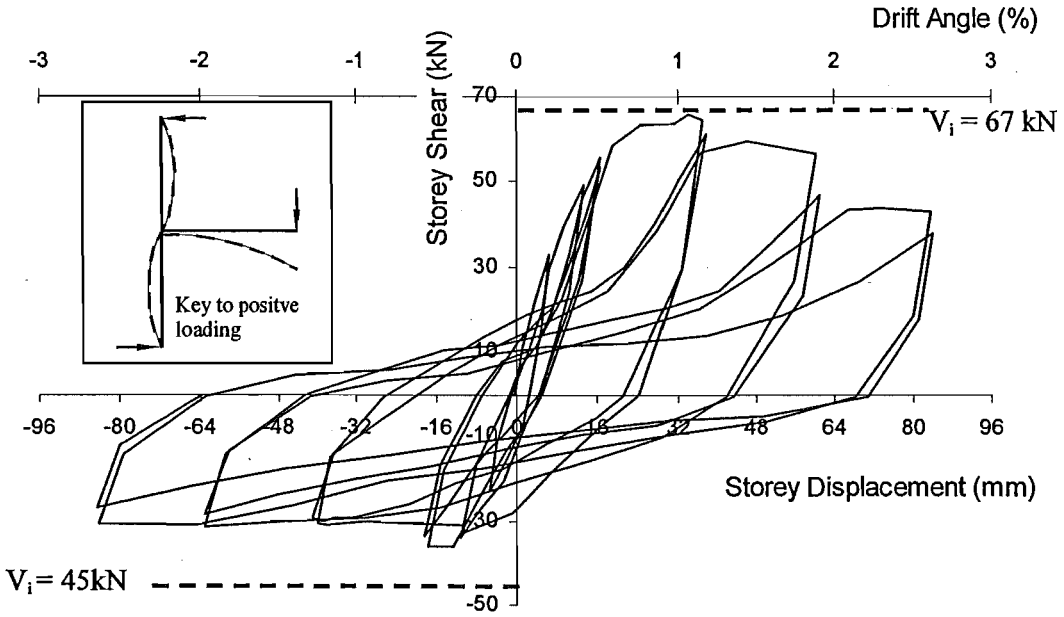

Fig. 7.46 Storey Shear Force versus Horizontal Storey Displacement Loops of EJ4

by test of Unit EJ4 was better when compared with that by test on Unit EJ3, and this was attributed to the more adequate configuration of the beam longitudinal bars in the exterior columns of Unit EJ4.

In Fig. 7.46, the theoretical storey shear strength determined at the attainment of negative beam flexural strength was attained during clockwise loading and it occurred at a storey drift of 1.1%, which was equal to a displacement ductility factor μ_Δ of 2. The attained storey shear strength by test on Unit EJ4 for anti-clockwise loading was about 16% less than the theoretical storey shear strength determined at the attainment of positive beam flexural strength and it occurred at a storey drift of 0.6%, which was equal to a displacement ductility factor μ_Δ of 1. Compared to test on Unit EJ2 where the attained storey shear strength was only about 75% of the theoretical storey shear strength for both loading directions, the attained storey shear force strength observed for test on Unit EJ4 increased by 9% to 25%. The compressive axial column load present for test on Unit EJ4 enhanced the force transfer from the beam tensile steel to the concrete by bond within the joint core, greatly relieving the opening action of the beam longitudinal bars and preventing the concrete tension cracking along the beam bar hooks, in comparison with test of EJ2. When compared to test on Unit EJ3 where the available storey shear strength

was about 90% of the theoretical storey shear strength, the increase in the attained storey shear strength by test of EJ4 was small. Unit EJ3 and Unit EJ4 were identical except the difference in beam bar hook arrangements and both units were tested with a constant compressive axial column load of 1800 kN present. This suggests that the beam bar hook details have no significant influence on the structural force strength performance of as-built exterior beam-column joint components if the concrete tension cracking failure associated with the interaction between column bar buckling and the opening action of the beam bar hooks can be prevented.

The measured displacement at first yield for test of Unit EJ4 using the method described in Section 5.3.2 was equivalent to a storey drift of 0.53% at first yield. The initial stiffness thus was 3.3 kN/mm on average for test on Unit EJ4 and it was 2.75 times the measured initial stiffness of 1.2 kN/mm for Unit EJ2. Significant improvement in the observed initial stiffness for test on Unit EJ4 was attributed to much reduced bond degradation along the beam longitudinal bars within the joint core owing to the presence of compressive axial column load. When compared to test of Unit EJ3 where the measured initial stiffness was 3.0 kN/mm, the improvement in the stiffness performance of test of EJ4 was very small. Hence if the premature concrete tension cracking along the beam bar hooks in tension can be totally prevented, the beam bar hook configuration in the exterior columns will not significantly influence the structural stiffness performance.

Some pinching of the storey shear force versus storey displacement hysteresis loops was observed in Fig. 7.46 for test of EJ4 and the pinching was observed to progress as the loading progressed. The low stiffness at the beginning of each load run was due to displacement across the major open beam flexural crack at the inner column face in the flexural compression zone of the beam, which was caused by tension in the previous loading run. Increase in the stiffness occurred mainly after the major beam flexural crack closed and the flexural compression started to be transmitted across the major beam flexural crack. Strength degradation was also observed in Unit EJ4, and it was of similar significance to that in Unit EJ3. However, the strength degradation observed for test on Unit EJ4 was much less significant than that for Unit EJ2. Progress of bond degradation along the beam longitudinal reinforcement adjacent to and within the joint core caused the attained beam flexural strength to reduce with the loading progress, leading to the observed strength degradation. The compressive axial column load for Unit EJ4 greatly

enhanced the bond mechanism to transfer the beam steel tension force to the surrounding concrete, leading to much improved energy dissipating capacity, when compared to test on Unit EJ2. Also compressive axial column load totally prevented the premature concrete tension cracking along the beam bar hooks in tension in Unit EJ4, consequently, the effect of the beam bar hook configuration in the exterior column became insignificant on the structural energy dissipating capacities, as demonstrated by Units EJ3 and EJ4.

In summary, test on Unit EJ4 demonstrated that the existence of compressive axial column load enhanced the available strength and stiffness of the unit, especially the stiffness, and also improved the structural energy dissipating capacity, when compared to test on Unit EJ2. Unit EJ4 reached the theoretical storey shear strength of the unit at a storey drift of approximately 1.1% for clockwise loading but it reached the storey shear strength which was about 15% less than the theoretical storey shear strengths at a storey drift of 0.6% for anti-clockwise loading. The observed attainment of the available storey shear strength by Unit EJ4 was at similar drift level to Unit EJ3. Softening with cyclic loading and pinching of the hysteresis loops observed for Unit EJ4 were of similar significance to Unit EJ3 and were not so significant as that observed for Unit EJ2. The compressive axial column load of $0.23 A_g f_c^{'}$ to $0.25 A_g f_c^{'}$ present for tests on Unit EJ3 and Unit EJ4 caused the influence of the beam bar hook details on the structural strength performance, stiffness performance and the energy dissipating capacity to be very insignificant.

7.6.4 Strains in Beam Longitudinal Reinforcement

For Unit EJ4, the beam was expected to develop a plastic hinge.

Fig.7.47 shows the measured strain profiles by electrical resistance strain gauges along beam bar 1 and beam bar 2 respectively. Compared with the measured steel strain profile along the beam longitudinal bars of Unit EJ2 (see Figs.7.25 and 7.26), bond degradation and bar slip along the beam longitudinal bars of Unit EJ4 were apparently improved within the joint region and the strains of beam flexural tensile reinforcement gradually decreased within the joint region relative to the steel strain at the inner column face. When compared to the observed strain profile of beam tension bars of Unit EJ3 (Fig.7.38 and Fig.7.39), it was found that units EJ3 and EJ4 had generally similar bond condition along the beam longitudinal bars within the joint region.

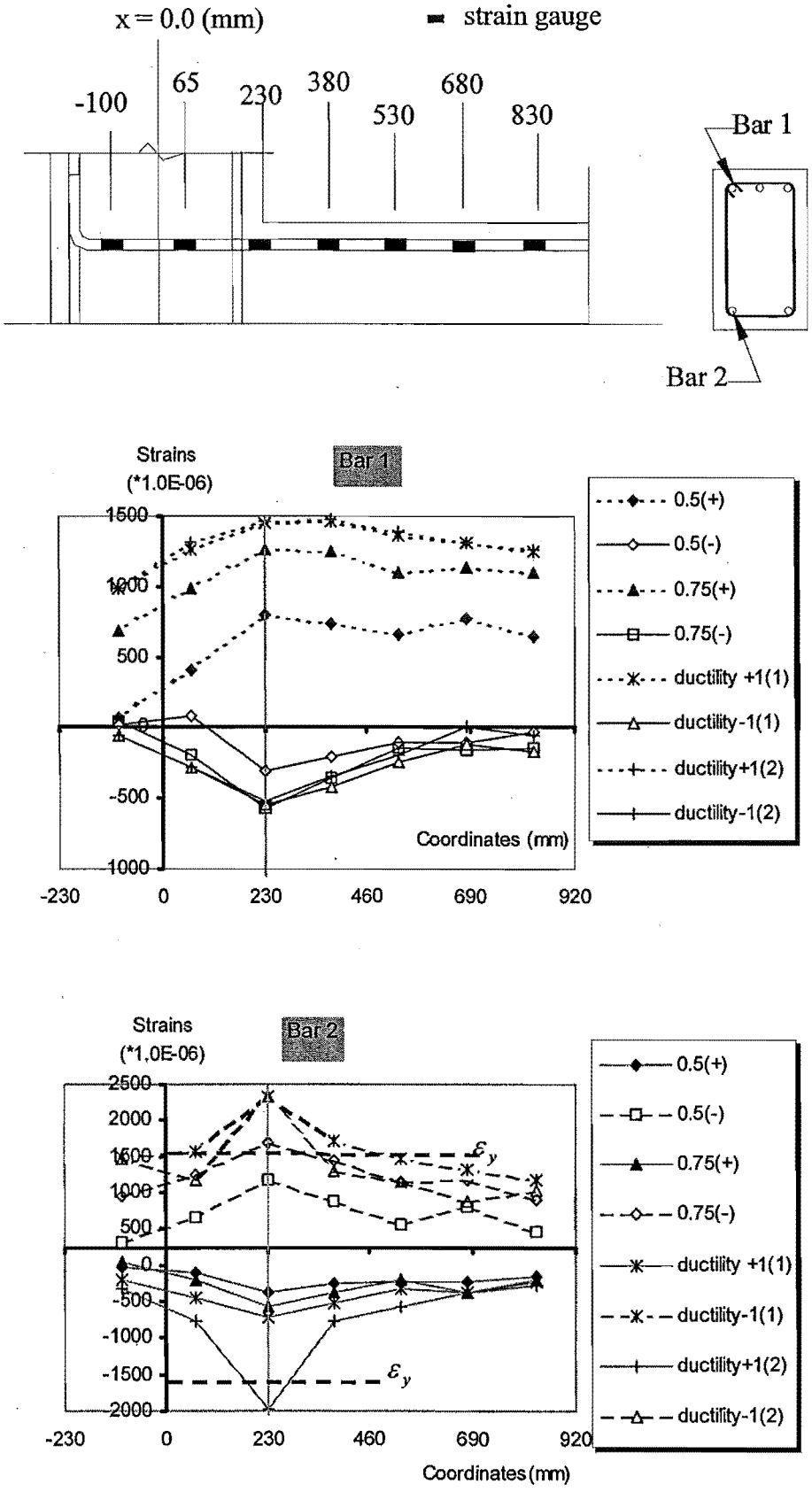

Fig. 7.47 Strain Profiles of Beam Bar 1 and Beam Bar 2 of Unit EJ4

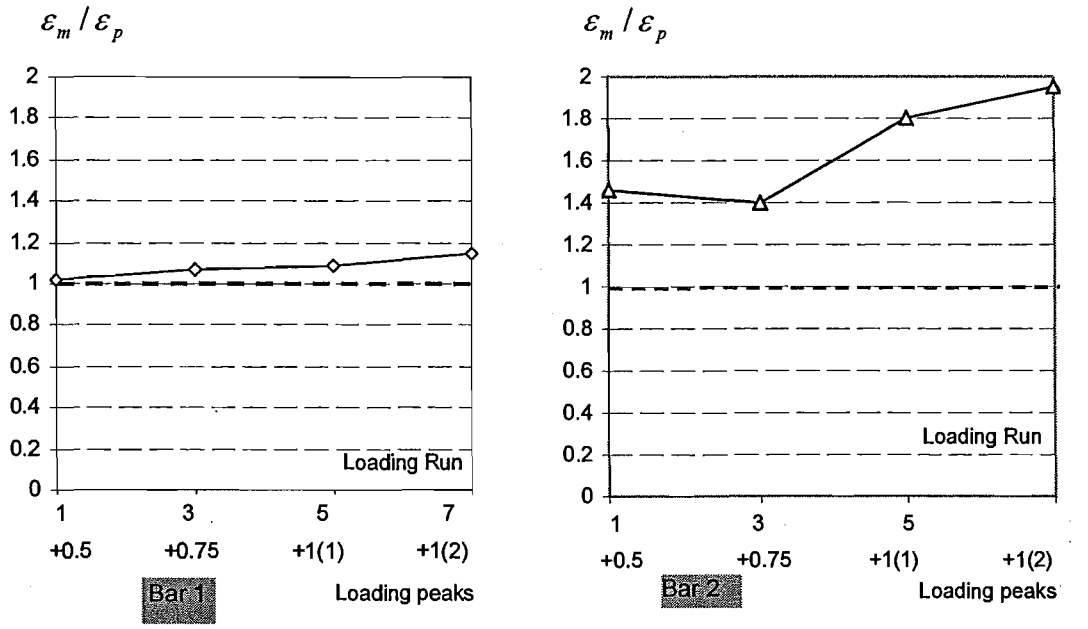

Fig.7.48 Comparison of measured and theoretical beam bar strains at column face

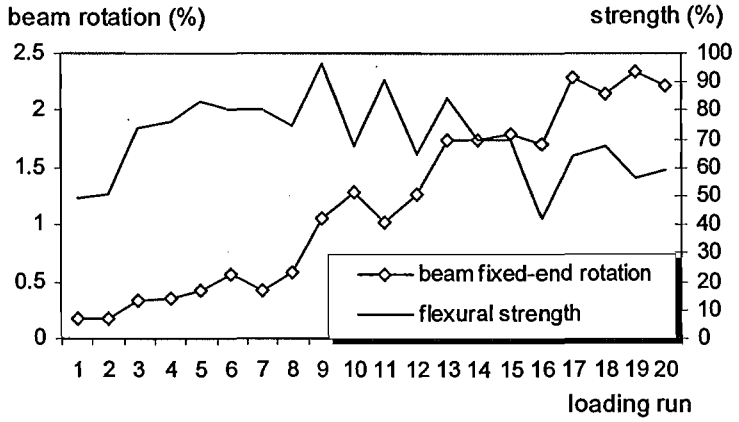

Fig. 7.49 Attained beam force strength and the observed beam rotation

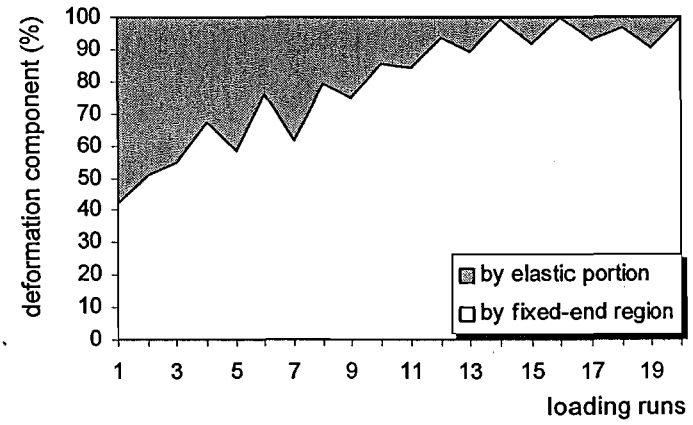

Fig. 7.50 Beam Deformation Components Measured for Unit EJ4

Fig. 7.48 compares the measured steel strains, ε_m, with the theoretically predicted strains, ε_p, for the beam flexural tension bars at the inner column face for Unit EJ4. The theoretical predictions were based on the measured beam shear forces and ordinary flexure theory established on the basis of plane-section assumption. The measured tension strains for the beam flexural tension bars at the column face were higher than the theoretical predictions and the discrepancies increased generally as the loading progressed. The measured tension strains, expressed as the percentages of the theoretical predictions, can vary from 105% to 200%. When compared with Unit EJ2, the discrepancies between the measured steel strain and the theoretically predicted strains were larger, even Unit EJ4 was expected to have better bond performance. The cause for this was not clear. However, very severe bond condition along the member longitudinal reinforcement could cause slippage between the longitudinal reinforcement and the concrete. As a result, the readings from the electrical resistance strain gauges could significantly deviate from the real steel strains.

7.6.5 Member Deformation Property

Unit EJ4 was a weak beam and strong column system. Fig. 7.49 shows the variation of the attained strength and deformation relationship for the beam of Unit EJ4. The observed beam rotation over the fixed-end region kept increasing at later loading stages even as the strength reduced. Hence the non-linear deformation was limited in the beam.

The measured member deformation was again concentrated into the member fixed-ends. Fig. 7.50 shows the measured deformation components for the beam. In Fig. 7.50, it is evident that the beam non-linear deformation was limited to the beam fixed-end.

Fig. 7.51 shows the observed rotational ductility in the fixed-end versus the attained flexural strength for the beam of Unit EJ4. It is seen that the beam can sustain a rotational ductility of 6 without significant strength degradation. Fig. 7.52 compares the observed beam behaviour, in terms of the strength versus non-linear deformation in the beam fixed-end, for Units EJ2 and EJ4. Units EJ2 and EJ4 were identical and both tests were expected to develop beam plastic hinges. Units EJ2 and EJ4 were tested with different column compressive axial load, zero for Unit EJ2 and $0.25A_g f_c'$ for Unit EJ4.

Fig. 7.52 shows that the beam flexural strength and the rotational ductility in the beam fixed-end was significantly affected by the compressive axial actions on the columns of

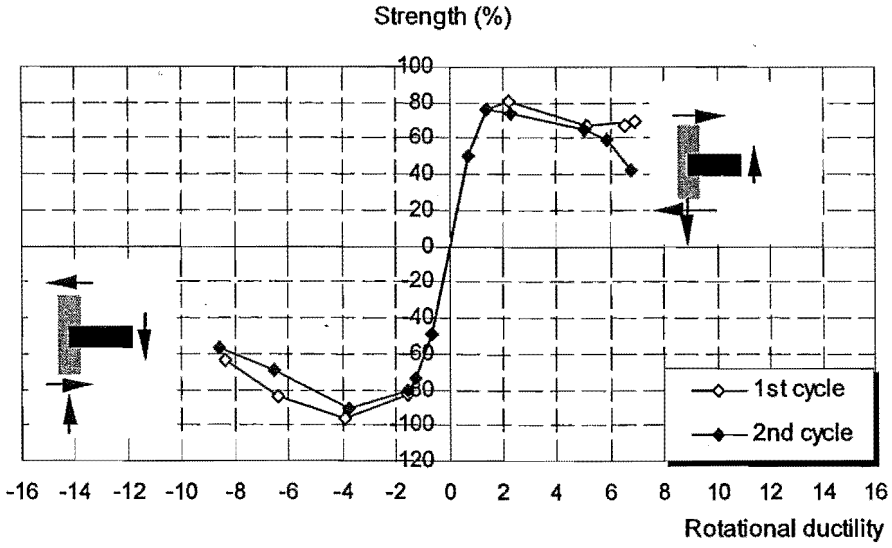

Fig. 7.51 Attained flexural strength versus rotational ductility in beam fixed-end of Unit EJ4

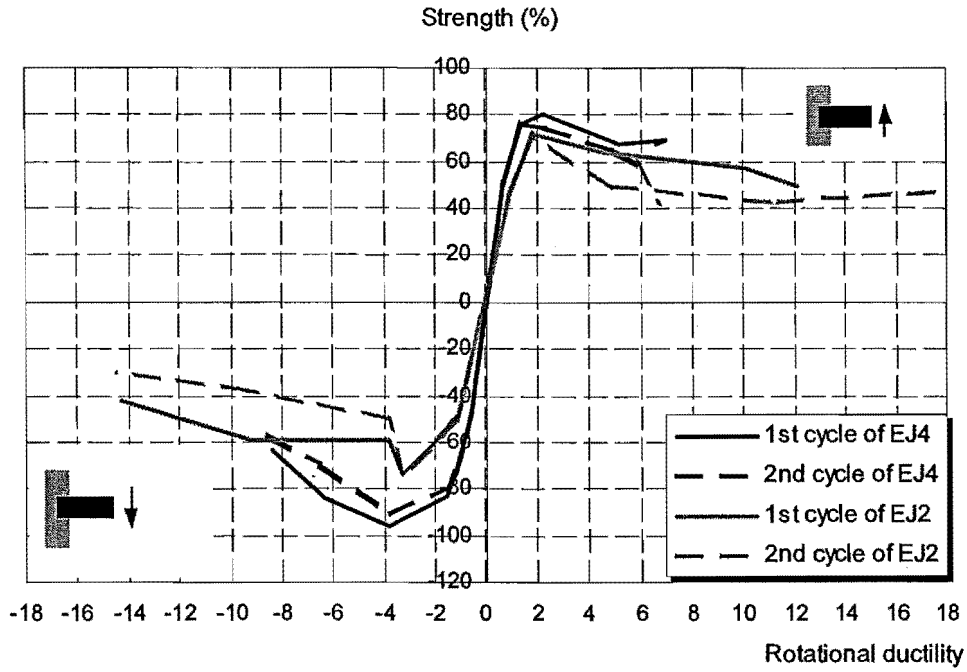

Fig. 7.52 Comparison of force strength and deformation capacity for Units EJ2 and EJ4

the unit. The observed initial stiffness for the beam of Unit EJ4, in terms of the flexural strength versus the rotational capacity, was 1.8 times that observed for the beam of Unit EJ2. The beam flexural strength of Unit EJ4 increased by more than 15%, when compared with Unit EJ2 due to the compressive column axial load. Enhancement of the beam initial stiffness due to compressive axial column load was much more significant,

when compared with the enhancement of the attained beam strength. This meant that the beam post-elastic flexural behaviour in the fixed-end was strongly dependent on the axial action on the columns transversely framing into the same joint. This evidence was similar to the finding obtained by comparing the observed beam force strength versus the rotations in the beam fixed-end for Units EJ1 and EJ3.

According to conventional flexural theory, the non-linear flexural deformation of a beam occurs due to the steel yielding penetration within the plastic hinge region. In this case, the non-linear force strength and the deformation behaviour of the beam is completely determined by the considered beam itself. However the observed evidence for Unit EJ4 was that severe bond degradation along the member longitudinal reinforcement occurred within and adjacent to the joint core and hence the post-elastic flexural deformation of the beam was concentrated into the fixed-end and it was mainly attributed to the long-sustaining steel tensile strain within and adjacent to the joint core. Therefore, the beam post-elastic flexural behaviour in the fixed-end was strongly dependent on the joint force transfer mechanism. The bond mechanism along the beam longitudinal reinforcement within the beam-column joint, namely, the joint force transfer mechanism, depends on not only the axial action on the columns but also the column cross sectional properties. As a result, the post-elastic behaviour of the beam in the fixed-end could be significantly influenced by the axial action and the cross sectional properties of the columns framing into the same joint, as observed for Units EJ2 and EJ4.

This is true even when the deformed longitudinal reinforcement is used because the flexural deformations of the reinforced concrete members in their fixed-ends are similarly strongly dependent on the joint force transfer mechanism.

7.6.6 Joint Behaviour

7.6.6.1 Joint Shear Stress

The estimated maximum nominal horizontal joint shear stresses for Unit EJ4, based on the measured member forces and the plane section assumption, were of similar magnitude to those of Unit EJ3 in both clockwise and anti-clockwise loading direction, and were 1.8 MPa, or $0.3\sqrt{f_c'}$ MPa in clockwise loading direction and 1.04 MPa, or

$0.17\sqrt{f_c'}$ MPa in anti-clockwise loading direction respectively. The maximum nominal horizontal joint shear stresses estimated for Unit EJ4 evidently were well below the joint shear capacity at the stage of diagonal tension cracking of the joint cores, which was $0.78\sqrt{f_c'}$ MPa, estimated using Mohr's circle for stress and assuming the concrete diagonal tension strength of $0.3\sqrt{f_c'}$ MPa [H1], if expressed in terms of nominal horizontal joint shear stress. The joint core of Unit EJ4 was of excellent integrity till the end of testing of EJ4.

7.6.6.2 Joint Shear Distortion and Joint Expansion

The maximum joint shear distortion measured for EJ4 was very small, being 0.0063%, which was of similar magnitude to Unit EJ3. Hence the joint core of Unit EJ4 was in excellent condition. In contrast, Unit EJ2, which was identical to Unit EJ4, had a maximum joint shear distortion of 0.52%. The significant improvement of the joint shear performance demonstrated by Unit EJ4 was due to the total prevention of the concrete tension cracking along the hooks of the beam bars in tension as a result of the enhancement of the beam steel tensile force transfer to the concrete by bond ahead of the bend, similar to the test of Unit EJ3.

Apparently, the contribution of the joint shear deformation to the storey deflection can be neglected should the compressive axial column load be greater than $0.2A_g f_c'$ for exterior beam-column joint components.

7.6.6.3 Joint Hoop Strains

Fig. 7.53 shows the measured strains in the joint hoops and the column transverse reinforcement adjacent to the joint core for test on Unit EJ4. All the measured strains were very small, and none of them was larger than 35×10^{-6}. Whereas in the case of the test on Unit EJ2 the joint hoop strains in the mid-depth of the joint core were up to the steel yield level of 1600×10^{-6}, the joint hoops of Unit EJ4 were not significantly strained. As described in section 7.5.6.2, the joint shear capacity prior to the diagonal concrete tension cracking is provided by a group of principal tensile and compressive

stresses generated in the concrete, and the joint shear reinforcement won't be highly stressed at this stage.

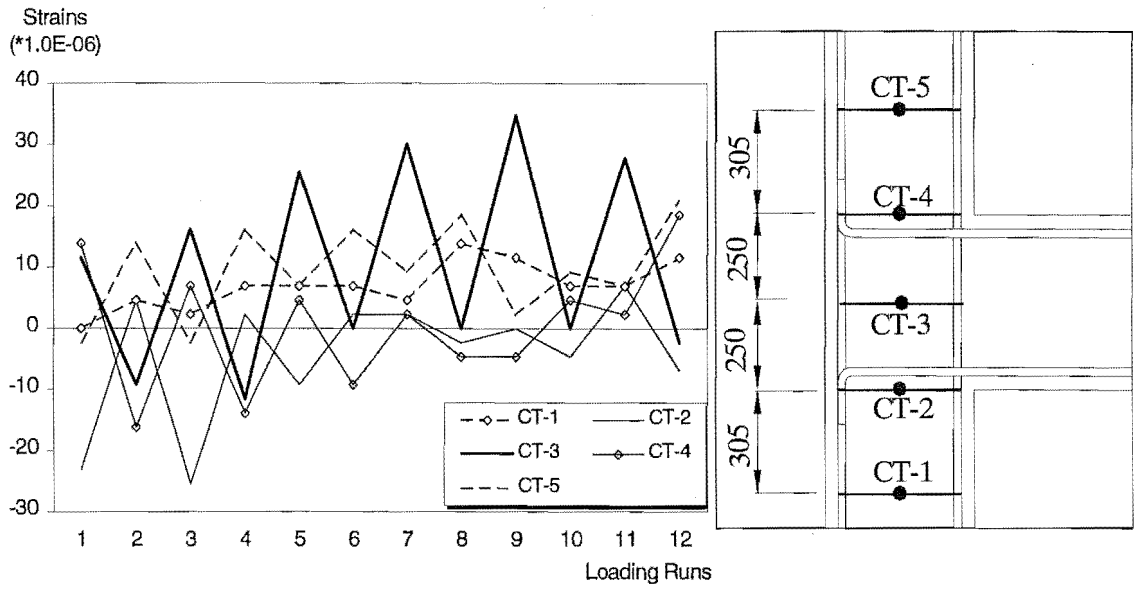

Fig. 7.53 Strains Measured for Joint Hoops and Column Transverse Reinforcement

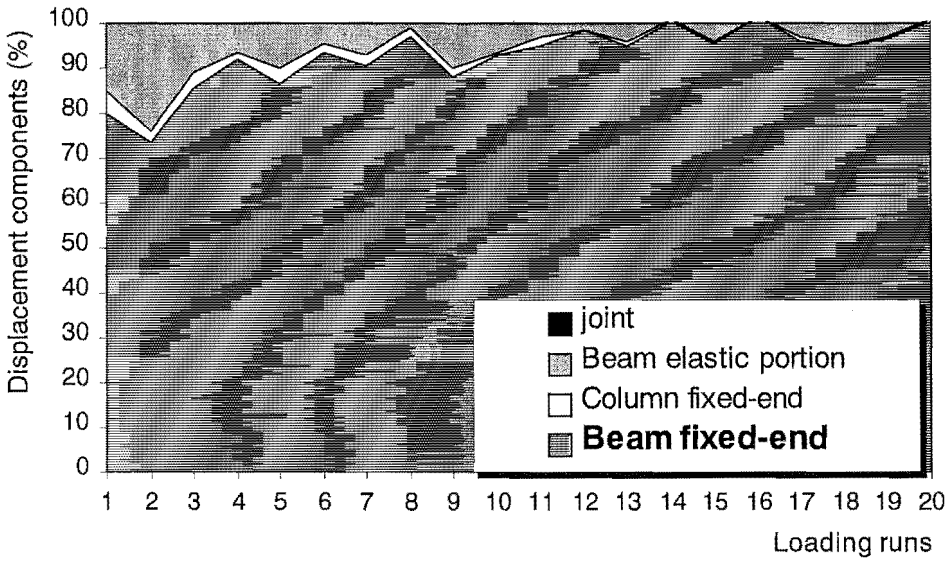

Fig. 7.56 Displacement Components Measured for Test of Unit EJ4

7.6.7 Displacement Components

Fig. 7.56 shows the measured displacement components for test of EJ4, where the contribution to storey displacement by the joint displacement was within 0.15 mm and it was ignored here. The contribution of column deformation to storey deflection considered here only came from the column deformation within the fixed-end region.

Fig. 7.54 clearly shows that the major contribution to storey deflection was from the beam deformation and it consisted of 80% to 99% of the total storey displacement. The contribution of column deformation to storey displacement was relatively small because the columns were basically only in the elastic range throughout the whole testing history. Evidently, the damage to the test unit EJ4 was limited to the beam.

7.6.8 Summary

A full-scale exterior beam-column joint unit EJ4 was fabricated and Unit EJ4 was identical to Unit EJ2. The plain round beam longitudinal reinforcing bars were bent into the joint core in the exterior columns as is current practice. Unlike Unit EJ2 which was tested under simulated seismic loading with zero axial column load, Unit EJ4 was tested under simulated seismic loading with the presence of a constant compressive axial column load of $0.23 A_g f_c^{'}$ in order to investigate the effect of axial column load on the seismic behaviour of exterior beam-column joint components. Unit EJ3 and Unit EJ4 were also identical except the arrangement of the beam bar hooks, and both units were tested with constant axial column load of 1800 kN present. Theoretical considerations showed that transverse reinforcement in the members could be very inadequate for Unit EJ4, especially in the beam, according to the requirement of shear resisting capacity and the requirement for preventing longitudinal bar buckling and confining the compressed concrete.

1. The test on Unit EJ4 showed that the overall performance of the unit was again dominated by flexure. The presence of a constant compressive axial column load of $0.23 A_g f_c^{'}$ for test of EJ4 greatly improved the seismic performance of the as-built exterior beam-column joint assembly, when compared to the test on the otherwise identical unit EJ2 but tested with zero axial column load.

2. The compressive axial column load on Unit EJ4 enhanced the force transfer by bond from the beam tension steel to the surrounding concrete ahead of the bend, and greatly reduced the beam steel tension force needed be transferred at the bend. Consequently, the premature concrete tension cracking failure along the beam bar hook, which was associated with the interaction between the column bar buckling and the opening action of the beam bar hooks as occurred for the test on Unit EJ2, was entirely prevented during the test on Unit EJ4. The final failure of Unit EJ4 was initiated by the degrading beam flexural behaviour as for Unit EJ3.

The storey shear strengths were attained by the test on Unit EJ4 at a storey drift of 1.1% during clockwise loading but at a storey drift of 0.6% during anti-clockwise loading. The storey shear strength during clockwise loading was equal to the theoretical storey shear strength determined at the attainment of negative beam flexural strength, and the storey shear strength during anti-clockwise loading was about 16% less than the theoretical storey shear strength determined at the attainment of positive beam flexural strength.

The measured displacement at first yield for test of Unit EJ4 was equivalent to a storey drift of 0.53%.

3. Results of Unit EJ4 were compared to the results of Unit EJ2. Such a comparison revealed that the presence of compressive axial column load of $0.23 A_g f_c^{'}$ for Unit EJ4 caused the initial stiffness to be 2.75 times the initial stiffness for Unit EJ2 and the storey shear strength of Unit EJ4 increased by about 15% of the theoretical storey shear strength. Furthermore, the compressive axial column load of $0.23 A_g f_c^{'}$ for Unit EJ4 also greatly improved the energy dissipating capacity of the system due to a significant improvement of beam flexural stiffness.

4. The results of Unit EJ4 were also compared to the results of Unit EJ3. The presence of the compressive axial column load of 1800 kN for the tests on Unit EJ3 and Unit EJ4 caused the effects of the different arrangements of the beam bar hooks in exterior column on the stiffness, strength and the energy dissipating capacity of the units to be very small.

5. Due to the use of plain round longitudinal reinforcement, the post-elastic flexural behaviour of the beam, which was weaker than the columns, was mainly limited into the

beam fixed-end. The beam post-elastic flexural behaviour in the fixed-end in this case was strongly dependent on the axial actions and the cross sectional details of the columns, which transversely framed into the same joint. This test finding disagrees with the conventional flexural theory but it was similar to the one revealed from test on Unit EJ3.

7.7 CONCLUSIONS

Simulated seismic load tests were conducted on four as-built reinforced concrete exterior beam-column joints and one retrofitted as-built exterior beam-column joint. The simulated seismic load tests on the as-built exterior beam-column joints were conducted as part of an investigation of the behaviour of existing reinforced concrete structures designed to pre-1970s codes when subjected to severe earthquake forces. The simulated seismic load test on the retrofitted as-built exterior beam-column joint was conducted to investigate the possible retrofit technique for existing reinforced concrete building structures. The four as-built full-scale exterior beam-column joint units, EJ1 to EJ4, were identical except the arrangement of the beam bar hooks in the exterior columns. The longitudinal and transverse reinforcement was from plain round bars. Two units, Units EJ1 and EJ3, had the beam bar hooks bent away from the joint cores as was not uncommon in existing reinforced concrete structures designed to pre-1970s codes, and the other two units, Units EJ2 and EJ4, had the beam bar hooks bent into the joint cores as required by current design codes. Units EJ1 and EJ2 were tested subjected to simulated seismic loading with zero column axial load but Units EJ3 and EJ4 were tested subjected to simulated seismic loading with the compressive column axial load of about $0.25 A_g f_c^{'}$ present. As-built Unit EJ1 was retrofitted by wrapping the column areas above and below the joint core using fibre-glass material after tested subjected to simulated seismic loading with zero axial column load, and the retrofitted unit, referred to as Unit REJ1, was tested subjected to simulated seismic loading with zero axial column load again. In addition, as-built test units EJ1 and EJ3 were identical to Hakuto's test units O7, and as-built test units EJ2 and EJ4 were identical to Hakuto's Unit O6, except that Hakuto used deformed longitudinal reinforcement.

Theoretical consideration shows that the shear force capacity of the beam-column joint was inadequate for the test of Unit EJ1. In addition, the beam and column transverse reinforcement was inadequate for all the tests, according to the requirements for preventing the longitudinal reinforcement from buckling and confining the compressed concrete, and/or the requirement for providing the shear force strength. Concrete tension cracking failure initiated by the opening of the beam bar hooks could occur due to insufficient column transverse reinforcement within beam bar hook ranges and the utilisation of plain round longitudinal reinforcement. Different beam bar hook details were expected to actuate different joint force transfer paths and therefore emphasise the need for column transverse reinforcement at different locations. The use of plain round longitudinal reinforcement and inadequate anchorage configuration of the beam bar hooks when bent away from the joint cores made it very critical to transfer the member forces across the joint core.

Comparison of the results of tests on Units EJ1 and EJ2 led to the following conclusions:

1. The overall seismic performance of the as-built exterior beam-column joint subassemblages was very poor. The final failure of the as-built units was dominated by premature concrete tension cracking along the beam bar hooks, which was initiated by the interaction between the column bar buckling and the opening action of the beam bar hooks, irrespective of the beam bar hook details.

2. Different beam bar hook details in the exterior columns significantly influenced the strength and stiffness performance of the unit, when the compressive axial column load was low.

The attained storey shear strength by the as-built exterior beam-column joint unit with the beam bar hooks bent away from the joint core was only 55% of the theoretical storey shear strength of the unit. In contrast, the attained storey shear strength by the as-built exterior beam-column joint unit with the beam bar hooks bent into the joint core was about 75% of the theoretical storey shear strength of the unit. The observed improvement in the available storey shear force strength due to more adequate beam bar hook configuration was as high as 20% of the theoretical storey shear strength when the axial column load was very low.

The attained stiffness in the elastic loading range by the unit with the beam bar hooks bent into the joint core was about 1.4 times the attained stiffness by the unit with the beam bar hooks bent away from the joint core.

3. Different beam bar hook details in the exterior columns were found to enhance the need for column transverse reinforcement at different locations. When the beam bar hook were bent away from the joint core, the column stirrups immediately above and below the joint core played an important role in actuating the postulated alternative force path across the joint core. When the beam bar hook were bent into the joint core, the shear reinforcement at the joint centre was more effective in controlling the opening of the beam bar hooks and actuating the corner to corner concrete strut mechanism, than the shear reinforcement far away from the joint centre.

4. When contrasted to the results from Hakuto's tests on Units O6 and O7 where the shear failure in the beam and/or the joint core triggered the final failure of the units, the use of plain round longitudinal reinforcement for Unit EJ4 totally suppressed the shear failure in the beam and the joint core, but it significantly enhanced the opening action of the beam bar hooks in tension, resulting in the premature failure of concrete tension cracking along the beam bar hooks and leading to low attainment and poor maintenance of the force strength and the stiffness of the unit, especially the stiffness.

When compared to the identical cases but with deformed longitudinal reinforcement, the decrease in the available strength of the unit due to the use of plain round longitudinal reinforcement was 20 to 25% of the theoretical strength of the units, when the units were tested with zero axial column load. Meanwhile, the decrease in the initial stiffness due to the use of plain round longitudinal reinforcement was about 70% for the exterior beam-column joint unit with the beam bar hooks bent into the joint core. Apparently, the use of plain round longitudinal reinforcement caused a much more significant decrease in the initial stiffness of the unit, compared to that in the storey shear strength of the unit. The adverse effect of the use of plain round longitudinal reinforcement on the initial stiffness was more significant for the as-built exterior beam-column joint units, than for as-built interior beam-column joint units.

Comparison of the results of tests on Units EJ3 and EJ4 led to the following conclusions:

5. The presence of a compressive axial column load of about $0.25 A_g f_c^{'}$ resulted in much improved seismic performance, in terms of the structural stiffness, strength and the energy dissipating capacity. Due to the presence of compressive axial column load of about $0.25 A_g f_c^{'}$, the force transfer by bond from the beam tension steel to the surrounding concrete was enhanced ahead of the bend. As a result, the beam steel tension force needed to be transferred at the bend reduced, premature concrete tension cracking failure along the beam bar hook was entirely suppressed and the seismic performance of the test units was completely dominated by the beam flexural behaviour.

The strengths attained by Unit EJ3 and Unit EJ4 were of similar magnitudes in terms of their theoretical storey shear strengths, and they were measured at similar storey drift levels. The storey shear strengths were attained by Unit EJ3 and Unit EJ4 at a storey drift of about 1.1 to 1.5% for clockwise loading direction but at a storey drift of about 0.6% for anti-clockwise loading, and they were approximately 10 to 12% less than the theoretical storey shear strengths. The initial stiffnesses measured for Unit EJ3 and Unit EJ4 were about 75% of the theoretical predictions based on the plane section assumption and the initial stiffnesses measured for Units EJ3 and EJ4 were equivalent to a storey drift of about 0.6% at first yield.

6. In comparison with the tests on the identical units but with zero axial column load, namely, Unit EJ1 and Unit EJ2, the presence of a compressive axial column load of 0.23 to $0.25 A_g f_c^{'}$ not only caused the measured initial stiffness to increase by 180% and the available storey shear strength to increase by about 20 to 33% of the theoretical storey shear strengths, but also greatly improved the energy dissipating capacity of the system by reducing softening and pinching of the hysteresis loops.

Simulated seismic load test on the retrofitted unit REJ1 led to the following conclusions:

7. When the column axial load was low, there was a need for actuating the alternative force path across the joint core when the beam bar hooks were bent away from the joint core. External wrapping the column areas above and below the joint core of the exterior beam-column joint subassemblage could actuate the postulated

alternative force path across the joint core, improving the general behaviour of the unit. Fibre-glass jacketing in the column areas above and below the joint core for Unit REJ1 controlled premature concrete tension cracking failure and actuated the alternative joint force transfer path.

The final failure trigger of the retrofitted unit became the degrading beam flexural behaviour. However, the available strength and stiffness of the retrofitted unit REJ1 were still low.

8. Should sufficient column transverse reinforcement be available immediately above and below the joint core, an alternative force transfer path across the joint core of the exterior beam-column joint subassmblages can be actuated if the beam bar hooks are bent away from the joint core. In this case, the overall seismic assessment of the system would be comparable to that with the beam bar hooks bent into the joint core.

Generalised strength and deformation behaviour for as-built reinforced concrete members are as follows:

9. Similar to the findings from the tests on two as-built interior beam-column joint units, the seismic performance of the as-built concrete members were totally governed by the degrading flexural behaviour, rather than by premature shear as observed for the members reinforced by deformed bars. Member deformation was concentrated in the fixed-ends at beam-column interfaces not only in post-elastic range but also in elastic range and this was due to severe bond degradation along the member longitudinal reinforcement within and adjacent to the joint core. Hence the post-elastic behaviour of an as-built reinforced concrete member was determined by the flexural behaviour at the fixed end of the member.

A rotational ductility in the member fixed-ends, rather than the curvature ductility associated with a certain plastic hinge length, becomes a proper index for member non-linear deformation.

Due to severe bond degradation along the longitudinal reinforcement resulting from the use of plain round longitudinal reinforcement, conventional flexural theory based on the plane section assumption would overestimate the member flexural strength and stiffness, especially the stiffness. The member non-linear property, in terms of the flexural

strength and rotational deformation in the fixed-ends, was found to be very strongly dependent on the members transversely framing into the same joint. For example, when compared with the cases with no column axial load, a column axial load of $0.25A_gf_c'$ could lead to the increase of about 15% in the strength and the increase of 50% to 80% in the initial stiffness for the beams. This evidence disagrees with the conventional flexure theory, which assumes the member's flexural behaviour to be completely determined by the member itself and it has nothing to do with other members.

CHAPTER 8

ANALYSIS OF TEST RESULTS AND SUGGESTIONS FOR SEISMIC ASSESSMENT AND RETROFIT OF EXISTING REINFORCED CONCRETE STRUCTURES

8.1 INTRODUCTION

A major earthquake imposes large deformations on structures and the structural deformation is usually well beyond the elastic response range in this case. Hence the key element in assessing the seismic performance of existing reinforced concrete structures during a major earthquake is the post-elastic seismic responses of the structures. The capacity design based seismic assessment procedure examines the global post-elastic structural behaviour by investigating the seismic performance of the critical post-elastic failure mechanism of the structure. Once the available lateral load strength and the available structural displacement capacity of the critical post-elastic collapse mechanism are determined, the structural performance in a major earthquake can be assessed.

The global non-linear behaviour of the whole structure depends on the local non-linear behaviour of individual reinforced concrete members. With an analytical model capable of reproducing the inelastic response of individual reinforced concrete components with reasonable accuracy, the global post-elastic behaviour of the whole structure can be adequately estimated by integrating the local behaviour of individual structural components, as demonstrated by tests and analysis conducted by Bracci et al [B2]. Hence, the information on the post-elastic behaviour of the individual reinforced concrete members is the fundamental element in conducting the seismic assessment of existing reinforced concrete structures, although the global behaviour is more relevant to the structural performance during a major earthquake. For the individual reinforced concrete components, it is necessary to identify the regions where non–linear deformations are expected, to find the available strengths of these identified regions, and also to check whether the available strengths of these regions can be maintained as the non-linear deformations progress.

Simulated seismic loading tests on as-built reinforced concrete components reinforced by deformed longitudinal reinforcement revealed that the current code methods were not

adequate, especially when used for estimating the shear performance and the stiffness performance of individual reinforced concrete components. The situation was even worse when the concrete components had plain round longitudinal bars (see Chapters 6 and 7). Also the seismic performance observed for as-built concrete beam-column joint components reinforced by plain round longitudinal bars was very different from that for similar test units reinforced by deformed longitudinal bars. Hence there is a need for developing new methods, which can be used for assessing the seismic behaviour of existing concrete components containing plain round longitudinal bars.

There are two main parts in this chapter. In the first part, the characteristics of the observed post-elastic responses for as-built concrete beam-column joint components reinforced by plain round longitudinal bars are outlined and the critical considerations in assessing the post-elastic behaviour of similar concrete components with plain bar reinforcement are identified. In the second part, suggestions for seismic assessment and retrofit wherever necessary of existing reinforced concrete frame structures are presented, including the suggestions for member modelling, the suggestions for the determination of the static flexural strength versus deformation relationship of as-built reinforced concrete members and the suggestions for possible retrofit techniques to improve the inadequate member flexural performance.

8.2 OUTLINES OF TEST RESULTS

8.2.1 Critical Aspects of Post-elastic Behaviour of Individual Existing Reinforced Concrete Subassemblages

As-built full-scale beam-column joint subassemblages, tested under simulated seismic loading in this test series, represent an existing reinforced concrete structure constructed in 1950s in New Zealand. Identical as-built test units but reinforced by deformed longitudinal bars had been tested under simulated seismic loading in the past at the University of Canterbury by Hakuto et al [H1]. Influences of the use of deformed longitudinal bars or plain round longitudinal bars on the seismic behaviour of beam-column joint components have been studied in Chapter 6 and Chapter 7. From Chapters 6 and 7, it is clear that whether the longitudinal reinforcement is from deformed bars or plain round bars can greatly influence the structural seismic behaviour. A detailed comparison of Hakuto's tests on as-built units and the tests conducted on as-built units in

Table 8.1 Comparison of Test Results of As-Built Units with Deformed Bars and As-Built Units with Plain Round Longitudinal Bars

Unit	$\frac{V_a}{V_i}$ (%)	$\frac{K_a}{K_e}$ (%)	R_y (%)	R_m		$\frac{V_a}{V_i}$(%)	Final failure trigger
				clock	Anticlock	at R ≤ 2%	
Unit 1	90	37	1.8	3.7	4	85	degrading column flexure in fixed-ends
Unit O1	95	50	1.2	2	2.3	90-100	joint shear
Unit 2	77	39	2	2.2	2	75	degrading beam and column flexure in fixed-ends plus joint shear
Unit EJ1	57	42*	33*	2	1	57	premature concrete tension cracking along beam bar hooks
Unit O7	77	40	0.5	0.48	1	87	premature concrete tension cracking along beam bar hooks and joint shear
Unit REJ1	75	50	0.8	0.5	0.8	75	degrading beam flexure
Unit EJ2	75	30	1.3	1.3	1.3	75	degrading beam flexure in fixed-end and premature concrete cracking along beam bar hooks
Unit EJ3	85	62	0.6	1.3	0.6	85	degrading beam flexure in fixed-end
Unit O6	100	47	0.42	1.8	1.8	100	shear failure in beam and joint
Unit EJ4	90	68	0.53	1.1	0.6	90	Degrading beam flexure in fixed-end

Note: values with * are measured in the loading cycle of $0.5V_i$, rather than in the loading cycle of $0.75V_i$,

V_a and V_i = the attained force strength and the theoretical force strength, respectively

K_a = the attained initial stiffness in terms of the storey shear versus the storey displacement,

K_e = estimated initial stiffness, which was the value using the sectional analysis for the beams and columns for the current test programme but was based on 0.5 times the gross sectional moment of inertia for Hakuto's tests.,

R_y = the storey drift at first yielding, the first yielding is determined by extrapolating the force and deformation line at $0.75V_i$ to V_i,

R_m = the storey drift when the maximum force strength was attained,

clock and anti-clock = the clockwise and anti-clockwise directions respectively,

R = storey drift

this test series was made in Table 8.1, in terms of the failure trigger of the system, the attainment of the force strength and stiffness.

For Hakuto's tests [H1], the concrete members yielded in flexure first, then the shear force strength in the potential plastic hinge regions degraded as the nonlinear deformation progressed. As a consequence, the possible premature shear failure due to the degradation of the shear force strength as the imposed non-linear deformation progressed could threaten the maintenance of the attained force strength. Typically, premature shear failure was observed in the beam-column joints and/or the beams for Hakuto's tests on as-built Unit O1, Unit O7, and Unit O6, and it triggered the final failure of the units. Hakuto's as-built units O1, Unit O7 and Unit O6 were otherwise identical to the current units 1, EJ1 and EJ2, respectively, except that Hakuto's units contained deformed longitudinal reinforcement. The beam-column joint cores of the as-built test units contained no or very small amounts of joint shear reinforcement and the beams of the test units contained very small quantities of transverse reinforcement. Hakuto et al concluded that the critical aspect present for the investigated reinforced concrete frame structure was the shear performance in the joints and the beams, and the shear performance after the flexural yielding could govern the overall seismic performance of the individual concrete members. Hence the information they tried to get was (1). the attainment of the shear force capacity of the beam-column joints without the joint shear reinforcement and the degradation of the joint shear force capacity with the increase in the imposed post-elastic deformation levels of the adjacent members; (2). the attainment of the beam shear force capacity and its maintenance with the increase in the imposed post-elastic deformation, which is limited to the plastic hinge regions.

However, the seismic performance observed for as-built concrete beam-column joint components reinforced by plain round longitudinal bars in the current project was very different. The shear performance in the beam-column joints and the beams was much less problematic, and the post-elastic behaviour of individual concrete components was due to the degrading member flexural behaviour, which was mainly limited in the fixed-ends. The degrading member flexural behaviour occurred as a result of progressive bond degradation along the plain round longitudinal bars with the increase in the imposed displacement levels and the loading cycles.

Apparently, for the individual reinforced concrete members with plain round bars, the attainment and maintenance of the flexural strengths and stiffnesses in the fixed-ends with the increase in the imposed post-elastic deformation levels and the cyclic loading cycles need to be investigated, rather than the degradation of the shear force strength as for the members reinforced by deformed bars.

8.2.2 Flexural Behaviour of As-built Reinforced Concrete Members Reinforced by Plain Round Longitudinal Bars

8.2.2.1 General

To investigate the flexure-dominated non-linear performance of an individual reinforced concrete member during a major earthquake, the key elements are the identification of the critical areas, which are expected to experience post-elastic deformation, and the determination of the flexural strength and deformation performance within the critical regions. The information on the locations of the critical areas is useful for modelling the stiffness distribution along the members, called member modelling. The information on the strength and deformation hysteretic behaviour within the critical regions is useful for modelling the member hysteretic behaviour, called hysteretic modelling.

8.2.2.2 Characteristics of Member Stiffness Distribution

For well-designed reinforced concrete members, energy-dissipation during a major earthquake is mainly by steel yielding penetration within the member over well-defined plastic hinge regions. Many methods have been developed to estimate the plastic hinge lengths [P1]. Modelling of the member non-linear behaviour focuses on the plastic hinge regions.

For as-built reinforced concrete members reinforced by plain round longitudinal bars, observed evidence showed that the member post-elastic deformation was mainly in the major flexural crack at beam-column interfaces, referred to as fixed-end rotation, with the remaining part of the member in the elastic range. A rotational ductility at the member fixed-end is demonstrated to be a proper index to the member non-linear deformation capacity. Member non-linear behaviour in this case should be better represented in terms of the flexural strength versus the rotational ductility in the fixed-end region.

Actually, even for reinforced concrete members reinforced by deformed longitudinal reinforcement, the observed magnitude of member fixed-end rotation, which occurred

mainly due to bond degradation within the beam-column joint region, was often too significant to be neglected [H1, K2, L4, T1]. Takeda [T1] reported that deflection caused by slip of the reinforcement and depression of the concrete at the beam-column interface was up to 31% of the total deformation.

Therefore, adequate modelling of the member's post-elastic behaviour in terms of the flexural strength versus the rotational ductility at the fixed-end region plays an important role in the seismic assessment of existing reinforced concrete structures in a major earthquake.

8.2.2.3 Characteristics of Member Flexural Behaviour at the Fixed-End

Conventional flexural theory assumes that the non-linear flexural deformation of an individual reinforced concrete member is due to steel yielding penetration over well-defined plastic hinge regions, the post-elastic flexural behaviour of the member in this case is completely determined by the cross sectional details of the member.

However, member flexural deformation in terms of the rotation in the fixed-end region is fundamentally different from the member flexural deformation in terms of curvature ductility associated with a given plastic hinge length. Observed significant lumping of member non-linear deformation in a major flexural crack at beam-column interfaces mainly occurred due to severe bond degradation along the plain round longitudinal reinforcement within the joint. As a result, the post-elastic flexural behaviour at the fixed-end was associated with the bond mechanism along the member longitudinal reinforcement within the joint region and hence was associated with the member force transfer across the joint core. A beam-column joint is the connection of the beams and the columns, hence the non-linear flexural behaviour of a member is also dependent on the actions and the cross sectional details of the other members framing into the same joint. For example, the tests on as-built units EJ2 and EJ4, which had plain round longitudinal reinforcement, demonstrated that a compressive column axial load of about 0.25 $A_g f_c'$ led to an increase up to 15% in the beam flexural strength and an increase in the initial stiffness of up to 80% in terms of the member flexural strength versus the member fixed-end rotation. Hence, a proper member model to represent the non-linear behaviour of the as-built member should capture the influences of other members framing into the same joint.

For plain round longitudinal reinforcement, the bond mechanism of the member longitudinal reinforcement within the joint region is developed due to friction and therefore is mainly developed over the flexural compressive zones of the member transversely framing into the same joint. The factors affecting the bond mechanism of plain round longitudinal reinforcement within the joint region include: (a). axial actions on the members framing into the same joint in transverse direction. Large axial action in compression on the transverse members will enhance the clamping action for the longitudinal reinforcement of the member within the joint region, and therefore enhanced the bond mechanism, leading to an enhanced member flexural behaviour in the fixed-end region, as revealed by the tests on the as-built units EJ1 to EJ4 in the current project. (b). the overall section depth of the members framing into the same joint in transverse direction. Member flexural compressive depth can be approximated to be a fraction of the member overall depth in the elastic range. The greater the flexural compressive depth of the transverse members are, the better the anchorage condition is along the member longitudinal reinforcement within the joint region. As a result, member strength would be slightly enhanced and member stiffness performance would be significantly improved. (c). confinement provided for the member adjacent to the joint. Member deformation in the fixed-ends are partially from the bond degradation in the member areas adjacent to the joint core. Transverse confinement for the members will enhance the bond mechanism along the plain round bars in the member areas adjacent to the joint core and subsequently enhance the member flexural strength and the stiffness performance.

Hence, the flexural behaviour of an as-built member at the fixed-end can be significantly affected by the axial actions and the cross sectional details of the transverse members at the same joint. However, except the tests conducted in this project, there have been no tests conducted to study the influences of the other members at the same joint on the member flexural behaviour at the fixed-end, when plain round longitudinal reinforcement is used. Evidently, more tests need to be conducted on the as-built reinforced concrete components reinforced by plain round longitudinal reinforcement in order to quantitatively study the influence of above-stated factors.

For deformed longitudinal reinforcement, the bond mechanism of the longitudinal reinforcement within the joint region is developed due to friction and mechanical mechanism. Usually the bond strength component from friction is very samll, compared to the mechanical mechanism. Many factors affect the bond mechanism of deformed bar

reinforcement. Apart from the above-stated factors which affect the bond mechanism of plain round bar reinforcement, the existence of joint horizontal and vertical shear reinforcement would actuate the force transfer mechanism from the steel to the concrete outside the main corner to corner concrete strut, easing the sustaining of large steel strain over a long range. Tests conducted by Lin et al [L4] demonstrated the beneficial effect of interior column bars on the enhancement of the bond mechanism along the beam longitudinal bars within the joint. Lin et al also studied the enhancement of the bond strength along the beam deformed longituidnal bars by column axial load [L4]. A database of seven test units, which were tested subjected to an axial load larger than $0.1A_gf_c'$, was used and all test units used Grade 300 deformed longitudinal reinforcement. It was found that the average bond stress along the beam deformed longitudinal reinforcement within the joint increased with the column compressive axial load. The average bond stress of the beam deformed longitudinal reinforcement is found to be $u_a = 1.2\sqrt{f_c'}$ when the compressive column axial load N^* is zero, and the effect of the compressive column axial load N^* on the average bond stress of the beam deformed longitudinal reinforcement was found to be:

$$u_a = 1.2\sqrt{f_c'}\left[1+\frac{N^*}{1.8A_gf_c'}\right] \qquad (8\text{-}1)$$

Although the extensive study on the bond mechanism along the deformed longitudinal reinforcement within the joint region, especially the effect of compressive axial column loads on the enhancement of the bond mechanism along the beam deformed longitudinal reinforcement, has been conducted, no research has been conducted by aiming at revealing the relationship between the bond mechanism along the deformed longitudinal reinforcement within the joint region and the member flexural behaviour at the fixed-ends. Apparently, extensive test study needs to be conducted on reinforced concrete beam-column joint components reinforced by deformed longitudinal bars in order to investiagte the member flexural behaviour at the fixed-ends.

8.2.2.4 Attainment and Maintenance of Member Flexural Strength and Stiffness

Measured storey shear versus storey displacement hysteresis curves for the as-built beam-column joints with plain bar reinforcement were characterised by the following:

(1). Very low initial stiffness and significant stiffness degradation.

The measured initial yield stiffness if plain round bars are used for longitudinal reinforcing bars was very low, being about 40% of the theoretical predictions for deformed bars. The stiffness degraded significantly as the loading progressed. Apart from this, the stiffness in the second cycle was apparently lower than that in the first cycle at the same displacement amplitude. The unloading stiffness was generally much higher than the correspondent loading stiffness.

(2). Low member flexural strength and significant strength degradation.

No shear failure was observed for the reinforced concrete linear members and the joint cores for the tested units, and the beams and columns with plain bar reinforcement were flexural-failure dominated. This means that the strength is determined by the available member flexural strength. However it is to be noted that the member flexural strength was less than the theoretical flexural strength based on the plane section theory for the conducted tests due to the violation of the plane section assumption resulting from severe bond degradation along the longitudinal reinforcement.

Also the flexural moment capacity in the second cycle was generally much lower than that in the first cycle at the same displacement amplitude.

(3). Significant pinching.

Significant pinching was observed to occur prior to the initial member yielding in both positive and negative directions for both as-built beams and columns. The pinching is characterised by very low stiffness at the beginning of the loading then a suddenly much increased stiffness after the wide crack formed during the previous tensile stress closes in the flexural compressive side. Such pinching is not associated with that often observed from a member failing in shear, but rather associated with a wide flexural crack at the beam-column interfaces due to previous tensile action. This wide flexural crack at the beam-column interface formed owing to severe bond deterioration along the longitudinal bars.

(4). Uneven moment strengths.

The available negative and positive flexural strengths for unsymmetrically reinforced beams were NOT proportional to the corresponding theoretical flexural strengths. Lower theoretical flexural strength corresponded to lower available strength in terms of the percentage of the theoretical flexural strength.

8.3 A PROPOSED METHOD FOR MODELLING FLEXURAL BEHAVIOUR OF AS-BUILT REINFORCED CONCRETE MEMBERS WITH PLAIN ROUND BAR REINFORCEMENT

8.3.1 A Member Model for Representing Member Flexural Behaviour at Fixed-end

As revealed by the tests in this project, when a reinforced concrete member contains plain round longitudinal reinforcement, the non-linear behaviour of the member is mainly dominated by the non-linear flexural behaviour at the fixed-end and a proper index to represent the member's non-linear behaviour is in terms of the flexural strength versus the rotational ductility in the fixed-end. In this case, member non-linear flexural behaviour at the fixed-end is strongly dependent on the axial actions and cross sectional details of the other members transversely framing into the same joint, (see Section 8.2.2.3).

Clearly, the above-stated concept contradicts the current understanding that the nonlinear behaviour of a member is completely determined by the member itself. Currently, no member models are capable of capturing the influences of other members framing into the same joint. A tentative suggestion for the development of such a proper member model at the member fixed-end is to use a joint member model to represent the member's non-linear flexural behaviour. A beam-column joint is the connection of the members with the transverse members at the joint and a joint member model can be a feasible option to interrelate the members framing into the same joint. Alternatively, a simplified method for modelling the member flexural behaviour could be the use of two separate flexural springs at one member end. The two flexural springs are connected in series and hence their bending moment actions are the same. One spring is used for representing the flexural behaviour associated with the steel yield penetration within the member's plastic hinge region and its properties are determined by the cross sectional details of the discussed member, as for the conventional theory. The other spring is used for representing the member flexural behaviour associated with the fixed-end rotation and its properties are determined by the considered member itself then are modified based on the cross sectional

details and the imposed axial actions on the members transversely framing into the same joint. In this latter way, the effect of the joint horizontal and vertical shear reinforcement on the bond mechanism along the member longituidnal reinforcement within the joint region could not be allowed for, but this is believed to be adequate because there is no or very limited joint shear reinforcement for as-built reinforced concrete structure and also such an effect would be very insignificant if the longitudinal reinforcement is from plain round bars. Development of such a member model is beyond the scope of this study.

8.3.2 Determination of Member Static Flexural Behaviour at Fixed-End

8.3.2.1 General

Non-linear flexural behaviour of reinforced concrete members is usually described in terms of the static (monotonic) force strength versus deformation skeleton curve and the internal hysteretic rules to allow for the cyclic loading effect. The static force strength versus the deformation skeleton curve is especially important and it gives all the information required by a non-linear static analysis. A non-linear static analysis (namely push-over analysis) is the core element for capacity design based seismic assessment and is also an important method recommended by design codes. This section aims at establishing the static non-linear behaviour in terms of the flexural strength versus the deformation behaviour for as-built reinforced concrete members.

It is common that the static flexural strength versus deformation skeleton curves for the reinforced concrete members are approximated by a tri-linear curve. The stiffness changes for the skeleton curves are the point at first yielding, the point at attainment of the ultimate force strength and the point after the attainment of the member flexural strength. Especially important is the determination of the flexural strength and the stiffness at first yield. Initial stiffness plays an important role in the success of the structural non-linear dynamic analysis [O4]. Studies frequently show that different hysteresis models with the same initial stiffness lead to similar final structural responses.

Although the tests in the current project showed severe violation of the plane section assumption for as-built reinforced concrete members, the theoretical predictions based on the plane section assumption are still used as a benchmark here in determining the static flexural strength and deformation skeleton curves of as-built reinforced concrete members.

8.3.2.2 Theoretical Determination of Member Properties at First Yield

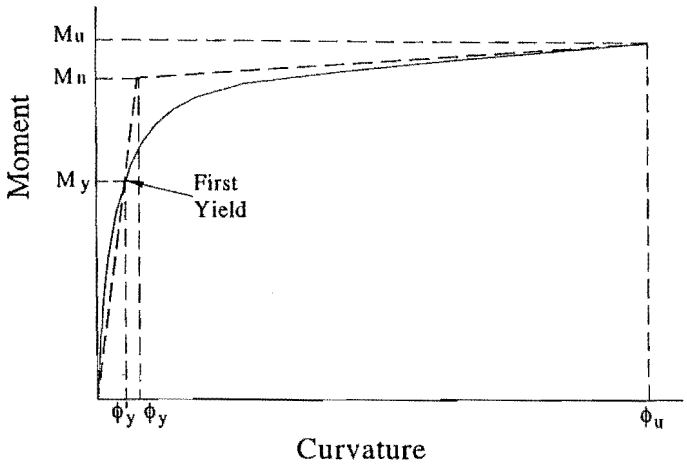

Fig.8.1 Typical Moment-Curvature Relationship [P18]

It is widely realised that the cracking effect on the yield stiffness is necessary to be taken into account [D2]. After concrete cracking, the member stiffness depends on the steel used and the sectional overall depth, rather than the gross sectional moment of inertia. This is obvious from the calculation of the concrete compressive depth at first yielding and the corresponding moment capacities according to conventional flexural theory [P1], see equations A1-1 and A1-2, reproduced from Appendix A.

$$k=[(\rho+\rho')^2 n^2+2(\rho+\frac{\rho' d'}{d})n]^{\frac{1}{2}}-(\rho+\rho')n \qquad \text{(A1-1)}$$

$$M_y=A_s f_y(\mathrm{d}-\frac{1}{3}kd)+A_s' f_s'(\frac{1}{3}kd-d') \quad \text{if } N^*=0.0 \qquad \text{(A1-2)}$$

$$M_y=A_s f_y(\mathrm{d}-\frac{1}{2}h)+A_s'\times f_s'(\mathrm{d}-\frac{1}{2}h)$$

$$+\frac{1}{2}kd\ f_c\,\mathrm{b}\,(\frac{1}{2}h-\frac{1}{3}kd) \quad \text{if } N^*\neq 0.0 \qquad \text{(A1-2')}$$

The determination of member yield stiffness is equivalent to the determination of equivalent moment of inertia, I_e, which is actually the yield stiffness in terms of concrete elastic modulus if the force-deformation relationship is a moment-curvature relationship. The choice of the moment of inertia, I_e, directly affects the estimated member yield stiffness.

Theoretically, the equivalent moment of inertia of a member can be found by conducting a sectional moment-curvature analysis, which can be done by employing the concrete and steel stress-strain relationships and using plane section theory. A typical moment-curvature relationship for a given section is shown in Fig.8.1. In Fig.8.1, the equivalent moment of inertia of the member can be found according to the member yield moment capacity M_y and the corresponding curvature ϕ_y as $I_e = M_y / \phi_y$.

In many design codes and general engineering practice, the equivalent moment of inertia of a member, after allowing for the effect of concrete cracking, is generally assumed to be proportional to the gross moment of inertia of a member. For reinforced concrete beams, the New Zealand concrete code NZS3101:1995 recommends a value of $I_e = 0.4\ I_g$ for rectangular beam sections, and $I_e = 0.35\ I_g$ for T- and L-beam sections. For reinforced concrete columns, the New Zealand concrete code recommends a value depending on the level of column axial load. According to NZS3101: 1995, $I_e = 0.8I_g$ when $N^* / A_g f_c' \geq 0.5$, $I_e = 0.6I_g$ when $N^* / A_g f_c' = 0.2$, and $I_e = 0.4I_g$ when $N^* / A_g f_c' = -0.05$. Paulay and Priestley [P11] proposed that equivalent member moment of inertia, I_e, of reinforced concrete members in calculating member initial stiffness be taken as $I_e = 0.35\ I_g$ for beams and $I_e = 0.6\ I_g$ for columns, where: I_g is moment of inertia of the gross concrete section. The same recommendations for assessing the seismic performance of pre-1970s reinforced concrete moment resisting frame structures were used by Park 1997 [P6] in the seismic assessment procedure outlined in Chapter 2.

In recent years, the above-stated engineering method for determining the equivalent moment of inertia of a member was extensively examined by many researchers [P17, P18]. Priestley et al found, after sectional moment-curvature analysis for some reinforced concrete members designed to current codes, that the member yield curvature is a function of member overall depth and the steel yield strain, rather than the gross moment of inertia of a member which was widely used in general engineering practice and design codes.

It is to be noted that such arguments about the equivalent moment of inertia of a member are on the basis of the sectional analysis using the plane section assumption. For the pre-1970s reinforced concrete moment-resisting frame structures, severe bond degradation and local bar slip along the member longitudinal reinforcement due to the use of plain bar reinforcement significantly violates the plane section assumption as observed for the as-built beam-column joint tests. Hence the determination of the equivalent moment of

inertia based on the sectional analysis as recently proposed by Pristley et al is not always expected to give adequate results for this specific case.

In this study, the theoretical flexural initial stiffness is determined by conducting sectional moment - curvature relationship at first yield, which is defined to be the stage when the longitudinal tensile reinforcement starts to yield, and it is then expressed as the ratio of the equivalent moment of inertia to the gross moment of inertia of the member section. The theoretically estimated initial stiffness is calibrated against the test evidence.

8.3.2.3 Proposed Skeleton Curve To Represent Flexural Behaviour of Members Reinforced by Plain Round Longitudinal Reinforcement

1. General

The tests conducted in the current project demonstrated that the non-linear deformations of the test units were mainly attributed to the theoretically predicted weak members. The non-linear flexural behaviour of an as-built reinforced concrete member was mainly limited to its fixed-end and it was strongly affected by the axial actions and the cross sectional details of the transverse members at the same joint. The effect due to the axial actions of the transverse members is especially important when the plain round longitudinal reinforcement is used, and it needs to be taken into account. This section proposes a method for determining the member non-linear flexural behaviour at the fixed-end and the proposed method can allow for the enhancement effect on the member flexural behaviour at the fixed-end due to the compressive axial actions of the transverse members at the same joint.

The test results of the weak members were employed here to calibrate the proposed skeleton curve. Theoretically, Units EJ2, EJ3 and EJ4 were expected to develop plastic hinges in the beams. For the tests on Units EJ2, Units EJ3 and EJ4, the overall post-elastic performance of the systems was totally or partially governed by the beam's non-linear flexural behaviour. Figs.8.2 and 8.3 show the observed member moment strength versus rotation skeleton curves for the beam of Unit EJ2, and the beams of Units EJ3 and EJ4, respectively. Fig.8.4 shows comparison of the observed monotonic moment strength versus rotation skeleton curve for the beams of Units EJ2, EJ3 and EJ4. Unit EJ2 was tested subjected to simulated seismic loading with zero column axial load, but Units EJ3 and EJ4 were tested subjected to simulated seismic loading with the presence of a

compressive column axial load of about $0.25A_gf_c'$. A study of the flexural behaviour of the beams of Unit EJ2, and Units EJ3 and EJ4 can identify the influence of column axial loads on the beam flexural behaviour at the fixed-end.

The theoretical beam flexural strengths at the ultimate limit state were 190kN-m and 129kN-m respectively for the negative bending and positive bending for Units EJ2 to EJ4. The theoretical initial stiffnesses of the beams at the first yield are calculated using sectional moment – curvature relationship as described in Section 8.3.2.2 and they are also shown in Fig.8.2 and Fig.8.3, correspondingly, in terms of the equivalent moment of inertia. The theoretical initial stiffness is equivalent to $I_e = 0.33I_g$ and $0.46I_g$ respectively for positive and negative bending for the beam of Units EJ2 to EJ4. I_e and I_g are the equivalent sectional moment of inertia and gross sectional moment of inertia of the member, respectively.

2. Flexural Strength Determination for the Proposed Skeleton Curves

Member flexural strength would be lower than the theoretical strengths when severe bond degradation occurs along the member longitudinal reinforcement and this was verified both by the tests in this study and by the theoretical analysis conducted by Hakuto et al [H1]. Hakuto assumed that the concrete compressive strain profile and the strain profile along the flexural tension reinforcement still satisfied the plane section assumption and he concluded that, under the extreme case where the tensile stress in the flexural compression steel reached the yield strength as the steel stress along the same bar but at opposite beam-column joint interface, the resulting decrease in the member flexural strength was about 15%. When there is the compressive column axial load at the joint, the bond mechanism along the beam longitudinal reinforcement and then the beam flexural strength will be enhanced. However the strength enhancement is insignificant, as shown in Fig.8.4 where the compressive column axial load was about $0.25\,A_g f_c^{'}$ and the beam flexural strengths were still about 10 to 12% less than the theoretical strengths. Hence, for the proposed member flexural strength versus the rotation at the fixed end curves, the flexural strengths of the members at the first yield state and at the ultimate limit state are taken as 85% of the theoretical strengths at the corresponding stages, irrespective of the magnitudes of the compressive axial actions of the transverse members. Equivalently, the flexural strengths of an as-built reinforced concrete member at the first yield state and at the ultimate limit state can be estimated using 85% of the steel yield strength.

3. Determination of Initial Flexural Stiffness for Proposed Skeleton Curves

For the beam of Unit EJ2, there was no compressive column axial action. Fig.8.2 shows that $I_e = 0.2I_g$, which is about 50% of the predicted initial stiffness based on sectional analysis, gives an adequate modelling of the initial stiffness of the observed skeleton curve. Hence, the initial stiffness of an as-built beam member at the first yield is taken as 50% of the theoretical prediction, when the columns at the same joint have zero axial load. Fig.8.3 shows that the initial stiffness of the observed skeleton curves for the beam of Units EJ3 and EJ4 are adequately represented by using of $I_e=0.3I_g$, which is about 75% of the theoretical predictions. Units EJ3 and EJ4 were tested subjected to simulated seismic loading with the presence of the compressive column axial load of about $0.25 A_g f_c^{'}$. Apparently, the enhancement of the beam flexural stiffness due to the compressive column axial load was much more significant, when compared to the enhancement effect on the flexural strength. This is more evident in Fig.8.4, which compares the skeleton curves for the beams of Units EJ2, EJ3 and EJ4. The initial stiffness of an as-built beam member at the first yield is taken as 75% of the theoretical prediction, when the compressive column axial load is not less than $0.25 A_g f_c^{'}$, where A_g and $f_c^{'}$ are respectively the gross sectional area and the compressive concrete strength of the columns. For the cases between, the enhancement effect on the beam initial stiffness due to the compressive column axial action can be estimated by using the interpolation method.

4. Proposed Skeleton Curves

The generalised skeleton curves proposed in this section are illustrated in Fig.8.5, in terms of the flexural strength versus the rotation at the fixed-end.

In Fig.8.5, θ_y is the theoretical member flexural deformation at first yield, in terms of the rotation at the fixed end, as defined in Chapter 6. θ_y is estimated based on the sectional analysis and hence is completely determined by the member itself. $\theta_{y,m}$ is the modified member flexural deformation in terms of the rotation at the fixed-end at first yield. $\theta_{y,m}$ is determined based on the theoretical initial stiffness and then modified according to the compressive axial action of the transverse members at the same joint, as described above in "Determination of Initial Flexural Stiffness for Proposed Skeleton Curves". The deformation at the attainment of the member flexural strength is taken as 2 times the

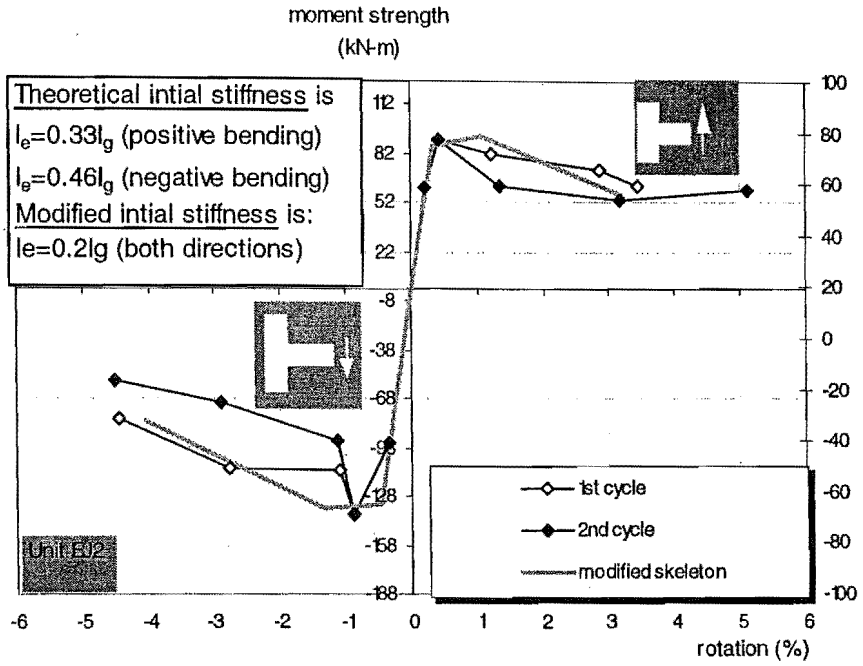

Fig.8.2 Skeleton Curve for the Beam of Unit EJ2

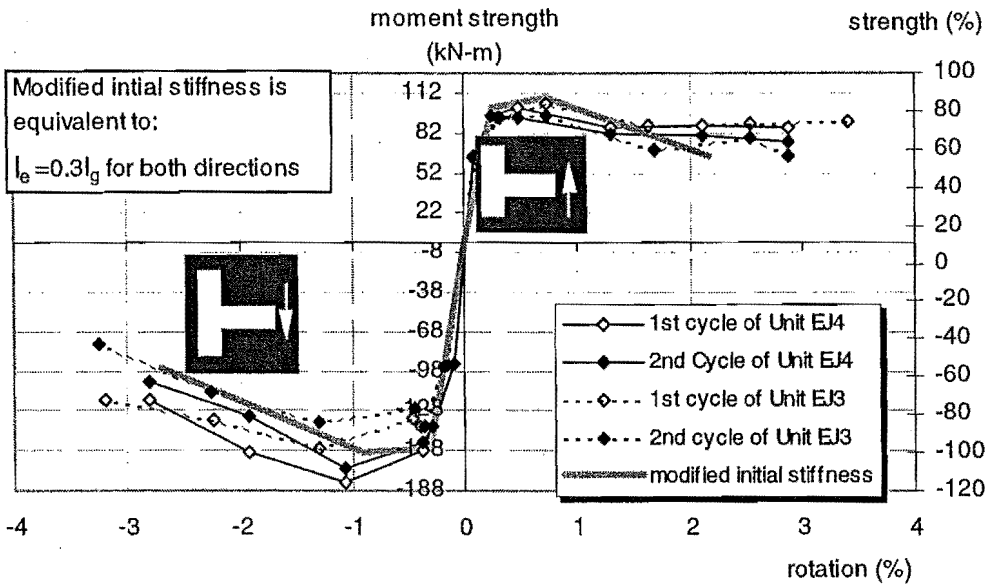

Fig.8.3 Skeleton Curves for the beams of Units EJ3 and EJ4

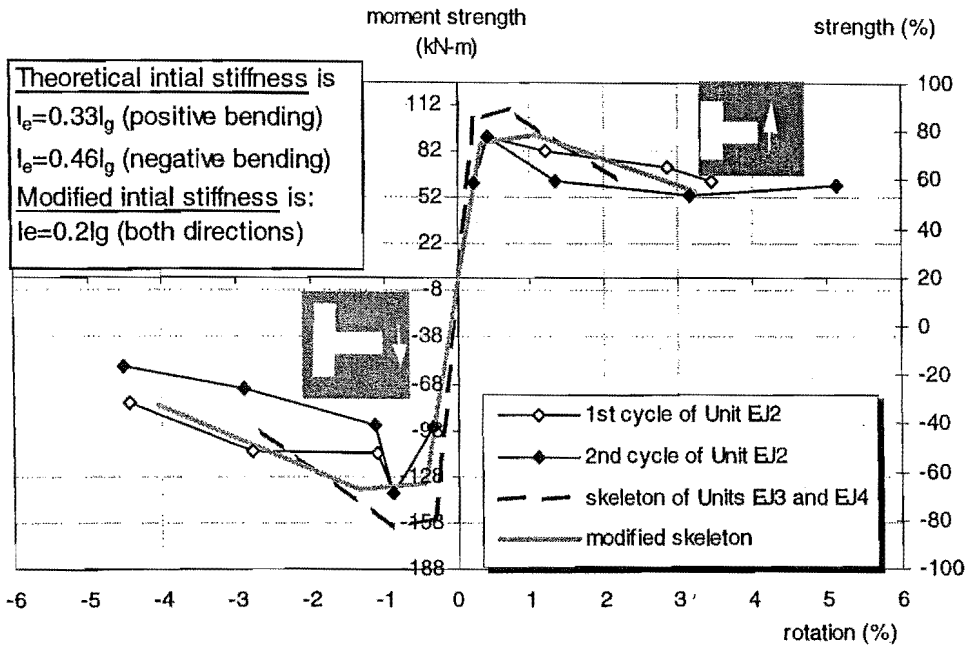

Fig.8.4 Comparison of Skeleton Curves for the Beam of Unit EJ2 with that for the Beams of Unit EJ3 and EJ4

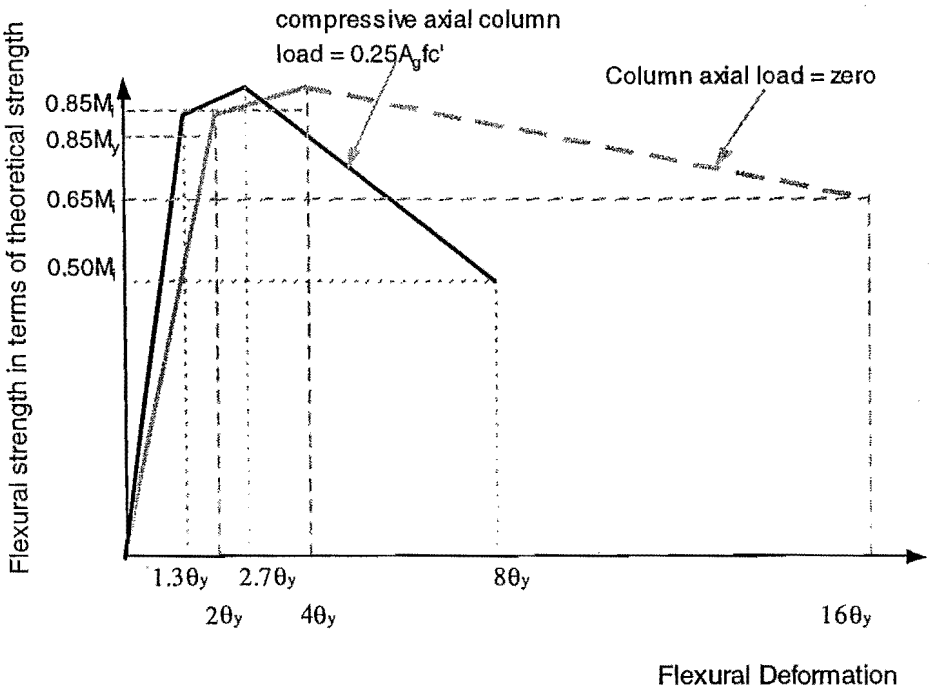

Fig.8.5 Generalised Beam Flexural Strength versus Rotation at Fixed-end Curves

flexural deformation at first yield, namely, $2\theta_{y,m}$, irrespective of the magnitudes of the compressive axial actions of the transverse members. The strength degradation after the attainment of the member ultimate moment strength varies with the axial load level on the transverse members. The compressive column axial load accelerated the degradation of the beam flexural strength. When the compressive axial load on the columns at the same joint is zero as for the beam of Unit EJ2, the beam flexural strength at the flexural deformation equivalent to $8\theta_{y,m}$ degrades to 65% of its ultimate theoretical strength. When the compressive axial load on the columns at the same joint is $0.25 A_g f_c^{'}$, the beam flexural strength at the flexural deformation equivalent to $6\theta_{y,m}$ degrades to 50% of its ultimate theoretical strength. If the member flexural strength degradation is limited to 20%, namely, the maintained member flexural strength is not less than 80% of the maximum strength, the rotational ductility capacity at the fixed-end of a member can be as high as 7 if the axial action on the members transversely framing into the same joint is zero, but it drops to less than 4 if the axial action on the members transversely framing into the same joint goes up to $0.25 A_g f_c^{'}$.

The skeleton curves modified in such a way for the beams of Units EJ2, EJ3 and EJ4 are also shown in Figs.8.2 to 8.4 correspondingly and they show a reasonable match to the test results.

Due to no test data available for the column members, the proposed method for determining the member flexural strength versus the rotation at the fixed end curves is only limited for beam members with plain round longitudinal reinforcement. For the as-built columns, the flexural behaviour in terms of the column flexural strength versus the rotation at the fixed end is assumed to be independent on the beams at the same joint. The initial flexural stiffness is taken as 75% of the theoretical prediction, the deformation at the ultimate state is 2 times the yield deformation and the flexural strength degrades to 50% of its theoretical prediction when the deformation reaches 6 times the yield deformation. This means that the column flexural behaviour at the fixed-end is similar to the beams where the bond mechanism along the beam longitudinal reinforcement is greatly enhanced within the joint region due to significant transverse clamping action.

8.4 SUGGESTIONS FOR STRUCTURAL RETROFIT

From the simulated seismic loading tests on as-built interior and exterior beam-column joints, it is clear that severe bond degradation along the member longitudinal bars within and adjacent to the joints would result in low attainment and poor maintenance of both the strength and stiffness and the non-linear deformation was only limited in a major flexural crack at beam-column interface, rather than in an area known as plastic hinge region. Deformation concentration over a narrow area means that the structural performance could not be ductile although the available deformation capacity could be very large. The real concern is the degradation of beam flexural behaviour, rather than the shear behaviour as for the case with deformed bars. Should the bond mechanism along the member longitudinal bars be improved, the member flexural performance will be upgraded.

External wrapping of the as-built lap-spliced reinforced concrete columns tested at the University of Canterbury conducted by Restrepo et al was demonstrated to be able to enhance the bond mechanism along the plain round column longitudinal bars. It is suggested that external wrapping, say fibre-glass wrapping, be applied to the beam area adjacent to the joint core for the existing exterior beam-column joint components when plain round longitudinal bars are used. Such a retrofit is expected to improve the bond mechanism along the beam longitudinal bars adjacent to the joint core, leading to the increases in the beam flexural strength and the beam flexural stiffness, especially the beam flexural stiffness. As a result, the degradation of the beam flexural behaviour can be greatly reduced and the overall seismic performance of similar weak beam-strong column systems can be greatly improved.

8.5 CONCLUSIONS

This chapter discusses the test results and proposes the method for assessing the seismic behaviour of as-built reinforced concrete members. The conclusions drawn are:

1. Unlike an as-built reinforced concrete member with deformed longitudinal reinforcement where the non-linear seismic behaviour of the member is likely to be dominated by the premature shear failure [H1], the non-linear seismic behaviour of an as-built reinforced concrete member with plain round longitudinal reinforcement is governed by the non-linear flexural behaviour at the fixed-end of the member.

Member non-linear flexural behaviour at the fixed-end is associated with the bond mechanism along the member longitudinal reinforcement within the joint region and therefore depends on not only the member itself but also strongly depends on the other members transversely framing into the same joint, especially the axial actions and the cross sectional details of the members transversely framing into the same joint. This concept differs from the conventional understanding that the non-linear flexural behaviour of a member is completely determined by the member.

2. A proper member model to represent the flexural behaviour at the member fixed-end could be a joint model in order to capture the influences from the other members framing into the same joint on the flexural behaviour at the member fixed-end. Alternatively, two separate flexural springs could be used to represent the flexural behaviour at one member end, one representing the non-linear flexural behaviour due to the steel yielding penetration within the plastic hinge region as for conventional flexural theory and the other representing the non-linear flexural behaviour at the member fixed-end. The properties of the former spring are determined based on the overall dimensions of the considered member itself and the properties of the latter spring are determined based on the considered member first then are modified based on the axial actions and the overall dimensions of the members transversely framing into the same joint.

3. Due to severe bond degradation along the member longitudinal reinforcement resulting from the use of plain round longitudinal bars, the flexural strength of an as-built reinforced concrete member is slightly lower than the theoretical flexural strength estimated based on the plane section assumption and the flexural initial stiffness of the member at the first yield is significantly lower than the theoretical predictions based on sectional analysis. When the members transversely framing into the same joint have compressive axial action present, the bond mechanism along the member longitudinal reinforcement is enhanced within the joint region. As a result, the member flexural strength and stiffness performance at the fixed-end, especially the stiffness performance, is improved. However, the compressive axial action on the transverse members will facilitate the member flexural strength degradation.

A tri-linear skeleton curve, in terms of the flexural strength versus the rotation at the fixed-end, is proposed to represent the non-linear static flexural behaviour at the fixed-end of an as-built reinforced concrete member, and the effect of the compressive column axial load on the beam flexural behaviour at the fixed-end is tentatively considered. It is

proposed that the flexural strengths of the member at different stages can be taken as 85% of the corresponding theoretical values, irrespective of the magnitudes of the compressive axial actions of the transverse members at the same joint. The beam flexural initial stiffness at the first yield can be taken as 50% of the theoretical prediction based on sectional analysis, when the column axial load at the same joint is zero, and it can be taken as 75% of the theoretical initial stiffness, when the compressive column axial load at the same joint is not less than $0.25 A_g f_c^{'}$, where A_g and $f_c^{'}$ are respectively the gross sectional area and the compressive concrete strength of the columns. For the cases between, the interpolation method is used to estimate the enhancement effect on the member flexural stiffness at the first yield due to the compressive axial action on the transverse members. For the as-built columns, the flexural initial stiffness can be taken as 75% of the theoretical initial stiffness, irrespective of the beam actions at the same joint.

The compressive column axial load, although enhances the available flexural strength and the initial stiffness for the beam at the same joint, significantly facilitates the flexural strength degradation of the beam. If the degradation of the member flexural strength is limited to 20%, the available rotational ductility at the beam fixed-end can reach up to 7 when the compressive column axial load is zero, but it drops to less than 4 when compressive column axial load is about $0.25 A_g f_c^{'}$.

4. The degrading flexural behaviour of the as-built reinforced concrete members can be upgraded by using external passive or active jacketing adjacent to the member areas adjacent to the joint core. External jacketing will enhance the bond mechanism along the plain round longitudinal reinforcement. As a consequence, the attained member flexural strength will be enhanced slightly, and the member fixed-end rotation and therefore the deformation at first yield will reduce, leading to the enhancement of the initial stiffness.

CHAPTER 9

EVALUATION OF A REINFORCED CONCRETE BUILDING CONSTRUCTED IN 1950S IN NEW ZEALAND

9.1 INTRODUCTION

The information on the non-linear behaviour of reinforced concrete members with plain round longitudinal reinforcement has been outlined in Chapter 8, based on the simulated seismic loading tests on as-built reinforced concrete beam-column joints in this test series. Hence, the probable seismic performance of a similar reinforced concrete structure in a major earthquake can be assessed by conducting the global non-linear analysis for the structure.

The as-built reinforced concrete components tested in this test series represented an existing reinforced concrete structure constructed in the late 1950s in New Zealand, referred as to the subject building. The seismic assessment of this subject building has been conducted in the past at the University of Canterbury by Hakuto et al [H1]. Hakuto et al assumed the use of deformed longitudinal bars and used the code equations for assessing the flexural and shear strengths of the members and beam-column joints.

Actually, plain round bar reinforcement was used in New Zealand until about the mid 1960s when deformed bar reinforcement became widely available. As outlined in Chapter 8, when plain round reinforcing bars are used, the code equations could not give adequate results, especially when used for estimating the shear-resisting capacity of as-built reinforced concrete members and beam-column joints. Due to severe bond degradation along the plain round longitudinal reinforcement within and adjacent to the beam-column joints, the premature shear failure in the linear members and the joints were precluded, however the flexural behaviour of the reinforced concrete members was greatly affected. Apparently, there is a need for re-assessing the seismic performance of the subject building in a major earthquake by employing the most updated information on the local behaviour of reinforced concrete members reinforced by plain round longitudinal bars, in order to identify how the local non-linear behaviour of individual members influences the global non-linear structural responses.

Both non-linear static analysis and non-linear dynamic analysis are conducted in studying the global behaviour of the subject building. Non-linear static analysis (also referred to as push-over analysis) of the subject building is carried out to determine the force strength and deformation capacity of the post-elastic critical collapse mechanism. This information is required by capacity design based seismic assessment procedures, such as the procedures proposed by Park and by Priestley (see Chapter 2). The structural capacities determined in this way are then compared with the seismic demands determined by New Zealand design code in order to investigate whether or not the subject building meets current code requirements. Non-linear dynamic analysis of the study building is carried out to provide information on the probable seismic force demand and the likely order of inelastic deformation demands of the subject reinforced concrete building during certain earthquake shakings. Global post-elastic structural analysis is essential in determining whether retrofit procedures need to be undertaken and whether the retrofit technique can really improve the structural seismic performance.

This chapter at first describes the subject building structure. Then the structural modelling and the analytical method for studying the global behaviour of the whole structure are described, accompanied with an extensive review in every aspect. Finally the results of non-linear static and non-linear dynamic analyses are presented.

9.2 STRUCTURAL MODELLING OF THE SUBJECT BUILDING

9.2.1 Description of the Building

The subject building is a reinforced concrete structure constructed in the late 1950's in New Zealand and it has been thoroughly investigated in the past. The typical floor plan and the elevation of the building are shown in Fig.9.1. There are 5 spans in the X (longitudinal) direction and the longitudinal span length is 4 meters. There are 3 spans in the Y (transverse) direction and the transverse span length is 4.9 meters. There are seven stories and the storey height is 3.2 meters except the first story where the storey height is 3.81 meters.

Regarding the plane configuration of the subject structure, three small service cores enclosed by reinforced concrete walls are eccentrically located within the building. Except this, the structural plane configuration is reasonably symmetric in both the X and Y directions. Regarding the elevation configuration of the subject building, there is an abrupt

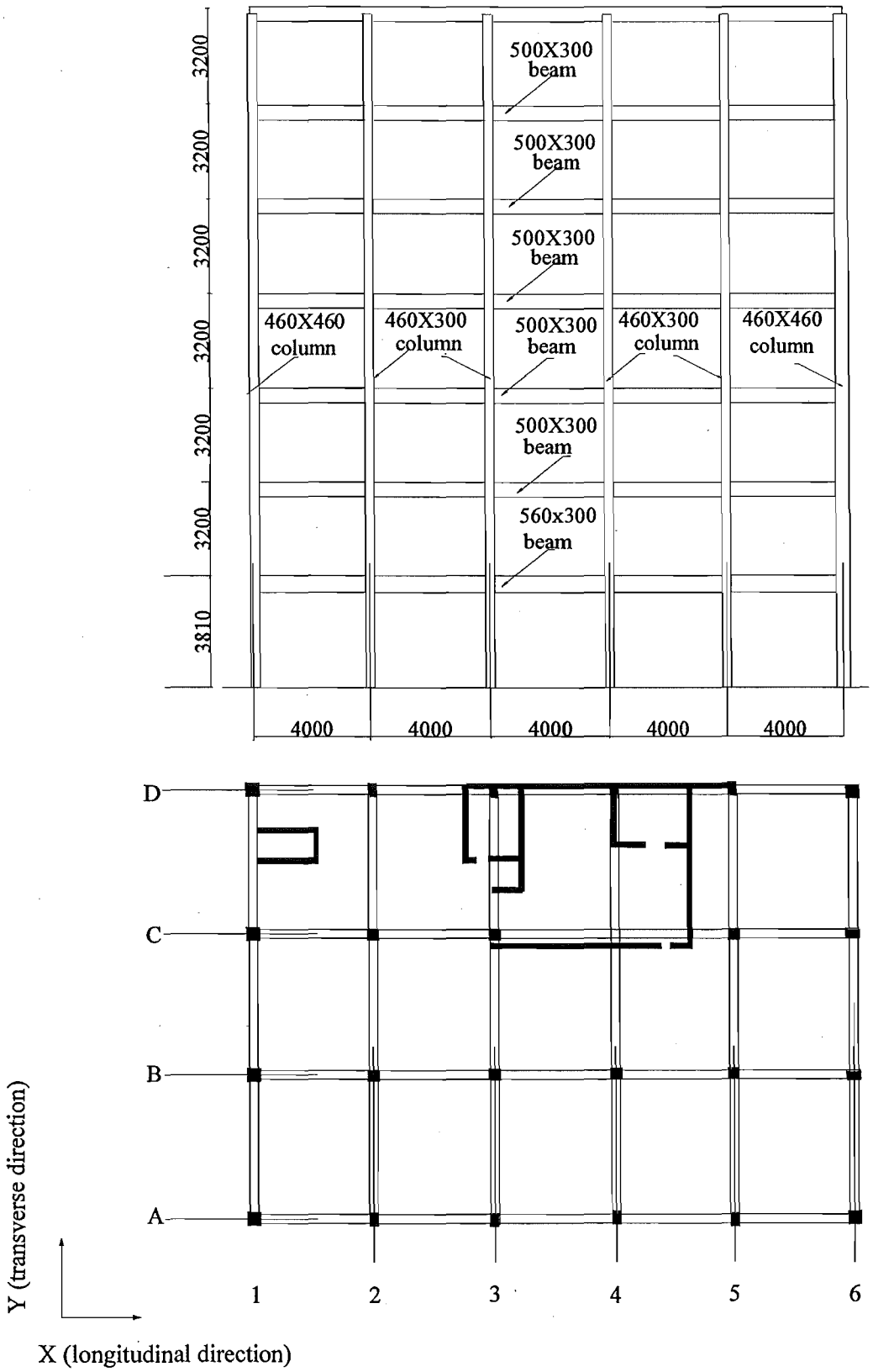

Fig.9.1 The Subject Reinforced Concrete Frame Structure

change in the load path at the sixth floor, where frame B has no interior columns at all and frame C has no interior columns at axis 2 and axis 5 either, possibly resulting in the concentration of structural actions at this level.

In addition, all the perimeter frames, longitudinal frames A, D and transverse frames 1 and 6, have masonry infills with small to medium openings. The masonry infills are two layer brick masonry infills with 100 mm gap between the two layers and the thickness of the masonry panels is 200 mm. The foundation system of the building consists of large foundation beams and reinforced concrete piles.

9.2.2 General Structural Assumptions

In conducting the non-linear static and dynamic analysis of the whole subject structure, some realistic assumptions are needed to develop a feasible but simple analytical model of the whole structure. The following assumptions are made in this analysis:

1. Two-dimensional analysis

For an unsymmetrical structure, the structural seismic response in one direction will couple with that in the orthogonal direction even when the building is subjected to the horizontal seismic loading in only one direction, referred to as structural torsional responses. For the subject building, the eccentrically located service cores are small, and except the eccentrically located service cores, the subject building is reasonably symmetric in both X and Y directions. To simplify the analysis, the horizontal earthquake motion is considered to be in the X direction only and the service cores are not considered, consequently, the torsional effects are eliminated. Hence, the seismic response of the subject building becomes a two-dimensional analysis.

It is noted that, due to the lack of the interior columns for the longitudinal internal frames B and C at the sixth floor, the load path from the longitudinal beams at the sixth floor must be adequately modelled. For the subject building, the loads on the longitudinal beams at the sixth floor are supported by the transverse beams at the same level and the load was then transferred from the transverse beams to the longitudinal external frames. Equivalently, the transverse beams provide vertical supports to the longitudinal beams at the axes 2, 3, 4, and 5 at the sixth floor. The structural model used by Hakuto in the seismic assessment of the subject building did not model the support actions at the sixth

floor, and the structural model used by Satyarno assumed that the longitudinal internal frames had interior columns at the sixth floor. In this study, such support actions are modelled as vertical shear springs between the longitudinal internal frames and the external frames. The properties of the shear springs are calculated based on the cross sectional details of the transverse beams, see Appendix B.

2. Rigid floor slabs

Tests on as-built reinforced concrete beam-column joint subassemblages representing the subject structure showed very low available lateral structural stiffness. Hence floor slabs can be assumed rigid in their own planes. As a consequence, the horizontal displacements of all the joints are the same at the same floor level if the horizontal earthquake motion is in the X direction. In this case, the analysis of the two-dimensional building in the X direction can be represented by two parallel plane frames, one external frame A and one internal frame B, connected by the vertical shear springs at the sixth floor.

However, contributions of the reinforced concrete floor slabs to the beam stiffness and flexural strength are allowed for and this can be found in Section 9.2.5.

3. Rigid beam-column joints

Beam-column joints are modelled infinitely rigid. This assumption is also believed adequate because simulated seismic loading tests on as-built reinforced concrete components representing the subject building showed good integrity of the joint panel when plain round longitudinal reinforcement was used.

4. No interaction between upper structure and foundation

The test results in the current test series showed that similar reinforced concrete frame structure would be very flexible during a major earthquake. Hence, it is assumed that the foundation is infinitely rigid and the columns are rigidly connected to the foundation at the ground floor.

5. Small deformation assumption

Deformations are considered to be sufficiently small to allow the original member dimensions to be unchanged throughout the analysis.

6. P-Δ effect allowance

It is known that the P-Δ effect, also referred as gravity load effect, increases the structural response significantly when a story drift exceeds 1%. In this study, P-delta effects are taken into account because very low available lateral stiffness was observed during this test scheme. The measured story drift at first yield reached 1.8-2% for the as-built interior beam-column joint assemblies with zero axial column load, 1.5% for the as-built exterior beam-column joint assemblies when tested with zero axial column load but 0.5-0.6% for the as-built exterior beam-column joint assemblies when tested with a compressive axial column load of 0.23-0.25 $A_g f_c'$. The storey drift at the maximum storey shear strength was about 2 to 4 % for the as-built interior beam-column joint tests and 1.2 to 1.5 % for the as-built exterior beam-column joint tests.

For the sake of comparison, the non-linear dynamic analysis of the structure was also conducted without the consideration of P-delta effect.

7. Base earthquake motions occur in the plane of the two-dimensional frame structure in the horizontal direction.

8. Allowance for masonry infills

Masonry infills are considered to be non-structural elements. Hence masonry infills are considered to contribute to the seismic weight but not to the structural stiffness for both the non-linear static analysis and the non-linear dynamic analysis.

It is also very common in general engineering practice that the structural analysis does not allow for the contribution of masonry infills to either the seismic weight or the structural stiffness. For the sake of comparison, the non-linear static analysis also studies the case where the masonry infills are not considered to contribute to the seismic weight, that is, the subject building is a reinforced concrete bare frame.

All the masses are lumped at each floor level. The analytical model of the subject building in the longitudinal direction is shown in Fig.9.2.

However, in Chapter 10, the subject building will be analysed as an infilled frame building where the masonry panels are considered in estimating both the seismic weight and the structural stiffness in order to investigate the effects of masonry infills on the structural global responses.

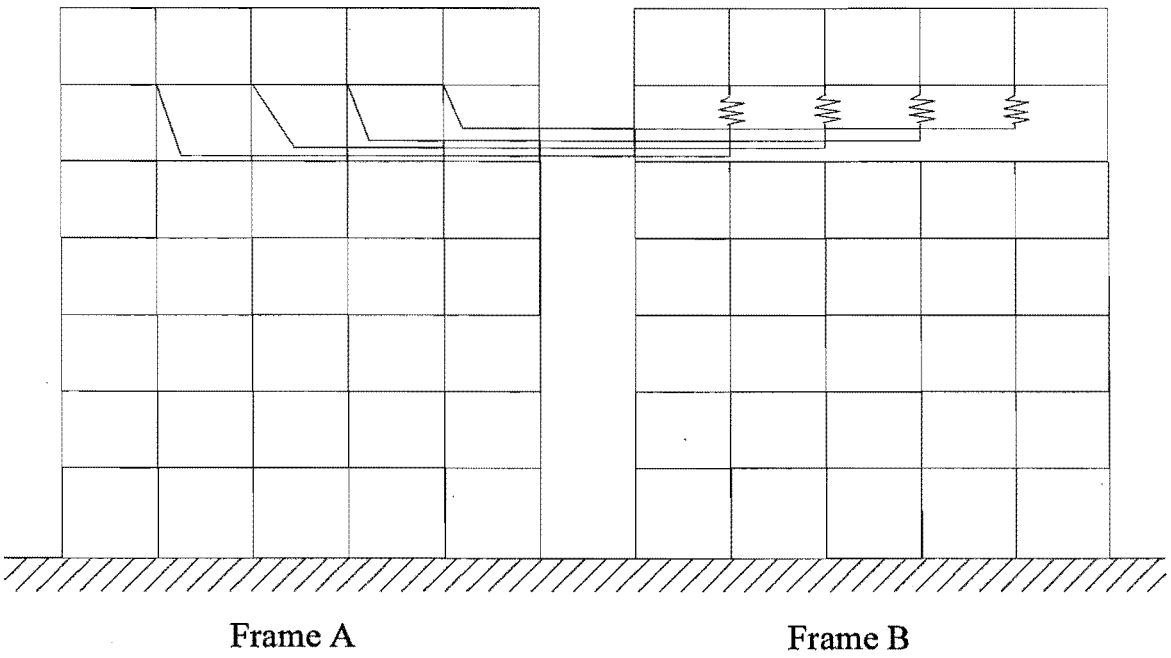

Fig.9.2 Structural model used for the analysis in longitudinal direction

9.2.3 Material Mechanical Properties

As described in section 2.5.1, probable material properties should be used here in order to give realistic seismic assessment result.

The specified concrete compressive strength in the original design was 20MPa for the subject building. Assuming the concrete strength increase of 50% due to conservative mix and the time effects, the probable concrete compressive strength is taken as 30 MPa. Specified steel yield strength in the original design was 275 MPa. Considering the likely steel yield strength is about 15% higher than the nominal strength, the probable steel yield strength is taken as 316 MPa. The material properties are summarised in Table 9.1.

Table 9.1 Material Properties

	Strength (MPa)	Elastic Modulus (MPa)	σ - ε Relationships
Concrete	$f_c^{'}=30$	25084	Parabolic as proposed by Hognestard
Steel	$f_y=316$	200000	Bi-linear curve with post-yielding stiffness of zero

Note: E_c = 25084 MPa is calculated using the equation for normal weight concrete recommended by the current New Zealand concrete design code NZS3101: 1995. $E_c = 3320\sqrt{f_c^{'}}+6900$ (MPa) where: $f_c^{'}$ is the compressive strength of concrete in MPa, $f_c^{'}$ = 30 MPa.

9.2.4 Estimation of Seismic Weight

Seismic weight includes the dead load and the seismic live load. The dead load includes the reinforced concrete frame members and the masonry infills. The sum of the seismic live load and the dead load of the frame members is assumed to be 8kPa and this is a slightly conservative estimation. The seismic weight on each node is calculated based on the floor area tributary method [P11]. In estimating the dead load of the brick masonry infills in the external frame A, the openings of the brick masonry infills are neglected and the masonry panels are treated as solid. For brick masonry panels, the volumetric weight varies from 130 kN/m^2 to 220 kN/m^2 [C5]. The volumetric weight of the masonry is taken as 150 kN/m^2 in this study.

9.2.5 Determination of Member Section Geometry

9.2.5.1 Beams (T- or L-Beams)

The reinforced concrete beams were analysed as T- or L- shaped beams in order that the contributions of slabs to the beam strength and stiffness, especially in the negative bending direction, can be allowed for.

The effective flange widths of T-shaped beams need to be determined with reasonable accuracy and the contribution of slab to stiffness and strength of a beam under negative bending is demonstrated to be very significant [P2, B2, K1, K2]. To increase the confidence when calculating beam sectional properties, a short review of the existing methods for determining the effective flange width of a beam is first presented.

Current New Zealand concrete design code (NZS 3101:1995) specifies that the width of slab assumed to be effective as a T-beam flange resisting stresses due to flexure shall not exceed one quarter the span length of the beam, and the effective overhanging slab width on each side of the web shall not exceed (a). eight times the slab thickness, nor (b). half the clear distance to the next web. For the investigated structure, the span length of the beam is 4 metres, the slab thickness is 120 mm and the clear distance between the webs is 3.7 metres. According to NZS3101: 1995, the equivalent width of a T-beam flange (namely for interior beams) is 1 metre, i.e. 500 mm on each side. In this case, the overhanging slab width on each side of the web is 500 mm and it is less than 960 mm (8 times 120 mm) and also less than 1850 mm (0.5 times 3.7 meters). In this way, the

equivalent flange width of a T- beam, according to NZS3101: 1995, is about one beam overall depth.

Pantazopoulou et al 1988 proposed a simple analytical model based on strain compatibility assumption of a plane section to account for the contribution of the slab to the strength and stiffness of beams under negative bending at a beam-column connection. They found that effective T-beam flange widths on either side of the beam depend on maximum beam strain at the column face, maximum available slab widths, the steel yielding and strain hardening property of the slab, and beam depth. They recommended that effective T-beam flange widths on either side of the beam are on the order of 1.5 beam depths for up to steel yielding, but increased to approximately three times beam overall depths for deformations that can be reasonably expected during severe earthquake loading.

A study conducted by Kebeyasawa et al [K2] reported that effective T-beam flange widths on either side of the beam were observed to progress with increased beam rotation and reached approximately four times beam overall depth during the test on the full-scale seven story reinforced concrete building specimen under pseudo-dynamic loading. This was about four times the values determined according to both current Japanese Design Standard and NZS3101: 1995 at a storey drift angle of 1/75 rad. The reported test also showed that contribution of the slab to the beam positive flexural strength was small and can be neglected.

The above review of existing methods for determining the effective T-beam flange width suggests that the current New Zealand design code tends to underestimate the real contribution of reinforced concrete slabs to beam negative moment capacities. Especially, when compared to the case with deformed bar reinforcement, much larger beam fixed-end rotational deformation occurred when plain bars are used for longitudinal reinforcement, as observed for the as-built beam-column joint tests conducted in this project. This means that the contribution of slab to the beam negative strength and stiffness could be quite large, as reported by Kebeyasawa [K2].

However, for the non-linear static and non-linear dynamic analyses conducted here, the method of NZS3101: 1995 is used to determine the effective widths of T -beam flanges, similar to the method used by Hakuto et al.

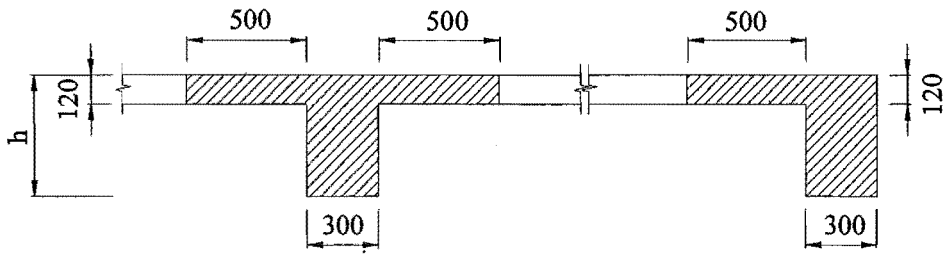

Fig.9.3 Determination of Effective Beam Widths

The determination of the effective widths of T- and L- beam flanges is illustrated in Fig. 9.3. In this case, the area of the floor slab reinforcement, which contributes to the beam negative flexural strength, is 700 mm^2 for the T-beams and 350 mm^2 for the inverted L-beam. A summary of the geometry of T- or L- beams and the reinforcing details is shown in Fig.9.4 for the longitudinal direction.

With the beam geometry defined and using the probable material properties, the beam stiffness at different stages could be determined.

9.2.5.2 Columns

A summary of the geometry and reinforcing details of the column cross sections for the subject building is also shown in Fig.9.4 for longitudinal direction analysis.

9.3 NON-LINEAR DYNAMIC ANALYSIS OF THE SUBJECT STRUCTURE

9.3.1 General

Apart from the structural modelling as discussed in section 9.2.2, the success of non-linear dynamic analysis of the analysed structure depends on two types of mathematical modeling: (a). modelling for the distribution of stiffness along the member; called "Member Models", and (b). modelling for the force-deformation relationship under stress reversals within the regions where non-linear deformation occurs, called "Hysteresis Models". Member modelling gives the information on member deformation (stiffness) distribution along the member and member hysteretic modelling gives the information on the hysteretic behaviour in the regions where potential non-linear deformation is expected.

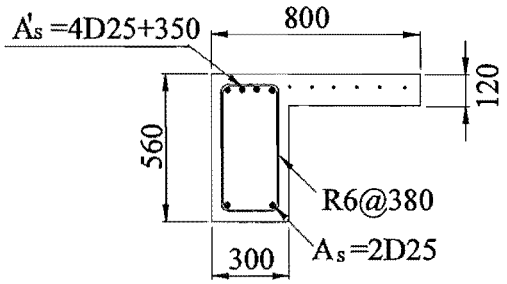

(a) Beams at Level 1

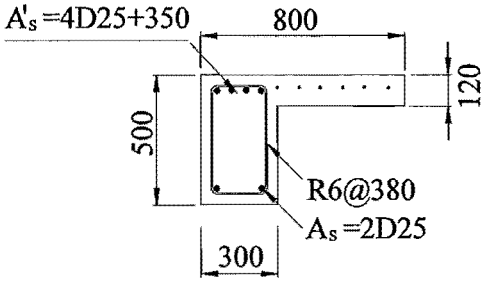

(b) Beams at Levels 2 and 3

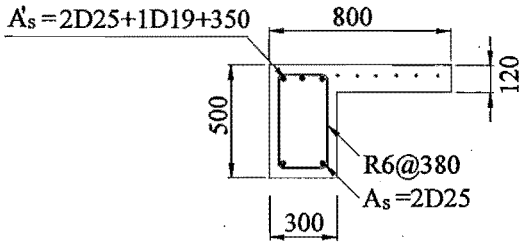

(c). Beams at Levels 4,5,6 and 7

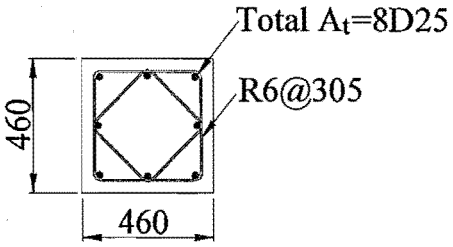

(d). Exterior columns at levels 1 and 2

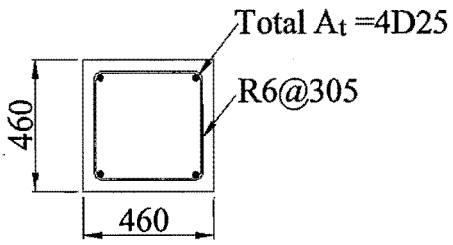

(e). Exterior columns at levels 3 to 7

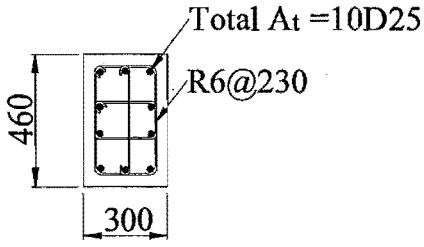

(f). Interior columns at Levels 1 and 2

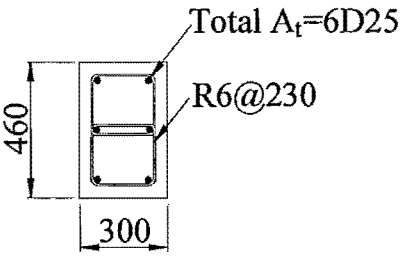

(g). Interior columns at Levels 3 to 7

Frame A in Longitudinal Direction

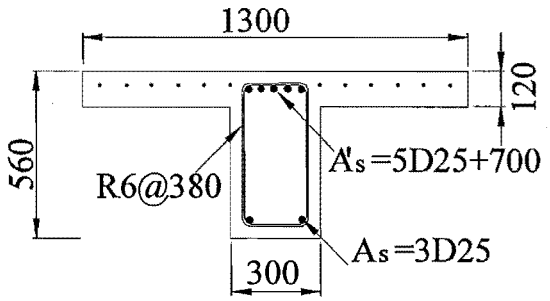

(a). Beams at level 1

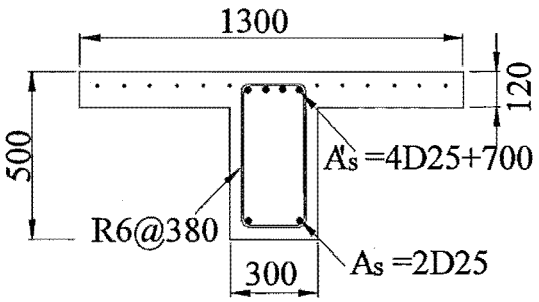

(b). Beams at levels 2 and 3

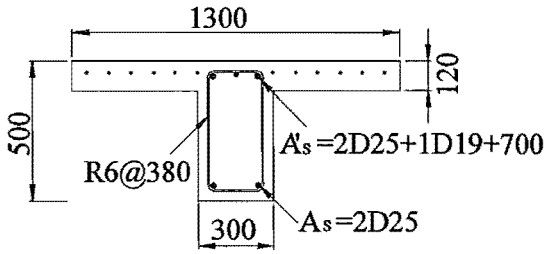

(c). Beams at levels 4 to 7

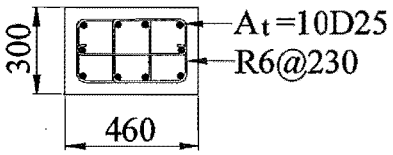

(d). Exterior columns at levels 1 and 2

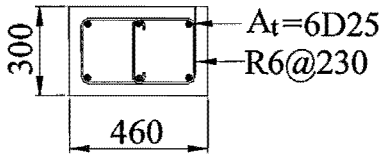

(e). Exterior columns at levels 3 to 7

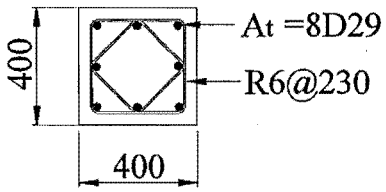

(f). Interior columns at levels 1 and 2

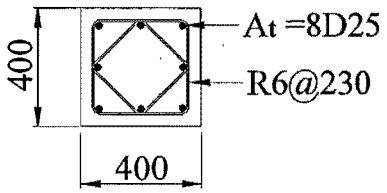

(g). Interior columns at levels 3 to 7

Frame B in Longitudinal Direction

Fig.9.4 Dimensions and Reinforcing Details of Beams and Columns

Therefore, the member model and hysteretic model used in the seismic assessment of the subject structure should be able to capture the observed characteristics in this test series of member deformation distribution and hysteretic behaviour in the regions where non-linear deformation occurs.

In this section, a short review of the existing member models and hysteresis models is presented and this background provides the necessary justification for selecting the member model and hysteresis models in this study. Finally, the member models and hysteresis models are proposed for the seismic assessment of the subject building, based on the outlined characteristics of the seismic behaviour of as-built reinforced concrete members with plain round longitudinal reinforcement.

9.3.2 Member Modelling

9.3.2.1 General

A reinforced concrete member may undergo non-linear deformation in a major earthquake and the member post-elastic deformation can have different components. Different deformation components can be in different regions of the member or they can be in the same region of the member. Also different deformation components may interact with each other.

Member modelling is to use subelements of different properties to represent different deformation components for a real structural member.

For the non-linear dynamic analysis of a reinforced concrete structure, it is very important to use the subelements to adequately represent the behaviour of the regions where non-linear deformation occurs. This is simply because the non-linear deformation is usually many times larger than the elastic deformation.

9.3.2.2 Outlines of Member Stiffness Distribution Characteristics

As outlined in Chapter 8, when the as-built reinforced concrete structures contain plain round longitudinal reinforcement, the non-linear deformation of the system is mainly attributed to the non-linear flexural deformation of the members. Hence there is no need to consider the shear deformation within a member and a beam-column connection panel in this study. The non-linear flexural deformation of an as-built reinforced concrete member is concentrated at the fixed-end of the member, and it is not only dependent on the

member itself but also is dependent on the axial action and the cross sectional details of the members transversely framing into the same joint. As described in Chapter 8, the effect of the axial action on the transverse members is especially significant, when the members have plain round longitudinal reinforcement. This suggests the need for the use of a specific flexural spring at each member fixed end, which is capable of capturing the interaction between the members at the same joint. Such a flexural spring is different from an ordinary flexural spring and this will be clear after the review of existing member models. The ordinary flexural spring used for a member cannot reflect the interaction between the members framing into the same joint.

9.3.2.3 Review of Existing Member Models

Various member models have been proposed to represent the stiffness distribution within a reinforced concrete member [O2]. For reinforced concrete beam and column members, the commonly used member models are as follows:

(1). One-component model [G1, G2]

One-component model idealises a reinforced concrete beam or column member as a perfectly elastic mass-less line element with two non-linear rotational springs at the two ends, and it is shown in Fig.9.5 [G2]. All inelastic deformations occur in these springs. The main features of the one-component model have (a). all inelastic deformation is lumped at member ends; (b). inelastic member-end deformation at one member end depends solely on the moment acting at that end. Due to the latter feature of this model, any moment versus rotation hysteresis model can be used for reproducing the non-linear behaviour of the member and this is a major advantage of the one-component model over the two-component model proposed by Clough et al in 1966 [C7]. Therefore, the one-component Giberson model is very versatile [G2] and is used widely in general engineering practice. However, for the reinforced concrete members, the moment-end rotation is usually dependent on the curvature distribution along the member, hence it is dependent on moments at both member ends. This means that the latter feature of this model is also one major disadvantage. Despite various disagreements, the performance of the one-component model is frequently demonstrated to be accurate enough for a relatively low-rise frame structure in which the inflection point of a column locates reasonably close to the mid-height.

Apparently, the one-component member model can model the concentration of the member non-linear flexural deformation at the member end as observed for as-built reinforced concrete member, but cannot model the effect of the axial action and the cross sectional details of the transverse members framing into the same joint. Hence, should the Giberson's one-component member model be used, some modifications are needed.

(2). Multi-component model [C1]

Multi-component model is actually the development of the two-component model proposed by Clough in 1966 [C7] by Aoyama and Sugano.

Originally, the two-component model proposed by Clough et al divided the member into two imaginary parallel elements: an elastic-plastic element to represent a yielding phenomenon and a fully elastic element to represent strain hardening behaviour. Inelastic member-end deformation at one member end depends on the moments acting at both member ends and this seems to be more rational, in comparison with one-component model. However, the imaginary fully elastic element has the same stiffness parameter along the whole length, as a result, this two-component model can deal with bilinear hysteresis model only, although the yield levels at two ends can be different. This is a major disadvantage for the two component model, compared with the one component model, as concluded in a discussion conducted by Giberson [G2].

Aoyama and Sugano adapted the two-component model proposed by Clough et al, proposing the multi-component model. The multi-component model divided the member into four parallel members to allow for flexural cracking, different yield levels at two member ends and strain hardening. Basically, the multi-component model has the same features as the two-component model. The stiffness of the multi-component model must be evaluated for a certain assumed moment distribution. This means that the stiffness parameters are only valid for a specific moment distribution.

(3). An isolated subelement member model proposed by Filippou et al [F2]

A new non-linear member model was proposed by Filippou et al in 1999 [F2]. This model isolates the basic mechanisms that control the hysteresis behaviour of reinforced concrete members into individual subelements. Currently, the subelemnts included elastic subelement, spread plastic subelement, interface bond-slip subelement and girder element. However, more subelements can be added into it if desired. All subelements are connected

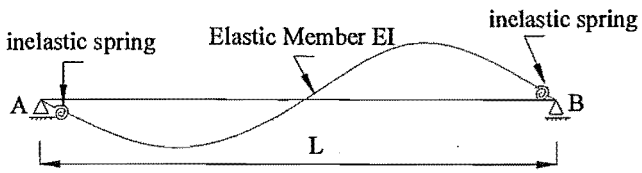

Fig.9.5 One-component member model

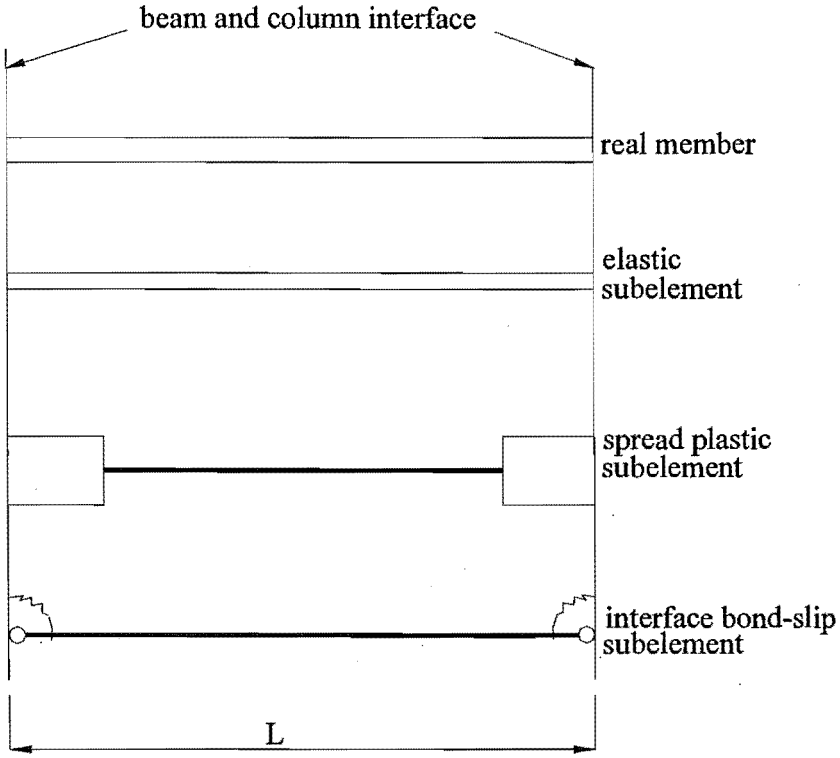

Fig.9.6 An isolated subelement member model [F2]

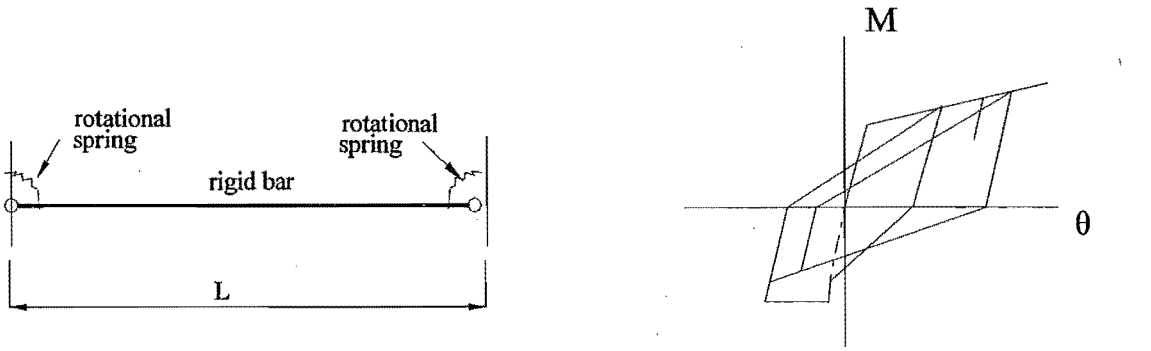

(a) interface bond-slip subelement

(b) hysteretic moment rotation model

Fig.9.7 Interface bond-slip subelement [F2]

in series. The proposed new model is shown in Fig.9.6. The flexibility matrix of each subelement is established and the flexibility matrixes of different subelements are added together to produce the flexibility matrix of the whole frame structure.

The flexibility coefficients of the proposed spread plastic subelement model depend on the extend of the plastic zones at the member ends, hence the coupling between the two plastic end zones can be considered.

Of particular interest is that this new model introduces the interface bond-slip subelement to account for the fixed-end rotation at the beam-column interfaces due to bond degradation and slip, which occurred within and adjacent to the joint core.

The proposed interface bond-slip subelement of this new model is shown in Fig. 9.7, and it consists of concentrated rotational springs at the member ends that are connected by a rigid bar. The fixed-end rotation at one member end is only dependent on the imposed moment at that member end in Fig.9.7.

It should be noted that the proposed interface bond slip subelement of this new model does not account for the effect of the transverse clamping actions from the members transversely framing into the joint. Therefore, this isolated subelement member model, which would be very useful when the member fixed-end rotation resulting from bond degradation and slip is significant, needs to be modified to capture the nature of the member fixed-end rotation due to severe bond degradation within the joint.

(4). Other member models

There are many other member models, for instance, connected two-cantilever model [O1] and distributed flexibility model et al. However these models are only dealing with the issues over the location of member inflection point, the continuity of displacement and rotation, and more detailed division of different segments of the members according to their stiffness.

9.3.2.4 Proposed Member Models

Apparently, none of the currently existing member models can directly deal with the interaction between the members framing into the same joints and a proper member model capable of capturing the interaction between different members framing into the same joint needs be developed. As suggested in Chapter 8, such a member model could be a

joint model or the use of a particular flexural spring at the member end, which has the properties determined by the member but modified by the axial action and the cross sectional details of the transverse members at the same joint. Current study is still based on the existing member model.

Among many existing member models, the one-component model could be the best approximation to represent the deformation lumping behaviour of as-built reinforced concrete beam and column members. Also the effect of column axial loads on the beam flexural behaviour at the fixed end, which is the most important effect from the transverse members at the same joint, can be approximately allowed for by estimating the beam flexural strength and the initial stiffness at first yield based on the column axial loads induced by gravity load, as described in Chapter 8. Hence, the beam and column members of the subject building are treated as one-component members in this study and they are idealised as perfectly elastic mass-less line elements with two non-linear rotational springs at the two ends.

For the flexural spring associated with one-component model, the plastic hinge length is specified and the hysteretic behaviour is in terms of moment and curvature relationship. For the member fixed-end rotation, the plastic hinge length is no longer needed. However, a flexural spring representing member fixed-end rotation can be incorporated in exactly the same manner. Hence the information on the rotational ductility versus the force strength in member fixed-ends can be easily used for the flexural spring at member ends in one-component member model.

9.3.3 Hysteretic Modelling

9.3.3.1 General

In conducting the non-linear dynamic analysis of the reinforced concrete structures, the information on the member cyclic force and deformation behaviour in the areas where the potential post-elastic deformation is expected to occur is required. Modelling of such information is referred to as hysteretic modelling.

A number of hysteretic models have been developed for reinforced concrete members in the past, and they range from the simple elasto-plastic and bilinear rules to more complicated rules that require over thirty parameters to keep track of the current stiffness. These hysteretic models are applicable to different circumstances due to different test

observations on which the development of the models was based. The hysteresis model used in this study should be capable of reproducing the observed hysteretic behaviour for the as-built reinforced concrete members.

9.3.3.2 Outlines of Hysteretic Characteristics of As-built Members

For a well-designed reinforced concrete member, the theoretical flexural moment capacity of the member can be attained and well maintained after the first yielding as the imposed post-elastic deformation increases. Typical lateral force versus deflection hysteresis loops observed for a well-designed flexure-dominated reinforced concrete beam are shown in Fig. 9.8 [O3]. In Fig.9.8, the flexural moment capacity after the first yielding was even larger than the theoretical flexural moment capacity due to the steel strain hardening, leading to the need for using a post-elastic stiffness larger than zero. When a deflection reversal is repeated, the attained flexural moment capacity in the second cycle at the same maximum deformation amplitude was nearly the same as that in the first cycle. Regarding the envelope curve of the hysteresis loops, apparent stiffness changes occur when the member flexural tensile reinforcement reaches yielding.

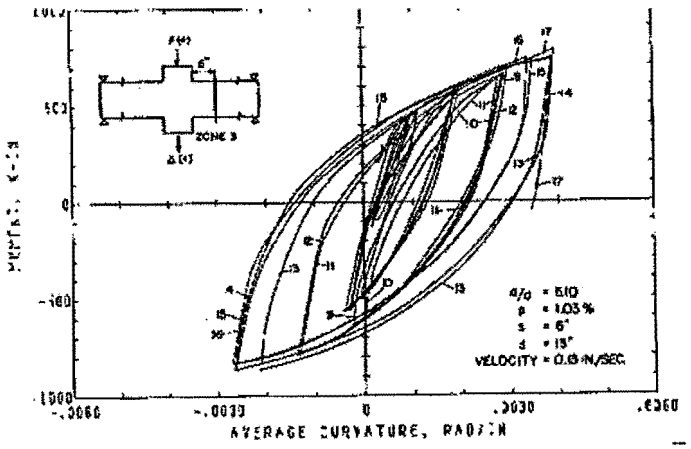

Fig.9.8 Typical Flexural Hysteresis Loops [O3]

Apart from flexure, many other factors can affect the load-deflection hysteresis loops of a reinforced concrete member subjected to large reversed inelastic deformations, such as, the deterioration of bond between concrete and steel under high-intensity cyclic loading and high shear forces.

As a result of shear distress in plastic hinge zones of reinforced concrete members, the member hysteretic behaviour can exhibit pronounced pinching. Apart from the shear distress, the pinching behaviour is also observed in "flexural" reinforced concrete members where severe bond deterioration along the longitudinal bars occurs within and adjacent to the beam-column interfaces. Pinching hysteretic behaviour is typically characterised by rapid strength degradation with load reversals and very low stiffness at a low stress level during reloading, such as shown in Fig.6.3.

For the as-built tests units, no shear failure was observed in the members and the joint cores, and the beams and columns with plain bar reinforcement were flexure-dominated. As outlined in chapter 8, the characteristics of observed flexural behaviour of the as-built reinforced concrete members with plain bar reinforcement are the low flexural strength and stiffness, and significant slip-type of pinching.

9.3.3.3 Review of Existing Hysteretic Models of Reinforced Concrete Members

The tests, on which the developments of different hysteresis models for reinforced concrete components are based, vary a lot. Consequently, the application of different hysteresis models may have a tight limit. According to the application range, existing hysteretic models of reinforced concrete members can be classified into two categories, one for flexure-dominated hysteretic behaviour and the other for significantly pinched hysteretic behaviour.

(1). Flexure-dominated hysteretic models

Quite a few flexure-dominated hysteretic models are developed, for example, (a). the widely used elastic-plastic hysteresis model, (b). bi-linear hysteretic model, (c). Clough model, et al.

The bi-linear hysteretic model is widely used in general engineering practice to simulate the flexure-dominate hysteretic behaviour, mainly because of its simplicity. However, the adequacy of this model is frequently questioned. For instance, the US-Japan Cooperative Research Program reported by Kabeyasawa [K2], which examined both full-scale pseudodynamic tests and scaled model shaking-table studies on a seven-story reinforced concrete frame wall structure of realistic size and complexity, concluded that the use of a

bilinear force-deformation relationship was incapable of reproducing true reinforced concrete frame component behaviour.

Otani also studied the effect of hysteretic characteristics of flexure-dominated hysteretic models on the predicted seismic response of reinforced concrete structures [O4]. He concluded (a). the stiffness properties of the used skeleton curve have very significant influences on earthquake response amplitude, especially, the stiffness at first yield, (b). the unloading stiffness degradation properties is also an important factor.

(2). Pinched hysteretic models (or Stiffness degrading hysteretic models)

The real hysteretic behaviour of a reinforced concrete member will be, to some extent, affected by shear or bond deterioration. Often, the influence of the shear or bond deterioration is so significant that the hysteretic behaviour of the reinforced concrete member will no longer be flexure-dominated. In this case, stiffness degrading hysteretic models should be used.

Many stiffness degrading hysteretic models have been developed, base on the experimental observations, for instance, (a). Clough's Degrading Stiffness Model [C3], (b). Takeda's Degrading Stiffness Model [T1], (c). Takeda's Slip hysteresis Model [K1], (d). Stewart's Pinching Model [S10], (e). Pivot Hysteresis Model proposed by Dowell, Seible and Wilson [D2].

In Clough's degrading stiffness model, the loading stiffness degradation in the bilinear elastic-plastic model is incorporated. The unloading stiffness slope remained parallel to the initial elastic slope. In comparison, Takeda's degrading stiffness model is a more refined hysteresis model for the reinforced concrete members. This model included stiffness changes at flexural cracking and yielding and also strain-hardening characteristics. The unloading stiffness is reduced by an exponential function of the previous maximum deflection. However the stiffness degradation simulated in both Clough's degrading stiffness model and Takeda's degrading stiffness model is the type of shear-induced stiffness degradation. The characteristics of stiffness degradation in association with bond degradation and bar slip are different from those associated with shear action.

The hysteretic models, which are capable of allowing for bond slip type of stiffness degradation, include Takeda's slip hysteresis model and Stewart's pinching model.

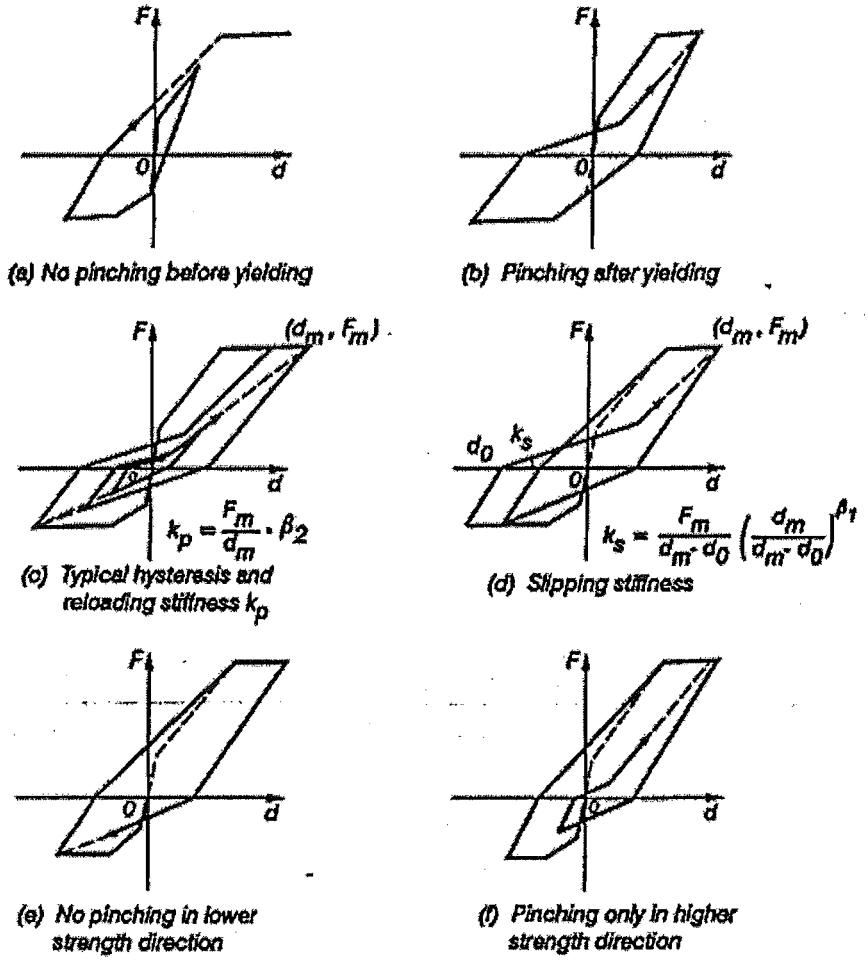

Fig.9.9 Takeda Slip Model

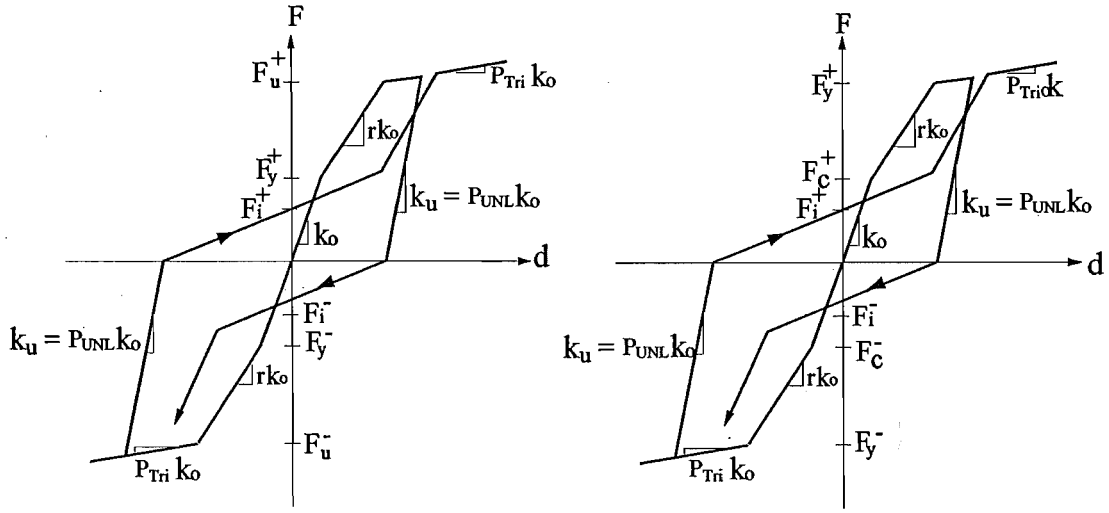

(a) Original model (b) Modified Model

Fig.9.10 Wayne Stewart Model

Takeda's slip hysteresis model was originally developed by Takeda and Eto, and then modified by Kabeyasawa et al [K2] to model the pinching due to bar slip within beam-column joint cores. The modified Takeda slip model is shown in Fig.9.9. This model, which is represented by a trilinear force-displacement envelope, is unsymmetrical in the positive and negative directions. The pinching occurrence is only in one direction where the yielding resistance is higher and the simulated pinching is due to bar slip within beam-column joint cores, as observed in the current test series. Such pinching is characterised by apparent increases in the loading stiffness after the crack closes under compressive stress action.

The Stewart's pinching model was originally developed based on test evidence of plywood sheathed shear walls where considerable pull out of the nails occurred. This model considers a symmetrical resistance envelope represented by a trilinear curve in both directions and pinching is mainly controlled by the force Vi at which the reloading curves intercept the axis of zero displacement. In this model, strength degradation and loading stiffness degradation as well as pinching behaviour due to bond degradation and bar slip can be represented. The considered pinching in this model is the initial slackness and subsequent degradation of the stiffness. The pinching occurs as the nails enlarge the holes and withdraw themselves from the framework. The characteristic stiffness change points are the yielding force point and ultimate force strength point, and strength hardening after the attainment of the theoretical flexural strength is allowed for. The Stewart's pinching model is shown in Fig.9.10.

Recently the original Stewart model was modified at the University of Canterbury [C4]. It is to be noted that the pinching in the original Stewart model was assumed to occur only after the yielding of the member and it is very common that reinforced concrete members exhibit significant pinching before the member yielding. The modified Stewart model is still symmetrical for positive and negative directions and is represented by a trilinear curve in both directions. However the three characteristic stiffness change points became the concrete cracking point, the yielding force point and ultimate force strength point. The modified Stewart model is shown in Fig. 9.10(b).

9.3.3.4 Proposed Hysteresis Models

The Stewart model and the Takeda slip model, which are employed in RUAUMOKO program [C4], can capture slip type pinching. The original or modified Stewart model has

a symmetrical trilinear skeleton curve and hence this model can only be used for the columns of the subject building, which are symmetrically reinforced concrete members. Unlike Stewart hysteresis model, the Takeda slip model has an unsymmetrical trilinear skeleton curve and hence it can be used for the beams of the subject building, which are unsymmetrically reinforced concrete members.

The original Stewart model allowed for the strength hardening after the achievement of the theoretical flexural strength. For existing reinforced concrete members with plain round longitudinal reinforcement, the flexural strength is generally lower than the theoretical strength and hence the strength hardening is not possible. Furthermore the observed evidence for existing reinforced concrete members with plain round longitudinal reinforcement was that the pinching occurred prior to the member yielding. Therefore the modified Stewart model, rather than the original Stewart model, is used.

The modified Stewart model has a symmetrical trilinear skeleton curve and the three stiffness changes represent the cracking, yielding and after the ultimate force strength stage. Similarly, Takeda slip model is also represented by a trilinear skeleton curve and the three stiffness changes represent the cracking, yielding, and after yielding of the member. However the skeleton curve of Takeda slip model is unsymmetrical for positive and negative directions and the pinching occurs only when the deformation reloads in the member strong direction.

The proposed tri-linear monotonic force strength and deformation skeleton curve for the as-built reinforced concrete members in chapter 8 includes the point at member first yield, the point at attainment of member ultimate strength and the strength degradation after attaining the ultimate force strength. In this study, strength degradation was considered externally, the tri-linear skeleton curve used for Takeda slip model and Wayne Stewart model need to introduce the cracking point.

9.3.4 Determination of the Skeleton Curves for the Used Hysteresis Models

9.3.4.1 Member Concrete Cracking Point

Ordinary theory is used to obtain the member flexural strength and deformation at concrete cracking.

According to NZS 3101:1995, member flexural strength at concrete cracking M_{cr} is

$$M_{cr} = f_r Z \qquad (9\text{-}1)$$

Where: f_r is the average concrete modulus of rupture, which is $f_r = 0.6 \sqrt{f_c'}$ (MPa) for normal weight concrete; Z is the section modulus of the considered element.

Member curvature at concrete cracking, ϕ_{cr}, is obtained using Equation 9-2.

$$\phi_{cr} = \frac{M_{cr}}{EI_g} \qquad (9\text{-}2)$$

9.3.4.2 Member Yield Point

For the beams of the subject building, the yield points of the static flexural strength versus the flexural deformation skeleton curves are determined using the proposed method in Chapter 8. That is, the beam flexural strength at first yield is taken as 85% of the theoretical prediction. The beam initial stiffnesses at first yield are respectively taken as 50% and 75% of the theoretical predictions based on the sectional analysis, when the compressive column axial load due to gravity load at the same joint is zero and not less than $0.25A_gf_c'$. Between the two limits, the interpolation method is used for determining the beam initial stiffness at the first yield. For the columns of the subject building, the flexural strength at first yield is taken as 85% of the theoretical prediction, and the initial stiffnesses at first yield are taken as 75% of the theoretical predictions based on the sectional analysis.

9.3.5 Determination of Hysteretic Parameters

For the selected hysteresis models used in this analysis, the hysteresis parameters for defining the internal rules will be calibrated against the test results of as-built concrete components in this test series by conducting verification using the program "Hysteresis" [C8], which was developed at the University of Canterbury.

Hysteresis models are used to represent the force and deformation relationship within the member regions where inelastic deformation is expected. Hence calibration was conducted for the columns of as-built Unit 1, the beams of Units EJ3 and EJ4. Unit 1 was expected to develop plastic hinges in columns, Units EJ3 and EJ4 were expected to develop plastic hinges in the beams.

For the calibration, the point at concrete cracking is determined using the method described in Section 9.3.4.1 and the point at the first yield is determined using the method

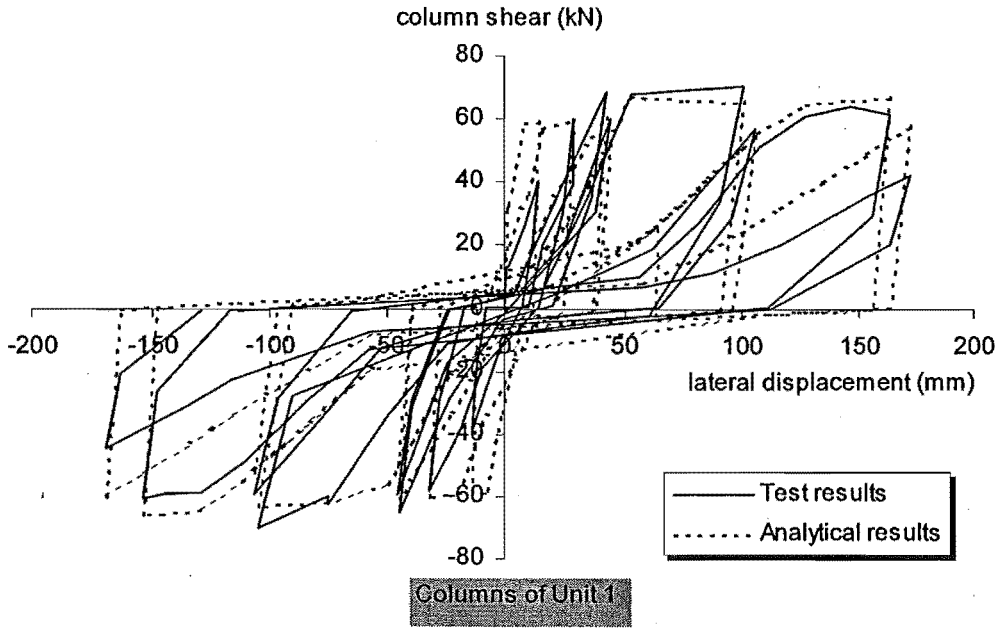

Fig.9.11 Verification of the Stewart model against the columns of tested Unit 1

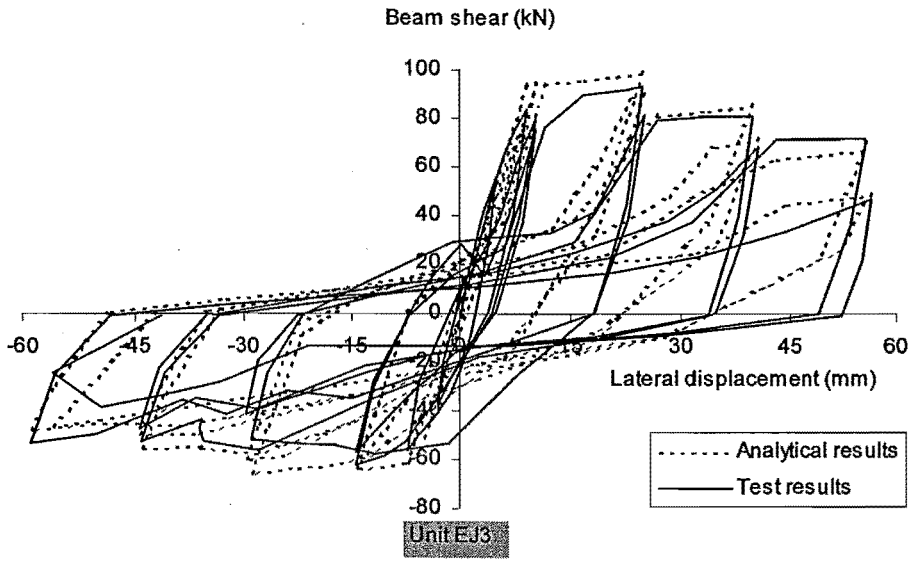

Fig.9.12 Verification of the Takeda slip model against the beam of tested Unit EJ3

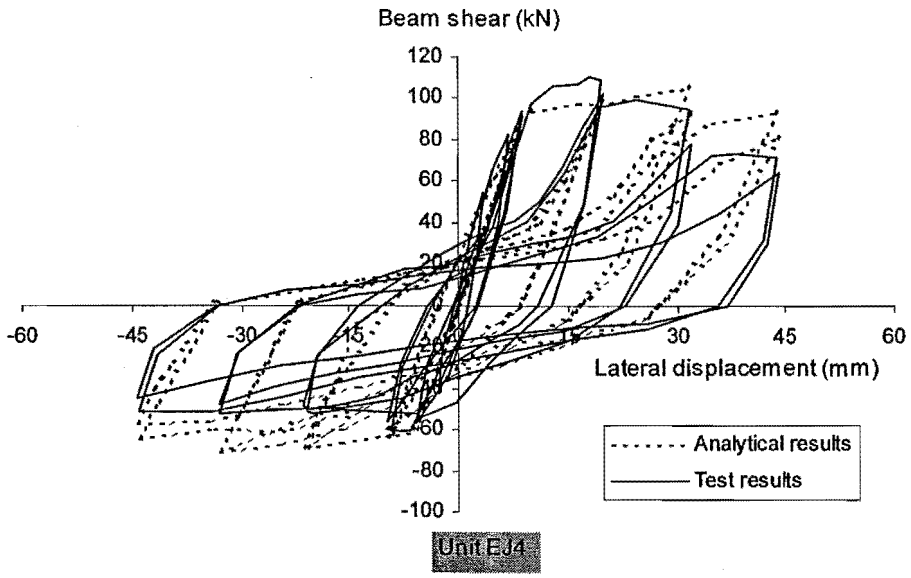

Fig.9.13 Verification of the Takeda slip model against the beam of tested Unit EJ4.

described in 9.3.4.2. Fig.9.11 shows the observed and analytical member force and deformation hysteresis curves for the columns of Unit 1. Figs.9.12 and 9.13 show the observed and analytical beam shear and beam lateral deformation hysteresis curves for the beam of Units EJ3 and EJ4, respectively. It is seen in Figs. 9.11, 9.12 and 9.13 that the member force and deformation hysteresis loops agree with the observed hysteresis loops reasonably well.

For the verification for the column of Unit 1 to the Modified Stewart Model, the bilinear factor and trilinear factor were 0.135 and 0.04 respectively. For the verification for the beams of Units EJ3 and EJ4 to the Takeda slip Model, the trilinear factor was 0.048.

Hence, the bilinear factor and trilinear factor of the modified Stewart model, which is to be used to represent the hysteretic behaviour of the as-built columns of the subject building, are taken as 0.135 and 0.04 respectively in this analysis. Similarly, the trilinear factor of the Takeda slip model, which is to be used for the as-built beams of the subject building, is taken as 0.048.

9.4 NON-LINEAR STATIC ANALYSIS

9.4.1 General

A non-linear static analysis, also referred as a push-over analysis, is of particular significance in general engineering practice. Unlike the non-linear dynamic analysis, which studies the structural performance during a certain earthquake motion, a non-linear static analysis can give the information on the probable structural strength capacity and

deformation capacity of the post-elastic failure mechanism. A non-linear static analysis is also conducted for the subject building.

As stated in Section 9.2.2, for the non-linear static analysis, the subject building is considered to have non-integral brick masonry infills in the external frames, similar to the non-linear dynamic analysis, and the infills are non-structural elements. Therefore, the masonry infills contribute to the seismic weight but not the structural stiffness. For the sake of comparison, the non-linear static analysis also studies the case, which does not allow for the masonry infills in estimating the seismic weight.

The difference between a non-linear static analysis and a dynamic analysis is that the studied building is subjected to a monotonic static loading history for a non-linear static analysis but is subjected to a dynamic cyclic loading history in a dynamic analysis. Basically, a non-linear static analysis and a dynamic analysis require the same information on individual member's behaviour, except that the non-linear static analysis does not require the information on a member's cyclic hysteresis behaviour.

In this study, the member model and the member's monotonic force versus deformation relationship representing the behaviour in non-linear deformation regions are the same as these proposed for the non-linear dynamic analysis, see section 9.3.

9.4.2 Lateral Force Pattern

The lateral force pattern used in a non-linear static analysis could influence the resulting strength and deformation capacity of the structure. For a low to medium regular frame structure, NZS4203: 1992 assumes that the 1st mode of vibration dominates the structural response. In this case, the lateral force pattern can be approximated using a triangular distribution. A method referred as an "Adaptive Push-Over" has been developed at the University of Canterbury [C1] and by using this method the results of any form of the initially assumed lateral force patterns can automatically converge to the ultimate displacement distribution.

In this study, the initial load pattern for the non-linear static analysis uses the method recommended by NZS4203: 1992 in evaluating the seismic action by the equivalent static method. The lateral load applied at level i of the structure is obtained from the following equation:

$$Fi = V \frac{W_i h_i}{\sum W_i h_i} \qquad (9\text{-}3)$$

where: V = the total horizontal base shear

W_i = seismic weight at level i

h_i = height of level i above the base of the structure

F_i = the lateral load at level, i

9.5 RESULTS OF NON-LINEAR DYNAMIC ANALYSIS

9.5.1 General

On the basis of the structural modelling and mathematical modelling as described in section 9.3, dynamic analysis was conducted for the subject structure to investigate the non-linear response of the structure when subjected to the first ten seconds of the El Centro 1940NS earthquake motion. For the dynamic analysis, the Rayleigh damping model was used, both the case with P-delta effect included and the case without P-delta effect included were conducted. The masonry infills were considered to be non-structural elements. Hence the infills contributed to the seismic weight but not to the structural stiffness. The fundamental period of the subject building is 1.85 (s), and this corresponds to a seismic acceleration coefficient of 0.17 for the 5% damping case from the acceleration spectra of the El Centro 1940NS earthquake motion. The design spectra according to NZS4203: 1992 should be not less than 0.16, when the fundamental period is 1.85(s) and the site is intermediate soil site. Therefore, the scale factor is taken as unity in conducting the dynamic analysis in order to match the design seismic action.

9.5.2 Maximum Base Shear Input

The observed maximum base shear input for the subject structure was the same and it was 1280 kN for both the case allowing for the P-Δ effect and the case without allowing for the P-delta effect. Theoretically, the inclusion of P-delta effect leads to a greater increase in the storey shear demands for the lower stories than that for the upper stories. This is because the axial load imposed on the columns due to gravity load was more significant at the lower stories than that at the upper stories. For the subject structure, the induced storey drifts were generally lower than 1%. Hence the P-Δ effect is not obvious.

9.5.3 Maximum Roof Deflection and Inter-Storey Drifts

The observed maximum roof displacements were basically the same for the case with allowance for P-Δ effect and the case without allowance for P-Δ effect and they were 184 mm, which was about 0.8% in terms of the roof drift.

Fig.9.14 shows the observed maximum inter-storey drifts when P-Δ effect is considered or not. From Fig.9.14, it is found that the observed maximum inter-storey drifts after taking into account of P-Δ effect were also basically the same as for the case without allowing for the P-Δ effect. For both cases, the maximum inter-storey drifts were within the deflection limit of NZS4203: 1992, which is 1.73% inter-storey drift [N5].

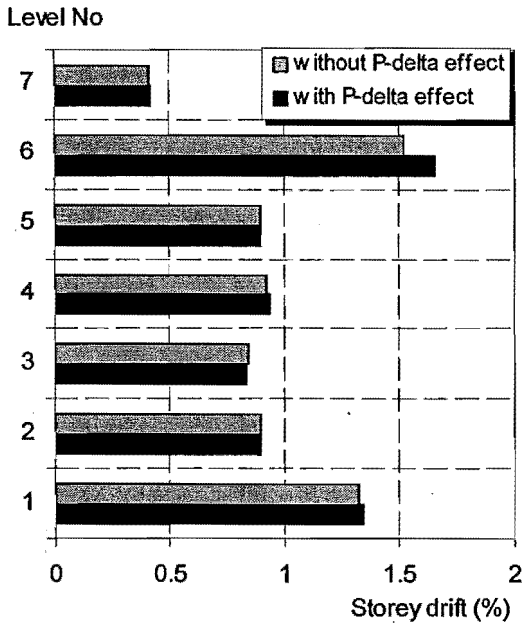

Fig.9.14 Observed maximum inter-storey drifts

This observation suggests that the influence of P-delta effect on the structural deflection performance would not be significant and can be ignored, should the code specified inter-storey drift limit be satisfied.

9.5.4 Maximum Deformations in Frame Members

Fig.9.15 and Fig.9.16 shows the required maximum curvature ductility in the beam and column members when the subject structure is subjected to El Centro 1940NS earthquake motion. For the non-linear dynamic analysis, plastic hinge regions were assumed to have a length of half the member depth.

The curvature ductility demand for the beam members varies a lot for a certain floor and it was generally larger in the first floor to the fifth floor. The maximum curvature ductility demand for the beams was 8.9 and it occurred in the fifth floor and the first floor. A curvature ductility of 8.9 for the beams corresponds to a rotational ductility of 5 when the member deformation capacity is evaluated using the equivalent rotational ductility in the beam fixed-ends, as stated in Chapters 6 and 7. Based on the tests in this project, the rotational ductility of 5 in the member fixed-ends can be achieved without much strength degradation.

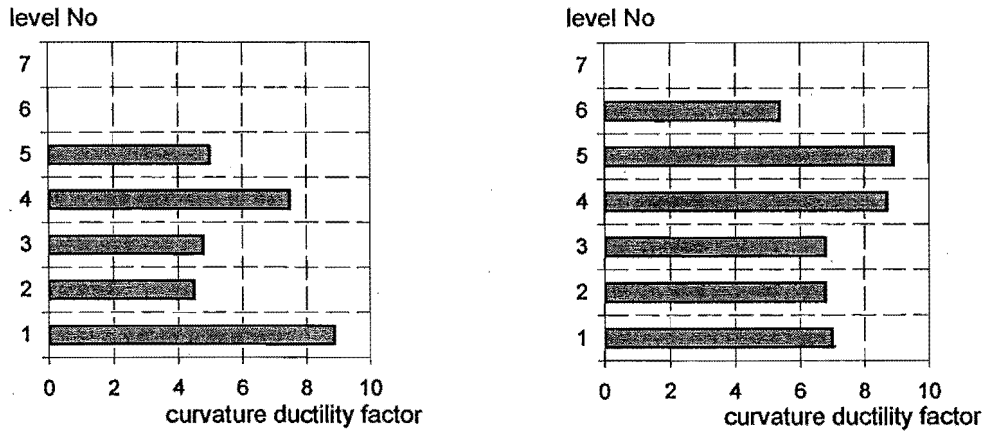

(a) Frame A (b) Frame B

Fig.9.15 Maximum curvature ductility in beam members

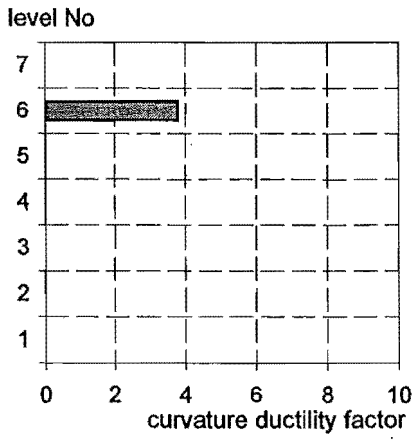

Fig.9.16 Maximum curvature ductility in column members

Only the two exterior columns in the sixth floor yielded. The column curvature ductility demand was small and the maximum column curvature demand was only 3.8. This is

equal to an equivalent rotational ductility less than 3 in the column fixed-end. Based on the test evidence the columns should be capable of achieving an equivalent rotational ductility in the fixed-end of 3 without causing much force strength degradation.

9.5.5 Possible Failure Mechanism

Fig.9.17 illustrates the probable failure mechanism of the structure. Flexural yielding occurred mainly in the beams. Only the two exterior columns in the sixth floor of frame A developed flexural plastic hinges at both end due to absence of interior columns in the sixth floor of frame B, and the other columns at the sixth floor were generally well away from the yielding. When the structure contains plain round longitudinal reinforcement, premature shear failure in the plastic hinge regions is unlikely. Hence the non-linear behaviour of the structure would be dominated by beam flexural plastic hinging and the formation of undesirable soft-storey failure mechanism is very unlikely.

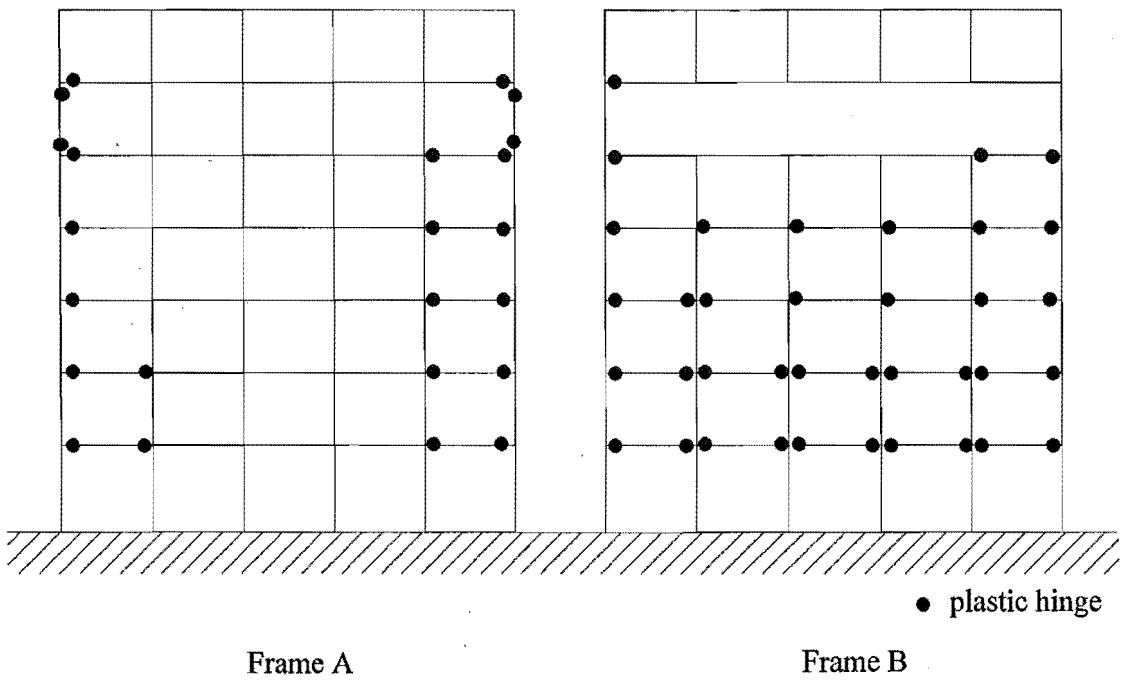

Fig.9.17 Probable mechanism of the structure in an earthquake similar to El Centro 1940NS earthquake motion

Therefore, the investigated subject structure should be able to survive when it is subjected to an earthquake with similar magnitude and similar vibration characteristics to 1940 El Centro North South earthquake motion.

Results of the dynamic analysis of the subject structure are summarised in Table 9-4.

Table 9-4 Summary of results of Dynamic Analysis of the Subject Structure

study cases	Demand				overall capacity/demand
	V_{max}	$\Delta_{r,max}$	R_{max}	μ_{ϕ},max	
with P-Δ effect	1280 kN	184 mm	1.73%	8.9 for beams 3.8 for columns	satisfactory
without P-Δ effect	1280kN	184 mm	1.73%	8.9 for beams 3.8 for columns	satisfactory

Note: V_{max} is the maximum base shear demand
$\Delta_{r,max}$ is the maximum roof displacement in mm
R_{max} is the maximum storey drift in %
μ_{ϕ},max is the maximum member curvature ductility demand

It needs to be clarified that the effect of cyclic loading on the maintenance of force strength is more significant than that of the imposed displacement levels (see Chapters 6 and 7). A number of cyclic loading at small displacement levels could lead to a great deal of reduction in the strength. The effect of cyclic loading on the structural response has been allowed for in this study by specifying the strength degradation dependent on the loading cycles. However, more study is needed to refine the information on the adverse effect of cyclic loading on the strength maintenance of the concrete members should the members contain plain round longitudinal reinforcement.

9.6 RESULTS OF NON-LINEAR STATIC ANALYSIS

For the non-linear static analysis of the subject building, two cases were analysed. One case was that the masonry infills were allowed for in estimating the seismic weight, as for the non-linear dynamic analysis. The other case was that the masonry infills were assumed not to exist and hence they were not allowed for in estimating the seismic weight, as was for the seismic assessment of the subject building conducted by Hakuto et al. Both cases did not allow for the contribution of masonry infills to the structural stiffness.

9.6.1 General Structural Strength and Deformation Capacity

Fig.9.18 shows the roof displacement and the base shear force relationship for the subject building, obtained by the non-linear push-over analysis for both cases.

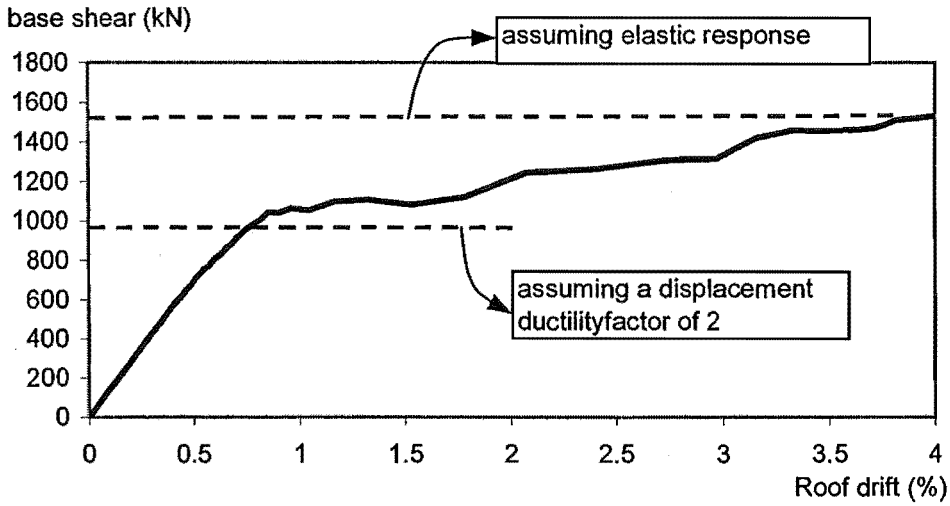

(a) Seismic weight did not allow for the contribution of masonry infills

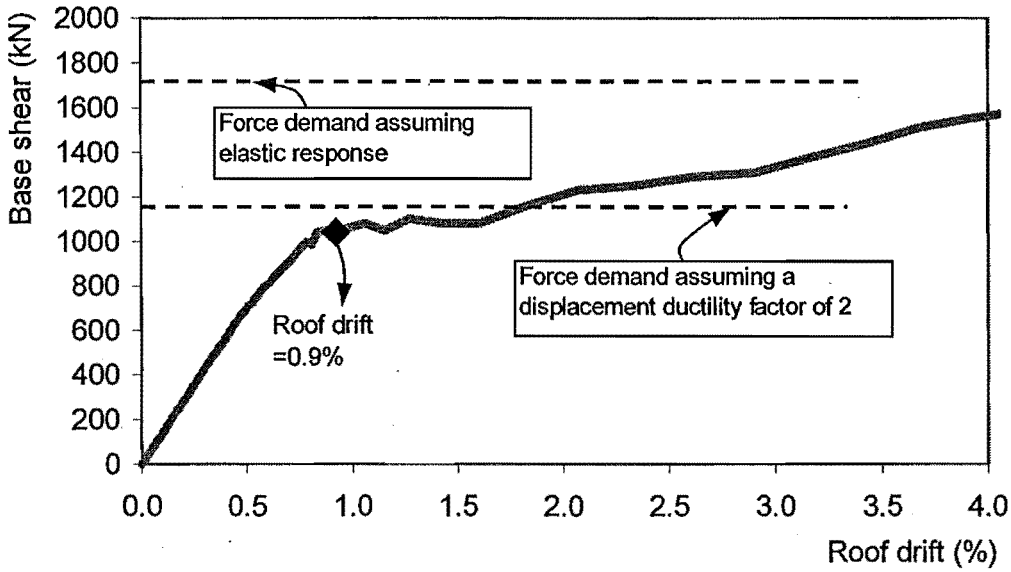

(b) Seismic weight has allowed for the contribution of masonry infills

Fig.9.18 Estimated structural capacity curve in terms of base shear versus roof drift

Fig.9.18 shows that the strength and deformation capacity curves had been nearly linear prior to the roof drift of 0.9% for both cases, so the structural displacement ductility at the roof drift of 0.9% was defined as $\mu_\Delta = 1$. The roof drift is defined as the ratio of the roof

displacement to the total building height. At the roof drift of 0.9%, the force strength of the structure in terms of the base shear force was 1050 kN and this gave a basic seismic acceleration coefficient of 0.13 if the seismic weight did not allow for the masonry infills, and it gave a basic seismic acceleration coefficient of 0.06 if the seismic weight allowed for the contribution of the masonry infills.

9.6.2 Strength and Deformation Capacity at Code-specified Deflection Limit

The New Zealand loading code NZS4203: 1992 permits a maximum inter-storey drift of 2.0% for $h_n \leq 15$m and 1.5% for $h_n > 30$m, where h_n is the total height of the building, with linear interpolation between, when equivalent static method or modal analysis is used; and a predicted drift of 2.5% is permitted regardless of height 2.5%, when inelastic time-history analysis is used to check the drift. For this structure, $h_n = 23.01$ metres, NZS4203: 1992 gives the maximum storey drift of 1.73% when equivalent static method is used.

So it was of significance to determine the stage when the maximum storey drift of 1.73% was reached. At the roof drift of 2%, the maximum storey drifts for all levels were shown in Fig. 9.19 for both the case with the masonry infills and the case without the masonry infills in estimating the seismic weight. Evidently, the inter-storey deformations for both cases were very similar.

In Fig.9.19, the maximum inter-storey drift occurred in the 3rd storey and it was nearly 3%, which was by far beyond the code limit. The maximum inter-story drift had been in the 3rd storey until the roof drift exceeded 4%. After that, the maximum inter-storey deformation shifted to level 6 where no interior columns existed for interior frame B. The occurrence of the largest inter-storey drift in the 3rd storey was due to the sudden column stiffness change in level 3 from levels 1 and 2. Apparently, the structural deflection performance was not be significantly affected by the absence of the interior column at level 6 in the practical deflection range.

In fact, to comply with the code specified inter-storey limit of 1.73%, the maximum roof drift needs to be within 1.4%. Fig.9.20 shows the maximum inter-storey drift at the roof drift of 1.4% for both cases. At the roof drift of 1.4% where the code-specified deflection limit was reached, the member yielding occurred only in the beams. The flexural plastic hinges are shown in Fig.9.21 and the structure has not developed a collapse mechanism at this stage. Hence, the overall structural strength versus the deformation capacity of the

subject building is more dominated by the code-specified deflection limit, than the formation of the collapse mechanism. That is, the code-specified deflection limit was reached before the formation of the collapse mechanism for the subject building.

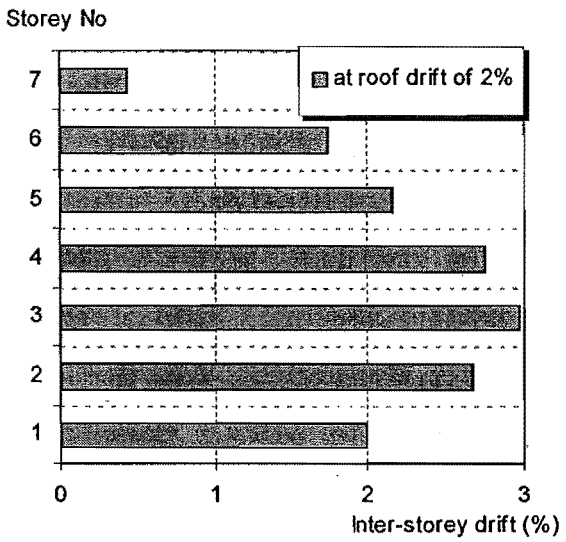

(a) Masonry infills are allowed for in estimating the seismic weight

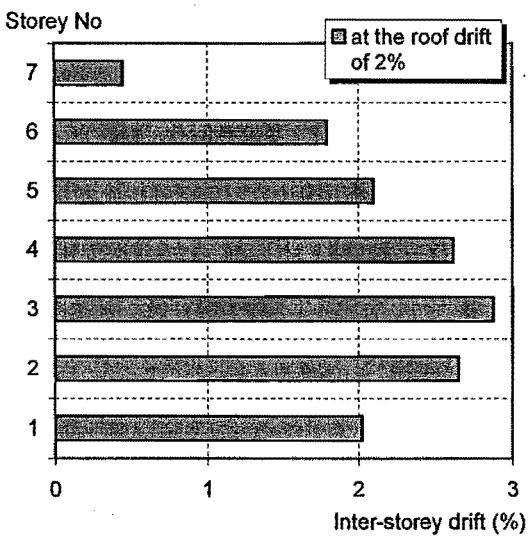

(b) Masonry infills are NOT allowed for in estimating the seismic weight

Fig.9.19 Maximum inter-storey drift at roof drift of 2%

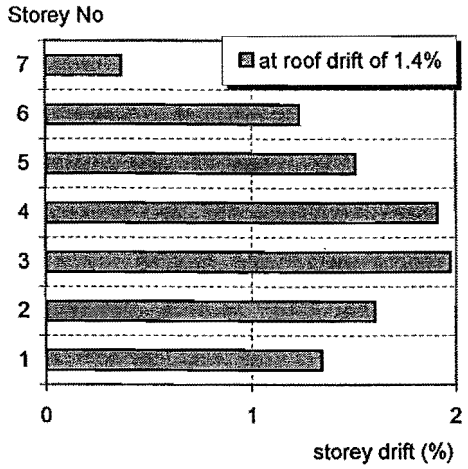

(a) Masonry infills are allowed for in estimating the seismic weight

(b) Masonry infills are NOT allowed for in estimating the seismic weight

Fig.9.20 Maximum inter-storey drifts at roof drift of 1.4%

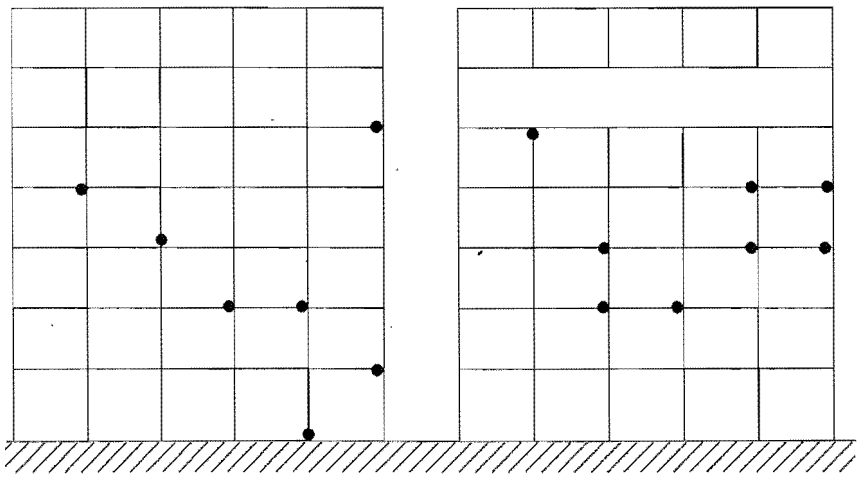

• plastic hinge

Frame A Frame B

Fig.9.21 Member yielding at roof drift of 1.4%

9.6.3 Check Member Deformation Capacity at the Code-specified Deflection Limit

At roof drift of 1.4%, the flexural yielding occurred only in the beams. The required maximum beam curvature ductility at the roof drift of 1.4% is shown in Fig. 9.22.

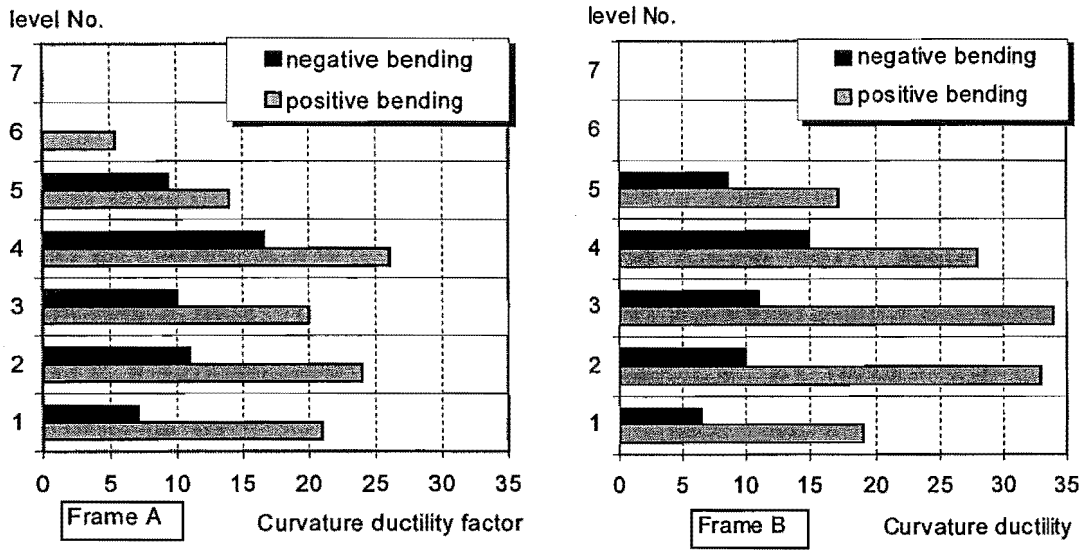

Fig.9.22 Maximum beam curvature ductility demand of each level

Fig.9.22 shows that the beam curvature ductility factor demand in the positive bending direction is much larger than that in the negative bending direction. There is a bigger demand for beam curvature ductility factor in the levels 2, 3 and 4. The maximum beam curvature ductility factor at this stage was 26 and 34 for frame A and Frame B respectively. For this analysis, it is assumed that the plastic hinge length is 50% of the member cross sectional depth. For the beams of exterior frame A, the curvature ductility factor demand of 24 is equal to a rotational ductility factor in the member fixed end of 10.8, where the rotational ductility factor is defined in the same way as in Chapter 6 and chapter 7. For the beams of interior frame B, the curvature ductility factor of 34 is equal to a rotational ductility factor of 14.7 in the beam fixed-end.

Based on the test results, the available strength for the interior beams showed a sudden drop when the rotational ductility factor is about 5 (see Fig.6.36). In addition, cyclic effects would cause the force strength to reduce significantly, so the force strength at a rotational ductility factor of more than 10 would be much lower than the 80% of the maximum strength. Hence the deformation capacity of the beams would be reached before the code-specified deflection limit.

In fact, at the roof drift of 1%, the beam curvature ductility factor demand in the positive bending direction in level 3 of Frame B was as high as 12 and this was equivalent to a rotational ductility factor at the fixed-end of 6. Hence, should the structural displacement ductility $\mu_\Delta = 1$ be defined to be at the roof drift of 0.9%, no structural displacement ductility factor could be relied on.

9.6.4 Structural Seismic Force Demands

According to NZS4203: 1992, the design horizontal seismic shear force for the ultimate limit state, acting at the base of the structure in the direction being consideration, can be calculated as follows:

$$V = C\, W_t \qquad (9\text{-}4)$$

where the lateral force coefficient, C, is calculated from Eq. 9-5 as follows:

$$C = C_h(T_1, \mu)\, S_p\, R\, Z\, L_u \qquad (9\text{-}5)$$

Table 9-5 Parameters used in calculating the seismic design base shear

S_p	0.67
R	1.0 for buildings of category IV
Z	0.8 in Christchurch
L_u	1.0 at ultimate limit state
T_1	1.16(s) if the masonry infills are NOT considered in estimating the seismic weight.
	1.86 (s) if the masonry infills are considered in estimating the seismic weight.
$C_h(T_1, \mu)_1$	0.34 for intermediate soil site and $\mu = 1.25$ for elastically responding reinforced concrete structure
$C_h(T_1, \mu)_2$	0.22 for intermediate soil site and $\mu = 1.25$ for elastically responding reinforced concrete structure
C_1	0.18 for elastically responding reinforced concrete structure
C_2	0.12 for elastically responding reinforced concrete structure

Note: $C_h(T_1, \mu)_1$ and C_1 are the obtained parameters when the masonry infills were NOT allowed for in estimating the seismic weight. $C_h(T_1, \mu)_2$ and C_2 are the obtained parameters when the masonry infills were allowed for in estimating the seismic weight.

In Table 9-5,

S_p = the structural performance factor

R = the risk factor

Z = the zone factor

L_u = the ultimate limit state factor

$C_h(T_1, \mu)$ = the basic seismic hazard acceleration coefficient

T_1 = the fundamental period of vibration

μ = the structural displacement ductility

The total seismic weight of the study frame structure is:

W_t = 8232 kN if the masonry infills were **not** considered in estimating the seismic weight;

W_t = 18765 kN if the masonry infills were considered in estimating the seismic weight.

As a result, the total horizontal seismic shear force acting at the base of the structure, namely, the design base shear, obtained using the equivalent static method and assuming elastic response is:

$V = C W_t = 1482$ kN for the case without allowance for the contribution of the masonry infills to the seismic weight

$V = C W_t = 2252$ kN for the case with allowance for the contribution of the masonry infills to the seismic weight

For the subject building, the deformation capacity of the individual members was reached before the code-specified deflection limit, and the code-specified deflection limit was reached before the formation of a collapse mechanism. Hence, the deformation capacity of the individual members dominated the overall structural performance. If the structural displacement ductility at the roof drift of 0.9% is defined as $\mu_\Delta = 1$, no structural displacement ductility can be relied on as discussed in Section 9.6.3. In this case, the subject building needs to elastically resist the design seismic force. At the roof drift of 0.9%, Fig.9.18 gives that the strength of the subject building in terms of the base shear force is 1050 kN and this is only 71% of the seismic demand for the case without the masonry infills in estimating the seismic weight and it is only 47% of the seismic demand for the case with the masonry infills in estimating the seismic weight. Apparently, the studied subject structure is not satisfactory according to current design code NZS4203: 1992. If the masonry infills are considered to contribute to the seismic weight, the available structural capacity is more inadequate, when compared to that without allowing for the infills in estimating the seismic weight.

9.7 CONCLUSIONS

Seismic performance of an existing reinforced concrete frame structure constructed in New Zealand in the late 1950s was assessed in this chapter by conducting non-linear static and non-linear dynamic analysis for the subject structure. The information on the seismic behaviour of individual reinforced concrete members was based on the simulated seismic loading tests conducted in the current project. The post-elastic behaviour of the beams and columns was modelled by using Giberson's one-component member model. However, for the flexural spring representing the beam's non-linear behaviour, the non-linear static properties were determined by the cross sectional details of the beams and then modified according to the compressive column axial load at the same joint, based on the proposed method in Chapter 8. Seismic assessment of the existing reinforced concrete frame structure led to the following conclusions:

1. Both non-linear dynamic and non-linear static analyses showed that the overall non-linear behaviour of the frame structure was mainly dominated by the flexural non-linear behaviour of the beams. The frame building was very unlikely to develop a soft-storey column failure mechanism in a major earthquake.

2. The P-Δ effect on the structural performance appeared to be insignificant, as long as the structure satisfied the deflection criteria specified by the code.

3. A non-linear static (push-over) analysis showed that the structural post-yielding performance was more governed by the local member deformation capacity than the code-specified deflection criteria.

When the attained maximum inter-storey drift reached the limit of 1.73% required by NZS4203: 1992, only beam plastic hinges had formed and a failure mechanism had not been achieved. At this stage, the maximum beam curvature ductility factor reached 34, which is equivalent to a rotational ductility factor of 15 in the member fixed-end. Based on the test evidence observed for as-built beam-column joints, it was difficult to achieve a rotational ductility factor of 15 in the member fixed-end. Hence, the individual members of the structure would reach their maximum deformation capacity before the maximum inter-storey drift reaches the code-specified limit. At the roof drift of 0.9%, the member curvature ductility factor had reached 12, and this was equivalent to a rotational ductility factor of about 6 in the member fixed-end, which was the maximum available member deformation capacity according to the tests.

No structural displacement ductility could be relied on at this stage. The available structural force strength in terms of base shear was only 71% of the design seismic force when masonry infills were not considered to contribute to the seismic weight, but only 47% of the design seismic force when the masonry infills were considered to contribute to the seismic weight. The design seismic force was determined according to current New Zealand design code NZS4203: 1992. This meant that the structure had a very inadequate performance according to the current seismic code.

4. The non-linear dynamic analysis of the structure was conducted when subjected to the first ten seconds of El Centro 1940 North South earthquake record. The maximum beam curvature ductility factor was 8.9 and this was equal to a rotational ductility factor less than 5 in the member fixed-ends, where the rotational ductility in the member fixed-end was defined in the same way as in chapters 6 and 7. Test evidence illustrated that the individual reinforced concrete members of the subject structure would be capable of achieving such a rotational ductility.

Hence it could be concluded that the subject structure would survive during a major earthquake of similar magnitude and similar vibration characteristics to the El Centro 1940NS earthquake motion.

5. Allowance for the masonry infills in estimating the seismic weight could make a significant difference in the estimated structural earthquake-resistant capacity. In reality, the frame structure contains these masonry panels and the masonry infills should be allowed for in calculating the seismic weight. Otherwise, the results could significantly deviate from the correct answers.

6. In establishing the analytical structural model, the realistic modelling of the transverse supports underneath the beams, where the interior columns in the 6^{th} floor are absent, was very important. In reality, the beams of the interior frame B at the sixth floor are supported by a transverse force resisting system. Without introducing the transverse supports, which were represented by springs in Fig.9.2, the subject structure would collapse even under gravity load.

CHAPTER 10

EFFECTS OF NON-INTEGRAL MASONRY INFILLS ON SEISMIC BEHAVIOUR OF REINFORCED COCNRETE BUILDINGS

10.1 INTRODUCTION

For the seismic assessment analysis conducted in Chapter 9, the masonry infills were treated as non-structural elements and the structural modelling did not allow for any masonry infills. The reality is that the building does contain masonry infills.

Presence of masonry infills not only affects the available structural capacity but also alters the structural demand. Masonry infilled frame structures are composite structures. Masonry infill panels provide stiffness to reduce the deformation demand whereas the surrounding frames provide ductility for the structure. As a consequence, masonry infilled frame structures exhibit a complicated behaviour. In addition, masonry infills significantly alter the dynamic characteristics of the infilled frames. Due to the presence of the masonry infill panels, the lateral stiffness, the mass and the damping ratio change markedly. As a result, the fundamental period of vibration of an infilled frame building is smaller than that of the corresponding bare frame building, leading to an increase in the seismic actions. Hence there is a need for investigating the combined effect on the seismic performance of the structure in a major earthquake.

Also of significance is that adding masonry infill walls (which usually have special connection between the frames and the infills, hence can be treated as integral masonry infill walls, rather than the non-integral infills) in the existing reinforced concrete frame structures is a common retrofit means, when the existing structures have inadequate stiffness and/or force strength behaviour. Adequate understanding of the seismic behaviour of the infilled frames is apparently very important in this case.

This chapter aims at investigating the possible effects of masonry infills on the seismic performance of the existing reinforced concrete structures, especially the failure mechanism and the force strength and deformation capacity of the final failure mechanism. At first, a brief review on the behaviour of masonry infilled frames is described based on test evidence and analysis results. Then, existing procedures for

analysing the infilled frames are outlined. As a result, a proper model for studying the seismic behaviour of the subject building with masonry infills is identified. A non-linear static (push-over) analysis is conducted for the subject frame building after taking into account the presence of masonry panels, possible effects of the presence of masonry infills on the seismic assessment results of the subject structure are summarised.

10.2 BEHAVIOUR OF MASONRY INFILLED FRAMES

10.2.1 General

Masonry infilled frame structures have been generally recognised to exhibit poor seismic performance, since numerous masonry infilled frame buildings have failed in past earthquakes. However, experimental observations, analytical studies and the performance of infilled frames in real earthquakes frequently indicate that masonry infills may produce some beneficial effects on the response of the building. The contradictory conclusions result from the difference in the uses of masonry infills in the earthquake-resistant structures.

Both non-linear dynamic analyses and experimental tests demonstrate that the strength of the composite structure is generally greater than the sum of the two components separately. This is due to the interaction between the infill panels and the surrounding frames. In addition, the initial stiffness of the composite structure is greater than that of the bare frame, due to the in-plane bracing action of the masonry panel. Tests on 1 / 2 scale single-storey infilled frame specimens, which was conducted by Schuller et al [S11] to study the influence of the relative strengths of infill panels and the surrounding frames, demonstrated that an infill panel increased both the lateral stiffness and load resistance of a reinforced concrete frame by a substantial amount.

However the presence of masonry infills also causes the degradation of stiffness, strength and energy dissipation capacity. This generalised degradation is mainly due to the progressive damage to the masonry panels and the gradual deterioration of the bond mechanism between the infill panels and the surrounding frames. As a consequence, infilled frame structures can only achieve low to medium displacement ductility.

10.2.2 Analysis of Masonry Infilled Frame Structures

Masonry panels are very brittle due to the brittle behaviour of the masonry materials. In comparison, the surrounding reinforced concrete frames are more ductile. The seismic performance of masonry infilled frames is markedly non-linear. Fig.10.1 shows two typical force-displacement hysteresis responses observed for infilled reinforced concrete frames by Kato et al [K4].

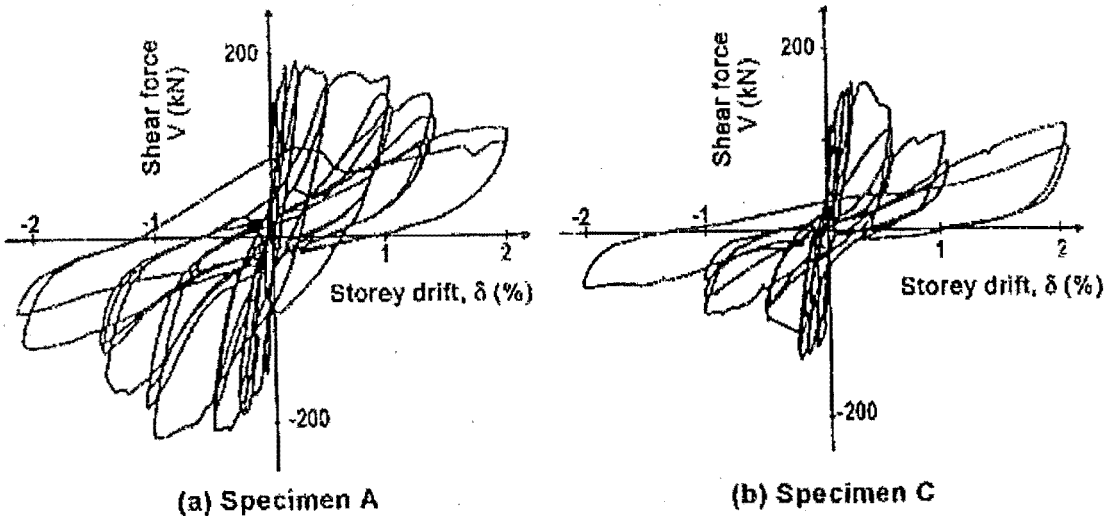

Fig.10.1 Typical force-storey drift curve under alternating forces, according to the test results by Kato et al

In analysing the non-linear seismic behaviour of masonry infilled reinforced concrete frames, apart from modelling of the reinforced concrete frame members in the same way as for bare frames, the masonry panels and the interfaces of the surrounding frames and the masonry panels also need to be adequately modelled.

10.2.3 Observed Failure Modes of Masonry Panels

To adequately model the masonry panels in conducting the analysis of the masonry infilled frames, possible failure modes of masonry panels need to be thoroughly understood.

Based on an extensive review of current research work into behaviour of infilled frames, Crisafulli et al [C5] summarised that there are two major failure mechanisms in masonry panels, shear associated failure and compression failure.

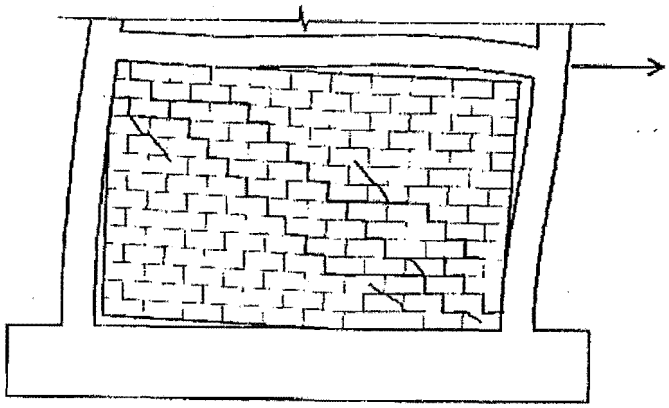

Fig.10.2 Shear cracking along the mortar joints, stepped cracks

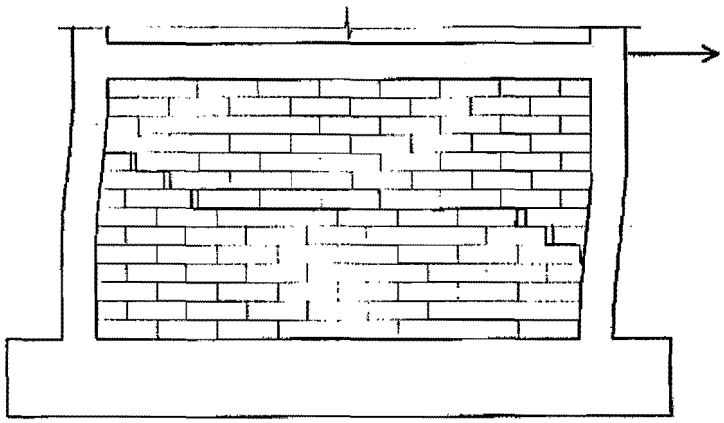

Fig.10.3 Shear failure due to horizontal sliding shear failure

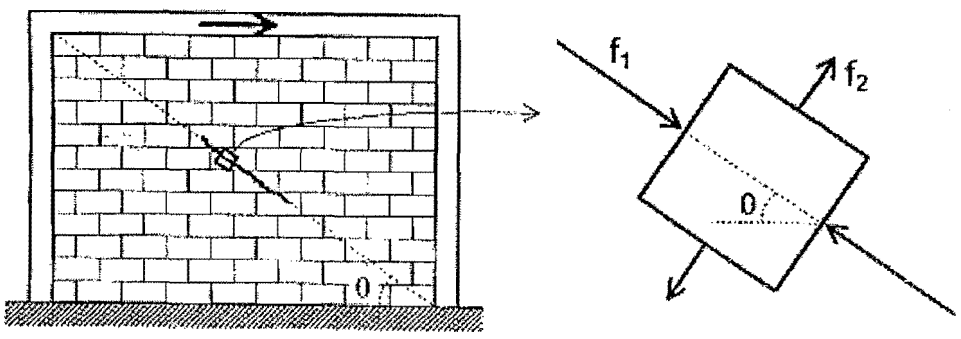

(a) cracking due to diagonal tension (b) biaxial compression-tension stress state

Fig.10.4 Cracking due to diagonal tension when the principal tensile stress exceeds the tensile strength of the masonry panels

(1). Shear cracking in the masonry panels.

This is a very common type of failure observed in experimental work and in the earthquake damage to infilled frame buildings during past earthquakes. This type of failure has different forms, depending on the shear strength of the mortar joints, the tensile strength of the masonry units and the relative values of the shear and normal stress. Figs.10.2, 10.3 and 10.4 illustrate some typical forms of shear failure, stepped cracking along the mortar joints (as illustrated in Fig.10.2); horizontal sliding failure along the mortar joints (in Fig.10.3); cracking due to diagonal tension (in Fig.10.4).

(2). Compressive failure of the masonry panels

Failure of the masonry panels due to compression is not so common as shear cracking failure. Compressive failure of the masonry panels is in the form of the crushing failure of the loaded corners and/or the compressive failure of the diagonal strut developed in the masonry panel.

10.3 ANALYSIS OF THE SUBJECT STRUCTURE AFTER TAKING INTO ACCOUNT OF EFFECT OF MASONRY PANELS

10.3.1 Possible Failure Modes of the Masonry Panels of the Subject Structure

Failure modes of the masonry panels are closely related to the construction technique. The subject reinforced concrete frame structure was constructed in the late 1950s in New Zealand. A commonly used technique in constructing the masonry infilled frame structures in New Zealand is that the reinforced concrete frames are erected first then the masonry panels are constructed. In this case, unintentional gaps between the masonry panels and the surrounding frames can form and the infilled frames are typical non-integral infilled frames. Tests on non-integral infilled frames demonstrate that a most likely failure mode for non-integral masonry infills is the horizontal sliding shear failure [D3, P26]. Therefore, it is assumed in this study that the horizontal sliding shear failure dominates the behaviour of the masonry panel.

10.3.2 Review of Methods for Modelling Masonry Panels

10.3.2.1 General

There are different methods for modelling the masonry panels in conducting the non-linear analysis of masonry infilled frames and they can be classified into two major categories, namely, micro-models and macro-models. Micro-models divide the masonry infills into numerous elements to allow for the local effects in details. Macro-models use a few elements to represent the effect of masonry infills as a whole.

10.3.2.2 Micro-Model Methods

A major representative of micro-model methods is finite element method. The finite element method has been extensively used for modelling infilled frames and it has major advantages for describing the structural local behaviour. In addition, finite element analysis also can give some information useful for macro-models methods, for instance, compression strut orientations and so on.

Crisafulli [C5] conducted the analysis of an infilled frame using a finite element model to study the possible effects of horizontal sliding shear failure in masonry panels. Fig.10.5 shows the deformed shape of the infilled frame after the formation of the horizontal sliding shear crack, which is located approximately at the middle height of the panel. In Fig.10.5, the masonry panel is divided into two parts by the horizontal crack and the masonry panel is in contact with the columns at each side. Consequently, the behaviour of the infilled frame can be approximately represented by a multi-braced frame, as suggested in Fig.10.6.

In addition, the actions induced in the surrounding frame are modified after the formation of the horizontal crack, as the comparison of Fig.10.7 and Fig.10.8 indicates. The variation of the shear and axial forces of the columns at mid height reflect the resulting effect due to the frame-panel interaction. The change in the column shear forces is much more pronounced than that in axial forces, indicating that the induced resultant force in the columns is mainly horizontal. The flexural demand in the columns at mid-height is significantly increased and could lead to plastic hinges in these regions.

One disadvantage of the finite element method is that it involves a much greater effort in preparing the input data and analysing the output results. More important is the difficulty

associated with adequate modelling of the masonry panels, which means that the results could be sometimes misleading.

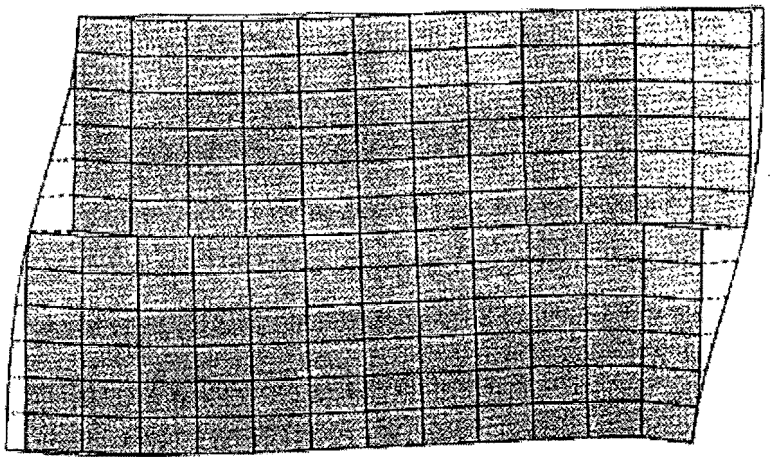

Fig.10.5 Deformed shape of an infilled frame with horizontal sliding shear failure in the masonry panel

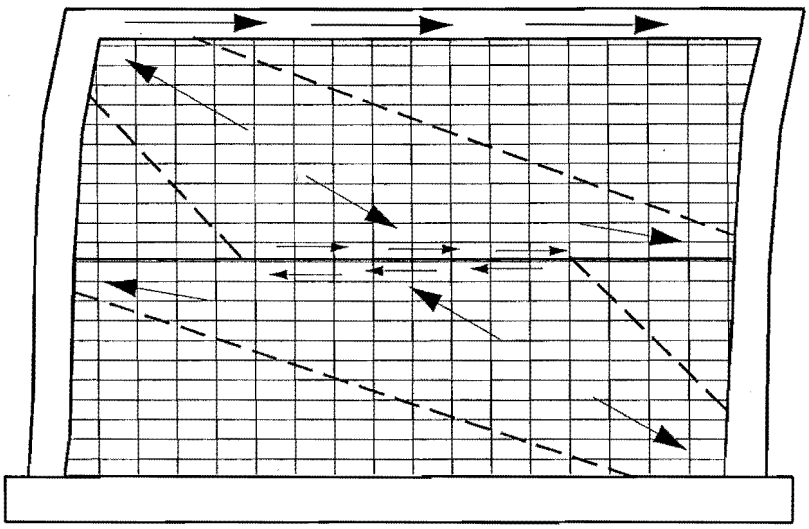

Fig.10.6 Approximate mechanism for describing the response of the infilled frame subjected to the horizontal sliding shear failure

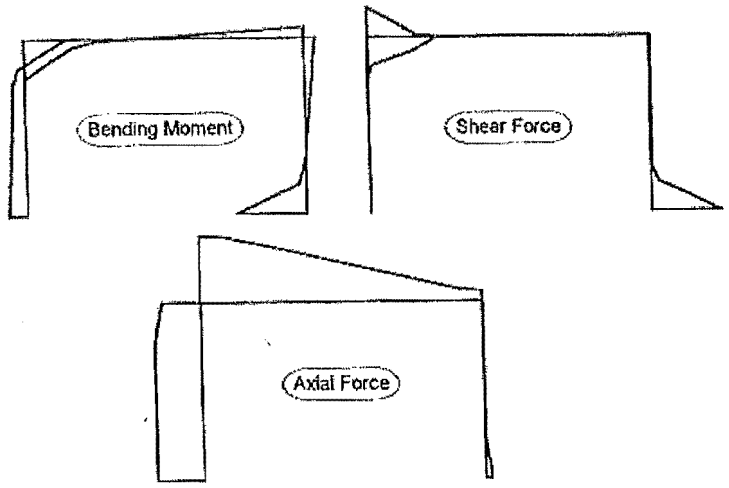

(a) Bending moment, shear and axial force diagrams for a typical infilled frame.

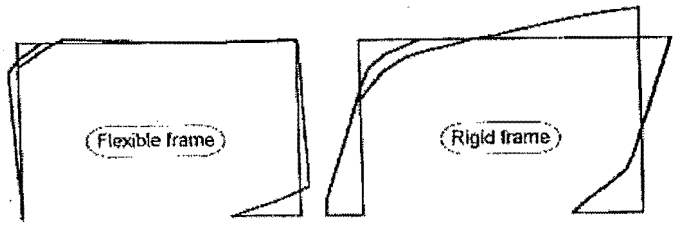

(b) Bending moment diagrams for flexible and rigid frame

Fig.10.7 Typical bending moments, shear and axial force diagrams obtained for the surrounding frame members, after separation occurs

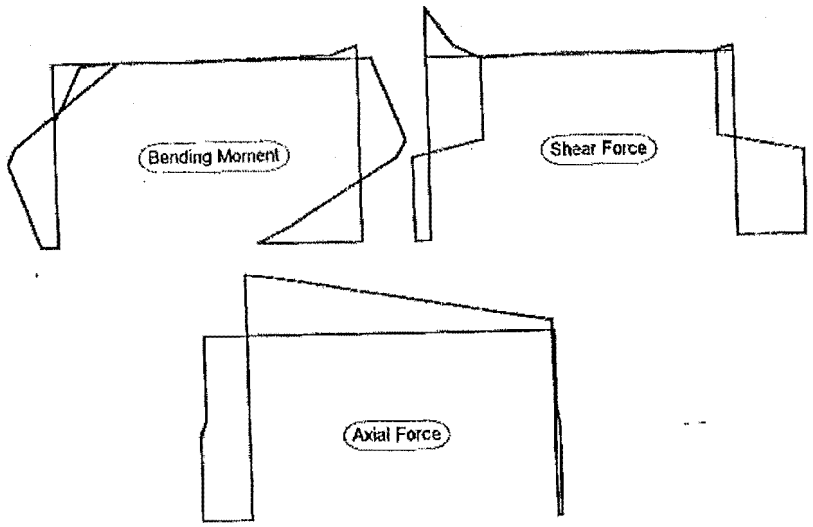

Fig.10.8 Typical bending moments, shear and axial force diagrams obtained for the surrounding frame members, after the formation of horizontal sliding shear crack

10.3.2.3 Macro-Model Methods

There are many macro-models available to model the masonry infilled frames and they can be classified into two categories, strut models, and strut and spring models.

Strut models aim at modelling the behaviour of masonry panels acting as compressive struts and they cannot deal with the shear failure in the masonry panels. Hence strut models cannot be used to study the effects of the horizontal sliding shear failure in masonry panels, which is supposed to be the case in this study, and they are not discussed in detail here.

Shear failure is more common when compared with the compressive failure in the masonry panels according to the discussion in section 10.3.1. A refined model, which aims at representing specifically the shear failure of the masonry panels, was proposed by Craisafulli et al [C5] and it is shown in Fig.10.9. This refined model consists of two struts and a shear spring in each direction and hence it can represent the shear behaviour and the compression behaviour of the masonry panels separately. The refined model has apparent improvement over the strut models.

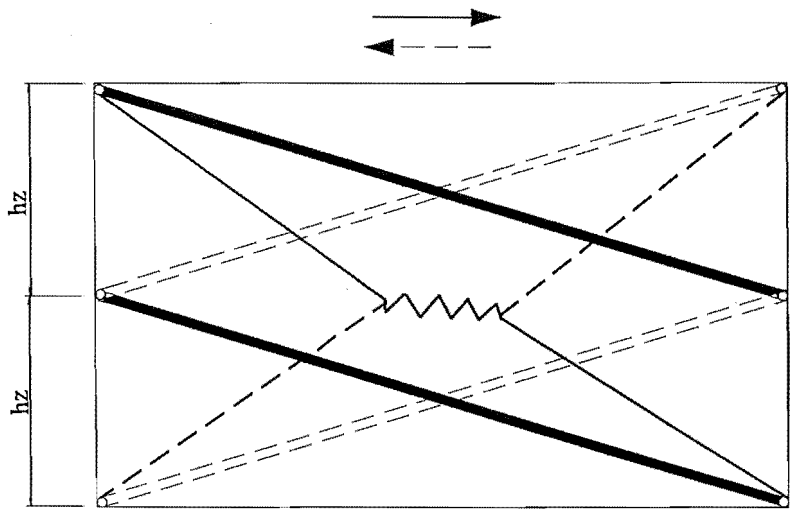

Fig.10.9 Refined mode for particular case of horizontal sliding shear failure [C5]

Crisafulli et al [C5] conducted the analysis on infilled reinforced concrete panels using the model illustrated in Fig.10.9. The study concluded that the response in the initial stage is primarily controlled by the shear spring. After the maximum shear strength in the masonry panels is reached, horizontal sliding shear failure starts and the mechanism changes,

resulting in significant increases in the actions induced in the frames. Therefore, the non-integral masonry infills of the subject structure can be represented by a shear spring to capture the effects of the horizontal sliding shear failure in masonry panels.

10.3.3 Modelling of the Subject Infilled Frame Structure

10.3.3.1 Assumptions

To model the subject structure after taking into account of masonry panels, the following two assumptions are made, apart from the assumptions made in chapter 9.

1. Modelling of the surrounding reinforced concrete frame members is exactly the same as that for the analysis of the bare frame in Chapter 9.

Beams and columns are treated as Giberson's one-component members. The determination of the skeleton curves for the beams and columns allows for the low attainment of the member flexural strength and the initial flexural stiffness due to severe bond degradation along the member longitudinal reinforcement.

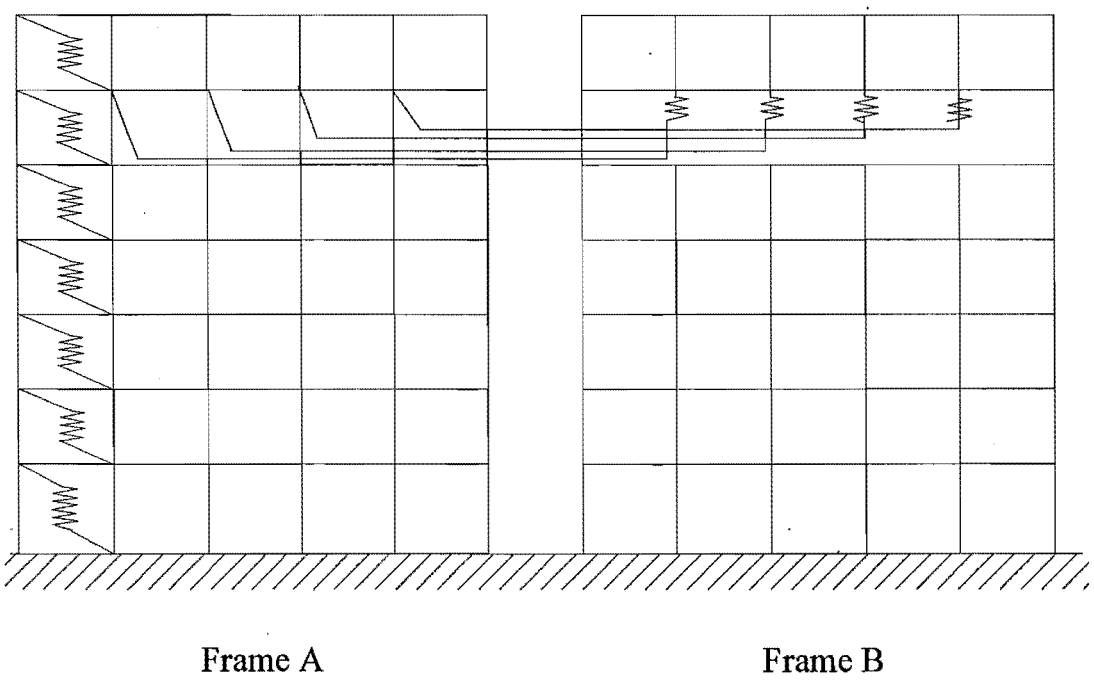

Fig.10.10 Structural Model for Analysis of Infilled Frame

2. The brick masonry panels in the external frame (frame A) are solid and the horizontal sliding shear failure in the masonry panels is assumed to be the dominant failure mode. This is because masonry panels are believed to be non-integral masonry panels and non-integral masonry panels are most likely to fail in a horizontal sliding shear failure. The seismic response is primarily controlled by the shear spring in the initial stage. After the shear strength is reached in the masonry panels, the horizontal sliding shear failure starts and the rapid strength degradation will occur due to the quick formation of the failure mechanism for the weak frame-strong infill system. Therefore, a shear spring, rather than the strut and spring model as shown in Fig.10.9, is used to represent the shear behaviour of the masonry panels.

Based on the above assumptions, the analytical model of the subject infilled frame is as shown in Fig.10.10.

10.3.3.2 Determination of Parameters for the Shear Spring

The shear spring is to represent the shear behaviour of non-integral brick masonry panels where the horizontal sliding shear failure is expected.

1. Force-deformation skeleton curve shape

Tests frequently demonstrate that the envelope of the hysteresis loops obtained from a cyclic test is very similar to the force-deformation relationship measured under a monotonic loading. Hence the force-deformation curve obtained from monotonic loading tests can be used as the skeleton curve of the hysteresis behaviour of the masonry panels.

Dawe and Seah [D3] tested an infilled non-integral steel frame and the horizontal sliding shear failure was observed. The monotonic response obtained for the infilled steel frame is illustrated in Fig.10.11.

Apparently, there are three stages, the initial uncracked stage (line O-A), the following behaviour with a slight decrease in stiffness until the peak force strength (line A'-B) and the final stage which leads to the collapse of the structural system (line B-C). The sudden drop from A to A' is a consequence of the relocation of the masonry panels after the first crack occurs and this effect is more significant for non-integral masonry infilled frames. Hence Klingner and Bertero [K7] concluded that the behaviour of the non-integral infilled frames until failure can be approximately assumed to be linear (O-A-A'-B).

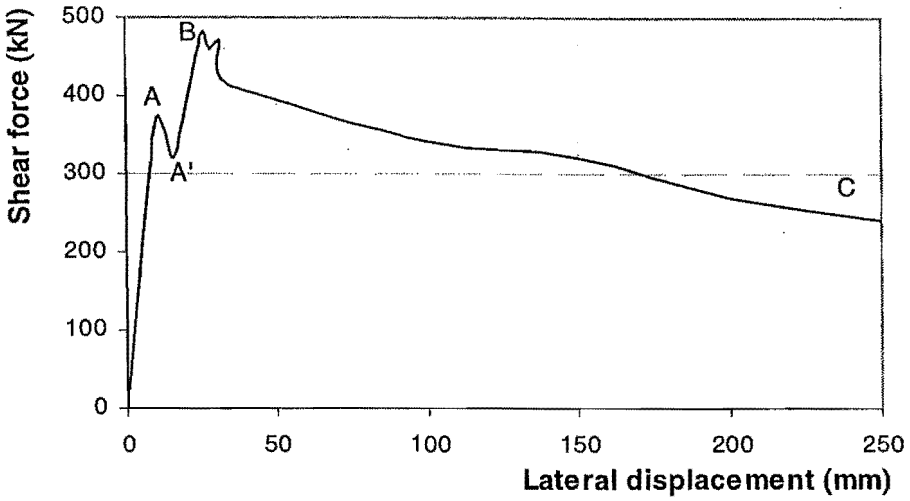

Fig.10.11 A typical force-displacement relationship for an non-integral infilled frame [D3]

In this study, the shear behaviour of non-integral masonry infills is assumed to be linear and the shear strength in the masonry infills is assumed to degrade rapidly after it reaches the maximum shear strength corresponding to the horizontal sliding shear failure. Hence, the skeleton curve for the shear spring is assumed to be as shown in Fig.10.12.

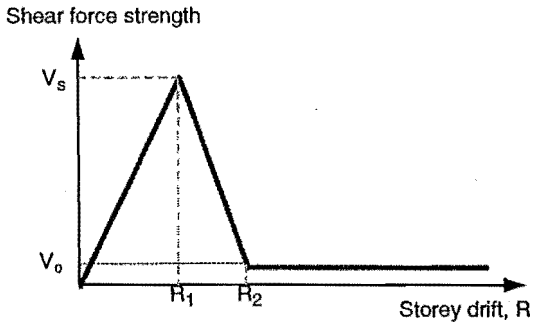

Fig.10.12 Skeleton curve for the shear spring of masonry infills

2. Determination of Characteristic Points of the Skeleton Curve for the Shear Spring

The characteristic points of the skeleton curve are the maximum shear force strength corresponding to the horizontal sliding shear failure in the masonry panels, V_s; the displacement level at developing the maximum shear force strength, R_1; the displacement level when the strength degradation finishes, R_2; and the residual strength V_o.

- Dimensions of masonry infills

For the subject structure, the masonry infills are two-layer brick masonry infills with 100 mm gap between two layers and the thickness of each masonry panel is 200 mm.

- Method for determining maximum shear force strength of the shear spring

Several methods have been developed to estimate the shear force strength when horizontal sliding shear failure initiates.

Assuming that the horizontal shear sliding failure initiates at the centre of the panel when the shear strength of the mortar joints is exceeded, Stafford Smith and Riddington [S12] found that the shear force to initiate the sliding shear cracking, V_s, is

$$V_s = \frac{\frac{\tau_o}{A_m}}{1.43 - \mu(0.8\frac{h_m}{L_m} - 0.2)} \qquad (10\text{-}1)$$

where A_m is the area of the masonry panel in the horizontal plane, τ_o is the bond shear strength, μ is a coefficient of friction, $\frac{h_m}{L_m}$ is the aspect ratio of the masonry panel.

Paulay and Priestley [P11] also proposed a method for estimating the shear strength at initiation of the horizontal sliding shear failure in the masonry panels as follows:

$$V_s = \frac{\tau_o A_m}{1 - \mu\frac{h_m}{L_m}} \qquad (10\text{-}2)$$

This approach allows for the clamping action of the vertical component of the diagonal compressive force in the strut and hence it is more rational.

Crisafulli [C5] also suggested a method for estimating the stiffness of the shear spring in the refined strut and spring model.

$$K_s = r_s \frac{A_{ms} E_m}{d_m} \cos^2\theta \qquad (10\text{-}3)$$

However the principle Equation 10-3 is based on is that the stiffness of the shear spring, K_s, is assumed to be a fraction r_s of the total stiffness of the masonry strut and it does not reflect the actual shear behaviour of the masonry panels.

Therefore, the method proposed by Paulay and Priestley is used for estimating the ultimate shear force strength of the shear spring.

- Determination of bond shear strength τ_o and the coefficient of friction μ

In using equation 10-2 to calculate the maximum shear strength of masonry panels, the bond shear strength, τ_o, and the coefficient of friction, μ, need to be determined first.

The mechanism of bond is incompletely understood although much research has been carried out on this aspect. According to Henrry's tests, this parameter can vary from 0.3 to 0.6MPa. Paulay and Priestley [P11] indicate that typical values of the bond shear strength range from 0.1 to 1.5 MPa. In this study, the bond shear strength is taken as 0.5MPa.

Similarly, the measured coefficient of friction, μ, varies widely and the factors affecting the coefficient of friction have not been clearly understood. The measured values of this coefficient range from 0.10 to 1.2 [C5]. Paulay and Priestley proposed the use of a value of μ =0.3 for design purposes.

In this study, μ = 0.5 is used because the values used for seismic design tend to be very conservative.

- Force strength reduction factors to allow for the effects of openings and non-integral interfaces between the masonry panels and frames

When using the approach proposed by Paulay and Priestley for estimating the maximum force strength of the shear spring, a strength reduction factor needs to be introduced to allow for the lower strength due to the openings and to the non-integral masonry panels.

Many tests have been conducted on integral and non-integral infilled reinforced concrete frames around the world and Crisafulli [C5] summarised the test results from different sources. The summarised test results are shown in Table 10-1.

From Table 10-1, it can be found that the maximum strength for non-integral infilled frames is 80% to 86% of that of integral masonry panels. Hence, a strength reduction factor of 0.8 is introduced to allow for the lower force strength attainment by the non-integral infilled frames.

Table 10-1 Statistical evaluation of test results for non-integral infilled frames

Type of infilled frame	ϕ		ϕ_{res}		δ_u		μ_Δ	
	MV	CV	MV	CV	MV	CV	MV	CV
No local damage in frame								
Integral masony infills	3.34	0.43	3.92	0.21	1.14	1.25	5.80	0.52
Non-integral masonry infills	3.80	0.40	2.01	0.15	3.66	0.59	4.88	0.35
Local damage in frame								
Integral masony infills	1.44	0.10	1.44	0.10	2.55	0.55	4.66	0.27
Non-integral masonry infills	1.79	0.26	1.49	0.05	0.88	0.98	7.07	0.71

ϕ : ratio of the shear resistance of the infilled frame to the shear resistance of the bare frame

ϕ_{res} : ratio of the residual resistance of the infilled frame, at δ=2-3%, to the residual resistance of the bare frame.

δ_u : storey drift corresponding to the maximum force, V_u.

μ_Δ : displacement ductility defined at $V = 0.85\ V_u$.

MV : mean value

CV : coefficient of variation

Openings in masonry panels affect the force transfer across the panels and hence affect the force strength of the masonry panels. Studies show that the dimensions and the positions of the openings in the panels are the most important factors in evaluating the influences of the openings on the masonry panels' behaviour. Study conducted by Durrani and Luo [D4] shows that the transfer of the shear force is possible with a diagonal strut mechanism for relative small openings. However, for large openings, the strut mechanism could not develop. Mallick and Garg [M8] studied the effect of opening position and concluded that stiffness and especially the lateral strength reduce when the opening is located along the loaded diagonal. They found that, in the most unfavourable case where the opening was provided in one of the loaded corners, the lateral strength was about 50% of that of a solid panel.

For the subject building, the openings in the masonry panels of the exterior frame are relatively small and located away from the corners. Hence the shear strength of the masonry panels in this study are taken as 80% of the corresponding shear strength for solid masonry panels.

In summary, the combined effect of openings in the masonry panels and the non-integral interfaces between the frames and masonry panels gives a force strength reduction factor

of 0.64. The maximum force strength of the shear spring is 64% of that given by Equation 10-2.

- Storey drift level at attainment of maximum shear force strength

Table 10-1 shows that the surrounding frame markedly influences the storey drift at failure, and the storey drift at failure can vary significantly, depending on whether there is damage to the surrounding frame and whether the masonry panels are integral or non-integral infills. For the subject frame structure, the frame structure is relatively weak and the confinement provided by the frame for the masonry infills is not expected to be very strong, therefore, the local damage to the frame is expected. In this case, the storey drift at the maximum shear strength of the masonry panels can be assumed to be $R_1 = 0.9\%$.

- Stiffness and strength degradation after attainment of the shear force strength in masonry panels

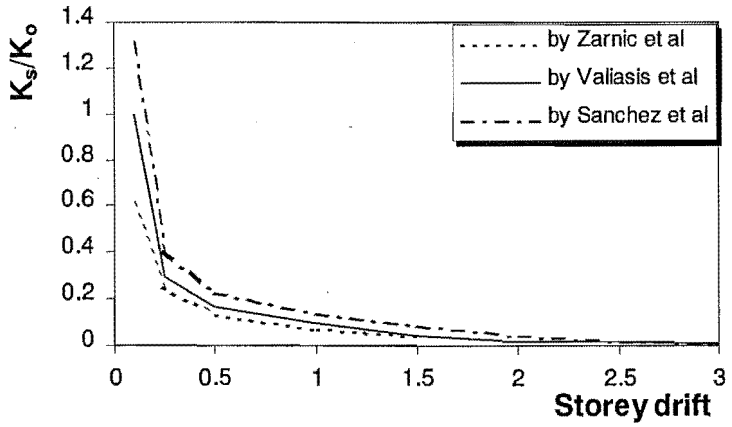

Fig.10.13 Stiffness degradation as a function of storey drift

As a consequence of the damage to the masonry infills and the deterioration of infills and frame interfaces, the attained stiffness significantly decreases as the lateral displacement increases. Fig.10.13 shows the variation of the secant stiffness as a function of the storey drift, δ. The test results for plotting Fig.10.13 are cited by Crisafulli [C5] from the tests on masonry infilled reinforced concrete frames, reported by Sanchez etal, Valiasis and Stylianidis and Zarnic and Tomazevic. The secant stiffness was calculated from peak to

peak on the hysteresis plots and normalised with a reference stiffness K_o defined at a δ = 0.05%, which is corresponding to the separation of the infill panel from the surrounding frames. Rapid stiffness reduction shown in Fig.10.13 after the separation of the infill panels from the surrounding frames suggests rapid strength degradation after the attainment of the maximum shear strength and hence it is assumed that, at a storey drift of 1.5%, the attained force strength drops to the 20% of the maximum force strength, namely, R_2 = 1.5%.

Detailed information on the parameters of the shear springs is summarised in Table 10-2. Slight difference in the maximum shear force strength of each panel, V_s, is either due to the slight difference in the net span lengths or due to the slight difference in the storey height.

Table 10-2 Parameters for the shear springs

Storey No		h_m/L_m	A_m (m^2)	τ_o (MPa)	μ	R	V_s (kN)	$\sum V_s$ (kN)
1	Interior panel	0.878	0.740	0.5	0.3	0.64	321.5	1599
	Exterior panel	0.898	0.724				317.1	
2 to 7	Interior panel	0.730	0.740				303.0	1506
	Exterior panel	0.746	0.724				298.5	

V_s = the maximum shear force strength of one panel and
$\sum V_s$ = the total shear force strength of the whole storey

10.3.4 Results of Non-Linear Static Analysis of Masonry Infilled Frames

10.3.4.1 Structural Force Strength and Deformation Capacities

A non-linear static analysis was conducted for the subject infilled frame structure. Fig.10.14 shows the structural strength and deformation capacity curve for the infilled frame structure, in terms of base shear and roof drift. Fig.10.14 also shows the force strength and deformation capacity curve under monotonic loading for the corresponding bare frame structure, which allowed for the contribution of masonry infills to the seismic weight but not to the stiffness and was reported in Chapter 9.

The maximum strength of the infilled frame, in terms of base shear, was 2452kN, which was equal to a basic seismic acceleration coefficient of 0.13. At the maximum strength of the infilled frame, the roof drift was 0.7%.

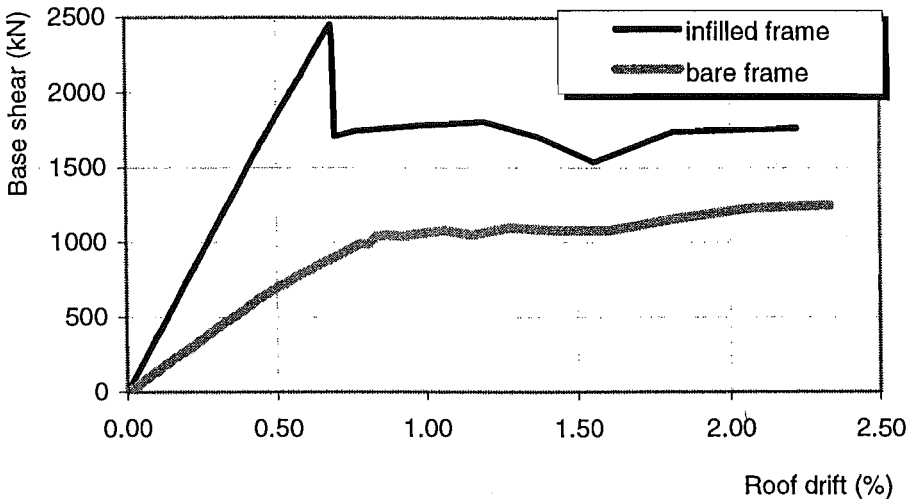

Fig.10.14 Structural Monotonic Force Strength and Deformation Capacity

In Fig.10.14 it is evident that the structural stiffness and strength performance was significantly improved when the masonry infills were considered to not only contribute to the seismic weight but also to the structural stiffness. When compared with the available strength of the bare frame, the maximum strength of the infilled frame, in terms of base shear, was doubled within the practical deflection range, and the initial structural stiffness in terms of base shear versus roof displacement, was nearly tripled. The code-specified deflection limit is about 1.5% in terms of roof drift, as discussed in Chapter 9.

It is very common in conventional structural analysis that masonry infills are treated as non-structural elements, and therefore masonry infills are not allowed for in estimating the structural stiffness. Apparently this could lead to significant errors in predicted structural stiffness and strength performance, especially the stiffness.

Another pronounced characteristic observed for the infilled frame is that, unlike the performance for the correspondent bare frame where the structural deformation capacity was large, the infilled frame demonstrated much smaller deformation capacity and it performed in a very brittle manner. This was due to the combined effect of the relatively weak frame and the non-integral construction technique for the masonry infills. Due to the

relatively weak frame, the confinement by the surrounding frame was not sufficient to maintain the integrity of the masonry infills after the horizontal sliding shear failure occurred. Due to the non-integral characteristic of the masonry infills, the performance of the masonry panels degrades significantly after the horizontal sliding shear failure starts in the masonry infills.

10.3.4.2 Structural Demands

The modal analysis of the infilled frame gives the fundamental period of vibration of T_1 =1.16 (s). This is much shorter than T_1 = 1.86 (s) for the corresponding bare frame. The analysis of the corresponding bare frame only allowed for the contribution of masonry panels to the seismic weight.

The design horizontal seismic shear force for the ultimate limit state, acting at the base of the structure in the direction being consideration, can be calculated using equation 9-4, according to NZS4203: 1992.

For the infilled frame, this gives a seismic design shear force of 6380 kN in terms of base shear for an intermediate soil site and μ_Δ = 1.25 which is for elastically responding reinforced concrete structures, and a seismic design shear force of 4128 kN in terms of base shear for an intermediate soil site and $\mu_\Delta = 2$.

In Fig.10.14, it can be seen that no structural ductility can be relied on. The available strength is 2452 kN in terms of the horizontal base shear and the design seismic force is 6380 kN in terms of required horizontal base shear force for an intermediate soil site and assuming an elastic structural response. Hence the ratio of the available structural force strength to the seismic force demand is only 38% for the infilled frame. For the bare frame analysis, which only allows for the contribution of masonry infills to the seismic weight but not to the stiffness, the available structural strength assuming elastic response of the structure is 47% of the seismic force demand. Hence, allowance for the masonry infills in estimating the structural stiffness and strength behaviour, although leading to much increased structural stiffness and strength, results in less inadequate structural seismic performance, when compared with the case where the masonry infills are only considered to contribute to the seismic weight but not to the stiffness. This was a consequence of much enhanced structural stiffness and therefore much increased seismic design force.

10.3.4.3 Maximum Inter-storey Drift

Fig.10.15 shows the maximum inter-storey drifts when the roof drift was 0.7% where the strength in terms of base shear dropped suddenly (see Fig.10.14). In Fig.10.15, the maximum inter-storey drift, which occurred in the 1st storey, is 0.9% and this corresponds to the specified stage where the shear strength of the masonry infills is attained and then starts to degrade significantly. Therefore, the rapid drop in the observed structural strength of the infilled frame at a roof drift of 0.7% was because of the horizontal sliding shear failure in the masonry panels of the first storey.

Although the infilled frame has no interior columns for the interior frame B at the level 6, the inter-storey drift in level 6 had been relatively very small, compared to the 1st and 2nd levels. For the bare frame analysis, the maximum inter-story drift was in the 3rd storey at the beginning and it then shifted to level 6 where no interior columns exist for interior frame B. This indicates that the critical part of the infilled frame is most likely in the first level. Once the sliding shear failure in the masonry panels occurs at the first level, a soft-storey mechanism forms and the frame building is effectively base-isolated.

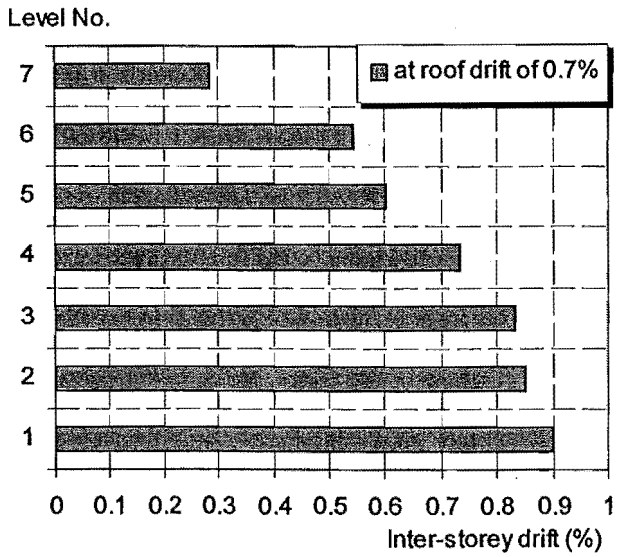

Fig.10.15 Inter-storey drift at roof drift of 0.7%, obtained for the Infilled Frame

10.3.4.4 Failure Mechanism

From Fig.10.14, it is seen that the infilled frame behaved linearly until the failure of masonry infills in the first level. After the horizontal sliding failure of masonry infills in the 1st level at the roof drift of 0.7%, the available force strength dropped significantly. Therefore, the stage at the roof drift of 0.7% can be defined as the structural failure stage.

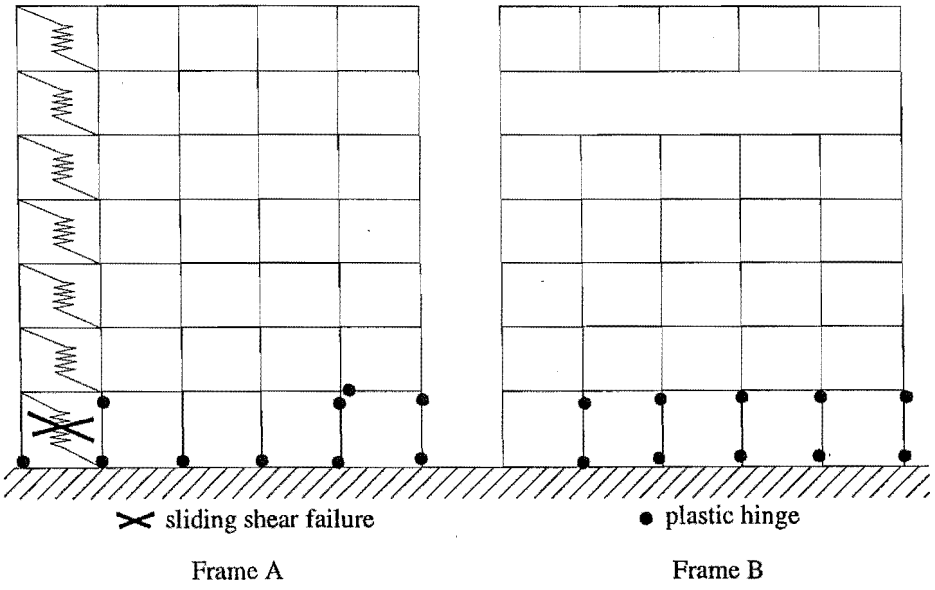

(a) at the attainment of maximum force strength

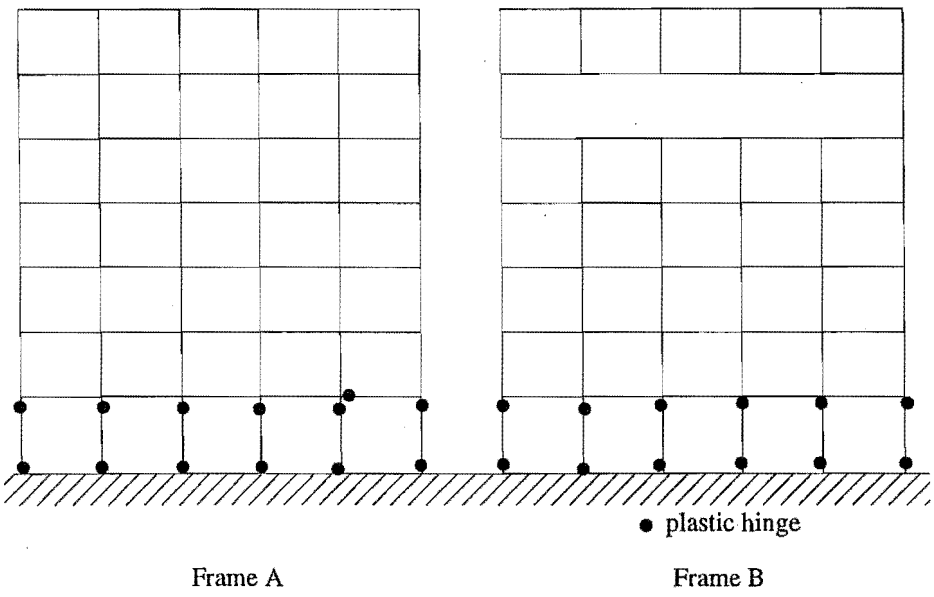

(b) after horizontal sliding shear failure

Fig.10.16 Failure mechanism of the infilled frame

The mechanism formed after the horizontal sliding shear failure at roof drift of 0.7% is shown in Fig.10.16, and it is a soft-storey column failure mechanism. Hence, unlike the bare subject frame structure where the structural response was terminated by the local member deformation capacity and a failure mechanism is very unlikely to form before the code-specified deflection criteria is reached, the structural response of the subject infilled frame structure was terminated by the formation of a soft storey failure mechanism.

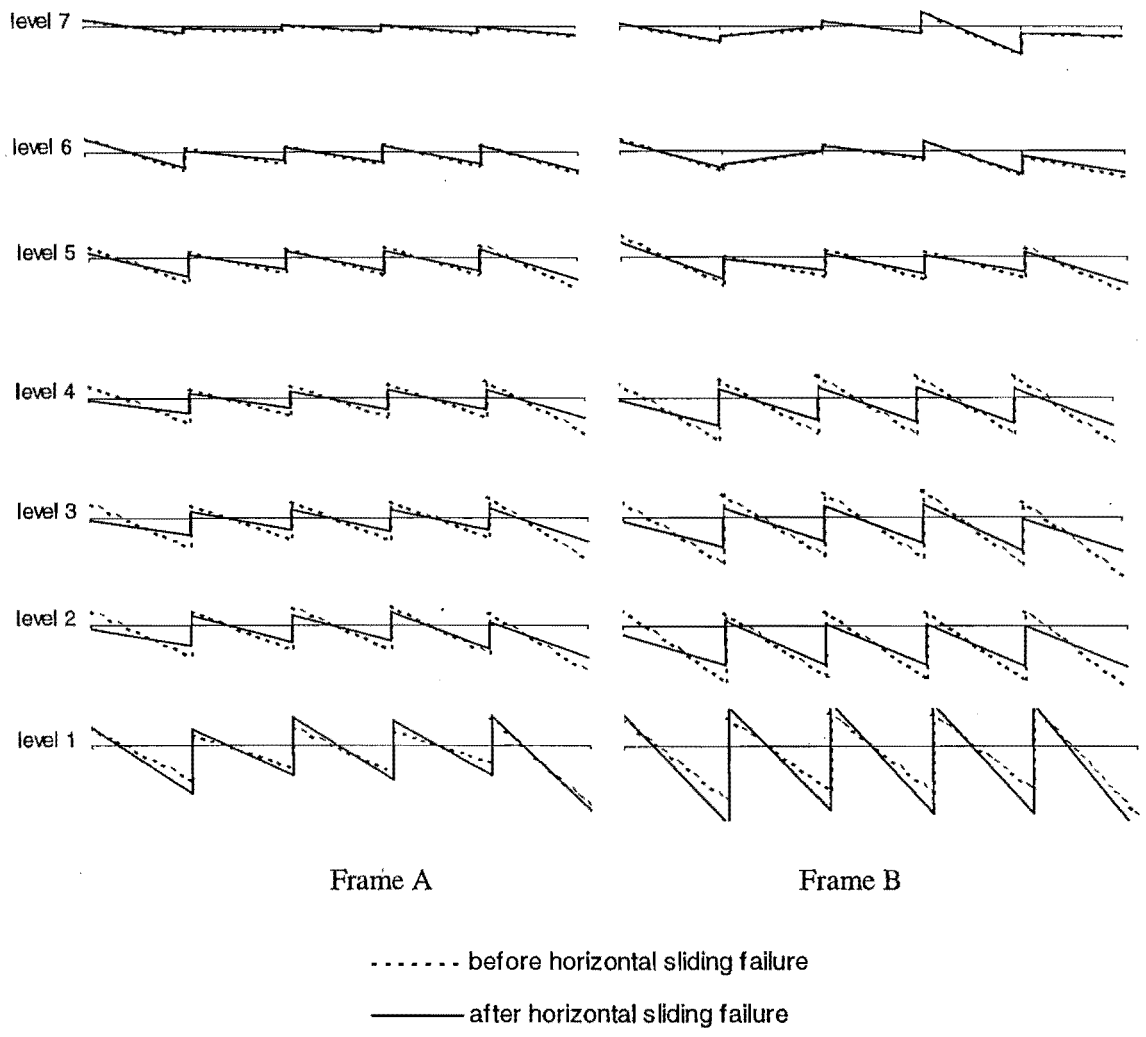

Fig.10.17 Bending moments of the beams before and after horizontal sliding shear failure

10.3.4.5 Bending Moment Profiles of Frame Members

Fig.10.17 shows the changes of induced bending moments in the beams of the infilled frame, just before and immediately after horizontal sliding shear failure in the masonry

panels. Fig.10.18 shows the changes of induced bending moments in the column members of the infilled frame due to the horizontal sliding shear failure in the masonry panels.

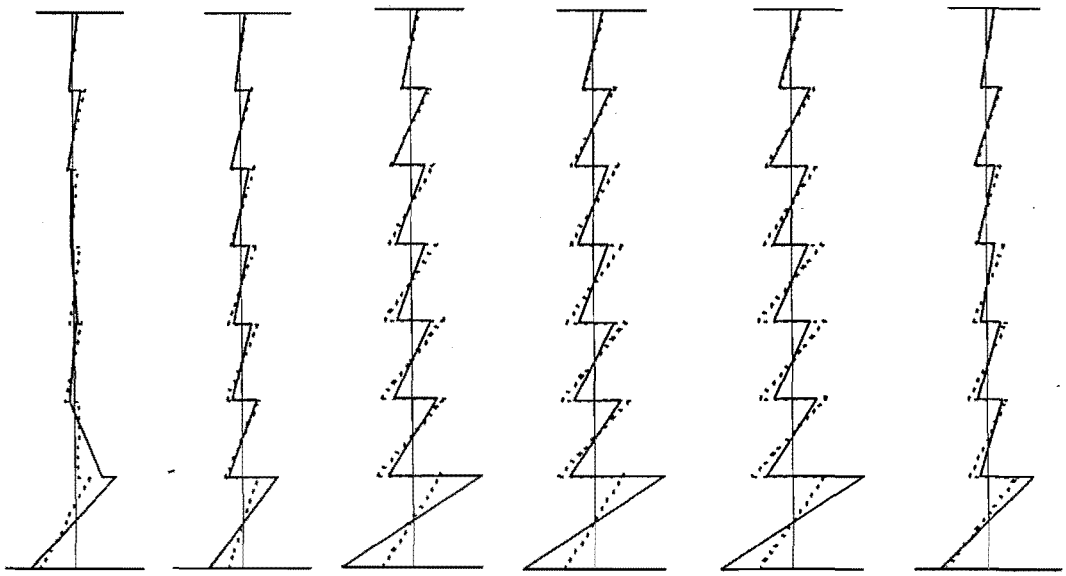

(a) Frame A

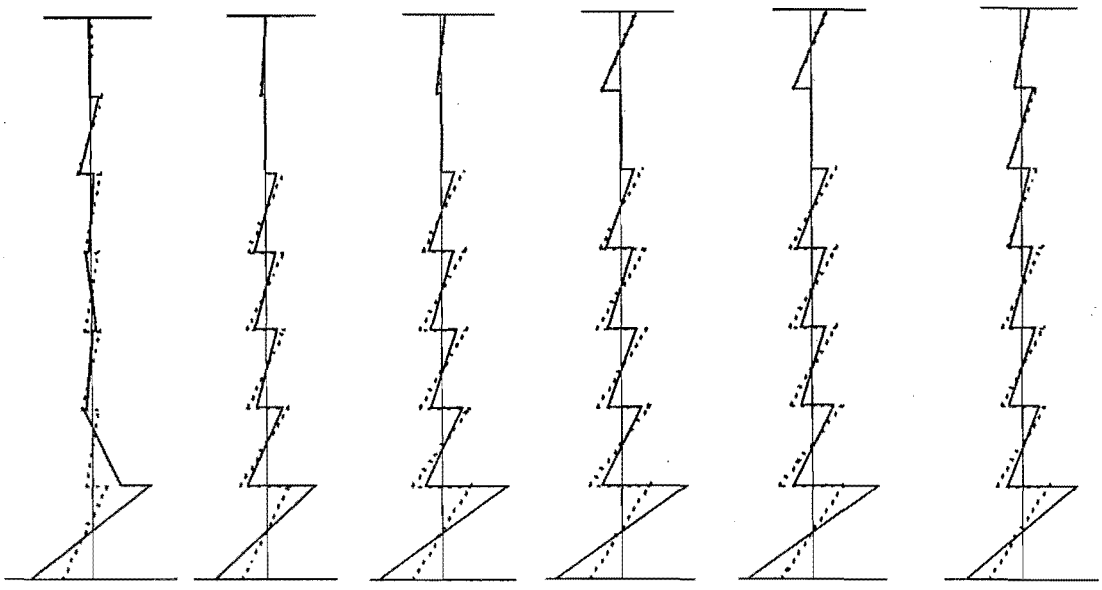

(b) Frame B

Fig.10.18 Bending moments of frame columns prior to and after horizontal sliding shear failure

From Fig.10.17 and 10.18, it is clear that the increase in the induced bending moment, due to the horizontal sliding shear failure in the masonry panels, concentrated in the frame members of the first storey. Meanwhile the frame members in other stories experienced a reduction in the induced bending moments, after the horizontal sliding shear failure occurred. This phenomenon is similar to the base isolation mechanism aimed at reducing the structural seismic responses.

Evidently, the most critical failure mechanism for the infilled frame structure is the soft-story column mechanism in the first storey when non-integral masonry infills exist. For a soft-story mechanism, no ductility can be relied on and the elastic performance has to be assumed.

10.4 CONCLUSIONS

A non-linear static analysis was conducted for the infilled frame structure. The infilled frame structure was otherwise identical to the subject structure except that the infilled frame allowed for the contribution of the masonry infills to the structural stiffness. The masonry infills were non-integral brick masonry panels and were of two-layers thick. Masonry infills were only present in the exterior frames. A brief review of the observed seismic behaviour of masonry infilled frame structures and the masonry panels clarified that the non-integral masonry infills are most likely to fail in horizontal sliding shear failure. Following a review of existing analytical approaches of the infilled frames, a shear spring was used to represent the shear behaviour of the masonry infills. A non-linear static analysis of the infilled frame led to the following conclusions:

1. When the infilled frame structure contained non-integral masonry infills, the most critical failure mechanism was the soft-storey column failure mechanism. The formation of the soft-storey column failure mechanism was due to the horizontal sliding shear failure in the masonry infills, which led to significant increase in the induced bending moments of the frame columns at that specific floor level. This suggests that the non-integral masonry infilled frame has a small deformation capacity and it is not expected to behave in a ductile way in a major earthquake. The available structural displacement ductility cannot be greater than 1.25.

2. Consideration of the contributions of masonry infills to the seismic weight and the stiffness resulted in an increased seismic demand and also the enhanced structural seismic capacity. The combined effect for this studied infilled frame was that the inclusion of masonry infills in estimating the structural stiffness gave a degraded structural capacity, in terms of the ratio of the available structural capacity to the design seismic demand. This indicated that the consideration of non-integral masonry infills as non-structural elements, therefore no allowance for the masonry infills in estimating the structural stiffness and the seismic weight, would be non-conservative.

3. In conducting a non-linear static analysis for an existing reinforced concrete infilled frame, it is adequate to use a shears spring to represent the shear behaviour of the non-integral masonry panels, which are most likely to fail in horizontal sliding shear failure. Prior to the horizontal sliding shear failure in the masonry panels, the behaviour of the masonry infills is dominated by the shear behaviour and this can be adequately represented by a shear spring. After the horizontal sliding shear failure occurs in the non-integral infills, the soft storey column failure mechanism will form and the structural analysis after this point is of little interest.

CHAPTER 11

CONCLUSIONS AND RECOMMENDATIONS FOR FUTURE RESEARCH

11.1 GENERAL

In a major earthquake, the structural deformation is usually well beyond the elastic range. Hence, the seismic assessment of an existing reinforced concrete structure focuses on examining the global post-elastic responses of the structure. The global post-elastic response of a structure is determined by the local post-elastic behaviour of the reinforced concrete components.

In this study, simulated seismic loading tests were conducted on as-built beam-column joint subassemblages in order to study the characteristics of the post-elastic behaviour of existing reinforced concrete members and obtain the information on modelling the local post-elastic behaviour of as-built reinforced concrete members. After employing the information on the post-elastic behaviour of individual reinforced concrete members obtained from this experimental programme, the seismic assessment of existing reinforced concrete structures designed to pre-1970s seismic design codes was carried out by conducting the non-linear analysis on an existing reinforced concrete frame structure constructed in the late 1950s in New Zealand. The emphasis of this study was placed on the effect of the plain round longitudinal bars used on the seismic performance of existing reinforced concrete structures.

Simulated seismic loading tests included two as-built full-scale interior beam-column joint units, four as-built full-scale exterior beam-column joint units and one retrofitted as-built exterior beam-column joint unit. The as-built test units contained the plain round longitudinal reinforcement and had the reinforcing details typical of an existing reinforced concrete structure constructed in the late 1950s in New Zealand. The two as-built interior beam-column joint units, Unit 1 and Unit 2, were identical, Unit 1 was tested with zero column axial load and Unit 2 was tested with a compressive column axial load of $0.12A_g f_c'$. The four as-built exterior beam-column joint units, Units EJ1 to EJ4, were identical except for the beam bar hook details in the exterior columns. Units EJ1 and EJ3

were identical and had the beam bar hooks bent away from the joint cores. They were tested respectively with zero column axial load and a compressive column axial load of $0.25A_gf_c'$ present. Units EJ2 and EJ4 were also identical and had the beam bar hooks bent into the joint cores. They were tested with zero column axial load and a compressive column axial load of $0.23A_gf_c'$ respectively. The retrofitted unit was the original as-built exterior beam-column joint unit with the beam bar hooks bent away from the joint core, and the retrofit was achieved by wrapping the column areas immediately above and below the joint core with fibre-glass to verify an alternative force path across the joint core. From the simulated seismic loading tests on as-built units, the characteristic of the local non-linear behaviour of as-built reinforced concrete components was investigated and the proper method for assessing the seismic behaviour of as-built reinforced concrete components was proposed. From the test on the retrofitted unit, the effectiveness of wrapping the columns adjacent to the joint core with fibre glass in actuating the alternative joint force path was studied.

For the non-linear analysis of the existing reinforced concrete frame building, the analytical models used were developed on the basis of the information on the post-elastic behaviour of existing reinforced concrete members obtained from the current test programme, and both non-linear static and dynamic analyses were conducted using the inelastic structural analysis program "RUAUMOKO" developed at the University of Canterbury [C4]. As a result, the likely seismic performance of pre-1970s reinforced concrete structures was evaluated. In addition, the non-linear static analysis of the corresponding infilled frame was conducted and the possible effects of non-integral brick masonry infills were studied.

Conclusions from this study and recommendations for future research are presented below.

11.2 CONCLUSIONS FROM SIMULATED SEISMIC LOADING TESTS

11.2.1 As-Built Interior Beam - Column Joint Units

1. The tests on Units 1 and 2 showed that the overall performance of the units was very poor, and it was dominated by the degrading flexural behaviour at the fixed-ends of the members, rather than by the premature shear failure as predicted by the code method. Due to the occurrence of severe bond degradation along the plain longitudinal

reinforcement and only small amount of column transverse reinforcement provided within and adjacent to the joint core, the compressive column axial load of $0.12A_g f_c'$ for Unit 2 caused significant column bar buckling within and adjacent to the joint core. As a result, the compressive column axial load for Unit 2 did not improve the system's stiffness performance and caused the strength to be reduced if it is expressed as the percentage of the theoretical strength.

The measured initial stiffness was about 40% of the theoretical predictions at first yield for both Unit 1 and Unit 2. The measured storey shear strength was about 90% and 67% of the theoretical predictions for Unit 1 and Unit 2 respectively. The theoretical stiffness and strength were determined based on the plane section assumption. Due to the very low measured initial stiffness, a storey drift index, rather than ordinary displacement ductility, becomes a proper index for the overall deformation capacity.

2. In respect to the seismic performance of as-built reinforced concrete members containing plain round longitudinal reinforcement, both tests showed that the post-elastic performance of the members was governed by the degrading flexural behaviour at the fixed-ends, rather than by the premature shear failure as indicated by the code method. Severe bond degradation along the plain round longitudinal reinforcement suppressed the premature shear failure but led to significant degradation of the flexural behaviour at the fixed-ends of the as-built members. Hence, the modelling of the post-elastic behaviour of existing reinforced concrete components focuses on the degradation of the flexural behaviour at the member fixed-ends.

Due to severe bond degradation along the longitudinal reinforcement, the plane section assumption was significantly violated. As a result, conventional flexural theory based on the plane section assumption overestimates the attained member flexural strength by 10% to 20% and underestimates the member flexural deformation at first yield by about 60%. Hence, the flexural stiffness and strength behaviour of existing reinforced concrete members with plain round longitudinal reinforcement would be less than the theoretical prediction based on the plane section assumption

However, bond degradation and bar slip along the longitudinal reinforcement greatly enhanced the shear force capacities associated with the compressive concrete strut mechanism in resisting shear for both the linear reinforced concrete members and the joints, resulting in much enhanced shear performance in the members and the joints.

Although the code method and/or the method recommended in Reference 6 predicted a very inadequate shear performance for the beams of Unit 2, the columns of Unit 1 and the joints of both units, no shear distresses were observed for both units. Hence, the shear behaviour of the existing reinforced concrete members with plain round longitudinal reinforcement would be much better than the theoretical prediction. The current code method and the method suggested in the current seismic assessment procedures could not give adequate result when used for predicting the shear performance.

3. One characteristic of the observed flexural behaviour for the existing reinforced concrete members was that the member deformation was concentrated at its fixed-ends at the beam-column interfaces due to severe bond degradation along the member longitudinal reinforcement within and adjacent to the joint core.

Therefore, in modelling the post-elastic flexural behaviour of as-built reinforced concrete members, which was limited to the fixed-ends of the members, the rotational ductility at the fixed-ends, rather than the curvature ductility associated with a certain plastic hinge length, becomes a proper index for the member non-linear deformation.

4. When plain round reinforcing bars are used, the transverse reinforcement requirements for preventing the bars from buckling and for confining the compressed concrete are very critical, rather than the requirement for resisting shear.

5. The test on Unit 1 was compared with the otherwise identical test but with deformed longitudinal bars, Hakuto's Unit O1, showed that the use of plain round longitudinal reinforcement suppressed the shear failure in the joint core, but led to lower attainment and poor maintenance of the flexural strength and the stiffness, especially the stiffness. The measured initial stiffness for Unit 1 was equivalent to 60% of that for Hakuto's O1 and the strength measured for Unit 1 reduced by about 10% when compared to that with deformed bars.

6. Compressive column axial load would not have beneficial effect on the joint shear performance if there is very small amount of column transverse reinforcement within and adjacent to the joint cores and the plain round longitudinal reinforcement is used, as was observed in the comparison between the results of Unit 2 and Unit 1.

11.2.2 As-Built and Retrofitted Exterior Beam - Column Joint Units

1. Seismic assessment of the as-built exterior beam-column joint units EJ1 to EJ4 using the current code method and the capacity design based assessment method showed that the beam and column transverse reinforcement was inadequate for all of the tests, according to the requirement for preventing the longitudinal reinforcement from buckling and confining the compressed concrete, and/or the requirement for providing shear force strengths. The beam shear force capacity for all the units was only 20% of the shear demand at the stage of developing the theoretical flexural strength of the systems, according to the New Zealand code NZS3101: 1995. The shear resisting capacity of the beam-column joint core of Unit EJ1 was only 38% of the shear demand at developing the theoretical flexural strength of the unit, which had the beam bar hooks bent away from the joint core and was tested with zero axial column load.

The examination of the member force transfer across the joint core showed that, when plain round longitudinal reinforcement was used and the beam bar hooks were bent away from the joint cores as for Units EJ1 and EJ3, it was very critical to transfer the member forces across the joint core if the amount of the column transverse reinforcement adjacent to the joint core was small as for Units EJ1 and EJ3. Concrete tension cracking failure initiated by the opening of the beam bar hooks could occur due to insufficient column transverse reinforcement within the beam bar hook ranges and the utilisation of plain round longitudinal reinforcement. Different beam bar hook details would actuate different joint force transfer paths and therefore emphasise the need for column transverse reinforcement at different locations.

Simulated seismic loading tests on Units EJ1 and EJ2, which were conducted with zero axial column load present

2. When the units were tested with zero column axial load, the overall seismic performance of the as-built exterior beam-column joint subassemblages was very poor. In this case, the final failures of the systems were dominated by premature concrete tension cracking along the beam bar hooks, which was initiated by the interaction between the column bar buckling and the opening action of the beam bar hooks, irrespective of the beam bar hook details. Different arrangements of the beam bar hooks in the exterior

columns had a significant influence on the structural strength and stiffness performance when the axial column compressive load was low.

The storey shear strength attained by the unit with the beam bar hooks bent away from the joint core was only 55% of the theoretical storey shear strength of the unit. In contrast, the storey shear strength attained by the as-built exterior beam-column joint unit with the beam bar hooks bent into the joint core was about 75% of the theoretical storey shear strength of the unit. The enhancement in the available strength due to more adequate beam bar hook configuration was as high as 20% of the theoretical storey shear strength when the axial column load was very low. The stiffness in the elastic loading range for Unit EJ2, which had the beam bar hooks bent into the joint core, was about 1.4 times the stiffness for Unit EJ1, which had the beam bar hooks bent away from the joint core.

3. When the column axial load was low, the transfer of the beam steel force across the joints was mainly at the beam bar bend. Different beam bar hook details in the exterior columns actuated different force paths across the joint cores and enhanced the need for column transverse reinforcement at different locations. When the beam bar hooks were bent away from the joint core, the transfer of the member forces across the joint core was mainly by a steeper concrete strut and the column stirrups immediately above and below the joint core played an important role in controlling the opening of the beam bar hooks and actuating the proposed alternative force path across the joint core. When the beam bar hooks were bent into the joint core, the transfer of the member forces across the joint core was mainly by the corner to corner concrete strut and the shear reinforcement at the joint centre was more effective in controlling the opening of the beam bar hooks and actuating the corner to corner concrete strut mechanism.

4. Compared with similar tests but reinforced by deformed bars, the use of plain round longitudinal reinforcement totally suppressed the shear failure in the beam and the joint core, but enhanced the premature failure of concrete tension cracking along the beam bar hooks when the column axial load is low. As a result, the attainment and maintenance of the strength and the stiffness were poor, especially the stiffness.

When compared with the case with deformed longitudinal bars, the decrease in the attained storey shear strength due to the use of plain round longitudinal reinforcement was 20 to 25% of the theoretical strength of the units, when the units were tested with zero axial column load. The decrease in the initial stiffness due to the plain round longitudinal

reinforcement used was about 70% for the exterior beam-column joint unit with the beam bar hooks bent into the joint core. Apparently, the plain round reinforcement used caused a much more significant decrease in the initial stiffness, in comparison to the adverse effect on the storey shear strength of the unit. The adverse effect of plain round longitudinal reinforcement used on the initial stiffness was more significant for the as-built exterior beam-column joint units than was for the as-built interior beam-column joint units.

Simulated seismic loading tests on Units EJ3 and EJ4, which were conducted with the compressive column axial load of 0.23 to 0.25 $A_g f_c^{'}$ present

5. The presence of compressive axial column load for Units EJ3 and EJ4 greatly improved the seismic performance of the as-built exterior beam-column joint units, and the post-elastic behaviour of the units in this case was governed by the degrading beam flexural behaviour at the fixed-end, rather than by the premature concrete tension cracking along the beam bar hooks as for the tests on Units EJ1 and EJ2. Different beam bar hook details made no apparent difference in the seismic performance of the systems.

The compressive axial column load of about $0.25 A_g f_c^{'}$ enhanced the force transfer by bond ahead of the bend from the beam tension steel to the surrounding concrete. As a result, the beam steel tension force needed to be transferred at the bend reduced, the premature concrete tension cracking failure along the beam bar hook was entirely precluded. Degrading beam flexural behaviour at the fixed-end occurred due to severe bond degradation along the beam longitudinal reinforcement within and adjacent to the joint core.

The strengths achieved by Units EJ3 and Unit EJ4 were of similar magnitude in terms of their theoretical storey shear strengths and they were approximately 10 to 12% less than the theoretical strengths.

The strengths of Units EJ3 and Unit EJ4 were attained at similar storey drift levels. The storey shear strengths for clockwise loading direction were attained at a storey drift of about 1.1 to 1.5% but the storey shear strengths for anti-clockwise loading were attained at a storey drift of about 0.6%. The initial stiffnesses measured for Unit EJ3 and Unit EJ4 were also similar, and they were equivalent to a storey drift of about 0.6% at first yield.

6. In comparison with the tests on the identical units but with zero axial column load, the presence of compressive axial column load of 0.23 to 0.25 $A_g f_c^{'}$ caused the initial stiffness to increase by 180% and caused the available storey shear strength to increase by about 20 to 33% of the theoretical storey shear strengths.

7. With respect to the seismic behaviour of as-built reinforced concrete members, the observed post-elastic behaviour of the members for Units EJ3 and EJ4 has similar characteristics to that observed for Units 1 and 2.

The beam post-elastic behaviour dominated the overall seismic performance for the tests on both Units EJ3 and EJ4, and the beam non-linear behaviour was determined by the flexural behaviour at the fixed-end for both Units EJ3 and EJ4. No beam shear distresses were observed although the code method predicted that the beam shear capacity for both units EJ3 and EJ4 was only 20% of the shear demand at the stage of developing the flexural strength. Due to severe bond degradation along the beam longitudinal reinforcement adjacent to the joint core, the plane section assumption was significantly violated. As a result, the beam flexural strength was slightly lower than the theoretical strength based on the plane section assumption, and the beam flexural stiffness at first yield was significantly lower than the theoretical prediction based on sectional analysis.

A rotational ductility in the beam fixed-end became a proper index for beam non-linear deformation. The beam non-linear property in terms of the flexural strength and rotational capacity at the fixed-end was found to be very strongly dependent on the axial load imposed on the columns transversely framing into the same joint. When compared with the cases with no column axial load, a column axial load of about $0.25A_gf_c'$ could lead to the increase of about 15% in the flexural strength and the increase of 50% to 80% in the initial stiffness for the beams.

This means that the conventional flexure theory, which assumes the member's flexural behaviour to be completely determined by the member itself, needs to be modified when used for assessing the flexural behaviour at the fixed-ends of as-built reinforced concrete members with plain round longitudinal reinforcement, or a model allowing for the deformation within the joint needs to be developed.

8. The danger of the column bar buckling for as-built columns only occurred when the columns were near the flexural yielding and this may be related to the steel's

Bauschinger effect. For the test of Unit 2, the compressive column axial load was only about $0.12 A_g f_c^{'}$ but apparent column bar buckling was observed. For the tests of Units EJ3 and EJ4, the compressive column axial load was about $0.25 A_g f_c^{'}$ but no evident column bar buckling was observed. The difference between Unit 2 and Units EJ3 and EJ4 was that, at the stage of developing the flexural strength of the test unit, the columns of Unit 2 approached the yielding stage, but the columns of Units EJ3 and EJ4 were still well in elastic range.

Simulated seismic loading test on the retrofitted as-built exterior beam-column joint unit REJ1

9. When the beam bar hooks are bent away from the joint core in the exterior columns, the theoretical examination of the force transfer mechanism across the joint core shows that an alternative force path across the joint core, which is a concrete strut running from the midway of the beam bar hook to the opposite joint corner, needs be actuated and this requires sufficient column transverse reinforcement above and below the joint core to control the opening of the beam bar hooks in the exterior columns.

The test on REJ1 showed that fibre-glass jacketing in the column areas above and below the joint core controlled the premature concrete tension cracking failure along the beam bar hooks and actuated the postulated force transfer path across the joint. The performance of Unit REJ1 was comparable to that of Unit EJ2, which had the beam bar hooks bent into the joint and was also tested with zero axial column load, suggesting that performance of the as-built exterior beam-column joint assemblies with inadequate beam bar hook configurations in the exterior columns would be similar to that with the beam bar hooks bent into the joint core, should sufficient confinement be provided for the column areas immediately above and below the joint cores.

The overall performance of Unit REJ1 was governed by the degrading beam flexural behaviour.

11.3 MODELLING OF SEISMIC BEHAVIOUR OF AS-BUILT CONCRETE MEMBERS WITH PLAIN ROUND LONGITUDINAL BARS

With adequate analytical model capable of reproducing the inelastic response of individual reinforced concrete components, the global post-elastic behaviour of a complete structure

can be adequately estimated by integrating the local behaviour of individual structural components. The conclusions below are associated with the modelling of the post-elastic behaviour of as-built reinforced concrete members with plain round longitudinal reinforcement and they are generalised based on the evidence of both the interior and exterior beam-column joint tests.

1. When an as-built reinforced concrete member has plain round longitudinal reinforcement, modelling of the post-elastic behaviour of the member should focus on the flexural behaviour at the member fixed-ends. A proper index to the member's non-linear deformation is the rotational ductility at the fixed-end, rather than the curvature ductility associated with a given plastic hinge length.

2. The member non-linear property, in terms of the flexural strength and rotational deformation at the fixed-end, was not only dependent on the member itself, but also strongly dependent on the member force transfer across the joint, especially dependent on the axial actions of the members transversely framing into the same joint. The compressive axial load imposed on the transverse members at the same joint would enhance the bond mechanism along the member longitudinal reinforcement within the joint region, leading to enhanced flexural strength and stiffness at the member fixed-end.

3. A method for determining the non-linear static flexural behaviour at the fixed-end of an as-built reinforced concrete member with plain round longitudinal reinforcement was proposed and the effect of the compressive column axial load on the beam flexural behaviour at the fixed-end was tentatively allowed for.

The non-linear static flexural behaviour at the fixed-end of an as-built reinforced concrete member was represented by a tri-linear monotonic skeleton curve. The three characteristic points were the point at the first yield, the point at the attainment of the member ultimate flexural strength, and the points at the finish of the flexural strength degradation.

The flexural strengths of as-built reinforced concrete members at first yield and at ultimate stage were suggested to be obtained using 85% of the steel yield strength, irrespective of the axial action on the transverse members at the same joint. For the beams, the initial stiffness at first yield was taken as 50% of the theoretical prediction based on the sectional analysis when the columns at the same joint had no axial load present, but it was taken as 75% of the theoretical predictions when the columns at the same joint were subjected to a

compressive column axial load of not less than $0.25A_gf_c'$. The deformation at developing the beam ultimate strength was suggested to be twice the yield deformation, based on the test evidence. The deformation and the available flexural strength at the finish of the degradation were also defined based on the test evidence, and the observed faster beam strength degradation due to the compressive column axial action had also been considered in the proposed model. When the compressive column axial load was zero, the beam flexural strength degraded to 65% of the theoretical flexural strength when the flexural deformation was 16 times the theoretical yield deformation. When the compressive column axial load was not less than $0.25A_gf_c'$, the beam flexural strength degraded to 50% of the theoretical flexural strength at the flexural deformation equal to 8 times the theoretical yield deformation. For situations between these limits, an interpolation method was used. For the columns, the initial stiffness was suggested to be 75% of the theoretical prediction without allowing for the effect of the axial load in the beams at the same joint. The deformation at developing the column ultimate flexural strength was also suggested to be twice the deformation at first yield as for the beams. Regarding the column strength degradation, it was suggested that the column flexural strengths degraded to 50% of the theoretical strengths when the flexural deformation was 8 times the theoretical yield deformation and the beams at the same joint were assumed to have no effect on column strength degradation.

11.4 CONCLUSIONS FROM GLOBAL NON-LINEAR ANALYSIS OF THE SUBJECT BUILDING

11.4.1 Seismic Assessment of The Subject Frame Building

Based on the information on the seismic behaviour of individual reinforced concrete members obtained from the simulated seismic loading tests, the seismic assessment of the subject reinforced concrete frame structure represented by the as-built test units was carried out by conducting the global non-linear static and dynamic analyses using the inelastic structural analysis program "RUAUMOKO". In estimating the seismic weight, two cases were considered. One case was that the external frame of the subject frame building had brick masonry infills, and the other case was that the subject frame building had no masonry infills. For both cases, it was assumed that the masonry infills were non-structural elements and thus they did not contribute to the structural stiffness. Seismic

assessment of the subject reinforced concrete frame structure led to the following conclusions:

1. The overall non-linear behaviour of the frame structure was dominated by flexure. The subject frame structure would be very unlikely to develop a soft-storey column failure mechanism in a major earthquake.

2. A non-linear static (push-over) analysis showed that the structural post-yielding performance was governed by the local member deformation capacity and the code specified deflection criteria. Before the code specified maximum deflection criteria was reached, the member fixed-end rotations were very likely to exceed their capacities.

3. The P-Δ effect on the structural performance was insignificant, as long as the structural deformation satisfied the deflection criteria specified by the code.

4. No level of structural ductility could be relied on and the structural assessment had to be based on an elastic response. In this case, the available structural strength in terms of base shear was only 71% of the design seismic force when masonry infills were not considered to contribute to the seismic weight, and only 47% of the design seismic force when the masonry infills were considered to contribute to the seismic weight. The design seismic force was determined according to the current New Zealand design code NZS4203: 1992. Inclusion of the contribution of masonry infills in estimating the seismic weight could make a significant difference in the estimated structural seismic performance. For this case, allowance for the masonry infills in estimating the seismic weight, although led to longer fundamental period thus a smaller seismic design force coefficient, gave a much larger seismic weight, resulting in much more inadequate seismic performance.

5. The non-linear dynamic analysis of the subject frame structure, which allowed for the contribution of masonry infills to the seismic weight but not for the structural stiffness, concluded that the investigated structure would survive during a major earthquake of similar magnitude and similar vibration characteristics to the El Centro 1940 North-South earthquake motion.

11.4.2 Seismic Assessment of The Subject Infilled Frame Building

A non-linear static analysis of the infilled frame was conducted. The subject building was considered to have non-integral brick masonry infills in the external frame and the infills not only contributed to the seismic weight but also contributed to the structural stiffness. Seismic assessment of the subject infilled frame building came to the following conclusions:

1. The non-integral masonry infills were most likely to fail in horizontal sliding shear failure and the masonry infills in this case could be adequately modelled as a shear spring.

2. The infilled frame building would immediately develop a soft story column failure mechanism in the first floor, following the horizontal sliding shear failure in the masonry panels. After that, the structural performance was similar to a base-isolated structure. No level of ductility could be relied on and the structural design had to be based on elastic response.

3. The analysis demonstrated that the earthquake–resistant capacity of the infilled frame structure was only 38% of the seismic design demand according to NZS4203: 1992, leading to the conclusion that the allowance for the masonry infills caused the structural seismic performance to degrade. Due to the presence of the masonry infills, the structural dynamic properties changed significantly, leading to a large increase in the seismic design force demand. The increase in the structural capacity due to the non-integral masonry infills did not match the increase in the seismic demand, resulting in the observed degradation in the earthquake – resistant capacity of the infilled frame structure.

11.5 MAIN CONTRIBUTIONS OBTAINED FORM THIS REASEARCH

11.5.1 Tests on As-Built Interior Beam-Column Joint Units

1. When the interior beam-column joint units with plain round longitudinal bars is a marginal weak beam-strong column system, the compressive column axial load won't improve the system's stiffness performance but causes the strength to be reduced if it is expressed as the percentage of the theoretical strength, as was observed for the tests on

Units 1 and 2. This is different from the case with deformed longitudinal bars where the compressive axial load could improve the system's stiffness performance,

2. When deformed longitudinal reinforcement is used, the compressive column axial load not higher than about $0.3A_gf_c'$ would improve the joint shear capacity. However, when the plain round longitudinal reinforcement is used, the compressive column axial load would not have a beneficial effect on the joint shear performance and performance could degrade greatly, if there is very small amount of column transverse reinforcement within and adjacent to the joint cores and the columns are only marginally stronger than the beams at the joint, as was observed for Units 1 and 2.

This is because the compressive column axial load could enhance the column bar buckling for this marginal weak beam-strong column system, resulting in extensive concrete spalling within and adjacent to the joint core and significantly reducing the joint shear resiting area. As a result, the joint shear performance could greatly degrade.

3. Compared with the otherwise identical test on as-built interior beam-column joint but with deformed longitudinal bars, the use of plain round longitudinal reinforcement suppressed the shear failure in the joint core, but led to less satisfactory flexural performance, especially the flexural stiffness.

The code methods do not give adequate results when used for assessing the seismic performance of the as-built reinforced concrete components. This is especially true when the code methods are used for assessing the shear performance.

11.5.2 Tests on As-Built and Retrofitted Exterior Beam - Column Joint Units

1. For the as-built exterior beam-column joint units, when plain round longitudinal reinforcement is used and the amount of the column transverse reinforcement is small, the premature concrete tension cracking failure along the beam bar hooks, which is initiated by the interaction between the column bar buckling and the opening action of the beam bar hooks, is the most critical aspect, irrespective of the beam bar hook details, when the column axial load was zero.

2. At an exterior beam-column joint, the columns are usually much stronger in flexure than the beam. The compressive column axial load can greatly improve the seismic performance of the as-built exterior beam-column joint units. When the compressive

column axial is about $0.25A_g f_c'$, the concrete tension cracking along the beam bar hooks can be precluded, consequently, causing the effect of different beam bar hook details on the seismic performance of the systems to become very insignificant. This can be seen by comparing the test results of Units EJ1 and EJ2 with the test results of Unit EJ3 and EJ4.

3. Whereas, in the case of as–built exterior beam-column joints with deformed bars, the shear failure in the beam and the joint core initiated the failure of the system, the use of plain round longitudinal reinforcement totally suppressed the shear failure in the beam and the joint core, but enhanced the premature concrete tension cracking along the beam bar hooks when the column axial load is low. The attainment and maintenance of the strength and the stiffness of the units were poor, especially the stiffness.

4. When the beam bar hooks are bent away from the joint core in the exterior columns and the compressive column axial load is low, the force transfer mechanism across the joint core will be an alternative force path across the joint core, which is a concrete strut running from the midway of the beam bar hook to the opposite joint corner. In this case, sufficient column lateral reinforcement above and below the joint core needs be provided, such as by wrapping the columns, in order to control the opening of the beam bar hooks in the exterior columns and actuate the alternative force path across the joint core. When the compressive axial load is high, external jacketing of the columns won't apparently improve the seismic performance because the member force transfer across the joint core in this case has changed.

11.5.3 Generalised Seismic Behaviour of As-Built Concrete Members with Plain Round Longitudinal Bars

1. When an as-built reinforced concrete member contains plain round longitudinal reinforcement, the post-elastic behaviour of the member is dominated by the flexural behaviour at the fixed-end of the member, rather than by the premature shear failure as was observed for the as-built member with deformed longitudinal reinforcement. Hence, the modelling of the post-elastic behaviour of existing reinforced concrete members focuses on the flexural behaviour at the member fixed-end.

A proper index for the non-linear deformation of the member is the rotational ductility at the fixed-end, rather than the curvature ductility associated with a given plastic hinge length.

The member flexural behaviour in terms of the flexural strength and the rotational deformation at the fixed-end is closely related to the bond mechanism along the member longitudinal reinforcement within the joint region and thus is related to the compressive axial load of transverse members at the same joint.

2. A method for determining the non-linear static flexural behaviour at the fixed-end of an as-built reinforced concrete member with plain round longitudinal reinforcement is proposed and the effect of the compressive column axial load at the same joint on the enhancement of the beam flexural behaviour at the fixed-end is tentatively allowed for.

The non-linear static flexural behaviour at the fixed-end of the member is suggested to be a tri-linear monotonic skeleton curve. The three characteristic points are the point at the first yield, the point at the attainment of the member ultimate flexural strength, and the points at the finish of the flexural strength degradation.

In determining the point at the first yield and the point at the attainment of the member ultimate flexural strength, the adverse effect of severe bond degradation along the member longitudinal reinforcement on the flexural strength and stiffness is allowed for. The enhancement of the beam flexural stiffness due to the compressive column axial load at the same joint is also allowed for. In determining the point at the finish of the strength degradation, the effect of the compressive column axial action on the beam flexural strength degradation is also incorporated in the proposed model.

11.5.4 Seismic Assessment of The Subject Reinforced Concrete Building

1. When a building has the plain round longitudinal reinforcement, the potential problem areas are the concrete tension cracking failure along the beam bar hooks in the exterior columns and the poor flexural behaviour at the member fixed-ends, rather than the premature shear failure in the beams and the joints as is the case with deformed longitudinal reinforcement.

2. When the as-built reinforced concrete frame structure has no masonry infills, which acts as structural elements, the structure is very unlikely to develop a soft-storey column failure mechanism in a major earthquake. The overall non-linear behaviour of the structure is dominated by flexure. The structure can have a large deformation capacity but it does not perform in a ductile manner. In this case, the use of a displacement ductility is

no longer meaningful and a inter-storey drift becomes a better index to the whole structure's deformation capacity, as revealed by the tests. No level of structural ductility can be relied on and the seismic assessment has to be based on the elastic response. The earthquake resisting capacity of the structure is not adequate, according to the current code demand.

3. When the frame building had non-integral masonry infills as structural elements, the building would develop a soft story column failure mechanism in the first floor, immediately after the attainment of the maximum shear strength in the infills. After that, the structure would perform in a similar way to a base-isolated structure. Unlike the bare frame, the structural deformation capacity of the infilled frame was small. No level of ductility could be relied on and the analysis has to be based on elastic response. The allowance for the non-integral masonry panels means that the structural earthquake-resisting capacity was more inadequate, compared to that without allowance for the masonry panels. However, if the masonry panels exist in a structure, they should be included in the analytical model in order that the assessment can have any validity for the real structure.

11.6 RECOMMENDATIONS AND SUGGETSIONS FOR FUTURE RESEARCH

1. It is suggested that degrading flexural behaviour of the as-built reinforced concrete members can be upgraded by using external passive or active jacketing adjacent to the member areas adjacent to the joint core. A quantitative study on the enhancement of the member flexural strength and the stiffness needs to be studied.

2. A proper member model capable of relating the non-linear flexural behaviour of the members with other members framing into the same joint should be developed. Such a member model would be very useful when the member fixed-end rotational deformation is significant.

3. Enhancement of the beam flexural behaviour in terms of the beam flexural strength versus the rotational deformation at the beam fixed-end due to the compressive column axial load varying over a broader range needs to be studied by conducting tests on both as-built and well-designed reinforced concrete members.

4. Influences of the column cross sectional details, including the column overall depth, the column bar arrangement etc, on the beam flexural behaviour at the fixed-end should be studied, when the deformed longitudinal bars are used (see Section 8.2.2.3).

Member deformation in the form of the rotation at the fixed-end is mainly associated with bond mechanism along the member longitudinal reinforcement within the joint region, therefore the member deformation at the fixed end is also affected by the other members at the same joint. For example, the bond mechanism along the beam deformed longitudinal reinforcement within the joint core would be enhanced should the columns have intermediate longitudinal bars going through the joint. As a result, the beam fixed-end rotational deformation would reduce and the beam flexural behaviour at the fixed-end would be enhanced.

5. For the seismic assessment of the subject structure conducted by Hakuto et al, the code equation was used for assessing the flexural and shear behaviour of the members and the joints. Hakuto's tests showed that the code equation was too conservative for predicting the shear performance. Hence, a non-linear two-dimensional analysis needs to be conducted for the subject structure, where the deformed longitudinal reinforcement is assumed and the information revealed by Hakuto et al on the post-elastic behaviour of the members is employed. Such an analysis could reveal the difference in the structural responses due to the effect of the steel type used.

6. A three-dimensional non-linear analysis should be conducted for this reinforced concrete structure to study the possible torsional effect on the global behaviour of the structure. Also a three-dimensional analysis would more properly model the peculiar geometry of the sixth floor of the prototype building.

7. The behaviour of masonry infills in these older structures needs more elaborate investigation under both push-over and time history analyses, with an emphasis on using a more appropriate model for the masonry infills.

REFERENCES

[A1] Aoyama, H., "A method for the Evaluation of the seismic Capacity of Existing Reinforced Concrete Buildings in Japan", *Bulletin of the New Zealand National Society for Earthquake Engineering*, Vol.14, No.3, Sept. 1981, pp105-130

[A2] Aoyama, H., "Outline of Earthquake Provisions in the Recently Revised Japanese Building Code", *Bulletin of the New Zealand National Society for Earthquake Engineering*, Vol.14, No.2, June 1981

[A3] ATC, " A Handbook for Seismic Evaluation of Existing Buildings ATC-22", *Applied Technology Council*, Redwood City, California, ATC21, 1989, 169pp

[A4] ATC, "Rapid Visual Screening of Buildings for Potential Seismic Hazards: A Handbook, *Applied Technology Council*, Redwood City, California, ATC21,1988

[A5] ATC, "Evaluating the Seismic Resistance of Existing Buildings ATC-14" *Applied Technology Council*, Redwood City, California, 1987,370pp

[A6] Aycardi, L. E., Mander, J. B., and Reinhorn, A. M., "Seismic Resistance of Reinforced Concrete Frame Structures Designed Only for Gravity Loads: Part II - Experimental Performance of Subassemblages", *Technical Report NCEER-92-0028*, December 1, 1992

[A7] Alcocer, S.M., and Jirsa, J.O., "Strength of Reinforced Concrete Frame Connections Rehabilitated by Jacketing" Structural Journal of American Concrete Institute, Vol.90, No.3, May 1993

[B1] Brunsdon, D. R and Priestly, M.J.N., "Assessment of Seismic Performance Characteristics of Reinforced Concrete Buildings Constructed Between 1936 and 1975", *Bulletin of the New Zealand National Society for Earthquake Engineering*, Vol. 17, No.3, Sept. 1984, pp.163—181

[B2] Benuska, L., "Loma Prieta Earthquake Reconnaissance Report", *Earthquake Spectra, EERI, Supplement* to Vol.6, No.1, 1990, pp 151-187

[B3] Beres, A., White, R.N., and Gergely,P., "Seismic Behaviour of Reinforced Concrete Frame Structures With Non-ductile Details: Part I - Summary of Experimental Findings of Full-Scale Beam-Column Joint Tests", *Technical Report NCEER-92-0024*, September 30, 1992

[B4] Beres, A., White, R.N., and Gergely,P., "Detailed Experimental Results of Interior and Exterior Beam-Column Joint Tests Related to Lightly Reinforced Concrete Frame Buildings", *Technical Report 92-7, Cornell University, Ithaca, NY*, 1992

[B5] Bracci, J.M., Reinhorn, A. M., and Mander, J. B., "Seismic Resistance of Reinforced Concrete Frame Structures Designed Only for Gravity Loads: Part I - Design and Properties of a One-Third Scale Model Structure", *Technical Report NCEER-92-0027*, December 1, 1992

[B6] Bracci, J.M., Reinhorn, A. M., and Mander, J. B., "Seismic Resistance of Reinforced Concrete Frame Structures Designed Only for Gravity Loads: Part III - Experimental Performance and Analytical Study of a Structural Model", *Technical Report NCEER-92-0029*, December 1, 1992

[C1] Collins, M.P., and Mitchell, D., *"Prestressed Concrete Structures"*, Response Republications, Canada, 1997

[C2] Cheung, P. C., Seismic Design of Reinforced Concrete Beam-Column Joints with Floor Slab, *Research Report 91-4, Department of Civil Engineering, University of Canterbury*, Oct. 1991

[C3] Clough, R.W., Benuska,K.L, Wilson,E.L.,"Inelstic Earthquake Response of Tall Building", *Proceedings of Third World Conference on Earthquake Engineering*, New Zealand, Vol. Section II, pp68-89(1965)

[C4] Carr, A. "*RUAUMOKO - Inelastic Dynamic Analysis*", Department of Civil Engineering, University of Canterbury, 1996

[C5] Crisafulli, F. J. et al, "Seismic Behaviour of Reinforced Concrete Structures with Masonry Infills", *Doctoral Thesis, Department of Civil Engineering, University of Canterbury*, 1997

[C6] Chapman, H.E., "Seismic Retrofitting of Highway Bridges", *Bulletin of the New Zealand National Society for Earthquake Engineering*, Vol.24, No.2, June 1991, pp186-201

[C7] Clough, R.W., Benuska, K.L., and Lin, T.Y., "FHA Study of Seismic Design Criteria for High Rise Buildings, HUDTS-3", Aug., 1966, *Federal Housing Administration, Washington, D.C.*

[C8] Carr, A. "*HYSTERESIS PROGRAM (1984-2000)*", Department of Civil Engineering, University of Canterbury, New Zealand

[C9] Carr, A. "*SPECTRA (1986-2001)*", Department of Civil Engineering, University of Canterbury, New Zealand

[D1] Dekker, D. R. and Park, R., " The Repair and Strengthenening of Reinforced Concrete Bridge Piers", *Research Report 92-1, Department of Civil Engineering, University of Canterbury,* March 1992.

[D2] Dowell, R. K., Seible, F. and Wilson, E. L., " Pivot Hysteresis Model for Reinforced Concrete Members", *ACI Structural Journal*, Vol.95, No.5, Sept-Oct. 1998 pp607-617

[D3] Dawe, J.L. and Seah,C.K., "Behaviour of Masonry Infilled Steel Frames", Canadian Journal of Civil Engineering, Vol.16, 1989, pp.865-876

[D4] Durrani, A.J. and Luo, Y.H., "Seismic Retrofitting of Flat-Slab buildings with Masonry Infills", proceedings from the NCEER Workshop on Seismic Response of Masonry, SanFrancisco, California, Feb. 1994, pp. 1/3-8

[E1] El - Attar, A. G., White, R. N., and Gergely, P., " Behaviour of Gravity Load Designed Reinforced Concrete Buildings Subjected to Earthquakes", *ACI Structural Journal,* Vol.94, No.2, March-April 1997, pp133-145

[F1] Fenwick, R.C. and Megget, L.M., "Elongation and Load Deflection Characteristics of Reinforced Concrete Members Containing Plastic Hinges", *Bulletin of the New Zealand National Society for Earthquake Engineering*, Vo.26, No.1, March 1993, pp28-41

[F2] Filippou, F.C., D'Ambrisi, A. and Issa,A., "Effects of Reinforcement Slip on hysteretic Behaviour of Reinforced Concrete Frame Members", *ACI Structural Journal*, Vol.96, No.3, May-June 1999, pp327-335

[G1] Giberson, M.F., "The Response of Nonlinear Multi-story Structures subjected to Earthquake Excitation", *Earthquake Engineering Research Laboratory, California Institute of Technology Pasadena, California, EERL Report* (1967).

[G2] Giberson, M.F., "Two Nonlinear Beams with Definitions of Ductility", *Journal of the Structural Division, Proceedings of the American Society of Civil Engineers*, Vol. 95, No.ST2, Feb. 1969, pp137-157.

[H1] Hakuto, S., Park, R. and Tanaka, H., "Retrofitting of Reinforced Concrete Moment Resisting Frames", *Research Report 95-4, Department of Civil Engineering, University of Canterbury,* August 1995

[H2] Hakuto, S., Park, R. and Tanaka, H., "Behaviour of As-Built and Retrofitted Beam-Column Joints of a 1950s Designed Reinforced Concrete Building Frame", *Proceedings of Technical Conference of New Zealand Concrete Society*, Taupo, New Zealand, March 1995

[H3] Hakuto, S., Park, R. and Tanaka, H., "Seismic Performance of Existing Reinforced Concrete Building Frames", *Proceedings of Technical Conference of New Zealand Concrete Society*, Taupo, New Zealand, March 1995

[H4] Hill, G., "Guild to Instrumentation, Transducers, and Data Loggers", *Department of Civil Engineering, University of Canterbury*, December 1995

[H5] Hakuto, S., Park, R. and Tanaka, H., "Effect of deterioration of Bond of Beam Bars Passing Through Interior Beam-Column Joints on Flexural Strength and Ductility", *ACI Structural Journal*, Vol.96, No.5, September-October 1999, pp858-864

[H6] Hwang, S. J. and Lee, H. J., "Analytical Model for Predicting Shear Strength of Exterior Reinforced Concrete Beam-Column Joints for Seismic Resistance", *ACI Structural Journal*, Vol.946, No.5, September-October 1999, pp846-857

[H7] Hsu, T.T.C., "Softening Truss Model Theory for Shear and Torsion", *ACI Structural Journal,* Vol. 88, No.5, pp552-561

[J1] Jury, R. D., " A Decade of Progress Since the Edgecumbe Earthquake-Buildings", *Bulletin of the New Zealand National Society for Earthquake Engineering*, Vol.30, No.2, June 1997, pp174-176

[J2] Jara, M., Hernandez, C., Garcia, R. and Robles, F., " The Mexico Earthquake of September 19, 1985. Typical Cases of Repair and Strengthening of Concrete Buildings", *Earthquake Spectra*, Vol. 5, No.1, California, USA, Feb.1989

[K1] Kunnath, Sashi K., Reinhorn Andrei M. and Park, Young J., "Analytical Modeling of Inelastic Seismic Response of R/C Structures", *Journal of Structural Engineering, ASCE*, Vol. 116, No.4 April 1990, pp996-1017

[K2] Kabeyasawa, T., Shiohara, H., Otani, S., and Aoyama, H., "Analysis of the Full-Scale Seven-Story reinforced Concrete Test Structure", *Journal of the Faculty of Engineering, the University of Tokyo (B)*, Vol. XXXVII-I, March 1983, pp431-478

[K3]. Kitayama, K., Otani,S., and Aoyama, H., "Earthquake Resistant Design Criteria for Reinforced Concrete Interior Beam-Column Joints", *Proceedings of Pacific Conference on Earthquake Engineering*, 1987, Wairakei, Vol. 1, pp315-326

[K4] Kato, H., Goto, T. and Mizuno, H., "Cyclic Loading Tests of Confined Masonry wall Elements for Structural Design Development of Apartment Houses in the Third World", Proceedings of the Tenth world Conference on Earthquake Engineering, Madrid, Spain, 1992, Vol.6, pp. 3539-3544

[K5] klingner, R.E. and Bertero, V.V., Infilled Frames in Earthquake-Resistant Construction, University of California, Berkeley, Report No. EERC 76-32, December, 1976

[L1] Liu, A. and Park, R., " Seismic Load Tests on Two Interior Beam-Column Joints Reinforced by Plain Round Bars Designed to Pre-1970s Seismic Codes", *Bulletin of the New Zealand National Society for Earthquake Engineering*, Vol.31, No.3, Sept. 1998.

[L2] Lees, J.M. and Burgoyne, C. J., "Experimental Study of Influence of Bond on Flexural Behaviour of Concrete Beams Pretensioned with Aramid Fiber Reinforced Plastics", *ACI Structural Journal*, Vol.96, No.3, May-June 1999, pp377-385

[L3] Lees, J.M. and Burgoyne, C. J., "Rigid Body Analysis of Concrete Beams Pre-Tensioned with Partially Bonded AFRP Tendons", Proceedings of the Third International Symposium on Non-Metallic (FRP) Reinforcement for Concrete Structures, Japan Concrete Institute, Japan, Oct. 1997, pp759-766

[L4] Lin, C.M., Restrepo, J.I. and Park, R., "Seismci Behaviour and Design of Reinforced Concrete Interior Beam-Column Joints", Research Report, 2000-1, University of Canterbury. pp471

[M1] Maffei, J., Seismic Evaluation & Retrofit Technology for Bridges, *Transfund New Zealand Research Report*, No.78, 1997

[M2] Maffei, J., Seismic Testing & Behaviour of A 1936-Designed Reinforced Concrete Bridge, *Transfund New Zealand Research Report*, No.78, 1997

[M3] Moehle, J.P., "Preliminary Report on the Seismological and Engineering Aspects of the January 17,1994 Northridge Earthquake", *Report UCB/EERC-94-01, Earthquake Engineering Research Center, University of California at Berkeley*, 1994

[M4] Mahin, S.A. and Bertero, V.V., "An Evaluation of Inelastic Seismic Design Spectra", *American Society of Civil Engineering*, Vol.107, No.ST9, Sept. 1981, pp1777-1795

[M5] Marti, P., "How To Treat Shear in Structural Concrete", *ACI Structural Journal*, Vol.96, No.3, May-June 1999, pp408-414

[M6] Moehle, J.P., Nicoletti, J.P., Lehman, D.E., "Review of Seismic Research Results on Existing Buildings", *Report No. SSC 94-03, Seismic Safety Commission, State of California,* Fall 1994.

[M7] Magenes and Calvi, "In-Plane Seismic Response of Brick Masonry Walls", Earthquake Engineering and Structural Dynamics, 1997

[M8] Mallick, D.V. and Garg, R.P, "Effect of Openings on the Lateral Stiffness of Infilled Frames", Proceedings of the Institution of Civil Engineering, Vol.49, 1971, pp.193-209

[M9] Marti, P., " Basic Tools of Reinforced Concrete Beam Design", *ACI Structural Journal*, Vol.82, No.1, Jan-Feb 1985, pp 46-56.

[N1] NZS3101: 1995, "The Design of Concrete Structures, NZS3101: 1995", *Standards New Zealand,* Wellington, 1995

[N2] Norena F, Castaneda C and Iglesias J "The Mexico Earthquake of September 19, 1985, Evaluation of the Seismic Capacity of Buildings in Mexico City" *Earthquake Spectra,* Vol.5, No.1 California, USA, February 1989

[N3] *"A draft document of Guidelines for the Seismic Assessment of pre-1975 Reinforced Concrete Structures and Structural Steel Buildings"*, prepared by a study group of the New Zealand National Society for Earthquake Engineering for the Building Industry Authority, April 1994.

[N4] *"The Assessment and Improvement of the Structural Performance of earthquake Risk Buildings, Draft for General Release",* New Zealand National Society for Earthquake Engineering, June 1996, pp122

[N5] NZS4203: 1992, "Code of Practice for general Structural Design and Design Loadings for Buildings", *Standards New Zealand,* Wellington, 1995

[O1] Ohkubo, M., "*A Note for the Seminar on the Method for Evaluating Seismic Performance of Existing Reinforced Concrete Buildings*", Kyushu Institute of Design, 1990

[O2] Otani, S. and Sozen, M.A.,"Behaviour of Multistory Reinforced Concrete Frames during Earthquakes", *Structural Research Series No.392, University of Illinois, Urbana, Illinois* (1972)

[O3] Otani, Shunsuke, "Nonlinear Dynamic Analysis of Reinforced Concrete Structures", *Canadian Journal of Civil Engineering*, Vol.7, No.2, pp333-344 (1980).

[O4] Otani, Shunsuke, "Hysteresis Models of Reinforced Concrete for Earthquake Response Analysis", *Journal of the Faculty of Engineering, The University of Tokyo (B)*, Vol. XXXVI, No.2, pp407 - 441 (1981).

[P1] Park, R. and Paulay, T., *Reinforced Concrete Structures*, John Wiley & Sons, New York, 1975, p769

[P2] Park, R "Review of Code Developments in New Zealand", *Bulletin of New Zealand National Society for Earthquake Engineering*, Vol 104, No.3, 1981

[P3] Park, R., "Seismic Assessment and Retrofit of Concrete Structures-United States and New Zealand Developments*", Proceedings of Technical Conference of New Zealand Concrete Society, Wairakei,* 1992, pp18-25

[P4] Priestley, M.J.N, and Calvi, G.M., "Towards a Capacity Design Assessment Procedure for Reinforced Concrete Frames", *Earthquake Spectra*, Vol.7, No.3, 1991, pp413-437

[P5] Priestley, M.J.N., " Displacement Based Seismic Assessment of Existing Reinforced Concrete Buildings", *Proceedings of Pacific Conference on Earthquake Engineering, Vol.2, Melbourne,* 1995, pp 225-244

[P6] Park, R., "A Static Force-Based Procedure for the Seismic Assessment of Existing Reinforced Concrete Moment Resisting Frames", *Bulletin of the New Zealand National Society for Earthquake Engineering*, Vol.30, No.3, 1997, pp213-226

[P7] Park,R, I J Billings, G C Clifton, J Cousins, A Filiatrault, D N Jennings, LCP Jones, N D Perin, S L Rooney, J Sinclair, D D Spurr, H Tanaka and G Walker (1995) " The Hyogo-ken Nanbu Earthquake(The Great Hanshin Earthquake) of 17 January 1995. Report of the NZNSEE Reconnaissance Team, *Bulletin of the New Zealand National Society for Earthquake Engineering*, Vol.28, No.1, 1995, pp1- 98

[P8] Park, R., "Evaluation of Ductility of Structures and Structural Assemblages from the Laboratory Testing", *Bulletin of the New Zealand National Society for Earthquake Engineering*, Vol.22, No.3, Sept. 1989, pp 155-166

[P9] Priestley, M.J.N., Seible, F., and Calvi, G. M., " *Seismic Design and Retrofit of Bridges*", John Wiley & Sons, Inc., New York, 1996, p686

[P10] Paulay, T., Equilibrium Criteria for Reinforced Concrete Beam-Column Joints, *ACI Structural Journal*, Nov.-Dec. 1989 P635-643

[P11] Paulay,T., and Priestley, M.J.N., *Seismic Design of Reinforced Concrete and Masonry Buildings*, John Wiley & Sons, Inc., New York, 1992

[P12] Priestley, M.J.N., Seible, F., and Calvi, G.M., *Seismic Design and Retrofit of Bridges*, John Wiley & Sons, Inc. USA, 1996

[P13] Paulay, T. and Scarpas, A., "The Behaviour of Exterior Beam-Column Joints", *Bulletin of the New Zealand National Society for Earthquake Engineering*, Vol.14, No.3, Sept. 1981, pp131-144

[P14] Park, R., Gaerty, L. and Stevenson, E. C., " Tests on an Interior Reinforced Concrete Beam-Column Joint", *Bulletin of the New Zealand National Society for Earthquake Engineering*, Vol.14, No.2, June 1981, pp81-92

[P15] Pessiki, S.P., Conley, C.H., Gergely, P., and White, R.N., " Seismic Behaviour of Lightly-Reinforced Concrete Column and Beam-Column joint Details", *Technical Report NCEER-90-0014*, August 2, 1990

[P16]. Pantazopoulou, S.J., Moehle, J.P., and Shahrooz, B.M., " Simple Analytical Model for T-Beams in Flexure", *Journal of Structural Engineering, ASCE*, Vol.114, No.7, July 1988, pp1507-1523

[P17] Priestley, M.J.N., and Kowalsky, M.J., "Aspects of Drift and Ductility Capacity of Rectangular Cantilever Structural Walls" *Bulletin of the New Zealand National Society for Earthquake Engineering*, Vol 31, No.2, 1998, p73-85

[P18] Priestley, M.J.N., "Brief Comments on Elastic Flexibility of Reinforced Concrete Frames and Significance to Seismic Design", *Bulletin of the New Zealand National Society for Earthquake Engineering*, Vol.31, No.4, 1998, p246-259

[P19] Park, R., "Ductility Evaluation from Laboratory and Analytical Testing", State –of- art Report in Special Theme Session SG on Ductility Evaluation and Design of Concrete Structures and Elements, *Proceedings of the 9th WCEE*, Tokyo/Kyoto, 1988, Vol. VIII, pp 605-615

[P20] Paulay, T., "Displacement Compatibility Considerations in the Seismic Design of Buildings", *Department of Civil Engineering, University of Canterbury*, Oct. 1998

[P21] Prietley, M.J.N and Calvi, G.M., "Concepts and Procedures for Direct Displacement-Based Design and Assessment", *Proceedings of the International Workshop on Seismic Design Methodologies for the Next Generation of Codes,* Belkema, Rotterdam, 1997, pp 171-181

[P22] Prietley, M.J.N. " Displacement-Based Seismic Assessment of reinforced Concrete Buildings", *Journal of Earthquake Engineering,* Vol.1, No.1, 1997, pp157-192

[P23] Priestley, M J N, Seible F and Chai Y H., " Design Guildlines for Assessment, Retrofit and Repair of Bridges for Seismic Performance" *Report SSRP92-01,* University of California, San Diego, 1992.

[P24] Priestley, M.J.N. and Seible, F., "Design of Seismic Retrofit Measures for Concrete Bridges", Seismic Assessment and Retrofit of Concrete Broidges, Report SSRP 91-03, *University of California,* San Diego, 1990, pp196-234

[P25] Priestley, M.J.N, Fyfe, E., and Seible, F.,"Column Retrofit Using Fiberglass-Epoxy Jackets", *First Annual Seismic Research Workshop,* California Department of Transportation, Sacamento, Dec.1991, pp 217-224

[P26] Pook, L.L. and Dawe, J.L., " Effects of Interface Conditions Between a Masonry Shear Panel and Surrounding Steel Frame", *Proceedings of the fourth Canadian Masonry Symposiu*m, 1986, Vol.2, pp.910-921

[P27] Pantazopoulou and Bonacci, "Consideration of Questions about Beam-Column Joint", *ACI Structural Journal*, Vol.89, No.1, Jan-Feb., 1992, pp27-36.

[R1] Rodriguez, M. and Park, R., "Repair and Strengthening of Reinforced Concrete Buildings for Earthquake Resistance", *Earthquake Spectra*, Vol. 7, No.3, 1991, pp439-459

[R2] Rodriguez, M. and Park, R., "Seismic Load Tests of Reinforced Concrete columns Strengthened by Jacketing", *Structural Journal of the American Concrete Institute*, Vol. 91, No.2, 1994, pp150-159

[R3] Rodriguez, M. and Park, R., "Seismic Load Tests of Reinforced Concrete Columns Strengthened by Jacketing*", Proceedings of the annual Technical Conference of the New Zealand Concrete Society*, Wairakei, Sept. 1990, pp72 - 83.

[S1] SANZ(1976), *Code of Practice for General Structural Design and Design Loadings for Buildings NZS 4203:1976*, Standards Association of New Zealand, Wellington

[S2] SANZ(1982), *Code of Practice for the Design of Concrete Structures NZS 3101 Part 1:1982, and Commentary on the Design of Concrete Structures NZS 3101 Part 2:1982*, Standards Association of New Zealand, Wellington

[S3] SNZ(1992), *Code of Practice for General Structural Design and Design Loadings for Buildings NZS 4203:1992, Volumn 1 Code of Practice and Volumn 2 Commentary,* Standards Association of New Zealand, Wellington

[S4] SNZ(1995), *Part 1 The Design of Concrete Structures and Part2 Commentary on the Design of Concrete Structures*, Concrete Structures Standard, NZS 3101:1995, Standards Association of New Zealand, Wellington

[S5] Sugano, S., "Seismic Capacity Evaluation of Existing Reinforced Concrete Buildings in Japan", *A Seminar Note at University of Canterbury*, April 1995

[S6] Satyarno, I., "Adaptive Pushover Analysis for the Seismic Assessment of Older Reinforced Concrete Buildings", Doctoral Thesis, Department of Civil Engineering, University of Canterbury, 2000, pp195

[S7] Shibata, A., and M.A. Sozen, "Substitute Structure Method for Seismic Design in Reinforced Concrete", *Journal of Mechanics Division, ASCE*, Vol. 102, No.ST1, 1976, pp1-18

[S8] Shiohara, Hitoshi "A New Model for Joint Shear Failure of Reinforced Concrete Interior Beam-Column Joints", *Journal of the School of Engineering, The University of Tokyo,* Vol. XLV (1998), pp15-40

[S9] Stoppenhagen, D.R.,and Jirsa, J.O., "Seismic Repair of a reinforced Concrete Frame using Encased Columns", University of Texas at Austin, PMFSEL, 1987 May, Report No.87-1

[S10] Stewart, W.G. "The Seismic Design of Plywood Sheathed Shear Walls", Ph.D Thesis, *Department of Civil Engineering, University of Canterbury, Christchurch, NZ*, 1987, pp395

[S11] Sculler, M., Mehrabi,A.B. et al, "Performance of Masonry-Infilled R/C Frames under In-Plane Lateral Loads: Experiments", *Proceedings from the NCEER Workshop on Seismic Response of Masonry,* San Francisco, California, February, 1994, pp.1/27-32.

[S12] Stafford Smith, B. and Riddington, J.R., "The Design of Masonry Infilled Steel Frames for Bracing Structures", The Structural Engineer, Vol.56B, No.1, 1978, pp.1-7

[T1] Takeda, T. Sozen, M.A. and Nielsen, N.N., "Reinforced Concrete Response to Simulated Earthquakes", *J. Struct. Engrg. Div., ASCE*, V.96, No.12, 1970, pp2257-2573

[W1] Wallace, J., " Behaviour of Beam Lap Splices under Seismic Loading, Master of Engineering Thesis, *Department of Civil Engineering, University of Canterbury*, 1996

APPENDIX A:

SEISMIC ASSESSMENT OF TEST UNITS

1. FLEXURAL STRENGTH CALCULATION OF BEAMS AND COLUMNS

Calculation Rules:

- Equilibrium equation using New Zealand Code Approach NZS3101:1995 was

$$\alpha_1 f_c' \, a \, b + A_s' \, f_s' = A_s \, f_y + N^* \qquad (1.1)$$

where: N^* is the applied axial load, N^* is positive if in compression and negative if in tension, see Fig.A-1; a is the depth of equivalent rectangular concrete compressive zone, a = β c, and c is the depth of concrete compressive zone in calculating the strains using plane section assumption; A_s' and f_s' are the flexural compressive steel area and the compressive steel stress in flexural compression steel respectively; A_s and f_y are the flexural tension steel area and the steel tension stress in flexural tension steel; b is the width of the member.

- β is 0.85 if $f_c' \le 30$ MPa, however, if $f_c' > 30$ MPa, $\beta = 0.85 - 0.008 \, (f_c' - 30)$

but $\beta \ge 0.65$ has to be satisfied.

- $\alpha_1 = 0.85$ for $f_c' \le 55$ MPa, and $\alpha_1 = 0.85 - 0.004(f_c' - 55)$ for $f_c' > 55$MPa, but α_1 must be not less than 0.75.
- Compressive flexural steel strain is found by using plane section theory and assuming the extreme concrete compressive strain is 0.003 as follows:

$$\varepsilon_s' = \frac{c - d'}{c} 0.003 \qquad (1.2)$$

$$f_s' = \varepsilon_s' E_s = 600 \, \frac{c - d'}{c} \qquad (1.3)$$

- Flexural strength can be found using the following equation:

$$M_b = A_s \, f_y (d - d') + \alpha_1 \, f_c' \, a \, b \, (d' - a/2) \qquad (1.4)$$

$$M_c = A_s \, f_y (d - \frac{h}{2}) + A_s' \, f_s' (d - \frac{h}{2}) + \alpha_1 \, f_c' \, a \, b \, (\frac{h}{2} - \frac{a}{2}) \qquad (1.5)$$

The diagrams for beam and column flexural strength calculation are illustrated in Fig. A-1.

The dimensions and reinforcing amounts used in beam and column strength calculation is listed in Table 1.1(a) and Table 1.1(b) for the interior beam column joint units and the exterior beam-column joint units respectively. It is noted that the two interior beam column joint units had the same dimensions and the same amount of reinforcing bars, and the four exterior beam-column

joint units had the same dimensions and the same amount of reinforcing bars except the beam bar hook details in exterior columns.

Table 1.1(a) Dimensions and Reinforcing Detail Parameters of Units 1 and 2

	For beam positive bending	For beam negative bending	For column bending
As (mm^2)	905	1809.6	1357
As'(mm^2)	1809.6	905	1357
p (%)	0.656	1.31	1.13
p' (%)	1.31	0.656	1.13
d (mm)	460	460	260
d'(mm)	40	40	40
b (mm)	300	300	460
$E_s(MPa)$	$2\times10^5 MPa$		

Table 1.1(b) Dimensions and Reinforcing Detail Parameters of Units EJ1 through EJ4

	For beam positive bending	For beam negative bending	For column bending
As (mm^2)	905	1357	905
As'(mm^2)	1357	905	905
p (%)	0.656	0.983	0.468
p' (%)	0.983	0.656	0.468
d (mm)	460	460	420
d'(mm)	40	40	40
b (mm)	300	300	460
$E_s(MPa)$	$2\times10^5 MPa$		

Table 1.2 Parameters f_c', f_y, f_{yt} N^*, α_1 and β for all units

Unit	f_c' (MPa)	f_y (MPa)	f_{yt} (MPa)	N^* (N)	α_1	β
Unit 1	43.8	321	318	0.0	0.85	0.74
Unit 2	48.9	321	318	800,000	0.85	0.70
Unit EJ1	34.0	321	318	0.0	0.85	0.82
Unit EJ2	29.2	321	318	0.0	0.85	0.85
Unit EJ3	34.0	321	318	1,800,000	0.85	0.82
Unit EJ4	36.5	321	318	1,800,000	0.85	0.80

To simplify the calculation of the member flexural strength, the parameters f_c', f_y, N^*, α_1 and β are summarised in Table 1.2 for all units, and the calculated member flexural strengths is summarised in Table 1.3 for all the units.

Table1.3 Member Flexural Strength of Test Units

Unit	Beam Negative Bending	Beam Positive Bending	Column
Unit 1	c = 53.6 mm a = 39 mm	c = 39 mm a = 29 mm	c = 38 mm a = 28 mm
	$M_b^- = 250$ *kN-m*	$M_b^+ = 129$ *kN-m*	$M_c = 108$ *kN-m*
Unit 2	c = 51.8 mm a = 36 mm	c = 38 mm a = 27 mm	c = 67 mm a = 47 mm
	$M_b^- = 251$ *kN-m*	$M_b^+ = 129$ *kN-m*	$M_c = 198$ *kN-m*
Unit EJ1	c = 48.2 mm a = 40 mm	c = 40.2 mm a = 33 mm	c = 34.5 mm a = 28.3 mm
	$M_b^- = 190$ *kN-m*	$M_b^+ = 129$ *kN-m*	$M_c = 120$ *kN-m*
Unit EJ2	c = 56.7 mm a = 43 mm	c = 41.4 mm a = 35.2 mm	c = 36.1 mm a = 30.6 mm
	$M_b^- = 189$ *kN-m*	$M_b^+ = 128$ *kN-m*	$M_c = 119$ *kN-m*
Unit EJ3	c = 48.2 mm a = 40 mm	c = 40.2 mm a = 33 mm	c = 154.8 mm a = 127 mm $f_s' = 600\frac{c-40}{c} > 321$ $f_s' = 321$MPa
	$M_b^- = 190$ *kN-m*	$M_b^+ = 129$ *kN-m*	$M_c = 392$ *kN-m*
Unit EJ4	c = 47.3 mm a = 37.8 mm	c = 39.8 mm a = 31.8 mm	c = 148.3 mm a = 118.7 mm $f_s' = 600\frac{c-40}{c} > 321$ $f_s' = 321$MPa
	$M_b^- = 190$ *kN-m*	$M_b^+ = 129$ *kN-m*	$M_c = 400.0$ *kN-m*

The ratio of the sum of column moment capacity to the sum of beam moment capacity, calculated at the centre-line of the joint core, is listed in Table 1.4 for all test units.

Table 1.4 Ratio of Column Flexural Strength to Beam Flexural Strength at a Joint

Units	Unit 1	Unit 2	Unit EJ1	Unit EJ2	Unit EJ3	Unit EJ4
$\sum M_c / \sum M_b$	0.63	1.16	2.07 (+) 1.40 (-)	2.07 (+) 1.40 (-)	6.76 (+) 4.59 (-)	6.90 (+) 4.68 (-)

(+) means that the value is associated with the positive beam bending direction and (-) means that the value is associated with the beam negative bending direction.

From Table 1.4, it is clear that Unit 1 would develop plastic hinges in columns, but Unit 2 would develop plastic hinges in beams. For all the four exterior beam-column joint units EJ1 through EJ4, the beam would develop plastic hinge.

2. CALCULATION OF MEMBER YIELD CURVATURES

(1). Depth of Concrete Compressive Zone at First Yield:

- **For Beams and Columns without Axial Load**

Members should be still in the elastic range at first yield stage. In this case, the depth of the concrete compressive zone can be found by assuming a triangular distribution of concrete compressive stress. Under this assumption, k can be found as follows for the member with zero axial load [P1]:

$$k = [(\rho + \rho')^2 n^2 + 2(\rho + \frac{\rho' d'}{d})n]^{\frac{1}{2}} - (\rho + \rho')n \qquad (1.6)$$

where k is the coefficient of the concrete compressive zone, kd is the depth of the concrete compressive zone, and n is the ratio of steel elastic modulus to concrete elastic modulus.

$E_s = 2\times10^5 MPa$ for all units, and $E_c = 3320\sqrt{f_c'} + 6900(MPa)$ = 28872, 30116, 26259, 24840, 26259 and 20958 MPa, according to NZS3101:1995, for Units 1, 2, EJ1, EJ2, EJ3 and EJ4 respectively. When ACI equation $E_c = 4730\sqrt{f_c'}(MPa)$ is used, E_c = 31303, 33076, 27580, 25560, 27580 and 28576 MPa, for Units 1, 2, EJ1, EJ2, EJ3 and EJ4 respectively. Using the second set of concrete elastic modulus, the ratio of steel elastic modulus to concrete elastic modulus is calculated and listed in Table 1.5.

Table 1.5 Ratio of Steel Elastic Modulus to Concrete Elastic Modulus

Unit	Unit 1	Unit 2	Unit EJ1	Unit EJ2	Unit EJ3	Unit EJ4
$n = E_s / E_c$	6.4	6.0	7.3	7.8	7.3	7.0

- **For Columns with Compressive Axial Load**

Say the compressive axial load is N^*, assuming that concrete compressive stress be in elastic range, so use the following equation to find k at the first yield stage (see Fig.A-2),

$$A_s f_y + N^* = A_s' \varepsilon_s' E_s + \frac{1}{2} kd\varepsilon_c E_c b \qquad (1.7)$$

$$\varepsilon_s' = (kd - d')/(d - kd)\varepsilon_y \qquad (1.8)$$

$$\varepsilon_c = kd/(d - kd)\times\varepsilon_y \qquad (1.9)$$

(2). Member Curvature and Moment Capacity at First Yield

$$\Phi_y = \frac{f_y}{E_s d(1-k)} \qquad (1.10)$$

$$M_y = A_s f_y (d - \frac{1}{3} kd) + A_s' f_s' (\frac{1}{3} kd - d') \quad \text{if } N^* = 0.0 \qquad (1.11)$$

$$M_y = A_s f_y (d - \frac{1}{2} h) + A_s' \times f_s' (d - \frac{1}{2} h)$$

$$+ \frac{1}{2} kd \, f_c b (\frac{1}{2} h - \frac{1}{3} kd) \quad \text{if } N^* \neq 0.0 \qquad (1.11)'$$

Calculated member curvatures at first yield using the method described above are summarised in Table 1.6 for all the units.

Calculation of yield curvatures of columns with axial load, such as, for Unit 2, Units EJ3 and EJ4, are described in detail below, because of its complexity.

Table 1.6 Member Curvatures at First Yield

Unit	Beam Negative Bending		Beam Positive Bending		Column	
	k	Φ_y ($\times 10^{-6}$)	k	Φ_y ($\times 10^{-6}$)	k	Φ_y ($\times 10^{-6}$)
Unit 1	0.311	5.0	0.213	4.4	0.288	8.6
Unit 2	0.304	5.0	0.209	4.4	0.43	10.7
Unit EJ1	0.288	4.9	0.23	4.5	0.21	4.8
Unit EJ2	0.30	5.0	0.24	4.6	0.22	4.9
Unit EJ3	0.29	4.9	0.23	4.5	0.52	7.9
Unit EJ4	0.28	4.9	0.23	4.5	0.50	7.7

(3). Detailed Calculation of Yield Curvature of Columns with Axial Load

The calculation of yield curvature of columns with axial load, such as the columns for Unit 2, Units EJ3 and EJ4 is described in detail as follows due to the complexity caused by the presence of column axial load.

- Column Yield Curvature of Unit 2

f_y =321MPa, $A_s = A_s'$ =1357 mm^2, f_c' = 48.9MPa, b = 460mm, d = 300-40 = 260 (mm)

$\rho = \rho' = 0.0113$, E_c =4730 $\sqrt{f_c'}$ MPa =33076 MPa, E_s = 200000 MPa, n = 6

Substituting the parameters above into Eqs.(1.7), (1.8) and (1.9) leads to

$$1357\times321 + 800000 = 1357\times\frac{260k-40}{260(1-k)}\times\varepsilon_y E_s + 0.5k\times\frac{260k}{1-k}\varepsilon_y E_c\times460$$

This gives k = 0.43

Check, $f_c = \frac{k}{1-k} f_y/n$ = 40.35 MPa < $f_c^{'}$=43.8 MPa, Approximately "ok"

Φ_y = 10.7E-06

- Column Yield Curvature of Unit EJ3

Substituting the relevant parameters of Unit EJ3 in Table 1.1(b), Table 1.2 and Table 1.5 into equations 1.7, 1.8 and 1.9 leads to

$$905\times321 + 1800000 = 905\times\frac{42k-4}{42(1-k)}\times\varepsilon_y E_s + 0.5k\times\frac{420k}{1-k}\varepsilon_y E_c\times460$$

This gives k = 0.48, $f_c = \frac{k}{1-k} f_y/n$ = 40.87 MPa > $f_c^{'}$=34MPa, so concrete is in non-linear state and linear concrete stress distribution is obviously not true. Hence using the following equation [C1]:

$$A_s^{'} f_s^{'} + \alpha_1 f_c^{'} \beta\, c\, b = A_s f_y + N^* \qquad (1.12)$$

where: $\varepsilon_s^{'} = (c-d^{'})/(d-c)\varepsilon_y$

$f_s^{'} = \frac{c-40}{420-c} f_y$, α_1 and β are listed for different concrete stress states in Reference C1, using trial method to find the "c".

For concrete of $f_c^{'}$, $\varepsilon_c^{'}$=0.00215 (Concrete Peak Strain)

(1). Try $\varepsilon_t/\varepsilon_c^{'}$=0.75, α_1=0.762, β=0.691

so: $A_s^{'} f_s^{'} + \alpha_1 f_c^{'} \beta\, c\, b = 905\frac{c-40}{420-c}\times321 + 0.691\times0.762\times34\times c\times460 = 2090505$

905(c-40) 321+8235.112 c(420-c) =2090505(420-c)

c^2-709.3c+108061 =0, c =221.6 mm

Check: $\varepsilon_s = \frac{d-c}{c}\varepsilon_t = 1.44368\times10^{-3}$, so below yield, try again

(2) Try $\varepsilon_t/\varepsilon_c^{'}$=1, α_1=0.884 β=0.728

so: $A_s^{'} f_s^{'} + \alpha_1 f_c^{'} \beta\, c\, b = 905\frac{c-40}{420-c}\times321 + 0.884\times0.728\times34\times c\times460 = 2090505$

c^2-656.7c+88414 =0, so c=189 mm

Check: $\varepsilon_s = \dfrac{d-c}{c}\,\varepsilon_t = 2.6266\times10^{-3}$, so much bigger than first yield strain. Use interpolation method to find a good c,

$$c = 221.6 + \frac{189-221.6}{2.6266\times10^{-3} - 1.44368\times10^{-3}}(1.605\text{-}1.44368)\times10^{-3} = 217 \text{ mm}$$

In that case, $f_s^{'}$=280 MPa, $\alpha_1 = 0.762 + \dfrac{0.884-0.762}{189-221.6}(217\text{-}221.6) = 0.779$

$$\beta = 0.691 + \frac{0.728-0.691}{189-221.6}(217\text{-}221.6) = 0.696$$

$$\Phi_{yc}^{+} = \Phi_{yc}^{-} = \varepsilon_y/(\text{d-c}) = \frac{1.605\times10^{-3}}{420-217} = 7.91\times10^{-6}$$

$M_{yc}^{+} = M_{yc}^{-} = 905\times321\times(230\text{-}40) + A_s^{'} f_s^{'}(230\text{-}40) + \alpha_1 f_c^{'} \beta\, c\, b\,(230 - 0.5\beta c)$

= 387609107 N-mm = 388 kN-m

- Column Yield Curvature of Unit EJ4

f_y =321MPa, $A_s = A_s^{'}$ = 905 mm^2, $f_c^{'}$=36.5 MPa, b= 460mm, d=460-40 =420 (mm)

$\rho = \rho^{'}$ = 0.468%, $E_c = 4730\sqrt{f_c^{'}}$ MPa =28576 MPa, E_s = 200000 MPa, n = 7

Substituting the parameters above into Eqs.(1.7), (1.8) and (1.9) leads to :

$$905\times321 + 1800000 = 905\times\frac{42k-4}{42(1-k)}\times\varepsilon_y E_s + 0.5k\times\frac{420k}{1-k}\varepsilon_y E_c\times460$$

This gives k = 0.473

Check: $f_c = \dfrac{k}{1-k} f_y/n$ = 41MPa > $f_c^{'}$=34MPa, so concrete is in non-linear state and Equation (1.12) should be sued, similar to that for Unit EJ3.

Using trial method to find the "c".

For concrete of $f_c^{'}$= 36.5 MPa, $\varepsilon_c^{'}$=0.00215 (Concrete Peak Strain), use the values associated with $f_c^{'}$= 34 MPa due to unavailable data for $f_c^{'}$= 36.5 MPa in Reference C1.

(1). Try $\varepsilon_t/\varepsilon_c^{'}$=0.75, α_1=0.762, β =0.691

so: $A_s^{'} f_s^{'} + \alpha_1 f_c^{'} \beta\, c\, b = 905\dfrac{c-40}{420-c}\times321 + 0.691\times0.762\times36.5\times c\times460 = 2090505$

c^2 -689.5c+100658.6 =0 so c =210 mm

Check: $\varepsilon_s = \dfrac{d-c}{c}\,\varepsilon_t = 1.6125\times10^{-3}$, and it is close to steel yield strain of $\varepsilon_y = 1.605\times10^{-3}$.

$$f_s' = \frac{c-40}{420-c} f_y = 260 \text{ MPa}$$

$$\Phi_{yc}^{+} = \Phi_{yc}^{-} = \varepsilon_y/(\text{d-c}) = \frac{1.605\times10^{-3}}{420-210} = 7.66\times10^{-6}$$

$$M_{yc}^{+} = M_{yc}^{-} = 905\times321\times(230\text{-}40) + A_s' f_s'(230\text{-}40) + \alpha_1 f_c' \beta c b (230 - 0.5\beta c)$$

= 392205015 N-mm = 392 kN-m

3. CALCULATION OF MEMBER ULTIMATE CURVATURE OF TEST UNITS

Member ultimate curvatures are calculated using the measured material strengths and assuming that the ultimate concrete compressive strain is 0.004. Similar to the flexural strength calculation, find the distance form the extreme compression fibre to the neutral axis, c, which satisfies the equilibrium equation (1.1).

$$\alpha_1 f_c' \text{ a b} + A_s' f_s' = A_s f_y + N^* \qquad (1.1)$$

The previous equations 1.2 and 1.3, in the case of using the ultimate concrete compressive strain of 0.004, become:

$$\varepsilon_s' = \frac{c-d'}{c}0.004 \qquad (1.2)'$$

$$f_s' = 800\frac{c-40}{c} \qquad (1.3)'$$

$$\Phi_u = \frac{0.004}{c} \qquad (1.13)$$

The calculated member ultimate curvature is listed in Tables 1.7 for tests on Units 1, 2, EJ1 through EJ4.

Table 1.7 Calculated Member Ultimate Curvature

Unit	Beam Negative Bending		Beam Positive Bending		Column	
	c (mm)	$\Phi_u (\times 10^{-5})$	c (mm)	$\Phi_u (\times 10^{-5})$	c (mm)	$\Phi_u (\times 10^{-5})$
Unit 1	50	8.0	39	10.3	37.8	10.6
Unit 2	50	8.0	37	10.8	62.8	6.4
Unit EJ1	46.7	8.6	40.2	9.9	35.3	11.3
Unit EJ2	48.6	8.2	41	9.8	36.7	10.9
Unit EJ3	46.2	8.7	40	10	165.1	2.4
Unit EJ4	46	8.7	40	10	157.7	2.5

Table 1.8 Calculated Member Curvature Ductility Factor μ_Φ

Unit	Part of the unit	Bending direction	$\Phi_y (\times 1.0E\text{-}06)$	$\Phi_u (\times 1.0E\text{-}06)$	μ_Φ
Unit 1	Beams	Negative bending	5.0	80	16
		Positive Bending	4.4	103	23
	Columns		8.6	106	12
Unit 2	Beams	Negative bending	5.0	80	16
		Positive bending	4.4	108	25
	Columns		10.7	64	6
Unit EJ1	Beam	Negative bending	4.9	86	18
		Positive bending	4.5	99	22
	Columns		4.8	113	24
Unit EJ2	Beam	Negative Bending	5.0	82	16
		Positive Bending	4.6	98	21
	Columns		4.9	109	22
Unit EJ3	Beam	Negative Bending	4.9	87	18
		Positive Bending	4.5	100	22
	Columns		7.9	24	3
Unit EJ4	Beam	Negative Bending	4.9	87	18
		Positive Bending	4.5	100	22
	Columns		7.7	25	3

4. Member Curvature Ductility Factor

Based on the calculated member curvature at first yield (Table 1.6) and at ultimate stage (Table 1.7), the curvature ductility factors of members are computed and listed in Table 1.8 for all the test units.

5. THE IMPOSED SHEAR FORCES ON THE MEMBERS:

5.1 Storey Shear Strength and Imposed Column Shear Forces

The storey shear strength, V_c of each unit is developed at the attainment of the theoretical flexural strengths of the critical members. For all the six tests, except the test on Unit 1, the theoretical storey shear force strength of the unit is dominated by the flexural strengths of the beams (beam). V_c is calculated as follows:

For interior beam-column joint units,

$$V_c = \frac{M_b^+ + M_b^-}{(1905-150)} \times \frac{1905}{3200} \text{(N)}$$ for weak beam-strong column systems, such as, Unit 2

$$V_c = \frac{M_c}{1600-250} \text{(N)}$$ for weak column-strong beam systems, such as, Unit 1

For exterior beam-column joint units, the storey shear force strength of the unit is dominated by the beam flexural strength,

$$V_c^+ = \frac{M_b^+}{1905-230} \times 1905/3200 \text{(N)}$$ for positive beam bending

$$V_c^- = \frac{M_b^-}{1905-230} \times 1905/3200 \text{(N)}$$ for negative beam bending

Note that the flexural moment capacity has a unit N-mm in above equations.

The theoretical storey shear force strength is summarised in Table 1.9 for all the units.

Table 1.9 Storey Shear Force Strength of Test Units

Unit	Unit 1	Unit 2	Unit EJ1		Unit EJ2		Unit EJ3		Unit EJ4	
			+	-	+	-	+	-	+	-
V_c (kN)	80	128	46	67	46	67	46	67	46	67
$v_{n,c}$ (MPa)	$0.10\sqrt{f_c'}$	$0.15\sqrt{f_c'}$	$0.06\sqrt{f_c'}$		$0.06\sqrt{f_c'}$		$0.06\sqrt{f_c'}$		$0.06\sqrt{f_c'}$	

The imposed shear forces on members should be calculated at the development of the theoretical storey shear strength of the unit. Therefore, the imposed column shear force is actually the storey shear strengths of the unit, V_c.

The maximum nominal column shear stress at the theoretical flexural strength of the unit is given by

$$v_{n,c} = \frac{V_c}{b_c d_c} \qquad (1.14)$$

Hence the nominal column shear stress at the theoretical flexural strength of the unit is $0.10\sqrt{f_c'}$, $0.15\sqrt{f_c'}$, $0.06\sqrt{f_c'}$, $0.064\sqrt{f_c'}$, $0.06\sqrt{f_c'}$ and $0.06\sqrt{f_c'}$ MPa for Units 1, 2, EJ1 to EJ4 respectively.

5.2 Imposed Beam Shear Force

The imposed beam shear force should be calculated according to the storey shear force strength of the unit.

For a weak beam-strong column system, the maximum imposed beam shear forces are usually obtained at the development of beam negative flexural strength because beam negative flexural strengths are larger than beam positive flexural strengths. For a weak column-strong beam system, the imposed beam shear forces are obtained at the development of the system's storey shear force strength using force equilibrium condition.

$V_b = V_c \times 3200/3810 = 67$ kN for Unit 1

$V_b = M_b^-$ (kN-mm) /(1905-$\frac{1}{2}h_b$)(mm) =143 kN for Unit 2

$V_b = M_b^-$ (kN-mm) /(1905-$\frac{1}{2}h_b$)(mm) =113 kN for Unit EJ1 through EJ4

The imposed beam shear forces for all test units are listed in Table 1.10.

Table 1.10 Imposed Beam Shear Force (kN)

Unit	Unit 1	Unit 2	Unit EJ1	Unit EJ2	Unit EJ3	Unit EJ4
V_b (kN)	67	143	113	113	113	113
$v_{n,b}$ (MPa)	$0.073\sqrt{f_c'}$	$0.15\sqrt{f_c'}$	$0.14\sqrt{f_c'}$	$0.15\sqrt{f_c'}$	$0.14\sqrt{f_c'}$	$0.14\sqrt{f_c'}$

The maximum nominal beam shear stress at the theoretical flexural strength of the units is given by

$$v_{n,b} = \frac{V_b}{b_w d} \qquad (1.15)$$

Hence the nominal beam shear stress at the theoretical flexural strength of the units is $0.073\sqrt{f_c'}$, $0.15\sqrt{f_c'}$, $0.14\sqrt{f_c'}$, $0.15\sqrt{f_c'}$, $0.14\sqrt{f_c'}$ and $0.14\sqrt{f_c'}$ MPa for Units 1, 2, EJ1 to EJ4 respectively.

5.3 Imposed Maximum Horizontal Joint Shear Force

The imposed horizontal joint shear force is

$$V_{jh} = T_1 + T_2 - V_c \quad \text{for interior beam-column joints} \qquad (1.16)$$

$$V_{jh} = T_b - V_c \quad \text{for exterior beam-column joint} \qquad (1.17)$$

where: T_1 and T_2 are the tensile forces in tension reinforcement of the left and right beams respectively for interior beam-column joints, when the storey shear strength is developed; T_b is the tensile forces in beam tension reinforcement for exterior beam-column joints, when the storey shear strength is developed.

For Unit 1, which was a weak column-strong beam system, the imposed horizontal joint shear force is estimated by assuming that the two beams share equally the imposed bending moment because the beams still in the elastic range. In elastic range, the beam steel tension stress, f_s, can be found by getting k using equation 1.6. With the known k and the known external bending moment, using equation 1.11 can give the correspondent beam steel tension stress. Beam steel tension forces, T_1 and T_2 then can be calculated based on beam steel tension stress.

Typically, external bending moment is 118 kN-m for the beams of Unit 1, the k is found to be k = 0.311 for beam negative bending of Unit 1 and k= 0.213 for beam positive bending of Unit 1. As a result, $\varepsilon_s = 7.88\times10^{-4}$ and ε_s=1.52E-03 for beam negative bending and positive bending respectively.

Therefore, $V_{jh} = T_1 + T_2 - V_c$ = 483 kN for Unit 1

For the rest five tests, including tests on Unit 2, Unit EJ1 through Unit EJ4, the storey shear force strength of the unit is governed by the beam flexural strength, so the beam steel tension forces are the steel forces at yield level.

$V_{jh} = (A_s + A_s')f_y - V_c = 6\times452\times321 - 128000$ (N) =744kN for Unit 2

$V_{jh} = A_s f_y - V_c = 1357\times321 - 67500$ (N) = 368 kN for Units EJ1 through EJ4

Table 1.11 Imposed horizontal joint shear force (kN)

Unit	Unit 1	Unit 2	Unit EJ1	Unit EJ2	Unit EJ3	Unit EJ4
V_{jh} (kN)	483	744	368	368	368	368
v_{jh}(MPa)	$0.5\sqrt{f_c'}$	$0.8\sqrt{f_c'}$	$0.3\sqrt{f_c'}$	$0.3\sqrt{f_c'}$	$0.3\sqrt{f_c'}$	$0.3\sqrt{f_c'}$

Similarly, the nominal horizontal joint shear stress at the development of the flexural strengths of the test units can be calculated using

$$v_{jh} = \frac{V_{jh}}{b_j h_c} \tag{1.18}$$

It gives $0.5\sqrt{f_c'}$, $0.8\sqrt{f_c'}$, $0.3\sqrt{f_c'}$, $0.3\sqrt{f_c'}$, $0.3\sqrt{f_c'}$ and $0.3\sqrt{f_c'}$ MPa for Units 1, 2 EJ1 to EJ4 respectively. Alternatively, the nominal horizontal joint shear stress at the development of the flexural strengths of the test units is $0.08\,f_c'$, $0.11\,f_c'$, $0.05\,f_c'$, $0.06\,f_c'$, $0.05\,f_c'$, $0.05\,f_c'$ MPa for Unit 1, Unit 2, Unit EJ1, Unit EJ2, Unit EJ3 and Unit EJ4 respectively.

The imposed joint horizontal shear forces and the nominal horizontal joint shear stress are summarised in Table 1.11 for all test units.

6. ESTIMATION OF SHEAR CAPACITY OF MEMBERS AND BEAM-COLUMN JOINTS

Estimation of the shear capacity was carried out using both the NZS3101 Method and the current seismic assessment procedures recommended by Park. Measured material strengths and a strength reduction factor of unity are used here.

6.1 NZS3101: 1995 Method

The probable shear force strengths of the plastic hinge regions are calculated using NZS3101: 1995 design provisions for structures designed for ductility. The shear strengths of other regions are calculated using the non-seismic design provisions of NZS3101: 1995. It is noted that NZS3101 does not have a method for calculating the shear strength of existing beam-column joints.

(1). Beam Shear Force Capacity

According to NZS3101:1995, the beam shear force capacity is calculated as follows:

$$V_{pb} = v_c b_w d + \frac{A_v f_{yt} d}{s} = \underline{k}\sqrt{f_c'} b_w d + \frac{A_v f_{yt} d}{s} \tag{1.19}$$

where: v_c =nominal shear stress carried by the concrete mechanism, f_c' = probable concrete compressive strength, b_w = width of beam web, d= effective depth of beam, A_v =area of transverse shear reinforcement, $\rho_w = A_s / b_w d$ and A_s is area of tension reinforcement.

In the non-seismic provisions of NZS3101: 1995,

$$v_c = (0.07+10\rho w)\sqrt{fc'} \qquad (fc' \text{ is in unit of MPa}) \qquad (1.20)$$

In plastic hinge regions,

$$v_c = 0.0 \qquad (1.21)$$

For the beams of Unit 1, non-seismic provision is applied because the beams were not expected to form plastic hinges. For other test units, including Unit 2 and Units EJ1 through EJ4, v_c is taken as zero in calculating the beam shear force capacity. The calculated beam shear force capacity for Unit 1, Unit 2, Unit EJ1 through EJ4 using the method of NZS3101: 1995 are respectively 146 kN, 22 kN, 22 kN, 22 kN, 22kN and 22 kN.

(2). Column Shear Force Capacity

According to NZS3101:1995, the column shear capacities are calculated as follows:

$$V_{pc} = v_c b_w d + \frac{A_v f_{yt} d}{s} = V_{pc,c} + V_{pc,s} \qquad (1.22)$$

$$v_c = (1+\frac{3N^*}{A_g f_c'}) v_b \qquad (1.23)$$

where: A_g = column gross sectional area, ρ_w = column tensile reinforcement ratio, b_w = column width, d= effective depth of column section, A_v = area of transverse reinforcement, f_{yt} = yield strength of transverse reinforcement.

In non-seismic provisions of NZS3101:1995,

$$v_b = \underline{k}\sqrt{f_c'} = (0.07+10\rho_w)\sqrt{f_c'} \qquad (1.24)$$

In plastic hinge regions where the axial load is less than $0.1 f_c'$,

$$v_c = 0.0 \qquad (1.25)$$

Hence,

$V_{pc,c}$ = 0.0 for Unit 1

$= (1+\frac{3N^*}{A_g f_c'})(0.07+10\rho_w)\sqrt{f_c'}\ b_w d$ = 209 kN for Unit 2

$$V_{pc,c} = (1+\frac{3N^*}{A_g f_c'})(0.07+10\rho_w)\sqrt{f_c'}\, b_w d$$

= 132 kN for Unit EJ1

= 122 kN for Unit EJ2

= 230kN for Unit EJ3

= 232 kN for Unit EJ4

The contribution of column transverse reinforcement to the total column shear force capacities is:

$$V_{pc,s} = \frac{A_v f_{yt} d}{s} = 56.6\times2\times318\times260/230 = 41 \text{ kN}$$ for Units 1 and 2

$$V_{pc,s} = \frac{A_v f_{yt} d}{s} = 56.6\times318\times420/305 = 25 \text{ kN}$$ for Units EJ1 to EJ4

Column shear force strength is the sum of the contribution of concrete to the shear strength and the contribution of column transverse reinforcement to the shear strength.

6.2 Method Proposed by Park in Reference P6

Detailed description of the method proposed by Park for estimating the shear force strength of members and beam-column joints can be seen in Chapter 2. For the members where plastic hinges were expected, the member shear strength will be estimated by taking into account of the imposed member curvature ductility. Generally, the method proposed by Park in Reference P6 will give less conservative estimations of the shear force capacity of the members and beam-column joints in existing reinforced concrete structures.

(1). Beam Shear Force Capacity

The beam shear capacities are estimated as follows, according to the method proposed by Park [P6]:

$$V_{pb} = V_{b,c} + V_{b,s} \qquad (1.26)$$

in which: $V_{b,c} = \underline{k}\sqrt{f_c'}\, b_w d$, $V_{b,s} = A_v f_{yt} d / s$

For the beams of Unit 1 where plastic hinges were not expected, $\underline{k}$ is taken as 0.2 (see Chapter 2). For the beams of Unit 2 and Units EJ1 through EJ4 where plastic hinges were expected, $\underline{k}$ is found according to the imposed ductility factor of the members (see Table 1.12 for all units).

Using the values of parameters summarised in Table 1.1(a) and Table 1.1(b) and the coefficient $\underline{k}$ in *Table 1.12*, the beam shear force capacity is estimated for all the units (see Table 1.12).

Table 1.12 Coefficient k for Estimating Beam Shear Force Capacity

Units	Unit 1	Unit 2	Unit EJ1	Unit EJ2	Unit EJ3	Unit EJ4
f_c'(MPa)	43.8	48.9	34	29.2	34	36.5
k	0.2	0.05	0.05	0.05	0.05	0.05
V_{pb}(kN)	204	70	62	59	62	63

(2). Column Shear Force Capacity

Using the proposed method for estimating the column shear force capacities by Priestley, rather than the method by Park, the column shear force capacities are estimated as follows (see Chapter 2):

Table 1.13 Estimation of Column Shear Force Capacity Using Method in P6

Units	Unit 1	Unit 2	Unit EJ1	Unit EJ2	Unit EJ3	Unit EJ4
f_c'(MPa)	43.8	48.9	34	29.2	34	36.5
N^*(kN)	0.0	800	0.0	0.0	1800	1800
a (mm)	28	47	28	31	127	119
tanα	NA	NA	NA	NA	0.104	0.107
k	0.1	0.29	0.29	0.29	0.29	0.29
$V_{c,c}$ (kN)	73	224	286	265	286.2	296.9
V_n(kN)	0	72	0	0	187.2	192.6
$V_{c,s}$(kN)	61	61	38.8	38.8	38.8	38.8
V_{pc}(kN)	134	358	325	304	512	528

$$V_{pc} = V_{c,c} + V_{c,s} + V_n \tag{1.27}$$

in which, $$V_{c,c} = v_c\ 0.8\ A_g = \underline{k}\sqrt{f_c'}\ 0.8\ A_g \tag{1.28}$$

$$V_{c,s} = \frac{A_v f_{yt} d''}{s}(\cot 30°) \tag{1.29}$$

$$V_n = N^* \tan\alpha \tag{1.30}$$

$\tan\alpha = (h_c - a)/l_c$

where: a is the equivalent depth of the rectangular compressive concrete block at ultimate state. Detailed calculation of column shear force capacity is listed in *Table 1.13* for all the units, based on the expected curvature ductility imposed as listed in *Table 1.8.*

(3). Horizontal Shear Force Capacity of Beam-Column Joints

The maximum horizontal shear capacity of beam-column joints is calculated using only the current seismic assessment procedures proposed by Park. NZS3101: 1995 gives no indication for estimating the shear force capacities of existing beam-column joint cores.

For both interior and exterior beam-column joints, the probable horizontal shear force capacity is obtained by the following equation [P6].

$$V_{Pjh} = v_c \; b_j \; h_j + V_{Pjh,S} \qquad (1.31)$$

where: $v_c = \underline{k}\sqrt{f_c'}\sqrt{1+\frac{N^*}{A_g \underline{k}\sqrt{f_c'}}}$ and $\underline{k}$ is the coefficient associated with the imposed ductility factor, b_j and h_j are the effective joint width and depth respectively, and they are determined based on NZS3101: 1995.

According to NZS3101:1995, h_j is taken as h_c, which is the overall depth of column in the direction of the horizontal joint shear to be considered, b_j is taken as:

I. where $b_c > b_w$: either $b_j = b_c$, or $b_j = b_w + 0.5 h_c$, whichever is the smaller;

II. where $b_c < b_w$: either $b_j = b_w$ or $b_j = b_c + 0.5 h_c$, whichever is the smaller.

As a result, b_j = 450 mm and h_j = 300 mm for two interior beam-column joints, but b_j = 460 mm and h_j = 460 mm for the four exterior beam-column joint units.

$V_{Pjh,S}$ = contribution of horizontal joint shear reinforcement, and it is zero for two interior beam-column joints and $V_{Pjh,S}$ =56.6×318 =18 kN for the four exterior beam-column joint units. Detailed calculation is seen in Table 1.14.

Table 1.14. Estimated Horizontal Joint Shear Capacity

Unit	Unit 1	Unit 2	Unit EJ1	Unit EJ2	Unit EJ3	Unit EJ4
N^* (kN)	0.0	800.0	0.0	0.0	1800.0	1800.0
f_c' (MPa)	43.8	48.9	34	29.2	34	36.5

k	0.3	0.3	0.1	0.3	0.1	0.3
v_c	1.99	4.07	0.583	1.621	2.302	4.325
V_{Pjh} (kN)	268	550	141	361	505	933

The estimated shear force capacity of beams, columns and beam-column joints, for all the units, is listed in Table 1.15. The investigation of the amount of transverse reinforcement for resisting the shear force is seen in Chapter 4.

Table 1.15 Shear Force Capacity of Beams, Columns and Beam-Column Joints (kN)

Part of Units	Unit 1	Unit 2	Unit EJ1	Unit EJ2	Unit EJ3	Unit EJ4
Beams, V_{pb} (kN)	146 (204)	22 (70)	22 (62)	22 (59)	22 (62)	22 (63)
Columns, V_{pc} (kN)	41 (134)	250 (358)	157 (325)	147 (304)	255 (512)	257 (528)
Beam-Column Joints, V_{Pjh} (kN)	(268)	(550)	(141)	(361)	(505)	(933)

Note: Values without bracket are given by NZS3101: 1995, and the values with brackets are given by the method proposed by Park [P6].

7. Requirement of Transverse Reinforcement Quantities for Anti-buckling

For all the tests, the axial load ratios on the columns are low. In this case (N*< $0.3 A_g f_c'$), the transverse reinforcement is more required for preventing buckling of longitudinal bars than that for confining the compressed concrete. Hence, apart from the investigation of the amount of transverse reinforcement according to the shear requirement as conducted before, the amount of transverse reinforcement is also investigated according to the requirement for preventing bar buckling using NZS3101: 1995. The procedure proposed in Reference P6 does not have a method in this regard.

7.1 Beams

- **Code Specification on Spacing Limit of Beam Transverse Reinforcement**

According to NZS3101: 1995, centre-to-centre spacing of stirrups or ties along the beam members shall not exceed the smaller of the least lateral dimension of the cross section or 16 times longitudinal bar diameter; centre-to-centre spacing of stirrups or ties in potential plastic hinge regions shall not exceed either d/4 or 6 times the diameter of any longitudinal compression bar to be restrained in the outer layers.

For Unit 1 where beams were not expected to form plastic hinges, b_w =300 mm< $16d_b$ =384 mm. Hence, s =300 mm governs.

For Unit 2 and Unit EJ1 through EJ4, beams were expected to develop plastic hinges, d/4 = 460/4 =115 mm < 6 d_b =144 mm. Hence, s = 115 mm governs.

- **Code Specification on Size Limit of Beam Transverse Reinforcement**

According to NZS3101: 1995, the diameter of the stirrup-ties in beams shall not be less than 5 mm. In addition, the area of one leg of a stirrup-tie placed in potential plastic hinge regions in the direction of potential buckling of the longitudinal bar shall not be less than:

$$A_{te} = \frac{\sum A_b f_y}{96 f_{yt}} \frac{s}{d_b} \qquad (1.32)$$

where $\sum A_b$ is the sum of the area of the longitudinal bars reliant on the tie.

For Unit 1 where beams were not expected to form plastic hinges, A_{te} = Area of D5 =19.6(mm^2). Area of per set shall not be less than 40 mm^2 for Unit 1.

For Unit 2 and Units EJ1 through EJ4, beams were expected to develop plastic hinges, the limit on area of one leg of a stirrup-tie shall be calculated by Equation 1.32.

$$A_{te} = \frac{\sum A_b f_y}{96 f_{yt}} \frac{s}{d_b}$$

$$= \frac{2D24 \times 321}{96 \times 318} \times \frac{115}{24} = 45.5 \text{ (mm}^2\text{)} \qquad \text{for Unit 2}$$

$$= \frac{1.5D24 \times 321}{96 \times 318} \times \frac{115}{24} = 34.2 \text{ (mm}^2\text{)} \qquad \text{for Units EJ1 to EJ4}$$

Area of per set shall not be less than 91 mm^2 for Unit 2 and 68 mm^2 for Units EJ1 to EJ4.

7.2 Columns

- **Code Specification on Spacing Limit of Column Transverse Reinforcement**

According to NZS3101: 1995, centre-to-centre spacing of stirrups or ties along the column members shall not exceed the smaller of 1/3 of the least lateral dimension of the cross section or 10 times longitudinal bar diameter; centre-to-centre spacing of stirrups or ties in potential plastic hinge regions shall not exceed either 1/4 of the least lateral dimension of the cross section or 6 times the diameter of any longitudinal compression bar to be restrained.

For Unit 1 where columns were expected to develop plastic hinges, $b_c/4$ = 75 mm < $6d_b$ =144 mm. Hence, s =75 mm governs.

For Unit 2 and Unit EJ1 through EJ4, columns were not expected to develop plastic hinges, $b_c/3$ = 100 mm < $10d_b$ =240 mm, so s = 100 mm governs for Unit 2

$b_c/3$ = 153 mm < $10d_b$ =240 mm, so s = 153 mm governs for Unit EJ1 to EJ4

- **Code Specification on Size Limit of Column Transverse Reinforcement**

According to NZS3101: 1995, the diameter of the stirrup-ties in columns shall not be less than 10 mm for the column longitudinal bars with diameter 20 mm to 32 mm. The area of one leg of a stirrup-tie, when governed by the requirement for anti-buckling, shall not be less than:

$$A_{te} = \frac{\sum A_b f_y}{135 f_{yt}} \frac{s}{d_b} \qquad (1.33)$$

In potential plastic hinge regions of columns, the area of one leg of a stirrup-tie, when governed by the requirement for anti-buckling, shall not be less than:

$$A_{te} \quad \frac{\sum A_b f_y}{96 f_{yt}} \frac{s}{d_b} \qquad (1.32)$$

where $\sum A_b$ is the sum of the area of the longitudinal bars reliant on the tie.

For Unit 1 where columns were expected to develop plastic hinges, the limit on area of one leg of a stirrup-tie is calculated using Equation 1.32.

$$A_{te} = \frac{\sum A_b f_y}{96 f_{yt}} \frac{s}{d_b} = \frac{D24 \times 321}{96 \times 318} \times \frac{75}{24} = 14.9 (\text{mm}^2) \qquad \text{for Unit 1}$$

For Unit 2 and Unit EJ1 through EJ4, columns were not expected to develop plastic hinges, the limit on area of one leg of a stirrup-tie shall be calculated by Equation 1.33.

$$A_{te} = \frac{\sum A_b f_y}{135 f_{yt}} \frac{s}{d_b} = \frac{D24 \times 321}{135 \times 318} \times \frac{100}{24} = 14.1 \ (\text{mm}^2) \quad \text{for Unit 2}$$

$$= \frac{D24 \times 321}{135 \times 318} \times \frac{153}{24} = 21.5 \ (\text{mm}^2) \quad \text{for Units EJ1 to EJ4}$$

In this case, area of per set shall not be less than 60 mm^2 for Unit 1, and shall not be less than 57 mm^2 for Unit 2, and shall not be less than 43 mm^2 for Units EJ1 to EJ4.

7.3 Beam-Column Joints

NZS3101: 1995 also has specification to limit the spacing and size of column transverse reinforcement within beam-column joints.

According to Clause 11.4.4.5 of NZS3101: 1995, the spacing of sets of column ties or hoops within a joint shall not exceed 10 times the column bar diameter or 200 mm, whichever is less.

$10d_b$ =10*24 = 240 mm for all the units

Hence, so s = 200 mm governs.

- Area Limit

According to Clause 11.4.4.5 of NZS3101: 1995, the quantities of horizontal joint reinforcement shall conform to that required by Eq.1.34.

The area of one leg of horizontal joint reinforcement shall not be less than:

$$A_{te} = \frac{\sum A_b f_y}{96 f_{yt}} \frac{s}{d_b} = \frac{452 \times 321}{96 \times 318} \frac{200}{24} = 39.6 \text{ (mm}^2\text{)}$$ for all the units

Hence, area of per set of horizontal transverse reinforcement within the joints shall not be less than 79 mm^2

Summary of the results obtained from this theoretical consideration is seen in Chapter 4 of the thesis.

7. Development of the Longitudinal Reinforcement within Joints

NZS3101: 1995 has the specifications on the maximum diameter of beam bars passing through the joints. Note that NZS3101: 1995 specifies the use of deformed longitudinal reinforcement.

According to NZS3101: 1995, the maximum diameter of beam bars passing through the interior joints should satisfy the following requirement by equation 1.34:

$$\frac{d_b}{h_c} \le 3.3 \alpha_f \frac{\sqrt{f_c'}}{\alpha_o f_y} \qquad (1.34)$$

where, α_f =1.0 for one-way frames and α_o is 1.0 when the plastic hinges are not expected in the beams, and α_o=1.25 when plastic hinges are expected to develop at column faces.

This gives $\frac{d_b}{h_c} \le 14.7$ for Unit 1 and $\frac{d_b}{h_c} \le 17.4$ for Unit 2.

NZS3101: 1995 also has the specifications on the maximum diameter of deformed column bars passing through the joints. According to NZS3101: 1995, when columns are designed to develop plastic hinges in the end regions, equation 1.34 needs to be satisfied; but when columns are not intended to develop plastic hinges in the end regions, the maximum diameter of column bars may exceed that given by equation 1.34 by 25%.

$$\frac{d_b}{h_b} \le 3.2 \frac{\sqrt{f_c'}}{f_y} \qquad (1.35)$$

For Unit 1, columns are expected to develop plastic hinges, $\frac{d_b}{h_b} \le 15.1$, and for Unit 2 and Units EJ1 to EJ4, columns are not expected to develop plastic hinges, $\frac{d_b}{h_b} \le 11.5, 13.8, 14.9, 13.8, 13.3$ respectively.

APPENDIX B

MODELLING OF RESTRAINTS BY TRANSVERSE BEAMS AT THE SIXTH FLOOR

This appendix describes in details for determining the properties of the vertical shear springs representing the restraints from the transverse beams at the sixth floor, when conducting the structural analysis in the longitudinal direction.

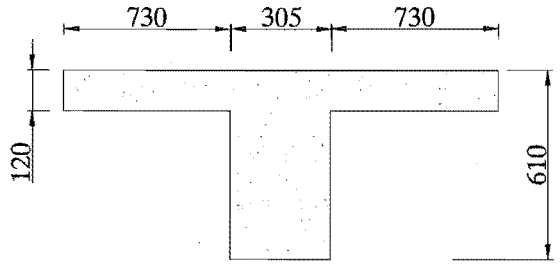

Fig.B.1 Overall Cross Sectional Dimensions of Transverse Beams at Sixth Floor

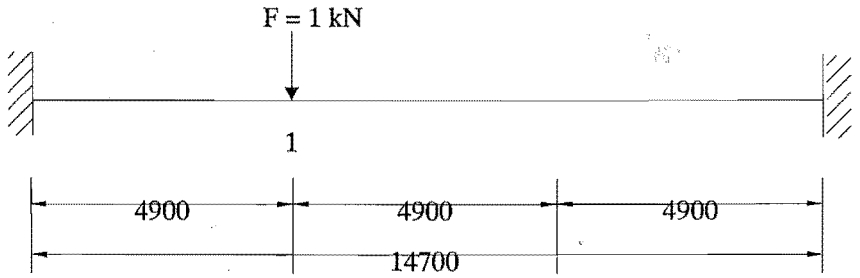

Fig.B.2 Analytical Model For Determining the Properties of Shear Springs

The cross section of the transverse beams of frame B at the sixth floor is a T beam as shown in Fig. B.1 and it is determined by allowing for the contribution of the floor slabs. The equivalent width of the T beam flange is taken as 1.2 times the beam overall depth, namely, 730 mm. The gross sectional moment of inertia of the transverse beam is 1.092E11 mm^4.

The shear spring stiffness is obtained by conducting elastic analysis of the structural model in Fig.B.2, where the two ends of the beam are fixed. A unit load is applied at location 1, where the longitudinal beam intersects with the transverse beam, then the stiffness of the shear spring is equal to $1/\Delta_{11}$, where Δ_{11} is the induced deflection at the location 1 due to the unit load. This gives that the vertical shear spring stiffness is 30240 kN/m.